Academic Press is an imprint of Elsevier
Radarweg 29, PO BOX 211, 1000 AE Amsterdam, The Netherlands
Linacre House, Jordan Hill, Oxford OX2 8DP, UK
32 Jamestown Road, London NW1 7BY, UK
30 Corporate Drive, Suite 400, Burlington, MA 01803, USA
525 B Street, Suite 1900, San Diego, CA 92101-4495, USA

First edition 2009

Copyright © 2009 Elsevier Inc. All rights reserved

No part of this publication may be reproduced, stored in a retrieval system or transmitted in any form or by any means electronic, mechanical, photocopying, recording or otherwise without the prior written permission of the publisher

Permissions may be sought directly from Elsevier's Science & Technology Rights Department in Oxford, UK: phone (+44) (0) 1865 843830; fax (+44) (0) 1865 853333; email: permissions @elsevier.com. Alternatively you can submit your request online by visiting the Elsevier web site at http://elsevier.com/locate/permissions, and selecting *Obtaining permission to use Elsevier material*

Notice
No responsibility is assumed by the publisher for any injury and/or damage to persons or property as a matter of products liability, negligence or otherwise, or from any use or operation of any methods, products, instructions or ideas contained in the material herein. Because of rapid advances in the medical sciences, in particular, independent verification of diagnoses and drug dosages should be made

ISBN: 978-0-12-374743-3
ISSN: 0065-2318

British Library Cataloguing in Publication Data
A catalogue record for this book is available from the British Library

Library of Congress Cataloging-in-Publication Data
A catalog record for this book is available from the Library of Congress

For information on all Academic Press publications
visit our website at books.elsevier.com

Printed and bound in USA

09 10 10 9 8 7 6 5 4 3 2 1

Working together to grow
libraries in developing countries
www.elsevier.com | www.bookaid.org | www.sabre.org
ELSEVIER BOOK AID International Sabre Foundation

LIST OF CONTRIBUTORS

Rosalía Agusti, CHIDECAR, Departamento de Química Orgánica, Facultad de Ciencias Exactas y Naturales, Universidad de Buenos Aires, Pabellón II, Ciudad Universitaria, 1428 Buenos Aires, Argentina

Feng Cai, Department of Chemistry, Wayne State University, Detroit, MI 48202, USA

Bruce Coxon, National Institutes of Health, Bethesda, MD 20892, USA

David Crich, Department of Chemistry, Wayne State University, Detroit, MI 48202, USA

Alexei V. Demchenko, Department of Chemistry and Biochemistry, University of Missouri - St Louis, One University Boulevard, St Louis, MO 63121, USA

Robin Ferrier, Gracefield Research Central Sciences, Industrial Research Ltd., Lower Hutt, New Zealand

Rosa M. de Lederkremer, CHIDECAR, Departamento de Química Orgánica, Facultad de Ciencias Exactas y Naturales, Universidad de Buenos Aires, Pabellón II, Ciudad Universitaria, 1428 Buenos Aires, Argentina

Mario A. Monteiro, Department of Chemistry, University of Guelph, Guelph, ON N1G 2W1, Canada

Roberto Rizzo, Department of Life Sciences, University of Trieste, Via Licio Giorgieri, 34127 Trieste, Italy

James T. Smoot, Department of Chemistry and Biochemistry, University of Missouri - St Louis, One University Boulevard, St Louis, MO 63121, USA

Dennis M. Whitfield, Institute for Biological Sciences, National Research Council of Canada, 100 Sussex Drive, Ottawa, ON K1A 0R6, Canada

Baolin Wu, Department of Chemistry, Wayne State University, Detroit, MI 48202, USA

PREFACE

Sugars played a key role at the dawn of the nuclear magnetic resonance era. Foremost was Lemieux's demonstration that the magnitude of vicinal proton–proton spin couplings was related to the spatial orientation of the hydrogen atoms. Subsequently, Karplus presented an equation that quantifies the relationship between the NMR coupling constants of sugars and related molecules to the dihedral angle between the coupled nuclei. In this issue, Coxon (Bethesda, Maryland) provides a comprehensive survey of the many empirical variants of the Karplus-type equation that have been proposed over the years as NMR spectroscopy has evolved to become the indispensable key tool in carbohydrate characterization. The treatment covers spin couplings over three, four, and five bonds, and includes both protons and heteronuclei. The equations range from simple, two-parameter versions that depict only the torsional dependence of coupling constants, to complex 22-parameter forms that simulate the variation of the coupling with many different molecular properties. Earlier applications of NMR in the carbohydrate field were surveyed in this series by Hall in Volumes 19 and 29, by Coxon in Volume 27, and later by Csuk and Glänzer in Volume 46, and by Tvaroška and Taravel in Volume 51.

Three articles in this volume, written from different perspectives, focus on a central theme in carbohydrate science, namely the glycosidic linkage, its formation and cleavage. The presumed intermediates or transition states in these reactions have considerable oxacarbenium ion character. Using a computational approach, Whitfield (Ottawa) employs quantum mechanics to study the bonding characteristics of such ions, which are difficult to study experimentally. Focusing on the 2,3,4,6-tetra-*O*-methyl-D-galactopyranosyl cation and its 2-*O*-acetyl analogue, his treatment examines their detailed conformations (half-chair and skew) and calculated energies to demonstrate the potential of *in silico* methodology in understanding the reactivity of glycopyranosyl oxacarbenium ions.

Although glycoscientists have learned over the years how to isolate certain classes of naturally occurring complex carbohydrates, the availability of pure natural compounds remains inadequate to address many ongoing challenges. Chemical synthesis remains the essential resource for accessing complex oligosaccharides and glycoconjugates, to provide significant quantities of the pure natural structures as well as unnatural mimetics that are often of interest. In this volume, Smoot and Demchenko (St. Louis, Missouri) survey the drawbacks of traditional oligosaccharide syntheses that require extensive protecting-group manipulations between each glycosylation step, and discuss significant recent improvements that have emerged to circumvent the shortcomings of earlier approaches. Their article complements the classic chapter in Volume 50 by Schmidt and Kinzy on the trichloroacetimidate methodology, the articles by Garegg in Volumes 52 and 59 focusing on thioglycoside procedures, and solid-state synthetic techniques as presented in Volume 58 by Plante, Palmacci, and Seeberger.

In a third related article, Cai, Wu, and Crich (Detroit, Michigan) focus on the particular situation in homoglycan synthesis where the glycon has an axial hydroxyl group at the 2-position. For the total synthesis of α-mannans and α-rhamnans the overall strategy involves construction of the 1,2-trans-axial glycosidic bond, whereas the β-mannans and β-rhamnans require additional steps post-glycosylation to generate the 1,2-*cis*-equatorial glycosidic linkage.

The glycobiology of *Trypanosoma cruzi*, the causative agent of Chagas' disease, has contributed significantly to the identification of target enzymes responsible for the construction of unique cell-surface molecules. Agusti and de Lederkremer (Buenos Aires) here discuss the structure of glycoinositolphospholipids in *T. cruzi*, both free and as protein anchors, that display unusual structural motifs, including galactofuranose, which are absent in mammals. The chemical synthesis of oligosaccharides containing Gal*f* is presented, as well as the use of the organism's trans-sialidase (TcTS) for synthetic purposes.

Many of the articles in earlier volumes of this *Advances* series remain of permanent reference value, but library holdings of the full series have not kept pace with growth of the carbohydrate field and the opening of many new research centers. In an important development, the publishers have now made full-text electronic access available, through *Science Direct,* to all previously published articles in every volume. Volume 1, which appeared in 1945 with the title *Advances in Carbohydrate Chemistry*, under the editorship of Ward Pigman and Melville L. Wolfrom, featured as its opening article a chapter on the classic Fischer cyanohydrin reaction for ascent of the sugar chain, authored by the great carbohydrate pioneer Claude S. Hudson. The series title was changed with Volume 24 to *Advances in Carbohydrate Chemistry and Biochemistry* to reflect the broadening impact of carbohydrates in the biological field.

Grateful thanks are expressed to three senior statesmen of the carbohydrate community, Laurens Anderson, Hans Baer, and John Brimacombe, who as members of the Board of Advisors have helped over the years to guide these *Advances* with their own contributions, their valuable insight, and their mentoring service to others providing significant articles to the series. With this issue, Robin Ferrier (New Zealand) and Mario Monteiro (Guelph, Ontario), the first and last doctoral students of the late Gerald Aspinall, pay tribute to the enormous contributions made by their mentor to the carbohydrate field, especially in the area of polysaccharide structural methodology. Roberto Rizzo (Trieste) provides an account of the life and work of Vittorio Crescenzi, and his notable investigations on polysaccharide technology and the physicochemical behavior of biopolymers in solution.

A sad note is of the recent deaths of several great carbohydrate pioneers of the twentieth century, including Roger Jeanloz, Bengt Lindberg, and Per Garegg, whose work will be commemorated in a future volume.

DEREK HORTON

Washington, DC
November, 2008

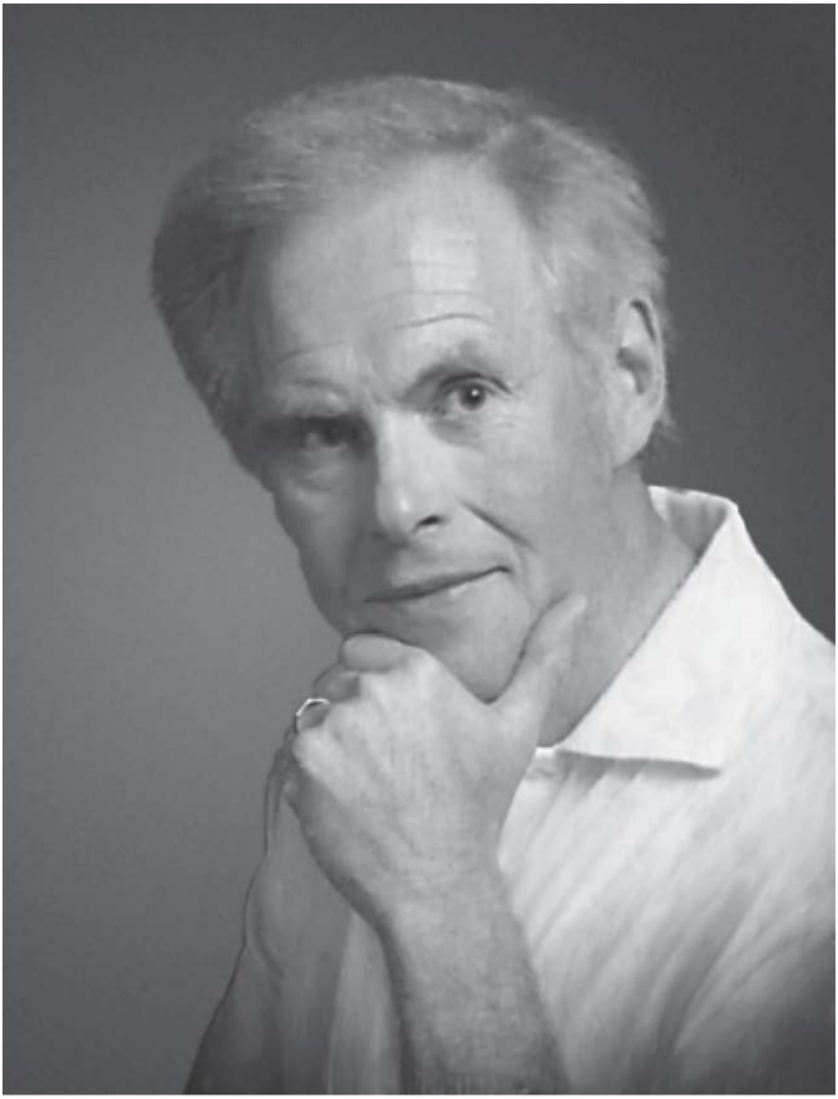

Gerald Aspinall.

GERALD ASPINALL

1924–2005

On the 30th of December, 1924, Gerald Oliver Aspinall was born to Leonard and Catherine (maiden name: Black) Aspinall in a small English village named Chesham Bois located between Amersham and Chesham, Buckinghamshire. During the beginning of the 1930s Gerald attended a nearby traditional kindergarten school, but when a boys' preparatory school, The Beacon, was founded in the district in 1933, his parents enrolled him in the new school. Gerald started early with the sharpening of his observational skills and, as a youngster, could regularly be found ‘‘playing with’’ his chemistry set on the kitchen table.

In 1937, Gerald entered the Merchant Taylors' School at Moor Park, Northwood, Middlesex, to which it moved in 1933 from London where it had been founded by the Worshipful Company of Merchant Taylors in 1561. On leaving, Gerald started his degree in chemistry at Bristol University, obtained his B.Sc. (first class honors) in 1944, and prolonged his stay at this University to carry out his Ph.D. studies.

Gerald's Ph.D. training (1945–1948) was in aromatic/alicyclic chemistry under Professor Wilson Baker, but an appointment as Lecturer to the Department of Chemistry, Edinburgh University in 1948 saw him change research fields completely upon joining the Hirst School of carbohydrate chemistry. He settled well, and was soon supervising research students carrying out structural studies of plant polysaccharides—an area to which he was to contribute massively during the following two decades in Edinburgh.

During this time in Edinburgh, Gerald met Joyce Brading, a doctoral student in the Department, and with whom many hours were spent carrying out convenient parallel chromatographic separations. In 1953 Gerald and Joyce married; their son John was born in 1957, and daughter Jill in 1963. These family additions were accompanied by a D.Sc. degree in 1958, awarded in recognition of Gerald's pioneering work on the structural chemistry of plant polysaccharides, and subsequently followed by

ISBN: 978-0-12-374743-3
DOI: 10.1016/S0065-2318(09)00001-8

© 2009 Elsevier Inc. All rights reserved.

promotion to Senior Lecturer in 1961 and Reader in 1963. In due course Gerald became the very proud grandfather of Michael Aspinall.

In Edinburgh, the Hirst School grew and thrived, with plant polysaccharides becoming the main focus of attention, and Gerald and his students and collaborators made major contributions to structural work. Concurrently, other departmental staff members directed research on relevant enzymic (D. J. Manners) and physical (C. T. Greenwood, D. A. Rees) methods applicable to polysaccharides, while E. E. Percival and D. M. W. Anderson and their students contributed much to knowledge of algal polysaccharides and commercially important plant gums. Together, under Sir Edmund Hirst, these people, and the ideas generator J. C. P. Schwarz, constituted a major internationally recognized center of carbohydrate expertise.

Methylation analysis of complex carbohydrates had been established in the 1940s in the carbohydrate schools at Bristol, Birmingham, and St Andrews, the names E. L. Hirst, J. K. N. Jones, W. N. Haworth, J. C. Irvine, and T. Purdie being associated with the development of this major tool for structural analysis of carbohydrates. However, inadequacies in the methods then available for the separation and characterization of the partially methylated sugar products made this approach unsuitable for use with polysaccharides—particularly those with complex structures based on several constituent sugars. Of critical importance was the advent of column chromatography, by the use of which it became possible to separate the partially methylated sugars in sufficient quantities to permit their quantification and characterization by classical methods, and the Edinburgh team made full use of this development. In consequence, the basic structures of polysaccharides, both simple and complex, were revealed, and the way was open to develop an understanding of the main architectures of this major group of natural products.

Work in the Aspinall group covered an extensive range of plant compounds, from relatively simple polymers based largely on one sugar to the very complex ones containing five or six monosaccharide components. Hemicelluloses were the focus of much attention, with products derived from a range of grasses, mosses, cereals, and trees being examined. Some comparative work on products derived from different parts of plants was done, with gums representing a particularly relevant class because of their special relationship to the materials produced elsewhere in the trees. Their commercial importance and the complexities of their molecular frameworks added to their interest as subjects for structural examination, and as the work developed it became apparent that a large proportion of these gums were components of mixtures which, of course, added to the complexities of the tasks addressed. More than 50 full papers describing research on plant polysaccharides were published by the Aspinall group, with the complexities of the work increasing over time and as a wider range of analytical tools became available.

While all of the natural products just referred to were heteropolysaccharides (although several of the hemicelluloses were largely xylose-based), some attention was paid to compounds composed of single hexoses. A minor amount of research was conducted on cellulose and starch chemistry, and callose, an unusual β-(1→3)-linked glucan, found in small amounts in the sieve plates of the phloem of the grape vine, was characterized. Two papers were published on ivory nut mannan and several on fructose-based polymers.

As if to preface his Canadian work that lay ahead, Gerald became involved in structural studies of the complex, highly branched extracellular polysaccharide of the microorganism *Aerobacter aerogenes*, which contains glucose, galactose, fucose, and glucuronic acid.

The research that the Aspinall group produced in Edinburgh over the period 1948–1967 helped substantially in taking the science of plant polysaccharide structure from its infancy to a moderately developed state. While a great deal of the information gathered was obtained by methylation/hydrolysis analysis, Gerald was always aware of the need to find and use other methods that would contribute to refining structures. He therefore made extensive use of such methods as partial hydrolysis and periodate oxidation, when appropriate.

Beyond his polysaccharide work, Gerald was always keenly aware that the chemistry of these polymers was based on the organic chemistry of simple carbohydrates and their derivatives, and he made several contributions to non-polymer carbohydrate research. Unless their anomeric centers are protected, mono-, oligo-, and polysaccharides are unstable at high pH values, since they are subject to base-catalyzed β-eliminations induced by the hemiacetal functions at the anomeric centers. In consequence, unstable intermediates are produced, which lead to further reactions. Gerald directed considerable effort into the base-induced degradation of several unsaturated and carbonyl/carboxyl-containing derivatives that modeled features of plant polysaccharides, the work leading to important understanding of the complex reactions of these compounds under basic conditions.

One of the most prominent papers to come from the Aspinall group, published with George Zweifel in 1957, reported on the selective tosylation of the 2,3-diols of methyl 4,6-*O*-benzylidene-α-D-mannopyranoside (with axial and equatorial hydroxyl groups, respectively, at C-2 and C-3), and 1,6-anhydro-β-D-mannopyranose (with a conformationally inverted pyranose chair, and therefore with equatorial and axial hydroxyl groups, respectively, at C-2 and C-3). In each case the equatorial hydroxyl group was esterified preferentially, consistent with the Barton/Cookson generalization, drawn from studies in the steroid field, that equatorial hydroxyl groups are more reactive toward substitution than are axial analogues. While this finding provided welcome evidence that, at least in this regard, carbohydrates behave in accord with comparable noncarbohydrate compounds, the result should not be accepted uncritically since several other factors, for example intramolecular hydrogen-bonding, could influence the relative reactivities of the hydroxyl groups in question.

The importance of the development and use of novel analytical methods applicable in the polysaccharide field was also recognized by the team in Edinburgh. For example, preliminary identification of specific partially methylated methyl glycosides was accomplished by comparison of their GLC retention times on two stationary phases with those of a large range of analogous reference compounds. An analytical technique, that has received considerable prominence is a microspectrophotometric procedure for monitoring the reduction of the periodate ion during the oxidation of 1,2-diol-containing carbohydrate compounds. It was developed to allow determination of the ratio of methyl 2- and 3-*O*-methyl-D-xylopyranosides in a mixture. Sugar tosylates and nitrates were subjected to infrared examination for analytical purposes.

In the course of their structural studies of polysaccharides, the Aspinall group isolated several oligosaccharide fragments and characterized them by comparison with specifically synthesized samples. Disaccharides made for this purpose were 2-*O*-*β*-D-xylopyranosyl-D-xylose, its monomethyl derivative with the substituent at O-3 of the nonreducing moiety, and 2-*O*-*β*-D-xylopyranosyl-L-arabinose. A biosynthetic investigation led to the establishment of the sugar ring size of natural uridine 5′-(L-arabinofuranosyl pyrophosphate).

In 1967, the Aspinall family crossed the Atlantic to take up residence in Peterborough, Ontario, Canada, where Gerald would serve, until 1972, as the Chemistry Department's Chair in the town's Trent University. During the years of 1971 and 1972 he also held the position of Conjunct Professor in the Department of Chemistry at Queen's University, Kingston, Ontario. In 1972, he moved to York University, North York (which is now part of the Greater Toronto Area), Ontario, to accept a position as Chair in the Department of Chemistry, an appointment he would hold until 1979. Whilst most of his energy was channeled toward administrative duties during his first several years in Canada, Gerald maintained an active research group that continued to make advances in the field of plant carbohydrates. Very importantly, his transition to full teaching and research duties in 1980 would see Gerald make an extraordinary return to the study of microbiological polysaccharides, which was to yield some of the most significant scientific results in this important field. His collaborations with biologists in this phase of his career and later were to enhance the caliber of his science and allow him demonstrate that an appreciation of the roles of the polysaccharides in natural processes could lead to new approaches to the control of some medical conditions.

His return to the laboratory was to yield major contributions to the chemistry of the complex polymers expressed by microorganisms. At this time, the structural elucidation of complex glycopeptidolipid antigens exhibited by *Mycobacterium spp.*, which contain novel glucuronic acid-based oligosaccharides, was completed. The first chemical synthesis of saccharide moieties expressed by *Mycobacterium spp.* was also accomplished. In 1986, Gerald was awarded the Claude S. Hudson Award in Carbohydrate Chemistry of the American Chemical Society in recognition of his contributions to the field. In 1988 his academic status was elevated to Distinguished Research Professor, and in 1992 he became a Fellow of the Royal Society of Canada, which is the Canadian Academy of the Sciences and Humanities, and the senior national body of distinguished Canadian scientists and scholars. In that year, Gerald formally retired, but his undiminished commitment to research and his energy would help him produce some of his best science in the following 13 years, which he spent as a Distinguished Research Professor Emeritus.

It could be said that Gerald left the best for last. During the 1990s, the fine structural investigations that delved into the complex cell-surface saccharides expressed by the *Campylobacter* and *Helicobacter spp.* revealed how these microorganisms exhibited molecular mimicry of the carbohydrate structures of the hosts. These structural findings would later explain many of the clinical features of *Campylobacter* and *Helicobacter spp.* infections.

In addition to being a leading cause of human enteritis, infections by *Campylobacter spp.*, especially *C. jejuni*, had been suspected of being an antecedent of severe neurological disorders, such as Guillain–Barré and Miller–Fisher syndromes. Gerald's observations that *C. jejuni* expressed structures homologous to human glycosphingolipids, especially the sialylated gangliosides of GM_1, GM_2, and GD_3, as components of their lipooligosaccharides, exposed the fact that *C. jejuni* infection possessed an autoimmune component, in which antibodies raised against this organism were disrupting the workings of cerebral peripheral nerves. Furthermore, *Campylobacter spp.* was also found to elaborate cell-surface capsular polysaccharides, which at the time, were thought to be O-chain regions of lipopolysaccharides. The most striking feature of *Campylobacter spp.* capsular polysaccharides was their incorporation of rare and previously unknown heptoses, and 6-deoxyheptoses of unusual configurations. The capsular polysaccharides of *C. jejuni* are now the basis for the development of a multivalent anti-*C. jejuni* neoglycoconjugate vaccine.

Gerald's last campaign focused on the lipopolysaccharide structures produced by the human gastric pathogen *Helicobacter pylori*, the lipopolysaccharides of which were found to express structures similar to human Lewis blood-group antigens. The potential role of molecular mimicry between *H. pylori* cell-surface carbohydrates and human gastric mucosa cells was the basis for the hypothesis that *H. pylori* ailments are a result of autoimmunity. Although this link has yet to be fully proved, recent studies continue to lend credibility to the autoimmune theory.

Altogether Gerald authored more than 200 research papers—about half of them from Edinburgh, and the others from his Canadian universities. Although the numerical balance is approximately even, the quality increased over the years, so that his Canadian work can be recognized as his best, and a fine exemplification of the benefits accruing from interdisciplinary collaboration.

As an acknowledged authority on carbohydrate chemistry over several decades, Gerald accepted the responsibility to review areas of his expertise, and he wrote extensively for *Advances in Carbohydrate Chemistry and Biochemistry*, *Annual Reports on the Progress of Chemistry*, *Annual Review of Biochemistry*, *Pure and Applied Chemistry* and several other reviewing journals and symposia proceedings. He served for more than 30 years on the Editorial Board of *Carbohydrate Research* since its inception in 1965, and his multi-author, three volume text ‘‘The Polysaccharides,’’ completed in 1985 for Academic Press, remains a benchmark publication in the field.

Gerald enjoyed sport, and rugby attracted his attention as a teenager, but first signs of knee trouble began appearing at this young age and he turned his interests to cricket and golf. He combined sporting activity with his love of the outdoors, and during his bachelor days his holidays were mainly spent mountaineering in the English Lake District and hiking in the Dolomite mountains of Northern Italy. Later, Aspinall family holidays were spent in Ardnamurchan in North West Scotland. In Canada, the family vacations usually consisted of camping in the provincial parks of Eastern Canada. The Adirondack Mountains of northern New York State were also a regular destination. In their later years, Joyce and Gerald would often combine vacation with attending carbohydrate conferences around the world. In 2001, double knee-replacement surgery slowed him down slightly, but, after recovering, he could often be seen taking the stairs while his students waited for the elevator. Gerald was a well informed and critical music listener with an extensive collection of recorded music, and he subscribed regularly to the Toronto Symphony, Tafelmusic, and the Toronto Opera Company. He was a devout churchman of the Anglican tradition and he felt no conflict between his faith and his science.

By nature Gerald was reserved and studious, but he was a fine teacher who treated his committed students with great respect which often developed into warm friendship. He was intensely dedicated to his work and set himself amazingly high standards, which his students did well to emulate. One year after skin-cancer surgery, Professor Aspinall was making plans for his next research campaign. He died on September 11th, 2005, in Toronto, Canada.

As one of his earliest Ph.D. students (RF) and the last (MAM), we readily acknowledge, on behalf of all his research students and colleagues, and also his many friends in the field, our great indebtedness to him.

We also acknowledge the assistance we have received in preparing this tribute from Professors J. G. Buchanan, A. M. Stephen, and, for personal material, John Aspinall.

ROBIN FERRIER
MARIO A. MONTEIRO

KEYNOTE PUBLICATIONS

G. O. Aspinall, M. A. Monteiro, R. T. Shaver, L. A. Kurjanczyk, and J. L. Penner, Lipopolysaccharides of *Helicobacter pylori* serogroups O:3 and O:6: Structures of a class of lipopolysaccharides with reference to the location of oligomeric units of D-*glycero*-α-D-*manno*-heptose residues, *Eur. J. Biochem.*, 248 (1997) 592–601.

G. O. Aspinall, and M. A. Monteiro, Lipopolysaccharides of *Helicobacter pylori* strains P466 and MO19: Structures of the O antigen and core oligosaccharide regions, *Biochemistry*, 35 (1996) 2498–2504.

G. O. Aspinall, M. A. Monteiro, H. Pang, E. J. Walsh, and A. P. Moran, Lipopolysaccharide of the *Helicobacter pylori* type strain NCTC 11637 (ATCC 43504): Structure of the O antigen chain and core oligosaccharide regions, *Biochemistry*, 35 (1996) 2489–2497.

G. O. Aspinall, D. Chatterjee, and P. J. Brennan, The variable surface glycolipids of mycobacteria: Structures, synthesis of epitopes, and biological properties, *Adv. Carbohydr. Chem. Biochem.*, 51 (1995) 169–242.

G. O. Aspinall, S. Fujimoto, A. G. McDonald, H. Pang, L. A. Kurjanczyk, and J. L. Penner, Lipopolysaccharides from *Campylobacter jejuni* associated with Guillain–Barré syndrome patients mimic human gangliosides in structure, *Infect. Immun.*, 62 (1994) 2122–2125.

G. O. Aspinall, A. G. McDonald, H. Pang, L. A. Kurjanczyk, and J. L. Penner, Lipopolysaccharides of *Campylobacter jejuni* serotype O:19: Structures of core oligosaccharide regions from the serostrain and two bacterial isolates from patients with the Guillain–Barré syndrome, *Biochemistry*, 33 (1994) 241–249.

G. O. Aspinall, A. G. McDonald, and H. Pang, Lipopolysaccharides of *Campylobacter jejuni* serotype O:19: Structures of O antigen chains from the serostrain and two bacterial isolates from patients with the Guillain–Barré syndrome, *Biochemistry*, 33 (1994) 250–255.

G. O. Aspinall, A. G. McDonald, T. S. Raju, H. Pang, A. P. Moran, and J. L. Penner, Chemical structures of the core regions of *Campylobacter jejuni* serotypes O:1, O:4, O:23, and O:36 lipopolysaccharides, *Eur. J. Biochem.*, 216 (1993) 1017–1027.

G. O. Aspinall, A. G. McDonald, T. S. Raju, H. Pang, S. D. Mills, L. A. Kurjanczyk, and J. L. Penner, Serological diversity and chemical structures of *Campylobacter jejuni* low-molecular-weight lipopolysaccharides, *J. Bacteriol.*, 174 (1992) 1324–1332.

G. O. Aspinall, N. K. Khare, R. K. Sood, D. Chatterjee, B. Rivoire, and P. J. Brennan, Structure of the glycopeptidolipid antigen of serovar 20 of the *Mycobacterium avium* serocomplex, synthesis of allyl glycosides of the outer di- and tri-saccharide units of the antigens of serovars 14 and 20, and serology of the derived neoglycoproteins, *Carbohydr. Res.*, 216 (1991) 357–373.

G. O. Aspinall, (Ed.), *The Polysaccharides,* Vol. 1, Academic Press, New York, 1982; Vol. 2, 1983; Vol. 3, 1985.

P. J. Brennan, G. O. Aspinall, and J. E. Shin, Structure of the specific oligosaccharides from the glycopeptidolipid antigens of serovars in the *Mycobacterium avium-Mycobacterium intracellulare-Mycobacterium scrofulaceum* complex, *J. Biol. Chem.*, 256 (1981) 6817–6822.

G. O. Aspinall, (Ed.), *Carbohydrates, MTP Review of Science,* Vol. 7, Butterworths, London, (1973).

G. O. Aspinall, Gums and mucilages, *Adv. Carbohydr. Chem. Biochem.*, 24 (1969) 333–379.

G. O. Aspinall, The exudate gums and their structural relationship to other groups of plant polysaccharides, *Pure Appl. Chem.*, 14 (1967) 43–55.

G. O. Aspinall, and K. M. Ross, The degradation of two periodate-oxidised arabinoxylans, *J. Chem. Soc.*, (1963) 1681–1686.

G. O. Aspinall, Gas–liquid partition chromatography of methylated and partially methylated methyl glycosides, *J. Chem. Soc.*, (1963) 1676–1680.

G. O. Aspinall, Structural chemistry of the hemicelluloses, *Adv. Carbohydr. Chem.*, 14 (1959) 429–468.

G. O. Aspinall, and R. J. Ferrier, A spectrophotometric method for the determination of periodate consumed during the oxidation of carbohydrates, *Chem. Ind.* (1957) 1216.

G. O. Aspinall, and G. Zweifel, Selective esterification of equatorial hydroxyl groups in the synthesis of some methyl ethers of D-mannose, *J. Chem. Soc.* (1957) 2271–2278.

J. F. Wilkinson, W. F. Dudman, and G. O. Aspinall, The extracellular polysaccharide of *Aerobacter aerogenes* A3 (S1), *Biochem. J.*, 59 (1955) 446–451.

G. O. Aspinall, The methyl ethers of hexuronic acids, *Adv. Carbohydr. Chem.*, 9 (1954) 131–148.

G. O. Aspinall, The methyl ethers of D-mannose, *Adv. Carbohydr. Chem.*, 8 (1953) 217–230.

G. O. Aspinall, E. L. Hirst, E. G. V. Percival, and I. R. Williamson, The mannans of ivory nut (*Phytelephas macrocarpa).* The methylation of mannan A and mannan B., *J. Chem. Soc.*, (1953) 3184–3188.

VIII CONVEGNO
SULLA CHIMICA DEI CARBOIDRATI
Università degli Studi di Milano
Comitato Scientifico
Alessandro Dondoni
Sergio Paoletti
Michelangelo Parrilli
Ugo Pfeiffer
Giangiacomo Torri
PROGRAMMA GIORNALIERO
Giovedì 13
Comitato Organizzatore
ilano 13-15 Giugno 2002

VITTORIO CRESCENZI

1932–2007

On June 12th, 2007, Vittorio Crescenzi passed away. The adult respiratory distress syndrome, a pathology whose direct causes are not well understood, interrupted his life and his constant and passionate engagement in research and teaching. He was full professor of Industrial Chemistry at the University of Rome (Italy) and internationally recognized as a distinguished scientist working on physicochemical and technological properties of polysaccharides.

Although near to retirement, Vittorio was still very active in the Department of Chemistry of the University of Rome, where he was coordinating a group of young Ph.D. students and postdoctorals engaged in research on novel biocompatible materials based on hyaluronic acid and designed for tissue engineering and controlled drug release.

Vittorio was born in 1932 in Rome, where in 1956 he graduated in Chemistry at the former Institute of General and Inorganic Chemistry with a thesis on the potential of gas-chromatographic analysis, under the guidance of Prof. Arnaldo Liberti. At that time, gas chromatography was a relatively new technique and commercial instruments were not available, so that Vittorio was obliged to assemble a home-made apparatus to carry out his experimental work. Soon he was attracted to research in macromolecular chemistry, which in Italy was being developed by such leading scientists as Alfonso M. Liquori, Paolo Corradini, and especially Giulio Natta, who was awarded the Nobel Prize in 1963. Alfonso Liquori, who worked in Cambridge (UK) during the same years as the pioneering studies on the crystal structure of DNA and proteins, invited Crescenzi to join him at the University of Bari, in the south east of Italy, where Liquori was a full professor.

Later on Vittorio moved, together with Liquori, to the University of Naples. There they met the group of Corradini, which was already active on the newly synthesized isotactic polypropylene. During these years a NATO fellowship allowed him to work at Stanford University in Palo Alto, California, with Paul J. Flory, who in 1974 also

ISBN: 978-0-12-374743-3
DOI: 10.1016/S0065-2318(09)00002-X

© 2009 Elsevier Inc. All rights reserved.

became a Nobel laureate. Vittorio crossed the Atlantic by ship and then traveled by train to California. In subsequent times of frequent airplane travels he enjoyed talking about those days spent on the ship playing ping-pong. Six months afterwards, his wife Ada, whom he had married in Rome in 1957, joined him in the USA, together with their first two daughters and also a third one, Laura, just newborn. Vittorio was very much impressed by the abundant research opportunities in the USA, and that country became his definitive reference point in making recommendations to any of his young collaborators.

In 1968, already back in Italy, Vittorio was called as full professor to the University of Trieste, where he founded the Macromolecular Chemistry Laboratory, leading a number of young scientists who still are active in the field of carbohydrate and polysaccharide chemistry. His main interest during this period was investigations on the polyelectrolytic properties of synthetic and natural polymers, including the very poorly studied ionic polysaccharides.

In 1976 Vittorio was called back to Rome as full professor of physical chemistry in the Department of Chemistry of ''La Sapienza'' University where this writer, as a young postdoctoral, met him and started to collaborate with him on the thermodynamic properties of ionic polysaccharides. In Rome, Vittorio started a local research group working on polysaccharides, but he also maintained a close collaboration with the Trieste group. He was very proud to be back in his beloved native town, as manifested by the company of numerous visiting scientists; they enjoyed his description of the most characteristic corners of the city, particularly those from the Roman Empire still remaining, and also the performance of the local soccer team. He worked in Rome until he died, not only as researcher but also as a well appreciated teacher, first in macromolecular chemistry and then in industrial chemistry. In this respect, he contributed greatly to the reorganization of the degree course in chemistry in line with modern developments of this discipline.

During the years 1983–1984 he spent a sabbatical leave at the Stevens Institute of Technology in Hoboken, New Jersey, USA, where, besides teaching and research, he organized jointly with S.S. Stivala the first ''International Meeting on Industrial Polysaccharides.'' The success of the meeting motivated him to organize the second such meeting, also at the Stevens Institute, while the third one was held in Italy at the newly founded ''Trieste Science Park.'' These meetings, together with the one held near Trieste in 1981 and focused on ''Polysaccharide Solutions and Gels,'' formed the basis for a fruitful scientific exchange between Italian scientists and scientists from other countries interested in various aspects of the chemistry of polysaccharides.

His continuous interest in applied research led him since 1980 to collaborate with a major Italian pharmaceutical company on problems related to polymeric biocompatible matrices, a field which he never abandoned.

Vittorio was a member of the Italian National Academy of Sciences, the so-called ‘‘Accademia dei XL’’ since it was founded in Verona (the town of Romeo and Juliet) in 1782 by Antonio M. Lorgna, an Italian mathematician and engineer, who brought together the 40 most prestigious Italian scientists, who at that time were citizens of different states, to provide them a common institution for scientific discussions. After the unification of all the Italian states, in 1875 the Academy moved to Rome.

Author of a large number of scientific publications in international journals, Vittorio was among the founders of two important Italian scientific associations: the ‘‘Macromolecular Science and Technology Association’’ (AIM) and the ‘‘Calorimetry and Thermal Analysis Association’’ (AICAT). He also stimulated the creation of the Italian Group of Carbohydrates, which is a section of the Italian Chemical Society. Vittorio is pictured here during his attendance at the 2002 meeting of the Italian Group of Carbohydrates.

As mentioned, Vittorio was near to retirement, although he would surely have continued to work closely with his research collaborators as well as dedicating time to his family, especially to Ada, his beloved wife. She graduated in pharmacy and biology at the University of Rome and, because of her scientific background, was from the outset the primary person with whom Vittorio discussed his research. Vittorio and Ada had a large family, with five daughters, Flavia, Fulvia, Laura, Fabiana, and Alberta, and six grandchildren: Giulia, Ilaria, Lorenzo, Lucrezia, Vittoria, and Chiara. A special relationship was established between the grandfather Vittorio and his granddaughter Vittoria; when she was 2 years old he spent time with her blowing soap bubbles and drawing with colored pencils. Vittorio drew very well and was mainly a caricaturist, as also demonstrated by his ironic self-portraits. Probably impressed by the tragic events of his youth, he was eager to know more about World War II, reading and collecting numerous books on this topic. However, science took up much of his attention, and colleagues were probably his best friends. In his study at home he hung pictures of those late scientists who, besides being friends, impressed him the most for their scientific achievements; these included notably J. P. Flory, A. M. Liquori, and J. J. Hermans. His profound belief in the necessity of proving every hypothesis drove Vittorio to agnosticism, but he was always respectful of people having different opinions.

Those who worked with him certainly remember his regular presence in the laboratory and his willingness to discuss scientific problems with passion. For his collaborators, perhaps their major difficulty was to keep pace with the numerous and interesting new research suggestions that he was able to produce. One of the most impressive aspects of his work was the international dimension of the research carried out in his laboratory. His numerous contacts with Dutch, English, French, and North American colleagues made research in his laboratory even more stimulating. His international contacts were fruitfully transmitted to those of us who continue to develop his main interests. We thank Vittorio for this inheritance.

ROBERTO RIZZO

ADVANCES IN CARBOHYDRATE CHEMISTRY AND BIOCHEMISTRY, VOL. 62

DEVELOPMENTS IN THE KARPLUS EQUATION AS THEY RELATE TO THE NMR COUPLING CONSTANTS OF CARBOHYDRATES

BY BRUCE COXON

National Institutes of Health, Bethesda, MD 20892, USA

I. Introduction 18
II. The Impact of Improved NMR Instrumentation 19
III. The Impact of Molecular Modeling 20
IV. Vicinal Coupling Constants 21
  1. Proton–Proton Couplings 21
  2. Proton–Carbon Couplings 36
  3. Proton–Nitrogen Couplings 45
  4. Phosphorus Couplings 47
  5. Carbon–Carbon Couplings 51
V. Other Types of Vicinal Couplings 60
  1. Fluorine Couplings 60
  2. Carbon–Tin Couplings 64
VI. Couplings Over Four Bonds 64
  1. Proton–Proton Couplings 64
VII. Couplings Over Five Bonds 68
  1. Proton–Proton Couplings 68
VIII. Online Calculators for Coupling Constants and Torsions 70
IX. Summary 72
References 73

ABBREVIATIONS

1D, one-dimensional; 2D, two-dimensional; 3D, three-dimensional; AMP, adenosine monophosphate; CNDO, complete neglect of differential overlap; COSY, correlation spectroscopy; CPMG, Carr-Purcell–Meiboom–Gill NMR pulse sequence; CT, constant time; dAMP, deoxyadenosine monophosphate; DFT, density functional

ISBN: 978-0-12-374743-3
DOI: 10.1016/S0065-2318(09)00003-1

© 2009 Published by Elsevier Inc.

theory; EHT, extended Hückel theory; FID, free induction decay; FPT, finite perturbation theory; FT, Fourier transform; HMBC, heteronuclear multiple bond correlation; HSQC, heteronuclear single quantum correlation; HSQMBC, heteronuclear single quantum multiple bond correlation; INADEQUATE, incredible natural abundance double quantum transfer experiment; INDO, intermediate neglect of differential overlap; INEPT, insensitive nuclei enhancement by polarization transfer; Kb, kilobyte; LCAO, linear combination of atomic orbitals; LRCC, long-range carbon–carbon correlation spectroscopy; MCSCF, multi-configurational self-consistent field; MD, molecular dynamics; MM, MM1, MM2, MMP2(85), MM2–85, MMX, various versions of Allinger's molecular-mechanics program; MO, molecular orbital; NOE, nuclear Overhauser effect; PCA, principal component analysis; PCILO, perturbative configuration interaction with localized orbitals; PFIDS, phosphorus fitting of coupling constants from doublets and singlets; PMR, proton magnetic resonance; RF, radio frequency; ROE, rotating-frame Overhauser effect; ROESY, rotating-frame Overhauser effect spectroscopy; SCF, self-consistent field; SCPT, self-consistent perturbation theory; SOPPA, second-order polarization propagator approximation; T_1, spin–lattice relaxation time; T_2, spin–spin relaxation time; VB, valence bond.

Single-letter abbreviations for ribonucleoside or ribonucleotide base-containing components, depending on context—A, adenosine; C, cytosine; G, guanosine; T, ribosylthymine; U, uridine.

I. INTRODUCTION

The Karplus equation has had a long association with carbohydrates. Apparently, in 1958, while Martin Karplus was in the process of completing his seminal 1959 paper on the theoretical dependence of vicinal NMR coupling constants on the dihedral angle of the coupled protons,[1] he attended a lecture by the late Raymond Lemieux at the University of Illinois in May, 1958 and recognized that Lemieux's new experimental data for such couplings in carbohydrates[2] and cyclohexenes[3] fitted his theoretical results very well.[4] It was not long before a number of other sugar chemists started exploiting this angular dependence of coupling constants in the conformational and configurational analysis of carbohydrates and their derivatives,[5–7] and the Karplus equation has found wide acceptance and utility throughout organic and inorganic chemistry.

In many instances, however, it has been sufficient merely to be aware of the angular dependence, and to use the experimental fact that the coupling constant is large or small, depending on whether the coupled nuclei are trans or gauche, an approach which Karplus himself recommended.[8] Responding to some criticism of the accuracy of dihedral angles calculated from coupling constants, Karplus published a second paper on the subject in 1963, in which the dependence of the couplings on substituent electronegativity and on bond length and bond angle were addressed.[8] Since that time, the original Karplus equation has been modified, extended, generalized, and reparametrized to include a large number of different nuclear pairs, and more-finely tuned dependences on a host of molecular properties, in addition to dihedral angle and electronegativity.

Because of the very large number of applications of the Karplus equation in chemistry, an effort has been made to restrict the scope of this chapter to the more fundamental investigations of the Karplus equation and the coupling constants that support it. Also, coupling constants over one and two bonds do not have dihedral angles between the coupled nuclei and so have largely not been included, even though they depend on the orientation of substituents.[9] Couplings over two bonds also have the practical disadvantage of a change in sign,[9] depending on structure, and are not as highly used as three-bond couplings for structural determination. On the other hand, following Perlin and Casu's discovery that one-bond ^{1}H–^{13}C coupling constants depend on anomeric configuration,[10] its detailed elaboration by Bock and Pedersen,[11–14] and angular dependence studies by Tvaroška, Taravel, and coworkers,[15–18] these couplings have constantly been used as a method for determination of anomeric configuration that complements the use of three-bond ^{1}H–^{1}H coupling constants from the anomeric center. Indeed, the use of $^1J_{\mathrm{CH}}$ is better in some cases than the use of $^3J_{\mathrm{H\text{-}1,H\text{-}2}}$, for example in α- and β-mannopyranose derivatives, where the $^3J_{1,2}$ values are very similar.

II. THE IMPACT OF IMPROVED NMR INSTRUMENTATION

In 1959, NMR spectroscopy was still in the primitive state of relying on continuous-wave, RF techniques, with magnetic field sweeps, and analogue spectral output on chart paper, from which coupling constants were determined by manual measurements of peak separations on the chart. Spectra were calibrated by the relatively crude procedure of placing audio modulation sidebands on the charts, which defined the frequency separations needed for measurements of coupling constants. Within 10 years, there were to be revolutions in both the practice of NMR spectroscopy and the computer field. The transition from continuous-wave techniques to Richard Ernst's pulse-FT NMR method[19,20] occurred rapidly, but the computer systems that were required for this new experimental procedure were at first slow, awkward, and suffered from extremely limited storage for data and programs;

for example, 4 Kb for data and 4 Kb for program space, with no permanent storage for data, except on punched, paper tape.

Fortunately, there have been enormous improvements in computer technology resulting in cheap memory and storage, with the result that the number of digital points that can be used to define a spectrum is now limited only by the decay rate $1/T_2^\star$ of the FID, which is given by the sum of the real, transverse relaxation rate $1/T_2$ and the rate $1/T_{2(\mathrm{inhomo})}$ due to magnetic field inhomogeneity. As a result, data tables of 256 Kb are now routinely possible for the 1D ^{1}H and ^{13}C NMR methods that are most commonly used to measure spin–spin coupling constants, as long as the FID does not decay to noise first.

Along with the computer revolution and digitization of data, there have been constant, iterative improvements in spectrometer and NMR probe performance. Competitive pressures have led to increasingly accurate phase and frequency synthesis, the adoption of more stable, digital lock systems for field–frequency regulation, and very large gains in NMR detection sensitivity, particularly from the development of cryoprobes (cold probes) that afford a sensitivity improvement of $\sim$4 over normal probes, corresponding to a reduction in acquisition time by a factor of 16.

By using the trade off of sensitivity versus resolution that is inherent in most spectral apodization methods, the improved sensitivity has allowed much more vigorous resolution enhancement to be used, allowing spectral multiplets to be split easily to the baseline, thus enhancing the measurement accuracy for the coupling constants.

Because the spacings used to measure the coupling constants are calculated as the difference of two frequencies, it is important that the spectra have adequate digital resolution, otherwise the experimental errors in the coupling constants could possibly be doubled. The larger data sets that are possible with modern equipment certainly allow this, together with such data extension methods as zero-filling and linear prediction, and the digital output of the peak positions by sophisticated algorithms that take into account several points near the top of the peak, and not just its maximum value. Enhanced computer processing speed has also been important for rapid computations of the Fourier transform and for other digital signal processing, which became essential once multidimensional NMR techniques were adopted.

III. THE IMPACT OF MOLECULAR MODELING

When the Karplus equation was first developed, few methods were in use for the specification of molecular geometry, and correlations of coupling constants with atomic dihedral angles were perforce often based on approximate methods such as measurement of Dreiding molecular models (±10°) or on assumptions that carbohydrate rings have dihedral angles that are similar to the ''idealized'' angles in related alicyclic molecules.[21] The wider use of X-ray crystal structure data has had the advantage that the dihedral angles that may be calculated from such data are obtained by experiment, but the disadvantage that they refer to the solid state, which may exhibit a different conformation from that present in solution. Other methods for the determination of molecular geometry such as high-quantum, local field solid-state NMR spectroscopy[22] suffer from the same disadvantage, if comparisons with the solution state are desired. A number of authors have clearly assumed, without proof, that the conformations in the solid and solution states are the same. Over the past 50 years, a number of powerful computational methods for the determination of molecular geometry have been adopted, including *ab initio* MO methods (such as Hartree–Fock), VB calculations, semiempirical (CNDO, INDO, and others), DFT (GAUSSIAN94, GAUSSIAN98, GAUSSIAN03), and MD/MM (such as Accelrys Insight/Discover, CHARMM, GROMOS96, PCMODEL, and others). VB methods are largely out of date at this point and do not always correctly reproduce the magnitudes and signs of coupling constants. Programs such as Insight/Discover that display values of dihedral angles merely by clicking on four atoms of a structure displayed on a computer monitor are particularly useful, since they avoid tedious manual calculations based on atomic coordinates. Of course, many of the methods of computational chemistry are based on approximations to a varying degree, but a realistic goal for the computation of dihedral angles appears to be ±0.5°.

IV. VICINAL COUPLING CONSTANTS

Vicinal ^1H–^1H coupling constants comprise the vast majority of coupling data that have been reported, and as the simplest case, substituted ethanes, have been exhaustively studied. These studies are described here because sugar chains may be regarded as a series of ethanic fragments, albeit with transannular stereoelectronic and anomeric effects, flanking group interactions, and other phenomena superimposed.

1. Proton–Proton Couplings

a. Proton–Proton Couplings, $^3J_{HCCH}$.— Initially, VB theory was used by Karplus to calculate $^3J_{HCCH}$ in ethane,[1] which could be fitted approximately by the equations:

$$\begin{aligned}{}^3J_{\mathrm{HCCH}} &= 8.5\cos^2\varphi - 0.28 \quad \text{for } 0^\circ \le \varphi \le 90^\circ \quad \text{and} \\ &9.5\cos^2\varphi - 0.28 \quad \text{for } 90^\circ \le \varphi \le 180^\circ\end{aligned} \tag{1}$$

where φ is the dihedral angle between the hydrogen atoms (also known as the projected valency angle, the torsion angle, or the torsion). For unsaturated systems, additional contributions from π-electrons were found to provide a quantitative explanation of the experimental results.[23] Later,[8] the results of the VB σ-electron calculation were restated in the equation:

$$^3J_{\mathrm{HCCH}} = A + B\cos\varphi + C\cos 2\varphi \tag{2}$$

For a C–C bond length of 1.543 Å, sp^3 hybridized carbon atoms, and an average energy, ΔE of 9 eV, the calculated constants were $A = 4.22$, $B = -0.5$, and $C = 4.5$ Hz.

A trigonometrically identical form of Eq. (2) has generally been used, namely,

$$^3J_{\mathrm{HCCH}} = A\cos^2\varphi + B\cos\varphi + C \tag{3}$$

because its quadratic form[21] allows an explicit calculation of φ from the coupling constant, despite a warning from Karplus.[8] In Eq. (3), the values of the constants A, B, and C are 9.0, −0.5, and −0.3 Hz, respectively. Dependences on substituent electronegativity, and on bond angle and length were also calculated,[8] although the latter two molecular properties have proved to have minor effects.

Efforts were soon made to incorporate an explicit electronegativity dependence. For example, Abraham and Pachler derived the expression

$$^3J_{\mathrm{HCCH}} = 8.0 - \sum \Delta\chi_i \tag{4}$$

where $\Sigma\Delta\chi_i$ is the sum of the electronegativity differences between the substituents i attached to the ethane molecule and hydrogen.[24] From data for tetrasubstituted aldopentopyranose derivatives, Durette and Horton formulated the expression:[25]

$$^3J_{\mathrm{HCCH}} = (7.8 - 1.0\cos\varphi + 5.6\cos 2\varphi)(1 - 0.1\Delta\chi) \tag{5}$$

This equation was modified by Streefkerk *et al.*[26] and used for calculation of $^3J_{\mathrm{HCCH}}$ values for 14 ideal conformations (two chair, six boat, and six skew forms) of per-*O*-trimethylsilyl derivatives of 6-deoxyhexoses,[27] and for structural studies of glycopeptides:[28]

$$^3J_{\mathrm{HCCH}} = (6.6 - 1.0\cos\varphi + 5.6\cos 2\varphi)\left(1 - \sum_{i=1}^{i=4} f_i\Delta\chi\right) \tag{6}$$

where φ is the dihedral angle between the protons in the fragment H–C–C′–H′, and where the electronegativity factor $f_i = 0.15$ when the torsion angle θ between R and H in H–C–C′–R is $> 90°$, and $f_i = 0.05$ when $\theta < 90°$. In effect, Eq. (6) includes an approximate dependence of $^3J_{\mathrm{HCCH}}$ on the angular orientation θ of the substituent R, a subject that is discussed next.

It was recognized as early as 1964 that there is a dependence of $^3J_{\mathrm{HCCH}}$ on substituent electronegativity orientation. In a study of steroid molecules, Williams and Bhacca found that J_{ae} 5.5 ± 1.0 Hz was about twice as large when there was an equatorial electronegative substituent attached to the coupling pathway, as the value J_{ea} 2.5–3.2 Hz measured when the substituent was attached axially.[29] These orientations correspond to a gauche relationship of the substituent to one of the coupled protons, and a trans arrangement, respectively (Fig. 1).

This significant dependence was also noted by others,[30,31] but was not fully addressed until 1979, when Haasnoot, Altona, and coworkers commenced the publication of a series of papers[32–34] in which the $^3J_{\mathrm{HCCH}}$ values of substituted ethanes and other molecules were investigated with great attention to accuracy and detail; studies that were assisted by the increasing sophistication of NMR instrumentation.

Meanwhile, Pachler calculated $^3J_{\mathrm{HCCH}}$ values for substituted ethyl derivatives using the Pople–Santry LCAO-MO method, a variant of EHT, and found (a) a linear dependence of the vicinal couplings on substituent electronegativity, and (b) that the couplings were described[35] well by the expression:

$$^3J_{\mathrm{HCCH}} = A + B\cos\varphi + C\cos 2\varphi + D\sin\varphi + E\sin 2\varphi \tag{7}$$

This relationship has been described as a truncated Fourier series containing a fundamental and one overtone.[33] Addition of the sine terms to the original Karplus equation was required to represent the asymmetry of the curves at $\varphi = 0°$.

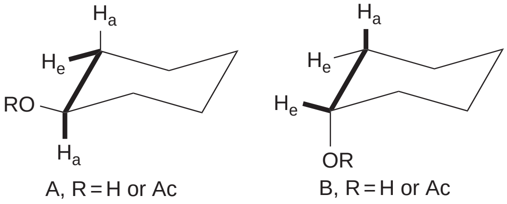

FIG. 1. Differing orientations of the electronegative substituent RO on the $^3J_{\mathrm{HCCH}}$ coupling pathway in steroid fragments. In type A, J_{ae} was observed to be 5.5 ± 1.0 Hz, whereas type B showed J_{ea} 2.5–3.2 Hz, thus illustrating enhancement of the coupling constant when the electronegative substituent is gauche to one of the coupled protons.

Pachler subsequently accounted for the dependence of the coupling on electronegativity and its orientation using equations[36] which were interpreted by Haasnoot *et al*.[33] as:

$$^3J_{\mathrm{HCCH}} = \left(A - a\sum\Delta\chi_i\right) + \left(B - b\sum\Delta\chi_i\right)\cos\left(\varphi - \varepsilon\sum{}'\Delta\chi_i\right) + \left(C - c\sum\Delta\chi_i\right)\cos 2\left(\varphi - \varepsilon\sum{}'\Delta\chi_i\right) \qquad (8)$$

where $\Sigma'\Delta\chi_i$ is a sum of the electronegativity differences that is given a positive or negative sign, depending on the gauche or trans orientation of the electronegative substituent just mentioned above. This reflects experimental observations that the gauche orientation of this substituent increases the magnitude of the coupling,[29] whereas the trans orientation decreases it.[37]

For reasons that have been described in detail,[33] it was proposed that Eq. (8) be replaced by a new relationship, now known as the Haasnoot or Altona equation:

$$^3J_{\mathrm{HCCH}} = P_1\cos^2\varphi + P_2\cos\varphi + P_3 + \sum\Delta\chi_i\left[P_4 + P_5\cos^2\left(\xi\varphi + P_6 \mid \Delta\chi_i \mid\right)\right] \qquad (9)$$

in which the sign parameter ξ takes the value +1 or −1, depending on the orientation of the electronegative substituent, which was now defined more carefully[33] to cover all possible values of φ (Fig. 2). By least-squares fitting of 315 coupling constants obtained from 109 compounds to dihedral angles calculated by molecular mechanics using Allinger's MM1 force field, the parameter values P_1 13.88, P_2 −0.81, P_3 0 (assumed), P_4 0.56, P_5 −2.32, and P_6 17.9 Hz were determined. A Macintosh desktop calculator program, SWEET J is available for Eqs. (3) and (9), which solves the

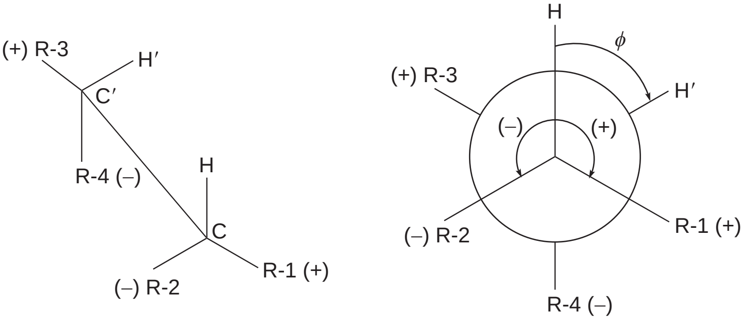

FIG. 2. Definition of positive and negative orientations of substituents R-1–R-4 with respect to the vicinally coupled protons in tetrasubstituted ethanes.

equations both numerically and graphically.[38] The program features include display of the fragment under consideration as a Newman projection, the dihedral angle can be changed with the mouse device, and the absolute configuration of stereogenic centers is determined by the computer.[38] An alternative PC desktop calculator program, ALTONA, has been written[39] for Eq. (9).

Although the first atom of the electronegative substituent has the greatest effect on the coupling constant (and also on ^{1}H and ^{13}C chemical shifts in general), the data and EHT-MO calculations of Haasnoot *et al.* and other data in the literature indicated the need for another parameter P_7 that would describe the moderating effect of the β-part of a substituent on its electronegativity, namely, a reduction in the electronegativity of the entire substituent, as the electronegativity of the β-part increased.[33] Therefore, an additional equation was introduced:

$$\Delta\chi^{\text{group}} = \Delta\chi^{\alpha\text{-substituent}} - P_7 \sum \Delta\chi^{\beta_i\text{-substituent}} \tag{10}$$

where the summation extends over all of the substituents attached to the α-substituent. Small values of P_7 were found, 0.14, 0.24, 0, and 0.19, depending on whether Eq. (10) was used with only the β-effect, or two, three, or four substituents, respectively.[33]

Equations (9) and (10) were applied initially to monosubstituted cyclohexanes with reasonable success,[33] and later to proline derivatives,[40] together with the ribose ring in nucleosides and nucleotides.[32,34] These equations readily allow the computation of a coupling constant from a torsion angle and the electronegativity factors, but do not offer an explicit solution for the reverse computation, namely the calculation of a torsion angle from a coupling constant.[33] For the latter computation, iterative, trial-and-error methods or graphical determination can be used, assisted by a computer program CAGPLUS.[33]

The conformations of five-membered rings have long been interpreted in terms of a classical equilibrium of North (N) and South (S) conformers, where these terms refer to the regions of conformational space at the top and bottom of the pseudorotational cycle, respectively.[34,40–42] While the cyclopentane conformation moves freely around the pseudorotational cycle, the placement of substituents on either homocyclic or heterocyclic five-membered rings raises the energy barriers between certain conformers, generally restricting them to the N and S regions.[34] By applying Eq. (9) to the sugar ring in a range of nucleoside and nucleotide derivatives, Haasnoot *et al.* demonstrated that, depending on substituent pattern and structure, the equilibrium can be biased toward either the N or S type.[34] For example, the 2′-deoxyribose ring with O-3′ pseudoaxial favors the S-type conformation, whereas the 3′-deoxy compound with O-2′ quasiaxial favors the N-form.[34]

Following the recognition that $^3J_{\mathrm{HCCH}}$ depends on both the group electronegativity value and its orientation, and the availability of a set of additive constants (ΔJ values) proposed for prediction of J_{gauche} in trisubstituted ($\mathrm{CH_2CH}$) fragments of polypeptides,[43] Altona and Haasnoot developed a simple additivity rule for prediction of anti and gauche $^3J_{\mathrm{HCCH}}$ values in pyranose rings.[44] This represents an alternative approach to the use of Eqs. (9) and (10). Good quality ^{1}H NMR data were tabulated or measured mostly at 270, 300, or 360 MHz for a large number of hexopyranoses, pentopyranoses, and 2-deoxy-pentopyranoses, and a few 4,6-*O*-benzylidene derivatives.[44] Analysis of the data allowed a table of additivity constants, $\Delta J(\mathrm{X})$ for substituents X in pyranose rings to be constructed.[44] These constants clearly demonstrate the incremental effect of $\mathrm{X}_{\mathrm{gauche}}$ on $^3J_{\mathrm{ae}}$ and $^3J_{\mathrm{ee}}$, and the decremental effect of $\mathrm{X}_{\mathrm{anti}}$ on $^3J_{\mathrm{ae}}$ and $^3J_{\mathrm{ee}}$, and of $\mathrm{X}_{\mathrm{gauche}}$ on $^3J_{\mathrm{aa}}$. The agreement between experimental and calculated coupling constants was characterized by a standard deviation $\sigma = 0.29$ Hz, so that in 95% of the cases, the experimental value would not deviate from the predicted value by more than ± 0.6 Hz. It was predicted that, for pyranose systems that bear an axial substituent at C-2 (e.g., mannosides, altrosides, and rhamnosides), the difference in $^3J_{1,2}$ of the α and β anomers will be determined exclusively by the electronegativity of this axial substituent.[44] The results also encompass Booth's rule that an electronegative substituent attached to an HCCH fragment exerts a maximum negative effect on $^3J_{\mathrm{gauche}}$ when positioned in an anti-periplanar orientation to one of the coupled protons,[37] and the observation of Abraham and Gatti that, in 1,2-disubstituted ethanes,[30] the coupling of two gauche protons flanked by two gauche electronegative substituents obeys Eq. (11):

$$^3J_{\mathrm{gauche}} = 4.1 + 0.63\sum_{i=1}^{i=2}\Delta\chi_i \qquad (11)$$

where the electronegativity difference $\Delta\chi_i = \chi_i - \chi_{\mathrm{H}}$.

Colucci *et al.* proposed the equation:

$$^3J_{\mathrm{HCCH}} = A + B\cos\varphi + C\cos 2\varphi + \sum_{i=1}^{i=4}\Delta s_i \cos\varphi \cos\varphi_{\mathrm{HX}(i)} \qquad (12)$$

where $\varphi_{\mathrm{HX}(i)}$ is the dihedral angle between the interacting proton and the substituent X_i, and Δs_i is a single, empirically determined constant of the substituent.[45] This equation was constructed on the premise that the torsional dependence of $^3J_{\mathrm{HCCH}}$ could be described as a simple perturbation of the ethane system. Torsion angles were determined from X-ray crystal structure data and MM2 molecular mechanics. If perfect tetrahedral geometry is assumed for the ethanic fragment, then $\varphi_{\mathrm{HX}(i)} = \varphi \pm 120°$ can be used, leading to a more useful expression:

$$
\begin{aligned}
{}^{3}J_{\mathrm{HCCH}} = {} & A + B\cos\varphi + C\cos 2\varphi + \cos\varphi[(\Delta S_1 + \Delta S_4)\cos(\varphi - 120) \\
& + (\Delta S_2 + \Delta S_3)\cos(\varphi + 120)]
\end{aligned}
\tag{13}
$$

The values of Δs_i were obtained from experimental coupling constants for monosubstituted ethanes,[45] and the values tabulated for 39 substituents covered a range from -0.92 Hz for a lithium substituent (electron donating), through 0.00 Hz for H, to 13.9 Hz for $\mathrm{OEt_2^+\ BF_4^-}$ (electron withdrawing). However, the authors commented that the variation of the Δs_i values defied a consistent explanation, and at that time had not been totally correlated with any other set of substituent constants or properties of the groups.[45]

In the foregoing discussion, the electronegativity values χ_i referred to are those of Huggins,[46] which are modifications of Pauling electronegativities.[47] In later work, Altona *et al.*[48] studied the electronegativity dependence of the torsion angle-independent term A in equations such as (7). They measured ${}^{3}J_{\mathrm{HCCH}}$ values for substituted ethanes even more carefully, with an estimated data-point accuracy of ≤ 0.02 Hz. Attempts to fit these data led to the conclusion that none of the existing χ tables would correlate well with the observed couplings.[48] On this basis, it was proposed that the use of χ electronegativities for coupling-constant correlations be abandoned in favor of a new electronegativity scale of λ_i values, derived from the data set at hand.[48] A least-squares fit was applied to the J values of 55 mono- and 38 1,1-di-substituted ethanes, including 22 isopropyl derivatives. Altona *et al.* also proposed that any nonadditivity or interaction effect on the coupling constants could be described well by the introduction of cross terms, including the product of either the electronegativity differences, $\Delta\chi_i\Delta\chi_j$, or of the substituent constants, $\lambda_i\lambda_j$. To correspond approximately to the Huggins electronegativity scale, the new λ_i values were scaled so that $\lambda_{\mathrm{H}} = 0$, and $\lambda_{\mathrm{OR}} = 1.40$, values that were part of a series for some 50 substituents, including many carbon-bound groups, and nitrogen, oxygen, halogen, phosphorus, silicon, and sulfur-containing groups.[48] It was proposed that the electronegativity dependence of the couplings of the substituted ethanes could be described by the expression:

$$
{}^{3}J_{\mathrm{HCCH}} = 7.84 - 0.59(\lambda_1 + \lambda_2) - 0.42(\lambda_1\lambda_2) \tag{14}
$$

where λ_1 and λ_2 are the new electronegativity values of up to two substitutents. A striking difference between the new λ_i scale and other empirical, electronegativity scales was found to be the inverse correlation of λ_i with the electronegativity of the β substituent, whereas in $\Delta\chi$ scales, the reverse obtains.[48] Equation (14) was found to fit 84 experimental couplings with an rms deviation of 0.018 Hz, and a maximum deviation of 0.06 Hz, but the parent ethane and monohalo- and 1,1-dihalo-ethanes were exceptions that had to be parametrized differently. The λ electronegativity approach was supported by theoretical calculations of 1404 coupling constants using a reparametrized EHT method for ethane and its derivatives, singly or multiply substituted with Cl, F, Me, and OH.[49] Pairwise interactions between substituents were accounted for by using specific quadratic cross terms to describe the electronegativity dependence of the coefficients in a truncated Fourier series, with simultaneous least-squares optimization of the Fourier coefficients and the electronegativity values.[49] The theoretical coupling constants generated in this study were fitted by expanding Pachler's equation [Eq. (7)] to include a $\cos 3\varphi$ term, and additional coefficients for the electronegativity cross terms, giving:

$$^3J_{\mathrm{HCCH}} = C_0 + C_1 \cos\varphi + C_2 \cos 2\varphi + C_3 \cos 3\varphi + S_1 \sin\varphi + S_2 \sin 2\varphi \tag{15}$$

where

$$\begin{aligned} C_0 &= C_{00} + C_{01}\sum_i \lambda_i + C_{012}(\lambda_1\lambda_2 + \lambda_3\lambda_4) \\ C_1 &= C_{10} + C_{11}\sum_i \lambda_i \\ C_2 &= C_{20} + C_{21}\sum_i \lambda_i + C_{214}(\lambda_1\lambda_4 + \lambda_2\lambda_3) \\ C_3 &= C_{30} \end{aligned}$$

and

$$\begin{aligned} S_1 &= S_{11}\sum_i \xi_i\lambda_i \\ S_2 &= S_{21}\sum_i \xi_i\lambda_i + S_{213}(\lambda_1\lambda_3 - \lambda_2\lambda_4) \end{aligned}$$

Definitions and values for the coefficients are given in the original publication.[49]

The rms deviation of the total set of couplings was reduced to 0.124 Hz, which was stated to be markedly improved over that for the Pachler and earlier Haasnoot–Altona studies.[49]

The non-bonded, through-space transmission of spin information, known as the Barfield transmission effect, has been investigated theoretically for five-membered rings by the FPT-INDO-SCF-MO method.[50] An early observation of this effect was the non-equivalence of $J_{\text{endo-endo}}$ and $J_{\text{exo-exo}}$ in norbornanes,[51,52] which was also predicted to occur in cyclopentane, tetrahydrofuran, and in 7-hetero-substituted norbornanes,[50] and also explains[50] the observed non-equivalence of cisoid H–C_β–C_γ–H and H–C_γ–C_δ–H couplings in prolines.[53,54] This effect is not described by the typical basic or generalized Karplus equations, and the computations of de Leeuw *et al.*[50] suggested that it could be approximated by the function:

$$\Delta J = T\,\cos^2\,(P - P_\mathrm{b}) \tag{16}$$

where ΔJ is a decrease in the size of the coupling due to the transmission effect, P is the phase angle of pseudorotation in the five-membered ring, P_b is the phase angle of the envelope form for which a maximum effect is reached, and T depends strongly on the nature of the atom through whose orbitals the effect is transmitted. T was estimated to be ~0.5 Hz for a furanose ring oxygen, and ~2 Hz for a carbon atom. Correction by Eq. (16) needs to be applied only to cisoidal coupling constants in five-membered rings calculated from a Karplus-like equation.[50] The correction is thought to be negligible for ribofuranose systems, where the maximum decreasing effect is small (~0.5 Hz) and occurs in a forbidden region of P ~270°. In 2-deoxyribose systems, the correction is more important, because the South-type conformer predominates.[50] The Barfield correction term has been incorporated in the PSEUROT program, with the assumption of a two-state, North–South equilibrium.[55] Transoid couplings are not affected by this Barfield effect.[50]

In an empirical *tour de force*, the Karplus equation has been expanded to contain 13 mutually independent structural terms and 22 adjustable parameters.[56] The terms were selected and evaluated individually, with the assumption of a linear additivity. A standard set of 198 vicinal coupling constants determined from 104 compounds dissolved in nonpolar solvents was selected from the literature, including mostly alkanes and halides, but with a number of other substituent types represented, and four sugars. An interesting, arbitrary assessment of coupling constants measured in different decades was made by assigning a precision of 0.2 Hz for data reported before 1969, 0.1 Hz for those from 1970–1979, and 0.05 Hz for those reported after 1980. In fitting data to the modified equation, the experimental coupling constants were weighted by the reciprocals of the assigned precisions. A number of group-electronegativity scales were considered, and that of Mullay was selected as being most suitable.[56] Plotting of Mullay's group electronegativities, χ_sub against 26 $^3J_\mathrm{HCCH}$ values for substituted ethanes revealed a good linear relationship:

$$^3J_\mathrm{HCCH} = A + B(\chi_\mathrm{sub} - \chi_\mathrm{H}) = A + B\Delta\chi_i \tag{17}$$

with $A = 7.520$ and $B = -0.2088$. Optimum molecular geometries were determined by Allinger's MM2/MMP2(85) program, and the consideration and rejection of many different molecular properties led to the equation:

$$\begin{aligned}{}^3J_{\mathrm{HCCH}} = {} & A\cos\varphi + B\cos 2\varphi + C\cos 3\varphi + D\cos^2 2\varphi + W(E\cos\varphi\sum\Delta\chi_i\cos\theta_i \\ & + F\sum\Delta\chi_i\cos 2\theta_i + G\sum\Delta\chi_i) + H[(\omega_1+\omega_2)/2 - 110] + I(r_{\mathrm{C-C}} - 1.5) \\ & + K\sum\Delta\chi_j^{\beta}\cos 2\psi_j + Lr^{-4} + M \qquad (18)\end{aligned}$$

where the summation with respect to i refers to all substituents on the H–C–C–H system, the summation pertaining to j to all β substituents, and ω_1 and ω_2 are the C–C–H bond angles.[56] The $\cos 3\varphi$ and $\cos^2 2\varphi$ terms represent testing of logical extensions of the series of terms in the original Karplus equation [Eq. (2)], and in Eq. (18), the angle θ_i subtended by the electronegative substituent with respect to a coupled proton has been parametrized separately from the HCCH dihedral angle φ, or the cos ($\varphi + 120°$) and cos ($\varphi - 120°$) terms used in other studies. As is evident in Eq. (18), combinations containing both φ and θ_i were also tested for the electronegativity terms, and the orientation of the β-part of the α-substituent to a coupled proton is described by a new torsion angle, ψ. The H term in Eq. (18) represents an average deviation of the C–C–H bond angles from the tetrahedral angle, and the Barfield transmission effect, which reflects the proximity effect of non-bonded substituent atoms to the coupled protons, is characterized by the Lr^{-4} term. The exponent in the latter term was tested exhaustively in the range -1 to -12, but was found to be meaningful only when the proximal atom was carbon or oxygen at a distance $r < 3.3$ Å. Fitting of Eq. (18) to the 198 values of ${}^3J_{\mathrm{HCCH}}$ led to the optimum parameters $A = -1.2246$, $B = 5.0935$, $C = -0.1055$, $D = 0.5711$, $E = 0.8319$, $F = 0.0433$, $G = 0.0345$, $H = -0.2058$, $I = -8.9222$, $K = 0.1438$, L(carbon) $= -8.9395$, and L(oxygen) $= 6.9202$. The parameter M took values of 7.5075, 7.0306, 6.4793, 6.5432, or 5.5319, depending on whether the compounds were mono-, 1,1-di-, 1,2-di-, tri-, or tetra-substituted, respectively.[56] Similarly, the W values found for these substitution patterns were 1.00, 2.55, 1.16, 2.29, and 1.40, respectively. The units used in Eq. (18) are Å for distances, degrees for valence and dihedral angles, and Hz for coupling constants.

This comprehensive study also tested the relative importance of the various terms in Eq. (18), and its relative performance when compared with modified Karplus equations of the Pachler, Haasnoot, and Colucci *et al.* types. Based on standard deviations of errors, the ranking of the four most important terms was found to be $\cos 2\varphi$, $\cos\varphi\ \Sigma\Delta\chi_i\ \cos\theta_i$, $\cos\varphi$, and $(\omega_1 + \omega_2)/2$. Thus, the second most important term is the combined electronegativity/electronegativity orientation term, and the fourth most significant one is the bond angle term, the first- and third-ranked terms being present in the original Karplus expression. An alternative equation containing these top four terms was proposed:

$$\begin{aligned}{}^3J_{\mathrm{HCCH}} = {} & A\cos\varphi + B\cos 2\varphi + WE\ \cos\ \varphi\sum\Delta\chi_i\cos\theta_i \\ & + H[(\omega_1+\omega_2)/2 - 110] + M\end{aligned} \tag{19}$$

which can be used with little loss of precision, if a computer program for Eq. (18) is unavailable.[56] However, Eq. (18) was found to have the lowest standard deviation (0.3255 Hz) of the four equations tested, when they were applied to the ${}^3J_{\mathrm{HCCH}}$ values of single conformation molecules in the standard set.[56]

Some 14 years after publication of the original Haasnoot equation, it was reparametrized to include a λ_i group electronegativity scale and specific parameters for substituted ethane derivatives,[57] regardless of degree of substitution:

$$\begin{aligned}{}^3J_{\mathrm{HCCH}} = {} & 14.63\cos^2\varphi - 0.78\cos\varphi + 0.60 \\ & + \sum_i \lambda_i\left[0.34 - 2.31\cos^2\left(s_i\varphi + 18.4|\lambda_i|\right)\right]\end{aligned} \tag{20}$$

where the sign parameter is now $s_i = \pm 1$. A slightly modified λ_i scale was constructed from the couplings to methyl in substituted ethanes and isopropyl derivatives, which were represented by the equation:

$${}^3J_{\mathrm{HCCH}} = 7.660 - 0.596(\lambda_1+\lambda_2) - 0.419(\lambda_1\lambda_2) \tag{21}$$

The parent ethane and its dihalo derivatives were now included, but norbornanes and molecules suspected to be conformationally inhomogeneous were excluded.[57] Molecular geometries were recalculated using the MM2-85 force field. By this means, the overall rms error for the ${}^3J_{\mathrm{HCCH}}$ values was lowered from 0.48 to 0.36 Hz. The λ_i values derived previously were found to be still valid for common organic solvents, but a slightly different λ_i scale was constructed for solutions in D_2O,[57] for compounds where the α-substituent carries one or two non-conjugated lone pairs of electrons that readily act as hydrogen-bond acceptors, so that $\Delta\lambda = -0.11 \pm 0.03$ for NH_2, NHR, NR_2, OH, OR, and R = alkyl. The λ_i values for the nucleic acid bases A, C, G, T, and U, as determined from *N*-isopropyl derivatives, were found to be 0.56 ± 0.01, irrespective of solvent.[57] The Pachler equation and equations such as (20) were stated to be valid for saturated HCCH fragments with approximately tetrahedral bond angles, but not for strained molecules such as norbornanes, in which large deviations from tetrahedral geometry occur.[57]

Various models for the interaction between pairs of substituents in ethanes have been discussed.[58,59] MCSCF *ab initio* calculations of ${}^3J_{\mathrm{HCCH}}$ in ethane have given the contributions from the Fermi contact, spin dipolar, orbital paramagnetic, and orbital diamagnetic mechanisms, of which only the Fermi contact contribution was found to be significant.[60]

In a different approach,[61] ${}^3J_{\mathrm{HCCH}}$ values (and also ${}^1J_{\mathrm{CH}}$ and ${}^2J_{\mathrm{HCH}}$) have been computed by DFT methods for exocyclic hydroxymethyl groups on aldopyranosyl rings, and the values compared with experiment and correlated with the O-5–C-5–C-6–O-6 torsion angle ω, according to the equations:

$$ {}^3J_{\mathrm{H-5,H-6R}} = 5.08 + 0.47\cos\omega + 0.90\sin\omega - 0.12\cos 2\omega + 4.86\sin 2\omega \tag{22}$$

$$ {}^3J_{\mathrm{H-5,H-6S}} = 4.92 - 1.29\cos\omega + 0.05\sin\omega + 4.58\cos 2\omega + 0.07\sin 2\omega \tag{23}$$

These relationships have been confirmed by DFT calculations on hydroxymethyltetrahydropyran analogues of aldohexopyranosides,[62] using a set of staggered and eclipsed geometries, which on least-squares fitting of the theoretical coupling constants yielded:

$$ {}^3J_{\mathrm{H-5,H-6R}} = 5.06 + 0.45\cos\omega + 0.80\sin\omega - 0.90\cos 2\omega + 4.65\sin 2\omega \tag{24}$$

$$ {}^3J_{\mathrm{H-5,H-6S}} = 4.86 - 1.22\cos\omega + 0.04\sin\omega + 4.32\cos 2\omega + 0.07\sin 2\omega \tag{25}$$

This study[62] also led to the equation:

$$ {}^2J_{\mathrm{H-6R,H-6S}} = -10.97 + 0.11\cos\omega + 0.59\cos 2\omega - 0.79\cos\theta + 2.00\cos 2\theta \tag{26}$$

reflecting the dependence of this geminal coupling on both of the torsion angles ω and θ, about C-5–C-6 and C-6–O-6, respectively, and the more significant dependence on θ.

Experimental values of ${}^3J_{\mathrm{HCCH}}$ were redetermined for the methyl α- and β-pyranosides of D-glucose and D-galactose, and were found to agree well with the results of the DFT computations.[62]

b. Proton–Proton Couplings, ${}^3J_{\mathrm{HCNH}}$.— Barfield and Karplus[63] combined a theoretical VB bond-order formulation of contact nuclear spin–spin coupling with a semiempirical approach based on Whiffen's measurements of proton hyperfine splitting data for π-electron radicals and radical ions of the form $\cdot$C-CHR$_2$, $\cdot$C-NHR, and $\cdot$C-OH, leading to the equation:

$$ {}^3J_{\mathrm{HCNH}} = 12\cos^2\varphi + 0.2 \tag{27}$$

However, equations such as this one were thought to have the limitation that because they were derived from the hyperfine interaction, which is symmetric about $\varphi = 90°$

no account was given of the asymmetry in the coupling constant.[63] $^3J_{\mathrm{HCNH}}$ is commonly observed to be 8.0–9.5 Hz in acetamidodeoxy sugars, and in secondary amines, such as *N*-2,4-dinitrophenyl derivatives of amino sugars.[64–66] For a long time, an explicit Karplus equation for $^3J_{\mathrm{HCNH}}$ in amino sugars was not available, and an equation with coefficients derived from model peptides by Bystrov *et al.*[67] was sometimes used. It has often been assumed that the 8.0–9.5 Hz coupling represents a trans arrangement of the coupled protons, for example H-2 and NH in the 2-acetamido-2-deoxy sugars. However, molecular dynamics simulations of tetrasaccharide fragments of hyaluronan suggested that a cis arrangement of the coupled protons sometimes occurs, and, therefore, that high values of $^3J_{\mathrm{HCNH}}$ cannot always be used to infer a purely trans form of the acetamido group.[68]

More recently, a very detailed theoretical study of 2-acetamido-2-deoxy-D-glucose and 2-acetamido-2-deoxy-D-galactose has been reported, in which DFT was used to calculate $^3J_{\mathrm{H\text{-}2,NH}}$ values of the pyranose anomers.[69] Karplus coefficients were then derived by least-squares fitting of the theoretical coupling constants to Eq. (3). The fitted Karplus parameters were found to be similar to those derived previously for peptide amide groups,[67] but were consistently larger. An implicit solvation model consistently lowered the magnitude of the calculated values, improving the agreement with experiment. However, an explicit solvation model worsened the agreement with the experimental data.[69] A detailed study of the effect of libration of the acetamido group on $^3J_{\mathrm{H\text{-}2,NH}}$ values was also performed.[69] The dynamical spread of the rotation of the acetamido group in free α-GlcNAc, *β*-GlcNAc, and α-GalNAc was estimated to be 32°, 42°, and 20°, with corresponding dihedral angles of 160°, 180°, and 146°, respectively. From DFT calculations containing mainly the important Fermi contact coupling term (but sometimes other interactions, too), the Karplus coefficients found for a $^3J_{\mathrm{H\text{-}2,NH}}$ version of Eq. (3) were $A = 9.45\text{–}10.02 \pm 0.21\text{–}0.26$, $B = -1.51$ to $-2.08 \pm 0.10\text{–}0.13$, and $C = 0.49\text{–}0.99 \pm 0.12\text{–}0.16$, depending on which GlcNAc or GalNac anomer was calculated. It was suggested that Karplus equations derived for proteins no longer be used for these sugars.[69]

c. Proton–Proton Couplings, $^3J_{\mathrm{HCOH}}$.— The VB bond-order–proton hyperfine splitting combination of Barfield and Karplus[63] also led to the equation:

$$^3J_{\mathrm{HCOH}} = 10\cos^2\varphi - 1.0 \tag{28}$$

However, this equation was considered to have the same failing as Eq. (27) in Section IV.1.b, in that the couplings for torsion angles of 0° and 180° are expected to be and are most commonly observed to be different.[63]

Based on two values of $^3J_{\mathrm{HCOH}}$ obtained by an exact analysis of the ABC system in the hydroxymethyl group of 3β-acetoxy-5β,6β-oxidocholestan-19-ol and three other literature values, Fraser *et al.*[70] formulated the expression:

$$^3J_{\mathrm{HCOH}} = 10.4\cos^2\varphi - 1.5\cos\varphi + 0.2 \tag{29}$$

However, the published spectrum of the steroid had significant noise on the peak maxima, and inspection of the ^{1}H shifts reported from an ABC analysis at 60 MHz revealed that this system would undoubtedly be AMX at current ^{1}H NMR frequencies of 500–950 MHz and would benefit from redetermination of the $^3J_{\mathrm{HCOH}}$ values. Until recently, this type of coupling had not been investigated in detail for sugars, despite many reported values, and the detection of such couplings in supercooled, aqueous solutions of carbohydrates.[71–73] For methyl β-D-gluco- and β-D-galacto-pyranosides, the latter studies reported averaging of the $^3J_{\mathrm{HCOH}}$ values (4.75–6.24 Hz), which was attributed to free rotor, hydroxyl groups.[72] However, other studies, for example, methyl 2,6-anhydro-3-deoxy-3-phthalimido-α-D-mannopyranoside in chloroform solution, have shown more extreme values ($^3J_{4,\mathrm{HO}\text{-}4}$ 11.6 Hz) that probably represent an anti arrangement of the coupled protons.[74]

A very detailed study of $^3J_{\mathrm{HCOH}}$ and other related coupling constants has recently been conducted.[75] Zhao *et al.* performed DFT calculations on a series of aldopyranosyl model structures, many of which were deoxygenated at C-3, C-4, and/or C-6, so as to eliminate any undesired hydrogen bonding.[75] DFT calculations were carried out with (a) only the Fermi contact contribution included and (b) non-Fermi contact terms included as well. For non-anomeric protons, inclusion of only the Fermi contact term resulted in a generalized Karplus equation:

$$^3J_{\mathrm{HCOH}} = 6.06 - 3.26\cos\varphi + 6.54\cos 2\varphi \tag{30}$$

which is similar to Eq. (29) of Fraser *et al.* The results from inclusion of all four contributions showed that the spin–dipolar term is negligible, whereas the paramagnetic spin–orbital and diamagnetic spin–orbital terms have comparable magnitudes, but opposite signs, thus leading to a slightly modified equation:

$$^3J_{\mathrm{HCOH}} = 5.76 - 2.05\cos\varphi + 6.78\cos 2\varphi \tag{31}$$

The situation is more complicated for $^3J_{\mathrm{HCOH}}$ involving the C-1–O-1 bond, because in one of the rotamers about this bond, HO-1 is anti to O-5, which (by Booth's effect) reduces the value of $^3J_{\mathrm{HCOH}}$ in this rotamer, causing the magnitudes of the two gauche couplings to be non-equivalent, and the derived Karplus curve to be phase-shifted relative to that predicted from Eq. (31). Because of this phenomenon, separate equations (Fig. 3A) are required for α- and β-pyranoses:

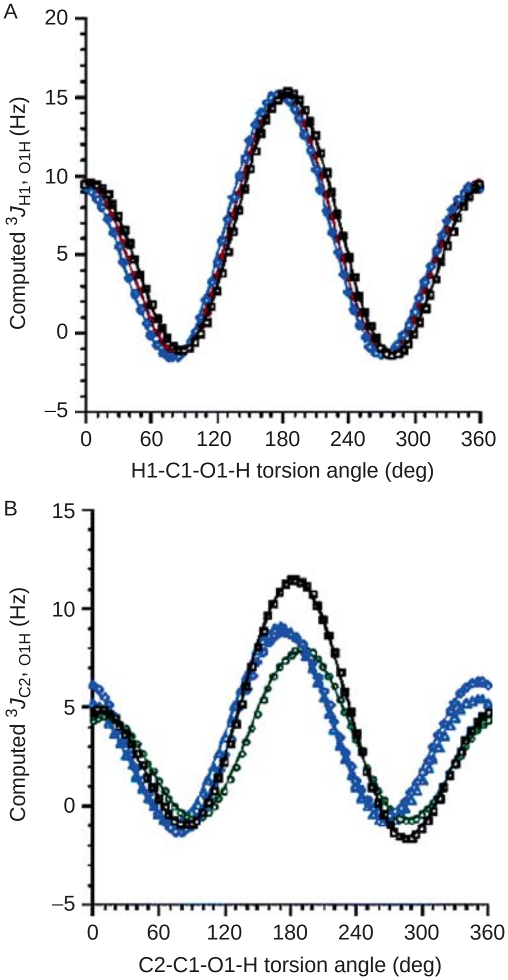

FIG. 3. (A) DFT calculated, four-quadrant plots of dependence of $^3J_{\text{H-1,HO-1}}$ on the torsion angle about C-1–O-1, for 3,4,6-trideoxy mimics of α-D-glucopyranose and α-D-mannopyranose (Eq. (32), blue triangles) and β-D-glucopyranose and β-D-mannopyranose (Eq. (33), black squares). The data are superimposed on a plot of Eq. (31), (red circles). (B) DFT dependence of $^3J_{\text{C-2,HO-1}}$ on the C-1–O-1 torsion angle in 3,4,6-trideoxy mimics of α-D-glucopyranose (Eq. (57), green circles), β-D-glucopyranose (Eq. (59), blue triangles), α-D-mannopyranose (Eq. (58), black squares), and β-D-mannopyranose (Eq. (60), purple diamonds).

$$^{3}J_{\mathrm{H-1,HO-1}}(\alpha) = 5.52 - 2.93\cos\varphi + 6.71\cos 2\varphi + 0.14\sin\varphi - 1.00\sin 2\varphi \quad (32)$$

$$^{3}J_{\mathrm{H-1,HO-1}}(\beta) = 5.71 - 2.88\cos\varphi + 6.65\cos 2\varphi + 0.076\sin\varphi - 1.17\sin 2\varphi \quad (33)$$

The theoretical studies of $^{3}J_{\mathrm{HCOH}}$ were supported by experimental measurements on methyl β-D-glucopyranoside, methyl β-galactopyranoside, methyl β-lactoside, methyl β-D-(4-^{13}C)glucopyranoside, methyl β-D-(1-^{13}C)galactopyranoside, and methyl β-(1,4′-$^{13}C_2$)lactoside at 600 MHz, using solutions of the sugars in a mixture of acetone-d_6 and highly purified water at −20 °C, to reduce the rate of hydroxyl-proton exchange.[75]

d. Proton–Proton Couplings, $^{3}J_{\mathrm{HCSiH}}$.— The angular dependence of $^{3}J_{\mathrm{HCSiH}}$ has been investigated by NMR studies of *cis*- and *trans*-3,5-dimethyl-1-silacyclohexanes, and 3-silabicyclo-[3.2.1]octane, the ^{1}H spectra of which afforded eight values of the coupling.[76] Torsion angles for the 1-silacyclohexane derivatives were assumed on the basis of electron-diffraction data for 1,1-dichloro- and 1,1-dimethoxy-1-silacyclohexane in the gas phase, and for 3-silabicyclo-[3.2.1]octane from literature data obtained by force-field methods, which together yielded φ values in the range 25°–165°. Least-squares fitting of the couplings to the angles resulted in the equation:

$$^{3}J_{\mathrm{HCSiH}} = 5.83\cos^{2}\varphi - 2.59\cos\varphi + 0.84 \quad (34)$$

An interesting corollary of this study was that the conformational free energy of the methyl group in 1-methyl-1-silacyclohexane is ~1.45 kJ mol^{-1} in favor of the axial orientation of this group.[76]

2. Proton–Carbon Couplings

The most important coupling constant of this type in carbohydrates is undoubtedly $^{3}J_{\mathrm{HCOC}}$, because this coupling occurs up to two times in the interglycosidic linkage, and, therefore, offers information on the transglycosidic angles φ and ψ. ^{13}C substitution is helpful in the measurement of these couplings, but is not mandatory, as a large number of NMR methods have been developed for measurements at natural abundance. Early data measured by Lemieux *et al.*[77] on uridine analogues substituted with ^{13}C at C-2 of the uracil residue and on 3,4,6-tri-*O*-acetyl-α-D-glucopyranose 1,2-(methyl 1-^{13}C-orthoacetate) suggested the existence of a Karplus relationship for $^{3}J_{\mathrm{HCOC}}$ and $^{3}J_{\mathrm{HCNC}}$, but no attempt was made to define any equations.

a. Proton–Carbon Couplings, $^3J_{\mathrm{HCOC}}$.— The early history of this coupling has been the subject of previous reviews, in which the Karplus-type relationship was illustrated graphically,[78,79] and later interpreted[80] by the equation:

$$^3J_{\mathrm{HCOC}} = -0.13(1 - \cos\varphi) - 2.80(1 - \cos 2\varphi) + 0.53(1 - \cos 3\varphi) + 5.32 \quad (35)$$

A Karplus equation of the three-parameter type was proposed by Tvaroška *et al.*[81] based on the precise measurement of $^3J_{\mathrm{HCOC}}$ in a series of conformationally rigid carbohydrate derivatives having known X-ray structures:

$$^3J_{\mathrm{HCOC}} = 5.7\cos^2\varphi - 0.6\cos\varphi + 0.5 \quad (36)$$

The compounds studied included 1,6-anhydro-aldohexo- and ketohexo-pyranoses, which contained X-ray defined dihedral angles in the range 86°–279° and $^3J_{\mathrm{HCOC}}$ 0–5.9 Hz. Literature data for cyclomaltohexaose, phenyl 3-*O*-acetyl-*β*-D-xylopyranoside, and 1,2-*O*-ethylidene-*β*-D-glucopyranoside, provided coupling values for estimated dihedral angles of 10° and 60°. The $^3J_{\mathrm{HCOC}}$ values were measured on natural-abundance ^{13}C by selective, 2D *J*-resolved spectroscopy, or by a modified, selective 2D INEPT experiment. Seventeen data pairs were used to construct 17 simultaneous equations which were solved for the values of *A*, *B*, and *C* in Eq. (3). In this study, the possible influence of electronegativity factors on the couplings was avoided by keeping the sum of the substituent electronegativities constant.[81]

A very similar study was submitted at almost the same time, but published sooner.[82] Mulloy *et al.* used the glycosidic linkages of cyclomalto-hexaose and -heptaose as the best source of data for dihedral angles in the range 0°–20°, and several H–C–O–C pathways in 1,6-anhydro-*β*-D-glucopyranose for angles of 100°–170°. The $^3J_{\mathrm{H\text{-}1,C\text{-}5}}$ values measured for *β*-D-Glc and *β*-D-Gal residues provided points for dihedral angles of ~60°, and the same coupling pathway for α-D-Glc residues gave data on dihedral angles of ~180°. Values of dihedral angles were obtained from X-ray crystal structures of the subject compounds, or from those of analogues. The resulting Eq. (37) obtained[82] by least-squares fitting of $^3J_{\mathrm{HCOC}}$ values measured by the 2D heteronuclear *J*-resolved method is very similar to that of Tvaroška *et al.*,[81] and these two studies confirm one another:

$$^3J_{\mathrm{HCOC}} = 5.5\cos^2\varphi - 0.7\cos\varphi + 0.6 \quad (37)$$

The resulting curve differed from that proposed by Hamer *et al.*[78] most significantly near 180°, where several *J* values were too large to be accommodated by their results or Eq. (35). The results of Mulloy *et al.*[82] suggested that for the interglycosidic bond angles φ and ψ, the prediction of $^3J_{\mathrm{HCOC}}$ from angles may be made to ±1 Hz, and the calculation of angles from $^3J_{\mathrm{HCOC}}$ to ±10°. These techniques were used to compare the conformations of sucrose, raffinose, and stachyose in solution and the solid state. The discrepancies between experimental values of $^3J_{\mathrm{HCOC}}$ and those predicted from the crystal structures indicated that sucrose and its homologous oligosaccharides do not exist in D_2O or Me_2SO-d_6 solutions in the conformation found in the solid state. Data from this study were also used to reassign the ^{13}C NMR spectrum of melezitose.[82] The general form of the equation is also supported by FPT-INDO calculations for the model compound 2-methoxytetrahydropyran, which when formulated as a superposition of dependences on φ and ψ yielded[83] the equation:

$$^3J_{\mathrm{HCOC}} = 6.3\cos^2\varphi - 1.2\cos\varphi + 0.1 \tag{38}$$

DFT calculations have been used to investigate the structures and conformations of four β-[1→4]-linked disaccharide mimics,[84] the method being used to compute both optimized geometries, and values of $^3J_{\mathrm{HCOC}}$ (and $^3J_{\mathrm{COCC}}$, see below) as a function of the interglycosidic torsion angles φ and ψ. The $^3J_{\mathrm{HCOC}}$ values computed by DFT were fitted by least squares to Eq. (3) giving:

$$^3J_{\mathrm{HCOC}} = 7.49\cos^2\varphi - 0.96\cos\varphi + 0.15 \tag{39}$$

A comparison of the theoretical $^3J_{\mathrm{HCOC}}$ values with Eq. (36) of Tvaroška *et al.*[81] indicated good agreement (Fig. 4), except for the extremes of the curve at $\varphi = 0°–20°$ and 160°–180°, where the computed couplings were larger, as implied by the larger *A* constant in Eq. (39). Re-measurement of the couplings for these angles was suggested.[84] Sufficient confidence was expressed in the theoretical computations of the coupling constants to suggest that the application of such computations to specific bonding structures might supersede the construction of generalized Karplus curves from experimental data for model compounds.[84]

Interglycosidic $^3J_{\mathrm{HCOC}}$ values have also been measured by non-selective, 2D *J*-resolved ^{1}H NMR of tri-, tetra-, and penta-saccharide fragments of the O-specific polysaccharide of *Shigella dysenteriae* type 1 substituted with ^{13}C at C-1 of the galactopyranose residues.[85]

More advanced NMR methods have also been used. Höög and Widmalm[86] measured transglycosidic $^3J_{\mathrm{HCOC}}$ of α-D-Man*p*-(1→3)-β-D-Glc*p*-OMe by selective excitation of ^{13}C resonances, followed by evolution of the heteronuclear couplings, and detection of ^{1}H resonances by two-site, Hadamard spectroscopy.[87,88] The $^3J_{\mathrm{HCOC}}$ values across the glycosidic linkage were extracted by a *J*-doubling procedure

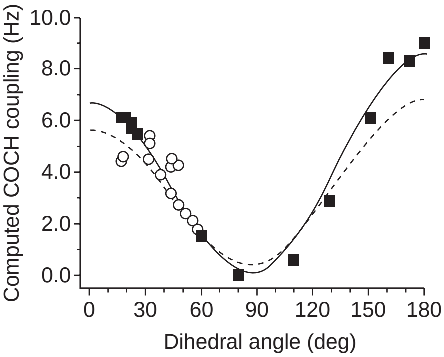

FIG. 4. Variation of trans-*O*-glycoside $^3J_{\mathrm{HCOC}}$ values (corrected) with dihedral angle φ, computed by DFT for four β-[1→4]-linked disaccharide mimics. The dashed line is a plot of the Karplus equation (Eq. (36)) defined experimentally by Tvaroška *et al.*,[81] and the solid line is the computed relationship (Eq. (39)), where ■ represents $^3J_{\mathrm{H\text{-}4',C\text{-}1}}$ data, and ○ is $^3J_{\mathrm{H\text{-}1,C\text{-}4'}}$ data.[84]

and were correlated with the interglycosidic angles φ and ψ by molecular dynamics/molecular mechanics using the CHARMM force field and Eqs. (36) and (39). The results indicated that the disaccharide adopts a preponderant conformation and has limited flexibility on a short timescale of less than the rotational correlation time τ_M, but on a timescale $> \tau_M$, excursions to other conformational states are required to obtain agreement between simulation and experiment.[86] In related work, trans-glycosidic $^3J_{\mathrm{HCOC}}$ values have been measured for eight α- or β-linked disaccharides by gradient-enhanced, multiple ^{13}C site-selective excitation, with ^{1}H decoupling after polarization transfer.[89] In most cases, good agreement was obtained between the experimental $^3J_{\mathrm{HCOC}}$ values and those calculated by application of Eq. (36) of Tvaroška *et al.*[81] to dihedral angles obtained by molecular-dynamics computations, with explicit water and the Amber–Homans forcefield.[89]

DFT calculations have been used to construct new Karplus curves for $^2J_{\mathrm{HH}}$, $^3J_{\mathrm{HH}}$ (as mentioned before) $^2J_{\mathrm{CH}}$, $^3J_{\mathrm{CH}}$, $^3J_{\mathrm{HCCC}}$, $^3J_{\mathrm{HCOC}}$, and $^3J_{\mathrm{HCSC}}$. A major focus of this investigation[62] was DFT computations for the exocyclic hydroxymethyl group of aldohexopyranoside derivatives, particularly in methyl α- and β-D-gluco- and -galacto-pyranosides, for which coupling constants were also determined experimentally by 2D ^{1}H–^{13}C heteronuclear zero- and double-quantum, phase-sensitive *J*-HMBC NMR. DFT on methyl β-D-glucopyranoside yielded $^3J_{\mathrm{HCOC}}$ values that fitted the equation:

$$^{3}J_{\mathrm{HCOC}} = 6.68\cos^{2}\varphi - 0.89\cos\varphi + 0.11 \tag{40}$$

in which the coefficient of the important $\cos^2 \varphi$ term lies in between the values in Eqs. (36) and (39). However, the DFT computations agree better with each other, than with the experimental data, possibly owing to solvation effects, basis set limitations in the DFT, and the use of a small set of geometries.[62]

Improved Karplus equations have been developed for $^{3}J_{\mathrm{C\text{-}1,H\text{-}4}}$ in aldopentofuranosides[90] by extension of the Haasnoot–Altona equation for $^{3}J_{\mathrm{HCCH}}$, to $^{3}J_{\mathrm{HCOC}}$. DFT calculations were performed for the eight methyl aldopentofuranosides using the GAUSSIAN98 program in the gas phase at the B3LYP/6–31G* level, thus generating 30 conformers for each structure. $^{3}J_{\mathrm{C\text{-}1,H\text{-}4}}$ values were then calculated for each optimized geometry by using the DEMON-KS program augmented by the DEMON-NMR code. These calculations furnished a data set of 240 $^{3}J_{\mathrm{C\text{-}1,H\text{-}4}}$ values comprised of 120 with the α configuration, and 120 with the β configuration. A three-step procedure was used to construct a Haasnoot–Altona equation. First, 240 scaled values of $^{3}J_{\mathrm{C\text{-}1,H\text{-}4}}$ were fitted to a three-parameter Karplus equation, giving:

$$^{3}J_{\mathrm{C-1,H-4}} = 8.14\cos^{2}\varphi - 0.61\cos\varphi - 0.15 \tag{41}$$

The need for scaling of the values of $^{3}J_{\mathrm{HCOC}}$ calculated by the *ab initio*, DEMON-NMR procedure was assessed by comparison of the theoretical and experimental values of four 1,6-anhydro-aldohexopyranose derivatives, which disclosed that the theory overestimated the couplings by an average of 16.7%, thus leading to a scaling factor of 0.833.

Secondly, by using the A, B, and C values from Eq. (41), the effect of anomeric configuration was accounted for by fitting the data for the α-furanosides to the full Haasnoot–Altona equation:

$$\begin{aligned}^{3}J_{\mathrm{C-1,H-4}} = {} & A\cos^{2}\varphi + B\cos\varphi + C\\ & + G\{D - E[\cos^{2}(\varphi(\xi) + F \times G)]\}\\ & + H\{D - E[\cos^{2}(-\varphi(\xi) + F \times H)]\}\end{aligned} \tag{42}$$

where G and H are the electronegativities of the substituents at C-1, thereby giving:

$$\begin{aligned}^{3}J_{\mathrm{C-1,H-4}}(\alpha) = {} & 8.14\cos^{2}\varphi - 0.61\cos\varphi - 0.15\\ & + G\{0.71 - 1.46[\cos^{2}(\varphi(\xi) + 44.3G)]\}\\ & + H\{0.71 - 1.46[\cos^{2}(-\varphi(\xi) + 44.3H)]\}\end{aligned} \tag{43}$$

In the same manner, an equation was constructed for the β-glycosides:

$$\begin{aligned} {}^3J_{\mathrm{C-1,H-4}}(\beta) = {} & 8.14\cos^2\varphi - 0.61\cos\varphi - 0.15 \\ & + G\{0.72 - 1.47[\cos^2(\varphi(\xi) + 40.1G)]\} \\ & + H\{0.72 - 1.47[\cos^2(-\varphi(\xi) + 40.1H)]\} \end{aligned} \tag{44}$$

Thirdly, the D–F values from the ${}^3J_{\text{C-1,H-4}}$ (α) and (β) equations were averaged to give:

$$\begin{aligned} {}^3J_{\mathrm{C-1,H-4}} = {} & 8.14\cos^2\varphi - 0.61\cos\varphi - 0.15 \\ & + G\{0.71 - 1.46[\cos^2(\varphi(\xi) + 42G)]\} \\ & + H\{0.71 - 1.46[\cos^2(-\varphi(\xi) + 42H)]\} \end{aligned} \tag{45}$$

The curve from this equation was similar to that from Eq. (39) of Cloran *et al.*,[84] the curve for the α-glycosides lying just below, and the curve for the β-glycosides slightly above, the curve from Eq. (39). The combination equation for α- and β-furanosides was used to investigate their conformational preferences further and could also be used to clarify the results of PSEUROT analyses based only on ${}^3J_{\mathrm{HCCH}}$ values.[90]

b. Proton–Carbon Couplings, ${}^3J_{\mathrm{HCCC}}$.— Bock and Pedersen performed a complete analysis of the ^{1}H-coupled ^{13}C spectrum of 1,6-anhydro-β-D-galactopyranose and some other sugars and found evidence of a Karplus dependence of ${}^3J_{\mathrm{HCCC}}$ and ${}^3J_{\mathrm{HCOC}}$, although only a limited range of dihedral angles (from Dreiding models) could be tested.[91] The complex ^{1}H-coupled ^{13}C spectra were simplified by selective, ^{1}H spin decoupling.

An unusual, indirect method was used by Aydin and Günther to determine ^{13}C, ^{1}H couplings over one, two, and three bonds in norbornanes.[92] They measured the corresponding ^{13}C, ^{2}H couplings in ^{1}H-decoupled, ^{13}C NMR spectra of deuterated isotopomers of norbornane-*d*, fenchane-2-*d*, and a number of deuterated, alkyladamantanes, thus avoiding the complexity of analyzing ^{1}H-coupled ^{13}C spectra.[92] The ^{13}C, ^{1}H couplings were calculated by multiplying the ^{13}C, ^{2}H couplings by the ratio of the magnetogyric constants, $\gamma_{\mathrm{H}}/\gamma_{\mathrm{D}} = 6.5144$. Dihedral angles were derived from MM2 force field calculations, and when substituent effects from branching and methyl substitution in the norbornanes were taken into account, the following equation was obtained:

$${}^3J_{\mathrm{HCCC}} = 4.50 - 0.87\cos\varphi + 4.03\cos 2\varphi \tag{46}$$

which may be rewritten as

$$^{3}J_{\mathrm{HCCC}} = 8.06\cos^{2}\varphi - 0.87\cos\varphi + 0.47 \tag{47}$$

Corrections to the coupling-constant measurements because of quadrupolar relaxation by deuterium were employed, and one disadvantage of this indirect method is that the $^{3}J_{\mathrm{DCCC}}$ values measured may be too small to be resolved, since they are a factor of 6.5 smaller than the corresponding $^{3}J_{\mathrm{HCCC}}$ values.[92] In sugars, the ^{13}C resonance of a deuterium-substituted carbon may disappear,[93] due either to quadrupolar relaxation by deuterium, and/or to saturation caused by lengthening of the ^{13}C T_1 on replacement of dipolar relaxation by a proton with the weaker effect of a deuteron.

The pendant hydroxymethyl group in sugars has been a popular vehicle for experimental and theoretical studies of coupling constants, and the application of FPT-INDO calculations to both anomers of the eight aldohexopyranoses yielded an equation for the dependence of $^{3}J_{\text{C-4,H-6}}$:

$$^{3}J_{\mathrm{C-4,H-6}} = 5.8\cos^{2}\omega - 1.6\cos\omega - 0.02\sin\omega + 0.28\sin 2\omega + 0.52 \tag{48}$$

where ω is the torsion angle of C-4 and H-6 about the C-5–C-6 bond.[94,95] The agreement of the calculated values and the experimental values available for mono- and oligo-saccharides was found to be satisfactory.[94]

Separate dependences have recently been computed[62] for H-6R and H-6S in 1,2,3-trideoxy analogues of D-gluco- and D-galacto-pyranose:

$$^{3}J_{\mathrm{C-4,H-6R}} = 0.10\cos\omega + 3.17\cos 2\omega + 0.27\sin\omega - 0.55\sin 2\omega + 3.34 \tag{49}$$

$$^{3}J_{\mathrm{C-4,H-6S}} = 0.49\cos\omega + 0.11\cos 2\omega - 0.13\sin\omega - 3.54\sin 2\omega + 3.64 \tag{50}$$

c. Proton–Carbon Couplings, $^{3}J_{\mathrm{HCSC}}$.— The application of a modified, 2D heteronuclear *J*-resolved NMR method to a set of eight conformationally rigid, thio sugar derivatives provided 17 values of $^{3}J_{\mathrm{HCSC}}$ that were used to define[96] the equation:

$$^{3}J_{\mathrm{HCSC}} = 4.44\cos^{2}\varphi - 1.06\cos\varphi + 0.45 \tag{51}$$

A crystal structure was available for one of the thio sugars studied, but for the others, no structural data were available, and dihedral angles for the H–C–S–C fragments were computed by the PCILO quantum chemical method. These angles covered the range $-155°$ to $179°$, with a gap from $-60°$ to $35°$. The experimental $^{3}J_{\mathrm{HCSC}}$ values spanned 0.3–8.1 Hz, but the latter value was rejected because its magnitude was thought to be enhanced by the π-electrons of a neighboring C=O group. Equation (51) was tested by application to methyl 4-thio-α-maltoside, for which it was found that the values $^3J_{\text{C-1,H-4}'}$ 5.15 Hz and $^3J_{\text{C-4}',\text{H-1}}$ 2.95 Hz measured for the H-1–C-1–S-4′–C-4′–H-4′ moiety differed from those, 3.8 and 3.1 Hz, respectively, predicted from the conformation in the crystal.[96] This discrepancy was rationalized by using the PCILO method to calculate a relaxed (φ, ψ) conformational energy surface for the thio disaccharide in aqueous solution, which revealed the existence of 15 conformers having five main minima for rotation about the glycosidic C–S bonds. Conformational averaging based on the populations computed for the five stable conformers and the $^3J_{\text{HCSC}}$ values calculated from Eq. (51) yielded the values $^3J_{\text{C-1,H-4}'}$ 5.2 Hz and $^3J_{\text{C-4}',\text{H-1}}$ 2.6 Hz.[96]

Taffazoli and Ghiasi performed DFT computations[62] on methyl 1-thio-β-D-glucopyranoside, yielding values of $^3J_{\text{HCSC}}$, which fitted the equation:

$$^3J_{\text{HCSC}} = 5.04\cos^2\varphi - 1.35\cos\varphi + 0.55 \tag{52}$$

which is in reasonable agreement with the experimental data of Tvaroška *et al.*[96]

d. Proton–Carbon Couplings, $^3J_{\text{HOCC}}$.— These couplings had previously been little studied,[97,98] but have recently been investigated in detail by DFT and experimental NMR.[75] Using the same deoxy-aldohexopyranoside models already described for $^3J_{\text{HCOH}}$, Zhao *et al.* used DFT results (Fig. 5) to construct the equation:

$$^3J_{\text{C}-1,\text{HO}-2} = 4.10 - 2.72\cos\varphi + 5.01\cos 2\varphi \tag{53}$$

which was derived by averaging the coefficients obtained from three model structures.

Fitting of the DFT data for a fourth structure generated an equation containing somewhat smaller coefficients:

$$^3J_{\text{C}-1,\text{HO}-2} = 3.28 - 0.93\cos\varphi + 3.74\cos 2\varphi \tag{54}$$

This result was interpreted[75] in terms of the absence of a terminal, in-plane electronegative substituent in the fourth structure, as compared with the other three models, in each of which, the magnitude of $^3J_{\text{C-1,HO-2}}$ was enhanced by the presence of an in-plane O-1, or O-5. Calculations using the GAUSSIAN03 program indicated that non-FC contributions to $^3J_{\text{C-1,HO-2}}$ were negligible. The applicability of Eqs. (53) and (54) to similar coupling pathways was investigated for $^3J_{\text{C-2,HO-1}}$, $^3J_{\text{C-3,HO-2}}$, $^3J_{\text{C-5,HO-4}}$, and $^3J_{\text{C-1,HO-2}}$ in additional model structures, using only staggered H–O–C–C torsion angles. Consideration of the presence or absence of terminal in-plane electronegative substituent effects led to a further equation for pathways without these effects:

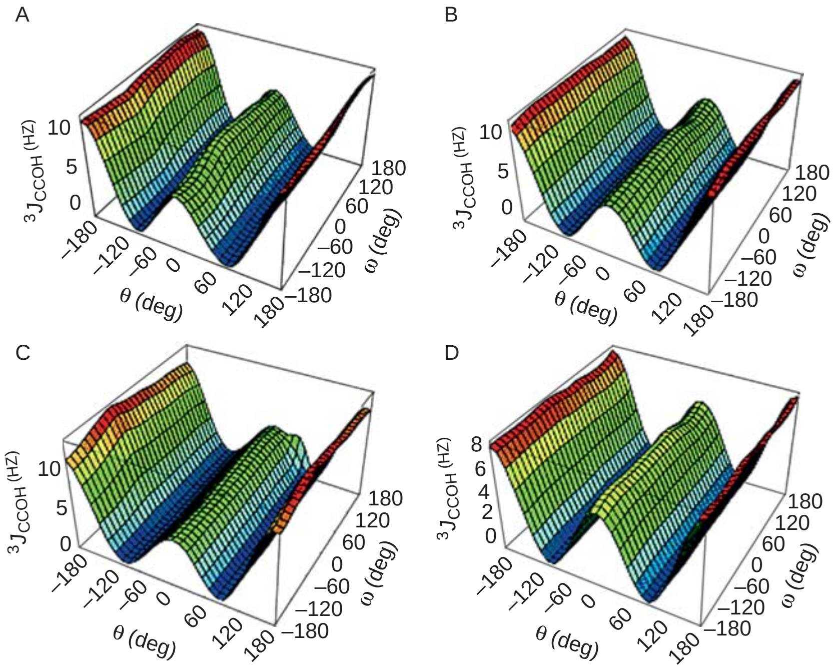

FIG. 5. Dependence of $^3J_{\text{C-1,HO-2}}$ on the glycosidic torsion angle ω and the C-1/HO-2 dihedral angle θ, as calculated by DFT for methyl α- and β-D-glucopyranoside mimics (curves (A) and (B), respectively) and. methyl α- and β-D-mannopyranoside mimics (curves (C) and (D), respectively), all having deoxy functions at C-3, C-4, and C-6. The curves display a strong dependence of $^3J_{\text{CCOH}}$ on θ, and a minimal dependency on ω.

$$^3J_{\text{HOCC}} = 3.49 - 1.41\cos\varphi + 4.18\cos 2\varphi \tag{55}$$

which on averaging with Eq. (54) gave

$$^3J_{\text{C}-1,\text{HO}-2} = 3.38 - 1.24\cos\varphi + 3.98\cos 2\varphi \tag{56}$$

Similar considerations for $^3J_{\text{C}-2,\text{HO}-1}$ led to non-symmetric equations (Fig. 3B) for specific configurations:

$$^3J_{\text{C}-2,\text{HO}-1}(\alpha-\text{Glc}) = 2.85 - 1.67\cos\varphi + 3.20\cos 2\varphi - 0.25\sin\varphi + 1.22\sin 2\varphi \tag{57}$$

$$^{3}J_{\mathrm{C-2,HO-1}}(\alpha-\mathrm{Man}) = 3.60 - 3.35\cos\varphi + 4.51\cos 2\varphi - 0.029\sin\varphi + 0.85\sin 2\varphi \tag{58}$$

$$^{3}J_{\mathrm{C-2,HO-1}}(\beta-\mathrm{Glc}) = 3.28 - 1.81\cos\varphi + 3.79\cos 2\varphi + 0.24\sin\varphi - 1.22\sin 2\varphi \tag{59}$$

$$^{3}J_{\mathrm{C-2,HO-1}}(\beta-\mathrm{Man}) = 3.39 - 1.31\cos\varphi + 4.08\cos 2\varphi - 0.26\sin\varphi - 0.98\sin 2\varphi \tag{60}$$

The latter two equations are very similar and were averaged[75] to give a combination:

$$^{3}J_{\mathrm{C-2,HO-1}}(\beta-\mathrm{Glc}/\beta-\mathrm{Man}) = 3.33 - 1.56\cos\varphi + 3.94\cos 2\varphi - 1.11\sin 2\varphi \tag{61}$$

$^{3}J_{\text{H-6R,HO-6}}$ and $^{3}J_{\text{H-6S,HO-6}}$ were calculated in GAUSSIAN03 by using appropriate torsion angles in a model structure, and the couplings were found to be consistent with Eq. (31). $^{3}J_{\text{C-5,HO-6}}$ values were found to be influenced by the O-5–C-5–C-6–O-6 and C-5–C-6–O-6–H torsion angles, and by the orientation of O-5. The computed couplings were consistent with Eq. (59) for *gg* and *gt* rotamers, and Eq. (53) for the *tg* rotamer.[75] $^{2}J_{\mathrm{HOC}}$ values were also examined, but were found to be small (-2 to -4 Hz), and showed non-systematic dependences on C–C and C–O torsion angles, suggesting that these couplings are not useful indicators of C–O conformation.[75]

3. Proton–Nitrogen Couplings

a. Proton–Nitrogen Couplings, $^{3}J_{\mathrm{HCCN}}$.— Coxon has measured the scalar ^{15}N–^{1}H NMR coupling constants of amino sugars over one to four bonds by three methods: (a) 1D ^{1}H NMR, (b) 1D and 2D ^{1}H–^{15}N HSQMBC[99,100] using an HCN cryoprobe,[66] and (c) 1D ^{1}H–^{15}N CPMG-HSQMBC[101] using a normal broadband probe. Method (a) was applied to organic-soluble, ^{15}N-substituted amino sugar derivatives synthesized by addition of phthalimide-^{15}N to carbohydrate epoxides,[74,102–103] method (b) to similar, unsubstituted derivatives, and method (c) to the 2-amino-2-deoxy-sugars common in biological systems, namely glucosamine, mannosamine, and galactosamine, as their *N*-acetyl and hydrochloride pyranose derivatives in D_2O and/or Me_2SO-d_6 solutions.[104] The precision of coupling constants measured by method (a) is probably better than ± 0.1 Hz, whereas methods (b) and (c) afford ± 0.3 Hz. The common amino sugars were usually present in the original crystal principally as a single pyranose anomer, either α or β, which underwent tautomeric interconversion to as many as four other forms on dissolution. The organic-soluble group included a number of aminodeoxy–hexopyranose derivatives that were conformationally restricted to chair, boat, or skew forms by the attachment of anhydro or 4,6-*O*-benzylidene rings.[74,102–103]

Dihedral angles φ_{HCCN} for the amino sugars were defined by molecular dynamics and mechanics calculations using either implicit solvent or explicit chloroform-*d*. Least-squares fitting of the angles of the organic-soluble derivatives in the range $\varphi_{\mathrm{HCCN}} = 10°–172°$, to experimental $^3J_{\mathrm{HCCN}}$ data with the assumption of positive values for the couplings allowed formulation[66] of a Karplus equation (Fig. 6) of the three-parameter type:

$$^3J_{\mathrm{HCCN}} = 3.1\cos^2\varphi - 0.6\cos\varphi + 0.4 \qquad (62)$$

However, because of the negative magnetogyric ratio of the ^{15}N nucleus, these couplings are likely to be negative, in which case Eq. (62) becomes

$$^3J_{\mathrm{HCCN}} = -3.1\cos^2\varphi + 0.6\cos\varphi - 0.4 \qquad (63)$$

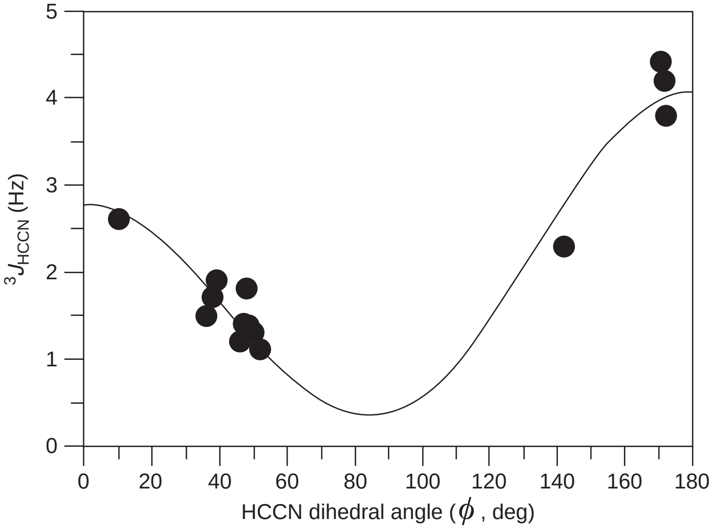

FIG. 6. Two-quadrant plot of Karplus equation $^3J_{\mathrm{HCCN}} = 3.1\cos^2\varphi - 0.6\cos\varphi + 0.4$ derived by fitting of experimental values of $^3J_{\mathrm{HCCN}}$ to the dihedral angle φ, with the assumption of positive values for $^3J_{\mathrm{HCCN}}$.

This equation (Fig. 7) is quite similar to the one developed[105] for ${}^3J_{\mathrm{HC\alpha C'N}}$ in peptides:

$$ {}^3J_{\mathrm{HC\alpha C'N}} = -4.6\cos^2\varphi + 3.0\cos\varphi + 0.8 \tag{64} $$

except that the magnitudes of the A, B, and C coefficients for the peptides appear to be enhanced by p-orbital contributions from the carbonyl group C′ in the coupling pathway.

The ${}^4C_1$ chair conformations of the water-soluble amino sugars that were defined by their ${}^3J_{\mathrm{HCCH}}$ values and molecular modeling provided a more restricted set of φ_{HCCN} angles (nominally 60° or 180°) than the conformationally limited, organic-soluble amino sugar derivatives. However, the ${}^3J_{\mathrm{HCCN}}$ values measured for the water-soluble ones are in reasonable agreement with Eq. (62). These couplings are potentially useful for characterization of amino sugar-containing, bacterial polysaccharides of interest in vaccine development, and for structural analysis of aminoglycoside antibiotics.

4. Phosphorus Couplings

a. Proton–Phosphorus Couplings, ${}^3J_{\mathrm{HCOP}}$ and Carbon–Phosphorus Couplings, ${}^3J_{\mathrm{CCOP}}$.— Reparametrized Karplus equations for these couplings were developed

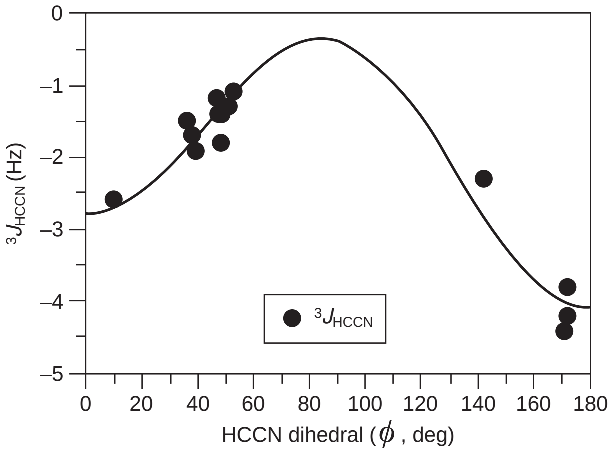

FIG. 7. Two-quadrant plot of Karplus equation ${}^3J_{\mathrm{HCCN}} = -3.1\cos^2\varphi + 0.6\cos\varphi - 0.4$ derived by fitting of experimental ${}^3J_{\mathrm{HCCN}}$ values to the dihedral angle φ, with the supposition of negative values for ${}^3J_{\mathrm{HCCN}}$.

simultaneously using a data set of 17 such couplings measured experimentally[106] for oligoribonucleotides:

$$^{3}J_{\mathrm{HCOP}} = 15.3\cos^2\varphi - 6.1\cos\varphi + 1.6 \tag{65}$$

$$^{3}J_{\mathrm{CCOP}} = 6.9\cos^2\varphi - 3.4\cos\varphi + 0.7 \tag{66}$$

The $^{3}J_{\mathrm{HCOP}}$ values were determined by direct extraction of splittings or by subtraction of the widths of multiplets in ^{31}P-decoupled, ^{1}H NMR spectra from those of the corresponding multiplets in ^{31}P-coupled spectra. $^{3}J_{\mathrm{CCOP}}$ values were measured directly from the ^{31}P splittings in ^{1}H-decoupled ^{13}C spectra. Other parametrizations had been developed earlier for these couplings, but were limited to one- or two-parameter equations by being based on too few values of the dihedral angle. For example, only parameters *A* and *B* in Eq. (3) could be derived from a data set containing only *J*(60) and *J*(180). These cases have been discussed in detail.[106] A study of the deoxyribonucleotide d(TpA), 3′,5′-cyclic AMP, and 3′,5′-cyclic dAMP showed that the different substitution of C-2′ in deoxyribonucleotides versus ribonucleotides does not change $^{3}J_{\mathrm{C\text{-}2'–C\text{-}3'–O\text{-}3'–P}}$ to a measurable extent, so that the same Karplus parameters may be used for such couplings in ribonucleotides and deoxyribonucleotides.[107] Backbone conformations of oligonucleotides have been characterized by six torsional angles, α, β, γ, δ, ε, and χ (Fig. 8), representing rotations about the P(*i*)–O-5′, O-5′–C-5′, C-5′–C-4′, C-4′–C-3′, C-3′–O-3′, and O-3′–P(*i*+1) bonds, respectively.[106] The results showed that the torsion angle $\varepsilon(t)$ of the trans conformer of right-handed ribo helices is confined to the range 214°–226°, the

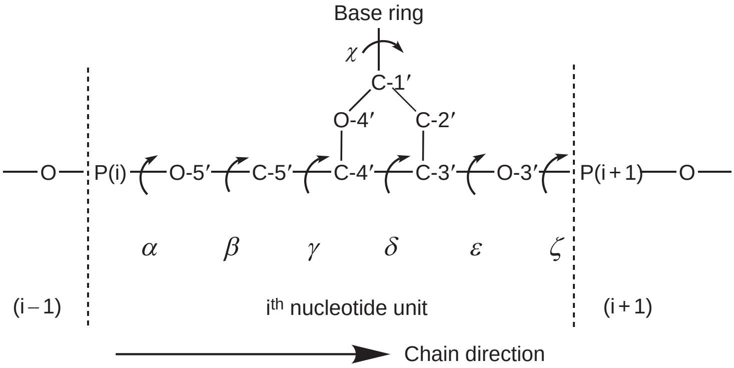

FIG. 8. Torsion angle descriptors α–ζ and χ for oligonucleotides.

average of which (219°) is in excellent agreement with the average value (218°) from single-crystal, X-ray studies, in contrast to that (208°) deduced from previous NMR data. Vicinal proton–phosphorus and carbon–phosphorus couplings have also been used to calculate the torsion angle ε (C-4′–C-3′–O-3′–P), in d(TpA), which was 195° in the trans conformer ε(*t*), and 261° in the gauche form ε(-). A two-state equilibrium of ε(*t*) and ε(-) was assumed in this study. Variable-temperature experiments demonstrated that the ε(*t*) form predominates at 1.5°–92 °C, and increases as the temperature is lowered.[107]

In an extension of this study to the oligodeoxynucleotides d(CT), d(CC), d(TA), d(AT), d(CG), d(GC), d(AG), d(AAA), d(TATA), and d(GGTAAT), the three coupling constants $^{3}J_{\text{C-4}'\text{–P}}$, $^{3}J_{\text{C-2}'\text{–P}}$, and $^{3}J_{\text{H-3}'\text{–P}}$ that are related to the backbone angle ε were analyzed in terms of a three-state equilibrium that took into account the N and S forms of the deoxyribose ring.[108] Depending on the N or S conformation of the deoxyribose ring, two ε(*t*) values occurred: ε(*t*, N) = 212° and ε(*t*, S) = 192°. The third rotamer was gauche and was associated exclusively with the S-type sugar ring, with the value ε(-, S) = 266°. Within experimental error, the magnitudes of these three angles were found to be independent of base sequence, with one exception: d(CG), which had ε(*t*, S) = 197°. Excellent agreement of the coupling constants was obtained with the three-state model, but poor agreement with a two-state analysis.[108]

Later, the application of more-sophisticated NMR experiments to a 10 base pair DNA duplex, uniformly ^{13}C,^{15}N-substituted in only one of the two strands was demonstrated:

$$\left[{}^{5'}\mathrm{G}_1\ \mathrm{G}_2\ \mathrm{C}_3\ \mathrm{A}_4\ \mathrm{A}_5\ \mathrm{A}_6\ \mathrm{A}_7\ \mathrm{C}_8\ \mathrm{G}_9\ \mathrm{G}_{10}\ -3'\right]\!-\mathrm{u}-{}^{13}\mathrm{C},\mathrm{u}-{}^{15}\mathrm{N}$$

$${}^{3'}\mathrm{C}_1\ \mathrm{C}_2\ \mathrm{G}_3\ \mathrm{T}_4\ \mathrm{T}_5\ \mathrm{T}_6\ \mathrm{T}_7\ \mathrm{G}_8\ \mathrm{C}_9\ \mathrm{C}_{10}\ -5'$$

Zimmer *et al.*[109] measured J_{HH} in the deoxyribose ring by 2D and 3D HCCH-E. COSY, J_{CH} couplings across the glycosidic torsion angle χ (see Fig. 8) by refocused HMBC, and $^{2}J_{\mathrm{CP}}$ and $^{3}J_{\mathrm{HP}}$ about the backbone torsion angle ε by a P-FIDS-CT-HSQC experiment. Using these experiments, a number of coupling constants in duplex DNA could be measured. Following the assumption by Lankhorst *et al.*[106] of trigonal projection symmetry about the ε torsion angle, their Karplus equations (Eqs. (65) and (66)) were expressed directly in terms of this angle:

$$^{3}J_{\mathrm{HCOP}} = 15.3\cos^2\,(\varepsilon + D) - 6.2\cos\,(\varepsilon + D) + 1.5, \quad \text{where } D = 120^\circ \tag{67}$$

$$^{3}J_{\mathrm{CCOP}} = 6.9\cos^2\,(\varepsilon + D) - 3.4\cos\,(\varepsilon + D) + 0.7, \quad \text{where } D = 0^\circ \tag{68}$$

A dependence of $^3J_{\text{H-3}',\text{P}}$ on position in the DNA sequence was noted, with the minimum value occurring at the 3′-end of the dA–dT tract.[109]

For the circular trinucleotide cr(GpGpGp), Mooren *et al.*[110] measured the value $^3J_{\text{C-4}'\text{–C-5}'\text{–O-5}'\text{–P}}$ 11.1 Hz, and similar values $^3J_{\text{C-4}'\text{–C-5}'\text{–O-5}'\text{–P}} = {}^3J_{\text{C-4}'\text{–C-3}'\text{–O-3}'\text{–P}} =$ 10.9 Hz had been observed earlier for the circular dinucleotide cd(ApAp). These large values did not fit the equations of Lankhorst *et al.*,[106] which were then reparametrized again according to 26 experimental calibration points based on dihedral angles obtained by molecular-mechanics energy minimization with the CHARMM force field.[110] The fitting of the coupling constant/dihedral angle pairs was achieved by least-squares optimization using a conjugate gradient minimization method, giving:

$$^3J_{\text{HCOP}} = 15.3\cos^2\varphi - 6.2\cos\varphi + 1.5 \tag{69}$$

$$^3J_{\text{CCOP}} = 8.0\cos^2\varphi - 3.4\cos\varphi + 0.5 \tag{70}$$

As expected, the main difference is in the A parameter (8.0 Hz) for $^3J_{\text{CCOP}}$, but since these equations were constructed in tandem, there is a small influence on $^3J_{\text{HCOP}}$. On the basis of this reparametrization,[110] seven equations were presented that related the populations of the β and γ conformers to the values of $^3J_{\text{H,P}}$ and $^3J_{\text{C,P}}$. It was recognized that the parametrization is a little weak in the 0°–60° region, as only one indirectly estimated value of $^3J_{\text{C,P}}$ was available, for $\varphi = 60°$.

The A, B, and C parameters were modified again by Plavec and Chattopadhyaya[111] based on 17 values of $^3J_{\text{C,P}}$ and the corresponding X-ray derived torsion angles for 3′,5′-cyclonucleotides, giving:

$$^3J_{\text{CCOP}} = 9.1\cos^2\varphi - 1.9\cos\varphi + 0.8 \tag{71}$$

Inclusion of the coupling constants of ‘‘strained’’ cyclonucleotides had been criticized earlier. Stating that the three-parameter Karplus equation applies only to a limited class of compounds, Plavec and Chattopadhyaya then accounted for the effects of the electronegativity of α-C and α-H attached to the second carbon atom of the CCOP pathway by constructing a five-parameter Karplus equation, according to the method used by Haasnoot and Altona for $^3J_{\text{HCCH}}$ (Eq. (9)). Least-squares, conjugate gradient minimization using 17 $^3J_{\text{C,P}}$ values, torsion angles, and electronegativities of α-substituents on the ‘‘middle’’ carbon yielded the equation:

$$^{3}J_{\mathrm{CCOP}} = 6.9\cos^{2}\varphi - 3.0\cos\varphi + 1.8 + \sum_{i=1,2}\Delta\chi_{i}\left[-3.2 + 6.2\cos^{2}\left(\xi_{i}\varphi + |\Delta\chi_{i}|\right)\right] \tag{72}$$

The first three terms describe the dependence of $^{3}J_{\mathrm{CCOP}}$ on torsion angle, whereas the summation term reflects the dependence on substituent electronegativity and its orientation. $\Delta\chi_i$ is the difference in electronegativity between the α-substituent and hydrogen on the Huggins scale and, as before, ξ is the ‘‘sign’’ parameter that takes values of +1 or −1, depending on the orientation of the substituent (see Fig. 2). $^{3}J_{\mathrm{CCOP}}$ input values were reproduced within $\Delta J \leq 0.4$ Hz, with an rms deviation of 0.2 Hz between experimental and back-calculated $^{3}J_{\mathrm{CCOP}}$ values. This deviation was slightly smaller than that achieved with the three-parameter Eq. (3), but it was acknowledged that a larger range of electronegativities and more data points are needed to give a more widely applicable relationship.[111]

5. Carbon–Carbon Couplings

Due to NMR sensitivity constraints, these coupling constants have most often been measured by use of selectively or uniformly ^{13}C-substituted compounds. The early, observational history of these couplings has been reviewed previously.[79] Sucrose and methyl α- and β-D-fructofuranoside have been prepared by chemical and/or enzymic methods with single sites of ^{13}C substitution at C-1, C-2, C-3, and C-6 of the fructofuranosyl rings.[112] Complete sets of $^{1}J_{\mathrm{CC}}$, $^{2}J_{\mathrm{CC}}$, and $^{3}J_{\mathrm{CC}}$ couplings constants were measured for sucrose and the methyl D-fructofuranosides by 1D ^{13}C NMR, with assistance from 1D ^{13}C INADEQUATE, for which various mixing times were used to observe selectively, carbon nuclei coupled to the ^{13}C-substituted site. Values for ^{13}C,^{1}H and ^{1}H,^{1}H couplings were also reported. The values of ^{13}C–^{1}H and ^{13}C–^{13}C couplings across the glycosidic linkage of sucrose suggested a ψ glycosidic torsion angle that was different from that in the crystal, although φ appeared to be similar.[112]

The signs of $^{3}J_{\text{C-1,C-6}}$ and $^{3}J_{\text{C-3,C-6}}$ coupling constants have been assumed to be positive and were used to determine the relative signs of $^{2}J_{\text{C-1,C-3}}$ and $^{2}J_{\text{C-1,C-5}}$ by application of a ^{13}C–^{13}C COSY-45 method to triply ^{13}C-substituted, D-aldopyranoses.[113] These sign determinations provided experimental confirmation of the relative signs of $^{2}J_{\mathrm{CCC}}$ and $^{2}J_{\mathrm{COC}}$ predicted by an empirical, projection resultant method.[114,115]

Xu and Bush measured the ${}^{2}J_{\mathrm{CC}}$ and ${}^{3}J_{\mathrm{CC}}$ coupling constants of a cell-wall lectin-receptor polysaccharide from *Streptococcus mitis* J22, uniformly substituted with ^{13}C to the extent of 96%.[116,117] The couplings were measured by 2D quantitative coherence transfer correlation spectroscopy,[118] the validity of which was confirmed by application of the method to the u-^{13}C-D-glucose growth precursor for the polysaccharide. The ${}^{2}J_{\mathrm{CC}}$ and ${}^{3}J_{\mathrm{CC}}$ values measured for the α and β anomers of the latter substrate were in good agreement with those reported by Serianni and coworkers, on the basis of direct, 1D ^{13}C NMR of single-site, ^{13}C-enriched glucoses.[119,120] Correlation of the ${}^{3}J_{\mathrm{CC}}$ couplings of the J22 polysaccharide was made by reference to the geometries of a three-conformation model determined by CHARMM molecular modeling.[117] Xu and Bush did not distinguish ${}^{3}J_{\mathrm{CCOC}}$ and ${}^{3}J_{\mathrm{CCCC}}$, but instead formulated[116] a combination equation:

$$ {}^{3}J_{\mathrm{CC}} = 2.24\cos^{2}\varphi - 1.3\cos\varphi + 0.5 \tag{73} $$

a. Carbon–Carbon Couplings, ${}^{3}J_{\mathrm{CCOC}}$.— Milton *et al.* synthesized ^{13}C-enriched α-Neu5Ac-(2→3)-β-Gal-(1→4)-Glc by enzymatic sialylation of a ^{13}C-enriched β-Gal-(1→4)-Glc acceptor using *Trypanosoma cruzi* trans-sialidase with *p*-nitrophenyl (u-^{13}C)Neu5Ac as a donor.[121] The ^{1}H NMR spectrum of this trisaccharide derivative is extremely complex because of substantial resonance overlap within a 0.4 ppm chemical-shift range, so that the interpretation of conventional 2D ^{1}H–^{1}H ROESY spectra is difficult. Therefore, the 3D ROESY-HSQC technique was used to separate the ROESY cross peaks according to their ^{13}C chemical shifts. This led to seven trans-glycosidic ROEs that were used in restrained MD with simulated annealing, using as input 10 pseudo-random geometries generated by a dynamical quenching procedure. Three families of structures that differed principally in the conformation about the α-Neu5Ac-(2→3)-Gal linkage resulted from the computations. The lowest-energy conformer in each family was selected as input for 5 ns restrained MD simulations *in vacuo*. Back calculation of theoretical ROEs from the global energy minimized MD simulation using a full relaxation matrix approach produced very good agreement with experiment.[121]

In this study, carbon–carbon coupling constants were found to be particularly valuable for additional validation of the predicted motional behavior, because only one ^{13}C–^{1}H coupling is available across the α-Neu5Ac-(2→3)-Gal linkage. Parametrization of the Karplus equation was implemented using only four ${}^{3}J_{\mathrm{CCOC}}/\varphi_{\mathrm{CCOC}}$ pairs, obtained from ^{13}C-substituted β-D-glucose (${}^{3}J_{\text{C-1–O-5–C-5–C-6}} = 3.8$ Hz/$\varphi = 180°$), methyl 4,6-*O*-(1-methylbenzylidene)-α-D-glucopyranoside, uniformly ^{13}C-substituted in the glucose moiety (${}^{3}J_{\text{Me–C–O-4–C-4}}$ 2.4 Hz/60°, ${}^{3}J_{\text{Me–C–O-6–C-6}}$ 1.9 Hz/60°), and (1-^{13}C)-1,6-anhydro-2,3-*O*-isopropylidene-β-D-mannopyranose (${}^{3}J_{\text{C-1–C-2–O-2–C-7}}$ 0.6 Hz/109°, the latter dihedral angle being determined from a crystal structure). Fitting of these data to the three-parameter Eq. (3) yielded[121] the equation:

$$^{3}J_{\mathrm{CCOC}} = 4.4\cos^{2}\varphi + 1.1\cos\varphi + 0.5 \tag{74}$$

which was thought to be semi-quantitative at best, due to the limited number of data points, and neglect of electronegativity effects.[121] Because α-Neu5Ac-(2→3)-β-Gal-(1→4)-Glc suffers from poor spectral dispersion in critical regions of its ^{13}C spectrum, 3D LRCC was used to measure six values of $^{3}J_{\mathrm{CCOC}}$ for the trisaccharide, which agreed very well with those calculated for the MD-simulated structure by use of Eq. (74). Two trans-glycosidic values of $^{3}J_{\mathrm{HCOC}}$ were also measured for the trisaccharide by heteronuclear, CT COSY and were in excellent agreement with those calculated using the equations of Tvaroŝka *et al.*[81] and Mulloy *et al.*[82] (Eqs. (36) and (37), respectively).

In a comprehensive study, Bose *et al.*[122] synthesized a large number of aldose derivatives selectively substituted with ^{13}C at C-1 or C-6, and ketoses similarly substituted at C-1, C-2, C-3, C-4, C-5, or C-6. Various ^{13}C–^{13}C coupling constants were measured for these derivatives by 1D ^{13}C/^{1}H decoupled NMR at 151/600 MHz. Many of the couplings were also calculated by DFT methods and were found to be mostly in close agreement with the experimental values, although some significant deviations (14%) of $^{1}J_{\text{C-1,C-2}}$ values were thought to be due to such possible limitations in the theoretical method as (a) the appropriateness of the functional procedure adopted, (b) the incompleteness of the chosen basis set, and (c) the omission of solvent effects from the computation. The types of coupling pathways were analyzed in detail, including such multiple pathways as $^{3+3}J_{\text{C-1,C-4}}$ and $^{3+3}J_{\text{C-2,C-5}}$, which in most ring configurations are observed to be very small or zero, leading to the conclusion that the coupling along each constituent pathway in these cases must be small or zero.[122] Dihedral angles for the atoms of interest were derived from geometrical optimizations using a modified GAUSSIAN94 program, with the B3LYP functional, and 6–31G basis set. Many of the aldo- and keto-pyranoses contained only φ_{CCOC} dihedral angles of ~180°, and so data for other values of φ_{CCOC} were measured or compiled from methyl 3,6-anhydro-α- and β-D-(1–^{13}C)glucopyranosides (~45°), methyl β-D-ribofuranoside (*ab initio* MO gave $\varphi_{\text{C-1–O-4–C-4–C-3}}$ ~123° for both forms), α-D-*erythro*- and -*threo*-2-pentulofuranoses ($\varphi_{\text{C-1–C-2–O-5–C-5}}$ ~154°), methyl α- and β-D-fructofuranosides ($\varphi_{\text{C-1–C-2–O-5–C-5}}$ ~164° and ~156° in the respective South (E_2) and North (^{2}E) conformations of these anomers), and sucrose, in which the $^{4}T_{3}$ form of the β-D-fructofuranosyl ring has $\varphi_{\text{C-1–C-2–O-5–C-5}} = \varphi_{\text{C-2–O-5–C-5–C-6}}$ ~133° in the crystalline state.[122] Theoretical calculations of coupling constants were also performed for three structural models, including one for a disaccharide as a function of the interglycosidic angle ψ. Careful attention was paid to the effects of rotameric populations about the C-1–O-1, O-1–C-4′, and C-5–C-6 bonds in the models.

An important result from this study was that the $^3J_{\mathrm{CCOC}}$ coupling constant is influenced by geometrical factors in addition to dihedral angle, the most critical being the orientation of terminal electronegative substituents on the coupling pathway.[122] For example, for HO–C–C–O–C–OH pathways, the magnitude of coupling between the terminal carbon nuclei is enhanced when the terminal oxygen atoms lie in the C–C–O–C plane ($\varphi_{\mathrm{CCOC}} = 180°$). Similar effects were observed for $\varphi_{\mathrm{CCOC}} = 60°$ when the terminal oxygen was in-plane (HO–C–O–C or O–C–C–OH plane). Out-of-plane terminal oxygen substituents and oxygen substituents on internal carbon atoms appeared to exert little effect on the magnitude of the coupling. For example, $^3J_{\mathrm{CC}}$ in a H_3C–C–O–C–OH was found to be virtually identical to $^3J_{\mathrm{CC}}$ in a HO–H_2C–C–O–C–OH pathway, when the hydroxymethyl oxygen atom in the latter moiety was oriented outside the C–C–O–C plane.[122] Similar phenomena had been reported earlier by Marshall *et al.* for $^3J_{\mathrm{CCCC}}$ couplings in C–C–C–CH_2OH pathways in butanol derivatives, although the effect of terminal substitution for eclipsed C–C–C–C fragments appeared to be smaller than expected from theoretical considerations.[123]

By excluding $^3J_{\text{C-1,C-6}}$ in ketopyranoses and also couplings enhanced by in-plane oxygen atoms, least-squares fitting of the $^3J_{\mathrm{CCOC}}$ data yielded the equation:

$$^3J_{\mathrm{CCOC}} = 3.70\cos^2\varphi + 0.18\cos\varphi + 0.11 \tag{75}$$

This equation yields a larger $^3J_{\mathrm{CCOC}}$ value for $\varphi = 0°$ than for $\varphi = \pm 180°$, which mirrors the behavior suggested for $^3J_{\mathrm{CCCC}}$ in HO–CH_2–C–C–C pathways,[123,124] with couplings of 3.5–6 Hz expected[122] for $\varphi_{\mathrm{CCOC}} = 0°$ and 2–4 Hz for $\varphi_{\mathrm{CCOC}} = 180°$. In most Karplus equations of the three-parameter type, the *B* coefficient (of the cosφ term) for positive coupling constants is negative, which leads to an increased value of the coupling for $\varphi = 180°$ over that for $\varphi = 0°$. Because of this anomaly and the paucity of data for $\varphi < 100°$, as an afterthought, Bose *et al.*[122] excluded the cos φ term from Eq. (75) and refitted their data to give a simplified equation:

$$^3J_{\mathrm{CCOC}} = 3.49\cos^2\varphi + 0.16 \tag{76}$$

which they stated was better supported by the available data, and which corresponds to identical maxima for $\varphi = 0°$ and 180°. It was pointed out that $^3J_{\text{C-1,C-6}}$ values in aldohexopyranosyl and ketohexopyranosyl rings do not obey the same Karplus relationship, that for the latter rings appearing to have decreased amplitude.[122]

The shortage of experimental data for $\varphi_{\mathrm{CCOC}} < 100°$ was soon addressed by a purely theoretical study of the four β-(1→4)-linked disaccharide mimics mentioned earlier.[84]

DFT-calculated $^3J_{\mathrm{CCOC}}$ couplings for φ_{CCOC} 0°–100°, together with geometries calculated likewise, suggested that the first Eq. (75) may be the more accurate relationship, namely, one where the couplings at $\varphi_{\mathrm{CCOC}} = 0°$ are somewhat larger than those at $\varphi_{\mathrm{CCOC}} = 180°$, at least in the absence of an in-plane electronegative substituent effect.[84] The latter effect was considered to be significant for the C-1–O-1–C-4′–C-5′ coupling pathway, where for some linkage geometries, O-5′ lies in the plane of this pathway. This led to the development of three parametrizations by least-squares fitting of the theoretically calculated coupling constants and geometries.[84] One used only $^3J_{\mathrm{C\text{-}1,C\text{-}5'}}$ data (Eq. (77)), another used just $^3J_{\mathrm{C\text{-}1,C\text{-}3'}}$ and $^3J_{\mathrm{C\text{-}2,C\text{-}4'}}$ (Eq. (78)), and one more employed all coupling data (Eq. (79)).

$$^3J_{\mathrm{CCOC}} = 6.17\cos^2\varphi - 0.51\cos\varphi + 0.30 \tag{77}$$

$$^3J_{\mathrm{CCOC}} = 4.96\cos^2\varphi + 0.63\cos\varphi - 0.01 \tag{78}$$

$$^3J_{\mathrm{CCOC}} = 4.96\cos^2\varphi + 0.52\cos\varphi + 0.18 \tag{79}$$

Interestingly, the first Eq. (77) contains a sign reversal for the *B* coefficient, which would indicate that for a possible in-plane oxygen atom, the coupling for $\varphi_{\mathrm{CCOC}} = 180°$ would be larger than that for $\varphi_{\mathrm{CCOC}} = 0°$.

Recent preliminary DFT calculations have shown that the two trans-glycosidic $^3J_{\mathrm{CCOC}}$ couplings in oligosaccharide linkages are not equivalent.[125] By using the GAUSSIAN03 program with structures that modeled the glycosidic linkage, Zhao *et al.* demonstrated that internal electronegative substituents in the coupling pathway cause a −15° phase shift of the Karplus curve (Fig. 9), so that the maximum coupling occurs at 165° instead of at 180°. This effect will need to be considered in the evaluation of linkage geometries by quantitative interpretation of $^3J_{\mathrm{CCOC}}$.[125]

Six spin-coupling pathways are subtended by typical glycosidic linkages, and in the structural analysis of oligo- and poly-saccharides, it would clearly be advantageous to use as many of these coupling constants as possible for the definition of molecular geometry, particularly in view of the limited number of NOEs observed in these systems.

b. Carbon–Carbon Couplings, $^3J_{\mathrm{CCCC}}$.— Early observations of the $^3J_{\mathrm{CCCC}}$ couplings of carbohydrates have been summarized previously.[79] The experimental determination and theoretical interpretation of such couplings in alicyclic compounds have been studied extensively by Barfield, Marshall, and coworkers.[123,124,126–129] For example, VB and MO studies of ^{13}C-substituted, 1-substituted butyl derivatives,

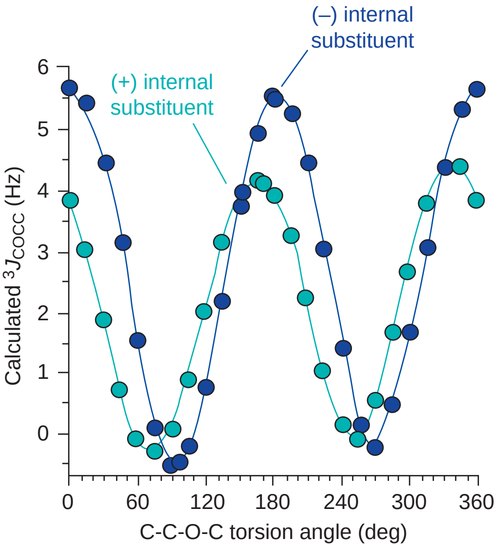

FIG. 9. Four-quadrant plots of DFT results for an ethyl β-D-glucopyranoside mimic of a disaccharide, showing phase shifting of $^3J_{CCOC}$ Karplus curves for C–C–O–C coupling pathways bearing an internal electronegative substituent. The mimic has deoxy functions at C-3, C-4, and C-6.

11-substituted 1-methyladamantane compounds, and methylcyclohexane indicated that a large number of direct (electron-mediated) and indirect coupling pathways contribute to vicinal $^{13}C–^{13}C$ coupling constants. The calculated Fermi-contact contributions for trans arrangements of carbon atoms in butane, methylcyclohexane, and 1-methyladamantane being 4.27, 3.72, and 3.32 Hz, respectively.[128,129] Coincidentally, the monotonic decrease in the magnitude of the coupling constant was found to parallel the increase in the number of impinging rear orbital lobes on carbon, the effect of which, may however, be small, and the observed decrease may be related to an increasing number of β methylene substituents in these systems.[131] With a cautionary note, Barfield *et al.*[128] suggested the equation:

$$^3J_{CCCC} = 5.00\cos^2\varphi - 1.58\cos\varphi + 0.31 \tag{80}$$

on the basis of INDO-FPT calculations with a number of overlap integrals set to zero. The *A* coefficient of this equation is very similar to that in Eq. (79) of Cloran *et al.*[84] for $^3J_{CCOC}$. According to a VB bond-order formulation of Barfield *et al.*,[128] there is a connection between $^3J_{\mathrm{CCCC}}$ and ^{1}H–^{1}H coupling constants that is not implied by any of the foregoing Karplus equations. Consideration of the direct and indirect contributions to $^3J_{\mathrm{CCCC}}$ in the all-trans arrangement in butane led to a 16-term expression,[128] containing one term that corresponded to $^3J_{\mathrm{HCCH}}$, six to long-range ^{1}H–^{1}H coupling over four bonds, and nine terms to long-range coupling over five bonds

$$\begin{aligned}{}^3J_{\mathrm{CCCC}}(\varphi) = {} & (K/K')[{}^3J_{\mathrm{HH'}}(\varphi) - {}^4J_{\mathrm{HH'}}(60°, \varphi) - {}^4J_{\mathrm{HH'}}(180°, \varphi) - {}^4J_{\mathrm{HH'}}(300°, \varphi) \\ & - {}^4J_{\mathrm{HH'}}(\varphi, 60°) - {}^4J_{\mathrm{HH'}}(\varphi, 180°) - {}^4J_{\mathrm{HH'}}(\varphi, 300°) + {}^5J_{\mathrm{HH'}}(60°, \varphi, 60°) \\ & + {}^5J_{\mathrm{HH'}}(60°, \varphi, 180°) + {}^5J_{\mathrm{HH'}}(60°, \varphi, 300°) + {}^5J_{\mathrm{HH'}}(180°, \varphi, 60°) \\ & + {}^5J_{\mathrm{HH'}}(180°, \varphi, 180°) + {}^5J_{\mathrm{HH'}}(180°, \varphi, 300°) + {}^5J_{\mathrm{HH'}}(300°, \varphi, 60°) \\ & + {}^5J_{\mathrm{HH'}}(300°, \varphi, 180°) + {}^5J_{\mathrm{HH'}}(300°, \varphi, 300°)] \end{aligned} \tag{81}$$

where φ is the dihedral angle about the C-2–C-3 bond in butane, and the fixed values of the angles in parentheses are the dihedral angles around the C-1–C-2 and C-3–C-4 bonds. This type of relationship has never been explored in carbohydrate chemistry, perhaps because of its complexity. In most studies of sugars, homo- and heteronuclear coupling constants have been considered in isolation.

Multiple coupling pathways are important for vicinal ^{13}C–^{13}C couplings in sugars (for example, $^{3+3}J_{\text{C-1–C-4}}$ and $^{3+3}J_{\text{C-2–C-5}}$), and in relevant work on dual-path couplings $^{2+3}J_{\mathrm{CCCC}}$ in ^{13}C-substituted 1-methylcyclopentanol, 1-methylcyclopentene, and polycyclic hydrocarbons, it has been proposed that the individual contributions of such pathways are algebraically additive, that is, the sum must take into account the relative signs of the couplings.[130] Evidently, the resultant of two simultaneous coupling pathways can be unexpectedly large, or anomalously small, as in the $^{3+3}J_{\text{C-1–C-4}}$ values of many aldohexopyranoses.[122]

Berger measured the $^3J_{\mathrm{CCCC}}$ values of 22 compounds, including ^{13}C-substituted derivatives of adamantane, bicyclo[2.2.2]octanes, bicyclo[3.2.1]octanes, *cis*-bicyclo [3.2.0]octanes, and bicyclo[2.2.1]heptanes, and fitted the values to ideal angles of 0°, 60°, 90°, 120°, and 180° that were close to angles obtained from force-field calculations, or from X-ray structure determinations.[132] His experimentally determined equation was determined by use of the additivity principle, if there was more than one pathway, giving

$$^3J_{\mathrm{CCCC}} = 1.67 + 0.176 \cos\varphi + 2.24 \cos 2\varphi \tag{82}$$

which may be rewritten as

$$^{3}J_{\mathrm{CCCC}} = 4.48\cos^{2}\varphi + 0.176\cos\varphi - 0.57 \tag{83}$$

Equation (82) was compared with one obtained from a different set of Barfield's theoretical data:

$$^{3}J_{\mathrm{CCCC}} = 2.73 + 0.579\cos\varphi + 2.17\cos 2\varphi \tag{84}$$

which can be reformulated as the alternative:

$$^{3}J_{\mathrm{CCCC}} = 4.34\cos^{2}\varphi + 0.579\cos\varphi + 0.56 \tag{85}$$

The agreement between experimental data and INDO-calculated couplings was thought to be rather good, within the error limits for both.[132]

$^{3}J_{\mathrm{CCCC}}$ values have been measured for the bicyclic monoterpenes, 3-carene, α-pinene, and camphene by selective 1D INADEQUATE, with ^{13}C at natural abundance, but the agreement between experimental data and the results of SCPT-INDO calculations was not satifactory.[133]

Wu *et al.* synthesized eight aldohexoses, four aldopentoses, and two aldotetroses, all substituted with ^{13}C at the terminal hydroxymethyl carbon atom.[120] Interpretation of the ^{13}C NMR spectra measured at 75 and 125 MHz was assisted by 1D INADEQUATE ^{13}C spectra, which can sometimes alleviate problems of spectral overlap, and enhance the detection of small ^{13}C–^{13}C couplings.[120] In the aldohexopyranoses, the dihedral angle $\varphi_{\text{C-3–C-4–C-5–C-6}}$ has a relatively fixed value of ~180°, and, therefore, these compounds provide a good model for the study of substituent effects along the coupling pathway. On the other hand, the interior dihedral angles of the pyranose ring are ~60°, thus offering alternative angles for studies of the angular dependence of $^{3}J_{\mathrm{CCCC}}$ (and $^{3}J_{\mathrm{CCOC}}$). The results of this study for $^{3}J_{\mathrm{CCCC}}$ mirror those obtained for $^{3}J_{\mathrm{CCOC}}$. Coupling is maximal when O-3 and O-4 are equatorial (3.6–4.4 Hz in glucopyranoses and mannopyranoses) or when O-3 is equatorial and O-4 is axial (3.4–4.1 Hz in galactopyranoses and talopyranoses), and minimal when these substituents are axial (1.8 Hz in gulopyranoses). Intermediate values were observed when O-3 is axial and O-4 equatorial (2.6–3.0 Hz in allopyranoses and β-altropyranose). Therefore, $^{3}J_{\text{C-3,C-6}}$ values may differ by a factor of 2 for coupled carbon nuclei having the same 180° dihedral angle, depending on the configuration of the hydroxyl groups attached to the terminal and intervening carbon atoms in the coupling pathway.[120] In the pentopyranoses, $^{3+3}J_{\text{C-2,C-5}}$ coupling (1.8 Hz) was observed in only one example,[120] behavior that is similar to that of $^{3+3}J_{\text{C-1,C-4}}$ in the aldohexopyranoses.[122]

An elaborate experimental and theoretical study of $^3J_{\mathrm{CCCC}}$ and many related coupling constants has recently been carried out. Thibaudeau *et al.*[134] prepared methyl α- and β-pyranosides of D-glucose and D-galactose containing single ^{13}C atoms at C-4, C-5, and C-6 (12 compounds) and measured complete sets of ^1J, ^2J, and ^3J couplings between the ^{13}C-substituted carbon, and nearby protons and carbons within the exocyclic hydroxymethyl group.[134] At the same time, these couplings were also computed by DFT methods by using a special basis set to obtain reliable Fermi-contact contributions. Complete hypersurfaces were calculated for $^1J_{\text{C-5,C-6}}$, $^2J_{\text{C-5,H-6R}}$, $^2J_{\text{C-5,H-6S}}$, $^2J_{\text{H-5,C-6}}$, $^2J_{\text{C-4,C-6}}$, $^3J_{\text{C-4,H-6R}}$, $^3J_{\text{C-4,H-6S}}$, $^3J_{\text{H-4,C-6}}$, $^2J_{\text{H-6R,H-6S}}$, $^3J_{\text{H-5,H-6R}}$, and $^3J_{\text{H-5,H-6S}}$.

The results were used to parametrize new equations correlating these couplings with the C-5–C-6 and C-6–O-6 dihedral angles ω and θ, respectively. Couplings computed by DFT were also tested by measuring them experimentally for ^{13}C-substituted 4,6-*O*-ethylidene derivatives of D-glucose and D-galactose, in which the values of ω and θ were constrained. Effects of substituents were also assessed by using DFT calculations for tetrahydropyran models containing a hydroxymethyl group, or this group plus a vicinal hydroxyl group in either an axial or an equatorial orientation. Favored rotamer populations about ω and θ in the methyl glycosides just mentioned were determined by use of a new computer program, CHYMESA, which was designed to analyze multiple *J*-couplings sensitive to exocyclic CH$_2$OH conformation. Due to the sensitivity of some couplings, especially $^2J_{\text{H-6R,H-6S}}$, $^2J_{\text{C-5,H-6R}}$, and $^2J_{\text{C-5,H-6S}}$ to both ω and θ, important information on correlated conformation about both torsion angles was obtained, which provides a method of evaluating such conformations in (1→6)-linked oligosaccharides, since ψ and θ are identical in these linkages.[134] The new equations for vicinal coupling constants included:

$$^3J_{\mathrm{C-4,H-6R}} = 3.58 + 0.11\cos\omega + 3.5\cos 2\omega + 0.35\,\sin\omega - 0.57\,\sin 2\omega \tag{86}$$

$$^3J_{\mathrm{C-4,H-6S}} = 3.60 + 0.50\cos\omega + 0.06\cos 2\omega + 0.13\,\sin\omega - 3.46\,\sin 2\omega \tag{87}$$

but several other equations reflecting the dependence of two-bond C–C and C–H couplings on the orientation of the hydroxymethyl gtoup were also developed. Both $^3J_{\text{C-4,H-6R}}$ and $^3J_{\text{C-4,H-6S}}$ display a Karplus dependence, as expected, but the curves are mutually phase-shifted by ~20°. Based on the good agreement between experimental and computed couplings, it was concluded that DFT provides an almost quantitative tool for the calculation of J_{HH}, J_{CH}, and J_{CC} values in saccharides, without the use of empirical scaling adjustments.[134]

V. OTHER TYPES OF VICINAL COUPLINGS

1. Fluorine Couplings

a. Proton–Fluorine Couplings, $^3J_{HCCF}$.— Studies of the dependence of $^3J_{HCCF}$ couplings on electronegativity have been a subject in their own right. Hall and Jones measured $^3J_{HCCF}$ for 16 geometrically constrained 1,2-disubstituted, fluorohaloacenaphthene derivatives, and, contrary to expectations based on $^3J_{HCCH}$, found that plots of the couplings against Huggins electronegativity values were described better by an exponential relationship than by a linear one.[135] Also, the dependences of cis and trans couplings were quite different,[135] according to

$$^3J_{HCCF}(\text{cis}) = 87.75\ \exp(-0.2522) \tag{88}$$

$$^3J_{HCCF}(\text{trans}) = 985.68\ \exp(-0.8749) \tag{89}$$

However, Hamman *et al.*[136] analyzed the rotameric populations of 2-fluoro-1,2-disubstituted ethanes and found that transoid $^3J_{HCCH}$ and $^3J_{HCCF}$ couplings could be described by linear fits

$$^3J_{HCCH}(\text{trans}) = 15.0 - 0.77\sum(\Delta\chi) \tag{90}$$

$$^3J_{HCCF}(\text{trans}) = 65.75 - 7.52\sum(\Delta\chi) \tag{91}$$

whereas $^3J_{HCCF}$ (gauche) displayed an exponential fit

$$^3J_{HCCF}(\text{gauche}) = 15.35\ \exp\left[-0.266\sum(\Delta\chi)\right] \tag{92}$$

where $\Sigma(\Delta\chi)$ is the sum of the differences in Huggins electronegativity between hydrogen and the six atoms or groups on the HCCF fragment.[136]

An elaborate study of the dependence of $^3J_{HCCF}$ on molecular properties was conducted by Thibaudeau *et al.*[137] who also summarized the early history of these couplings in which the three-parameter Karplus equation was used to describe the couplings. By using experimental values of $^3J_{HCCH}$ in the Haasnoot–Altona equation, these authors calculated the corresponding ^{1}H–^{1}H torsion angles, from which endocyclic torsion angles v_0–v_4 were obtained from a detailed analysis of the temperature-dependent North–South equilibria of the pentofuranose rings in 11 monofluorinated nucleosides, by use of the PSEUROT program.[137] The equilibria were used to calculate the phase angle and pucker values that characterized the major conformers. These values were used to calculate the proton–fluorine torsion angle φ_{HF} from the linear relationship

$$\varphi_{\mathrm{HF}} = A_{\mathrm{F}} v_j + B_{\mathrm{F}} \tag{93}$$

where $j = 0$–4, and the A_{F} and B_{F} parameters were obtained from a series of *ab initio* geometry optimizations on eight of the monofluorinated nucleosides, by means of the GAUSSIAN94 program at the HF/3–21G level.[137] Values of $^3J_{\mathrm{HCCF}}$ were measured for the nucleosides by 1D ^{1}H NMR, and the values were supplemented by literature values for four fluorocyclohexane derivatives, six geometrically constrained fluorobicycloalkanes, and a fluoro-*cis*-decalin, giving a data set of 57 $^3J_{\mathrm{HCCF}}/\varphi_{\mathrm{HF}}$ pairs. This data set could not readily be fitted to a Karplus equation of the three-parameter type, nor could an accurate fit to a six-parameter, generalized Haasnoot–Altona equation be achieved. Finally, the introduction of bond-angle terms a_{FCC} and a_{HCC} led to a seven-parameter equation:

$$\begin{aligned} {}^3J_{\mathrm{HCCF}} = {} & 40.61\cos^2\varphi - 4.22\cos\varphi + 5.88 \\ & + \sum \lambda_i[-1.27 - 6.20\cos^2(\xi_i\varphi + 0.20\lambda_i)] \\ & - 3.72[(a_{\mathrm{FCC}} + a_{\mathrm{HCC}})/2 - 110]\cos^2\varphi \end{aligned} \tag{94}$$

The difference between experimental and back-calculated $^3J_{\mathrm{HCCF}}$ values was $<$2.9 Hz, with an overall rms deviation of 1.38 Hz. Graphical analysis of the conformational preferences of the 11 fluronucleosides indicated that the use of $^3J_{\mathrm{HCCF}}$ and $^3J_{\mathrm{HCCH}}$ values gave qualitatively similar results. These two types of coupling constants were combined in a modified version of the PSEUROT program: PSEUROT + J_{HF} in which $^3J_{\mathrm{HCCH}}$ values can be used alone or in combination with $^3J_{\mathrm{HCCF}}$. The application of the seven-parameter Eq. (94) in conjunction with the PSEUROT + J_{HF} program was tested further on two more fluoronucleosides, on four difluorinated nucleosides, and on a fluoro-*trans*-decalin derivative, giving reasonable results in each case.[137]

b. Proton–Fluorine Couplings, $^3J_{\mathrm{HCNF}}$ and $^4J_{\mathrm{HCC'NF}}$.— As models for peptides, Hammer and Chandrasegaran[138] synthesized a series of nine *N*-fluoroamide derivatives by reaction of trifluoromethyl hypofluorite with the corresponding amides and measured their $^3J_{\mathrm{HCNF}}$ values by 1D ^{1}H and ^{19}F NMR. However, the observation of $^3J_{\mathrm{HCNF}} < 5$ Hz in the ^{19}F NMR spectra was not feasible, because of quadrupolar broadening by the ^{14}N nucleus. The compounds were chosen partly for their rigidity (as in four bicycloalkanes), expected dihedral angles, or ease of preparation. Dihedral angles were taken either from X-ray data for NH analogs, or with the assumption of a planar amide group, were estimated from ''carefully straightened'' Dreiding models, with a suggested accuracy of ±5°. Nonlinear, least-squares fitting of the coupling constants using the MLAB implementation of the PROPHET program yielded[138] the equation:

$$^{3}J_{\mathrm{HCNF}} = 70.8\cos^{2}\varphi - 44.1\cos\varphi - 7.2 \tag{95}$$

In these *N*-fluoroamides, the coupling pathway differs from those previously discussed in that it contains an sp^2-hybridized carbonyl carbon atom, which may enhance the magnitude of the coupling. The shape of the fitted curve is highly skewed, apparently reflecting the fact that the values estimated for $^{3}J_{\mathrm{HCNF}}$ (180°) are approximately five times as large as those measured for $^{3}J_{\mathrm{HCNF}}$ (0°), thus producing comparable values of the *A* and *B* constants.[138] By using similar methods, this study also yielded a Karplus equation for $^{4}J_{\mathrm{HCC'NF}}$:

$$^{4}J_{\mathrm{HCC'NF}} = -19.5\cos^{2}\psi + 8.8\cos\psi + 4.9 \tag{96}$$

where ψ is the dihedral angle about the C–C′ (C$_\alpha$–CO) bond. Presumably, only one torsion angle is required to describe this four-bond coupling, because of restricted rotation about the amide bond. The best fit to the experimental data generated a highly skewed, inverted Karplus curve in which $^{4}J_{\mathrm{HCC'NF}} = \sim -5$ Hz for $\psi = 0°$ and $^{4}J_{\mathrm{HCC'NF}} = \sim -23$ Hz for $\psi = 180°$, with the curve crossing zero twice.[138]

c. Carbon–Fluorine Couplings, $^{3}J_{\mathrm{CCCF}}$ and $^{3}J_{\mathrm{COCF}}$.— In a study of glycosyl fluorides, Bock and Pedersen found evidence of a Karplus dependence of $^{3}J_{\mathrm{CCCF}}$, since the $^{3}J_{\mathrm{C\text{-}3,F\text{-}1}}$ values (4–10 Hz) of β-pyranosyl fluorides in which C-3 and F-1 are trans are larger than those (0–6 Hz) of the α-fluorides, in which these coupling nuclei are gauche.[139] However, the same could not be said for $^{3}J_{\mathrm{COCF}}$, because in all pyranosyl fluorides, $^{3}J_{\mathrm{C\text{-}5,F\text{-}1}}$ was found to be in the range 2–5 Hz, regardless of anomeric configuration.[139] Additional examples of the $^{3}J_{\mathrm{CF}}$ couplings of fluorinated carbohydrates have been reviewed.[140]

d. Fluorine–Fluorine Couplings, $^{3}J_{\mathrm{FCCF}}$.— These couplings have been found not to obey a simple dependence on dihedral angle, as noted by Hall *et al.* on the basis of measurements on the anomeric 3,4,6-tri-*O*-acetyl-2-deoxy-2-fluoro-D-gluco- and D-manno-pyranosyl fluorides, and 7,7,8-trifluoro-2(3),5(6)-dibenzobicyclo[2.2.2] octane and its 7-chloro derivative.[141] Thus, approximate ^{19}F–^{19}F dihedral angles of 0°, 60°, 120°, and 180° showed $^3J_{\mathrm{FCCF}}$ values in the ranges $+9.4$ to $+11.4$, -13.5 to -18.8, -1.2 to -2.2, and -20.0 Hz, respectively. The reversal in sign was unexpected, and various attempts have been made to explain these and similar observations theoretically. Kurtkaya *et al.*[142] performed DFT computations for 1,2-difluoroethane in which the four Ramsey contributions, Fermi contact, spin–dipolar, diamagnetic spin–orbit, and paramagnetic spin–orbit to the spin coupling were characterized separately. The positive region of the curve from 0° to 40° was determined by a Fermi-contact term, but the negative section from 40° to 180° originated from reinforcing negative Fermi-contact and paramagnetic spin–orbit terms. More importantly, the Fermi-contact term in the range 90°–180° was found to contain an extremely strong negative contribution from the three non-bonded lone pairs of electrons on the fluorine atoms.[142]

Various theoretical treatments, including DFT and two high-level *ab initio* methods, MCSCF and SOPPA, have been tested recently by San Fabián and Westra Hoekzema.[143] These authors represented contributions to the angular dependence of $^3J_{\mathrm{FCCF}}$ in 1,2-difluoroethane by a truncated Fourier series:

$$^3J_{\mathrm{FCCF}} = C_0 + \sum_{n=1}^{m} (C_n \cos n\varphi) \tag{97}$$

where this general expression could be used to describe either the total contributions or any of the component Fermi contact, spin–dipolar, diamagnetic spin–orbit, or paramagnetic spin–orbit terms. Owing to the symmetry in unsubstituted 1,2-difluoroethane, $^3J_{\mathrm{FCCF}}\,(+\varphi) = {}^3J_{\mathrm{FCCF}}\,(-\varphi)$, and so sine coefficients were not included in Eq. (97). When $m = 2$, this equation simplifies to the familiar Karplus equation, which suggests that the latter equation is a subset of a more complex relationship. The lack of a traditional Karplus dependence for $^3J_{\mathrm{FCCF}}$ values of saturated fluorocarbons is reflected in the interpretation that (a) higher order Fourier coefficients are needed in Eq. (97) to reproduce these couplings correctly and (b) the values of the first three coefficients differ from the usual large C_0 and C_2 coefficients, and small C_1 value.[143] It was concluded that the deviation of $^3J_{\mathrm{FCCF}}$ from the Karplus equation arises mainly from through-space interaction in the Fermi-contact contribution, and that the description of this contribution by Eq. (97) requires at least six coefficients (that is, $m = 5$ in Eq. (97)). As a result, an explicit, analytical expression is not available for the dependence of $^3J_{\mathrm{FCCF}}$ on torsion angle. Moreover, the dependence of the $^3J_{\mathrm{FCCF}}$ coupling on substituents is generally complex and not well understood.

2. Carbon–Tin Couplings

a. Carbon–Tin Couplings, $^3J_{\mathrm{CCCSn}}$.— Vicinal ^{13}C–^{119}Sn couplings have been measured for geometrically constrained, *exo*- and *endo*-2-norbornyl-, 1- and 2-adamantyl-, and 3-nortricyclyl-trimethylstannane.[144] Fitting of the $^3J_{\mathrm{CCCSn}}$ values to a three-parameter Karplus equation using CCCSn torsion angles 35°, 70°, 85°, 120°, 160°, 170°, and 180° obtained from Dreiding models of the stannane derivatives gave the equation:

$$^3J_{\mathrm{CCCSn}} = 30.4 - 7.6\cos\varphi + 25.2\cos 2\varphi \qquad (98)$$

which may be rewritten as

$$^3J_{\mathrm{CCCSn}} = 50.4\cos^2\varphi - 7.6\cos\varphi + 5.2 \qquad (99)$$

VI. COUPLINGS OVER FOUR BONDS

These couplings may certainly be described as long range, but two definitions of long-range coupling constants have been used. Some authors refer to long-range couplings as those transmitted over more than one bond, while others mean the couplings over more than three or even four bonds. In sugars, this group of couplings includes those over pathways containing four saturated bonds, or three saturated and one unsaturated bond (allylic couplings), which have different dependences on dihedral angle.

1. Proton–Proton Couplings

a. W and non-W Couplings, $^4J_{\mathrm{HCCCH}}$.— W-type couplings are rather common in saturated, carbohydrate structures, occurring whenever the coupling pathway has a near planar W shape,[145] as in pyranose and furanose rings having a 1,3-diequatorial arrangement of protons, or of different pairs of magnetically active nuclei.[66] $^4J_{\mathrm{HCCCH}}$ couplings were first observed in carbohydrates by Hall and Hough, who found $^4J_{1,3}$ 1.3, 1.4, and 1.8 Hz for three 2,3,4-tri-*O*-acetyl-1,6-anhydro-β-D-hexopyranoses in which H-1 and H-3 were both equatorial.[146] At that time, the long-range coupling was not observable in 1,6-anhydro derivatives in which H-3 was axial, thus indicating a stereochemical dependence. Other early examples were $^4J_{1,3}$ 0.7–0.9 Hz in $^4C_1$ chair conformations of methyl 4,6-*O*-benzylidene-α-D-altropyranoside derivatives,[64] and $^4J_{2,4}$ 0.8–1.0 Hz in $^3S_5$ skew conformations of 1,2-*O*-alkylidene-α-D-glucopyranosides[147,148] and similar derivatives having a five-membered ring fused to C-1 and C-2.[149]

On the basis of a semi-empirical VB theory, Barfield soon indicated that the maximum long-range coupling (if positive) should correspond to a planar zigzag (that is, W) arrangement in which the relevant dihedral angles φ_1 and φ_3 are both 180°, with a sharp decrease in magnitude expected as either proton H-1 or H-3 is moved out of the plane.[150] For the $^4J_{1,3}$ couplings in the 1,6-anhydrohexopyranoses, φ_1 and φ_3 are subtended by H-1–C-1–C-2–C-3 and C-1–C-2–C-3–H-3, respectively.

At the time of our report on the observation of an unusually large coupling $^4J_{2,4}$ +2.45 Hz in the ^{1}H NMR spectrum of 3-*O*-benzoyl-1,2,4-*O*-benzylidyne-α-D-ribopyranose,[151] the theoretical interpretation of these couplings was somewhat inexplicit, and rather confusing. Barfield's early VB theory[150] did not account satisfactorily for the variation of the sign of $^4J_{\mathrm{HCCCH}}$ with the 1,3-diequatorial or 1,3-equatorial-axial orientations of ring protons in the chair conformations of pyranose sugars[152] The theory was interpreted[153] either in terms of the equation:

$$^4J_{\mathrm{HCCCH}} = 0.7\left(\cos^2\varphi_1 + \cos^2\varphi_3\right) - 0.3 \tag{100}$$

or an alternative:

$$^4J_{\mathrm{HCCCH}} = A\left(\cos^2\varphi_1 \cos^2\varphi_3\right) - B \tag{101}$$

where $B = 0.35$, and $A = 0.31$ for $0° \le \varphi_1, \varphi_3 \le 90°$, 1.07 for $0° \le \varphi_1 \le 90° \le \varphi_3 \le 180°$, or 3.61 for $90° \le \varphi_1, \varphi_3 \le 180°$. The latter equation agreed more closely with $^4J_{\mathrm{HCCCH}} = +2.45$ Hz of the 1,2,4-*O*-benzylidyne-α-D-ribopyranose derivative,[151] whereas the former equation predicts the couplings more accurately for $^4J_{1,3}$ +1.6 Hz and $^4J_{3,5}$ +1.5 Hz in 1,6-anhydro-β-D-mannopyranose triacetate, and other similar derivatives.[152] However, $^4J_{\mathrm{HCCCH}}$ couplings in conformationally locked ring-systems have frequently been observed to be abnormally large, for example, reaching $^4J_{1,3}$ 18.2 Hz in bicyclo[1.1.1]pentane.[154] In this derivative, H-1 and H-3 are collinear and may be expected to couple strongly through overlap of the rear lobes of their H–C bonding orbitals.

In a reprise, almost 40 years later, Barfield has clarified the situation by a study of the structural dependencies of $^4J_{\mathrm{HCCCH}}$ in propanic and allylic systems by DFT/FPT methods, which were used to obtain the Fermi-contact contributions to the couplings.[154] The theoretical contributions to the coupling constants were dissected according to dependences on various molecular properties, including the φ_1 and φ_3 torsion angles, the central C-1–C-2–C-3 bond angle θ_2, and the C-1–C-3 distance $r_{\text{C-1,C-3}}$. Barfield has published a very revealing 3D plot of $^4J_{\mathrm{HCCCH}}$ as a function of both φ_1 and φ_3 (Fig. 10).

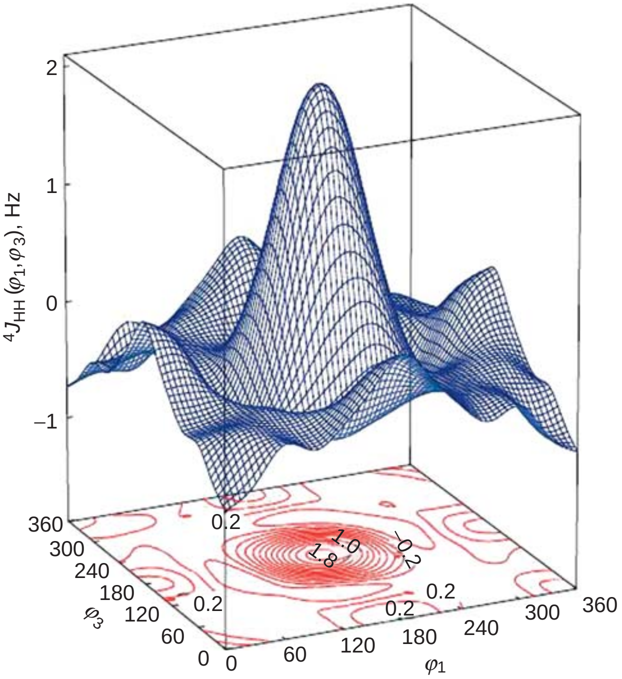

FIG. 10. 3D plot and contour map for $^4J_{HCCCH}$ in propane, calculated as a function of the dihedral angles φ_1 and φ_3 by DFT/FPT at 30° intervals of the angles. 3D spline interpolations were used to create the graphs, which illustrate how the coupling constant changes sign, depending on the values of φ_1 and φ_3. A maximum positive value is seen for $\varphi_1 = \varphi_3 = 180°$.

The data for this plot were calculated by DFT/FPT for 30° intervals of φ_1 and φ_3 and show that $^4J_{HCCCH}$ reaches a maximum of +2.11 Hz for $\varphi_1 = \varphi_3 = 180°$, and a minimum value of −0.73 Hz for $\varphi_1 = \varphi_3 = 0°$, thus adequately interpreting the variation of the signs of the experimental couplings with geometrical factors.[154] For propane, the following expression was proposed:

$$^4J_{HCCCH}(\varphi_1,\varphi_3) = 0.82\cos^2\varphi_1\cos^2\varphi_3 - 0.62\cos\varphi_1\cos\varphi_3 \times(\cos\varphi_1 + \cos\varphi_3) + 0.21\cos\varphi_1\cos\varphi_3 - 0.32 \qquad (102)$$

Unfortunately, the choice of trigonometric functions still seems a little arbitrary, perhaps reflecting the difficulty of translating the theory into practical equations.

The dependence of $^4J_{HCCCH}$ on φ_1, φ_3, θ_2, and $r_{\text{C-1,C-3}}$ was investigated by a DFT/FPT procedure in which φ_1 and φ_3 were stepped by 60° increments, and θ_2 by 10°

intervals in the range 70–130°. Fitting of the theoretical results for the trans–trans (*tt*) conformation of propane (W-form, $\varphi_1 = \varphi_3 = 180°$) yielded[154] the equation:

$$\begin{aligned} {}^4J_{\mathrm{HCCCH}}\left(tt, \theta_2, r_{\mathrm{C-1,C-3}}\right) = \left[-95.4 \sin^4(\theta_2/2) + 17.6 \sin^2(\theta_2/2)\right] \\ \times \exp\left[-5.20\left(r_{\mathrm{C-1,C-3}} - r(0)_{\mathrm{C-1,C-3}}\right)\right] - 1.19 \end{aligned} \tag{103}$$

where $r(0)_{\text{C-1,C-3}}$ is the smallest value (1.978 Å) in the series, occurring for $\theta_2 = 70°$.

A simple alternative to Eq. (102) was formulated to represent W-couplings in bicycloalkanes:

$$\begin{aligned} {}^4J_{\mathrm{HCCCH}}\left(\varphi_1, \varphi_3, r_{\mathrm{C-1,C-3}}\right) = 18.15 \cos^2 \varphi_1 \cos^2 \varphi_3 \\ \times \exp\left[-1.70\left(r_{\mathrm{C-1,C-3}} - r(0)_{\mathrm{C-1,C-3}}\right)\right] - 1.10 \end{aligned} \tag{104}$$

For example, using $r_{\text{C-1,C-3}} = 1.872$ Å in this equation leads to a computed value ${}^4J_{1,3}$ 20.6 Hz in bicyclo[1.1.1]pentane, which may be compared with its experimental value of 18.2 Hz.[154]

The ${}^4J_{\mathrm{HCCCH}}$ values of 28 cyclopentane and cyclohexane derivatives have been subjected to PCA, by using the couplings, the corresponding torsion angles, and the $\cos^2 \varphi_1 \cos^2 \varphi_3$ product as variables in a multivariate data analysis.[155] The torsion angles were calculated by use of three different molecular-mechanics packages, PC MODEL (MMX), CS MOPAC PRO (AM1), and GAUSSIAN98 [HF/6–31g(d,p)]. PCA was performed by using the PIROUETTE software package, the application of which to GAUSSIAN98 data yielded seven clusters of compounds, where the clustering reflected structural similarities in the compounds. Two significant principal components were described by the equations:

$$\mathrm{PC1} = 0.4125\,{}^4J_{\mathrm{HCCCH}} + 0.5352 \cos^2 \varphi_1 \cos^2 \varphi_3 + 0.5175\,\varphi_1 + 0.5250\,\varphi_3 \tag{105}$$

$$\mathrm{PC2} = 0.8734\,{}^4J_{\mathrm{HCCCH}} - 0.2921 \cos^2 \varphi_1 \cos^2 \varphi_3 - 0.2897\,\varphi_1 - 0.0042\,\varphi_3 \tag{106}$$

The most important variables in the separation of the seven clusters were found to be the coupling-constant values and the calculated products, $\cos^2 \varphi_1 \cos^2 \varphi_3$, which together had the highest modeling-power indices, and the largest coefficients in PC1 and PC2.[155] Two trends in clustering were observed, one owing to similarities in torsion angle (four groups of samples) and another to values of the four-bond coupling, including the small or zero couplings resulting from 1,3-diaxial arrangements of protons. It was proposed that substituents positioned on the same side of the ring as the coupled protons have a greater influence in diminishing the W-coupling than does the orientation of these protons,[155] a somewhat surprising result, in view of the known dependence of $^4J_{\mathrm{HCCCH}}$ values of carbohydrates on the stereochemistry of the protons.

As the resolution of NMR spectrometers has improved and resolution enhancement by such methods as Gaussian multiplication of the FID has been more widely used, non-W values of $^4J_{\mathrm{HCCCH}}$ have been detected more frequently.[156] For example, $^4J_{1,5}$ 0.5–0.7 Hz in a series of methyl 4,6-*O*-benzylidene-α-D-hexopyranosides, in which φ_1 and φ_3 have values of ~180° and ~60°, respectively.[66] In partially protected galactopyranosides, the observation of $^4J_{\mathrm{HO\text{-}4,H\text{-}5}}$ 1.0 Hz was more reasonably interpreted by a W coupling to a hydroxyl proton,[157] than by a through-hydrogen-bond-coupling $^{\mathrm{h}}J$ involving a pathway via the ring oxygen,[158] as supported by DFT calculations.[157]

b. Allylic Couplings, $^4J_{\mathrm{HC{=}CCH}}$.— The early history of these couplings has been reviewed before.[21,145] Fermi-contact contributions to the transoid and cisoid allylic couplings in propene have recently been calculated by DFT/FPT and fitted[154] to the equations:

$$^4J_{\mathrm{trans}} = -4.76\sin^2\varphi - 0.60\cos\varphi + 0.53 \tag{107}$$

$$^4J_{\mathrm{cis}} = -3.52\sin^2\varphi - 0.02\cos\varphi - 0.37 \tag{108}$$

These couplings are theoretically expected to have largest numeric magnitudes of approximately –4 Hz for $\varphi = 90°$, although the experimental values have been found to be 1–2 Hz smaller.[154]

VII. COUPLINGS OVER FIVE BONDS

1. Proton–Proton Couplings

a. Extended W Couplings, $^5J_{\mathrm{HCCCCH}}$.— An especially favorable geometry for the detection of these couplings is when the protons are separated by five bonds in a planar, zigzag (extended W) arrangement.[145] For example, methyl 4,6-*O*-benzylidene-α-D-altropyranosides having the pyranose ring in a $^4C_1$ form (Fig. 11) exhibited values $^5J_{3e,6e}$ 0.5–0.7 Hz, whereas in similar derivatives in which H-3 and H-6 were not in a planar, extended W, the $^5J_{3,6}$ coupling was not detectable.[66] However, couplings of 0.4–1.3 Hz have also been measured for chair forms of 1,3-dioxanes and pyranoid compounds in which the 1,4-protons are diequatorial, but not precisely in an extended W orientation.[159] According to Barfield *et al.*,[128] $^5J_{\mathrm{HCCCCH}}$ couplings

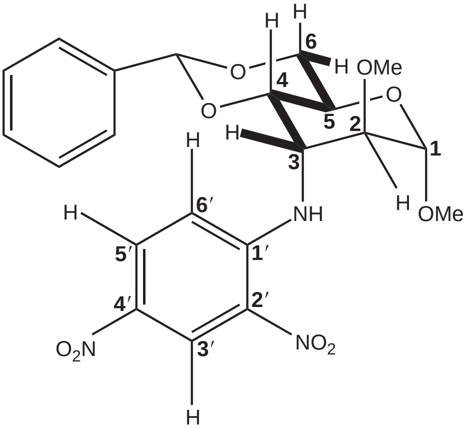

FIG. 11. A planar, extended W coupling pathway (heavy bonds) in methyl *N*-2′,4′-dinitrophenyl-3-amino-4,6-*O*-benzylidene-3-deoxy-2-*O*-methyl-α-D-altropyranoside, which results in a long-range coupling constant of $^5J_{3,6}$ 0.5 Hz.

may be expected to have a functional dependence on cos $\varphi_{1,2}$, cos $\varphi_{2,3}$, and cos $\varphi_{3,4}$, where $\varphi_{1,2}$, $\varphi_{2,3}$, and $\varphi_{3,4}$ are the dihedral angles about C-1–C-2, C-2–C-3, and C-3–C-4, respectively.

b. Biallylic Couplings, $^5J_{\mathrm{HCC{=}CCH}}$.— These couplings have been reviewed previously[66,145] Based on measurements of the magnitudes and relative signs of $^5J_{1,4}$ in methyl 3,4-dichloro-4-deoxy-D-*glycero*-pent-2-enopyranosides,[160] Eq. (109) was proposed

$$^5J_{\mathrm{HCC{=}CCH}} = 3.25\,\sin^2\varphi_1\,\sin^2\varphi_4 \tag{109}$$

where φ_1 and φ_4 are the torsion angles of the terminal protons with respect to the coupling pathway.[66] For the important π-electron contribution to homo-allylic (biallylic) couplings, Barfield and Sternhell suggested[161,162] Eq. (110) on the basis of VB formalism:

$$^5J^{\pi}_{\mathrm{HCC{=}CCH}} = 4.99\,\sin^2\varphi_1\,\sin^2\varphi_4 \tag{110}$$

However, σ-electron contributions were not included because the size of the secular determinants increases enormously with the size of the basis set, and it was difficult to find suitable empirical parameters for the σ-electron system.[162]

VIII. ONLINE CALCULATORS FOR COUPLING CONSTANTS AND TORSIONS

Stenutz has provided a number of useful tools for the online calculation of homo- and heteronuclear coupling constants, torsion angles, rotameric populations, and puckering phase. Two calculations of $^3J_{\mathrm{HCCH}}$ are available, using either the Haasnoot,[163] or Pachler[164] relationships. Both implementations depend on the relative orientation of the substituents, and turning a molecular model so that the proton on the near side is pointing up is recommended. Each online program requires four substituents to be selected from drop-down menus of atom types. The implementation of the Haasnoot procedure automatically selects one of three equations, depending on the number of attached hydrogen atoms. Entry of a φ_{HCCH} value then allows the corresponding $^3J_{\mathrm{HCCH}}$ to be calculated, or conversely, the insertion of a coupling constant value results in the computation of one to four torsion angles, depending on the size of the coupling.

A generalized online calculation of the three-parameter Eq. (3) is also available, which can be used to compute either homo- or heteronuclear coupling constants from given dihedral angles.[165] Users of this calculation either type in new values of the A, B, and C coefficients or select these coefficients automatically by choosing a literature reference from a list, many of which have been discussed in this chapter. Conversely, the entry of a coupling constant permits the calculation of four solutions for a torsion angle, which are comprised of ± a smaller angle, and ± a larger angle. If there are only two torsions that will reproduce the coupling constant, or if the ^3J value lies outside the range of the Karplus equation, then ''not a number'' is displayed.

Another online module allows the calculation of $^3J_{\mathrm{HCCH}}$ values specifically for β-ribofuranosides (or nucleosides/nucleotides) from the puckering phase or determines the puckering phase from experimental coupling constants.[166] There may be more than one phase that reproduces the experimental couplings, but only one is found by the program. An rmsd > 0.5 suggests that there is an equilibrium of two conformers, namely, N $\leftrightarrow$ S, and for comparison purposes, such an equilibrium is calculated. If the ribofuranose ring is rigid, then the rmsd for the fitted pseudorotation angle (P) should be lower than for the two-state model. To calculate the coupling constant, either the pseudorotation angle is entered in degrees or a conformer, such as $^3T_2$ and the like, is selected by clicking on a button.[166] The program output displays the calculated values of $J_{1,2}$, $J_{2,3}$, and $J_{3,4}$, as well as the best P, the rmsd values, and the best N $\leftrightarrow$ S equilibrium in terms of the %N conformer (^3E).

A module for unsubstituted 2-deoxy-*erythro*-β-pentofuranose permits the calculation from the pseudorotation angle of all the $^1J_{\mathrm{CH}}$, $^2J_{\mathrm{CH}}$, and $^3J_{\mathrm{CH}}$ couplings around the furanose ring, except that, in some cases, the relative proportions of the two dominant C-4–C-5 rotamers (*gg* and *gt*) are required.[167] In nucleic acids, the *gg* rotamer is the only one present.

Yet another module can be used to calculate hydroxymethyl coupling constants related to the ω torsion angle, O-5–C-5–C-6–O-6 in hexopyranoses. By entering this angle together with a value for the θ torsion, C-5–C-6–O-6–HO-6, the magnitudes of $^1J_{\text{C-5,C-6}}$, $^2J_{\text{C-4,C-6}}$, $^1J_{\text{C-6,H-6R}}$, $^1J_{\text{C-6,H-6S}}$, $^2J_{\text{C-5,H-6R}}$, $^2J_{\text{C-5,H-6S}}$, $^2J_{\text{C-6,H-5}}$, $^3J_{\text{C-4,H-6R}}$, $^3J_{\text{C-4,H-6S}}$, $^2J_{\text{H-6R,H-6S}}$, $^3J_{\text{H-5,H-6R}}$, and $^3J_{\text{H-5,H-6S}}$ can be estimated.[168]

Two useful tables of rotameric populations for the hydroxymethyl groups in hexopyranoside derivatives are available online. In the first,[169] two protocols have been used to calculate rotameric distributions from experimental values of $^3J_{\text{H-5,H-6R}}$ and $^3J_{\text{H-5,H-6S}}$, using either application of the Haasnoot equation to the data of Bock and Duus,[170] or the results of the quantum-mechanical calculations of Stenutz *et al.*[61] The populations of the *gt* rotamer obtained by the two methods are in good agreement, but those of the *gg* and *tg* rotamers agree less well. In the second table,[171] a single set of populations of the *gt, gg*, and *tg* rotamers has been calculated from the experimental $^3J_{\text{H-5,H-6R}}$ and $^3J_{\text{H-5,H-6S}}$ values of a larger collection of both hexopyranoside and disaccharide derivatives, by using the limiting values of Stenutz *et al.*[61]

An online calculator is available that relates ^{13}C chemical shifts on glycosylation to the ^{1}H–^{1}H distance $r_{\text{H,H}}$ across the glycosidic linkage, and the ψ_{H} torsion angle.[172] The method applies to α-linked disaccharides containing galacto, gluco, and manno residues, and is based on the work of Bock *et al.*[173] Entry of the glycosylation shifts (ppm) for the non-reducing end, $\Delta\delta_{\text{C-1}}$ and for the reducing end, $\Delta\delta_{\text{C-}n}$ into the calculator gives estimates of ψ_{H} (in degrees) and $r_{\text{H,H}}$ (in Å). Examples of results are given for 11 α-linked disaccharide methyl glycoside derivatives.[172]

An interactive plotting program for Eq. (2) is available online which allows the entry of different sets of the parameters *A, B*, and *C* and then displays up to five plots simultaneously, together with the parameters for each plot. The values of *J* and φ at any value of φ on each plot can be inspected by moving the cursor to the location, followed by clicking and holding the left mouse button at that location.[174,175]

A free graphical tool, MestRe-J for Windows-32 platforms, is available for the prediction of $^3J_{\text{HCCH}}$ from torsion angles[176,177] using either the Haasnoot–Altona equation[33] with Huggins electronegativities $\Delta\chi$, the Colucci–Jungk–Gandour equation,[45] or the more recent and precise Díez–Altona–Donders equations with λ electronegativities.[58] The latter equations include the effects of nonadditive interactions between substituents, and the equations for $^3J_{\text{HCCH}}$ can also be solved for the torsion angles. This graphical application works with a Newman projection of the molecular fragment and displays a plot of *J* values versus the torsion angle. Computation of the Barfield–Smith equation[178,179] has also been implemented,[177] for which a significant erratum has been published.[180] Other programs are also available for the calculation of torsion angles from NMR data, including the MULDER program,[181] and a module in the AURELIA program.[182]

IX. SUMMARY

Karplus equations of varying complexity are available for most of the three- and four-bond spin–spin coupling constants that are commonly measured for carbohydrates. Similar equations have also been developed for one- and two-bond couplings between pairs of nuclei that are not directly connected by a dihedral angle, but instead depend on the relative torsion angles of substituents either inside, or outside the coupling pathway. The coefficients in the equations have in most cases been determined by fitting of experimental data and are specific for particular pairs of nuclei separated by various coupling pathways. These coefficients are summarized in Table I

TABLE I

Coefficients[a] in Selected Three-Parameter Karplus Equations, $^3J = A\cos^2\varphi + B\cos\varphi + C$, for Vicinal NMR Coupling Constants, Ranked According to the Magnitude of *A*

^3J	A	B	C	References
$^3J_{\mathrm{HCNF}}$	70.8	−44.1	−7.2	138
$^3J_{\mathrm{CCCSn}}$[b]	50.4	−7.6	5.2	144
$^3J_{\mathrm{HCOP}}$	15.3	−6.2	1.5	110
$^3J_{\mathrm{HCOH}}$	13.56	−2.05	−1.02	75
	10.4	−1.5	0.2	70
$^3J_{\mathrm{CCOP}}$	9.1	−1.9	0.8	111
$^3\mathrm{J}_{\mathrm{HCCH}}$	9.0	−0.5	−0.3	8
$^3J_{\mathrm{HC\alpha NC'}}$	9.0	−4.4	−0.8	105
$^3J_{\mathrm{HOCC}}$	8.36	−1.41	−0.69	75
$^3J_{\mathrm{HCCC}}$	8.06	−0.87	0.47	92
$^3J_{\mathrm{HCSiH}}$	5.83	−2.59	0.84	76
$^3J_{\mathrm{HCOC}}$	5.7	−0.6	0.5	81
	5.5	−0.7	0.6	82
$^3J_{\mathrm{CCCC}}$	4.48	0.18	−0.57	132
$^3J_{\mathrm{HCSC}}$	4.44	−1.06	0.45	96
$^3J_{\mathrm{CCOC}}$	4.4	1.1	0.5	121
	3.70	0.18	0.11	122
$^3J_{\mathrm{HCCN}}$[c]	3.1	−0.6	0.4	66
$^3J_{\mathrm{HC\alpha C'N}}$[c]	−4.6	3.0	0.8	105

[a] The entries in the table are illustrative, rather than comprehensive, and do not take into account the recent trend to develop multiple Karplus equations for different structural elements. The main text or original publications should be consulted for full details.

[b] ^{119}Sn.

[c] ^{15}N.

for Karplus equations of the three-parameter type that describe vicinal couplings, for which the important *A* coefficient varies from a maximum value of 70.8 Hz for $^3J_{\mathrm{HCNF}}$, to a minimum of 3.1 Hz for $^3J_{\mathrm{HCCN}}$. Many of the three-parameter equations have been constructed from quite small experimental data sets, especially for the heteronuclear couplings. A notable exception is the work of Serianni and coworkers, who have generated vast quantities of coupling-constant data, experimentally from ^{13}C-substituted sugars, and theoretically by DFT methods. The inclusion, in the Karplus equation, of other admittedly important molecular properties such as atomic or group electronegativity, electronegativity orientation, valence-bond angle, and bond length requires large experimental (or theoretical) data sets and has not been performed for all combinations of nuclei, and of coupling pathway.

As the quantity of available experimental and theoretical data has increased, there has been a trend towards parametrization of multiple Karplus equations for various structural elements, especially for different coupling pathways, and anomeric configurations.

As an alternative to the use of these empirically derived equations, Serianni *et al.* have suggested that spin couplings could instead be calculated for molecules of interest by DFT, which with the correct choice of basis sets, now seems to give theoretical coupling values that agree well with experimental measurements, often without the need for scaling adjustments.

Interactive, online programs are available for the calculation of coupling constants, dihedral angles, and the ^{1}H–^{1}H distance across thr α-linkages of some disaccharides, as well as a program for plotting up to five Karplus curves.

REFERENCES

1. M. Karplus, Contact electron–spin coupling of nuclear magnetic moments, *J. Chem. Phys.*, 30 (1959) 11–15.
2. R. U. Lemieux, R. K. Kullnig, H. J. Bernstein, and W. G. Schneider, Configurational effects on the proton magnetic resonance spectra of six-membered ring compounds, *J. Am. Chem. Soc.*, 80 (1958) 6098–6105.
3. R. U. Lemieux, R. K. Kullnig, and R. Y. Moir, The configuration of the 3-methoxycyclohexene oxides. A novel application of proton magnetic resonance spectroscopy to the determination of structure and configuration, *J. Am. Chem. Soc.*, 80 (1958) 2237–2242.
4. L. Dalton, Karplus equation. Theoretical calculation links NMR coupling constant to molecular geometry, *Chem. Eng. News*, 81 (2003) 37–39.
5. J. W. Lenz and J. P. Heeschen, The application of nuclear magnetic resonance to structural studies of carbohydrates in aqueous solution, *J. Polymer Sci.*, 51 (1961) 247–261.
6. R. J. Abraham, L. D. Hall, L. Hough, and K. A. McLauchlan, A proton resonance study of the conformations of carbohydrates in solution. Part I. Derivatives of 1,2-*O*-isopropylidene-α-D-*xylo*-hexofuranose, *J. Chem. Soc.* (1962) 3699–3705.

7. L. D. Hall, Nuclear magnetic resonance, *Adv. Carbohydr. Chem.*, 19 (1964) 51–93.
8. M. Karplus, Vicinal proton coupling in nuclear magnetic resonance, *J. Am. Chem. Soc.*, 85 (1963) 2870–2871.
9. I. Tvaroška and F. R. Taravel, Carbon–proton coupling constants in the conformational analysis of sugar molecules, *Adv. Carbohydr. Chem. Biochem.*, 51 (1995) 15–61.
10. A. S. Perlin and B. Casu, Carbon-13 and proton magnetic resonance spectra of D-glucose-^{13}C, *Tetrahedron Lett.* (1969) 2921–2924.
11. K. Bock, I. Lundt, and C. M. Pedersen, Assignment of anomeric structure to carbohydrates through geminal ^{13}C-H coupling constants, *Tetrahedron Lett.* (1973) 1037–1040.
12. K. Bock and C. M. Pedersen, A study of ^{13}CH coupling constants in hexopyranoses, *J. Chem. Soc. Perkin II* (1974) 293–297.
13. K. Bock and C. M. Pedersen, A study of ^{13}CH coupling constants in pentopyranoses and some of their derivatives, *Acta Chem. Scand.*, B 29 (1975) 258–264.
14. K. Bock and C. M. Pedersen, Determination of one-bond carbon–proton coupling constants through ^{13}C-satellites in ^{1}H-n.m.r. spectra, *Carbohydr. Res.*, 145 (1985) 135–140.
15. M. Hricovini and I. Tvaroška, Conformational dependence of the one-bond carbon–proton coupling constants in oligosaccharides, *Magn. Reson. Chem.*, 28 (1990) 862–866.
16. I. Tvaroška and F. R. Taravel, One-bond carbon–proton coupling constants: Angular dependence in α-linked oligosaccharides, *Carbohydr. Res.*, 221 (1991) 83–94.
17. I. Tvaroška, Theoretical aspects of structure and conformation of oligosaccharides, *Curr. Opin. Struct. Biol.*, 2 (1991) 661–665.
18. I. Tvaroška and F. R. Taravel, One-bond carbon–proton coupling constants: Angular dependence in *β*-linked oligosaccharides, *J. Biomol. NMR*, 2 (1992) 421–430.
19. R. R. Ernst, Sensitivity enhancement in magnetic resonance, *Advan. Magn. Reson.*, 2 (1966) 1–135.
20. R. R. Ernst and W. A. Anderson, Application of Fourier transform spectroscopy to magnetic resonance, *Rev. Sci. Instrum.*, 37 (1966) 93–102.
21. B. Coxon, Conformational analysis via nuclear magnetic resonance spectroscopy, *Methods Carbohydr. Chem.*, 6 (1972) 513–539.
22. M. Edén, A. Brinkmann, H. Luthman, L. Eriksson, and M. H. Levitt, Determination of molecular geometry by high-order multiple-quantum evolution in solid-state NMR, *J. Magn. Reson.*, 144 (2000) 266–279.
23. M. Karplus, Theory of proton coupling constants in unsaturated molecules, *J. Am. Chem. Soc.*, 82 (1960) 4431–4432.
24. R. J. Abraham and K. G. R. Pachler, The proton magnetic resonance spectra of some substituted ethanes. The influence of substitution on CH–CH coupling constants, *Mol. Phys.*, 7 (1964) 165–182.
25. P. L. Durette and D. Horton, Conformational studies on pyranoid sugar derivatives by NMR spectroscopy. Correlations of observed proton–proton coupling constants with the generalized Karplus equation, *Org. Magn. Reson.*, 3 (1971) 417–427.
26. D. G. Streefkerk, M. J. A. De Bie, and J. F. G. Vliegenthart, Conformational studies on pertrimethylsilyl derivatives of some mono- and disaccharides by 220 MHz PMR spectroscopy, *Tetrahedron*, 29 (1973) 833–844.
27. D. G. Streefkerk, M. J. A. De Bie, and J. F. G. Vliegenthart, Conformational studies of pertrimethylsilyl derivatives of some 6-deoxyaldohexopyranoses and four less-common aldohexopyranoses by 220-MHz P.M.R. spectroscopy. Substituent and configurational effects on the chemical shifts of the ring protons, *Carbohydr. Res.*, 38 (1974) 47–59.
28. L. Dorland, B. L. Schut, J. F. G. Vliegenthart, G. Strecker, B. Fournet, G. Spik, and J. Montreuil, Structural studies on 2-acetamido-1-*N*-(4-L-aspartyl)-2-deoxy-*β*-D-glucopyranosylamine and 2-acetamido-6-*O*-(α-L-fucopyranosyl)-1-*N*-(4-L-aspartyl)-2-deoxy-*β*-D-glucopyranosylamine, *Eur. J. Biochem.*, 73 (1977) 93–97.

29. D. H. Williams and N. S. Bhacca, Dependency of vicinal coupling constants on the configuration of electronegative substituents, *J. Am. Chem. Soc.*, 86 (1964) 2742–2743.
30. R. J. Abraham and G. Gatti, Rotational isomerism. Part VII. Effect of substituents on vicinal coupling constants in XCH_2-CH_2Y fragments, *J. Chem. Soc. (B)* (1969) 961–968.
31. L. Phillips and V. Wray, The structural dependence of the inductive effect. Part VI. The calculation of vicinal proton–proton spin–spin coupling constants in substituted ethanes, *J. Chem. Soc. Perkin II* (1972) 536–539.
32. C. A. G. Haasnoot, F. A. A. M. de Leeuw, H. P. M. de Leeuw, and C. Altona, Interpretation of vicinal proton–proton coupling constants by a generalized Karplus relation. Conformational analysis of the exocyclic C-4′–C-5′ bond in nucleosides and nucleotides, *Recueil, J. Roy. Netherlands Chem. Soc.*, 98 (1979) 576–577.
33. C. A. G. Haasnoot, F. A. A. M. de Leeuw, and C. Altona, The relationship between proton–proton NMR coupling constants and substituent electronegativities-I. An empirical generalization of the Karplus equation, *Tetrahedron*, 36 (1980) 2783–2792.
34. C. A. G. Haasnoot, F. A. A. M. de Leeuw, H. P. M. de Leeuw, and C. Altona, The relationship between proton–proton NMR coupling constants and substituent electronegativities. II-Conformational analysis of the sugar ring in nucleosides and nucleotides in solution using a generalized Karplus equation, *Org. Magn. Reson.*, 15 (1981) 43–52.
35. K. G. R. Pachler, Extended Hückel theory MO calculations of proton–proton coupling constants-II. The effect of substituents on vicinal couplings in monosubstituted ethanes, *Tetrahedron*, 27 (1971) 187–199.
36. K. G. R. Pachler, The dependence of vicinal proton–proton coupling constants on dihedral angle and substituents, *J. Chem. Soc. Perkin II* (1972) 1936–1940.
37. H. Booth, The variation of vicinal proton–proton coupling constants with orientation of electronegative substituents, *Tetrahedron Lett.* (1965) 411–416.
38. G. Balacco, A desktop calculator for the Karplus equation, *J. Chem. Inf. Comput. Sci.*, 36 (1996) 885–887.
39. C. M. Cerda-Garcia-Rojas, L. G. Zepeda, and P. Joseph-Nathan, A PC program for calculation of dihedral angles from ^{1}H NMR data, *Tetrahedron Comput. Methods*, 3 (1990) 113–118.
40. C. A. G. Haasnoot, F. A. A. M. de Leeuw, H. P. M. de Leeuw, and C. Altona, Relationship between proton–proton NMR coupling constants and substituent electronegativities. III. Conformational analysis of proline rings in solution using a generalized Karplus equation, *Biopolymers*, 20 (1981) 1211–1245.
41. C. Altona and M. Sundaralingam, Conformational analysis of the sugar ring in nucleosides and nucleotides. A new description using the concept of pseudorotation, *J. Am. Chem. Soc.*, 94 (1972) 8205–8212.
42. C. Altona and M. Sundaralingam, Conformational analysis of the sugar ring in nucleosides and nucleotides. Improved method for the interpretation of proton magnetic resonance coupling constants, *J. Am. Chem. Soc.*, 95 (1972) 2333–2344.
43. R. J. Abraham, P. Loftus, and W. A. Thomas, Rotational isomerism-XXI. The conformation of 2-amino-3-fluoropropanoic acid (2AFP) and 2-fluoro-3-aminopropanoic acid (3-AFP) as the zwitterion, cation, and anion, an NMR and MO study, *Tetrahedron*, 33 (1977) 1227–1234.
44. C. Altona and C. A. G. Haasnoot, Prediction of *anti* and *gauche* vicinal proton–proton coupling constants in carbohydrates: A simple additivity rule for pyranose rings, *Org. Magn. Reson.*, 13 (1980) 417–429.
45. W. J. Colucci, S. J. Jungk, and R. D. Gandour, An equation utilizing empirically derived substituent constants for the prediction of vicinal coupling constants in substituted ethanes, *Magn. Reson. Chem.*, 23 (1985) 335–343.
46. M. L. Huggins, Bond energies and polarities, *J. Am. Chem. Soc.*, 75 (1953) 4123–4126.

47. L. Pauling, The nature of the chemical bond. IV. The energy of single bonds and the relative electronegativity of atoms, *J. Am. Chem. Soc.*, 54 (1932) 3570–3582.
48. C. Altona, J. H. Ippel, A. J. A. Westra Hoekzema, C. Erkelens, M. Groesbeek, and L. A. Donders, Relationship between proton–proton NMR coupling constants and substituent electronegativities. V. Empirical substituent constants derived from ethanes and propanes, *Magn. Reson. Chem.*, 27 (1989) 564–576.
49. L. A. Donders, F. A. A. M. de Leeuw, and C. Altona, Relationship between proton–proton NMR coupling constants and substituent electronegativities. IV. An extended Karplus equation accounting for interaction between substituents and its application to coupling constant data calculated by the extended Hückel method, *Magn. Reson. Chem.*, 27 (1989) 556–563.
50. F. A. A. M. de Leeuw, A. A. van Beuzekom, and C. Altona, Through-space effects on vicinal proton spin–spin coupling constants mediated via hetero atoms: Nonequivalence of *cis*-couplings in five-membered rings, *J. Comput. Chem.*, 4 (1983) 438–448.
51. A. P. Marchand, N. W. Marchand, and A. L. Segre, NMR studies of rigid bicyclic systems. II. Evidence for the nonequivalence of *exo–exo* and *endo–endo* coupling constants in 7-substituted-1,4-dichloro-2,2,3,3-tetradeuterionorbornanes, *Tetrahedron Lett.*, 59 (1969) 5207–5210.
52. J. L. Marshall, S. R. Walter, M. Barfield, A. P. Marchand, N. W. Marchand, and A. L. Segre, Reasons for the nonequivalence of the *exo–exo* and *endo–endo* vicinal NMR coupling constants in norbornanes, *Tetrahedron*, 32 (1976) 537–542.
53. H. Kessler, A. Friedrich, and W. E. Hull, Peptide conformation. 12. Conformation of cyclo-(L-Pro$_3$) in solution, *J. Org. Chem.*, 46 (1981) 3892–3895.
54. H. Kessler, W. Bermel, A. Friedrich, G. Krack, and W. E. Hull, Peptide conformation. 17. *cyclo*(L-Pro-L-Pro-D-Pro). Conformational analysis by 270- and 500-MHz one- and two-dimensional ^{1}H NMR spectroscopy, *J. Am. Chem. Soc.*, 104 (1982) 6297–6304.
55. F. A. A. M. de Leeuw and C. Altona, Computer-assisted pseudorotation analysis of five-membered rings by means of proton spin–spin coupling constants: Program PSEUROT, *J. Comput. Chem.*, 4 (1983) 428–437.
56. K. Imai and E. Ōsawa, An empirical extension of the Karplus equation, *Magn. Reson. Chem.*, 28 (1990) 668–674.
57. C. Altona, R. Francke, R. de Haan, J. H. Ippel, G. J. Daalmans, A. J. A. Westra Hoekzema, and J. van Wijk, Empirical group electronegativities for vicinal NMR proton–proton couplings along a C–C bond: Solvent effects and reparameterization of the Haasnoot equation, *Magn. Reson. Chem.*, 32 (1994) 670–678.
58. E. Díez, J. San-Fabián, J. Guilleme, C. Altona, and L. A. Donders, Vicinal proton–proton coupling constants. I. Formulation of an equation including interactions between substituents, *Molec. Phys.*, 68 (1989) 49–63.
59. J. Guilleme, J. San-Fabián, E. Díez, F. Bermejo, and A. L. Esteban, Vicinal proton–proton coupling constants. II: Analysis of the effect of interaction between geminal substituents upon vicinal couplings to methyl groups, *Molec. Phys.*, 68 (1989) 65–85.
60. J. Guilleme, J. San-Fabián, J. Casanueva, and E. Díez, Vicinal proton–proton coupling constants: MCSCF *ab initio* calculations of ethane, *Chem. Phys. Lett.*, 314 (1999) 168–175.
61. R. Stenutz, I. Carmichael, G. Widmalm, and A. S. Serianni, Hydroxymethyl group conformation in saccharides: Structural dependencies of $^2J_{\mathrm{HH}}$, $^3J_{\mathrm{HH}}$, and $^1J_{\mathrm{CH}}$ spin–spin coupling constants, *J. Org. Chem.*, 67 (2002) 949–958.
62. M. Tafazzoli and M. Ghiasi, New Karplus equations for $^2J_{\mathrm{HH}}$, $^3J_{\mathrm{HH}}$, $^2J_{\mathrm{CH}}$, $^3J_{\mathrm{CH}}$, $^3J_{\mathrm{COCH}}$, $^3J_{\mathrm{CSCH}}$, and $^3J_{\mathrm{CCCH}}$ in some aldohexopyranoside derivatives as determined using NMR spectroscopy and density functional theory calculations, *Carbohydr. Res.*, 342 (2007) 2086–2096.
63. M. Barfield and M. Karplus, Valence-bond bond-order formulation for contact nuclear spin–spin coupling, *J. Am. Chem. Soc.*, 91 (1969) 1–10.

64. B. Coxon, Conformations and proton coupling constants in some methyl 4,6-*O*-benzylidene-α-D-hexopyranosides, *Tetrahedron*, 21 (1965) 3481–3503.
65. B. Coxon, Deuterium isotope effects in carbohydrates revisited. Cryoprobe studies of the anomerization and NH to ND deuterium isotope induced ^{13}C NMR chemical shifts of acetamidodeoxy and aminodeoxy sugars, *Carbohydr. Res.*, 340 (2005) 1714–1721.
66. B. Coxon, A Karplus equation for $^{3}J_{\mathrm{HCCN}}$ in amino sugar derivatives, *Carbohydr. Res.*, 342 (2007) 1044–1054.
67. V. F. Bystrov, V. T. Ivanov, S. L. Portnova, T. L. Balashova, and Y. A. Ovchinnikov, Refinement of the angular dependence of the peptide vicinal NH-C(alpha)H coupling constant, *Tetrahedron*, 29 (1973) 873–877.
68. A. Almond, A. Brass, and J. K. Sheehan, Dynamic exchange between stabilized conformations predicted for hyaluronan tetrasaccharides: Comparison of molecular dynamics simulations with available NMR data, *Glycobiology*, 8 (1998) 973–980.
69. M. Mobli and A. Almond, *N*-Acetylated amino sugars: The dependence of NMR $^{3}J(\mathrm{H}^{\mathrm{N}}\mathrm{H}^{2})$-couplings on conformation, dynamics, and solvent, *Org. Biomol. Chem.*, 5 (2007) 2243–2251.
70. R. R. Fraser, M. Kaufman, P. Morand, and G. Govil, Stereochemical dependence of vicinal H–C–O–H coupling constants, *Can. J. Chem.*, 47 (1969) 403–409.
71. L. Poppe and H. van Halbeek, Nuclear magnetic resonance of hydroxyl and amido protons of oligosaccharides in aqueous solution. Evidence for a strong intramolecular hydrogen bond in sialic acid residues, *J. Am. Chem. Soc.*, 113 (1991) 363–365.
72. L. Poppe and H. van Halbeek, NMR spectroscopy of hydroxyl protons in supercooled carbohydrates, *Nature Struct. Biol.*, 1 (1994) 215–216.
73. H. van Halbeek, NMR developments in structural studies of carbohydrates and their complexes, *Curr. Opin. Struct. Biol.*, 4 (1994) 697–709.
74. B. Coxon, Boat conformations: Synthesis, NMR spectroscopy, and molecular modeling of methyl 2,6-anhydro-3-deoxy-3-phthalimido-α-D-mannopyranoside and its ^{15}N-labeled analog, *Carbohydr. Res.*, 322 (1999) 120–127.
75. H. Zhao, Q. Pan, W. Zhang, I. Carmichael, and A. S. Serianni, DFT and NMR studies of $^{2}J_{\mathrm{COH}}$, $^{3}J_{\mathrm{HCOH}}$, and $^{3}J_{\mathrm{CCOH}}$ spin-couplings in saccharides: C–O torsional bias H-bonding in aqueous solution, *J. Org. Chem.*, 72 (2007) 7071–7082.
76. R. Carleer and M. J. O. Anteunis, Angular dependence of the vicinal interproton spin–spin coupling in silacyclohexanes. The conformational energy term of the methyl group in 1-methyl-1-silacyclohexane, *Org. Magn. Reson.*, 12 (1979) 673–678.
77. R. U. Lemieux, T. L. Nagabhushan, and B. Paul, Relationship of ^{13}C to vicinal ^{1}H coupling to the torsion angle in uridine and related structures, *Can. J. Chem.*, 50 (1972) 773–776.
78. G. K. Hamer, F. Balza, N. Cyr, and A. S. Perlin, A conformational study of methyl *β*-cellobioside-d_8 by ^{13}C nuclear magnetic resonance spectroscopy: Dihedral angle dependence of $^{3}J_{\mathrm{C\text{-}H}}$ in ^{13}C–O–C–^{1}H arrays, *Can. J. Chem.*, 56 (1978) 3109–3116.
79. B. Coxon, Carbon-13 Nuclear magnetic resonance spectroscopy of food-related disaccharides and trisaccharides, *In Developments in Food Carbohydrate-2*, (C. K. Lee, Ed.), pp. 351–390. Applied Science Publishers Ltd, Barking, Essex, England (1980).
80. I. Tvaroška and L. Václavík, Stereochemistry of nonreducing disaccharides in solution, *Carbohydr. Res.*, 160 (1987) 137–149.
81. I. Tvaroška, M. Hricovíni, and E. Petráková, An attempt to derive a new Karplus-type equation of vicinal proton–carbon coupling constants for C–O–C–H segments of bonded atoms, *Carbohydr. Res.*, 189 (1989) 359–362.
82. B. Mulloy, T. A. Frenkiel, and D. B. Davies, Long-range carbon–proton coupling constants. Application of conformational studies of oligosaccharides, *Carbohydr. Res.*, 184 (1988) 39–46.

83. I. Tvaroška, Dependence on saccharide conformation of the one-bond and three-bond carbon–proton coupling constants, *Carbohydr. Res.*, 206 (1990) 55–64.
84. F. Cloran, I. Carmichael, and A. S. Serianni, DFT calculations on disaccharide models: Studies of molecular geometries and trans-*O*-glycoside $^3J_{\mathrm{COCH}}$ and $^3J_{\mathrm{COCC}}$ spin-couplings, *J. Am. Chem. Soc.*, 121 (1999) 9843–9851.
85. V. Pozsgay, N. Sari, and B. Coxon, Measurement of interglycosidic $^3J_{\mathrm{CH}}$ coupling constants of selectively ^{13}C-labeled oligosaccharides by 2D *J*-resolved ^{1}H NMR spectroscopy, *Carbohydr. Res.*, 208 (1998) 229–238.
86. C. Höög and G. Widmalm, Conformational flexibility of the disaccharide α-D-Man*p*-(1→3)-*β*-D-Glc*p*-OMe employing molecular dynamics simulations and *trans*-glycosidic $^3J_{\mathrm{C,H}}$ from NMR experiment, *J. Phys. Chem.*, 104 (2000) 9443–9447.
87. T. Nishida, G. Widmalm, and P. Sandor, Hadamard long-range proton–carbon coupling constant measurements with band-selective proton decoupling, *Magn. Reson. Chem.*, 33 (1995) 596–599.
88. T. Rundlöf, A. Kjellberg, C. Damberg, T. Nishida, and G. Widmalm, *Magn. Reson. Chem.*, 36 (1998) 839–847.
89. N. W. H. Cheetham, P. Dasgupta, and G. E. Ball, NMR and modelling studies of disaccharide conformation, *Carbohydr. Res.*, 338 (2003) 955–962.
90. J. B. Houseknecht, T. L. Lowary, and C. M. Hadad, Improved Karplus equations for $^3J_{\mathrm{C1,H4}}$ in aldopentofuranosides: Application to the conformational preferences of the methyl aldopentofuranosides, *J. Phys. Chem.*, 107 (2003) 372–378.
91. K. Bock and C. M. Pedersen, Two- and three-bond ^{13}C–^{1}H couplings in some carbohydrates, *Acta Chem. Scand. B*, 31 (1977) 354–358.
92. R. Aydin and H. Günther, ^{13}C, ^{1}H spin–spin coupling. X.-Norbornane: A reinvestigation of the Karplus curve for $^3J_{(13\mathrm{C},1\mathrm{H})}$, *Magn. Reson. Chem.*, 28 (1990) 448–457.
93. H. J. Koch and A. S. Perlin, Synthesis and ^{13}C NMR spectroscopy of D-glucose-3-*d*. Bond-polarization differences between the anomers of D-glucose, *Carbohydr. Res.*, 15 (1970) 403–410.
94. I. Tvaroška and J. Gajdoŝ, Angular dependence of vicinal carbon–proton coupling constants for conformational studies of the hydroxymethyl group in carbohydrates, *Carbohydr. Res.*, 271 (1995) 151–162.
95. F. R. Taravel, V. Durier, C. Gouvion, K. Mazeau, and I. Tvaroška, Conformational analysis of carbohydrates inferred from carbon–proton coupling constants, *J. Chim. Phys.*, 91 (1994) 798–805.
96. I. Tvaroška, K. Mazeau, M. Blanc-Muesser, S. Lavaitte, H. Driguez, and F. R. Taravel, Karplus-type equation for vicinal carbon–proton coupling constants for the C–S–C–H pathway in 1-thioglycosides, *Carbohydr. Res.*, 229 (1992) 225–231.
97. I. Carmichael, D. M. Chipman, C. A. Podlasek, and A. S. Serianni, Torsional effects on the one-bond ^{13}C–^{13}C spin coupling constant in ethylene glycol: Insights into the behavior of $^1J_{\mathrm{CC}}$ in carbohydrates, *J. Am. Chem. Soc.*, 115 (1993) 10863–10870.
98. G. Batta and K. E. Kövér, Heteronuclear coupling constants of hydroxyl protons in a water solution of oligosaccharides: Trehalose and sucrose, *Carbohydr. Res.*, 320 (1999) 267–272.
99. R. T. Williamson, B. L. Márquez, W. H. Gerwick, and K. E. Kövér, One- and two-dimensional gradient-selected HSQMBC NMR experiments for the efficient analysis of long-range heteronuclear coupling constants, *Magn. Reson. Chem.*, 38 (2000) 265–273.
100. B. L. Márquez, W. H. Gerwick, and R. T. Williamson, Survey of NMR experiments for the determination of $^{\mathrm{n}}J_{(\mathrm{C,H})}$ heteronuclear coupling constants in small molecules, *Magn. Reson. Chem.*, 39 (2001) 499–530.
101. K. E. Kövér, G. Batta, and K. Fehér, Accurate measurement of long-range heteronuclear coupling constants from undistorted multiplets of an enhanced CPMG-HSQMBC experiment, *J. Magn. Reson.*, 181 (2006) 89–97.

102. B. Coxon and R. C. Reynolds, Synthesis of nitrogen-15-labeled amino sugar derivatives by addition of phthalimide-^{15}N to a carbohydrate epoxide, *Carbohydr. Res.*, 110 (1982) 43–54.
103. B. Coxon and R. C. Reynolds, Boat conformations. Synthesis, NMR spectroscopy, and molecular dynamics of methyl 4,6-*O*-benzylidene-3-deoxy-3-phthalimido-α-D-altropyranoside derivatives, *Carbohydr. Res.*, 331 (2001) 461–467.
104. B. Coxon, unpublished.
105. V. F. Bystrov, Y. D. Gavrilov, and V. N. Solkan, Stereochemical dependence of the vicinal ^{13}C'–NC$^{\alpha}$–^{1}H and ^{1}H–C$^{\alpha}$C'–^{15}N proton–heteroatom coupling constants in the NMR spectra of peptides. Comparison of experimental and theoretical data, *J. Magn. Reson.*, 19 (1975) 123–129.
106. P. P. Lankhorst, C. A. G. Haasnoot, C. Erkelens, and C. Altona, Carbon-13 NMR in conformational analysis of nucleic acid fragments. 2. A reparametrization of the Karplus equation for vicinal NMR coupling constants in CCOP and HCOP fragments, *J. Biomol. Struct. Dyns.*, 1 (1984) 1387–1405.
107. P. P. Lankhorst, C. A. G. Haasnoot, C. Erkelens, and C. Altona, Carbon-13 NMR in conformational analysis of nucleic acid fragments. 3. The magnitude of torsional angle ε in d(TpA) from CCOP and HCOP coupling constants, *Nucleic Acids Res.*, 12 (1984) 5419–5428.
108. P. P. Lankhorst, C. A. G. Haasnoot, C. Erkelens, H. P. Westerink, G. A. van der Marel, J. H. van Boom, and C. Altona, Carbon-13 NMR in conformational analysis of nucleic acid fragments. 4. The torsion angle distribution about the C3′-O3′ bond in DNA constituents, *Nucleic Acids Res.*, 13 (1985) 927–942.
109. D. P. Zimmer, J. P. Marino, and C. Griesinger, Determination of homo- and heteronuclear coupling constants in uniformly ^{13}C,^{15}N-labeled DNA oligonucleotides, *Magn. Reson. Chem.*, 34 (1996) S177–S186.
110. M. M. W. Mooren, S. S. Wijmenga, G. A. van der Marel, J. H. van Boom, and C. W. Hilbers, The solution structure of the circular trinucleotide cr(GpGpGp) determined by NMR and molecular mechanics calculation, *Nucleic Acids Res.*, 22 (1994) 2658–2666.
111. J. Plavec and J. Chattopadhyaya, Reparametrization of Karplus equation relating $^{3}J_{\mathrm{CCOP}}$ to torsion angle, *Tetrahedron Lett.*, 36 (1995) 1949–1952.
112. J. M. Duker and A. S. Serianni, (^{13}C)-Substituted sucrose: ^{13}C–^{1}H and ^{13}C–^{13}C spin coupling constants to assess furanose ring and glycosidic bond conformations in aqueous solution, *Carbohydr. Res.*, 249 (1993) 281–303.
113. S. Zhao, G. Bondo, J. Zajicek, and A. S. Serianni, Two-bond ^{13}C–^{13}C spin-coupling constants in carbohydrates: New measurements of coupling signs, *Carbohydr. Res.*, 309 (1998) 145–152.
114. T. Church, I. Carmichael, and A. S. Serianni, Two-bond ^{13}C–^{13}C spin coupling constants in carbohydrates: Effect of structure on coupling magnitude and sign, *Carbohydr. Res.*, 280 (1996) 177–186.
115. A. S. Serianni, P. B. Bondo, and J. Zajicek, Verification of the projection resultant method for two-bond ^{13}C–^{13}C coupling sign determinations in carbohydrates, *J. Magn. Reson., B*, 112 (1996) 69–74.
116. Q. Xu and C. A. Bush, Measurement of long-range carbon–carbon coupling constants in a uniformly enriched complex polysaccharide, *Carbohydr. Res.*, 306 (1998) 335–339.
117. Q. Xu and C. A. Bush, Molecular modeling of the flexible cell wall polysaccharide of *Streptococcus mitis* J22 on the basis of heteronuclear NMR coupling constants, *Biochemistry*, 35 (1996) 14521–14529.
118. A. Bax, D. Max, and D. Zax, Measurement of long-range ^{13}C–^{13}C J couplings in a 20-kDa protein–peptide complex, *J. Am. Chem. Soc.*, 114 (1992) 6923–6925.
119. M. J. King-Morris and A. S. Serianni, ^{13}C NMR studies of [1-^{13}C]aldoses: Empirical rules correlating pyranose ring configuration and conformation with ^{13}C chemical shifts and ^{13}C–^{13}C spin couplings, *J. Am. Chem. Soc.*, 109 (1987) 3501–3508.
120. J. Wu, P. B. Bondo, T. Vuorinen, and A. S. Serianni, ^{13}C–^{13}C Spin coupling constants in aldoses enriched with ^{13}C at the terminal hydroxymethyl carbon: Effect of coupling pathway structure on J_{CC} in carbohydrates, *J. Am. Chem. Soc.*, 114 (1992) 3499–3505.

121. M. J. Milton, R. Harris, M. A. Probert, R. A. Field, and S. W. Homans, New conformational constraints in isotopically (^{13}C) enriched oligosaccharides, *Glycobiology*, 8 (1998) 147–153.
122. B. Bose, S. Zhao, R. Stenutz, F. Cloran, P. B. Bondo, G. Bondo, B. Hertz, I. Carmichael, and A. S. Serianni, Three-bond C–O–C–C spin-coupling constants in carbohydrates: Development of a Karplus relationship, *J. Am. Chem. Soc.*, 120 (1998) 11158–11173.
123. J. L. Marshall, S. A. Conn, and M. Barfield, Vicinal ^{13}C–^{13}C spin-spin coupling constants of 1-butanols, *Org. Magn. Reson.*, 9 (1977) 404–407.
124. J. L. Marshall,, Carbon–carbon and carbon–proton NMR couplings. Applications to organic stereochemistry and conformational analysis, *Methods in Stereochemical Analysis* Vol.2. (1983) Verlag Chemie International, Deerfield Beach, FL.
125. H. Zhao, I. Carmichael, and A. S. Serianni, Oligosaccharide trans-glycoside $^3J_{\mathrm{CCOC}}$ Karplus curves are not equivalent: Effect of internal electronegative substituents, *J. Org. Chem.*, 73 (2008) 3255–3257.
126. D. Doddrell, I. Burfitt, J. B. Grutzner, and M. Barfield, Experimental and theoretical studies of vicinal ^{13}C–^{13}C coupling oonstants, *J. Am. Chem. Soc.*, 96 (1974) 1241–1243.
127. M. Barfield, I. Burfitt, and D. Doddrell, Conformational and substituent dependencies of ^{13}C–^{13}C coupling constants, *J. Am. Chem. Soc.*, 97 (1975) 2631–2634.
128. M. Barfield, S. A. Conn, J. L. Marshall, and D. E. Miiller, Experimental and theoretical studies of the conformational and substituent dependencies of vicinal ^{13}C–^{13}C coupling constants. Impinging multiple rear-lobe effects, *J. Am. Chem. Soc.*, 98 (1976) 6253–6260.
129. M. Barfield, J. L. Marshall, E. D. Canada, and M. R. Willcott, III, γ-Methyl substituent effect on vicinal coupling constants involving carbon-13, *J. Am. Chem. Soc.*, 100 (1978) 7075–7077.
130. J. L. Marshall, L. G. Faehl, and R. Kattner, The additivity of NMR carbon–carbon spin–spin coupling constants, *Org. Magn. Reson.*, 12 (1979) 163–168.
131. V. Wray, An INDO MO study of substituent effects upon $^3J_{\mathrm{CC}}$, *J. Am. Chem. Soc.*, 100 (1978) 768–770.
132. S. Berger, The conformational dependence of vicinal ^{13}C^{13}C spin–spin coupling constants in alicyclic compounds, *Org. Magn. Reson.*, 14 (1980) 65–68.
133. A. Y. Denisov, A. V. Tkachev, and V. I. Mamatyuk, Vicinal ^{13}C–^{13}C coupling constants in bicyclic monoterpenes, *Magn. Reson. Chem.*, 30 (1992) 95–100.
134. C. Thibaudeau, R. Stenutz, B. Hertz, T. Klepach, S. Zhao, Q. Wu, I. Carmichael, and A. S. Serianni, Correlated C–C and C–O bond conformations in saccharide hydroxymethyl groups: Parametrization and application of redundant ^{1}H–^{1}H, ^{13}C–^{1}H, and ^{13}C–^{13}C NMR *J*-couplings, *J. Am. Chem. Soc.*, 126 (2004) 15668–15685.
135. L. D. Hall and D. L. Jones, Observations on the electronegativity dependence of vicinal ^{19}F-^{1}H coupling constants, *Can. J. Chem.*, 51 (1973) 2925–2929.
136. S. Hamman, C. Béguin, C. Charlon, and C. Luu-Duc, Conformational studies on 2-fluoro-1, 2-disubstituted ethanes by NMR spectroscopy. Influence of electronegativity on vicinal proton–proton and fluorine–proton coupling constants, *Org. Magn. Reson.*, 21 (1983) 361–366.
137. C. Thibaudeau, J. Plavec, and J. Chattopadhyaya, A new generalized Karplus-type equation relating vicinal proton–fluorine coupling constants to H–C–C–F torsion angles, *J. Org. Chem.*, 63 (1998) 4967–4984.
138. C. F. Hammer and S. Chandrasegaran, Determination of $^3J_{\mathrm{HF}}$ and $^4J_{\mathrm{HF}}$ Karplus relationships for the φ and ψ angles of peptides using *N*-fluoroamides as models, *J. Am. Chem. Soc.*, 106 (1984) 1543–1552.
139. K. Bock and C. M. Pedersen, A study of ^{13}C–^{19}F coupling constants in glycosyl fluorides, *Acta Chem. Scand. B*, 29 (1975) 682–686.
140. M. Michalik, M. Hein, and M. Frank, NMR spectra of fluorinated carbohydrates, *Carbohydr. Res.*, 327 (2000) 185–218.

141. L. D. Hall, R. N. Johnson, J. Adamson, and A. B. Foster, Observations on the angular dependence of vicinal ^{19}F–^{19}F coupling constants, *Chem. Commun.*, (1970) 463–464.
142. S. Kurtkaya, V. Barone, J. E. Peralta, R. H. Contreras, and J. P. Snyder, On the capriciousness of the FCCF Karplus curve, *J. Am. Chem. Soc.*, 124 (2002) 9702–9703.
143. J. San Fabián and A. J. A. Westra Hoekzema, Vicinal fluorine–fluorine coupling constants: Fourier analysis, *J. Chem. Phys.*, 121 (2004) 6268–6276.
144. D. Doddrell, I. Burfitt, W. Kitching, M. Bullpitt, C.-H. Lee, R. J. Mynott, J. L. Considine, H. G. Kuivila, and R. H. Sarma, Karplus-type dependence of vicinal ^{119}Sn–^{13}C coupling, *J. Am. Chem. Soc.*, 96 (1974) 1640–1642.
145. S. Sternhell, Correlation of interproton spin–spin coupling constants with structure, *Quart. Rev.*, 23 (1969) 236–270.
146. L. D. Hall and L. Hough, Proton magnetic resonance spectra of 2,3,4-tri-*O*-acetyl-1,6-anhydro-D-hexopyranoses: A long-range coupling, *Proc. Chem. Soc.*, (1962) 382.
147. B. Coxon and L. D. Hall, The conformations of cyclic compounds in solution-II. Some 1,2-*O*-alkylidene-pyranose derivatives, *Tetrahedron*, 20 (1964) 1685–1694.
148. J. A. Heitmann, G. F. Richards, and L. R. Schroeder, Carbohydrate orthoesters. III. The crystal and molecular structure of 3,4,6-tri-*O*-acetyl-1,2-*O*-[1-(*exo*-ethoxy)ethylidene]-α-D-glucopyranose, *Acta Cryst.*, B30 (1974) 2322–2328.
149. T. Ito, Synthesis and nuclear magnetic resonance spectrum of 3′,4′,6′-tri-*O*-acetyl-2-(methylthio)-D-glucopyrano[2′,1′:4,5]-2-thiazoline, *Can. J. Chem.*, 44 (1966) 94–97.
150. M. Barfield, Angular dependence of long-range proton coupling constants across four bonds, *J. Chem. Phys.*, 41 (1964) 3825–3832.
151. B. Coxon, Model parameters for the analysis of skew conformations of carbohydrates by PMR spectroscopy, *Carbohydr. Res.*, 13 (1970) 321–330.
152. L. D. Hall and J. F. Manville, Studies of carbohydrate derivatives by nuclear magnetic double-resonance. Part II. A determination of the signs of proton–proton coupling-constants of saturated and unsaturated carbohydrates, *Carbohydr. Res.*, 8 (1968) 295–307.
153. V. F. Bystrov and A. U. Stepanyants, The stereochemical significance of the long-range proton spin coupling constant of the σ-fragment H–C–C–C–H, *J. Mol. Spectrosc.*, 21 (1966) 241–248.
154. M. Barfield, DFT/FPT studies of the structural dependencies of long-range ^{1}H,^{1}H coupling over four bonds ^4J(H,H’) in propanic and allylic systems, *Magn. Reson. Chem.*, 41 (2003) 344–358.
155. M. G. Constantino, V. Lacerda Jr., G. V. J. da Silva, L. Tasic, and R. Rittner, Principal component analysis of long-range ‘W’ coupling constants of some cyclic compounds, *J. Mol. Struct.*, 597 (2001) 129–136.
156. K. C. Ramey and J. Messick, Stereospecific long range couplings in the NMR spectra of substituted 1,3-dioxanes, *Tetrahedron Lett.*, (1965) 4423–4428.
157. E. A. Larsson, J. Ulicny, A. Laaksonen, and G. Widmalm, Analysis of NMR *J* couplings in partially protected galactopyranosides, *Org. Lett.*, 4 (2002) 1831–1834.
158. O. Kwon and S. J. Danishefsky, Synthesis of asialo GM$_1$. New insights in the application of sulfonamidoglycosylation in oligosaccharide assembly: Subtle proximity effects in the stereochemical governance of glycosylation, *J. Am. Chem. Soc.*, 120 (1998) 1588–1599.
159. J. C. Jochims, G. Taigel, and W. Meyer zu Reckendorf, Fernkopplungen bei glucopyranosen in der 1-C-konformation, *Tetrahedron Lett.*, (1967) 3227–3234.
160. B. Coxon, H. J. Jennings, and K. A. McLauchlan, Structures and conformations of some D-*glycero*-pent-2-enopyranosyl derivatives and determination of the relative signs of some associated long-range proton coupling constants, *Tetrahedron*, 23 (1967) 2395–2412.
161. M. Barfield, R. J. Spear, and S. Sternhell, Interproton spin–spin coupling across a dual path in five-membered rings, *J. Am. Chem. Soc.*, 93 (1971) 5322–5327.

162. M. Barfield and S. Sternhell, Conformational dependence of homoallylic H–H coupling constants, *J. Am. Chem. Soc.*, 94 (1972) 1905–1913.
163. R. Stenutz, Scalar coupling constants – $^3J_{HH}$ Haasnoot, $^3J_{HH}$ calculation, http://www.stenutz.eu/conf/jhh.html.
164. R. Stenutz, Scalar coupling constants – $^3J_{HH}$ Pachler, $^3J_{HH}$ calculation, http://www.stenutz.eu/conf/pachler.html.
165. R. Stenutz, Scalar coupling constants, hetero- and homo-nuclear coupling constant calculation, http://www.stenutz.eu/conf/karplus.html, http://www.casper.organ.su.se/ke3690/karplus.html. The latter format does not require an active network connection, as it can be saved to the computer desktop, and run from there.
166. R. Stenutz, Scalar coupling constants, β-ribose, http://www.stenutz.eu/conf/rib2.html.
167. R. Stenutz, Scalar coupling constants, β-2-deoxyribose (2-deoxy-*erythro*-pentose), http://www.stenutz.eu/conf/rib.html.
168. R. Stenutz, Scalar coupling constants, coupling constants related to the ω torsion, http://www.stenutz.eu/conf/hm_rscalc.html.
169. R. Stenutz, Hydroxymethyl groups, conformation of hydroxymethyl groups determined from $^3J_{H\text{-}5,H\text{-}6}$, http://www.stenutz.eu/conf/hm_bock.html.
170. K. Bock and J. Ø. Duus, A conformational study of hydroxymethyl groups in carbohydrates investigated by ^{1}H NMR spectroscopy, *J. Carbohydr. Chem.*, 13 (1994) 513–543.
171. R. Stenutz, Hydroxymethyl groups, conformation of hydroxymethyl groups from $^3J_{H\text{-}5,H\text{-}6}$, http://www.stenutz.eu/conf/hm_div.html.
172. R. Stenutz, Chemical shifts, ^{13}C glycosylation shifts and conformation, http://www.stenutz.eu/conf/hm_div.html.
173. K. Bock, A. Brignole, and B. W. Sigurskjold, Conformational dependence of ^{13}C nuclear magnetic resonance chemical shifts in oligosaccharides, *J.C.S. Perkin Trans. II*, (1986) 1711–1713.
174. P. Atkins and J. de Paula Living graphs, Karplus equation, http://www.oup.com/uk/orc/bin/9780199280957/01student/graphs/graphs/lg_14.14.html.
175. P. Atkins and J. de Paula, *Physical Chemistry for the Life Sciences*, Chapter 14 (2005) Oxford University Press, Oxford.
176. A. Navarro-Vázquez, J. C. Cobas, and F. J. Sardina, A graphical tool for the prediction of vicinal proton–proton $^3J_{HH}$ coupling constants, *J. Chem. Inf. Comput. Sci.*, 44 (2004) 1680–1685.
177. J. C. Cobas, MestReJ: A free tool for the prediction of vicinal proton–proton $^3J_{(HH)}$ coupling constants, http://nmr-analysis.blogspot.com/2008/10/mestrej-free-tool-for-prediction-of.html(includes a link to download the program).
178. M. Barfield and W. B. Smith, Internal H–C–C angle dependence of vicinal ^{1}H–^{1}H coupling constants, *J. Am. Chem. Soc.*, 114 (1992) 1574–1581.
179. W. B. Smith and M. Barfield, Predictions of ^3J(HH) near 180° – Reparameterization of the sp^3–sp^3 equation, *Magn. Reson. Chem.*, 31 (1993) 696–697.
180. W. B. Smith and M. Barfield, Predictions of ^3J(HH) near 180° – Reparameterization of the sp^3–sp^3 equation, erratum, *Magn. Reson. Chem.*, 34 (1996) 740.
181. P. Padrta and V. Sklenář, Program Mulder – A tool for extracting torsion angles from NMR data, *J. Biomol. NMR*, 24 (2002) 339–349.
182. K.-P. Neidig, M. Geyer, A. Goerler, C. Antz, R. Saffrich, W. Beneicke, and H. R. Kalbitzer, Aurelia, a program for computer aided analysis of multidimensional NMR spectra, *J. Biomol. NMR*, 6 (1995) 255–270.

ADVANCES IN CARBOHYDRATE CHEMISTRY AND BIOCHEMISTRY, VOL. 62

COMPUTATIONAL STUDIES OF THE ROLE OF GLYCOPYRANOSYL OXACARBENIUM IONS IN GLYCOBIOLOGY AND GLYCOCHEMISTRY

BY DENNIS M. WHITFIELD

Institute for Biological Sciences, National Research Council of Canada, 100 Sussex Drive,
Ottawa, ON K1A 0R6, Canada

I. Introduction 83
  1. Importance of Glycopyranosyl Oxacarbenium Ions 83
II. Galactopyranosyl Oxacarbenium Ion as an Illustrative Model 84
  1. Background 84
  2. Isolated Cations—Ring and C-5–C-6 Side-Chain Conformations 89
  3. Facially Selective Methanol–Oxacarbenium Ion Complexes 98
  4. The Orientations and Conformations of Side Chains at C-2, C-3, C-4, and C-5 109
  5. The Role of C-2–O-2 Rotations, Including Neighboring-Group Participation 118
  6. The Role of Proton Transfer in the Transition State for Glycosylation Reactions 130
  7. Differences in Ionization Between α- and β-Donors 136
III. Conclusions and Future Directions 140
  1. Summary of Glycosylation Reaction Mechanisms 140
  2. Further Calculations Based on Existing Methodology 145
  3. Future Calculations Requiring Methodology Development 145
  4. Experimental Studies of Glycosylation 146
  Acknowledgments 147
  References 147

I. INTRODUCTION

1. Importance of Glycopyranosyl Oxacarbenium Ions

Unraveling the mechanistic details of the myriad of glycosyl processing enzymes (GPEs)[1–4] is a major endeavor of numerous scientists since these enzymes are essential to many industries, ranging from such biomass utilization industries as bioethanol and paper

ISBN: 978-0-12-374743-3
DOI: 10.1016/S0065-2318(09)00004-3

© 2009 Elsevier Inc. All rights reserved.

production through the varied fermentation processes of the food and beverage industries, to the production of aminoglycoside antibiotics and carbohydrate conjugate vaccines by the pharmaceutical industries.[5] Behind all this glycobiology are the decades of developments by carbohydrate chemists to isolate, identify, and synthesize the substrates and products of many of these enzymes. Such studies are an integral part of elucidating the fundamental structure–function relationships that underlie the practical application of these compounds.[6–8] Many of these processes involve the formation or breaking of glycosidic bonds. Consequently, an understanding of the formation and breaking of glycosidic linkages is at the core of both glycobiology and glycochemistry.

With only a few exceptions, both the formation and breaking of glycosidic linkages involve processes that proceed through species having a high degree of oxacarbenium ion character. Thus, in the chemistry of, glycofuranosyl and glycopyranosyl groups, as the two commonest ring forms of sugars, an understanding of oxacarbenium ions is a very important area of research. Because of the transient nature of oxacarbenium ions, their properties are very difficult to establish experimentally.[9,10] For this reason one of the strategies for establishing their structures and their conformational preferences is to perform quantum mechanical (QM) studies. QM is the computational method of choice, since the ions by definition contain a trigonal carbon atom and one must consider subtle charge-delocalization effects, and neither factor is readily amenable to any other computational method. In the past 10 or so years computational resources and software have become available that allow for the practical study of such species.[11,12] Since a number of these studies have been conducted in the author's laboratory in Ottawa, this chapter presents a study of the D-galactopyranosyl system, prepared specifically for this contribution. It should enable those readers having access to the appropriate software and hardware, to perform their own studies of sugars of interest. Here the results for the galactopyranosyl system are compared and contrasted with published results for other carbohydrates, and in this way pertinent examples from the literature are presented. A diligent attempt has been made to provide both recent and classical references to the fundamental principles and relevant experimental studies. No detailed understanding of computational chemistry is expected of the reader, but some familiarity with either or both of chemical glycosylation reactions and GPE-catalyzed reactions is helpful.

II. GALACTOPYRANOSYL OXACARBENIUM ION AS AN ILLUSTRATIVE MODEL

1. Background

In what is generally considered a classic paper in carbohydrate chemistry, Edwards provided compelling evidence that galactopyranosides are hydrolyzed faster than their *gluco* counterparts.[13] In a variety of other situations this higher reactivity seems to be general; galactopyranosyl donors are almost always more reactive than glucopyranosyl donors having the same protecting and leaving groups, in chemical glycosylations under similar reaction conditions.[14] The simplest explanation of this trend is to assume that the corresponding galactopyranosyl oxacarbenium ion is more reactive than its glucopyranosyl isomer.[15] This expectation was originally ascribed to greater steric hindrance at the anomeric center from the axial substituent at O-4 (Gal) as compared to the equatorial substituent at O-4 (Glc). Subsequent experimental evidence argues against a steric origin of this difference in reactivity.[16] Further studies suggest a through-space stabilizing electronic effect to explain this reactivity difference,[17] including an effect on the facial selectivity of nucleophilic attack at C-1, the anomeric carbon atom (see Scheme 1).[18–20] It is anticipated that further insights into these observations will become apparent during these studies.

The first question to decide is which derivative of galactose should be studied. Naively, the fully hydroxylated cation **1** might be chosen, since it is clearly the prototype of all related cations, and should be the ion formed by GPEs that form or degrade galactopyranosides (see Scheme 2). However, there are several problems with this choice, all relating to the conformations of the pendant hydroxyl groups. QM calculations of hydroxylated sugars consistently demonstrate rings of $\mathrm{O-H\ldots O}$ groupings as minimum-energy species.[21–23] The total energy is typically lower the more hydroxyl groups there are involved in the rings. There is even recent experimental evidence that supports the existence of these ring structures for isolated sugars in the gas phase.[24–27] Many groups describe such interactions as hydrogen bonds (H-bonds), even though the associated bond lengths and bond angles are at the edge of the accepted norms for H-bonding.[28–30] Recent QM calculations using the atoms in molecules (AIM) approach to study this phenomenon do not find the necessary bond-critical or ring-critical points that would allow these interactions to be considered H-bonds.[31,32] An experimental determination of the electron density of sucrose crystals by X-ray diffraction methods finds the expected bond- and ring-critical points associated with long-range H-bonding, but not those among vicinal ring hydroxyl groups, in agreement with the data of Klein et al.[33] Further, the trigonal anomeric carbon atom is expected to distort the pyranosyl ring in the oxacarbenium ions toward the half-chair ring conformations, thus deviating from the nearly perfect $^4C_1$ chair conformations of most D-galactopyranosides.[34] Consequently, it could be anticipated that true, in the sense that such interactions have the requisite critical points in AIM studies, intramolecular H-bonding, such as found with 1,3-diaxial hydroxyl groups might occur.[35] The best studied of such interactions is the strong H-bonding between O-4 and O-2 in 1,6-anhydro-β-D-glucopyranose.[36] Both of these hydroxyl–hydroxyl interactions tend to obscure the questions of

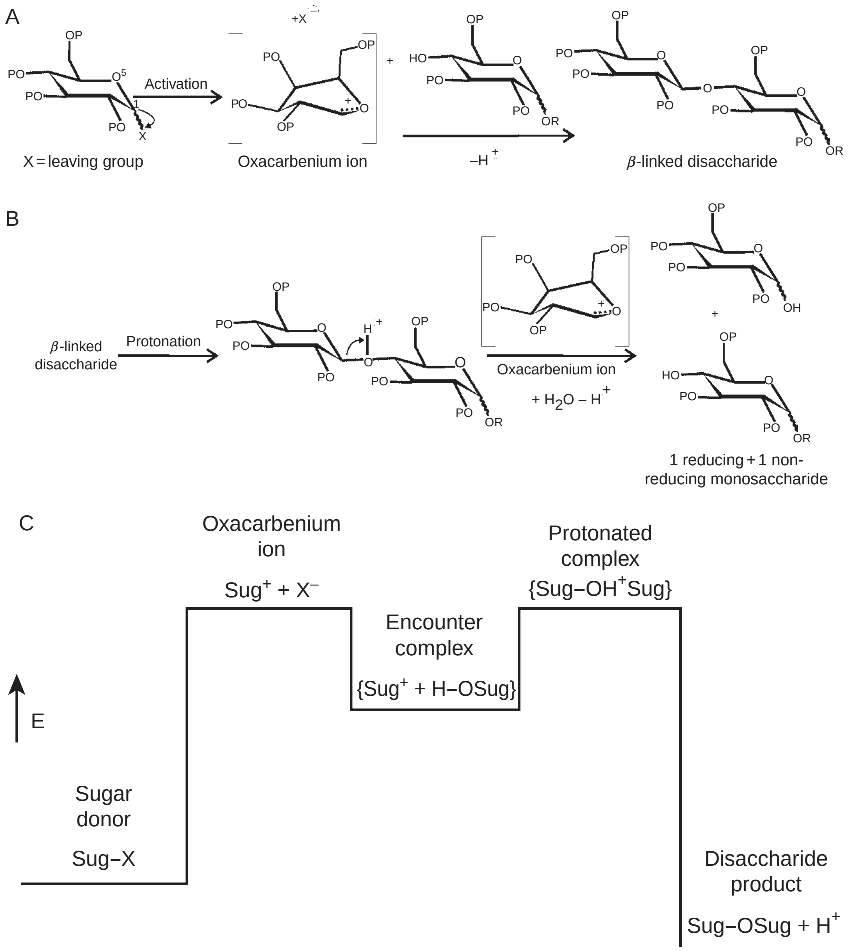
A
Activation
X = leaving group
+X⁻
Oxacarbenium ion
−H⁺
β-linked disaccharide
B
β-linked disaccharide
Protonation
Oxacarbenium ion
+ H₂O − H⁺
1 reducing + 1 non-reducing monosaccharide
C
Oxacarbenium ion
Sug⁺ + X⁻
Protonated complex
{Sug–OH⁺Sug}
Encounter complex
{Sug⁺ + H–OSug}
E
Sugar donor
Sug–X
Disaccharide product
Sug–OSug + H⁺

SCHEME 1. (A) Top, A typical glycosylation reaction that proceeds by activation of a leaving group attached to C-1 of a suitably protected (P) glycopyranosyl donor, which leads via transient formation of an oxacarbenium ion that has considerable double-bond character between C-1 and O-5, and a positive charge, followed by nucleophilic attack and loss of a proton leading in this example to a *β*-linked disaccharide. Activation can be spontaneous, but usually requires a Lewis acid promoter. (B) Middle, Similarly protonation of the same disaccharide leads to breaking of the glycosidic linkage via the same glycopyranosyl oxacarbenium ion and, in the presence of water, to the formation of a reducing and a non-reducing monosaccharide. (C) Bottom, schematic bar graph of energy (E) versus reaction-coordinate for a typical glycosylation reaction. Sug–X is equivalent to the donor in (A) and SugOH to the acceptor in (A). Relative energies are arbitrarily chosen and may vary from case to case.

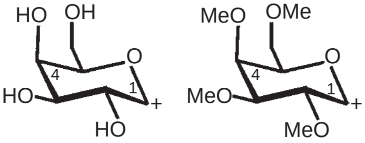

1 **2**

Scheme 2. Chemical structure of fully hydroxylated **1** and its tetra-*O*-methyl analogue **2** the D-galactopyranos-1-yl oxacarbenium ion.

intrinsic reactivity that the researcher is trying to address. Further, most studies have as an ultimate objective the details of either a GPE-catalyzed or a purely chemical reaction. In the former case most, if not all, of the hydroxyl groups act as either H-bond acceptors or donors, and frequently both, to active-site residues of the enzyme.[37] In the case of chemical glycosylation, most of the hydroxyl groups are derivatized with protecting groups. To achieve either of these objectives it is therefore necessary to consider non-isolated hydroxyl groups. For all of these reasons we have chosen to study 2,3,4,6-tetra-*O*-methyl-D-glycopyranosides instead of the fully hydroxylated species. In this case, the methyl group in ion **2** (Scheme 2) can be viewed as either a prototypic protecting group or as a crude model of an enzyme-complexed sugar.

In many cases, after prototypic studies such as the current ones, more-detailed studies should include the actual protecting groups used in the chemical reaction, or the active-site residues thought to be important for the GPE-catalyzed reaction. At present, such studies are at the cutting edge of purely QM resources and are typically done by treating the enzyme with a lower level calculation, such as molecular mechanics (MM) that is to say, QM-MM studies.[38] For MM calculations it is necessary to have a force field that accurately describes the molecules, in this case carbohydrates and proteins. The development of force fields applicable with carbohydrates is an active area of research.[39–41] For many purposes, such as studying the effect of solvation and counterions it is beneficial to have a force field that allows for the time-dependence of conformations, and this entails molecular dynamics (MD).[42,43] A final caveat is that few, if any, of the current force fields have been simultaneously parameterized for carbohydrates and proteins.[44,45] Thus there are a number of challenges to be overcome before these QM-MM studies become routine.

No QM study of a glycopyranosyl oxacarbenium ion with a full complement of ‘‘normal’’ protecting groups appears yet to have been done. The Ottawa group has performed some limited studies, varying the protecting group at O-2.[46] Some relatively rigid fused rings, such as isopropylidene and benzylidene protecting groups, have been considered, but otherwise methyl or acetyl as prototypic protecting groups have been used in the calculations.[47,48] This is due in part to the need for increased computational resources, as QM calculations using conventional software scale as n^3, where n is the number of atoms. It is also attributable to the multiple minima problem, posed by having flexible protecting groups, which can in principle populate large numbers of conformations having small energy differences. Addressing this problem of multiple minima in a realistic way is a current challenge for computational chemists. For example, such protecting groups as benzyl, allyl, or propargyl all have two C–O bonds and a spC- or $sp^2C–Csp^3$ bond which, even considering only staggered minima,[49–50] leads to more conformers (27^n where n is the number of such protecting groups) than can be readily considered by one-at-a-time calculations.

Returning to the QM study of **2**, the next decision is what level of QM to use. There are notably the Hartree–Fock (HF) or density functional theory (DFT) methods, and within each of these there has to be determined what basis set to use and what type of each to use. This is a very challenging question, and even with access to very large computer hardware resources the use of the biggest basis set with the highest level of theory possible may not be correct. Full discussion of this dilemma is outside the scope of this chapter, but the simple answer is that it depends on the question the researcher is interested in. For example, if the user is mostly interested in ring conformations and side-chain conformations (the present objective), then the standard commercial packages should be adequate. If however the interest is in more subtle effects, as for example through-space interactions between protecting groups and the anomeric center, then a proper preliminary study to select the appropriate QM method is recommended. Certainly for such charged systems as oxacarbenium ions, a moderate to large basis set is necessary, with at least some polarization and diffuse functions such as 6–31+G(d,p) as the minimum basis to obtain reliable results.[51] Recent QM studies on glucopyranose provide compelling evidence that each extension: adding additional polarization (d,p) to (2d,2p), adding diffuse functions 1+G to 1++G, and adding extra valence functions 6–31 to 6–311 all assist, and thus the basis set 6–311++G(2d,2p) is recommended for carbohydrates.[52] In fact, a number of current QM studies of carbohydrates use this basis set.[53,54] Since oxacarbenium ions also exhibit charge delocalization and hence can be expected to be sensitive to electron correlation, HF methods with some level of correlation such as the popular Møller–-Plesset approach are recommended.[55–57] Since DFT intrinsically includes some electron correlation, many groups use one of the variants of DFT. A number of deficiencies in DFT have been pointed out, including a failure to properly account for such medium-range interactions as 1,3 interactions.[58–60] It is hoped that these problems can be solved, and there is some evidence that newer functionals are indeed better.[61,62]

Two current reports have studied model systems for glycopyranosides, namely 2-methoxytetrahydropyran[63] and 2-ethoxytetrahydropyran,[64] with special emphasis on determining precisely the anomeric effect. To achieve these goals, a so-called complete basis set (CBS) calculation was performed in the gas phase at 0 K. To reach agreement with experiment, the standard corrections of including the zero point energy (ZPE), a temperature correction to room temperature, and estimating the entropy to get $\triangle G^{298}$ were added. However, even this was not sufficient, and an estimate of the solvation energy also had to be included to obtain high agreement with experiment. These works point out the deficiencies of several of the standard QM procedures.[65] Since it is scarcely feasible to calculate most chemical species at this high level, it must always be realized that most calculations contain errors and the temptation to overinterpret small energy differences should be resisted. The intention of the calculations in the author's laboratory has always been to identify trends which can in turn be manipulated by synthetic chemists to improve glycosylation efficiency and/or eliminate unwanted side reactions.

Since one of the early collaborators had considerable experience with the DFT program Amsterdam density functional (ADF), our group has mostly used this program. In a few cases results were compared with a number of other QM programs utilizing roughly equivalent basis sets, and no substantial differences in geometries or relative energies for minima were found.[66] However, great care should be taken, as already noted. The calculations currently use the TPZ basis set with the local part of the V_{xc} potential (LDA) described using the VWN parametrization,[67] in combination with the gradient corrected (CGA) Becke's functional[68] for the exchange and Perdew's function for correlation (BP86).[69,70] The ADF program used is mounted on a standard UNIX/LINUX-based PC cluster, that uses eight processors for standard jobs. It is maintained in Ottawa by the organization's computer-support group. For scientists for whom computational chemistry is not their sole project, it is highly recommended that they use standard QM packages operating on computers that are maintained by computer professionals, otherwise such scientists may spend an inordinate amount of time managing the computer and not doing calculations.

2. Isolated Cations—Ring and C-5–C-6 Side-Chain Conformations

For the current study the next question is how to choose a starting geometry, since an initial set of coordinates is needed for any QM calculation. Operationally, the simplest approach is to draw the structure of interest, in this instance starting with a 2,3,4,6-tetra-*O*-methyl-D-galactopyranoside, such as the methyl glycoside of either anomer and doing a simple MM optimization, which should find the $^4C_1$ chair minimum.

Then, the glycosidic oxygen and the attached atoms can be deleted. This process can be done with any commercial MM package or one of the many MM programs available over the Internet. The only potential complication is that the coordinates must be saved in a format that the QM program will accept as input. The Ottawa group usually prefers to do QM calculations using internal coordinates, where a set of the bond lengths, bond angles, and torsion angles are used to define the molecule's geometry, instead of the more usual *xyz* Cartesian coordinates. Internal coordinates allow for such operations as side-chain optimization since, for example, the torsion angle to be varied can be immediately found in the input file. The same process can be done using Cartesian coordinates by making use of the *xyz* coordinates of the four atoms that define the torsion angle of interest. Exact procedures can usually be found in the operation manuals of most QM programs or by searching online. Internal coordinates are also reported to lead to faster geometry optimization, and since such optimization is often the rate-limiting factor in QM studies, this has obvious advantages.[71]

Scientists rarely work in totally unexplored fields, and often something is known about the expected answer at the outset. In this case, since the expected trigonal geometry at C-1 in the cation will lead to a significant flattening of the ring, chemical intuition and/or a perusal of suggestions in the literature suggests that a $^4H_3$ half chair is a highly plausible ring conformation for **2**. It could be also surmised that the inverted $^3H_4$ half chair might be populated, since O-4 is of opposite configuration to most common pyranosides.[72,73] Similarly, there have been reports for other 2,3,4,6-tetra-*O*-methyl-D-glycopyranosyl oxacarbenium ions, notably the *gluco* (**3**) and *manno* (**4**) isomers. For both **3** and **4**, two minimum-energy ring conformations have been reported.[74,75] In both cases a $^4H_3$ half-chair conformation plus for **3** a ring-inverted $^5S_1$ skew boat and for **4** a ring inverted ^3E envelope conformation have been reported; see Fig. 1. The ^3E conformation is adjacent to the exactly inverted $^3H_4$ half chair, whereas $^5S_1$ is on the equator and more closely related to $^5H_4$, in conformational space; see Fig. 2.

Following from Hendrickson's original proposal, the conformations of 6-membered rings can be plotted as 3D spheres or as 2D projections of the 3D spheres. These 2D representations are sometimes called Stoddart diagrams, as they were first introduced to carbohydrate chemistry in Stoddart's classic book on carbohydrates.[76] A full discussion of this topic is outside the scope of this chapter, and the reader is referred to various books and papers.[77–79] Both representations are used here as necessary. A canonical vector representation of 6-membered ring conformations we developed is explained later in more detail, but one of its advantages is that is allows all 38 IUPAC-defined conformations of 6-membered rings to be described by idealized geometries; see Fig. 2.[80,81]

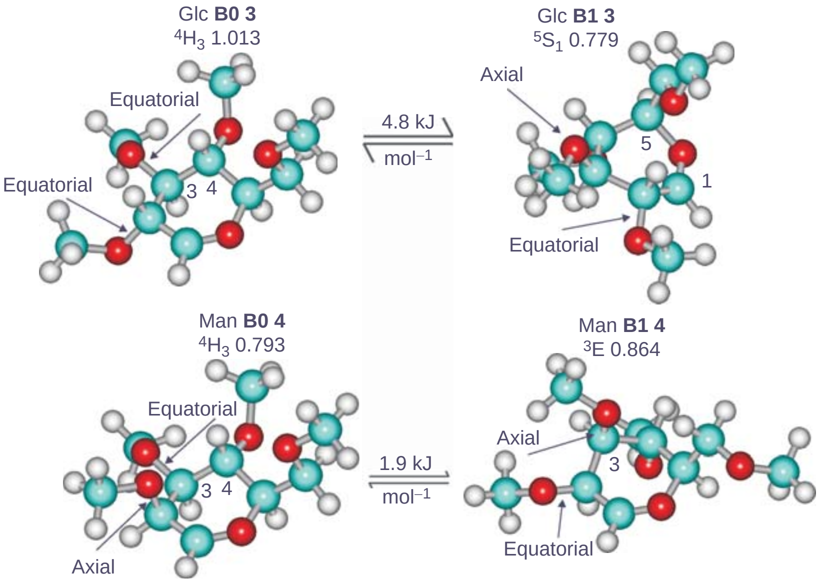

FIG. 1. ADF–DFT (DPZ-frozen core)-optimized conformers of the *gluco* (**3**) and *manno* (**4**) isomers of **2**. Note the quasi-equatorial orientation of C-2–O-2 in all but **4 B0** and the *syn* CH-2-C-2–O-2C(H_3) conformation in all cases. The canonical vector with the highest coefficients is also shown. A coefficient of 1.0 equals a perfect match to that particular idealized conformation.

Hence this study starts with five different starting geometries of **2**, namely: the one drawn and four derived from those idealized $^4H_3$, $^3H_4$, ^3E, and $^5S_1$ coordinates that have the *O*-methyl and hydroxymethyl substituents added to the tetrahydropyran ring in the D-*galacto* configuration, or by modification of the configurations of the literature results. These additions can usually be done with a MM program. It is helpful, but not strictly necessary, to partially optimize the new side-chain conformations to approximate the expected values, otherwise spurious results can be obtained in the subsequent QM geometry optimization. For example, in this case C–O and O–CH_3 bond lengths should be in the 1.35–1.45 Å range and the corresponding C–O–C bond angle near the tetrahedral value. Table I shows a part of a typical ADF input file, indicating the methods used.

Scheme 3 shows the five starting geometries in the top row and the four QM-optimized geometries in the middle row. The hand-drawn geometry and the $^4H_3$ derived geometry optimized to very similar conformations. These four optimized species were then characterized by frequency calculations. This consists of taking the second derivative of the energy in the three *xyz* dimensions of positional space.

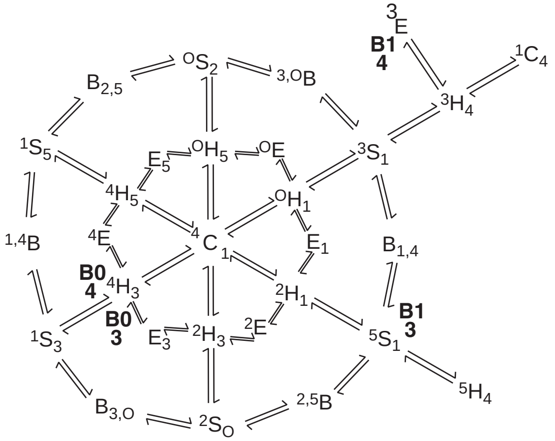

FIG. 2. 2D projection of the top half of the 3D spherical representation of the conformations of pyranosyl rings. The 12 boats and skew boats are on the equator (outer circle) and 12 of the half chairs and envelopes are on the inner circle. One chair is at the center (pole). The extensions to the upper right show a small portion of the bottom half. The approximate positions in conformational space of the **B0** and **B1** conformations of **3** and **4** are indicated.

There are a number of computational approaches to doing frequency calculations, but all share the characteristic of being computationally demanding. This is one of the most CPU-intensive parts of the overall process. Three of the initial four optimized structures had all positive frequencies and hence are minima, whereas the fourth had several negative frequencies. Several attempts were made to find a minimum near this conformation. First, the *xyz* coordinates of the atoms having the largest negative frequency were moved to new input values by using the coefficients of the imaginary frequency as guides, and were then reoptimized, but the resulting conformation was not lower in energy. Secondly, an intrinsic reaction coordinate (IRC) calculation was done, using default values in both the forward and reverse directions. IRC calculations are designed to start from transitions states (TSs) and follow the imaginary (negative) frequency to the local minimum. However, in this instance neither resultant conformation was lower in energy, and so this conformation was omitted from the list of candidates.

Next, the ω_H (H-5-C-5–C-6-O-6) dihedral angle was systematically varied, starting from the first found minimum for each of the $^4H_3$, ^3E, and $^5S_1$ conformations. The variation is straightforward in internal coordinates, since this torsion angle is in the coordinate file. So all that needs to be done is define this torsion angle as a variable and set the starting value, which is usually the value found as the minimum and the

TABLE I
Part of Standardized Optimization Input File

```
GEOVAR (This means to perform a full Geometry Optimization using default values)
END
BASIS (The basis set for DFT taken from the ADF library)
type TZP
core none (None of the inner core orbitals are frozen as is sometimes done)
END
XC (exchange corrections)
LDA SCF VWN (Local-Density Approximation, Self-Consistent Field)
END
METAGGA (exchange)
SOLVATION (A version of COSMOS)
   Surf Klamt
   Solv eps=9.03 rad=2.4 emp=0.0 cav0=1.321 cav1=0.0067639 (parameterized to CH2Cl2)
   Charged method=CONJ conv=1e-6 iter=300 omega=1.0
   C-Mat POT
   radii
   C=1.989 (the size of the atoms is necessary for the COSMOS procedure)
   O=1.7784
   H=1.3
END
SYMMETRY tol=0.001
INTEGRATION 6.5 6.0 6.5 (This is a grid size, the default is 5.0 therefore the number of points has been
increased for higher precision. In ADF this variable greatly affects the CPU time and the accuracy)
A1FIT 10.0
```

Comments in parentheses are not in the actual file.

end value, which in this case is the starting value plus 360° and the number of increments. Trial and error in this case led to the use of 60 increments for such studies, and hence each point of the calculation varies the torsion angle by 6°; see Fig. 3 for a representative example. In Fig. 3, some points near the first maximum may be anomalous (near $\omega_H = -120°$) and suggest the use of a smaller step size or a higher level of calculation to find this maximum accurately. Since this study is interested in finding minima, the reported calculation is adequate. With eight processors per job, these 60 points took about 72 CPU hours to calculate. Similar calculations found lower-energy species for the ${}^3E$ conformation, but not for the ${}^5S_1$ case. As shown in Fig. 3, two minima are lower in energy then the starting conformation, which had ω_H approximately equal to 180°. This C-5–C-6 (ω_H =180°) conformer is often called *gg* as O-6 is *gauche* to both C-4 and O-4. For D-galactopyranosyl species, with O-4 axial or quasi-axial, this ω_H conformation creates a unfavorable steric interaction between O-6 and O-4 (the Hassel–Ottar effect),[83] see Fig. 4. Thus, it is not surprising that both

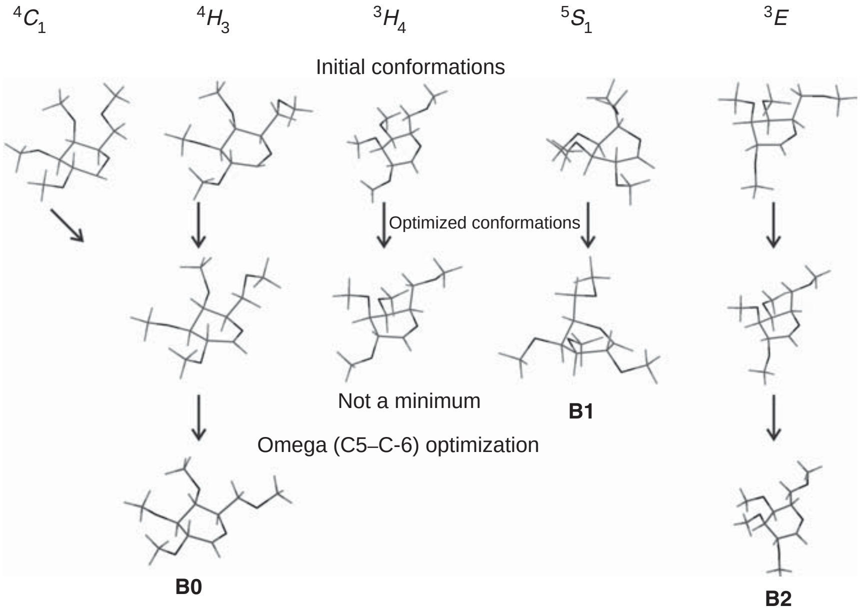
$^4C_1$
$^4H_3$
$^3H_4$
$^5S_1$
^3E
Initial conformations
Optimized conformations
Not a minimum
B1
Omega (C5–C-6) optimization
B0
B2

SCHEME 3. Five sources of input conformations for **2** along upper row: far left, drawn structure $^4C_1$,$^4H_3$ and $^3H_4$ taken from idealized geometries,[82] $^5S_1$ from *gluco* configured analogues of **2**[80,81] and ^3E from *manno* configured analogues, by *in silico* modification. Middle row: after initial optimization and frequency calculations it was found that the $^3H_4$ conformation was not a minimum, even after multiple optimizations (see text for details). Systematic ω_H variation found lower energy conformers for $^4H_3$ and ^3E but not for $^5S_1$ conformations, lower row.

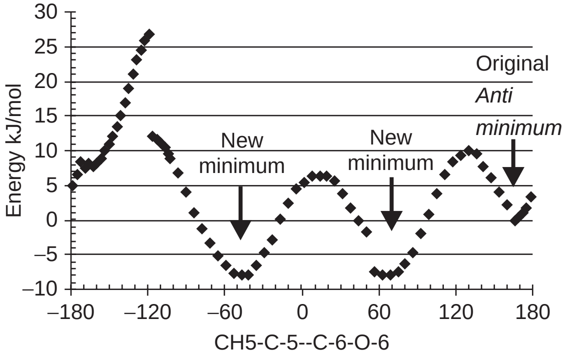

FIG. 3. Rotation about the CH-5-C-5–C-6-O-6 (ω_H) torsion angle of **2 B0**, starting from the *anti* minimum and moving to higher numbers. Note the two new minima near *gauche*$^-$ and *gauche*$^+$ conformations. The original *anti* minimum is arbitrarily set to 0.0 kJ mol^{-1} to show the energy difference of the new minimum.

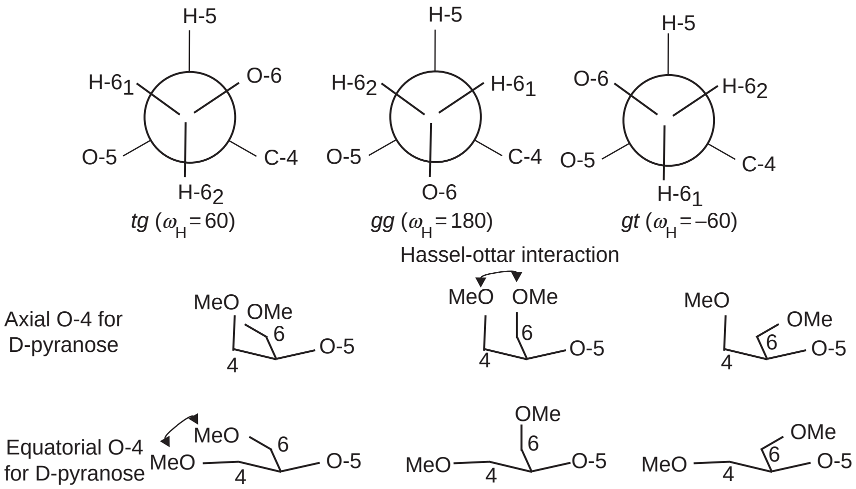

FIG. 4. Top, Newman projection of the three rotamers about C-5–C-6 of a D-glycopyranose. Middle, schematic representations of the O-6–O-4 interactions in the various C-5–C-6 rotamers for axial substituents at C-4. Bottom is the same as the middle one but for a equatorial substituent at C-4.

of the other two staggered conformers are lower in energy. After reoptimization and correction for ZPE the *gt* conformer having O-6 *gauche* to O-5 and *trans* to C-4 ($\omega_H = -40.5°$) is slightly lower in energy (4.2 kJ mol^{-1}) than the *tg* conformer having O-6 *trans* to O-5 and *gauche* to C-4 ($\omega_H = 67.7°$). This is reasonable since this conformer allows more-efficient electron donation to the vacant p-orbital at C-1 than the *tg* conformer.[84] For **3 B0**, the relative energies for the *gt, gg*, and *tg* conformers are 0.0, 5.9 and 18.0 kJ mol^{-1}. Similarly for **3 B1** the values are 0.0, 3.3, and 8.9 kJ mol^{-1}, for **4 B0** 0.0, 3.8, and 17.4 kJ mol^{-1}, and for **4 B1** 0.0, 9.4, and 8.1 kJ mol^{-1} suggesting that this effect is general.

For exact ω_H values and other geometric parameters for these species, see Table II. Following from the terminology used with other glycopyranosyl oxacarbenium ions, this conformation is called **B0**. The $^5S_1$ inverted conformer is called **B1**, and in this case, since three conformers were found and not the usual two, the $^3H_4$ conformer is termed **B2**. For both **B1** and **B2**, O-4 is quasi-equatorial and the classic Hassel–Ottar analysis of ω_H fails. This is why it was important to check all three ω_H minima. In this case **B1** has $\omega_H = -159.3°$ as the minimum and **B2** has $\omega_H = -35.1°$ as its minimum.

The canonical vector representation allows an easy as well as exact description of the ring conformations of these species; see Table II. Each conformer is characterized by its projection on to idealized Chair (**C**), Boat (**B**), and Skew boat (**S**) conformations

TABLE II

Selected Geometric Parameters and Relative Energies of All Species of 2

Species	C-1–O-5	O_M–C-1	τ_5	ω_H	CH-2-C-2–O-2-C(H_3)	Chair	Boat	Skew Boat	Intermediate	Energy
Gal **B0**[a]	1.26	–	−5.5	67.7	27.3	$^{4}C_{1}$ 0.587	$^{2,5}B$ 0.023	$^{1}S_{3}$ 0.489	**$^{4}H_{3}$ 0.978**	4.2
Gal **B0**	1.26	–	−3.8	−40.5	27	$^{4}C_{1}$ 0.566	$^{2,5}B$ 0.049	$^{1}S_{3}$ 0.497	**$^{4}H_{3}$ 0.994**	0.0[b]
Gal **B1**	1.27	–	−8.7	−159	−33	$^{1}C_{4}$ 0.261	$^{0,3}B$ 0.012	**$^{5}S_{1}$ 0.803**	–	10.4
Gal **B2**	1.26	–	1.6	−35.1	−10.2	$^{1}C_{4}$ 0.571	$^{2,5}B$ 0.077	$^{3}S_{1}$ 0.417	**$^{3}H_{4}$ 0.834**	15.4
Gal 1,6-anhydro	1.35	1.54[c]	66.8	−147	−42.1	**$^{1}C_{4}$ 0.944**	$^{1,4}B$ 0.043	$^{2}S_{0}$ 0.264	–	−25.7
Gal **F0**	1.38	1.46	51.4	−166	−44.3	$^{4}C_{1}$ 0.156	$^{2,5}B$ 0.158	**$^{1}S_{3}$ 0.992**	–	−148.3
Gal **F1**	1.33	1.45	52.7	−177	−47.8	**$^{1}C_{4}$ 0.825**	$^{0,3}B$ 0.003	$^{1}S_{5}$ 0.091	–	−155.3
Gal **F2**	1.37	1.47	42.8	168.2	28.6	$^{4}C_{1}$ 0.101	$B_{0,3}$ 0.077	**$^{1}S_{5}$ 0.994**	–	−142.8
Gal **F2**[d]	1.37	1.46	50.8	−180	−38.3	$^{4}C_{1}$ 0.115	$B_{2,5}$ 0.224	**$^{1}S_{3}$ 0.942**	–	−150.2
Gal **G0**	1.35	1.47	−45	61.7	84.7	**$^{4}C_{1}$ 0.863**	$B_{0,3}$ 0.033	$^{1}S_{5}$ 0.161	–	−116.3
Gal **G0**[e]	1.35	1.47	−45	63.2	84.1	**$^{4}C_{1}$ 0.860**	$B_{0,3}$ 0.036	$^{1}S_{5}$ 0.153	–	0.3
Gal **G1**	1.35	1.47	−45	61.7	84.7	$^{1}C_{4}$ 0.193	$^{0,3}B$ 0.068	**$^{5}S_{1}$ 0.838**	–	−118.8
GalAc **B0**	1.27	–	−3.8	−40.1	11.3	$^{4}C_{1}$ 0.584	$^{2,5}B$ 0.123	$^{1}S_{3}$ 0.509	**$^{4}H_{3}$ 1.019**	0.0[f]
GalAc **B1**	1.27	–	−8.2	−157	2.2	$^{1}C_{4}$ 0.280	$^{0,3}B$ 0.024	**$^{5}S_{1}$ 0.801**	–	7.6
GalAc 1,6Anhydo	1.36	1.54[c]	65.1	−146	31.7	**$^{1}C_{4}$ 0.937**	$B_{1,4}$ 0.001	$^{2}S_{0}$ 0.298	–	−10.8
GalAc **B2**	1.27	–	−6.6	−41.8	8.5	$^{1}C_{4}$ 0.316	$^{0,3}B$ 0.065	**$^{5}S_{1}$ 0.735**	–	23.2
GalAc **C0**	1.32	1.57[g]	−31	57.5	−139.7	**$^{4}C_{1}$ 0.763**	$B_{0,3}$ 0.077	$^{1}S_{5}$ 0.324	–	−57.8
GalAc **C1**	1.32	1.58[g]	−37	−42	−127.1	$^{1}C_{4}$ 0.224	$^{2,5}B$ 0.018	**$^{3}S_{1}$ 0.827**	–	−46.4
GalAc **B0 C0** TS	1.26	2.64[g]	−6.9	−40.4	−104.1	$^{4}C_{1}$ 0.604	$^{2,5}B$ 0.092	$^{1}S_{3}$ 0.483	**$^{4}H_{3}$ 0.966**	30.3
GalAc **D0**	1.33	2.22[h]	−33	60	−133.64	**$^{4}C_{1}$ 0.764**	$B_{0,3}$ 0.057	$^{1}S_{5}$ 0.328	–	−107.7
GalAc **D1**	1.33	2.52[h]	−36	−37.5	−118	$^{1}C_{4}$ 0.251	$B_{2,5}$ 0.044	**$^{3}S_{1}$ 0.834**	–	−94.1
GalAc **E0**	1.33	2.76	−31	63.5	−122	**$^{4}C_{1}$ 0.631**	$B_{2,5}$ 0.436	$^{1}S_{3}$ 0.114	–	−115
GalAc **E1**	1.32	2.67	−30	−171	−124.8	$^{1}C_{4}$ 0.235	$^{2,5}B$ 0.053	**$^{3}S_{1}$ 0.713**	–	−94.8

[a] Second minimum in Fig. 3, note different ω_H from **B0**.

[b] Energy arbitrarily set to 0.0 kJ mol^{-1} absolute energy (TZP, no core, etc., see Table I) −7.28392305 a.u. (ZPE = 0.281895 a.u.), 1 a.u. 2645.4985 kJ.

[c] C-6–O-1 distance.

[d] 2nd minimum from reverse LT in Figs.7C and 8C.

[e] Not a minimum see Fig. 5F—**G0′** CH4-C-4–O-4-C(H_3) 18.5° **G0** 26.1°.

[f] Energy arbitrarily set to 0.0 kJ mol^{-1} absolute energy (TZP, no core, etc., see Table I) −7.93876972 a.u. (ZPE = 0.290508 a.u).

[g] C-1–O-7 distance where O-7 = former C=O oxygen.

[h] O_M–C-7 distance where C-7 = former C=O carbon.

where a perfect match has a coefficient of 1.0 and a complete mismatch a coefficient of 0. Intermediate ring conformations can be described by permutations of the original three vectors. The capitalization terminology is used to indicate vector quantities whereas the lower-case terminology is a generic conformational label. For the **B0** conformation, it is calculated from the ring dihedral angles[80,81] to be almost exactly half a chair ($^4C_1$ 0.566) and a half a skew boat ($^1S_3$ 0.497), which means after permutation that it is almost exactly a perfect half chair ($^4H_3$ 0.994). The **B1** conformation is a skew boat ($^5S_1$ 0.803) distorted toward the inverted chair ($^1C_4$ 0.261), with almost no boat contribution. The **B2** conformation is again close to half a chair, but note the inverted chair ($^1C_4$ 0.571) and half a skew boat ($^3S_1$ 0.417), and therefore after permutation there is a different half chair ($^3H_4$ 0.834). Thus, in the first two cases, optimization brought it close to the input conformations, but in the third case the conformation changed to the adjacent (in conformational space) half chair, which was the one that failed by direct optimization. The reason for the failure of the direct optimization is not clear, but this result strongly emphasizes the need to start from a wide variety of input structures. Results like this also suggest that other minima probably exist on the potential energy surface (PES) of **2**.

Table II shows some geometric variables such as τ_5 (pyranose ring torsion C-5-O-5–C-1-C-2), which is expected to be near zero if C-1 is perfectly sp^2 hybridized. The values for **B0** (−3.8°), **B1** (−8.7°), and **B2** (1.6°) support this proposition. Similarly, the short values for the C-1–O-5 bond length: **B0** (1.25 Å), **B1** (1.27 Å), and **B2** (1.26 Å) support considerable double-bond character, again consistent with conventional descriptions of glycopyranosyl oxacarbenium ions; see Scheme 1. The energy differences, with stability decreasing in the order **B0** $>$ **B1** $>$ **B2** suggest importance of the through-space interaction between O-4 and C-1, which is maximal in the **B0** conformation (O-4–C-1 is 3.00, 3.58, 4.08 Å for **B0, B1**, and **B2,** respectively). However, the quasi-axial O-3 in **B2** (O3–C-1 3.17 Å) is almost as close as O-4 in **B0**, casting some doubt on this simple explanation for the stability of **B0**.[85] Further, the **B0** versus **B1** energy difference (10.4 kJ mol^{-1}) is larger than for the *gluco*-configured **3** (4.8 kJ mol^{-1}), or *manno*-configured **4** (1.9 kJ mol^{-1}) which do not have this interaction. Thus, the axial O-4 to C-1 interaction in **2 B0** can be estimated to contribute 5.6 kJ mol^{-1} to its stability. The greater stability of **B1** versus **B2** (5.0 kJ mol^{-1}) points to the importance of the quasi-equatorial orientation of O-2 in the $^5S_1$ conformation found for **3** and the **2 B1** and **B0** conformations, but not for the **2 B2** conformation.

Finally, during the ω_H optimization for **B1**, a species of much lower energy (−25.7 kJ mol^{-1} compared to **2 B0**) was observed, which is the 1,6-anhydro dioxocarbenium species **5** (see Scheme 4). The extra stability arises from the new C–O covalent bond. Neutral 1,6-anhydro species are often isolated as byproducts in

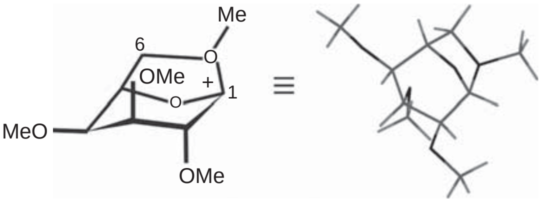

SCHEME 4. Chemical structure and ball-and-stick representation of 1,6-anhydrodioxolenium ion **5**.

glycosylation reactions.[86] During the *ab initio* molecular dynamics (AIMD) studies of **3** and **4**, analogous 1,6-anhydrodioxocarbenium species were also found.[74] The probable explanation is that such species form if the oxacarbenium ion is not intercepted by a nucleophile. Also, the species must lose an alkyl cation to form a neutral species, which is a process that must have an energy barrier. For **2**, CH_3^+ would be the cation lost, and in many of the known experimental cases it is the benzyl cation which is lost. Presumably, the barrier to this alkyl cation loss minimizes this otherwise exothermic pathway in many cases. The barriers to rotation about C-5–C-6 that allow for 1,6-anhydro formation are also probably higher for steric reasons in glycosyl donors having substituents larger than methyl and thereby also diminish the viability of this side reaction. The discussion in this section has been about ‘‘isolated’’ cations in the sense of no solvent, no counterions, or any other nucleophiles to interact with. In glycosylation reactions, all of these interactions must be considered, and this is the focus of the next sections.

3. Facially Selective Methanol–Oxacarbenium Ion Complexes

If it is accepted that many glycosylation reactions, both chemical and biological, proceed through oxacarbenium ions at some point during the reaction, then it is necessary to consider the probable modes of interaction of such ions with any nucleophiles present in the reaction mixture. Combining this assumption with the new computational studies that have found probable conformations of three low-energy species of such ions, it is also necessary to connect these species to reactants and products to obtain any significant insight into the reaction under consideration. In this section, possible sites of reactivity of **2** and hence connection to the products are presented, and in Section II.7 some aspects of ionization and hence the connection to starting materials are presented.

Under glycosylation conditions there are often several nucleophiles present that may potentially react with the oxacarbenium ion once formed, in addition to the hydroxyl group that is the glycosylation target. These include (1) the intramolecular processes leading to 1,6 anhydro bond formation, (2) the intermolecular processes where a nucleophile other than the hydroxyl group reacts, for example the so-called thio exchange reactions,[87–89] (3) the leaving group such as the classical halides, (4) any anionic component or negative dipole of, or derived from, the promoter, such as triflate anions,[90–92] (5) such additives as molecular sieves or hindered bases such as 2-chloropyridine,[93,94] and (6) the solvent, such as acetonitrile[95] or ethers, see Scheme 5.[96] Further, based on a classical S_N1 reaction mechanism,[97,98] a model has been developed where a neutral species is in equilibrium with a contact ion pair (CIP) and a solvent-separated ion pair (SSIP) which is in further equilibrium with an oxacarbenium ion. In this model, the reactivity with nucleophiles increases as the species become more charged, that is, the order of reactivity is neutral < CIP < SSIP

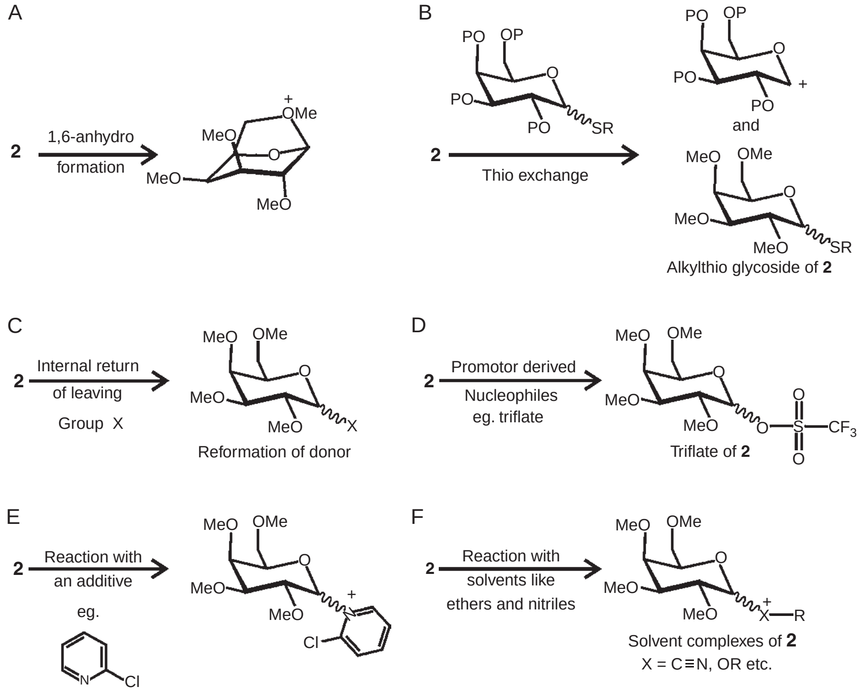
A
2
1,6-anhydro formation
MeO
+
OMe
O
MeO
MeO
B
PO
OP
O
PO
PO
SR
2
Thio exchange
PO
OP
O
PO
+
PO
and
MeO
OMe
O
MeO
MeO
SR
Alkylthio glycoside of 2
C
2
Internal return of leaving Group X
MeO
OMe
O
MeO
MeO
X
Reformation of donor
D
2
Promotor derived Nucleophiles eg. triflate
MeO
OMe
O
MeO
MeO
O
S
O
O
CF3
Triflate of 2
E
2
Reaction with an additive
eg.
N
Cl
MeO
OMe
O
MeO
MeO
+
Cl
F
2
Reaction with solvents like ethers and nitriles
MeO
OMe
O
MeO
MeO
+
X
R
Solvent complexes of 2
X = C≡N, OR etc.

SCHEME 5. Examples of nucleophiles often present in glycosylation reactions that can compete with the nucleophilic hydroxyl group (A) 1,6-anhydro formation, (B) thio exchange, (C) leaving-group return, (D) promoter-derived components such as triflate anions, (E) additives such as added bases, (F) solvents.

$<$ oxacarbenium ion.[99] Experimental support for this model includes the observation that thioglycosides anomerize faster then they react.[100] Also, in accord with early experiments true S_N2 kinetics for a glycosylation reaction is only observed with very strong nucleophiles, see Scheme 6.[101,102] Thus, most glycosylations are thought to proceed through a continuum of species that ranges from CIPs to free oxacarbenium ions. Furthermore, Dewar showed that a pure S_N2 reaction at the carbon atom of α-hydroxy substituted carbon atoms such as C-1 of pyranoses is forbidden because of electron–electron repulsion between the nucleophile and oxygen at the TS.[103] Consequently, both experiment and theory suggest an S_N1-like mechanism for glycosylation reactions.

Since by definition the overall TS for S_N1-like mechanisms is ionization, facial selectivity (which leads to stereospecificity) is thought to depend on the facial specificity of the post-TS nucleophile–carbenium ion encounter complex.[104] Little is known at present about the possible structures of CIPs or SSIPs. However, the free oxacarbenium ions can be modeled by QM as already shown. By extending these studies to allow model nucleophiles (typically methanol), to complex with one face or the other, it may be possible to find models of such encounter complexes. Such a study

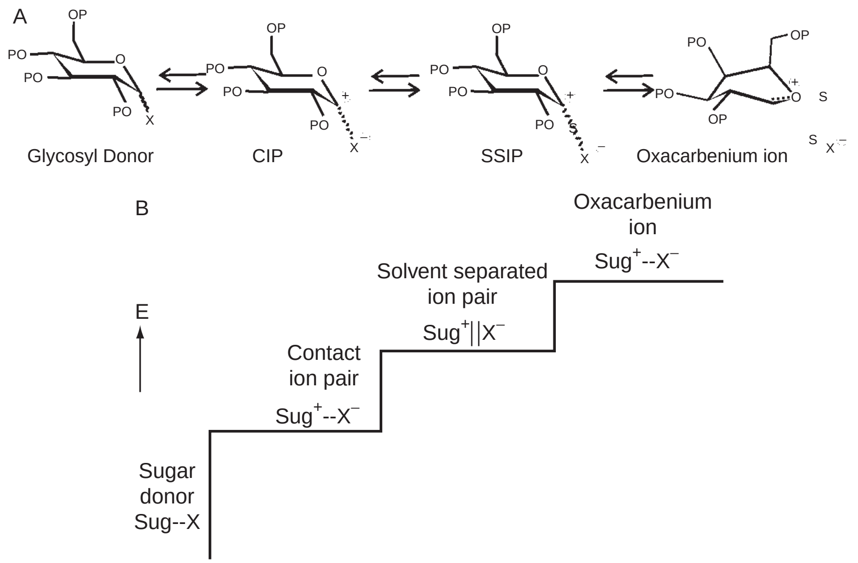

SCHEME 6. (A) Top, classical S_N1 ionization pathway. For most common glycosylation reactions the reactive species probably resemble SSIPs and oxacarbenium ions, although this is not proved. (B) Revised schematic: ionization energy versus reaction-coordinate model (compare Fig.1C left side). Relative energies are arbitrarily chosen, and may vary from case to case.

was done for **2** by arbitrarily placing a methanol molecule on the α face or β face of the three conformers **B0, B1**, and **B2**. The species were then optimized as before, including frequency calculations and ω_H optimization. This optimization process led to two different α-face complexes **G0** and **G1**, and three different β-face complexes **F0, F1**, and **F2**, see Fig. 5A–E.

Figure 5F shows an example from the optimization procedure where a partially optimized **G0** structure is superimposed on a fully **G0** optimized structure. These two

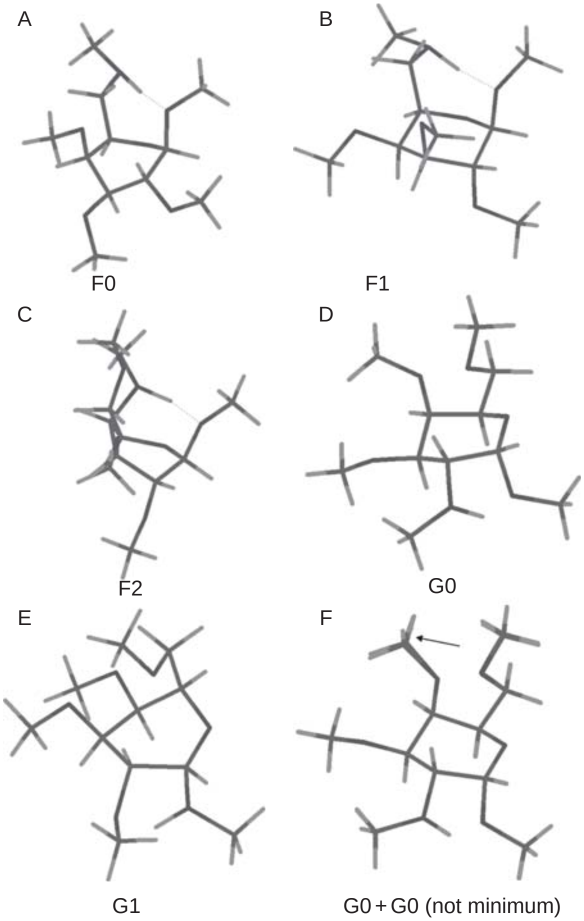

FIG. 5. Stick representations of methanol complexes of **2:** (A) **F0**, (B) **F1** and (C) **F2** (D) **G0**, (E) **G1**, (F) a superimposition of **G0** and a conformer of **G0** with one small imaginary frequency. The arrow in (F) indicates the small reorientation of the O–CH_3 bond necessary to find a true minimum.

structures differ only by subtle differences in the orientation of the *O*-methyl side-chain at C-4. The differences in energy between such species are typically <1 kJ mol^{-1}; and in this case 0.3 kJ mol^{-1}. These observations place some limits on the energy differences that can be considered to be indicative of significant differences, that is $\gg 2$kJmol^{-1}. These differences also relate to the difficulty of modeling flexible protecting groups as already discussed for *O*-benzyl and related protecting groups.

None of these minima correspond to encounter complexes, but rather to species with considerable hydronium ion character.[105] In fact, all three **F** species have the methanolic hydroxyl proton transferred to O-6 or O-4 (**F2**), and exhibit strong H-bonds from O^{+}-6(4)-H to the new O-1 glycosidic oxygen atom. In other words they have undergone proton transfer. All **G** species are optimized to conformers having the methanolic hydroxyl group oriented toward O-2, or even transferred to O-2 but with geometric values at the edge of accepted H-bonding criteria.

The relative energetics are somewhat skewed by the presence of H-bonding in the **F** species.[48] This H-bonding arises since these complexes all have considerable hydronium ion character. Such acidic hydrogen atoms will almost undoubtedly favor association with some electronegative group, as long as these species exist long enough to equilibrate with solvent and/or internal bond rotations. These species are minima on the PES, and so this degree of stability is probable. In previous studies the value of such an interaction was estimated as 28 kJ mol^{-1} although there are considerable sources of error in this number, notably that there is no *a priori* reason to expect that all such H-bonds should have the same energy. Similar species have been postulated during theoretical studies of protic acid-catalyzed hydrolysis of glycosides.[106–109] However, there appears to be no experimental evidence for the presence of such species, other than the observation by mass spectrometry of MH^{+} ions of O-glycosides in the gas phase.[110–115] Figure 6 shows ball-and-stick representations of the same complexes as well as their relative energies, with the correction for H-bonding in parentheses. After correction for H-bonding, the energy difference between **G0** or **G1** and any **F** species is too small to predict facial selectivity.

Table II also has some geometric parameters that assist in the characterization of such complexes. For example the bond between the anomeric carbon atom and methanol nucleophile, C-1–O$_{M}$, is close to 1.46 Å for all **F** and **G** species, and thus indicative of the hydronium ion character. Since typical methyl glycosides have C-1–O$_{M}$ bond lengths close to 1.38 Å, then protonation causes a bond lengthening of only <0.1 Å. It is noteworthy that τ_5 deviates appreciably from planarity, an indication of little similarity to the isolated oxacarbenium ion **B** species. Thus, in terms of conformation, such hydronium ion species can be quite close to the parent glycosides. However, except for **G0**, none of these species have ring conformations close to $^{4}C_{1}$, and this is probably a discriminating factor among these species.

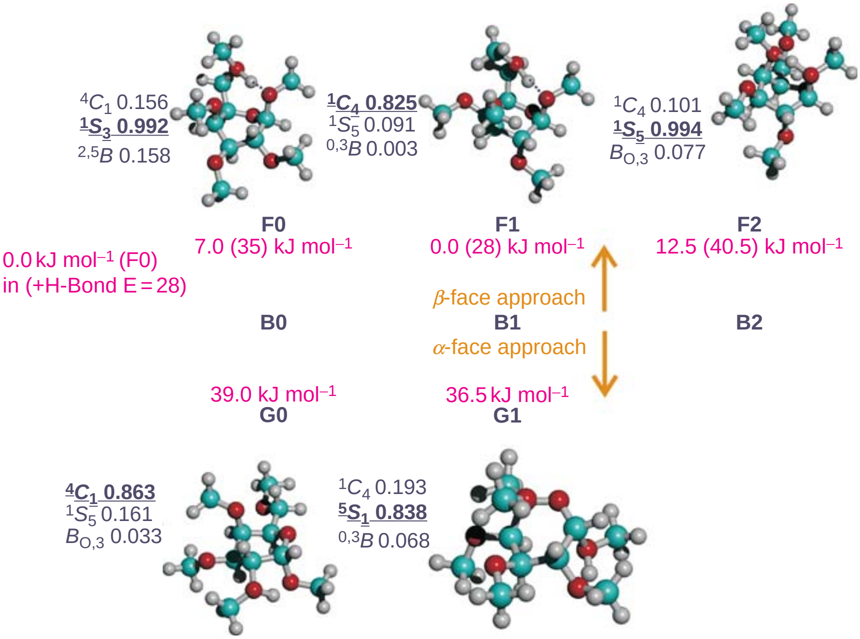
$^4C_1$ 0.156
$^1S_3$ 0.992
$^{2,5}B$ 0.158
$^1C_4$ 0.825
$^1S_5$ 0.091
$^{0,3}B$ 0.003
$^1C_4$ 0.101
$^1S_5$ 0.994
$B_{O,3}$ 0.077
F0
7.0 (35) kJ mol^{-1}
F1
0.0 (28) kJ mol^{-1}
F2
12.5 (40.5) kJ mol^{-1}
0.0 kJ mol^{-1} (F0)
in (+H-Bond E = 28)
β-face approach
B0
B1
B2
α-face approach
39.0 kJ mol^{-1}
G0
36.5 kJ mol^{-1}
G1
$^4C_1$ 0.863
$^1S_5$ 0.161
$B_{O,3}$ 0.033
$^1C_4$ 0.193
$^5S_1$ 0.838
$^{0,3}B$ 0.068

FIG. 6. Ball-and-stick representation of **2 F0, F1, F2**, and **G0** and **G1**. The top structures correspond to *β*-attack and the bottom structures to *α*-attack. The relative energies are also shown, with the values corrected for H-bonding shown in parentheses.

From a synthetic point of view this lack of inherent facial selectivity suggests that small differences in protecting-group strategies can be predicted to alter stereospecificity. Indeed, early experimental studies support this premise.[116–118] At least three mechanisms can be readily deduced. The first is that increasing the steric bulk of the nucleophile, especially in comparison with the nucleophile methanol, will disfavor the formation of H-bonds and hence the propensity for *β*-glycosides whereas increasing the electronegativity of O-4 or O-6 as compared to *O*-methyl will have a favorable effect. The experimental data that address the issue of remote protecting-group effects on glycosylation stereochemistry is scattered throughout the literature and does not appear to have been systematically assembled or analyzed. One relevant observation is that bulky protecting groups at O-6, especially for D-glucopyranosyl donors, favor *α*-glycosylation, although to achieve very high levels of stereoselectivity very bulky protecting groups had to be introduced at O-6.[119–121] Secondly, similar changes in stereoelectronics of the nucleophile or the protecting groups also directly affect the relative energetics of all species, irrespective of H-bonding, by through-space interactions. Thirdly, different protecting groups may alter the ring conformation of these species, which can lead to through-bond as well as through-space differences from such altered ring conformations.

Returning to the energy differences between **F0, F1, F2, G0**, and **G1** and the question of facial selectivity and hence stereoselectivity of glycosylation reactions, see Fig. 6; there is no *a priori* reason to expect that the facial selectivity observed in these complexes should reflect the experimentally observed selectivity. However an experimental correlation between gas-phase carbocation stability and solvolytic reactivity has been shown.[122] One non-sugar study has concluded that diastereoselection of 2-adamantyl cations depends on a *E* to *Z* flipping motion equilibrium.[123] This model resembles the current two-conformer glycopyranosyl model for one possible factor controlling the α/β selectivity in glycosylation reactions.[75] It is notable that the same glycosyl donors and acceptors can lead to different stereochemical outcomes, depending on the method of activation and the solvent used in the experiment. Among the mechanisms proposed to account for this variability is that the method of activation affects the ultimate leaving group. Two classic examples are the halide-ion procedure, which is thought to proceed by transient formation of the more-reactive β-halides[124,125] and pre-activation of usually anomeric alkyl(aryl)-thio or -sulfoxide donors to α-triflate species.[92] The standard explanation for this reactivity is based on the equilibration of neutral species, CIPs, SSIPs, and oxacarbenium ions, as already discussed. Secondly, it has also been postulated that ionization of different leaving groups may lead to different ring conformations of the oxacarbenium ions, and hence in some cases to different facial selectivity; this is the two-conformer hypothesis.[75] A third commonly invoked mechanism, for which there is considerable experimental evidence, is direct participation of such solvents as nitriles and ethers.[126,127] There are also many examples where solvent change does not change anomericity or even changes it in the direction opposite to that expected by solvent participation.[128,129] The usual explanation of solvent participation is that the nucleophile should attack from the face opposite the complexed solvent. Nitriles have been shown to favor the α face of D-glycopyranos-1-yl oxacarbenium ions, leading to β-glycosides whereas alkyl ethers have been suggested to favor the β face and hence lead to α-glycosides. A fourth possibility, later suggested, is that the leaving group acts as a hydrogen-bonding acceptor for the hydroxylic proton of alcohol nucleophiles. This hypothesis applies particularly to reactions of CIPs or SSIPs, and could lead to retention of configuration by an S_Ni mechanism,[130] or inversion if a relay proton-transfer chain is invoked (see Scheme 7).[131,132] Since there is experimental and/or theoretical evidence for all four of these mechanisms, it is probable that all should be considered, with their relative importance depending on the exact experimental conditions.

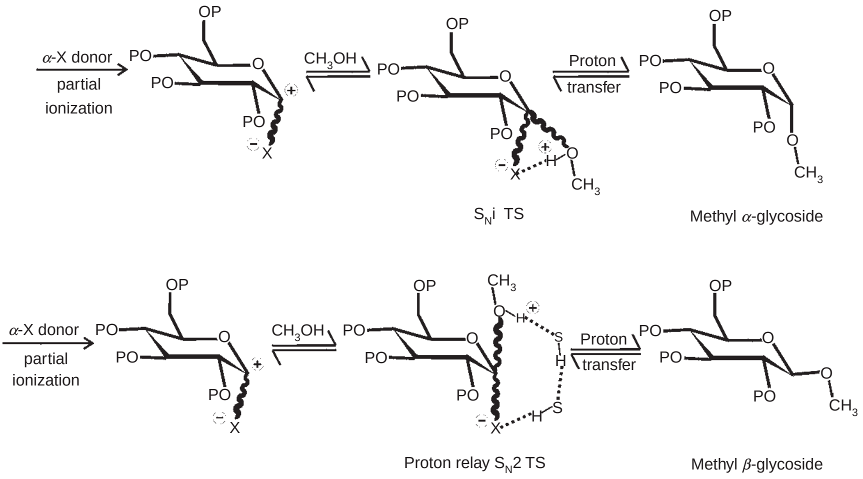
α-X donor
partial
ionization
OP
PO
PO
O
PO
X
CH3OH
OP
PO
PO
O
PO
X
H
O
CH3
SNi TS
Proton
transfer
OP
PO
PO
O
PO
O
CH3
Methyl α-glycoside
α-X donor
partial
ionization
CH3OH
CH3
O
H
S
H
S
H
X
Proton relay SN2 TS
Proton
transfer
Methyl β-glycoside

Scheme 7. Possible examples of the anionic leaving-group acting as the ultimate proton acceptor in either a S_Ni type mechanism that leads to retention of configuration or, in a reaction mixture that contains exchangeable protons (SH), via a S_N2-like mechanism involving a proton relay. The former is plausible for cases where X = triflate or similar very good leaving groups that can spontaneously ionize, whereas the later is more appropriate to solvolysis conditions.

Since direct optimization failed to find classical encounter complexes, another type of QM study called linear transit (LT) was conducted. This LT study varied the C-1–O_M bond length ($O_M = OCH_3$) in small increments, starting from the **G0** and **F2** minima of **2** and either shortening this bond to 1.36 Å or lengthening it to 3.0 Å, using 119 points in total. The results are shown in Fig. 7A and B, respectively.

The results for the α species (**G0**) show that as the C-1–O_M bond is shortened the methanolic proton is transferred to O-2, resulting in glycosylation, but this process is endothermic. Thus, as is required for chemical balance in a glycosylation reaction, the formation of a neutral glycoside requires proton transfer to some external base. Hydronium ions have pK_As of roughly 0 to -4, so that many additives, including molecular sieves or hindered bases which are often present in the glycosylation reaction mixture, are sufficiently basic to receive such protons. Also, notable is that the pyranose ring of the OH-2 hydronium species is near the most stable $^4C_1$ chair of the neutral α-glycoside. Bond lengthening of **G0** leads to a species of close similarity to the **B0**$^4H_3$ conformation. The 119 points of this trajectory are plotted in 3D-conformational space in Fig. 8A and show this smooth conversion from near $^4C_1$ to near $^4H_3$. The methanol stays close to

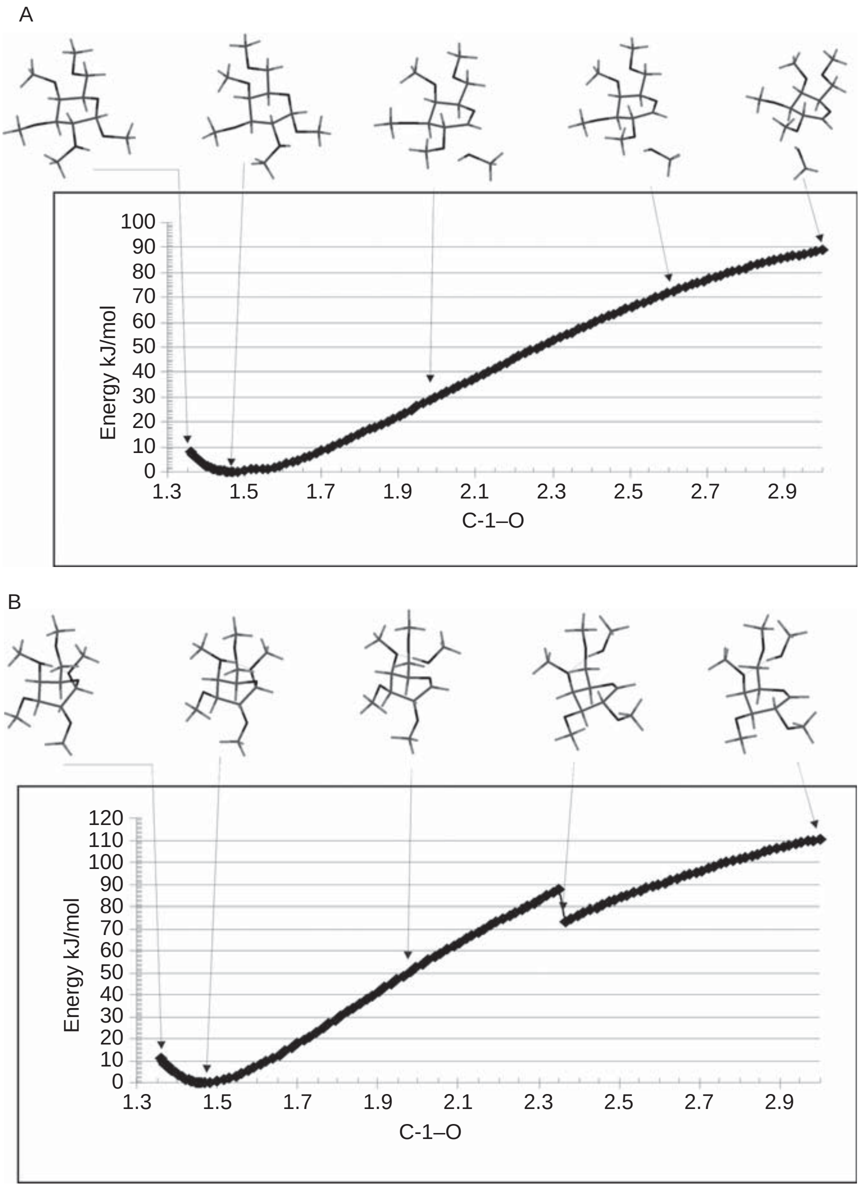

FIG. 7. Continued

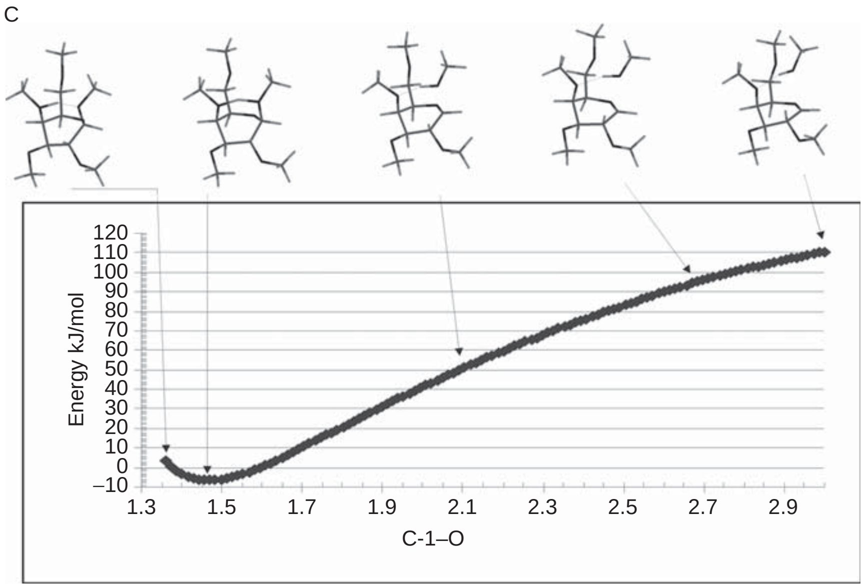

FIG. 7. Relative energy versus C-1–O bond length for an LT study of varying the C-1–O_M bond length in Å, starting from the minimum and stretching or contracting this bond (A) top α (**G0**), (B) middle β (**F2**), and (C) bottom β (**F2**) starting from the conformer found in (B) at 3.0 Å and shortening the bond. Energies in (C) relative to **F2** which was set to 0.0 kJ mol^{-1} as was **F2** in (B) and **G0** in (A). Selected structures are shown for clarity from the points indicated by arrows on the graphs.

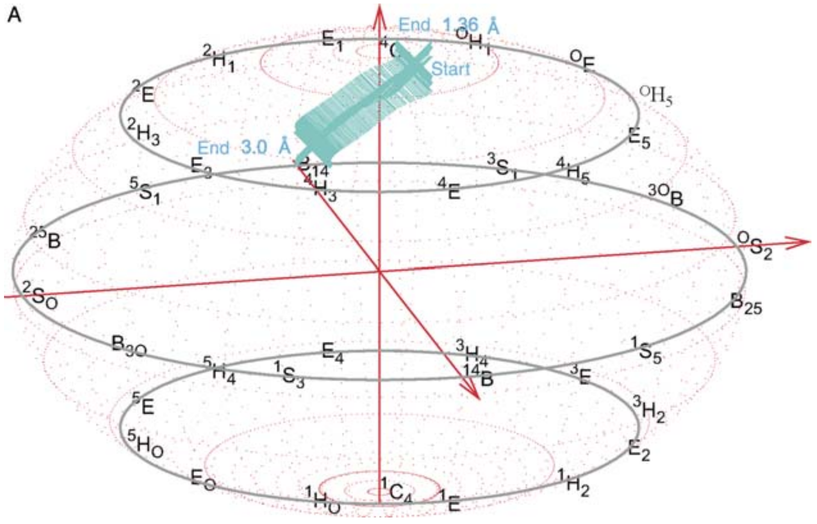
A
End 1.36 Å
Start
End 3.0 Å
E_1
$^{4}C_1$
$^{O}H_1$
$^{2}H_1$
^{O}E
$^{O}H_5$
^{2}E
$^{2}H_3$
E_5
E_3
B_{14}
$^{4}H_3$
$^{3}S_1$
$^{4}H_5$
^{4}E
^{3O}B
$^{5}S_1$
^{25}B
$^{O}S_2$
$^{2}S_O$
B_{25}
B_{3O}
$^{5}H_4$
$^{1}S_3$
E_4
$^{3}H_4$
^{14}B
^{3}E
$^{1}S_5$
^{5}E
$^{3}H_2$
$^{5}H_O$
E_2
E_O
$^{1}H_O$
$^{1}C_4$
^{1}E
$^{1}H_2$

FIG. 8. Continued

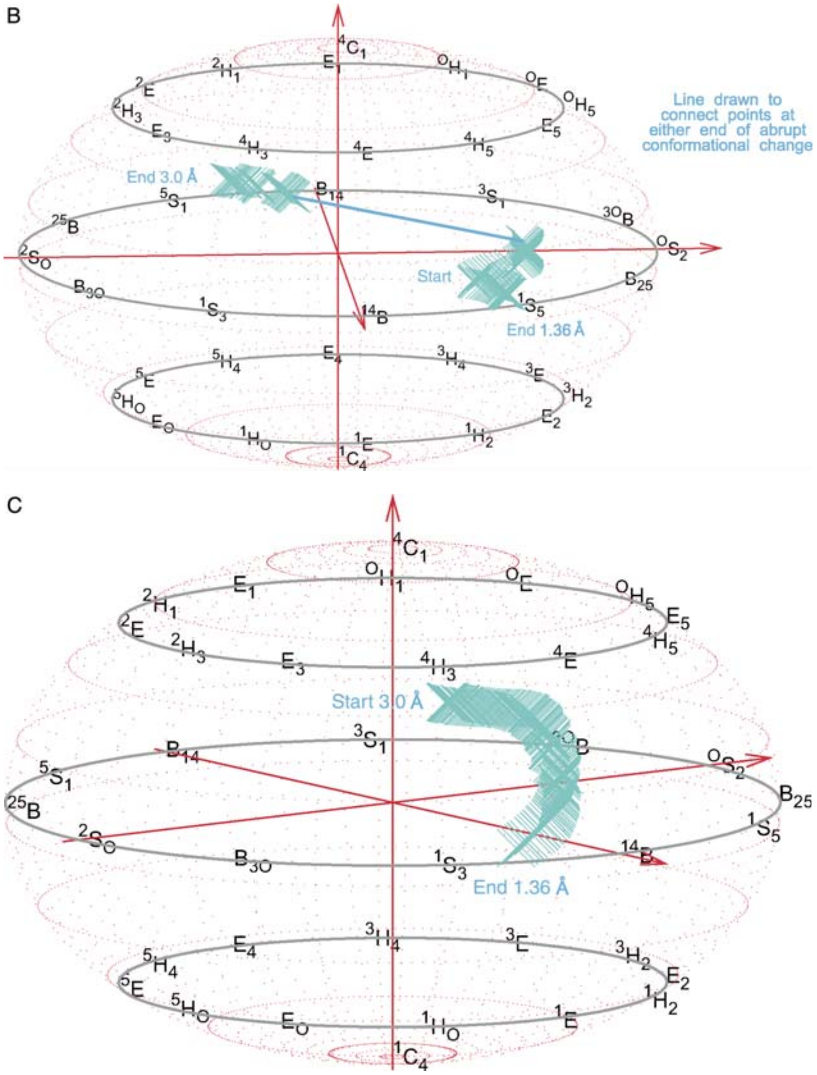
B
$^4C_1$
E_1
$^2H_1$
$^OH_1$
^2E
^OE
$^OH_5$
$^2H_3$
E_5
E_3
$^4H_3$
^4E
$^4H_5$
Line drawn to connect points at either end of abrupt conformational change
End 3.0 Å
B_{14}
$^5S_1$
$^3S_1$
^{25}B
^{3O}B
^2S_O
$^OS_2$
Start
B_{3O}
B_{25}
$^1S_3$
$^1S_5$
^{14}B
End 1.36 Å
E_4
$^5H_4$
$^3H_4$
^5E
^3E
$^3H_2$
^5H_O
E_O
E_2
^1H_O
^1E
$^1H_2$
$^1C_4$
C
$^4C_1$
$^OH_1$
E_1
^OE
$^2H_1$
$^OH_5$
^2E
E_5
$^2H_3$
$^4H_5$
E_3
$^4H_3$
^4E
Start 3.0 Å
$^3S_1$
^{3O}B
B_{14}
$^OS_2$
$^5S_1$
^{25}B
B_{25}
$^1S_5$
^2S_O
^{14}B
B_{3O}
$^1S_3$
End 1.36 Å
$^3H_4$
E_4
^3E
$^3H_2$
$^5H_4$
E_2
^5E
$^1H_2$
^5H_O
E_O
^1H_O
^1E
$^1C_4$

FIG. 8. Position on the conformational sphere from the linear transit study in Fig. 7A–C for (A) top, α (**G0**) (B) middle β (**F2**); (C) bottom, starting from the end of (B) β (**F2**). The start arrow indicates the minimum, and the end arrow corresponds to C-1–O$_M$ = 3.0 Å.

O-2 even at the longest separation. Although no clear minimum, which would correspond to an encounter complex, is found in these studies this result does suggest that noncovalent bonding between the incoming nucleophile and (in this case) O-2 could orient the nucleophile, thus promoting stereospecificity.

The LT study of the β species (**F2**) shows many similarities to the α species, as at short bond length the methanolic hydroxyl proton is transferred to O-4 and at long bond lengths the nucleophile exhibits the orienting effect of H-bonding to O-4. However, two notable differences between α and β are apparent. One, the species closest to a glycoside is not in a chair conformation and at C-1–O_M equal to approximately 2.32 Å the β species exhibits an abrupt conformational change. This corresponds to the discontinuity in Fig. 7B and is most dramatically seen in the 3D-conformational space plot (Fig. 8B). However, the final species is still close in conformational space to the **B0**$^4H_3$ conformation.

The smooth transformations are fully reversibly (not shown) for the α species **G0** to **B0**, and **B0** to **G0**. However, as shown in Figs. 7C and 8C the β species are not reversible and the discontinuity is not found for the reverse LT for the β species, and a different **F** species (**F2′**) is found as the minimum. As shown in Table II its ring conformation and other geometric parameters are closest to **F0**. These species differ in that, in **F0**, the H-bond interaction is with O-6 whereas in **F2′** it is with O-4. This is a result of the long-range orientation modeled in the LT study. It is hypothesized that this orientation effect could be utilized by synthetic chemists to optimize stereoselectivity.

4. The Orientations and Conformations of Side Chains at C-2, C-3, C-4, and C-5

Following from the discussions in Section II.3, one of the many factors that affect the reactivity and stability of the glycopyranosyl oxacarbenium ion is the orientation and the conformation of the side chains attached to C-2, C-3, C-4, and C-5. In this study the implications for reactivity of the different stereochemistry and hence orientation at C-4 of *galacto*- versus *gluco*-configured ions (**2** versus **3**) are one of the main considerations. This section considers some of these implications.

That substituent at O-2 favor the equatorial orientation has already been presented. This disposition puts them in the same plane as the C-1–O-5 double bond. The physical basis of this preference is currently unknown and is a subject for future experimental and computational study. The magnitude of this effect may be estimated by comparing the stability for **2** of **B1** versus **B2**, which suggests a stabilization of about 5 kJ mol^{-1}. A similar value for this energy difference is also apparent by comparing **B0** versus **B1** for

3 and **4**. This effect has only been briefly discussed by other workers, where in most cases it has been argued that *O*-pyranosyl substituents are less electron withdrawing than they would otherwise be if they were axially or quasi-axially disposed. That is, the ''normal'' O-substituents of sugars are electron withdrawing since for example glucopyranosides are about 10^8 less reactive than their fully deoxygenated counterparts, namely ''glycosides'' of tetrahydropyran with each hydroxyl contributing in the order O-2>O-4>O-3>O-6.[133–135] Sugar numbering is used here for all species to avoid confusion. The axial versus equatorial difference as already discussed for the galactose versus glucose example is attributed largely to a through-space dipole effect. For example, it has been shown by the Woerpel group that both the 4-methyl-tetrahydropyranyl (**6**) and 4-benzyloxy-tetrahydropyranyl (**7**) oxacarbenium ions can undergo ring inversion under the conditions of reaction before nucleophilic attack.[136] Furthermore, both **6** and **7** exhibit facial selectivity based on a favored 4-methyl quasi-equatorial conformation for **6** and a favored 4-benzyloxy quasi-axial conformation for **7**. The calculated energy difference is 25.9 (**6**) and 19.9 (**7**) kJ mol^{-1} with a barrier from the $^{3}H_{4}$ conformers of 19.0 and 31.3 kJ mol^{-1}.[74] The backward barrier for **7** is close to 19 kJ mol^{-1} and so these calculations provide a good estimate of the barrier to the ring inversion, namely 19 kJ mol^{-1} which allows for equilibration under glycosylation conditions.

It was this question of the magnitude of the ring-inversion barrier that prompted development of a method for finding the ring-inversion barrier for 6-membered rings including **3** and **4**. Use of the AIMD method for this problem involved developing two fundamental additional procedures. QM-based MD, namely AIMD, is the method of choice, since this allows the molecule to follow the pathway of lowest free energy, whereas static QM calculations such as already made for **2** can only find the free energy after extensive additional calculations.[137–139] Importantly the free energy is not part of conventional optimization procedures that optimize for energy that is closely related to enthalpy that is, they do not consider the entropy. As more complex molecules such as fully protected sugars and enzyme active sites are considered the neglect of entropy during optimization could be a serious deficiency. Secondly, in order to do MD, a coordinate system is needed that is compatible with the equations of motions for molecules. This necessity prompted the development of the canonical-vector coordinate system. In this new system, a displacement in any of the dimensions of Chair, Boat, or Skew boat moves the atoms of the molecule an equivalent amount. This is not true in the older Cremer–Pople and related representations of 6-membered rings.[82] Further, these canonical vectors can be used as constraints to force either ring inversion or ring pseudorotation. Without some type of constraint, the MD would have to be run for a long time until a spontaneous ring inversion or rotation occurred. By using, for example, the Chair vector as a constraint for ring inversion, the

MD naturally finds the lowest free-energy pathway. This works because many combinations of ring dihedrals have the same ring constraint. In the 3D representations shown in Figs. 8 and 9, for example, for the Chair component any specific value of the *z*-Chair component corresponds to a plane parallel to the equator. Pseudorotation involves movement about the equator that is the *x*–*y* plane in these representations. Since these canonical vectors are directly derived from the normal modes of 6-membered rings, the physical movements of a Boat versus a Skew boat constraint are different (*x*–*z* versus *y*–*z* planes) but the result in the 3D spherical representation is movement around the equator, namely pseudorotation. Looking in detail at the trajectories in Fig. 9 which use the Chair constraint, both start on the lower left-hand side (^4E and $^4H_3$) with initial movement toward the equator. Near the equator both molecules pseudorotate and then again move vertically toward $^3H_4$. The scattering of points on the upper right reflects the high-energy movement toward the $^1C_4$ chair. The absolute energies are plotted in the right-hand graph and show that the TS near $^OS_2$ is similar for both species. The experimental conformation of this TS appears to be unknown, and so this aspect of the trajectories can not be directly validated.

Since few experimental data were available before embarking on the AIMD studies of **3, 4, 6**, and **7** an extensive series of validations with neutral 6-membered rings were

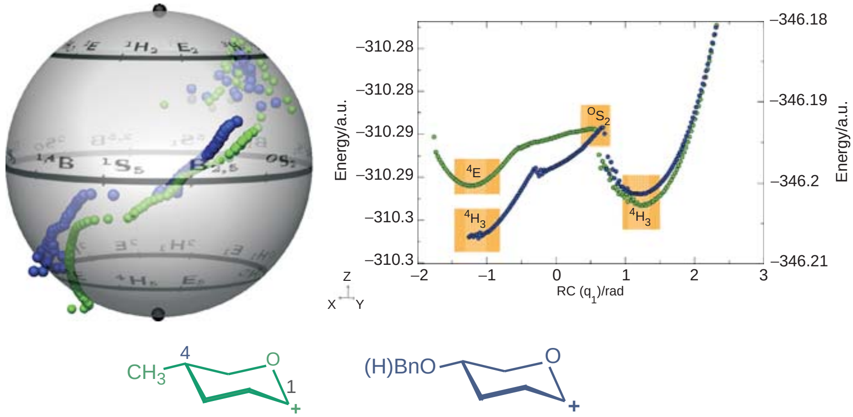

6

7 calculation done for H analogue

FIG. 9. Ab initio molecular dynamic (AIMD) calculations, which can be used to estimate the barrier to ring inversion of about 19 kJ mol^{-1} for both **6** and **7** in 4-substituted tetrahydropyranos-1-yl oxacarbenium ions. Note the greater stability of the axially substituted ion for **7** (blue points $^4H_3$ versus $^3H_4$) and the equatorially substituted ion for **6** (green points ^4E versus $^3H_4$). These calculations use the projector-augmented wavefunction (PAW) AIMD method with constraints based on the canonical vectors already described, for details see Ref. 74.

made. In all cases agreement with experiment for both the conformation and the energy barrier of the TS was found.[140] As an intermediate test, the pathway for inversion of methyl 2,3,4,6-tetra-*O*-methyl-α-D-glucopyranoside (**8**) and its β anomer (**9**) were studied. The results are summarized in Table III and the trajectory for **9** is plotted in Fig. 10. The inversion barrier of these molecules is of interest in regard to the experimental force versus extension measurements of polymers of glucose by atomic force microscopy (AFM) measurements.[141] These barriers and the pathway are also of interest to persons studying the numerous GPE enzymes that form or degrade glucosides, as these pathways could be followed by some of these enzymes.[142,143] The results for **8** and **9** suggest that neutral glucosides invert via similar but distinct TSs near ${}^{O}E$ and have similar but distinct skew boats near ${}^{O}S_2$ as the lowest secondary minimum.

TABLE III

Ring-Inversion Barriers as Estimated by AIMD Studies Using PAW for 3, 4, 8, and 9

Species	**Conformational Descriptors at TS**	**Energy Barrier (kJ mol^{-1})**
3	${}^{1}S_3$ (**B0** to **B1**)	23.6
4	${}^{1}S_3$ (**B0** to **B1**)	44.6
8	${}^{O}E$ 0.757, ${}^{O,3}B$ 0.046, ${}^{1}S_5$ 0.087	51.9
9	${}^{O}E$ 0.830, ${}^{O,3}B$ 0.253, ${}^{1}S_5$ 0.098	37.3

For details see Refs. 74 and 140.

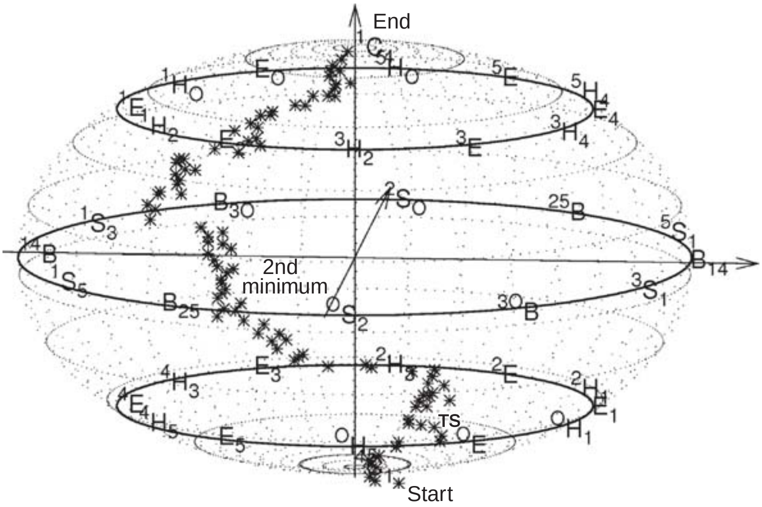

FIG. 10. AIMD trajectory for ring inversion of neutral **9** using the Chair constraint. The start and end points are indicated, as is the approximate position of the TS and the secondary minimum.

Again few experimental data are available for comparison. A recent publication presents another variant of AIMD to study this question.[144]

Subsequent AIMD studies of **3** and **4** were made designed to test if the barriers to interconversion are low enough that glycopyranosyl oxacarbenium ions can interconvert under glycosylation conditions. The results shown in Table III show barriers close to the 19 kJ mol^{-1} found for **6** and **7** for **3**, and so the tentative answer is yes. Thus, once formed, and as long as none of the potential nucleophiles in the system trap the ions, then interconversion can occur to more stable and or more accessible conformations. One of the AIMD trajectories of **3** is shown in Fig. 11. It is readily apparent that the general features are similar to **6** and **7**, that is, initial movement is along the *z*-axis perpendicular to the equator, followed by pseudorotation and then another perpendicular movement. As shown for the corresponding energy versus reaction-coordinate trace, the pseudorotation portion is effectively isoenergetic. That is, in the absence of external constraints which might, for example, be present in the active site of a GPE, glucopyranosyl oxacarbenium ions exist on a PES with a large isoenergetic space. This suggests that many different sites of reactivity are accessible. As already discussed a number of GPEs that degrade glucopyranosides

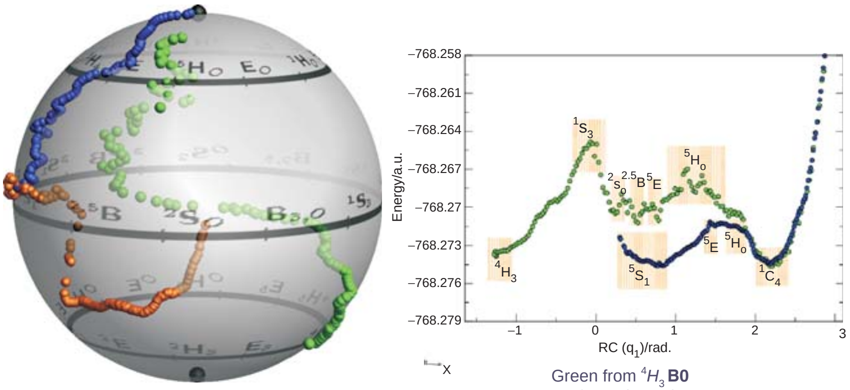

Green from $^4H_3$ **B0** conformation using q1 chair constraint, blue from $^5S_1$ **B1** conformation using q1 chair constraint and orange from ^2S_O using the q2 Boat constraint.

Green from $^4H_3$ **B0** conformation using q1 chair constraint and blue from $^5S_1$ **B1** conformation using q1 chair constraint.

FIG. 11. AIMD trajectories of **3**. Left side: representative points plotted in 3D, and right side, corresponding absolute energies in a.u. The colors on the left and right are for the same trajectories. The $^1C_4$ minima in the right-hand side are for the 1,6-anhydro species as described above, for details see Ref. 74.

have had the conformation of their TSs deduced from kinetic isotope effect (KIE) studies,[145,146] diffraction studies of enzyme inhibitors[147–149] and other experimental methods. For all such GPEs examined, the corresponding TS can be found on the trajectory in Fig. 11. This result suggests a way of classifying GPEs by the position of their TSs on the trajectory. An AIMD study of **2** is too time-consuming for this chapter, but it is anticipated that the barriers from **B0** to **B1**, and **B2**, and back should be comparable to those for **3** and **4**.

The axial versus equatorial disposition for alkoxy-substituents at C-4 of glycopyranosyl oxacarbenium ions has been shown to favor axial substituents by at least 5 kJ mol^{-1}. Further, the comparison of **B2** versus **B1** for **2** suggests that quasi-axial O-3 to C-1 is less important then O-4 to C-1. This further suggests that either through-space interactions are less efficient or that other mechanisms are also important. One such possible alternative mechanism is direct neighboring-group participation by such electronegative substituents as the carbonyl oxygen of esters. Such long-range neighboring-group interactions have long been postulated, and some experimental data strongly support their existence as intermediates or TSs.[150] Their feasibility was tested computationally by comparing the possible dioxolenium ions formed by participation from O-4 (**10**) or O-3 (**11**) acetates of L-fucopyranosyl oxacarbenium ions, and these were further compared to their corresponding **B0** oxacarbenium ion.[151] In both cases the dioxacarbenium ions are more stable then their oxacarbenium ion isomers. The dioxacarbenium ion from **11** was predicted to be more stable then its isomer from **10**. Further, the ring conformation of this ion is close in conformational space to its corresponding **B0** ion, suggesting that it is readily populated, see Scheme 8. In agreement with these observations are experimental studies that showed that O-3 acyl-substituted fucopyranosyl donors are highly α-selective.

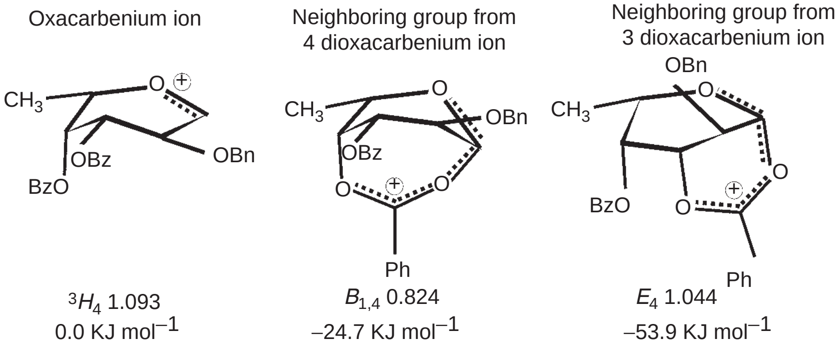

SCHEME 8. Neighboring-group participation from O-3 acyl-substituted L-fucopyranosyl donors is calculated by ADF–DFT (DPZ frozen core) to be more plausible than from O-4. The canonical vector having the highest coefficients is also shown.

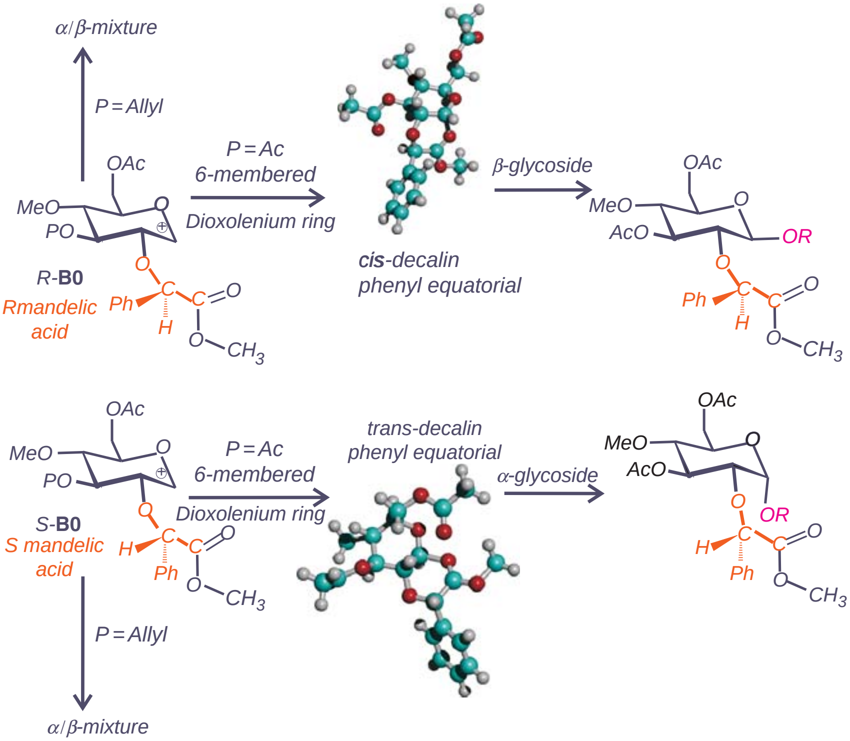
α/β-mixture
P=Allyl
OAc
MeO
PO
O
R-B0
Rmandelic acid
Ph
C
H
C
O
O
CH3
P=Ac
6-membered
Dioxolenium ring
cis-decalin
phenyl equatorial
β-glycoside
OAc
MeO
AcO
O
OR
O
Ph
C
H
C
O
O
CH3
OAc
MeO
PO
O
S-B0
S mandelic acid
H
C
Ph
C
O
O
CH3
P=Ac
6-membered
Dioxolenium ring
trans-decalin
phenyl equatorial
α-glycoside
OAc
MeO
AcO
O
O
OR
H
C
Ph
C
O
O
CH3
P=Allyl
α/β-mixture

FIG. 12. The *R*-mandelic acid (in gold)-based chiral auxiliary at O-2 can form a more-stable 6-membered dioxolenium ion, *trans*-decalin-like (32.9 kJ mol^{-1} relative to its **B0**), whereas its epimer can lead to a *cis*-decalin type of dioxolenium ion (72.8 kJ mol^{-1}), ADF–DFT (DPZ frozen core). The *trans*-decalin leads to α glycosides, whereas the *cis*-decalin leads to β glycosides. Both 6-membered-ring dioxolenium ions are more stable then any dioxolenium ion based on participation from O-3 (*R* 43.9 kJ mol^{-1} and *S* 46.7 kJ mol^{-1}). If R = allyl, then it is hypothesized that non-facially selective glycosylation takes place through the oxacarbenium ion (**B0** or **B1**). Note that the experiment used *O*-benzyl and not the *O*-methyl, which was used for the calculation to avoid complications of multiple minima.

A more subtle experimental effect has been reported where the substituent at O-3 affects stereoselectivity. In this case the O-3 acetyl derivative (**12**) is more selective than its O-3 allyl analogue (**13**), see Fig. 12. Although participation from the O-3 acetyl group appeared plausible, it was calculated to be significantly less stable than the participation from O-2 that formed the basis of the novel stereodirecting properties of the O-2 mandelic acid ethers.[152] The current hypothesis is that through-bond activation from the electron-donating O-3 allyl ether is significant enough that the less stereospecific glycosylation reaction of the oxacarbenium ion (**B0** or **B1**), efficiently competes with the stereoselective O-2 neighboring-group participation (**C0** or **C1**).

Yet another hypothesis has been presented regarding the stereoselectivity of glycosylation reactions, which depends on the nature of the substituents at O-3 and O-2. This is a steric argument named steric buttressing. This has as its basis that, in the TS for glycosylation, the τ_1 (C-1-C-2–C-3-C-4) dihedral angle approaches planarity, and hence any combination of protecting groups on O-2 or O-3 that hinders this conformational movement can lead to both lower reactivity and lower stereospecificity.[153] These studies present evidence for the beneficial use of propargyl ethers in combination with benzyl or trialkylsilyl ethers to minimize these unfavorable interactions.[154,155] This effect has not been studied computationally. Some indication can be gleaned from a recent QM study of the ionization (see Section II.7 later) of 4,6-*O*-benzylidene-2,3-di-*O*-methyl-α-D-mannopyranosyl triflate, **14**. At a short C-1–O-S bond length of 1.52 Å, where the bonding in **14** can be described as predominantly covalent, $\tau_1 = -51.8°$. At a much longer C-1–O-S 2.48 Å bond length, where the bonding is significantly more ionic, $\tau_1 = -40.5°$. Between these two points the O-2 methyl to O-3 methyl C–C separation decreases from 5.18 to 4.91 Å. These numbers suggest that the buttressing effect is real, but it is not possible to ascertain from this analysis if this is sufficient to affect the outcome of glycosylation reactions.

Finally the effect of the substituent at C-5, which for hexopyranosyl sugars would either interconvert D and L in the same configuration or, as in **B0** versus **B1** of pentopyranosyl sugars by ring inversion, has not been studied in much detail. A few indicative studies have been made. Notably the **B0, B1, F0, F1, G0**, and **G1** species of the D-lyxopyranosyl oxacarbenium ion (**15**) have been calculated to compare with the same species for the *manno*-configured **4**. This directly compares the effect of the substituent at C-5 to its absence. As in **2**, β-glycosylation is favored by H-bonding to O-6 in **4**, and this is not possible in **15**. It is also favored by the movement of the ring in the **B1** species toward chair species and is disfavored by movement of the ring in the **B0** species toward boat and skew-boat conformers. The opposite trends are observed for α-glycosylation. In fact for all D-glycopyranosyl oxacarbenium ions studied thus far, these trends have been found, that is for **B0** conformers ring movements favor α-glycosylation, whereas for **B1** conformers ring movements favor β-glycosylation. Returning to **15** in its **F0** species, H-bonding to axial O-2 is found, and for its **F1** species, H-bonding to axial O-3 is found. Experimentally 2,3,4-tri-*O*-benzyl-D-lyxopyranosyl donors give predominantly β-glycosides.[81] Since the analogous 2,3,4,6-tetra-*O*-benzyl-D-mannopyranosyl donors typically yield α/β mixtures favoring α, a stereodirecting effect for C-5 substituents can be deduced.

Perhaps the best studied instance of stereospecificity in a glycosylation reaction that can be related to remote protecting groups is the β-directing effect of 4,6-alkyl (aryl)idene protecting groups for *manno*-configured donors.[156–158] The same protecting groups also lead to an α-directing effect for *gluco*- and *galacto*-configured donors. These effects can be abrogated by bulky protecting groups at O-2 and particularly at O-3. These latter observations led in part to the steric buttressing hypothesis just discussed. The conventional hypothesis is that the fused ring forces the ω_H dihedral angle to adopt the conformation disfavored by the Hassel–Ottar effect, namely *tg* (*gluco* or *manno*) or *gg* (*galacto*), which destabilizes the progression to the oxacarbenium ion and favors reaction through CIPs leading to the observed β-stereoselectivity. This hypothesis also requires that the favored anomeric configuration of the actual CIP related to the glycosyl donor is α (compare **14**), and that the actual reaction has a high degree of S_N2 character.

The observed selectivities are readily accommodated by the two recurring factors that emerge from QM calculations, namely favorable ring movement from the oxacarbenium ion to the hydronium-ion species, and H-bonding in the hydronium-ion species. That is the *trans*-decalin-like ring fusion across C-4–C-5 leads to ring conformations that are stabilized by α-attack on *gluco*-configured ions, whereas β-attack is favored for *manno*-configured ions (**14**). The β-attack on *manno*-configured ions is also favored by H-bonding to O-3, possibly explaining the sensitivity of the stereospecificity to the protecting group at O-3 presented earlier.

The C-5–C-6 conformation has been extensively studied in neutral oligosaccharides, as after the interglycosidic torsion angles it is the most important conformational determinant. Most early studies using MM or low level QM calculations failed to reproduce the experimental observations. In particular, conformations that suffer from Hassal–Ottar interactions were commonly calculated to be more stable than they actually are. In recent years, higher level QM and better parameterized MM force fields have led to much better agreement with experiment.[159] In particular, the accounting for solvation minimizes the formation of intramolecular H-bonds, which often overestimate the stability of Hassal–Ottar C-5–C-6 conformations. Based on these literature observations, and combined with the use of *O*-methyl substituents and moderately large basis sets, it is suggested that QM calculations such as those for **2** give reasonable estimates of the C-5–C-6 torsion-angle dependence.

There are undoubtedly other factors and consequences of the orientations of side chains on glycopyranosyl donors and their related reactive intermediates that could be productively studied by QM calculations. Thus, nothing has been described concerning amino sugars, an important subdivision of known carbohydrates. Also, except for the multiple minimum problem, nothing has been described about protecting group–protecting group interactions. For **2** this means analyzing the O–CH_3 rotamers and any possible methyl–methyl interactions. For **2** the secondary methyl groups at O-3 and O-4 all adapt *gauche*$^+$ or *gauche*$^-$ conformations, with absolute values nearer to 40° than 60°. This preference has been found for most of the species studied. It also well precedented by the work of Anderson.[160,161] As in Fig. 5G, small rotations of O–C(H_3) bonds affect the total energy, presumably by subtle combinations of through-space steric and hyperconjugative through-bond interactions.[162,163] Furthermore, in only a few circumstances, while examining rotations about exocyclic bonds, have methyl–methyl steric interactions been observed. It is readily appreciated, since most protecting groups are larger then methyl, that unfavorable steric interactions are probable. Less easily recognized is that in some situations protecting group–protecting group interactions could be favorable; plausible examples are dipole–dipole interactions, aromatic stacking interactions or hydrophobic interactions. Another type of long-range interaction that almost undoubtedly affects reactivity in carbohydrates is OH to pi interactions. Such interactions are strongly orientation-dependent, would be difficult to recognize, but such interactions are readily calculated to be stabilizing.[164,165] Such a juxtaposition of the hydroxyl group of a glycosyl acceptor and the aromatic ring of a benzyl or similar protecting group predictably leads to anomalous unreactivity. These types of protecting group–protecting group and hydroxyl–protecting group interactions are amenable to QM study, but require special attention to computational details to obtain results. Such studies could be highly fruitful in discerning synthetic factors that a chemist can control to minimize the problematic use of unreactive donor–acceptor combinations in glycosylation reactions.

5. The Role of C-2–O-2 Rotations, Including Neighboring-Group Participation

A special feature, only recently recognized, is that rotation about C-2–O-2, in particular for *O*-methyl but also for a wide range of other substituents, changes from a threefold rotor for neutral species to a twofold rotor for glycopyranosyl oxacarbenium ions, with a *syn* minimum.[166] Absolute values of the CH-2-C-2–O-2-C(H_3) torsion angle are usually <20°. For **2 B0**, Fig. 13 shows a rotation profile of the methyl group at O-2, which provides another example of this phenomenon with a *syn* minimum at CH-2-C-2–O-2-C(H_3) of 27.3° (Table II), about 5 kJ mol^{-1} below the secondary *anti* minimum. This conformational bias has been suggested to arise from a unimodal hyperconjugative interaction between one lone pair on O-2 and the C-1–O-5 double-bond orbital. The latter is the lowest unoccupied molecular orbital (LUMO) of glycopyranos-1-yl oxacarbenium ions and is therefore the most likely orbital to be involved in hyperconjugative interactions. Thus, there is a subtle conformational

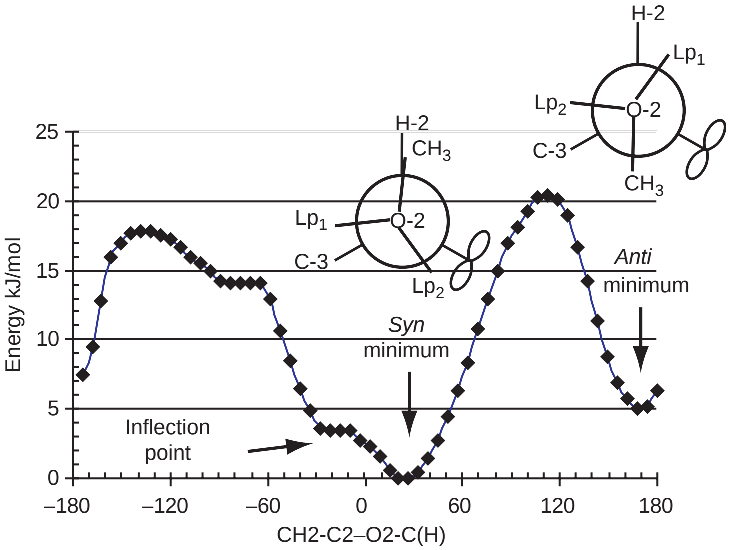

FIG. 13. Rotation about the CH-2-C-2–O-2-C(H_3) torsion angle of **2 B0**. Note the two minima at *syn* and *anti* conformations. The inflection point near −40° is indicative of the gauche$^-$ minimum found for neutral analogues of **2**.

control of the glycosylation reactivity from the O-2 substituent via C-2–O-2 bond rotation at the point of formation of an oxacarbenium ion; see Fig. 14.[167] DFT studies of the ionization of glycopyranosyl donors (see Section II.7) suggest that this rotation is a consequence rather then the origin of ionization, that is rotation follows rather then precedes ionization. This effect is still of interest to synthetic chemists, as the judicious choice of ether protecting groups at O-2 should influence the conformational preference about C-2–O-2 and hence the reactivity of the corresponding glycopyranosyl oxacarbenium ion.

The better known hyperconjugative interaction that relates to all C–O torsions, including C-2–O-2 is the Bohlmann effect first identified from characteristic conformationally dependent shifts in the IR spectra of amines.[168,169] This effect is a result of electron donation from lone pairs on N or O to the $\sigma^\star$ orbital of adjacent C–H bonds. This effect is maximal for an *anti* relationship between the relevant lone pair and the C–H bond. One such interaction is always present in *gauche* H-C–O-C conformations and is one of the factors that stabilize such conformations.

Indeed, the protecting group at O-2 is well known to affect the reactivity of glycosyl donors. This effect was most eloquently stated by Paulsen based on decades

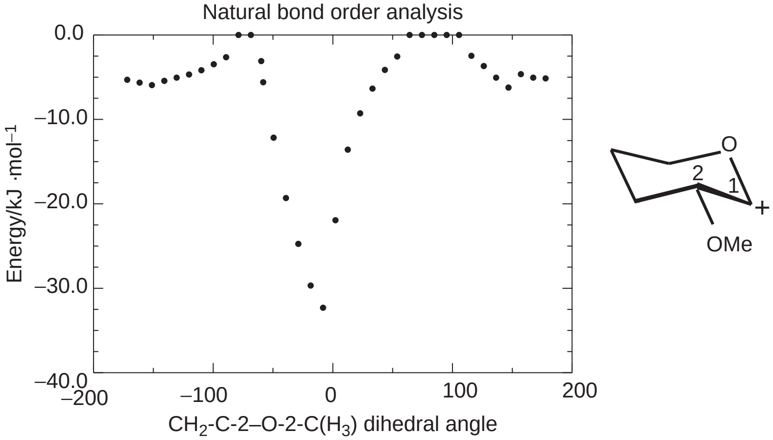

FIG. 14. π-type lone pair on oxygen, LP2, and the C-1–O-5 π-bond with a unimodal angular dependence with a maximum near CH-2-C-2–O-2-C(H$_3$) = 0°. Gaussian 98[170] (B3LYP/6–311+G** basis set) using the NBO 3.1 program.[171]

of experimental results in a classic review[7,172] and then shown by direct experimental comparisons of acyl versus ether O-2 protecting groups that led to the discovery of the armed–disarmed effect.[173,174] That is O-2 electron-donating groups are more reactive then O-2 electron-withdrawing groups, which is further hypothesized to arise from a greater ease of formation of the glycopyranos-1-yl oxacarbenium ion. This effect is kinetic. Subsequent experimental work on comparing the reactivity of glycosyl donors while keeping the acceptor constant has led to a useful scale that at least approximately assesses reactivity at the synthetic planning stage.[175,176] In recent years, more-subtle effects of regioselective glycosylation of diols have been found, which are less amenable to simple explanations.[177–179] These new phenomena depend on the acceptor as well as the donor and strongly support models of glycosylation reactions where the TS for glycosylation involves both the donor and acceptor, that is, it is not pure S$_N$1. In fact Paulsen in his review[7,172] postulated that the reactivities of the donor and acceptor must be matched. Not long afterward, van Boeckel published a related concept of matched and mismatched TSs for glycosylation. This concept was further extended to the concept of double stereo-differentiation.[180,181] This kinetic effect can be rationalized by postulating equilibria between neutral donor, CIP, SSIP, and oxacarbenium ion. As the nucleophilic acceptor becomes weaker and weaker, the donor must be more ionized to react. However if the donor is activated by, for example, the presence of electron-donating protecting groups, then it may be too kinetically unstable to last long enough to react with the acceptor. Instead the donor may either decompose or react with other components in the reaction mixture. A further example of what could be described as misreactivity rather then unreactivity is the observation that electron-rich aromatic groups, especially at O-2 can in fact undergo electrophilic aromatic substitution reactions presumably via glycopyranos-1-yl oxacarbenium ion intermediates.[182] Many of these ideas have been combined into the concept of one-pot glycosylation strategies which have become widely used in recent years.[183–187]

The substituents, particularly at O-2, are also known to affect dramatically the reactivity of GPEs. In most cases the substituent effects follow the arming disarming concept in that electron-withdrawing groups retard the reaction and electron-donating groups accelerate it.[188–190] There are fewer examples of substituent effects on GPEs that affect stereo- or regioselectivity.

Since the pioneering work of Winstein, Isbell, and many others[191–193] it has been recognized that groups capable of neighboring-group participation, such as esters, provide a powerful stereodirecting method leading to 1,2- trans glycosides, often exclusively and often in high yields. The original formulation of this participatory mechanism focused on the kinetic aspect, as exemplified by the greater reactivity of 1,2-β-diacetates of D-glucopyranose as compared to their α anomers.[72,73] In recent years, where leaving groups much more reactive than acetate are typically used in glycosylation reactions, the thermodynamic aspects of bicyclic dioxolenium ion formation leading to 1,2-trans glycosides has gained more importance. A contemporary example of the greater reactivity of *trans* 2-*O*-acyl-β-D-benzothiooxazoles (SBOX) glycosides as compared to their *cis* α-D-isomers in Cu^{2+}-mediated glycosylation reactions illustrates the importance of this kinetic versus thermodynamic distinction.[194] In cases where stereoselectivity is not complete and a certain amount (even occasionally predominantly) of the 1,2-*cis* glycosides are formed, the most frequent explanation is that the *cis*-glycosylation reaction proceeds through the monocyclic oxacarbenium ion.[195–201] Since 2-*O*-acyl groups are electron withdrawing, and dioxolenium ions are stable enough to be isolated and characterized by X-ray diffraction or NMR, there is little doubt that in these cases that glycosylation reactions proceed through oxa- or dioxa-carbenium ion intermediates.[202–204] Further corroboration of these assertions comes from the pressure dependence of the reaction where stereoselectivity increases with pressure, presumably because of the lower volume of activation of the more stereoselective dioxolenium ion.[205] For the analogous 2-amino-2-deoxyglucopyranosyl derivatives, where 5-membered oxazolinium ions can be formed, experimental conditions that lead to β-selective glycosylation without oxazolinium ion formation have been determined.[206]

From a synthetic point of view, lowering the barrier to dioxolenium ion formation in these examples where neighboring-group participation fails could lead to higher *trans* stereoselectivity. This goal prompted a search to find a plausible TS that would link the **B0** or **B1** conformations of 2-*O*-acetyl-3,4,6-tri-*O*-methyl-D-gluco- (**15**), and mannopyranos-1-yl (**16**) oxacarbenium ions with their corresponding bicyclic dioxolenium ions **C0** and **C1** (see Fig. 15 for structures). These studies led to a procedure that starts by determining the C-2–O-2 bond-rotation profiles, followed by TS optimization and demonstrated TSs connecting **B0** to **C0** (38.7 and 22.4 kJ mol^{-1}) and **B1** to **C1** (27.6 and 31.2 kJ mol^{-1}) for **15** and **16**, respectively. Each of these TS has the CH-2-C-2–O-2-C(=O) torsion angle near ±90°: **B0** to **C0** **15** −82.2°, **16** 42.2° and **B1** to **C1** **15** −111.6° and **16** 109.6°

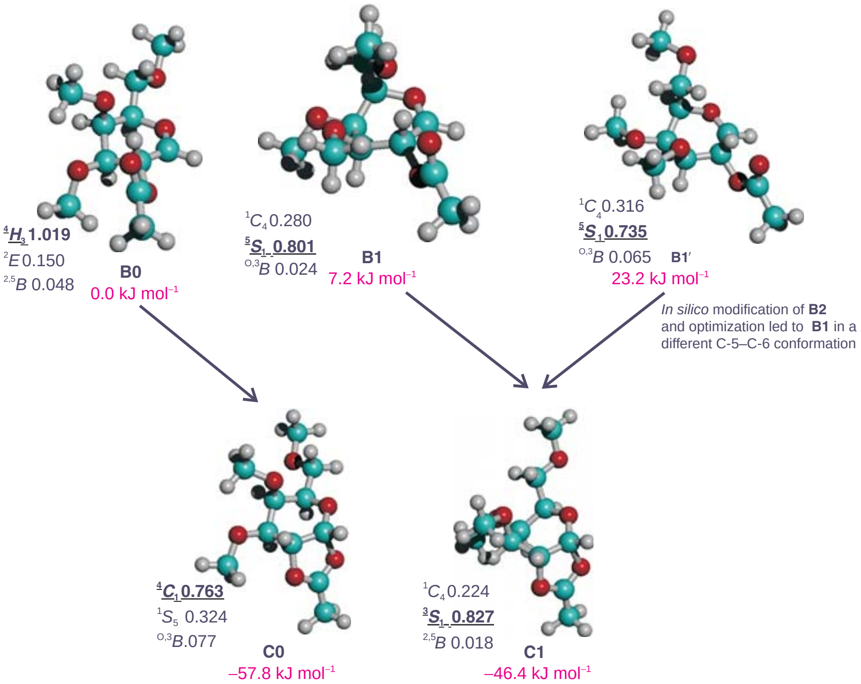
$^{4}H_{3}$ 1.019
^{2}E 0.150
$^{2,5}B$ 0.048
B0
0.0 kJ mol^{-1}
$^{1}C_{4}$ 0.280
$^{5}S_{1}$ 0.801
$^{O,3}B$ 0.024
B1
7.2 kJ mol^{-1}
$^{1}C_{4}$ 0.316
$^{5}S_{1}$ 0.735
$^{O,3}B$ 0.065
B1′
23.2 kJ mol^{-1}
$^{4}C_{1}$ 0.763
$^{1}S_{5}$ 0.324
$^{O,3}B$.077
C0
–57.8 kJ mol^{-1}
$^{1}C_{4}$ 0.224
$^{3}S_{1}$ 0.827
$^{2,5}B$ 0.018
C1
–46.4 kJ mol^{-1}

In silico modification of **B2** and optimization led to **B1** in a different C-5–C-6 conformation

FIG. 15. The ADF–DFT (TPZ) optimized **B0, B1**, and **B2** conformations of **17** and the related ring-closed dioxolenium ions **C0** and **C1**. The canonical-vector coefficients are also shown as well as the relative energies.

This method is illustrated for the 2-*O*-acetyl-3,4,6-tri-*O*-methyl-D-galactopyranos-1-yl oxacarbenium ion (**17**). Thus, the **B0, B1**, and **B2** conformations were optimized as for **2** (see Table II and Fig. 15). In Fig. 16, bond rotation about C-2–O-2 is shown for the **B0** conformer, which goes through a maximum followed by a sharp drop to a new minimum for the **C0** dioxolenium ion. The procedure then involves performing a frequency calculation for the species nearest the maximum. The imaginary frequency is then used in a transition-state optimization. Most QM packages have options to allow for such calculations. A second frequency calculation is then performed on the new species as shown in Table IV where the coefficients of the one imaginary frequency are shown. It may be readily seen that atoms listed in bold in Table IV are those expected to be involved in dioxolenium ring closure, and so with some confidence this TS can be assigned to ring closure. Of course other pathways, perhaps even with lower barriers, may exist but this is clearly a viable pathway.

The standard model of neighboring-group participation recognizes that, after formation of the dioxolenium ion, the former carbonyl carbon (C-7) becomes the site of reactivity. In fact, early work showed that the LUMO of this type of ion can be described as a vacant p-type orbital centered on C-7, strongly supporting this assertion.[47] This fact creates a dilemma; if C-7 is the site of nucleophilic attack, then how are glycosides at C-1 formed?[207–211] The **D0, D1, E0** and **E1**, formed from C-7 or C-1 approach by CH_3OH, are shown in Fig. 17. It is readily seen from the corresponding canonical-vector coefficients that the ring conformations do not change much, and the relatively long C-1–O_M or C7–O_M bond lengths suggest that these species are much closer to classical encounter complexes.

Direct attack at C-7 should lead, after proton transfer, to neutral orthoesters, and in fact neutral orthoesters have been postulated to be intermediates in neighboring-group glycosylation reactions.[207] Such neutral orthoesters are often isolated as side products in glycosylation reactions. A related observation is that sometimes the O-2 acyl group can be transferred to the acceptor, which is the so-called acyl-transfer side reaction; see Scheme 9. In additions to the acyl-transfer product, 2-OH glycosides of both anomers, and even (1→2)-linked oligosaccharides are sometimes formed. A synthetic example has been reported in which donor **18** led besides the expected glycoside **19**, to the acyl-transfer product **20**, the 2-OH glycosides **21ab**, and (1→2)-linked oligosaccharides **22**.[212] This side reaction has also been ascribed to the intervention of neutral orthoesters as intermediates.[213–216] Also, under either Lewis acid or Brønsted acid conditions, neutral orthoesters can sometimes be isomerized to neutral glycosides, and this reaction can be accompanied by acyl transfer and all of the foregoing associated side products.[212] During a study of the methanol adducts of the relatively rigid 2,6-di-*O*-acetyl-3,4-*O*-isopropylidene-D-galactopyranos-1-yl oxacarbenium ion

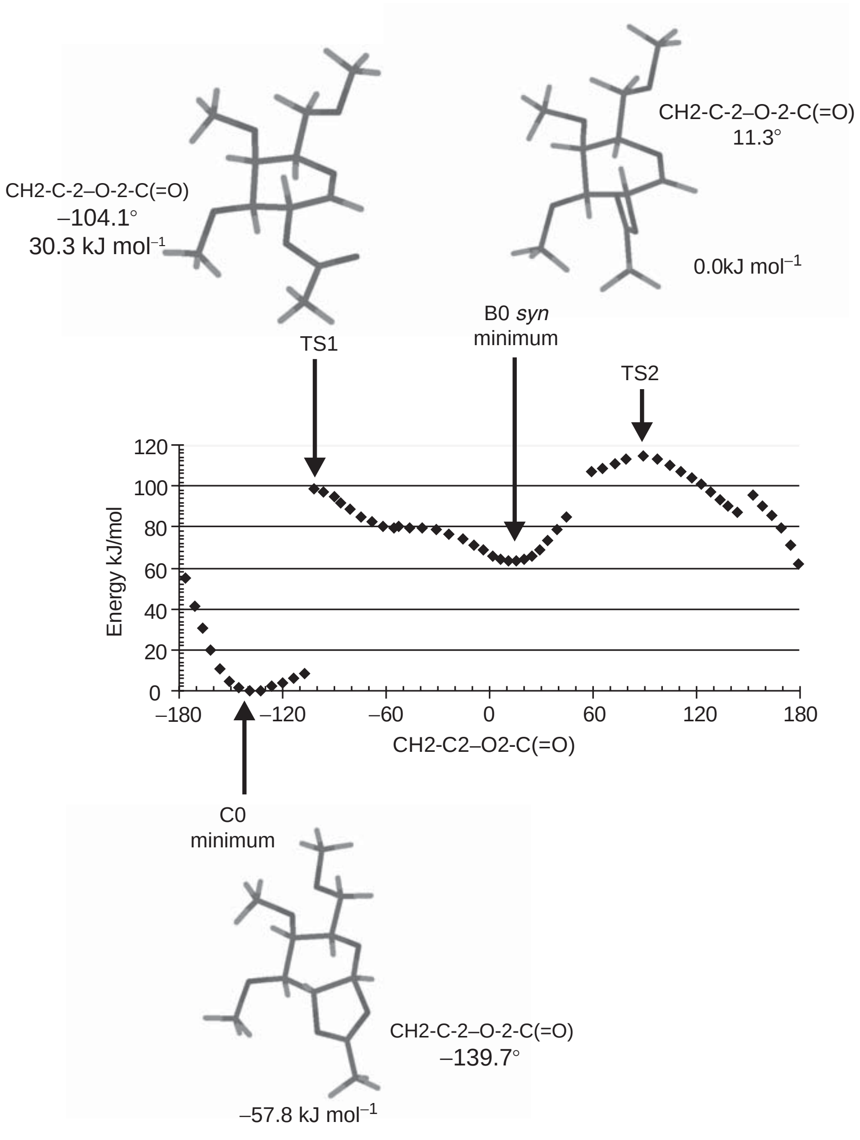

FIG. 16. Rotation about the CH-2-C-2–O-2-C(=O) torsion angle of **17 B0**. Note the two minima at *syn* **B0** and the ring-closed dioxolenium ion **C0** conformations. Also note the two TSs separating **B0** from **C0**. Rotation was made starting at the *syn* **B0** minimum and moving in the direction of TS1. The small discontinuity near 150° is a result of this rotation. Missing points failed to converge. The 60th point did, however, return to almost exactly the starting conformation. The structures shown are for the associated stationary points, and the reported energies which differ from the graph reflect the optimization without the bond-rotation constraints.

TABLE IV

Coefficients of the Imaginary Frequency −85.971 cm^{-1} for B0 to C0 Conversion of 17[a]

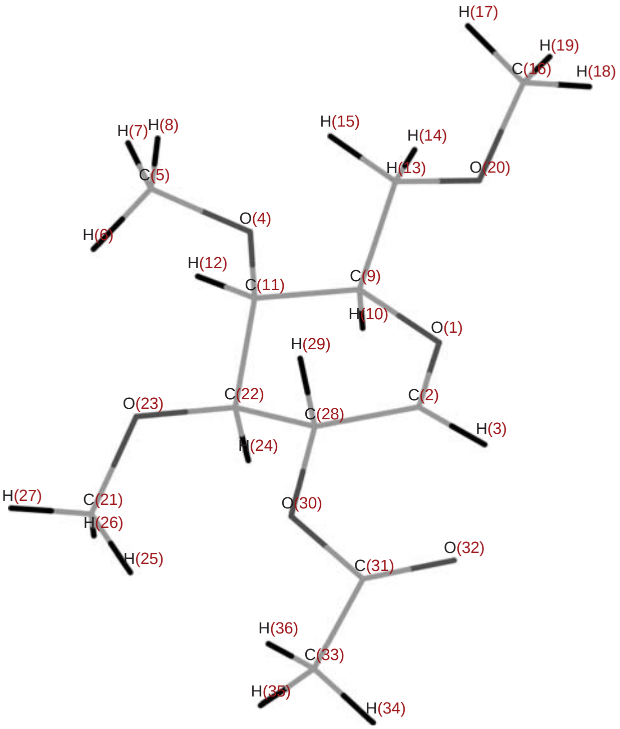
H(17)
H(19)
C(16)
H(18)
H(7)
H(8)
H(15)
H(14)
C(5)
H(13)
O(20)
O(4)
H(6)
H(12)
C(11)
C(9)
H(10)
O(1)
H(29)
C(22)
C(2)
O(23)
C(28)
H(3)
H(24)
H(27)
C(21)
O(30)
H(26)
H(25)
O(32)
C(31)
H(36)
C(33)
H(35)
H(34)

1. O	**0.039**	**0.011**	**0.145**
2. C	**0.043**	**0.002**	**0.255**
3. H	**0.028**	**0.005**	**0.475**
4. O	−0.020	0.002	−0.004
5. C	−0.022	0.002	−0.003
6. H	−0.019	0.003	0.003
7. H	−0.021	0.002	−0.008
8. H	−0.029	0.005	−0.002
9. C	0.029	0.028	−0.007
10. H	0.090	0.086	−0.027
11. C	0.008	0.012	−0.013
12. H	0.016	0.016	−0.033
13. C	−0.015	−0.017	−0.049
14. H	−0.053	−0.072	−0.017
15. H	−0.024	−0.023	−0.122
16. C	0.002	0.001	−0.031

(continued)

TABLE IV (*continued*)

17. H	−0.012	0.002	−0.064
18. H	0.018	0.023	−0.016
19. H	−0.003	−0.031	−0.014
20. O	0.010	0.015	−0.028
21. C	0.044	0.043	0.024
22. C	0.030	0.029	0.026
23. O	0.004	0.006	0.005
24. H	0.068	0.077	0.028
25. H	0.050	0.047	0.078
26. H	0.079	0.071	0.000
27. H	0.039	0.037	0.007
28. C	**0.022**	**−0.019**	**0.123**
29. H	**−0.048**	**−0.108**	**0.106**
30. O	**0.065**	**−0.012**	**0.270**
31. C	**−0.065**	**−0.027**	**−0.176**
32. O	**−0.180**	**−0.022**	**−0.586**
33. C	−0.041	−0.042	−0.088
34. H	−0.038	−0.059	−0.132
35. H	−0.025	−0.074	−0.064
36. H	−0.068	−0.021	−0.061

[a] The largest coefficients are shown in bold and correspond to atom numbers shown in the stick figure.

23, nearly isoenergetic charged intermediates **D** and **E**, resulting from nucleophilic attack at C-7 and C-1, respectively, were found. Related 2,6-di-*O*-acyl donors (see **18** in Scheme 9) exhibited a strong tendency to undergo the acyl-transfer side reaction. These observations prompted a detailed study of the interconnection between **D** and **E**, as well as the progression of **D** to acyl-transfer products and **E** to glycosides. To date no conclusive connection between such intermediates as **E** and glycosides has been found. Some plausible TSs that involve proton transfer (see later) have been found, but this still remains an unresolved issue.

A more clear-cut case for the progression of **D** species to acyl-transfer products was found by using a LT study with a complex constraint; (see Scheme 10). The key to this pathway is proton transfer from the alcohol in charged intermediate **D** to O-2. Two subsequent TSs lead to acyl transfer and a 2-OH charged intermediate **H**. Intermediate **H** is presumably the precursor of the anomeric mixture of 2-OH glycosides and eventually the (1→2)-linked oligosaccharides, although this is not proved. Examination of progression to the first TS along the route to acyl transfer for the benzoyl analogue suggested that the phenyl ring of the benzoate needed to rotate. This computational result led to the idea that placing substituents at the 2- and 6-positions of the benzoate should hinder this rotation and hence increase the barrier to acyl transfer. This was reduced to practice by synthesizing the 2,6-dimethylbenzoate

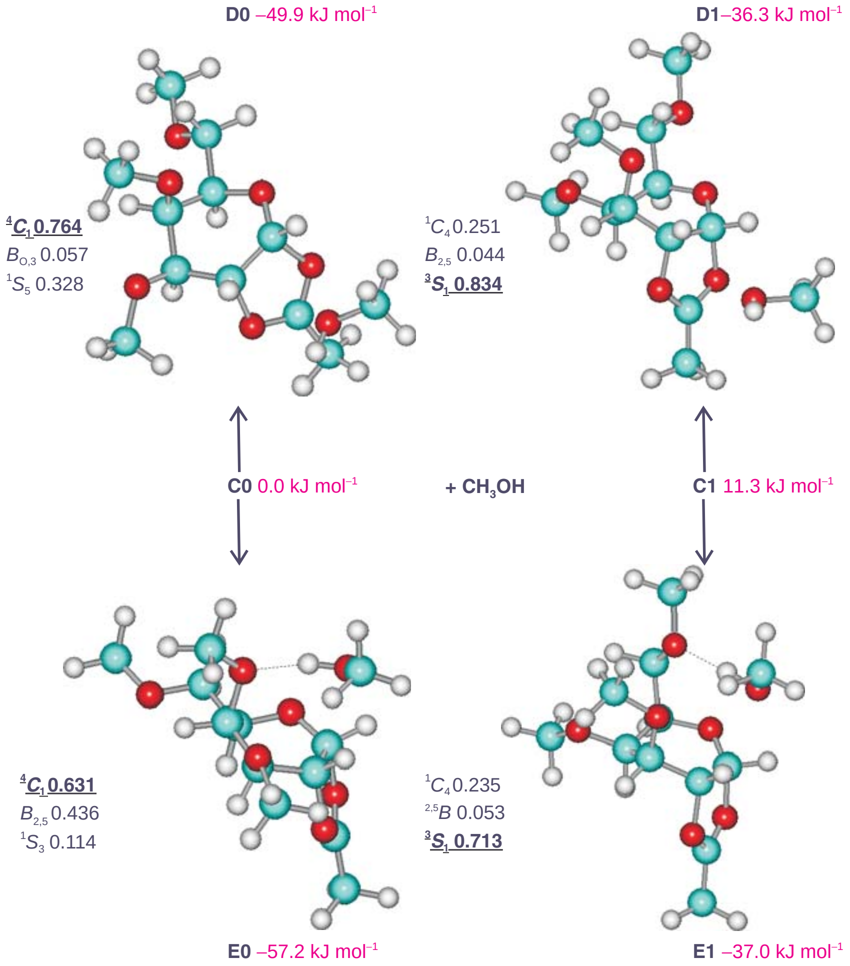
D0 –49.9 kJ mol^{-1}
D1–36.3 kJ mol^{-1}
$^4C_1$ 0.764
$B_{O,3}$ 0.057
$^1S_5$ 0.328
$^1C_4$ 0.251
$B_{2,5}$ 0.044
$^3S_1$ 0.834
C0 0.0 kJ mol^{-1}
+ CH$_3$OH
C1 11.3 kJ mol^{-1}
$^4C_1$ 0.631
$B_{2,5}$ 0.436
$^1S_3$ 0.114
$^1C_4$ 0.235
$^{2,5}B$ 0.053
$^3S_1$ 0.713
E0 –57.2 kJ mol^{-1}
E1 –37.0 kJ mol^{-1}

FIG. 17. Ball and stick representation of the **D0, D1, E0**, and **E1** methanol complexes of **17**.

(DMB) analogue of **24**, namely donor **25** (see Scheme 11). Glycosylation with this donor led only to glycoside, **26**, and no acyl transfer. Further, if less triflic acid promoter was used, a mixture of neutral orthoester (**27**) and glycoside **26** could be formed. If this mixture was treated with more triflic acid then only glycoside **26** and a small amount of hydrolysis product were isolated. This example clearly decouples neutral orthoester formation from acyl transfer, at least for such donors as **24**.

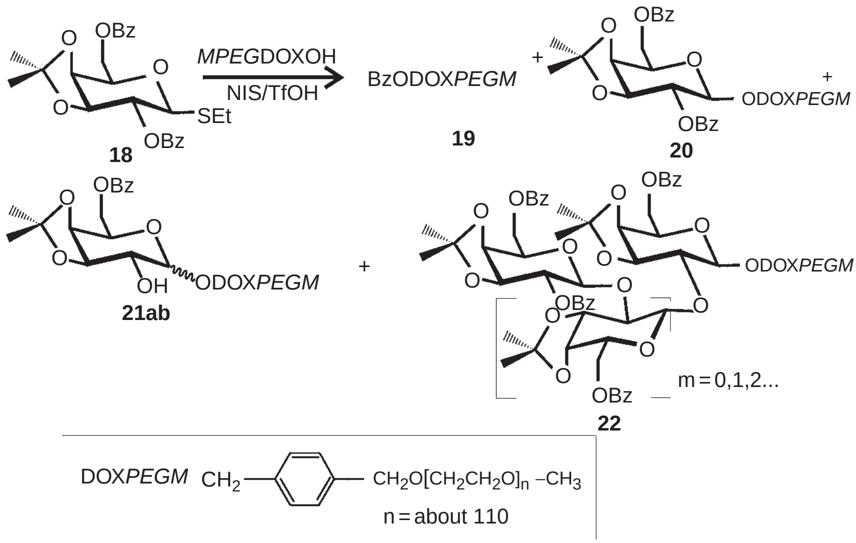
MPEGDOXOH
NIS/TfOH
OBz
SEt
18
BzODOXPEGM
19
ODOXPEGM
20
OH
ODOXPEGM
21ab
22
m = 0,1,2...
DOXPEGM CH2
CH2O[CH2CH2O]n –CH3
n = about 110

SCHEME 9. Acyl (benzoyl in this case)-transfer from a glycosyl donor (**18**) to the acceptor (MPEG-DOXOH), accompanied by formation of 2-OH glycosides (**21ab**) and (1→2)-linked oligosaccharides **22**.

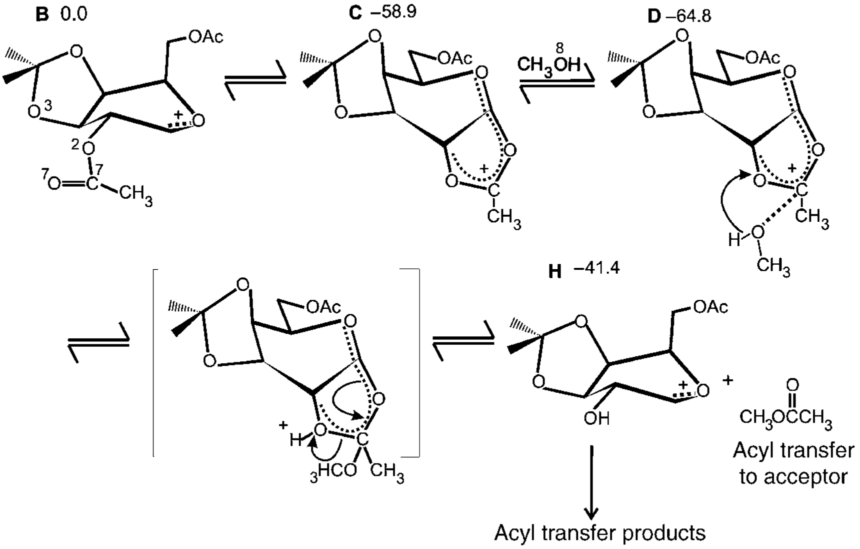
B 0.0
C −58.9
D −64.8
H −41.4
OAc
CH3OH
8
CH3
OH
CH3OCCH3
Acyl transfer to acceptor
Acyl transfer products

SCHEME 10. Plausible mechanism for acyl transfer, based on a proton transfer to O-2 triggering mechanism, ADF–DFT (DPZ frozen core).

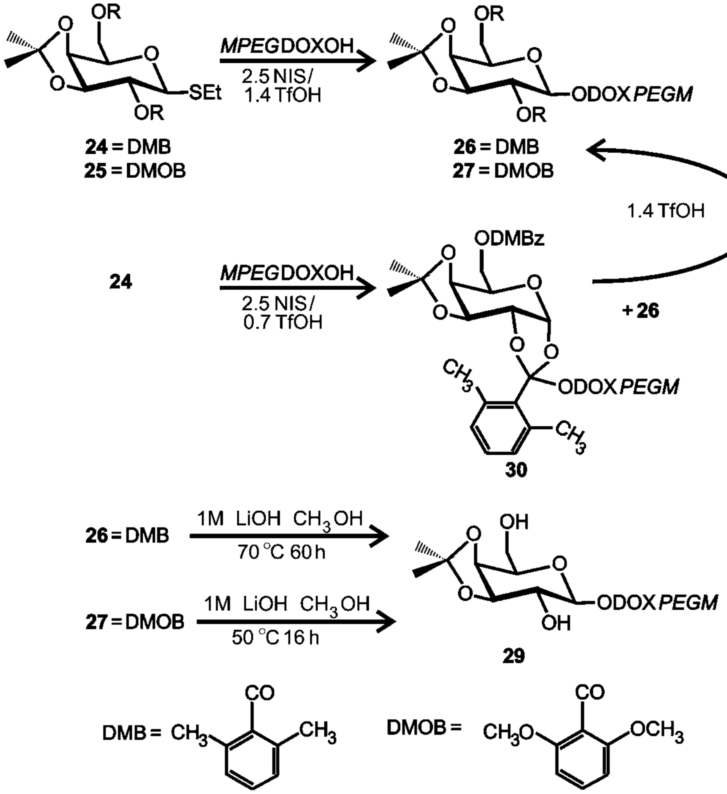
OR
SEt
24 = DMB
25 = DMOB
MPEGDOXOH
2.5 NIS/
1.4 TfOH
ODOXPEGM
26 = DMB
27 = DMOB
1.4 TfOH
24
MPEGDOXOH
2.5 NIS/
0.7 TfOH
ODMBz
+26
CH3
ODOXPEGM
30
26 = DMB
1M LiOH CH3OH
70 °C 60 h
27 = DMOB
1M LiOH CH3OH
50 °C 16 h
OH
29
DMB =
CO
CH3
DMOB =
CH3O
OCH3

SCHEME 11. 2,6-Dimethylbenzoyl (DMB) and 2,6-dimethoxybenzoyl (DMOB) acyl-protecting groups developed from computational chemistry.

The 2,6-dimethoxybenzoyl (DMOB) analogue was also synthesized and tested. It also minimized acyl transfer dramatically, but was significantly easier to cleave to diol **29**. Synthetic work in a variety of contexts has shown that 2-*O*-acyl substituents in *β*-galactosides are difficult to hydrolyze.[217] Glycosides **26** and **27** probably represent extreme cases, and in most other synthetic contexts these groups should undergo hydrolysis more readily. It is also probable that an electron-withdrawing group at the 4-position of the benzoate should assist hydrolysis without affecting the acyl-transfer minimizing properties. There is also a report in the literature of the 3-acetoxy-2,2-dimethylpropanoate protecting-group (donor **30**) that internally blocks reaction at C-7 during glycosylation (see Scheme 12).[218] The routine use of such protecting groups should assist synthetic chemists to make purer products.

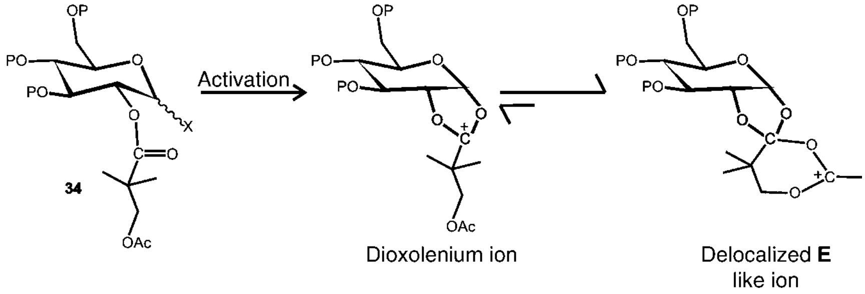

Scheme 12. The 3-acetoxy-2,2-dimethylpropanoyl protecting group internally quenches the **C**-like dioxolenium ion to lead to a highly delocalized **E**-like ion. This prevents acyl transfer and promotes stereoselectivity.

6. The Role of Proton Transfer in the Transition State for Glycosylation Reactions

There appear to have been no definitive studies of the TS for any chemical glycosylation reaction. In balancing the classical glycosylation reaction (Scheme 1A) the alcohol acceptor must lose a proton, which nominally combines with the leaving group (X) to form the other product, HX. In other words, proton transfer must be part of any glycosylation reaction mechanism. But proton transfer could in principle precede or succeed the TS. Sugar hydroxyl groups typically have pK_As well above 10 and are unlikely to be ionized in the absence of a strong base. Chemical glycosylations are almost always conducted in the presence of Brønsted or Lewis acids unless very reactive leaving groups are used, that is to say, not under basic conditions. Glycosylation reaction models that require pre-TS alkoxide formation are therefore unlikely. Therefore the possibility that proton transfer is post-TS has some credence. Classical S_N1 reaction mechanisms require that ionization of the glycosyl donor is the TS such that nucleophilic attack and proton transfer must occur post-TS.[219] Computational results that consistently find hydronium ion species on the PES as minima have necessitated consideration of the possibility that these are not artifacts of particular computational protocols, but might actually be transient intermediates on the path to glycosides. This would require a subsequent proton transfer, which as shown in Fig. 7A–C is an endothermic process, that has an activation barrier.

Since GPEs can use a variety of mechanisms to promote enzymatic glycosylation, the timing of proton transfer could in principle be different. This of course is at least partly due to the wide variety of substrates that GPEs utilize. Current modeling of glycosyltransferase mechanisms by QM-MM methods finds late TSs with relatively short C-1–$O_{acceptor}$ (1.5–1.9 Å) and relatively long C-1–X (> 2.5 Å) bond lengths.[220,221] The sugar rings of the donor adopt conformations consistent with a high degree of oxacarbenium character.[222,223] For retaining glycosyltransferases, the leaving group acts as proton acceptor.[224]

The possibility that proton transfer rates might in some cases affect the outcome of glycosylation reactions was first raised by consideration of galactosylation reactions of 5′-OH of nucleoside acceptors; see Scheme 13.[164] In this case acyl-transfer reaction products were isolated as the main products under standard glycosylation conditions. Spectroscopic and computational studies led to the conclusion that the predominant conformation of the acceptor **31** under the conditions of the glycosylation reaction is *syn* about the glycosidic linkage. This *syn* conformation is stabilized by an intramolecular H-bond between the 5′-OH group and the pyrimidine base.[164,225] Reaction conditions that broke up this H-bond led to higher yields of glycosylation products. This led to a proposal that inhibition of proton transfer could adversely affect glycosylation reactions.[226] In related synthetic examples, two acceptors (**32** and **33**) that were also found to have hydroxyl groups that are probably intramolecularly H-bonded under glycosylation reaction conditions led to the formation of α-linked disaccharides instead of *β*-linked ones under conditions where neighboring-group participation was expected to lead to *β*-glycosides.[227] Combined with the concepts of matched TS for glycosylation reactions already discussed, these results prompted consideration the probable role of proton transfer in the TS for glycosylation reactions.

Further impetus for consideration of the role of proton transfer came with the discovery of the mechanism for acyl-transfer involving proton transfer to O-2. This led to consideration of the possibility that glycoside formation under neighboring-group participation conditions might be triggered by an analogous pathway of proton

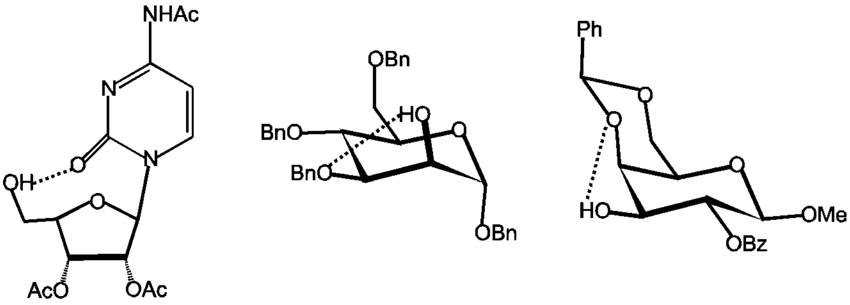

31 **32** **33**

SCHEME 13. Intramolecularly H-bonded acceptors, which led to misreactivity in glycosylation reactions.

transfer to O-1 or O-5. However, computational results with **15** showed that, unlike acyl transfer where the O-2 protonated species is not a minimum but rather spontaneously optimizes to **H** in an exothermic process, protonated O-1 and O-5 species are minima but the processes are endothermic; see Scheme 14. Further unpublished studies have not led to a low-energy pathway to glycosides from such species. Whether this results from inadequate computational protocols or is real that is a subject for further studies.

A further role for proton transfer was found during studies that followed from considerations of C-2–O-2 bond rotation during neighboring-group participation. Following the discovery that the TS to dioxolenium ion formation probably involves C-2–O-2 bond rotation, at least in some cases, it was suggested that the opening of the dioxolenium ion to form glycosides might also involve C-2–O-2 bond rotation. The ''classic'' model of dioxolenium ion S_N2 reactivity invokes a 5-coordinate TS with bond stretching and contracting motions along the incoming nucleophilic C-1 directions and C-1–O-7 bonds. Using constrained LT methods such as those for unraveling the acyl-transfer mechanism failed to find such a TS. However, simple LT calculations as shown in Fig. 18 for **17 E0** and **17 E1** readily found possible TS structures. Similar

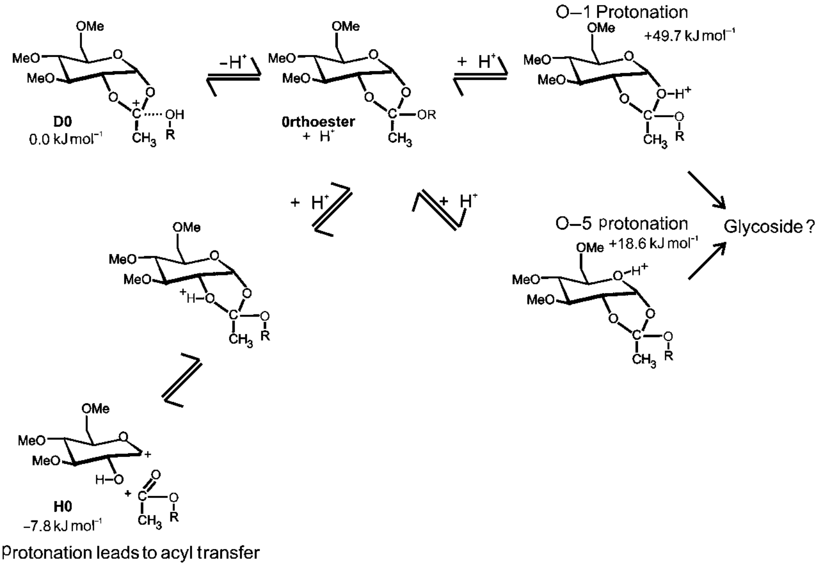

Scheme 14. Possible role for proton transfer from **D**-type intermediates to glycosides, noting that **D** species are orthoesters protonated on the former alcohol oxygen. Results are shown for methanol plus 2-*O*-acetyl-3,4,6-tri-*O*-acetyl-D-glucopyranos-1-yl (**15**). Proton transfer to O-1 or O-5 is endothermic ADF–DFT (TPZ), but transfer to O-2 triggers acetyl transfer.

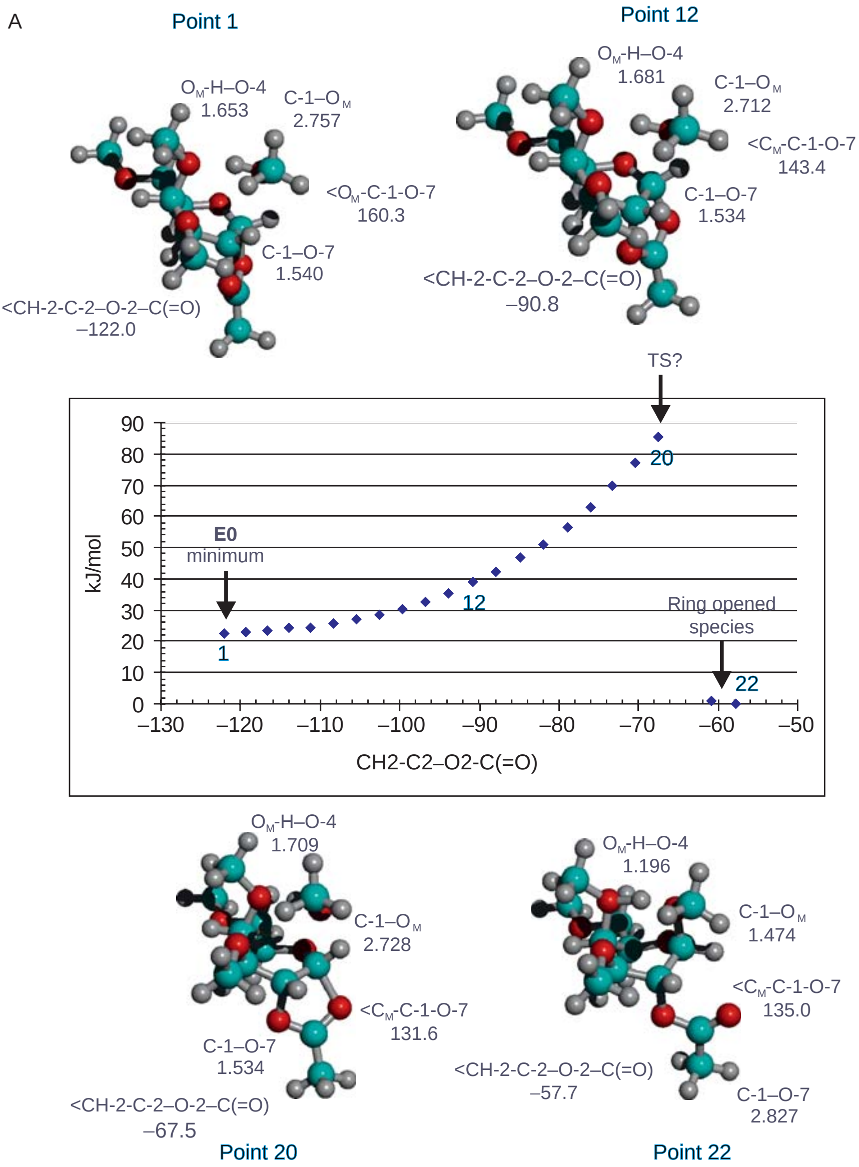

FIG. 18. (A) Top: partial rotation about the CH-2-C-2–O-2-C(=O) torsion angle of **17 E0**. Note the apparent TS at point 20, which occurs after passing CH-2-C-2–O-2-C(=O) = about −90°. The four structures correspond to points 1, 12, 20, and 22 respectively. Also note the apparent proton transfer to O-4 after ring opening.

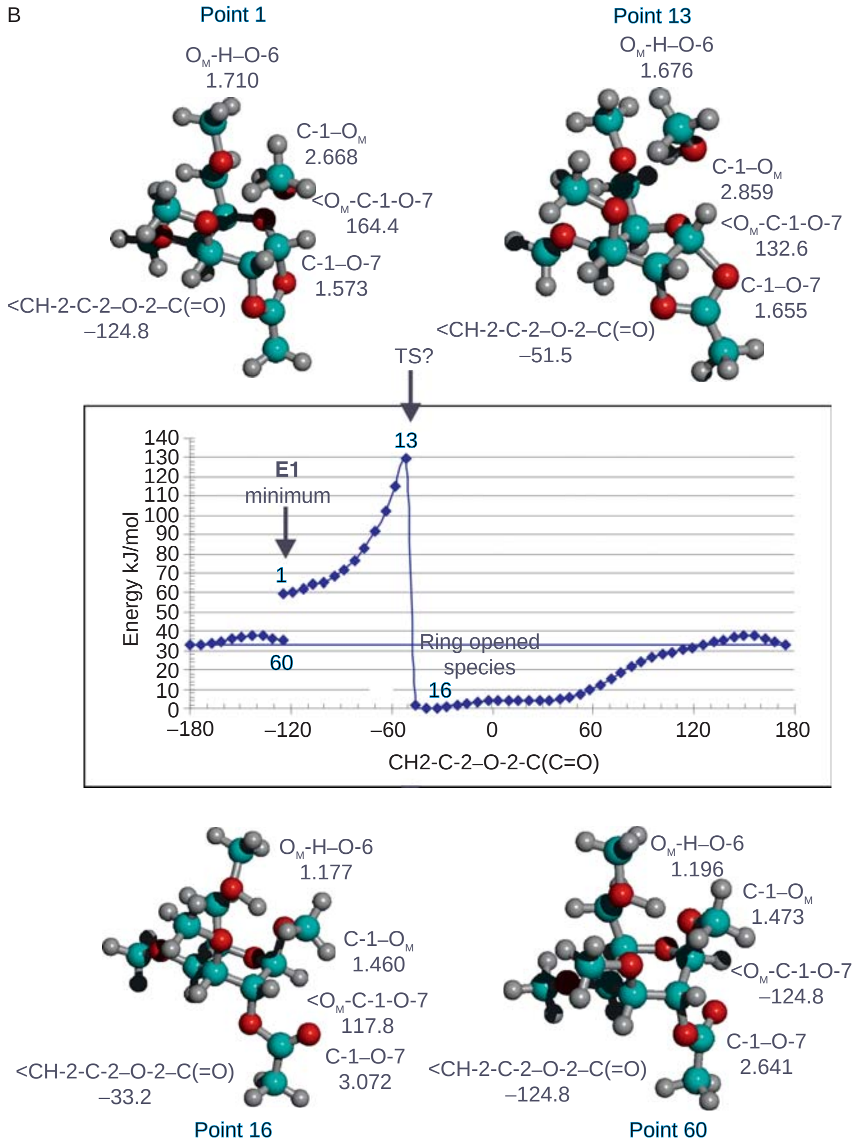

FIG. 18. (B) Bottom: rotation about the CH-2-C-2–O-2-C(=O) torsion angle of **17 E1**. Note the apparent TS at point 13. The four structures correspond to points 1, 13, 16, and 60, respectively. Also to be noted is the apparent proton transfer to O-6 after the ring opening.

transition states were also found for **16** and **15**.[74] In all instances the CH-2-C-2–O-2-C (=O) torsion angle is near 90°. In all cases where a TS could be found, the hydroxylic proton of the nucleophile is strongly H-bonded. This unanticipated result led to support for the hypothesis that at least in some cases, proton transfer could be involved at or near the TS of glycosylation reactions. Further considerations have led to further hypotheses, as shown in Schemes 15 and 7, that the leaving group or other polar species present in glycosylation reactions might function as proton acceptors in the TS when intramolecular H-bonding is not present. In fact, other groups studying by computations S_N2, reactions at carbon under solvolysis conditions have invoked proton-transfer relays such as the one presented in Scheme 7 at the TS.[228,229]

The energetic magnitude of these effects is difficult to discern from the present data but the misreactivity in glycosylation reactions with acceptors **31, 32,** and **33** suggests that it is large enough to have significant effects on the outcome of a glycosylation reaction. The energy diagram of Fig. 1C is redrawn in Scheme 16 to illustrate this possibility. It is surmised that, in some cases, intramolecular H-bonds may raise the proton-transfer barrier and possibly in other cases intermolecular H-bonds may lower the barrier. The energetic barrier to ionization depends on an interaction with a promoter or some other form of activation of the leaving group, and so experimentally determining the reaction barrier is complex. The process of acid hydrolysis of glycosides is more amenable to study, as the mechanism in most cases is glycosidic O-protonation followed by ionization and subsequent quenching of the oxacarbenium ion by water.[230] The corresponding enthalpy of activation is on the order of 140 kJ mol^{-1} for many alkyl glycopyranosides,[231] whereas the H-bonding effects

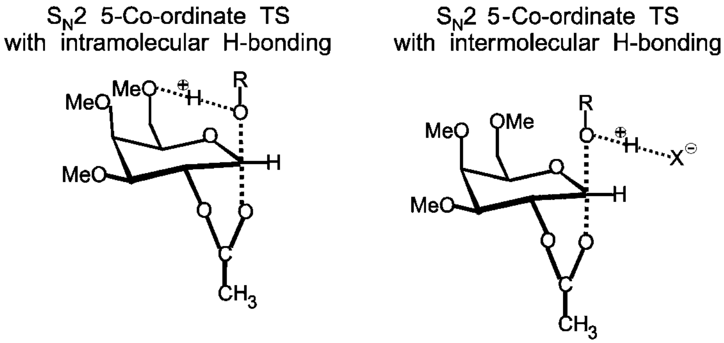

SCHEME 15. S_N2-like TS for **17** which involves (A) left, intramolecular H-bonding or (B) right, intermolecular H-bonding. In (B) the H-bond is shown to the anionic leaving group, but it could be to solvent molecules or other weakly basic species present in the reaction mixture.

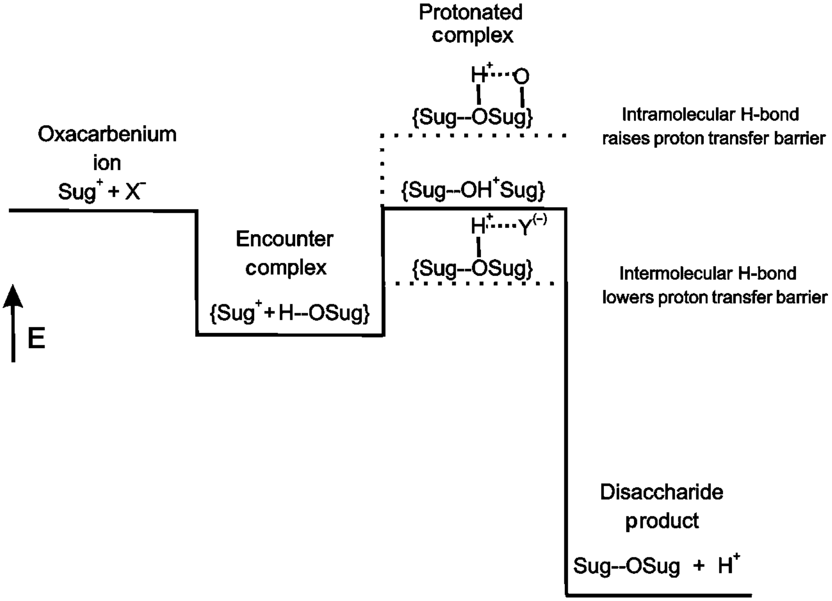
Protonated complex
H+···O
{Sug--OSug}
Intramolecular H-bond raises proton transfer barrier
Oxacarbenium ion
Sug+ + X−
{Sug--OH+Sug}
Encounter complex
{Sug+ + H--OSug}
H+····Y(-)
{Sug--OSug}
Intermolecular H-bond lowers proton transfer barrier
E
Disaccharide product
Sug--OSug + H+

SCHEME 16. Revised schematic: energy versus reaction-coordinate model for progression from an encounter complex to disaccharide taking into account H-bonds from the acceptor (compare Fig.1C, right side). Species Y may be the anionic leaving-group X^-, or some other electronegative reaction component. Relative energies are arbitrarily chosen, and may vary from case to case.

described here are on the order of 5–10 kJ mol^{-1}. Proton transfer can be modulated by additives and by judicious choice of protecting groups, both of which are under the control of synthetic chemists. Indeed it seems probable that both the reactivity and the stereochemical outcome of glycosylation reactions could be productively manipulated by appropriate modulation of these parameters.

7. Differences in Ionization Between *α*- and *β*-Donors

Although ionization is the first step of S_N1-like reaction mechanisms, it is not clear how to study this step computationally. The origin of this dilemma is that ionization starts from a neutral glycosyl donor and precedes to a charged oxacarbenium ion and an anionic leaving group. Even under the computational conditions used, in which the solvent is considered as a continuum dielectric that can help to stabilize charged species, the absence of either specific solvation or some other charge neutralization mechanism leads to minimum-energy species that maximize charge neutralization. In early LT studies, such as those in Fig. 7 (except that the leaving group was neutral) led to species where the anionic leaving-group complexed to C–H bonds and, in extreme cases, led to E_2-like elimination reactions. It is not clear if in some cases this type of interaction actually occurs, but if it is considered that most glycosylation reactions require promoters, it is probable that charge neutralization occurs by other mechanisms in most glycosylation reactions. Once a cycle of glycosylation starts, the hydroxylic proton is available for charge neutralization.

Further complexities include the intermediate CIPs and SSIPs. Since such species are only stable in solution, computational methods that include solvation are necessary. This is a research area where both experimental and computational developments are to be encouraged. Some preliminary studies have been made in this area by using an arbitrarily placed and fixed Li^+ cation as promoter for studying the ionization of a series of prototypic glycosyl donors. For these purposes there is no differentiation between activation of the leaving group and ionization.[232] Ionization is achieved by lengthening the C-1–X bond in small increments, with full geometry optimization of all other variables at each point.

The same computational experiment was performed for α/β 2-*O*-acetyl-3,4,6-tri-*O*-methyl-D-galactopyranosyl triflates (**18ab**) and the results closely parallel the previous ones; see Fig. 19. That is, the α anomer smoothly and reversibly (not shown) ionizes to a conformer near the **B0** conformer of **17**. In contrast, the β anomer undergoes an abrupt conformational change at C-1–O bond length of 1.71 Å to a conformation near $B_{O,3}$, and then slowly moves in conformational space toward the same **B0** conformation of **17**. The trajectory is not reversible, and a different, higher energy, neutral species is formed at short C-1–O bond lengths. That is, the two anomers ionize to the same conformation, but by different pathways. Plausibly if a good nucleophile is present that reacts before ionization is complete then different facial selectivity could be observed. Further, if only poor nucleophiles are present, then the selectivity should be the same, as the same **B0** ion should be the reactive species.

Selected frames for the β anomer are shown in Fig. 20, along with some selected geometric parameters. Besides the coefficients of the canonical vectors, the ring change can be monitored by the value of τ_5 which changes by 87.4° after C-1–O changes by 0.04 Å on going from frame 2 to frame 3. At this point O-5–C-1 has shortened, but not to the point that it can be considered a double bond such that this conformational change precedes ionization. Also of note is that the CH-2-C-2–O-2-C-7 dihedral angle hardly changes at all in any frame. Although not directly tested by this computational procedure, it suggests that ionization can proceed directly in this

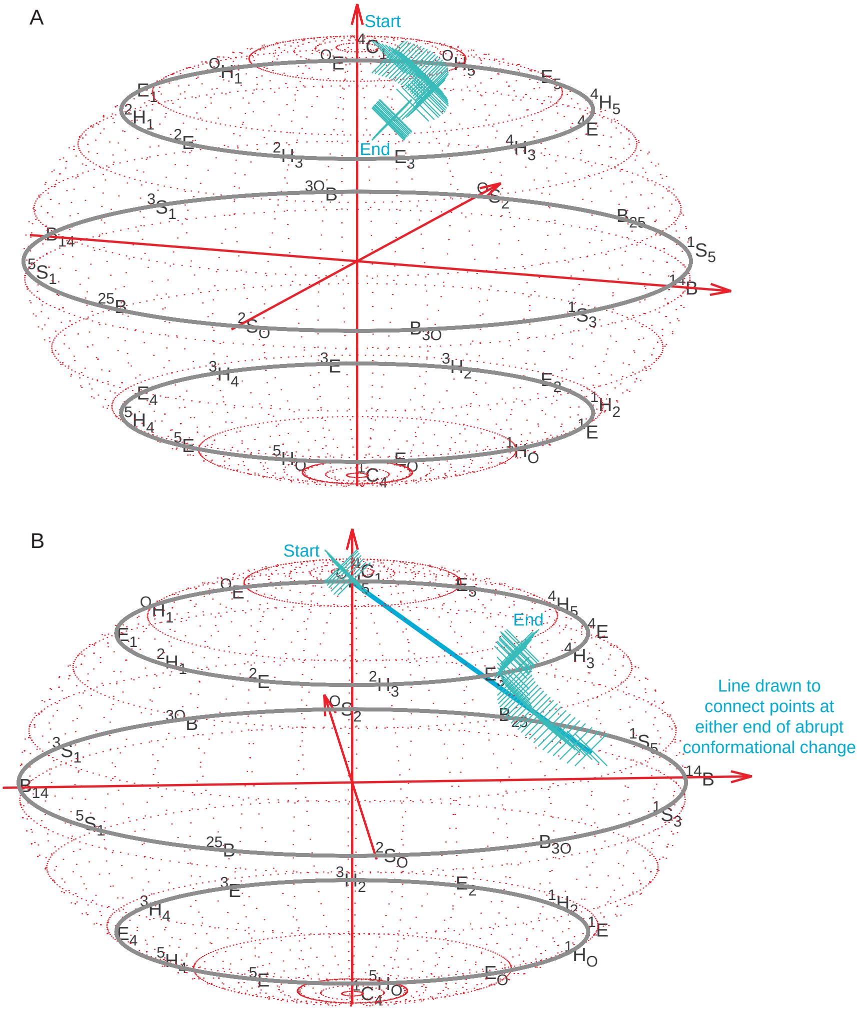

FIG. 19. (A) Top: the α-donor **18a** ionizes smoothly to a conformation near E_3, which is close in conformational space to the $^4H_3$ minimum for the isolated **17**. (B) Bottom: the β-donor **18b** starts to ionize smoothly, but at a C-1–O-1 bond length of 1.71 Å undergoes an abrupt conformational change to close to $B_{O,3}$ on the conformational equator, and then slowly moves toward E_3 as ionization increases.

case to a **B0** conformation without anchimeric assistance. Nucleophilic attack from the α face before dioxolenium ion formation would compromise the expected β-stereoselectivity.

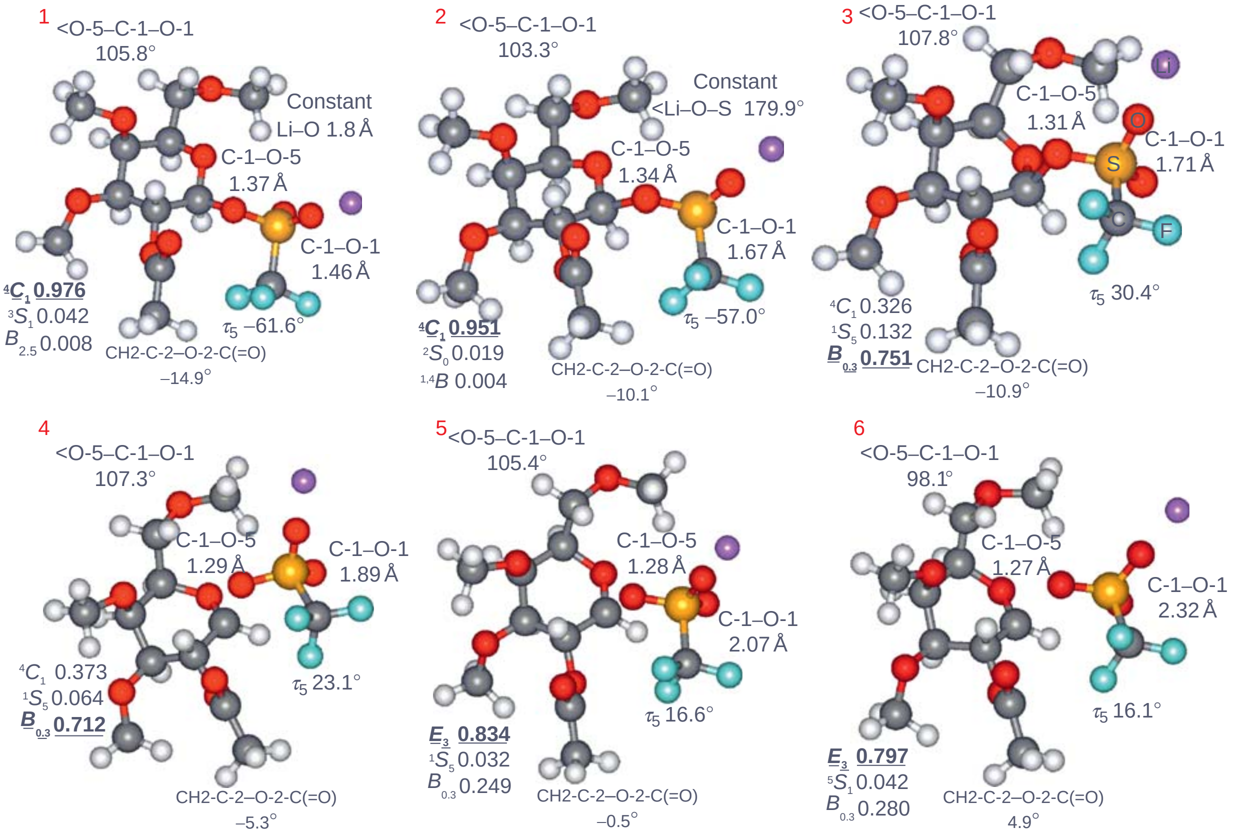
1
<O-5–C-1–O-1
105.8°
Constant
Li–O 1.8 Å
C-1–O-5
1.37 Å
C-1–O-1
1.46 Å
⁴C₁ 0.976
³S₁ 0.042
B₂.₅ 0.008
τ₅ –61.6°
CH2-C-2–O-2-C(=O)
–14.9°
2
<O-5–C-1–O-1
103.3°
Constant
<Li–O–S 179.9°
C-1–O-5
1.34 Å
C-1–O-1
1.67 Å
⁴C₁ 0.951
²S₀ 0.019
¹,⁴B 0.004
τ₅ –57.0°
CH2-C-2–O-2-C(=O)
–10.1°
3
<O-5–C-1–O-1
107.8°
Li
C-1–O-5
1.31 Å
O
C-1–O-1
1.71 Å
S
C
F
⁴C₁ 0.326
¹S₅ 0.132
B₀.₃ 0.751
τ₅ 30.4°
CH2-C-2–O-2-C(=O)
–10.9°
4
<O-5–C-1–O-1
107.3°
C-1–O-5
1.29 Å
C-1–O-1
1.89 Å
⁴C₁ 0.373
¹S₅ 0.064
B₀.₃ 0.712
τ₅ 23.1°
CH2-C-2–O-2-C(=O)
–5.3°
5
<O-5–C-1–O-1
105.4°
C-1–O-5
1.28 Å
C-1–O-1
2.07 Å
E₃ 0.834
¹S₅ 0.032
B₀.₃ 0.249
τ₅ 16.6°
CH2-C-2–O-2-C(=O)
–0.5°
6
<O-5–C-1–O-1
98.1°
C-1–O-5
1.27 Å
C-1–O-1
2.32 Å
E₃ 0.797
⁵S₁ 0.042
B₀.₃ 0.280
τ₅ 16.1°
CH2-C-2–O-2-C(=O)
4.9°

FIG. 20. Snapshots (1–6) from LT ionization (ADF-TPZ) of the β-triflate **18b** which is done by slow increments of the C-1–O-1 bond length. The Li^+–O (1.8 Å) and <S–O–Li^+ (179.9°) are kept constant. Relevant geometric parameters are indicated. Note the abrupt conformational change apparent in frame 3. Color code grey C, white H, blue F, yellow S, red O and purple Li.

Among the donors previously studied were neutral D-glycopyranosyl donors related to **3** and **4**, where X was fluoride, chloride, and triflate, as well as donors related to **14** where X = triflate. In all cases the α-configured donors ionized smoothly and reversibly from conformations near $^4C_1$ to near $^4H_3$. However in all examples the β-configured isomers exhibited abrupt conformational changes when the C-1–X bond length reached a value about 12–15% greater than its equilibrium value. Further, most trajectories were not reversible, and the resulting conformation was different if the maximally stretched bond was contracted back to its original value. The species formed after the abrupt change were different in all cases and, among this small selection of leaving groups, were leaving-group dependent. In the literature it has long been postulated that β-D-glycopyranosyl donors should undergo a pre-ionization conformational change to allow the C-1–X bond to become antiperiplanar to a lone pair on O-5.[233,234] The present computational results differ from this model in two ways. First the conformational change does not occur until the C-1–X bond has lengthened, and secondly the resulting conformation depends on the leaving group.

The ionization of anomeric triflates by lengthening the C-1–O bond may occur spontaneously for example by thermal vibrational excitation. However, the necessity to include the Li^+ ion as a promoter to obtain reliable computational results and experiments such as the following raise the possibility that a promoter is necessary; see Scheme 17. In this case, attempted glycosylation of acceptor **33** under a variety of standard conditions was not successful. However, when 2,6-di-*tert*-butyl-4-methylpyridine (DTMP), a hindered base, was added the disaccharide **35** could be isolated in good yield.[235] A possible mechanism is shown in Scheme 17 in which the protonated DTMP acts as a promoter for the anomeric triflate, which is in turn formed by anion exchange. This could be especially true for such highly deactivated donors as the phthalimide donor **34**. Progress toward unraveling these complexities would be assisted by having a reliable method to assess computationally the reactivity of donors, such as a much more sophisticated approach to ionization studies than the prototypes presented in this section.

III. CONCLUSIONS AND FUTURE DIRECTIONS

1. Summary of Glycosylation Reaction Mechanisms

Selected points from the vast glycosylation literature have been presented which are intended to complement the results shown for galactopyranosyl oxacarbenium ions related to **2** and **17**. A number of little recognized parameters previously described for other glycopyranosyl oxacarbenium ions have been identified for **2** and **17** that help to suggest their generality. A summary is made below:

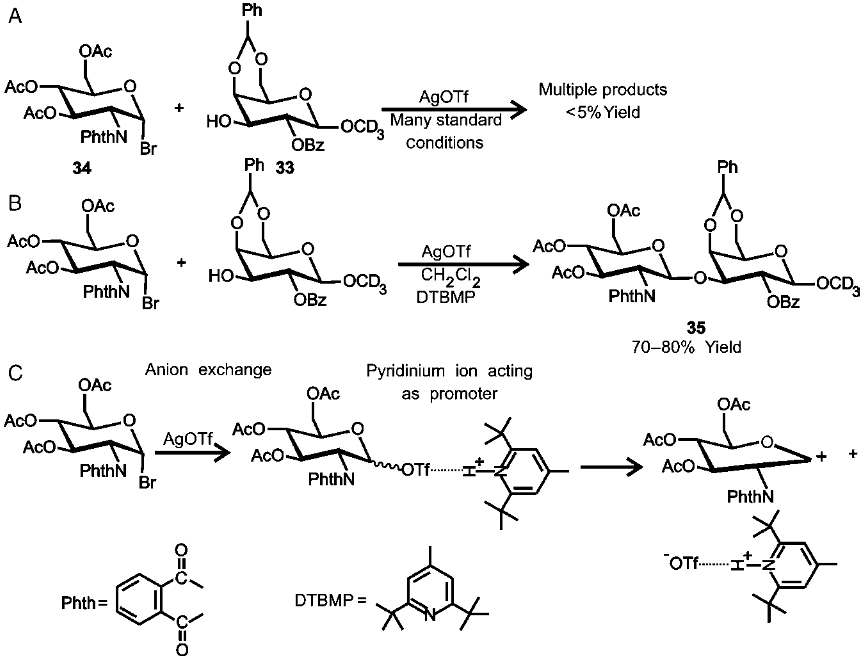
A
OAc
AcO
AcO
O
PhthN
Br
34
+
Ph
O
O
O
HO
OCD3
OBz
33
AgOTf
Many standard conditions
Multiple products
<5% Yield
B
OAc
AcO
AcO
O
PhthN
Br
+
Ph
O
O
O
HO
OCD3
OBz
AgOTf
CH2Cl2
DTBMP
OAc
AcO
AcO
O
PhthN
O
Ph
O
O
O
OCD3
OBz
35
70–80% Yield
C
OAc
AcO
AcO
O
PhthN
Br
Anion exchange
AgOTf
OAc
AcO
AcO
O
PhthN
OTf
Pyridinium ion acting as promoter
H
N
+
OAc
AcO
AcO
O
PhthN
+
+
-OTf
H
N
+
Phth=
O
C
C
O
DTBMP=
N

Scheme 17. (A) Top: failed glycosylation reaction under many conventional conditions. (B) Middle: experimental solution by use of the hindered base 2,6-di-*tert*-butyl-4-methylpyridine (DTMP); (C) possible mechanism for this glycosylation invoking promotion of the anomeric triflate by the pyridinium ion.

(1) The $^5S_1$ conformation of glycopyranosyl oxacarbenium ions with O-2 equatorial and the remaining substituents quasi-axial is important, especially for *gluco, galacto*, and related configurations.

(2) Facial selectivity of nucleophilic attack on glycopyranosyl oxacarbenium ions is determined by ring conformation and H-bonding. The latter depends especially on the lifetime of the oxacarbenium ions.

(3) The *syn* conformation about C-2–O-2 is an important feature of glycopyranosyl oxacarbenium ions.

(4) Neighboring-group participation occurs by C-2–O-2 bond rotation in both the forward **B** to **C** direction or in the reverse glycosylation reaction, except for some rigid cases.

(5) The transition states for glycosylation reactions involve proton transfer in most cases. The acidity of the alcoholic nucleophile increases as the degree of ionization of the glycosyl donor increases (see Scheme 18).

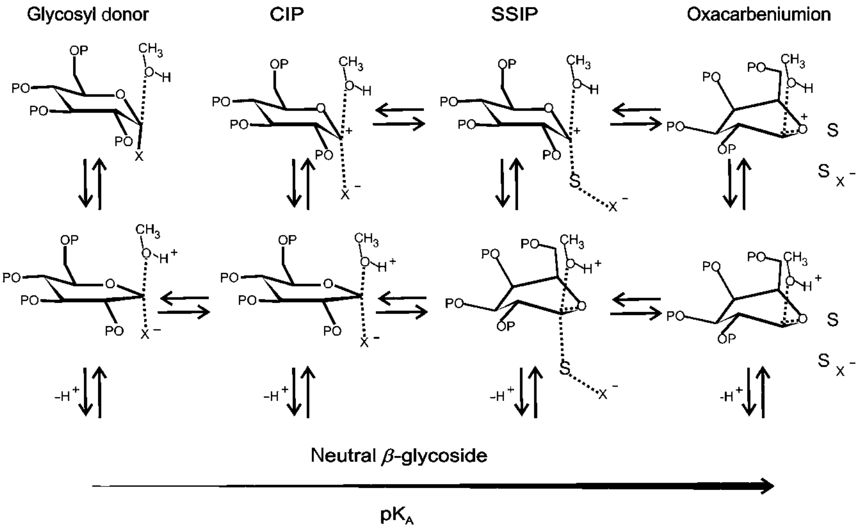

SCHEME 18. Schematic representation of the concept that, as the nucleophilic alcohol acceptor attacks a progressively ionized glycosyl donor, the acidity (pK_A) of the corresponding complex increases.

(6) Ionization appears to precede ring closure to dioxolenium ions, and hence loss of stereoselectivity can occur by at least two mechanisms: (i) Reactive nucleophiles can react before ring closure or (ii) The barrier height of the TS to ring closure becomes raised by steric or other factors, and the oxacarbenium ion is therefore the reactive species under kinetic control.

(7) Ionization of *β* anomers occurs by an abrupt conformational change before total ionization. This may also lead to altered stereoselectivity in the glycosylation reaction.

(8a) Unreactive donors lead to long-lived oxacarbenium ions that can equilibrate and hence have many routes of reactivity; and selectivity is therefore highly dependent on reaction conditions.

(8b) Reactive donors can react before ionization is complete and therefore selectivity is highly dependent on reaction conditions, but for different reasons than stated in 8a.

(9) Stereoselectivity can be optimized by channeling reaction into one pathway by appropriate combinations of protecting groups and leaving groups.

These combined results are summarized in Scheme 19 for such non-participating glycosyl donors as **2**, and in Scheme 20 for O-2 participating donors such as **17**.

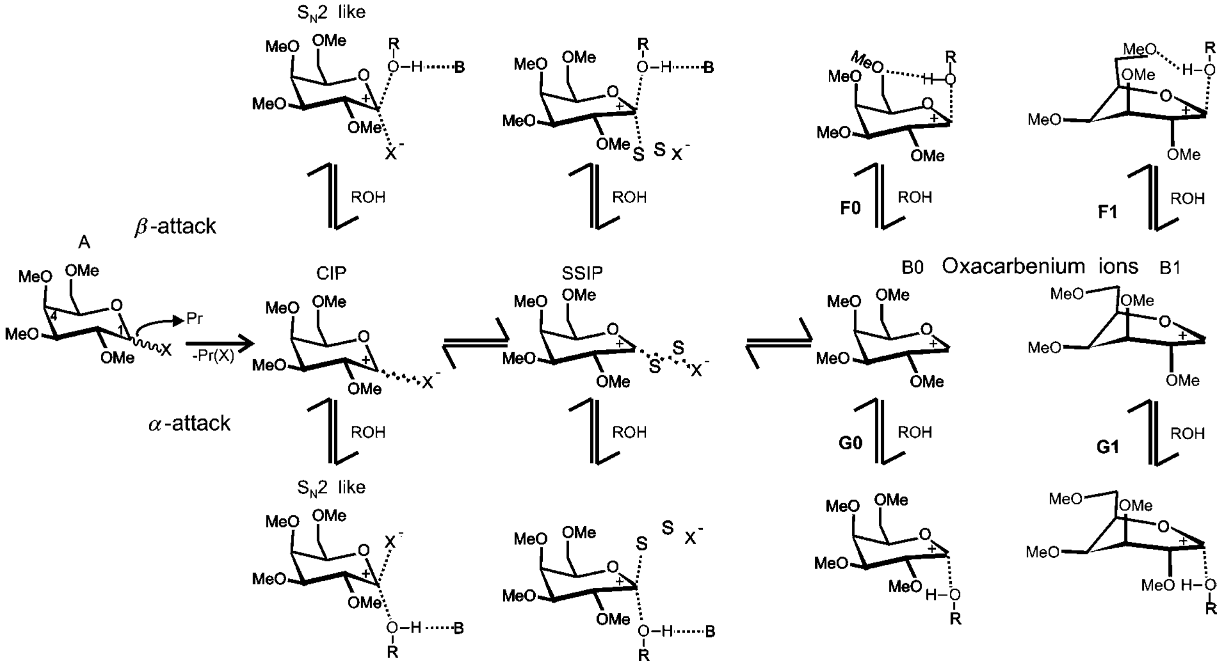
SN2 like
A
β-attack
α-attack
-Pr(X)
Pr
CIP
SSIP
ROH
F0
F1
G0
G1
B0 Oxacarbenium ions B1
SN2 like

SCHEME 19. Simplified mechanistic reaction scheme for non-participating glycosylation reactions of **2** not involving neighboring-group participation.

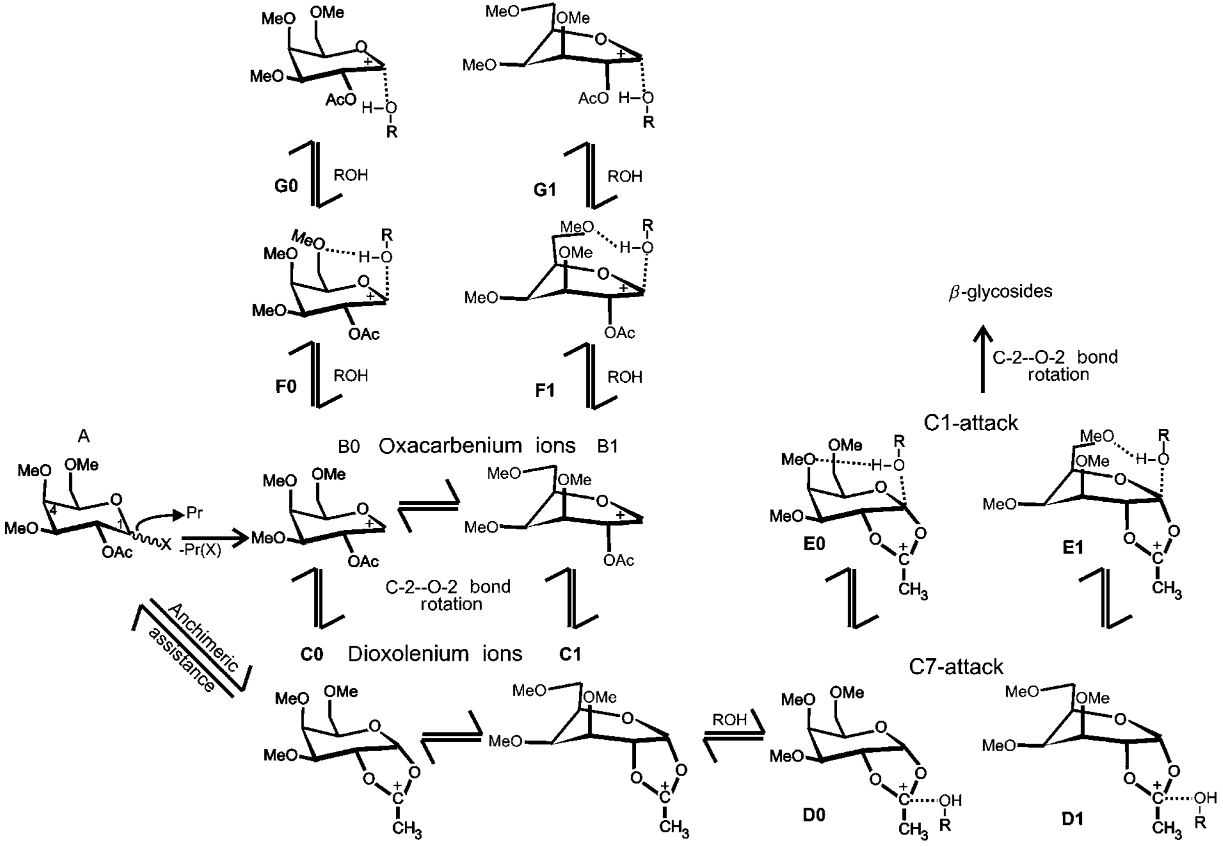
A
B0 Oxacarbenium ions B1
C0 Dioxolenium ions C1
Pr
-Pr(X)
Anchimeric assistance
C-2--O-2 bond rotation
G0
G1
F0
F1
ROH
E0
E1
D0
D1
C1-attack
C7-attack
β-glycosides
C-2--O-2 bond rotation

SCHEME 20. Simplified mechanistic scheme for glycosylation reactions of **17** involving neighboring-group participation.

2. Further Calculations Based on Existing Methodology

These discussions have also led to ideas listed here for future studies, and these are divided into computational and experimental. The computational studies have also been further subdivided into those using existing methodologies and those that require methodology development. Even those using existing methodologies may, of course, benefit from improvements in hardware, software, algorithms, and the like.

(1) CBS calculations of important quantities, notably **B0** versus **B1**, and **B1** versus **B2**, and so on, for a selection of glycopyranosyl oxacarbenium ions. Such studies should give a more accurate number for the following effects: (i) O-2-equatorial effect, (ii) O-2 *syn* versus *anti*. Experimental studies of such glycopyranosyl oxacarbenium ions should also be encouraged.

(2) Further studies of O-2 substituent effects, including the TS barrier to neighboring-group participation and the possibilities of using chiral protecting groups to take advantage of the O-2 *syn* preference.

(3) Since encounter complexes of alcohol donors and glycopyranosyl oxacarbenium ions were not found, nor were CIPs of partially ionized glycopyranosyl donors, it is hypothesized that including solvent molecules in such studies is necessary. Such studies may require methodology development, but are included here since these are extrapolations of existing studies.

(4) The ionization of leaving groups other than protonated OMe, triflate, and halide already studied. This includes thioglycosides and acetimidates. Such studies require more attention to the method of activation and should include such promoters as BF_3 and AgOTf.

3. Future Calculations Requiring Methodology Development

The following suggestions for study areas are much more speculative since they require, as a minimum, extensive model studies to arrive at a method. In many cases this will require extensive modifications to the existing software.

(1) Protecting-group–protecting group interactions, such as the steric buttressing effect. This requires a protocol for dealing with the problem of multiple minima of flexible protecting groups. It also requires assessing the reliability of computing through-space interactions, which probably require large basis sets and accurate evaluation of correlation effects.

(2) Experimental and/or theoretical studies to assess the role of H-bonding and proton transfer at or near the TS of glycosylation reactions. This not only requires reliable models of TSs, but also good computational methods for H-bonding.

(3) The study of CIPs and SSIPs and their reactivity with alcoholic nucleophiles. This includes the specific inclusion of solvent as in Section III.2, point 3. It also entails solving many body interactions such as in point (1).
(4) Related to (3) but still a separate issue is the inclusion of nucleophiles in ionization studies. At present, ionization is modeled by increasing the C-1–X bond length, but it is not clear if other degrees of freedom also contribute to ionization. Notably, it is plausible that conformational changes of the glycopyranosyl ring may in some cases initiate ionization rather than result from it. It would thus be beneficial if ways to implement complex constraints that include ring conformation, such as the canonical vector representation and for example C-1–Onuc bond length in the same calculation.
(5) Develop ways to determine the relative reactivity of glycosyl donors by calculation only and similarly to rank the reactivity of the hydroxyl groups of glycosyl acceptors. The ultimate goal would be to find unreactive or misreactive species without performing experiments.

4. Experimental Studies of Glycosylation

The overriding objective of these computational studies is to assist synthetic chemists in developing better experimental methodology. Similarly, studies of glycosyl processing enzymes are aimed at elucidating factors that industries using these enzymes can utilize to improve their processes. Next are some suggestions for experimental work derived from the computational studies presented in this chapter.

(1) To prepare glycopyranosyl donors having chiral protecting groups at O-2, to assess if the O-2 *syn* preference can be used productively to either increase reactivity or enhance stereoselectivity.
(2) To develop novel protecting groups or some other strategy to promote proton transfer in the TS of glycosylation reactions. These should be particularly aimed at activating unreactive hydroxyl groups.
(3) To further develop protecting-group strategies that would strongly bias the ring conformation of the glycopyranosyl oxacarbenium ion, and permit nucleophilic attack at one face to be strongly favored over the other.
(4) Experiments to determine what is the ‘‘real’’ leaving group in glycosylation reactions, and to ascertain if these react spontaneously or require a promoter. This relates particularly to anomeric triflates, as there is credible evidence for their participation in glycosylation reactions. It is not apparent whether these species react spontaneously or if they require some sort of promotion (see Scheme 17). Such studies could lead to a suite of such leaving groups and promoters that match most glycosylation reaction scenarios.

(5) Assess the role of trace amounts of water or other possible proton-relay molecules in glycosylation reactions. In the acyl-transfer model a relay molecule was found to lower the barrier for proton transfer.

ACKNOWLEDGMENTS

The author acknowledges the assistance of various collaborators, visiting scientists, and postdoctoral fellows who have made this research possible. These include J. J. Krepinsky, T. Nukada, A. Bérces, M. Z. Zgierski, L.-J. Wang, and A.R. Ionescu.

REFERENCES

1. G. E. Whitworth, M. S. Macauley, K. A. Stubbs, R. J. Dennis, E. J. Taylor, G. J. Davies, I. R. Greig, and D. J. Vocadlo, Analysis of PUGNAc and NAG-thiazoline as transition state analogues of human *O*-GlcNAcase: Mechanistic and structural insights into inhibitor selectivity and transitions state poise, *J. Am. Chem. Soc.*, 129 (2007) 635–644.
2. M. L. Sinnott, Catalytic mechanisms of enzymatic glycosyl transfer, *Chem. Rev.*, 90 (1990) 1171–1202.
3. A. J. Bennet and T. E. Kitos, Mechanisms of glycopyranosyl and 5-thioglycopyranosyl transfer reactions in solution, *J. Chem. Soc. Perkin Trans II* (2002) 1207–1222.
4. V. L. Schramm, Enzymatic transition states and transition state analogues, *Curr. Opin. Struct. Biol.*, 15 (2005) 604–613.
5. C.-H. Wong, Ed., *Carbohydrate-based Drug Discovery*, Wiley–VCH, Weinheim, 2003.
6. D. M. Whitfield and S. P. Douglas, Glycosylation reactions – Present status future directions, *Glycoconjugate J.*, 13 (1996) 5–17.
7. H. Paulsen, Advances in selective chemical syntheses of complex oligosaccharides, *Angew. Chem. Int. Ed.*, 21 (1982) 155–175.
8. N. K. Kochetkov, Recent developments in the synthesis of polysaccharides and stereospecificity of glycosylation reactions, in A. Rahman, (Ed.), *Studies in Natural Products Chemistry*, Vol. 14, Elsevier Science B. V, 1994, pp. 201–266.
9. N. S. Banait and W. P. Jencks, Reactions of anionic nucleophiles with α-D-glucopyranosyl fluoride in aqueous solutions through a concerted A_ND_N (S_N2) mechanism, *J. Am. Chem. Soc.*, 113 (1991) 7951–7958.
10. T. L. Amyes and W. P. Jencks, Lifetimes of oxocarbenium ions in aqueous solution from common ion inhibition of the solvolysis of α-azido ethers by added azide ion, *J. Am. Chem. Soc.*, 111 (1989) 7888–7900.
11. A. G. Gerbst, A. A. Grachev, A. S. Shashkov, and N. E. Nifantiev, Computation techniques in the conformational analysis of carbohydrates, *Russ. J. Bioorg. Chem. (Bioorganicheskaya Khimiya pp. 28–43)*, 33 (2007) 24–37.
12. C. O. da Silva, Carbohydrates and quantum chemistry: How useful is this combination? *Theor. Chem. Acta*, 116 (2006) 137–147.
13. J. T. Edward, Stability of glycosides to acid hydrolysis, *Chem. Ind.*, (1955) 1102–1104.

14. F. H. Newth and G. O. Phillips, The reactivity of the *O*-acylglycosyl halides. Part III. Steric effects, *J. Chem. Soc.*, (1953) 2904–2909.
15. K. N. Kirschner and R. J. Woods, Solvent interactions determine carbohydrate conformation, *Proc. Natl. Acad. Sci.*, 98 (2001) 10541–10545.
16. H. H. Jensen and M. Bols, Steric effects are not the cause of the rate difference in hydrolysis of stereoisomeric glycosides, *Org. Lett.*, 5 (2003) 3419–3421.
17. M. Miljković, D. Yeagley, P. Deslongchamps, and Y. L. Dory, Experimental and theoretical evidence of through-space electrostatic stabilization of the incipient oxocarbenium ion by an axially oriented electronegative substituent during glycopyranoside acetolysis, *J. Org. Chem.*, 62 (1997) 7597–7604.
18. D. M. Smith and K. A. Woerpel, Electrostatic interactions in cations and their importance in biology and chemistry, *Org. Biomol. Chem.*, 4 (2006) 1195–1201.
19. C. G. Lucero and K. A. Woerpel, Stereoselective *C*-glycosylation reactions of pyranoses: The conformational preference and reactions of mannosyl cation, *J. Org. Chem.*, 71 (2006) 2641–2647.
20. S. R. Shenoy, D. M. Smith, and K. A. Woerpel, Nucleophilic additions of trimethylsilyl cyanide to cyclic oxocarbenium ions: Evidence for the loss of stereoselectivity at the limits of diffusion control, *J. Am. Chem. Soc.*, 128 (2006) 8671–8677.
21. S. E. Barrows, F. J. Dulles, C. J. Cramer, A. D. French, and D. G. Truhlar, Relative stability of alternative chair forms and hydroxymethyl conformations of ß-D-glucopyranose, *Carbohydr. Res.*, 276 (1995) 219–251.
22. D. M. Whitfield, Orientations of carbohydrate substituents, *J. Mol. Struct.(Theochem)*, 395 (1997) 53–59.
23. G. A. Jeffrey, Modeling OH···O hydrogen bonds in carbohydrates, *J. Mol. Struct.*, 237 (1990) 75–79.
24. J. Screen, E. C. Stanca-Kaposta, D. P. Gamblin, B. Liu, N. A. Macleod, L. C. Snoek, B. G. Davis, and J. P. Simons, IR-spectral signatures of aromatic-sugar complexes: Probing carbohydrate–protein interactions, *Angew. Chem. Int. Ed.*, 46 (2007) 3644–3648.
25. R. A. Jockusch, R. T. Kroemer, F. O. Talbot, L. C. Snoek, P. Çarçabal, J. P. Simons, M. Havenith, J. M. Bakker, I. Compagnon, G. Meijer, and G. von Helden, Probing the glycosidic linkage: UV and IR ion-dip spectroscopy of a lactoside, *J. Am. Chem. Soc.*, 126 (2004) 5709–5714.
26. P. Çarçabal, I. Hünig, D. P. Gamblin, B. Liu, R. A. Jockusch, R. T. Kroemer, L. C. Snoek, A. J. Fairbanks, B. G. Davis, and J. P. Simons, Building up key segments of *N*-glycans in the gas phase: Intrinsic structural preferences of the α(1,3) and α(1,6) dimannosides, *J. Am. Chem. Soc.*, 128 (2006) 1976–1981.
27. R. A. Jockusch, F. O. Talbot, and J. P. Simons, Sugars in the gas phase part 2: The spectroscopy of jet-cooled phenyl *ß*-D-galactopyranoside, *Phys. Chem. Chem. Phys.*, 5 (2003) 1502–1507.
28. J.-Y. Salpin and J. Tortajada, Gas-phase acidity of D-glucose. A density functional theory study, *J. Mass Spectrom.*, 39 (2004) 930–941.
29. Y. K. Sturdy, C.-K. Skylaris, and D. C. Clary, Torsional anharmonicity in the conformational analysis of *ß*-D-galactose, *J. Phys. Chem. B*, 110 (2006) 3485–3492.
30. M. M. Deshmukh, L. J. Bartolotti, and S. R. Gadre, Intramolecular hydrogen bonding and cooperative interactions in carbohydrates via the molecular tailoring approach, *J. Phys. Chem. A*, 112 (2008) 312–321.
31. R. A. Klein, Lack of intramolecular hydrogen bonding in glucopyranose: Vicinal hydroxyl groups exhibit negative cooperativity, *Chem. Phys. Lett.*, 433 (2006) 165–169.
32. R. A. Klein, Electron density topological analysis of hydrogen bonding in glucopyranose and hydrated glucopyranose, *J. Am. Chem. Soc.*, 124 (2002) 13931–13937.
33. D. M. M. Jaradat, S. Mebs, L. Chęcińska, and P. Luger, Experimental charge density of sucrose at 20 K: Bond topological, atomic, and intermolecular quantitative properties, *Carbohydr. Res.*, 342 (2007) 1480–1489.

34. A. Vasella, G. J. Davies, and M. Böhm, Glycosidase mechanisms, *Curr. Opin. Chem. Biol.*, 6 (2002) 619–629.
35. T.-H. Tang, E. Deretey, S. J. Knak Jensen, and I. G. Csizmadia, Hydrogen bonds: Relation between lengths and electron densities at bond critical points, *Eur. Phys. J. D*, 37 (2006) 217–222.
36. M. Sládkovićová, P. Mach, L. Smrćok, and H. Rundlöf, DFT and neutron diffraction study of 1,6-anhydro-*ß*-D-glucopyranose (levoglucosan), *Cent. Eur. J. Chem.*, 5 (2007) 55–70.
37. C. Breton, L. Šnajdrová, C. Jeanneau, J. Koća, and A. Imberty, Structures and mechanisms of glycosyltransferases, *Glycobiology*, 16 (2006) 29R–37R.
38. I. Tvaroška, Molecular modeling insights into the catalytic mechanism of the retaining galactosyltransferase LgtC I, *Carbohydr. Res.*, 339 (2004) 1007–1014.
39. R. D. Lins and P. H. Hünenberger, A new GROMOS force field for hexopyranose-based carbohydrates, *J. Comput. Chem.*, 26 (2005) 1400–1412.
40. M.-J. Hwang, X. Ni, M. Waldman, C. S. Ewig, and A. T. Hagler, Derivation of Class II force fields. VI. Carbohydrate compounds and anomeric effects, *Biopolymers*, 45 (1998) 435–468.
41. M. Kuttel, J. W. Brady, and K. J. Naidoo, Carbohydrate solution simulations: Producing a force field with experimentally consistent primary alcohol rotational frequencies and populations, *J. Comput. Chem.*, 23 (2002) 1235–1243.
42. K. Ueda, T. Ueda, T. Sato, H. Nakayama, and J. W. Brady, The conformational free-energy map for solvated neocarrabiose, *Carbohydr. Res.*, 339 (2004) 1953–1960.
43. J. Gonzalez-Outeiriño, K. N. Kirschner, S. Thobhani, and R. J. Woods, Reconciling solvent effects on rotamer populations in carbohydrates - a joint MD and NMR analysis, *Can. J. Chem.*, 84 (2006) 569–579.
44. M. Basma, S. Sundara, D. Calgan, T. Vernali, and R. J. Woods, Solvated ensemble averaging in the calculation of partial atomic charges, *J. Comput. Chem.*, 22 (2001) 1125–1137.
45. R. J. Woods, R. A. Dwek, C. J. Edge, and B. Fraser-Reid, Molecular mechanical and molecular dynamical simulations of glycoproteins and oligosaccharides. 1. GLYCAM-93 parameter development, *J. Phys. Chem.*, 99 (1995) 3832–3846.
46. A. Bérces, D. M. Whitfield, T. Nukada, Z. I. do Santos, A. Obuchowska, and J. J. Krepinsky, Is acyl migration to the aglycon avoidable in 2-acyl assisted glycosylation reactions? *Can. J. Chem.*, 82 (2004) 1157–1171.
47. T. Nukada, A. Bérces, M. Z. Zgierski, and D. M. Whitfield, Exploring the mechanism of neighbouring group assisted glycosylation reactions, *J. Am. Chem. Soc.*, 120 (1998) 13291–13295.
48. T. Nukada, A. Bérces, and D. M. Whitfield, Can the stereochemical outcome of glycosylation reactions be controlled by the conformational preferences of the glycosyl donor? *Carbohydr. Res.*, 337 (2002) 765–774.
49. T. Schaefer, K. J. Cox, C. L. Morier, C. Beaulieu, R. Sebastian, and G. H. Penner, Motion about the $C_{sp}2$–$C_{sp}3$ bond in benzyl OR ($R = CH_3$, CH_2CH_3, $CH(CH_3)_2$, $C(CH_3)_3$). Solvent and substituent dependence, *Can. J. Chem.*, 68 (1990) 1553–1558.
50. H.-S. Im, E. R. Bernstein, H. V. Secor, and J. I. Seeman, Supersonic jet studies of benzyl alcohols: Minimum energy conformations and torsional motion, *J. Am. Chem. Soc.*, 113 (1991) 4422–4431.
51. G. I. Csonka, Proper basis set for quantum mechanical studies of potential energy surfaces of carbohydrates, *J. Mol. Struct. (Theochem)*, 584 (2002) 1–4.
52. N. Miura, T. Taniguchi, K. Monde, and S. I. Nishimura, A theoretical study of α- and *ß*-D-glucopyranose conformations by the density functional theory, *Chem. Phys. Lett.*, 419 (2006) 326–332.
53. U. Schnupf, J. L. Willet, W. B. Bosma, and F. A. Momany, DFT studies of the disaccharide, α-maltose: Relaxed isopotential maps, *Carbohydr. Res.*, 342 (2007) 196–216.
54. Y. Kurihara and K. Ueda, An investigation of the pyranose ring interconversion path of α-L-idose calculated using density functional theory, *Carbohydr. Res.*, 341 (2006) 2565–2574.

55. T. Flieg, S. Knecht, and C. Hättig, Quantum-chemical investigation of the structures and electronic spectra of the nucleic acid bases at the coupled cluster CC2 level, *J. Phys. Chem. A*, 111 (2007) 5482–5491.
56. O. Guvench and A. D. MacKerell, Jr., Quantum mechanical analysis of 1,2-ethanediol conformational energetics and hydrogen bonding, *J. Phys. Chem. A*, 110 (2006) 9934–9939.
57. J. Antony and S. Grimme, Is spin-component scaled second-order Møller–Plesset perturbation theory an appropriate method for the study of noncovalent interactions in molecules? *J. Phys. Chem. A*, 111 (2007) 4862–4868.
58. Y. R. Huang, S. Knippenberg, B. Hajgató, J.-P. François, J. K. Deng, and M. S. Deleuze, Imaging momentum orbital densities of conformationally versatile molecules: A benchmark theoretical study of the molecular and electronic structures of dimethoxymethane, *J. Phys. Chem. A*, 111 (2007) 5879–5897.
59. M. D. Wodrich, C. Corminboeuf, P. R. Schreiner, A. A. Fokin, and P. R. von Ragué Schleyer, How accurate are DFT treatments of organic energies? *Org. Lett.*, 9 (2007) 1851–1854.
60. P. R. Schreiner, Relative energy computations with approximate Density Functional Theory – A caveat!, *Angew. Chem. Int. Ed.*, 46 (2007) 4217–4219.
61. Y. Zhao and D. G. Truhlar, How well can new-generation density functionals describe protonated epoxides where older functionals fail, *J. Org. Chem.*, 72 (2007) 295–298.
62. T. A. Rokob, A. Hamza, and I. Pápai, Computing reliable energetics for conjugate addition reactions, *Org. Lett.*, 9 (2007) 4279–4282.
63. A. J. Weldon, T. L. Vickrey, and G. S. Tschumper, Intrinsic conformational preferences of substituted cyclohexanes and tetrahydropyrans evaluated at the CCSD(T) complete basis set limit: Implications for the anomeric effect, *J. Phys. Chem. A*, 109 (2005) 11073–11079.
64. H. L. Woodcock, D. Moran, R. W. Pastor, A. D. MacKerell, Jr., and B. R. Brooks, *Ab initio* modeling of glycosyl torsions and anomeric effects in a model carbohydrate: 2-ethoxy tetrahydropyran, *Biophys. J.*, 93 (2007) 1–10.
65. I. Tvaroška and J. P. Carver, The anomeric and *exo*-anomeric effects of a hydroxy group and the stereochemistry of the hemiacetal linkage, *Carbohydr. Res.*, 309 (1998) 1–9.
66. A. R. Ionescu, L.-J. Wang, M. Z. Zgierski, T. Nukada, and D. M. Whitfield, Two unexpected effects found with 2,3,4,6-tetra-*O*-methyl-D-gluco- and mannopyranosyl oxacarbenium ions: An O-2 pseudo-equatorial preference and a large H-2-C-2–O-2-CH_3*syn* preference, in H. Vliegenhart and R. J. Woods, (Eds.), *NMR Spectroscopy and Modeling of Carbohydrates, Am. Chem. Soc. Symp. Ser. 930,* Oxford University Press, 2006, pp. 302–319.
67. S. H. Vosko, L. Wilk, and M. Nusair, Accurate spin-dependent electron liquid correlation energies for local spin density calculations: A critical analysis, *Can. J. Phys.*, 58 (1980) 1200–1211.
68. A. D. Becke, Density-functional exchange-energy approximation with correct asymptotic behavior, *Phys. Rev. A*, 38 (1988) 3098–3100.
69. J. P. Perdew, K. Burke, and Y. Wang, Generalized gradient approximation for the exchange-correlation hole of a many-electron system, *Phys. Rev. B*, 54 (1996) 16533–16539.
70. M. Hricovíni, B3LYP/6–311++G** study of structure and spin-spin coupling constants in methyl 2-*O*-sulfo-α-L-iduronate, *Carbohydr. Res.*, 341 (2006) 2575–2580.
71. J. Baker, Constrained optimization in delocalized internal coordinates, *J. Comput. Chem.*, 18 (1997) 1079–1095.
72. R. U. Lemieux, The mercaptolysis of glucose and galactose pentaacetates, *Can. J. Chem.*, 29 (1951) 1079–1091.
73. R. U. Lemieux, Some implications in carbohydrate chemistry of theories relating to the mechanisms of replacement reactions, *Adv. Carbohydr. Chem.*, 9 (1954) 1–57.

74. A. R. Ionescu, D. M. Whitfield, M. Z. Zgierski, and T. Nukada, Investigations into the role of oxacarbenium ions in glycosylation reactions by ab initio molecular dynamics, *Carbohydr. Res.*, 341 (2006) 2912–2920.
75. T. Nukada, A. Bérces, L.-J. Wang, M. Z. Zgierski, and D. M. Whitfield, The two conformer hypothesis: 2,3,4,6-tetra-*O*-methyl- mannopyranosyl- and -glucopyranosyl oxacarbenium ions, *Carbohydr. Res.*, 340 (2005) 841–852.
76. J. F. Stoddart, *Stereochemistry of Carbohydrates*, Wiley-Interscience, New York, 1971.
77. E. Juaristi, *Conformational Behavior of Six-Membered Rings Analysis, Dynamics, and Stereoelectronic Effects Methods in Stereochemical Analysis*, Wiley–VCH, Weinheim, 1995.
78. D. Cremer and J. A. Pople, A general definition of ring puckering coordinates, *J. Am. Chem. Soc.*, 97 (1975) 1354–1358.
79. J. B. Hendrickson, Molecular geometry. VII. Modes of interconversion in the medium rings, *J. Am. Chem. Soc.*, 89 (1967) 7047–7061.
80. For a fully working version see http://www.sao.nrc.ca/ibs/6ring/.
81. T. Nukada and D. M. Whitfield, Practical applications of computational studies of the glycosylation reaction, in A. A. Klyosov, Z. J. Witczak, and D. Platt, (Eds.) *Carbohydrate Drug Design - ACS Symp. Ser.*, Vol. 932. Wiley–VCH, Weinheim, 2006, pp. 265–300.
82. A. Bérces, T. Nukada, and D. M. Whitfield, Quantitative description of six-membered ring conformations following the IUPAC conformational nomenclature, *Tetrahedron*, 57 (2001) 477–491.
83. O. Hassel and B. Ottar, The structure of molecules containing cyclohexane or pyranose rings, *Acta Chem. Scand.*, 1 (1947) 929–942.
84. H. H. Jensen, L. U. Nordstrøm, and M. Bols, The disarming effect of the 4,6-acetal group on glycoside reactivity: Torsional or electronic? *J. Am. Chem. Soc.*, 126 (2004) 9205–9213.
85. R. J. Woods, C. W. Andrews, and J. P. Bowen, Molecular mechanical investigations of the properties of oxocarbenium ions. 2. Application to glycoside hydrolysis, *J. Am. Chem. Soc.*, 114 (1992) 859–864.
86. N. N. Malysheva, V. I. Torgov, E. M. Klimov, and N. K. Kochetkov, Intramolecular glycosylation of 6-*O*-benzyl-substituted glucose derivatives, *Izvestiya Akademii Nauk SSSR, Seriya Khimicheskaya*, 9 (1974) 2153–2155Engl. Trans 1975 2075–2077.
87. Z. Li and J. C. Gildersleeve, An armed-disarmed approach for blocking aglycon transfer of thioglycosides, *Tetrahedron Lett.*, 48 (2007) 559–562.
88. Z. Li and J. C. Gildersleeve, Mechanistic studies and methods to prevent aglycon transfer of thioglycosides, *J. Am. Chem. Soc.*, 128 (2006) 11612–11619.
89. R. Geurtsen and G.-J. Boons, Chemoselective glycosylations of sterically hindered glycosyl acceptors, *Tet. Lett.*, 43 (2002) 9429–9431.
90. G. Wulff and G. Röhle, Results and problems of *O*-glycoside synthesis, *Angew. Chem. Int. Ed.*, 13 (1974) 157–170.
91. D. Crich, Chemistry of glycosyl triflates: Synthesis of *ß*-mannopyranosides, *J. Carbohydr. Chem.*, 21 (2002) 667–690.
92. D. Crich and S. Sun, Are glycosyl triflates intermediates in the sulfoxide glycosylation method? A chemical and ^{1}H, ^{13}C, and ^{19}F NMR spectroscopic investigation, *J. Am. Chem. Soc.*, 119 (1997) 11217–11223.
93. B. A. Garcia and D. Y. Gin, Dehydrative glycosylation with activated diphenyl sulfonium reagents. Scope, mode of *C*(1)-hemiacetal activation, and detection of reactive glycosyl intermediates, *J. Am. Chem. Soc.*, 122 (2000) 4269–4279.
94. A. Demchenko, T. Stauch, and G.-J. Boons, Solvent and other effects on the stereoselectivity of thioglycoside glycosidations, *SYNLETT*, (1997) 818–820.
95. I. Braccini, C. Derouet, J. Esnault, C. H. du Penhoat, J.-M. Mallet, V. Michon, and P. Sinaÿ, Conformational analysis of nitrilium intermediates in glycosylation reactions, *Carbohydr. Res.*, 246 (1993) 23–41.

96. V. Magnus, D. Vikić-Topić, S. Iskrić, and S. Kveder, Competitive formation of peracetylated α-L-arabinopyranosides and β-L-arabinose 1,2-(alkyl orthoactetates) in Koenigs-Knorr condensations, *Carbohydr. Res.*, 114 (1983) 209–224.
97. J. P. Richard, K. B. Williams, and T. L. Amyes, Intrinsic barriers for the reactions of an oxocarbenium ion in water, *J. Am. Chem. Soc.*, 121 (1999) 8403–8404.
98. J. P. Richard and Y. Tsuji, Dynamics for reaction of an ion pair in aqueous solution: The rate constant for ion pair reorganization, *J. Am. Chem. Soc.*, 122 (2000) 3963–3964.
99. D. Crich and O. Vinogradova, On the influence of the C2–O2 and C3–O3 bonds in 4,6-*O*-benzylidene-directed β-mannopyranosylation and α-glucopyranosylation, *J. Org. Chem.*, 71 (2006) 8473–8480.
100. G.-J. Boons and T. Stauch, T. Stereoselectivity in glycosidic bond formation: Studies on the anomerisation of thioglycosides, *SYNLETT*, (1996) 906–908.
101. A. J. Rhind-Tutt and C. A. Vernon, Mechanisms of reactions in the sugar series. Part II. Nucleophilic substitution in 2,3,4,6-tetra-*O*-methylglycopyranosyl chlorides, *J. Chem. Soc. Part 2*, (1960) 4637–4643.
102. T. Bowden, P. J. Garegg, J. L. Maloisel, and P. Konradsson, A mechanistic study: Nucleophilic dependence in glucosylations with glucosyl bromides, *Israel J. Chem.*, 40 (2000) 271–277.
103. M. J. S. Dewar and R. C. Dougherty, *The PMO Theory of Organic Chemistry;* Plenum, New York, 1975, p. 263.
104. J. P. Richard, A consideration of the barrier for carbocation–nucleophile combination reactions, *Tetrahedron*, 51 (1995) 1535–1573.
105. H. Perst, in *Oxonium Ions in Organic Chemistry*, Verlag Chemie, Weinheim, 1971.
106. Y. Blériot, A. Genre-Grandpierre, A. Imberty, and C. Tellier, Structure and conformation of mannoamidines by NMR and molecular modeling: Are they good transition state mimics? *J. Carbohydr. Chem.*, 15 (1996) 985–1000.
107. C. W. Andrews, B. Fraser-Reid, and J. P. Bowen, An ab initio study (6–31G$^{☆}$) of transition states in glycoside hydrolysis based on axial and equatorial 2-methoxytetrahydropyrans, *J. Am. Chem. Soc.*, 113 (1991) 8293–8298.
108. P. Deslongchamps, Y. L. Dory, and S. Li, 1994 R.U. Lemieux award lecture hydrolysis of acetals and ketals. Position of reaction states along the reaction coordinates, and stereoelectronic effects, *Can. J. Chem.*, 72 (1994) 2021–2027.
109. M. Mohr, R. A. Bryce, and I. H. Hillier, Quantum chemical studies of carbohydrate reactivity: Acid catalyzed ring opening reactions, *J. Phys. Chem. A*, 105 (2001) 8216–8222.
110. S. Suzuki, K. Matsumoto, K. Kawamura, S. Suga, and J.-I. Yoshida, Generation of alkoxycarbenium ion pools from thioacetals and applications in glycosylation chemistry, *Org. Lett.*, 6 (2004) 3755–3758.
111. S. Suga, K. Matsumoto, K. Ueoka, and J.-I. Yoshida, Indirect cation pool method. Rapid generation of alkoxycarbenium ion pools from thioacetals, *J. Am. Chem. Soc.*, 128 (2006) 7710–7711.
112. T. A. Boebel and D. Y. Gin, Probing the mechanism of sulfoxide-catalyzed hemiacetal activation in dehydrative glycosylation, *J. Org. Chem.*, 70 (2005) 5818–5826.
113. C. Denekamp and Y. Sandlers, Anomeric distinction and oxonium ion formation in acetylated glycosides, *J. Mass Spectrom.*, 40 (2005) 765–771.
114. C. Denekamp and Y. Sandlers, Formation and stability of oxocarbenium ions from glycosides, *J. Mass Spectrom.*, 40 (2005) 1055–1063.
115. V. Kovacik, J. Hirsch, D. Thölmann, and H.-F. Grützmacher, Fourier transform ion cyclotron resonance study of ion-molecule reactions of $[\mathrm{M\text{-}OCH_3}]^+$ ions of methyl 2,3,4,6-tetra-*O*-methyl-D-hexopyranosides with ammonia, *Org. Mass. Spectrom.*, 26 (1991) 1085–1088.
116. V. Maroušek, T. J. Lucas, P. E. Wheat, and C. Schuerch, The influence of reactant structure and solvent on galactoside syntheses from galactosyl sulfonates, *Carbohydr. Res.*, 60 (1978) 85–96.

117. R. Eby and C. Schuerch, The use of positively charged leaving-groups in the synthesis of α-D-linked glucosides. Synthesis of methyl 2,3,4-tri-*O*-benzyl-6-*O*-(2,3,4,6-tetra-*O*-benzyl-α-D-glucopyranosyl)-α-D-glucopyranoside, *Carbohydr. Res.*, 39 (1975) 33–38.
118. J. M. J. Fréchet and H. H. Baer, Concerning the problem of stereospecific glycosylation. Synthesis and methanolysis of some 2-*O*-benzylated D-galactopyranosyl and D-galactofuranosyl halides, *Can. J. Chem.*, 53 (1975) 670–678.
119. H. Tokimoto, Y. Fujimoto, K. Fukase, and S. Kusumoto, Stereoselective glycosylation using the long-range effect of a [2-(4-phenylbenzyl)oxycarbonyl]benzoyl group, *Tet. Asymm.*, 16 (2005) 441–447.
120. S. Houdier and P. J. A. Vottero, Steric effect of a bulky 6-substituent in the I^+-promoted glycosylation with pent-4-enyl and thioethyl glycosides, *Carbohydr. Res.*, 232 (1992) 349–352.
121. J. M. Fréchet and C. Schuerch, Solid-phase synthesis of oligosaccharides. II. Steric control by C-6 substituents in glucoside syntheses, *J. Am. Chem. Soc.*, 94 (1972) 604–609.
122. J.-L. M. Abboud, I. Alkorta, J. Z. Davalos, P. Müller, E. Quintanilla, and J.-C. Rossier, Influence of carbocation stability in the gas phase on solvolytic reactivity: Beyond bridgehead derivatives, *J. Org. Chem.*, 68 (2003) 3786–3796.
123. D. Kaneno and S. Tomoda, Origin of facial diastereoselection in 2-adamantyl cations. Theoretical evidence against the Felkin-Anh and the Cieplak models, *Tetrahedron Lett.*, 45 (2004) 4559–4562.
124. M. Dejter-Juszynski and H. M. Flowers, Studies on the Koenigs-Knorr reaction Part II. Synthesis of an α-linked disaccharide from tri-*O*-benzyl-α-fucopyranosyl bromide, *Carbohydr. Res.*, 18 (1971) 219–226.
125. R. U. Lemieux, K. B. Hendriks, R. V. Stick, and K. James, Halide ion catalyzed glycosidation reactions. Syntheses of α-linked disaccharides, *J. Am. Chem. Soc.*, 97 (1975) 4056–4062.
126. J. P. Richard, M. M. Toteva, and T. L. Amyes, What is the stabilizing interaction with nucleophilic solvents in the transition state for solvolysis of tertiary derivatives: Nucleophilic solvent participation or nucleophilic solvation, *Org. Lett.*, 3 (2001) 2225–2228.
127. C. Fraschetti, F. R. Novara, A. Filippi, N. A. Trout, W. Adcock, T. S. Sorensen, and M. Speranza, Gas-phase diastereoselectivity of secondary 5-substituted (X)-adamant-2-yl ($X = F, Si(CH_3)_3$) cations, *J. Org. Chem.*, 72 (2007) 4077–4083.
128. D. Crich and H. Xu, Direct stereocontrolled synthesis of 3-amino-3-deoxy-*β*-mannopyranosides: Importance of the nitrogen protecting group on stereoselectivity, *J. Org. Chem.*, 72 (2007) 5183–5192.
129. T. H. Schmidt and R. Madsen, Glycosylations directed by the armed-disarmed effect with acceptors containing a single ester group, *Eur. J. Org. Chem.*, (2007) 3935–3941.
130. D. M. Whitfield and T. Nukada, DFT Studies of the role of C-2–O-2 bond rotation in neighboring-group glycosylation reactions, *Carbohydr. Res.*, 342 (2007) 1291–1304.
131. S. Morpurgo, M. Bossa, and G. O. Morpurgo, A theoretical study of hydrogen bonding, proton transfer and kinetic isotope effects in the dimer of 2-tetrahydropyranol and in 2-tetrahydropyranol-H_2O adducts, *Phys. Chem. Chem. Phys.*, 3 (2001) 4898–4906.
132. S. Morpurgo, M. Brahimi, M. Bossa, and G. O. Morpurgo, A theoretical study on proton transfer in the mutarotation of sugars, *Phys. Chem. Chem. Phys.*, 2 (2000) 2707–2713.
133. K. E. S. Dean, A. J. Kirby, and I. V. Komarov, Torsional effects on reactivity in glycosyl transfer, *J. Chem. Soc. Perkin Trans. II*, (2002) 337–341.
134. C. M. Pedersen, L. U. Nordstrøm, and M. Bols, ''Super Armed'' glycosyl donors: Conformational arming of thioglycosides by silylation, *J. Am. Chem. Soc.*, 129 (2007) 9222–9235.
135. H. H. Jensen, C. M. Pedersen, and M. Bols, Going to extremes ''Super'' armed glycosyl donors in glycosylation chemistry, *Chem. Eur. J.*, 13 (2007) 7576–7582.
136. S. R. Shenoy and K. A. Woerpel, Investigations into the role of ion pairing in reactions of heteroatom-substituted cyclic oxocarbenium ions, *Org. Lett.*, 7 (2005) 1157–1160.
137. V. van Speybroeck and R. J. Meier, A recent development in computational chemistry: Chemical reactions from first principles molecular dynamics simulations, *Chem. Soc. Rev.*, 32 (2003) 151–157.

138. O. Coskuner, Preferred conformation of the glycosidic linkage of methyl-ß-mannose, *J. Chem. Phys.*, 127 (2007) 15101–15107.
139. J. M. Stubbs and D. Marx, Aspects of glycosidic bond formation in aqueous solution: Chemical bonding and the role of water, *Chem. Eur. J.*, 11 (2005) 2651–2659.
140. A. R. Ionescu, A. Bérces, M. Z. Zgierski, D. M. Whitfield, and T. Nukada, The conformational pathways of saturated six-membered rings. A static and dynamical density functional study, *J. Phys. Chem. A*, 109 (2005) 8096–8105.
141. P. E. Marszalek, H. Li, A. F. Oberhauser, and J. M. Fernandez, Chair-boat transitions in single polysaccharide molecules observed by force-ramp AFM, *Proc. Natl. Acad. Sci.*, 99 (2002) 4278–4283.
142. G. J. Davies, V. M.-A. Ducros, A. Varrot, and D. L. Zechel, Mapping the conformational itinerary of ß-glycosidases by X-ray crystallography, *Biochem. Soc. Trans*, 31 (2003) 523–527.
143. T. M. Gloster, P. Meloncelli, R. V. Stick, D. L. Zechel, A. Vasella, and G. J. Davies, Glycosidase inhibition: An assessment of the binding of 18 putative transition-state mimics, *J. Am. Chem. Soc.*, 129 (2007) 2345–2354.
144. X. Biarmés, A. Ardèvol, A. Planas, C. Rovira, A. Laio, and M. Parrinello, The conformational free energy landscape of ß-D-glucopyranose. Implications for substrate preactivation in ß-glucoside hydrolases, *J. Am. Chem. Soc.*, 129 (2007) 10686–10693.
145. J. K. Lee, A. D. Bain, and P. J. Berti, Probing the transitions states of four glucoside hydrolyses with ^{13}C kinetic isotope effects measured at natural abundance by NMR spectroscopy, *J. Am. Chem. Soc.*, 126 (2004) 3769–3776.
146. P. J. Berti and S. E. Tanaka, Transitions state analysis using multiple kinetic isotope effects: Mechanisms of enzymatic and non-enzymatic glycoside hydrolysis and transfer, *Adv. Phys. Org. Chem.*, 37 (2002) 239–314.
147. P. K. Qasba, B. Ramakrishnan, and E. Boeggeman, Substrate-induced conformational changes in glycosyltransferases, *Trends Biochem. Sci.*, 30 (2005) 53–62.
148. D. M. A. Guérin, M. B. Lascombe, M. Costabel, H. Souchon, V. Lamzin, P. Béguin, and P. M. Alzari, Atomic (0.94 Å) resolution structure of an inverting glycosidase in complex with substrate, *J. Mol. Biol.*, 316 (2002) 1061–1069.
149. V. M. A. Ducros, D. L. Zechel, G. N. Murshudov, H. J. Gilbert, L. Szabó, D. Stoll, S. G. Withers, and G. J. Davies, Substrate distortion by a ß-mannanase: Snapshots of the Michaelis and covalent intermediate complexes suggest a $B_{2,5}$ conformation for the transition state, *Angew. Chem. Int. Ed.*, 41 (2002) 2824–2827.
150. A. V. Demchenko, E. Rousson, and G.-J. Boons, Stereoselective 1,2-*cis*-galactosylation assisted by remote neighboring group participation and solvent effects, *Tetrahedron Lett.*, 40 (1999) 6523–6526.
151. A. G. Gerbst, N. E. Ustuzhanina, A. A. Grachev, E. A. Khatuntseva, D. E. Tsvetkov, D. M. Whitfield, A. Bérces, and N. E. Nifantiev, Synthesis, NMR and conformational studies of fucoidan fragments 3: Effect of benzoyl group at O-3 on stereoselectivity of glycosylation by 3-*O*- and 3,4-di-*O*-benzoylated 2-*O*-benzyl-fucosyl bromides, *J. Carbohydr. Chem.*, 20 (2001) 821–831.
152. J.-W. Kim, H. Yang, V. Khot, D. M. Whitfield, and G.-J. Boons, Stereoselective glycosylations using (*R*)- or (*S*)-(ethoxycarbonyl)benzyl chiral auxiliaries at C-2 of glycopyranosyl donors, *Eur. J. Org. Chem.*, (2006) 5007–5028.
153. D. Crich and V. Y. Dudkin, An unusual example of steric buttressing in glycosylation, *Tetrahedron Lett.*, 41 (2000) 5643–5646.
154. D. Crich and P. Jayalath, 2-*O*-Propargyl ethers: Readily cleavable, minimally intrusive protecting groups for ß-mannosyl donors, *Org. Lett.*, 7 (2005) 2277–2280.
155. D. Crich, P. Jayalath, and T. K. Hutton, Enhanced diastereoselectivity in ß-mannopyranosylation through the use of sterically minimal propargyl ether protecting groups, *J. Org. Chem.*, 71 (2006) 3064–3070.

156. D. Crich and N. S. Chandrasekera, Mechanism of 4,6-*O*-benzylidene-directed *β*-mannosylation as determined by α-deuterium kinetic isotope effects, *Angew. Chem. Int. Ed.*, 43 (2004) 5886–5889.
157. R. Weingart and R. R. Schmidt, Can preferential *β*-mannopyranoside formation with 4,6-*O*-benzylidene protected mannopyranosyl sulfoxides be reached with trichloroacetimidates? *Tetrahedron Lett.*, 41 (2000) 8753–8758.
158. K. Worm-Leonhard, K. Larsen, and K. J. Jensen, 4,6-*O*-benzylidene directed *β*-mannosylation without intermediate trfilate formation? Comparison of trichloroacetimidate and DISAL donors in microwave promoted glycosylations under neutral conditions, *J. Carbohydr. Chem.*, 26 (2007) 349–368.
159. I. Tvaroška, F. R. Taravel, J. P. Utille, and J. P. Carver, Quantum mechanical and NMR spectroscopy studies on the conformations of the hydroxymethyl and methoxymethyl groups in aldohexosides, *Carbohydr. Res.*, 337 (2002) 353–367.
160. C. H. Marzabadi, J. E. Anderson, J. Gonzalez-Outeirino, P. R. J. Gaffney, C. G. H. White, D. A. Tocher, and L. J. Todaro, Why are silyl ethers conformationally different from alkyl ethers? Chair–chair conformational equilibria in silyloxycyclohexanes and their dependence on the substituents on silicon. The wider roles of eclipsing, of 1,3-repulsive steric interactions, and of attractive steric interactions, *J. Am. Chem. Soc.*, 125 (2003) 15163–15173.
161. A. Mendonca, G. P. Johnson, A. D. French, and R. A. Laine, Conformational analyses of native and permethylated disaccharides, *J. Phys. Chem. A*, 106 (2002) 4115–4124.
162. I. V. Alabugin, M. Manoharan, and T. A. Zeidan, Homoanomeric effects in six-membered heterocycles, *J. Am. Chem. Soc.*, 125 (2003) 14014–14031.
163. E. Kleinpeter, N. Rolla, A. Koch, and F. Taddei, Hyperconjugation and the increasing bulk of $OCOCX_3$ substituents in trans-1,4-disubstituted cyclohexanes destabilize the diequatorial conformer, *J. Org. Chem.*, 71 (2006) 4393–4399.
164. T.-H. Tang, D. M. Whitfield, S. P. Douglas, I. G. Csizmadia, and J. J. Krepinsky, Differential reactivity of carbohydrate hydroxyls in glycosylation reactions I: Intramolecular interaction of the 5′-hydroxyl group with the heteroaromatic base in a model compound of 2-deoxy-cytidine, *Can. J. Chem.*, 70 (1992) 2434–2448.
165. K. Oku, H. Watanabe, M. Kubota, S. Fukuda, M. Kurimoto, Y. Tsujisaka, M. Komori, Y. Inoue, and M. Sakurai, NMR and quantum chemical study on the $OH\cdots\pi$ and $CH\cdots O$ interactions between trehalose and unsaturated fatty acids: Implications for the mechanism of antioxidant function of trehalose, *J. Am. Chem. Soc.*, 125 (2003) 12739–12748.
166. A. R. Ionescu, D. M. Whitfield, and M. Z. Zgierski, O-2 Substituted pyranosyl oxacarbenium ions are C-2–O-2 rotors with a strong *syn* preference, *Carbohydr. Res.*, 342 (2007) 2793–2800.
167. F. Bravo, A. Viso, E. Alcázar, P. Molas, C. Bo, and S. Castillón, Computational insight into the reaction intermediates in the glycosylation reaction assisted by donor heteroatoms, *J. Org. Chem.*, 68 (2003) 686–691.
168. S. Wolfe, H. B. Schlegel, M.-H. Whangbo, and F. Bernardi, On the origin of the Bohlmann bands, *Can. J. Chem.*, 52 (1974) 3787–3792.
169. J.-H. Lii, K.-H. Chen, and N. L. Allinger, Alcohols, ethers, carbohydrates, and related compounds part V. The Bohlmann torsional effect, *J. Phys. Chem. A*, 108 (2004) 3006–3015.
170. M. J. Frisch, G. W. Trucks, H. B. Schlegel, G. E. Scuseria, M. A. Robb, J. R. Cheeseman, V. G. Zakrzewski, J. A. Montgomery, Jr., R. E. Stratmann, J. C. Burant, S Dapprich, J. M. Millam, *et al.*, *Gaussian 98, Revision A.11.3*, Gaussian, Inc, Pittsburgh PA, 2002.
171. E. D. Glendening, A. E. Reed, J. E. Carpenter, F. Weinhold, NBO Version 3.1.
172. H. Paulsen, Haworth memorial lecture: Synthesis of complex oligosaccharide chains of glycoproteins, *Chem. Soc. Rev.*, (1983) 15–45.
173. B. Fraser-Reid, U. E. Udodong, Z. Wu, H. Ottosson, J. R. Merritt, C. S. Rao, C. Roberts, and R. Madsen, *n*-Pentenyl glycosides in organic chemistry: A contemporary example of serendipity, *SYNLETT*, (1992) 927–942.

174. B. Fraser-Reid, J. R. Merritt, A. L. Handlon, and C. W. Andrews, The chemistry of *n*-pentenyl glycosides: Synthetic, theoretical, and mechanistic ramifications, *Pure Appl. Chem.*, 65 (1993) 779–786.
175. Z. Zhang, I. R. Ollman, X.-S. Ye, R. Wischnat, T. Baasov, and C.-H. Wong, Programmable one-pot oligosaccharide synthesis, *J. Am. Chem. Soc.*, 121 (1999) 734–753.
176. N. L. Douglas, S. V. Ley, U. Lucking, and S. L. Warriner, Tuning glycoside reactivity: A new tool for efficient oligosaccharide synthesis, *J. Chem. Soc. Perkin Trans. I*, (1998) 51–65.
177. K. N. Jayaprakash and B. Fraser-Reid, A study of *n*-pentenyl orthoesters having *manno, gluco,* and *galacto* configurations in regioselective glycosylations, *Carbohydr. Res.*, 342 (2007) 490–498.
178. K. N. Jayaprakash, J. Lu, and B. Fraser-Reid, Synthesis of a lipomannan component of the cell-wall complex of *Mycobacterium tuberculosis* is based on Paulsen's concept of donor/acceptor ''match,'' *Angew. Chem. Int. Ed.*, 44 (2005) 5894–5898.
179. B. Fraser-Reid, S. Grimme, M. Piacenza, M. Mach, and U. Schlueter, Orthoester versus 2-*O*-acyl glycosides as glycosyl donors: Theoretical and experimental studies, *Chem. Eur. J.*, 9 (2003) 4687–4692.
180. N. M. Spijker, H. M. Zuurmond, P. Westerduin, and C. A. A. van Boeckel, Studies directed towards the synthesis of sulphated and non-sulphated glyco-conjugate fragments using insoluble silver-salt promoters, *Recl. Trav. Chim. Pays-bas*, 108 (1989) 360–368.
181. N. M. Spijker, C. A. A. van Boeckel, Double stereodifferentiation in carbohydrate coupling reactions: The mismatched interaction of donor and acceptor as an unprecedented factor governing α/β ratio of glycoside formation, *Angew. Chem. Int. Ed.*, 30 (1991) 180–183.
182. S. S. Kulkarni, Y.-H. Liu, and S.-C. Hung, Neighboring group participation of 9-anthracenylmethyl group in glycosylation: Preparation of unusual *C*-glycosides, *J. Org. Chem.*, 70 (2005) 2808–2811.
183. A. V. Demchenko, 1,2-*cis O*-Glycosylation: Methods, strategies, principles, *Curr. Org. Chem.*, 7 (2003) 35–79.
184. H. Tanaka, N. Matoba, H. Tsukamoto, H. Takimoto, H. Yamada, and T. Takahashi, Automated parallel synthesis of a protected oligosaccharide library based upon the structure of dimeric Lewis X by one-pot sequential glycosylation, *SYNLETT*, (2005) 824–828.
185. J. D. C. Codée, R. E. J. N. Litjens, L. J. van den Bos, H. S. Overkleeft, and G. A. van der Marel, Thioglycosides in sequential glycosylation strategies, *Chem. Soc. Rev.*, 34 (2005) 769–782.
186. X. Huang, L. Huang, H. Wang, and X.-S. Ye, Iterative one-pot oligosaccharide synthesis, *Angew. Chem. Int. Ed.*, 116 (2001) 5221–5224.
187. Y. Wang, X.-S. Ye, and L.-H. Zhang, Oligosaccharide assembly by one-pot multi-step strategy, *Org. Biomol. Chem.*, 5 (2007) 2189–2200.
188. M. N. Namchuk, J. D. McCarter, A. Becalski, T. Andrews, and S. G. Withers, The role of sugar substituents in glycoside hydrolysis, *J. Am. Chem. Soc.*, 122 (2000) 1270–1277.
189. J. P. Richard, D. A. McCall, C. K. Heo, and M. M. Toteva, Ground-state, transitions-state, and metal-cation effects of the 2-hydroxy group on β-D-galactopyranosyl transfer catalyzed by β-galactosidase (*Escherichia coli, lac Z*), *Biochemistry*, 44 (2005) 11872–11881.
190. M. Terinek and A. Vasella, Synthesis of tetrahydropyridoimidazole-2-acetates: Effect of carboxy and methoxcarbonyl groups at C(2) on the inhibition of some β- and α-glycosidases, *Helv. Chim. Acta*, 87 (2004) 3035–3049.
191. S. Winstein and R. E. Buckles, The role of neighboring groups in displacement reactions. 1. Retention of configuration in the reaction of some dihalides and acteoxyhalides with silver acetate, *J. Am. Chem. Soc.*, 64 (1942) 2780–2801.
192. H. L. Frush and H. S. Isbell, Sugar acetates, acetylglycosyl halides, and orthoacetates in relation to the Walden inversion, *J. Natl. Bur. Stand.*, 27 (1941) 413–428.
193. M. Tichý and M. Pánková, Diequatorial chair transition state in cyclisation of a diequatorial benzamido methanesulphonate, *Coll. Czech. Chem. Commun.*, 40 (1975) 647–657.

194. D. Crich and M. Li, Revisiting the armed–disarmed concept: The importance of anomeric configuration in the activation of *S*-benzoxazolyl glycosides, *Org. Lett.*, 9 (2007) 4115–4118.

195. Y. Zeng, J. Ning, and F. Z. Kong, Remote control of α- or *β*-stereoselectivity in (1→3)-glucosylations in the presence of C-2 ester capable of neighboring-group participation, *Tet. Lett.*, 43 (2002) 3729–3733.

196. Y. Zeng, J. Ning, and F. Z. Kong, Pure α-linked products can be obtained in high yields in glycosylation with glucosyl trichloroacetimidate donors with a C2 ester capable of neighboring group participation, *Carbohydr. Res.*, 338 (2003) 307–311.

197. F. Yang, H. He, Y. Du, and M. Lü, Unexpected α-stereochemical outcome of attempted *β*-glycosylations, *Carbohydr. Res.*, 337 (2002) 1165–1169.

198. A. Imamura, H. Ando, S. Korogi, G. Tanabe, O. Muraoka, H. Ishida, and M. Kiso, Di-*tert*-butylsilylene (DTBS) group-directed α-selective galactosylation unaffected by C-2 participating functionalities, *Tet. Lett.*, 44 (2003) 6725–6728.

199. L. Chen and F. Z. Kong, Unusual α-glycosylation with galactosyl donors with a C2 ester capable of neighboring group participation, *Tet. Lett.*, 44 (2003) 3691–3695.

200. A. Imamura, A. Kimura, H. Ando, H. Ishida, and M. Kiso, Extended applications of di-*tert*-butylsilylene-directed α-predominant galactosylation compatible with C-2-participating groups toward the assembly of various glycosides, *Chem. Eur. J.*, 12 (2006) 8862–8870.

201. D. Crich and P. Jayalath, Stereocontrolled formation of *β*-glucosides and related linkages in the absence of neighboring group participation: Influence of a *trans*-fused 2,3-*O*-carbonate group, *J. Org. Chem.*, 70 (2005) 7252–7259.

202. J. E. Wallace and L. R. Schroeder, Koenigs–Knorr reactions. Part 3. Mechanistic study of mercury(II) cyanide promoted reactions of 2-*O*-acetyl-3,4,6-tri-*O*-methyl-α-D-glucopyranosyl bromide with cyclohexanol in benzene–nitromethane, *J. Chem. Soc. Perkin Trans II*, (1977) 795–802.

203. H. Paulsen and E. Schüttpelz, *Endo*-Envelope-Konformation bei 2-methyl-*cis*-4,5-trimethylen-1,3-dioxolan-2-ylium-tetrafluoroborat, *Chem. Ber.*, 112 (1979) 3214–3220.

204. D. Crich, Z. Dai, and S. Gastaldi, On the role of neighboring group participation and orthoesters in *β*-xylosylation: ^{13}C NMR observation of a bridging 2-phenyl-1,3-dioxolenium ion, *J. Org. Chem.*, 64 (1999) 5224–5229.

205. N. K. Kochetkov, V. M. Zhulin, E. M. Klimov, N. N. Malysheva, Z. G. Makarova, and A. Y. Ott, The effect of high pressure on the stereoselectivity of the glycosylation reaction, *Carbohydr. Res.*, 164 (1987) 241–254.

206. G. Hodosi and J. J. Krepinsky, Polymer-supported solution synthesis of oligosaccharides: Probing glycosylation of MPEG-DOX-OH with 2-acetamidoglycopyranosyl derivatives, *SYNLETT*, (1996) 159–161.

207. J. Banoub and D. R. Bundle, 1,2-orthoacetate intermediates in silver trifluoromethanesulphonate promoted Koenigs–Knorr synthesis of disaccharide glycosides, *Can. J. Chem.*, 57 (1979) 2091–2097.

208. P. J. Garegg and T. Norberg, Observations on silver trifluoromethanesulfonate-promoted syntheses of 1,2-*trans*-glycosides from acylated glycosyl bromides, *Acta Chem. Scand. B*, 33 (1979) 116–118.

209. P. J. Garegg, P. Konradsson, I. Kvarnström, T. Norberg, S. C. T. Svensson, and B. Wigilius, Studies on Koenigs–Knorr glycosidations, *Acta Chem. Scand. B*, 39 (1985) 569–577.

210. P. J. Garegg and I. Kvarnström, The orthoester glycosylation method. Variations in the anomeric composition of the product with aglycone basicity in the two step procedure, *Acta Chem. Scand. B*, 30 (1976) 655–658.

211. P. J. Garegg and I. Kvarnström, The orthoester glycosylation method. Part II. Variation in the anomeric composition of the product with aglycone basicity and accessibility, *Acta Chem. Scand. B*, 31 (1977) 509–513.

212. T. Nukada, A. Bérces, and D. M. Whitfield, Acyl transfer as a problematic side reaction in polymer-supported oligosaccharide synthesis, *J. Org. Chem.*, 64 (1999) 9030–9045.

213. A. F. Bochkov, V. I. Betaneli, and N. K. Kochetkov, Sugar orthoesters 16. Mechanism of the isomerization of protected α-D-glucopyranose 1,2-orthoacetates by mercuric bromide in nitromethane, *Bioorg. Khim.(Engl.)*, 3 (1977) 30–35.
214. A. F. Bochkov, V. I. Betaneli, and N. K. Kochetkov, Sugar orthoesters XV. Dependence on the conditions and mechanisms of the proton-catalyzed reactions of substituted α-D-glucopyranose 1,2-(alkyl orthoacetate)s in media of low polarity, *Bioorg. Khim.(Engl.)*, 2 (1976) 671–682.
215. N. F. Samoshina and N. I. Uvarova, Preparation of acetates of glucosides of steroid and triterpene alcohols via the isomeric orthoesters, *Khim. Prirodnykh Soedinenii (Engl.)*, 3 (1979) 289–294.
216. F. Z. Kong, Recent studies on reaction pathways and applications of sugar orthoesters in synthesis of oligosaccharides, *Carbohydr. Res.*, 342 (2007) 345–373.
217. E. Eichler, F. Yan, J. Sealy, and D. M. Whitfield, 1-Methyl 1′-cyclopropylmethyl – An acid labile *O*-protecting group for polymer-supported oligosaccharide synthesis, *Tetrahedron*, 57 (2001) 6679–6693.
218. H. Yu, D. L. Williams, and H. A. Ensley, 4-Acetoxy-2,2-dimethylbutanoate: A useful carbohydrate protecting group for the selective formation of *β*-(1 3)-D-glucans, *Tetrahedron Lett.*, 46 (2005) 3417–3421.
219. W. Hao and V. D. Parker, Rapid formation and slow collapse of a carbocation–anion pair to a neutral molecule, *J. Org. Chem.*, 73 (2008) 48–55.
220. I. Tvaroška, I. André, and J. P. Carver, Ab initio molecular orbital study of the catalytic mechanism of glycosyltransferases: Description of reaction pathways and determination of transition-state structures for inverting *N*-acetylglucosaminyltransferases, *J. Am. Chem. Soc.*, 122 (2000) 8762–8776.
221. I. Tvaroška, I. André, and J. P. Carver, Catalytic mechanism of the inverting *N*-acetylglucosaminyltransferase I: DFT quantum mechanical model of the reaction pathway and determination of the transition state structure, *Glycobiology*, 13 (2003) 559–566.
222. M. Raab, S. Kozmon, and I. Tvaroška, Potential transition-state analogs for glycosyltransferases. Design and DFT calculations of conformational behavior, *Carbohydr. Res.*, 340 (2005) 1051–1057.
223. X. Biarmés, J. Nieto, A. Planas, and C. Rovira, Substrate distortion in the Michaelis complex of *Bacillus* 1,3–1,4-*β*-glucanase. Insight from first principles molecular dynamics simulations, *J. Biol. Chem.*, 281 (2006) 1432–1441.
224. I. André, I. Tvaroška, and J. P. Carver, On the reaction pathways and determination of transitionm-state structures for retaining α-galactotransferases, *Carbohydr. Res.*, 338 (2003) 865–877.
225. T.-H. Tang, D. M. Whitfield, S. P. Douglas, J. J. Krepinsky, and I. G. Csizmadia, Differential reactivity of carbohydrate hydroxyls in glycosylation reactions III: Structure, stability and reactivity of 2′-deoxycytidine model compound–BF_3 complexes, *Can. J. Chem.*, 72 (1994) 1803–1825.
226. D. M. Whitfield, S. P. Douglas, T.-H. Tang, I. G. Csizmadia, H. Y. S. Pang, F. L. Moolten, and J. J. Krepinsky, Differential reactivity of carbohydrate hydroxyls in glycosylation reactions II: The effect of intramolecular hydrogen bonding on the rate-limiting step in glycosylation reactions. Galactosylation of nucleoside 5′-hydroxyls for the syntheses of novel potential anticancer agents, *Can. J. Chem.*, 72 (1994) 2225–2238.
227. D. M. Whitfield, M. Y. Meah, and J. J. Krepinsky, Ultrasonic agitation accelerates *cis*-glycosylation with heterogeneous promoters, *Collect. Czech. Chem. Comm.*, 58 (1993) 159–172.
228. X. Lin, C. Zhao, and D. L. Phillips, Modeling S_N2 reactions in methanol solution by ab initio calculation of nucleophile solvent–substrate clusters, *J. Org. Chem.*, 70 (2005) 9279–9287.
229. J. Chandrasekhar, S. F. Smith, and W. L. Jorgensen, Theoretical examination of the S_N2 reaction involving chloride ion and methyl chloride in the gas phase and aqueous solution, *J. Am. Chem. Soc.*, 107 (1985) 154–163.
230. A. J. Bennet and M. L. Sinnott, Complete kinetic isotope effect description of transition states for acid-catalyzed hydrolyses of methyl α- and*β*-glucopyranosides, *J. Am. Chem. Soc.*, 108 (1986) 7287–7294.

231. T. E. Timell, The acid hydrolysis of glycosides 1. General conditions and the effect of the nature of the aglycone, *Can. J. Chem.*, 42 (1964) 1456–1472.
232. A. Bülow, T. Meyer, T. K. Olszewski, and M. Bols, The C-4 configuration as a probe for the study of glycosidation reactions, *Eur. J. Org. Chem.*, (2004) 323–329.
233. L. Hosie, P. J. Marshall, and M. L. Sinnott, Failure of the the antiperiplanar lone pair hypothesis in glycoside hydrolysis. Synthesis, conformation, and hydrolysis of a α-D-xylopyranosyl- and α-D-glucopyranosyl-pyridinium salts, *J. Chem. Soc. Perkin Trans. II*, (1984) 1121–1131.
234. P. Deslongchamps, S. Li, and Y. L. Dory, Hydrolysis of α- and β-glycosides. New experimental data and modeling of reaction pathways, *Org. Lett.*, 6 (2004) 505–508.
235. D. M. Whitfield, C. J. Ruzicka, J. P. Carver, and J. J. Krepinsky, Synthesis of model oligosaccharides of biological significance. 9. Synthesis of trideuteriomethyl di-3,6-*O*-(2-acetamido-2-deoxy-β-D-glucopyranosyl)-β-D-galactopyranoside: The I antigen branch-point trisaccharide and related disaccharides, *Can. J. Chem.*, 65 (1987) 693–703.

ADVANCES IN CARBOHYDRATE CHEMISTRY AND BIOCHEMISTRY, VOL. 62

OLIGOSACCHARIDE SYNTHESIS: FROM CONVENTIONAL METHODS TO MODERN EXPEDITIOUS STRATEGIES

BY JAMES T. SMOOT and ALEXEI V. DEMCHENKO

Department of Chemistry and Biochemistry, University of Missouri - St Louis, One University Boulevard,
St Louis, MO 63121, USA. Email: demchenkoa@umsl.edu

I. Introduction 162
II. Chemical Glycosylation and Conventional Oligosaccharide Synthesis 165
  1. Principles of Chemical Glycosylation 165
  2. Traditional Linear Oligosaccharide Synthesis 167
  3. Convergent Block Synthesis 169
III. Selective (Leaving-Group Based) Strategies 177
  1. Selective Activation 177
  2. Two-Step Activation and the *In situ* Preactivation 182
  3. Active–Latent Strategy 185
  4. Orthogonal and Semi-orthogonal Strategies 188
  5. Deactivation by Steric Hindrance 193
  6. Temporary Deactivation Concept 193
IV. Chemoselective (Protecting-Group Based) Strategies 196
  1. Arming and Disarming with Neighboring Substituents 198
  2. Reactivity-Based Programmable Strategy 201
  3. Disarming by the Remote Substituents 202
  4. Disarming by Torsional Effects 203
  5. Super-Armed Glycosyl Donors 206
V. Regioselectivity-Based Strategies 208
  1. Hydroxyl Reactivity 208
  2. Triphenylmethyl Reactivity 210
  3. Bidirectional Approaches 211
VI. Novel Technologies for the Rapid and High-Throughput Oligosaccharide Synthesis 213
  1. One-Pot Strategies 214
  2. Polymer-Supported, Solid-Phase, and Automated Synthesis 219
  3. Fluorous Tag-Supported and Microreactor Synthesis 226
VII. Enzymatic Approach 228
  1. Oligosaccharide Synthesis with Glycosyltransferases 230
  2. Oligosaccharide Synthesis with Glycosidases (Hydrolases) 233
VIII. Outlook 234
References 236

ISBN: 978-0-12-374743-3
DOI: 10.1016/S0065-2318(09)00005-5

© 2009 Elsevier Inc. All rights reserved.

ABBREVIATIONS

Alloc, allyloxycarbonyl; AMB, 2-(azidomethyl)benzoyl; BSP, benzenesulfinyl piperidine; CMP, cytidine monophosphate; COD, cyclooctadienyl; Cp, cyclopentadienyl; CSA, camphorsulfonic acid; DAST, (diethylamino)sulfur trifluoride; DBU, 1,8-diazabicyclo[5.4.0]undec-7-ene; DCC, *N*,*N*′-dicyclocarbodiimide; DABCO, 1,4-diazabicyclo[2.2.2]octane; DDQ, 2,3-dichloro-5,6-dicyanobenzoquinone; DEIPS, diethylisopropylsilyl; Dimedone, 5,5-dimethyl-1,3-cyclohexanedione; DIPEA, diisopropylethylamine; DMAP, dimethylaminopyridine; DMDO, dimethyl dioxirane; DMTST, dimethyl(thiomethyl)sulfonium friflate; DTBMP, di(*t*-butyl)methylpyridine; Fmoc, fluorenylmethoxycarbonyl; GDP, guanosine diphosphate; IDCP, iodonium(di-δ-collidine)perchlorate; Lev, levulinoyl; LG, leaving group; MBn, *p*-methylbenzyl; MBz, *p*-methylbenzoyl; MPEG, methoxypolyethylene glycol; NBS, *N*-bromosuccininide; NIS, *N*-iodosuccininide; PFBz, pentafluorobenzoyl; Pfp, pentafluorophenyl; Phth, phthalimido; Piv, pivaloyl; RRV, relative reactivity value; SBox, *S*-benzoxazolyl; STaz, *S*-thiazolinyl; TBDMS, *t*-butyldimethylsilyl (also TBS); TCA, trichloroacetyl; TESOTf, triethylsilyl triflate; TFA, trifluoroacetic acid; TIPS, triisopropylsilyl; TMS, trimethylsilyl; TMSOTf, trimethylsilyl trifluoromethanesulfonate (triflate); Tol, tolyl; Tr, triphenylmethyl (trityl); Troc, 2,2,2-trichloroethyloxycarbonyl; TTBP, *tris*(tribromoneopentyl)phosphate; UDP, uridine diphosphate; Z, benzyloxycarbonyl.

I. INTRODUCTION

Complex carbohydrates are involved in a broad variety of biological phenomena, and in particular their involvement in life-threatening processes, has associated this class of natural compounds with tremendous diagnostic and therapeutic potential. The main scientific effort in the past two decades has focused upon those carbohydrates associated with diseases that rank consistently among the leading causes of death worldwide. These include in particular cardiovascular disease, cancer, and septicemia, bacterial, viral, and parasitic infections. At the core of this tremendous effort is the concept that, if a comprehensive knowledge of the structure, conformation, and properties of these carbohydrates were available, elucidation of the mechanisms for the pathogenesis of the associated disease could be facilitated. Consequently, this could lead to the development of effective tools for the prevention, diagnosis, treatment, and healing of these diseases.

Over the years, glycoscientists have mastered techniques for the isolation of certain classes of naturally occurring carbohydrates. The availability of pure natural isolates, however, is still inadequate to address all of the challenges presented by modern glycoscience. As a result, glycoscientists have turned to chemical synthesis as a means for accessing complex carbohydrates. In principle, the efficient chemical synthesis of carbohydrates should yield significant quantities of the pure natural compounds and constitutes the only means for accessing their unnatural mimetics that are often needed for screening purposes. Due to the enormous progress made in the area of synthetic and analytical chemistry, many classes of organic compounds are now relatively accessible by broadly applicable methods. However, carbohydrates of even moderate complexity still represent a significant challenge. A few representative examples are shown in Fig. 1.

The majority of biologically important and therapeutically active carbohydrates exist as polysaccharides or as complex glycoconjugates in which oligosaccharides are connected to peptides, proteins, or fatty acids. This account discusses only methods and strategies for the synthesis of the oligosaccharide sequences. The first attempts to address the challenges of oligosaccharide synthesis emerged in the mid-1980s and 1990s, and resulted in the development of a number of revolutionary approaches. These innovative strategies significantly shortened oligosaccharide assembly by minimizing the need for protecting-group manipulations between glycosylation steps. Nicolaou's selective activation,[1] Fraser-Reid's armed-disarmed approach,[2] Danishefsky's glycal assembly,[3] Ogawa's orthogonal technique,[4,5] Roy's[6] and Boons'[7] active–latent concept, Wong's and Ley's programmable strategies[8–11] are just a few examples to mention.

The excellent innovations just surveyed have allowed scientists to synthesize complex oligosaccharides and glycoconjugates that for decades were practically inaccessible. For example, the total syntheses of tumor antigens of the Globo-series–Globo-H by Danishefsky,[12] Schmidt,[13] Boons,[14] Wong,[15] and Seeberger[16] have become modern classics of synthetic carbohydrate chemistry. Nevertheless, these syntheses remain very complex: their successful accomplishment required significant resources, and kept these targets accessible only to an elite circle of glycoscientists. Moreover, it has become apparent that only certain selected sequences can be accessed by these novel techniques. Furthermore, each target still required careful selection of methods, conditions, and strategies. On many occasions, the use of advanced oligosaccharide building blocks was required for successful execution of these strategies.

These notable gaps have stimulated additional scientific efforts that have led to the development of a new pool of methods for the stereoselective synthesis of challenging

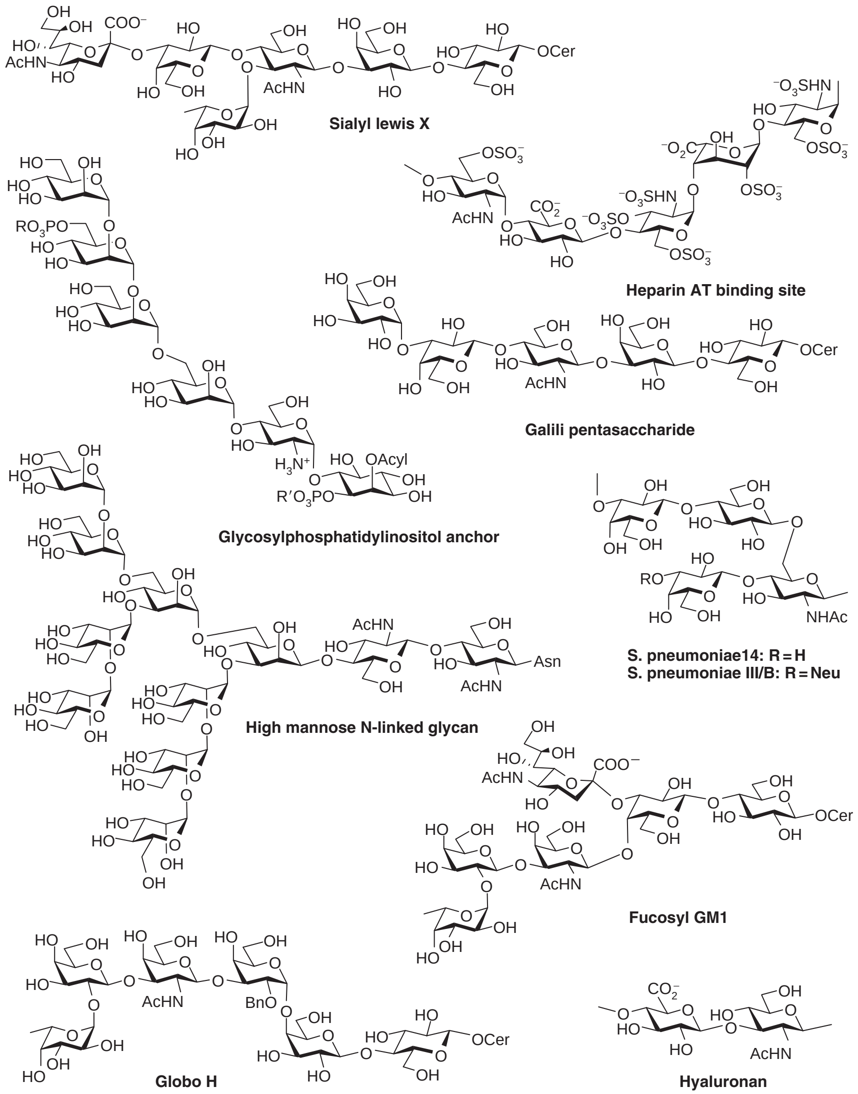
Sialyl lewis X
Heparin AT binding site
Galili pentasaccharide
Glycosylphosphatidylinositol anchor
S. pneumoniae14: R = H
S. pneumoniae III/B: R = Neu
High mannose N-linked glycan
Fucosyl GM1
Globo H
Hyaluronan

FIG. 1. Representative oligosaccharide targets.

glycosidic linkages and strategies for expeditious oligosaccharide synthesis. Preactivation-based sequential couplings by Huang's[17–19] and van der Marel's groups,[20] Crich's synthesis, detailed elsewhere in this volume (p. 251), of β-mannosides,[21] Gin's dehydrative method,[22] Seeberger's polymer-supported automated synthesis,[23,24] Lowary's work on furanosides,[25] Gervay's glycosyl iodide approach,[26,27] Hung's work of one-pot protection of sugars,[28,29] and Boons' stereodirected synthesis of α-glycosides[30,31] are some key examples of significant recent breakthroughs. Most of these studies have already been used in targeted oligosaccharide syntheses, which are a clear indication of the demand for these improvements and the keen interest of the broad chemical community drawn to this topic.

The current account is dedicated solely to strategies that have been developed for the synthesis of oligosaccharides. This topic has been previously reviewed, and for a comprehensive survey the reader is encouraged to refer to other articles discussing this subject.[32–38] Related topics, such as glycosylation[39] and synthesis of glycoconjugates,[40–46] are mentioned only briefly herein, whereas comprehensive contemporary accounts should provide additional insight into these important subjects.

II. CHEMICAL GLYCOSYLATION AND CONVENTIONAL OLIGOSACCHARIDE SYNTHESIS

In spite of significant progress made in the area of glycoside synthesis,[39] the necessity of forming either a 1,2-*cis* or a 1,2-*trans*-glycosidic bond with high stereocontrol remains the main reason that chemical O-glycosylation is ranked among the most challenging problems of modern synthetic chemistry. The achievement of high yield and stereocontrol is difficult, because of the complexity of the glycosylation process, which often proceeds together with a variety of side reactions. In oligosaccharides containing multiple linkages, the stereocontrol of glycosylation becomes particularly critical.

1. Principles of Chemical Glycosylation

A typical chemical glycosylation is based on the nucleophilic displacement of a leaving group on the glycosyl donor by a hydroxyl moiety of the glycosyl acceptor. The remaining hydroxyl groups of both components are temporarily masked with protecting groups. Full details of the glycosylation mechanism have not yet been elucidated, and the speculations and diagrams presented herein are the commonly accepted prototype of the glycosylation mechanism. Upon promoter-assisted departure of the leaving group, the flattened oxacarbenium ion (see Whitfield's account elsewhere in this volume on glycopyranosyl ions) is formed (Scheme 1), and as a result, the nucleophilic attack is almost equally possible from either the top (*trans*, β for the

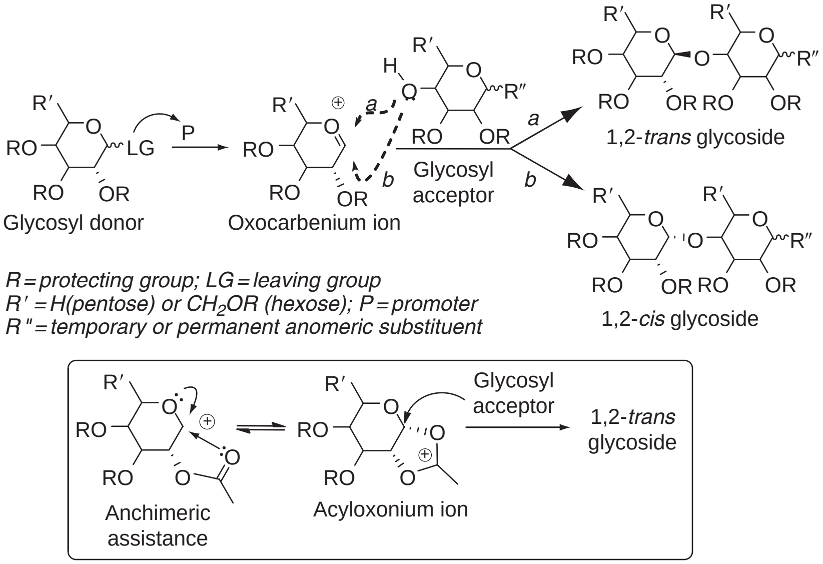

R = protecting group; LG = leaving group
R′ = H(pentose) or CH_2OR (hexose); P = promoter
R″ = temporary or permanent anomeric substituent

SCHEME 1. Outline of chemical glycosylation.

D-gluco series) or the bottom face (*cis*, α) of the ring. Even though the α product is thermodynamically favored (anomeric effect),[47] a substantial amount of the kinetic *β*-linked product is often obtained, because the glycosylation of carbohydrate acceptors is irreversible. Uncontrolled glycosylation reactions commonly result in the formation of mixtures of diastereomers (*cis*/*trans* or α/*β* anomers).

Various factors such as temperature, pressure, structure, conformation, solvent, promoter, steric hindrance, or leaving group can affect the stereoselectivity of glycosylation. Some of these factors influence the stereoselectivity dramatically, others only to certain extent; undoubtedly, the neighboring substituent at C-2 is one of the major players. If the use of a base-labile ester-protecting groups is permitted, 1,2-*trans* glycosides can be prepared with the assistance by a neighboring participating group.[48,49] These glycosylations proceed primarily via a bicyclic acyloxonium ion intermediate that can only accept nucleophilic attack from the top face, resulting in the stereoselective formation of a 1,2-*trans* glycoside (Scheme 1). Many traditional glycosyl donors such as halides, thioglycosides, or O-imidates provide excellent stereoselectivity and high yields.[39]

Another important factor affecting the outcome of glycosylations is the nature of the leaving group at the anomeric position. As a result, a large number of glycosyl donors have been developed.[39,50] In addition to the traditionally used chlorides or bromides,[51,52] more recent glycosyl donors such as Schmidt's O-trichloroacetimidates,[53] Mukaiyama's fluorides,[1,54] alkyl/aryl thioglycosides pioneered by Ferrier, Nicolaou and Garegg,[55,56] Fraser-Reid's O-pentenyl glycosides,[57,58] and Danishefsky's glycal-epoxide system[3] have become valuable alternatives.

The development of efficient coupling reactions is largely responsible for the progress that has been made in the area of oligosaccharide synthesis. When the arsenal of the glycosylation techniques was limited to Fischer and Koenigs–Knorr approaches (or their variations), the assembly of oligosaccharides was limited to the linear and block techniques. However, when such stable glycosyl donors as fluorides, thioglycosides or O-alkenyl glycosides emerged, the question arose of selective or chemoselective activation of one leaving group over another.

2. Traditional Linear Oligosaccharide Synthesis

A linear oligosaccharide synthesis consists of the glycosylation of a monosaccharide donor with a monosaccharide acceptor, in the presence of a promoter (activator), to give the desired disaccharide. There are two possible pathways that can then follow (Scheme 2). The first possible route involves the conversion of the intermediate disaccharide into the second-generation glycosyl acceptor via liberation a specific hydroxyl group. The acceptor is then allowed to react with a glycosyl donor, resulting in the formation of trisaccharide A. The deprotection–glycosylation sequence can be then reiterated to yield a tetrasaccharide and so on. Alternatively, the temporary anomeric protection (T, Scheme 2) of the disaccharide intermediate could be removed and a new leaving group installed, resulting in the formation of the second-generation glycosyl donor. The latter is then allowed to react with a new glycosyl acceptor, leading to the formation of trisaccharide B. As in the first variation, the reprotection–glycosylation reaction sequence is then repeated until an oligosaccharide of the desired chain length is obtained.

In spite of the need for additional synthetic manipulations between glycosylation steps, which often results in an increased number of total steps that is inversely correlated with the efficiency and overall yield, this strategy is still in use.[59–62] A few examples of this strategy for oligosaccharide synthesis have been selected to illustrate the state of the art. The first example depicted in Scheme 3 is the synthesis of the tetrasaccharide **9** corresponding to the repeating unit of pneumococcal oligosaccharide serotype 6A.[63] It makes use of both versions of the traditional approach, implying the generation of the intermediate glycosyl donor and glycosyl acceptor. The thioglycoside donor **1** was glycosidated with the rhamnose acceptor **2** in the presence of methyl triflate (MeOTf) to form the disaccharide **3** in 61% yield. The resulting disaccharide

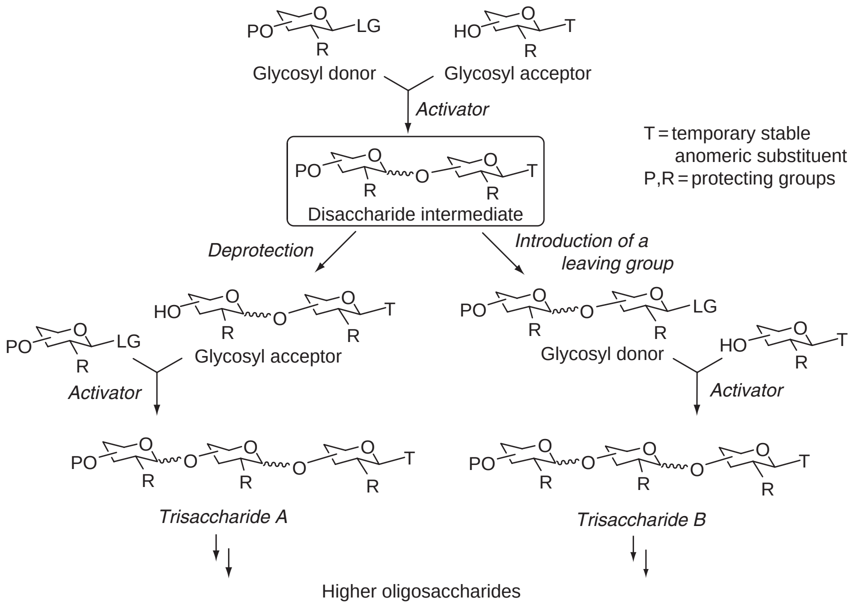
Glycosyl donor
Glycosyl acceptor
Activator
T = temporary stable anomeric substituent
P,R = protecting groups
Disaccharide intermediate
Deprotection
Introduction of a leaving group
Glycosyl acceptor
Glycosyl donor
Activator
Activator
Trisaccharide A
Trisaccharide B
Higher oligosaccharides

SCHEME 2. Conventional (linear) approach.

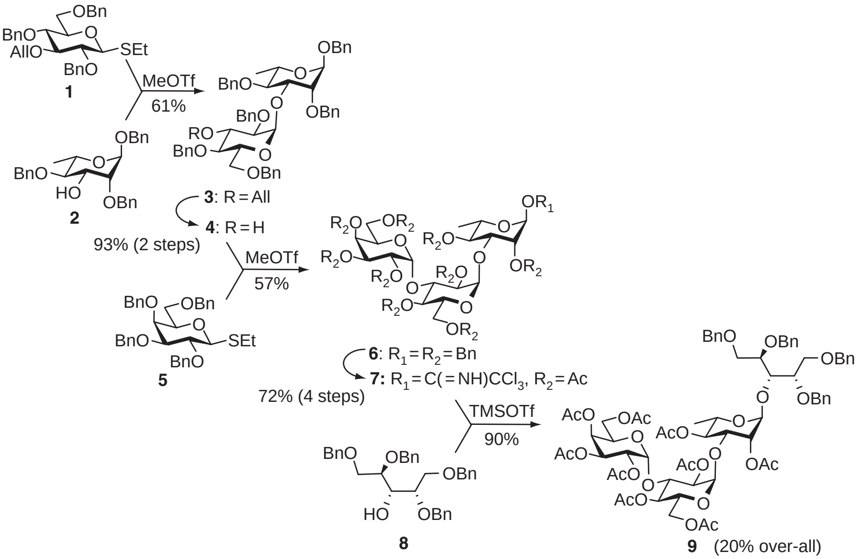
1
MeOTf
61%
2
3: R = All
4: R = H
93% (2 steps)
MeOTf
57%
5
6: R1 = R2 = Bn
7: R1 = C(=NH)CCl3, R2 = Ac
72% (4 steps)
TMSOTf
90%
8
9 (20% over-all)

SCHEME 3. Synthesis of pneumococcal oligosaccharide serotype 6A.[63]

was then deallylated over two steps in 93% yield to provide glycosyl acceptor **4**. The latter was glycosylated with the galactose donor **5** in the presence of MeOTf, producing the trisaccharide **6** in 57% yield. The latter was then converted into the glycosyl donor **7** by sequential debenzylation, acetylation, liberation of the hemiacetal, and insertion of the trichloroacetimidoyl anomeric moiety in 72% overall yield. Glycosyl donor **7** was glycosidated with the ribitol acceptor **8** in the presence of trimethylsilyl triflate (TMSOTf) to provide tetrasaccharide **9** in 90% yield (20% overall).

Another relevant example is the synthesis of the blood-group determinant H-type II pentasaccharide **21** (Scheme 4).[64] The assembly began with monosaccharide building blocks: the glycosyl phosphate **10** and a pentenyl glycoside **11** obtained from glycal precursors. The phosphate leaving-group in the glycosyl donor **10** was activated by addition of *t*-butyldimethylsilyl (TBDMS) triflate. The resulting disaccharide **12** was then converted into glycosyl acceptor **13** by removal of the levulinoyl (Lev) group, and glycosylated with the trichloroacetimidoyl donor **14** in the presence of TMSOTf to provide trisaccharide **15** in 87% yield. The trisaccharide was then deprotected to provide glycosyl acceptor **16**. The chain growth was continued by the glycosylation with the glycosyl phosphate donor **17** in the presence of TMSOTf to provide tetrasaccharide **18** in 92% yield. Selective removal of the 2-(azidomethyl)benzoyl (AMB) group was accomplished with tributyl phosphine to provide glycosyl acceptor **19** in 92% yield. The latter was subsequently glycosylated with glycosyl donor **20** to afford pentasaccharide **21** in 94% yield. As clearly illustrated by this example, the traditional approach offers the benefit of its simplicity, as in principle the same anomeric and protective groups can be used repeatedly.

Along with the long history of the traditional approach, numerous improvements have been incorporated. Nevertheless, it has become apparent that stereoselective synthesis of the glycosidic bond is only part of the challenge that synthetic chemists confront during the synthesis of oligosaccharides. For the most part, the traditional stepwise approach significantly decreases the overall efficiency of the oligosaccharide assembly, and this is especially apparent when applied to the synthesis of large oligosaccharides. As a result, the past two decades have witnessed a dramatic improvement of the methods and strategies used for oligosaccharide synthesis.

3. Convergent Block Synthesis

The first attempt to address challenges associated with the linear stepwise approach was the development of a convergent building-block approach. Pioneering studies by Zen,[65] Paulsen,[66] and Ogawa[67] should be acknowledged in particular. According

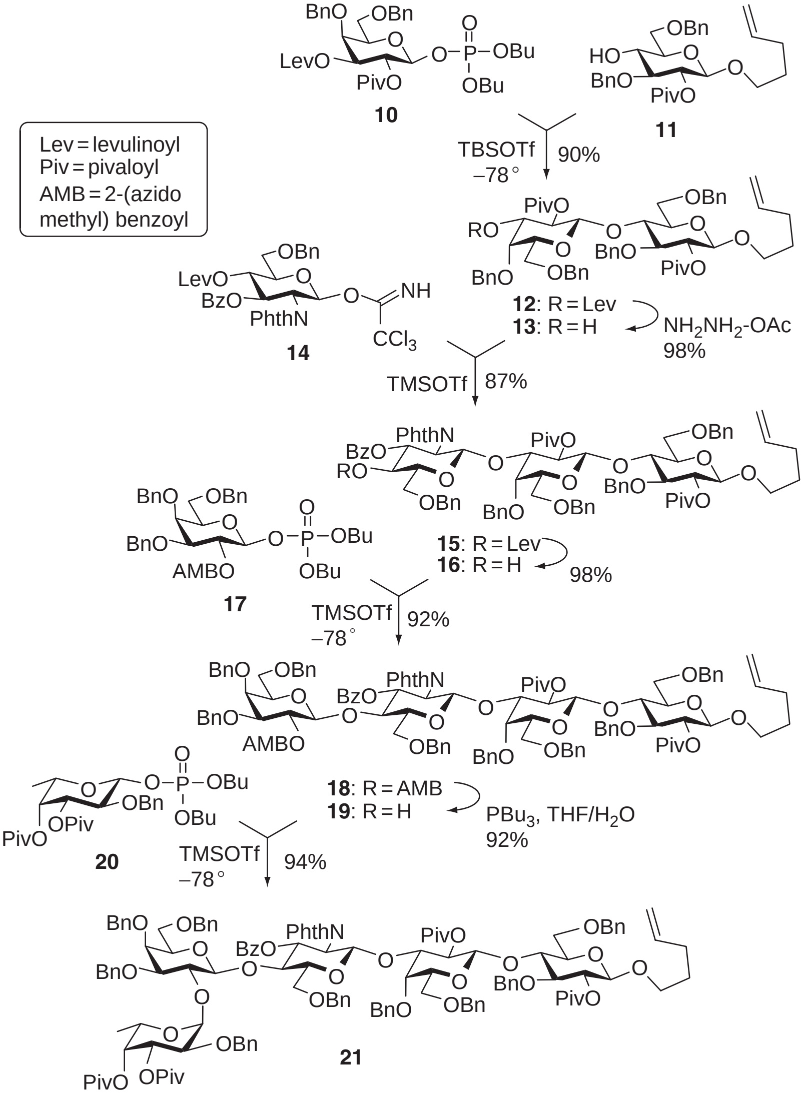
Lev = levulinoyl
Piv = pivaloyl
AMB = 2-(azido methyl) benzoyl
10
11
TBSOTf
–78°
90%
12: R = Lev
13: R = H
NH2NH2-OAc
98%
14
TMSOTf
87%
15: R = Lev
16: R = H
98%
17
TMSOTf
–78°
92%
18: R = AMB
19: R = H
PBu3, THF/H2O
92%
20
TMSOTf
–78°
94%
21

SCHEME 4. Linear synthesis of H-Type II pentasaccharide **21**.[64]

to this strategy, oligosaccharide building blocks are obtained separately and then coupled together (converged) by means of a glycosylation reaction (Variation A). As highlighted in Scheme 5, this method employs the coupling of ''clusters'' of the

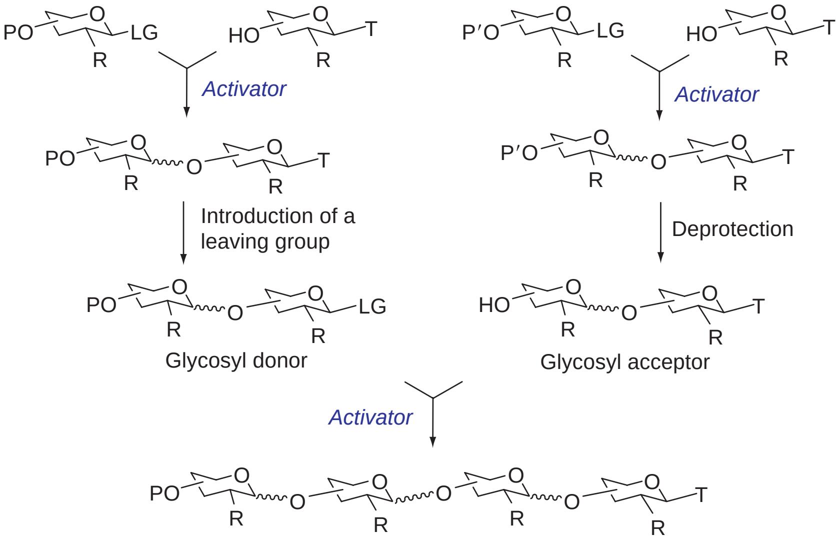

SCHEME 5. Convergent block synthesis. Variation A.

sugar residues. Two disaccharides are constructed individually: the first disaccharide is then converted into the glycosyl donor by the transformation of a stable temporary anomeric substituent into a suitable leaving group. Meanwhile, the second disaccharide is deprotected to expose a hydroxyl group to be used as the glycosyl acceptor for the subsequent glycosylation, leading to the corresponding tetrasaccharide. A major benefit of such block synthesis is the decreased number of steps required for the overall assembly. Thus, in comparison to the linear approach, convergent block synthesis allows formation of larger saccharides in the same number of synthetic steps (compare Schemes 2 and 5). Another key feature of variation A of the convergent approach is that it allows for the introduction of a ‘‘difficult’’ glycosidic linkage, such as 1,2-*cis*, at an earlier stage of the saccharide assembly thus avoiding the complicated separation of diastereomers at the later stage.[66,67]

A convergent synthesis of the pentasaccharide derivative **33** of the triterpeniod saponin obtained from the plant *Spergularia ramosa* was achieved as outlined in Scheme 6.[68] The entire assembly relied on use of the trichloroacetimidate protocol and was accomplished in a three plus two fashion. The assembly of the trisaccharide was initiated by the glycosidation of glucosyl trichloroacetimidate donor **22** with rhamnosyl diol acceptor **23** to provide disaccharide **24** in 63% yield. The latter could be used directly as the glycosyl acceptor for the reaction with xylosyl donor **25**, leading

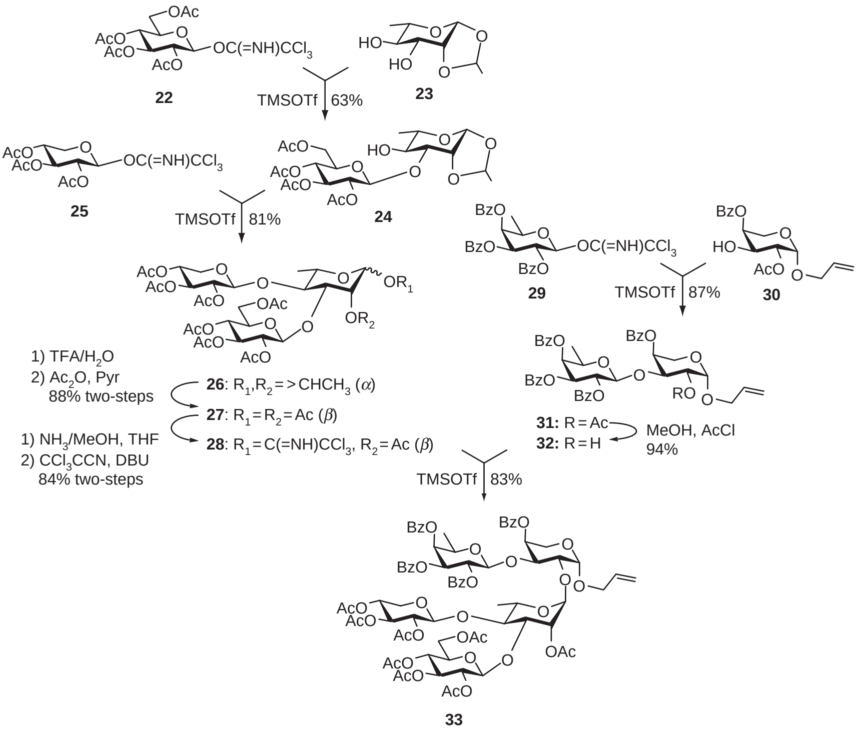
22
23
TMSOTf 63%
25
24
TMSOTf 81%
29
30
TMSOTf 87%
1) TFA/H2O
2) Ac2O, Pyr
88% two-steps
26: R1,R2 = >CHCH3 (α)
27: R1 = R2 = Ac (β)
28: R1 = C(=NH)CCl3, R2 = Ac (β)
1) NH3/MeOH, THF
2) CCl3CCN, DBU
84% two-steps
31: R = Ac
32: R = H
MeOH, AcCl
94%
TMSOTf 83%
33

SCHEME 6. Convergent synthesis of the pentasaccharide of *Spergularia ramosa*.[68]

to trisaccharide **26** in 81% yield. The 1,2-ethylidene moiety of trisaccharide **26** was then cleaved with trifluoroacetic acid–water (TFA–H_2O) and the resulting diol was acetylated with Ac_2O in pyridine to give trisaccharide **27** in 88% yield. The anomeric acetate in compound **27** was selectively removed by reaction with NH_3/MeOH, and the resulting hemiacetal was converted into a trichloroacetimidoyl derivative **28** by treatment with CCl_3CN in the presence of 1,8-diazabicyclo[5,4,0]undec-7-ene (DBU) in 84% yield. In the mean time, glycosyl donor **29** was coupled with glycosyl acceptor **30** to provide disaccharide **31** in 87% yield. The latter was then deacetylated with AcCl–MeOH to provide glycosyl acceptor **32** in 94% yield. The oligosaccharide building blocks, glycosyl donor **28** and glycosyl acceptor **32**, were coupled in the presence of TMSOTf to provide the target pentasaccharide **33** in 83% yield.

Another relevant example is the convergent assembly of a biantennary heptasaccharide motif **39** of a human glycoprotein isolated from seminal plasma. It was accomplished by Ley's and Wong's groups in a 2 + 3 + 2 fashion as depicted[69] in Scheme 7. The glycosyl bromide donor **34**, obtained from lactosamine, was glycosidically coupled to the trimannosyl acceptor **35** using buffered AgOTf as the promoter, producing pentasaccharide **36** in 71% yield. The allyloxycarbonyl (Alloc) group in compound **36** was then removed with $Pd(PPh_3)_4$ to provide glycosyl acceptor **37** in 88% yield, which was then glycosylated with glycosyl donor **38** using the buffered AgOTf to produce the target heptasaccharide **39** in 76% yield.

The convergent approach is particularly advantageous if the construction of one or more challenging bonds is required. It is often used for the purpose of the introduction of a ''difficult'' linkage, such as 1,2-*cis*, at an earlier stage of the saccharide assembly to avoid complicated diastereomer separation at the later stage.[66,67] A representative example illustrating the introduction of a number of ''difficult'' linkages at the early stage is the synthesis of the high mannose-type oligosaccharide **50** illustrated[70] in Scheme 8. For instance, building block **45**, containing the challenging β-mannosyl

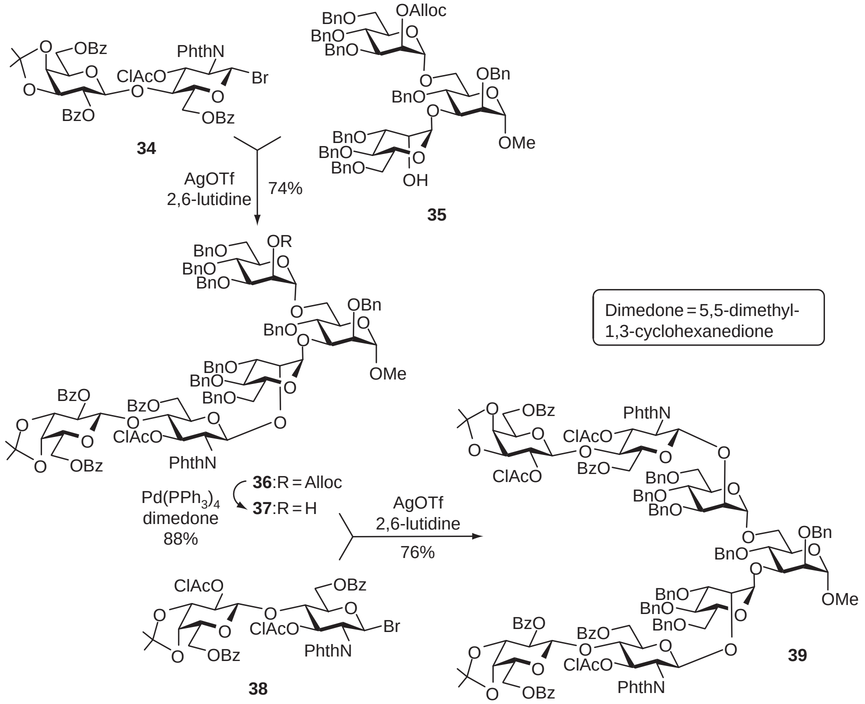

Dimedone = 5,5-dimethyl-1,3-cyclohexanedione

SCHEME 7. Convergent block synthesis of heptasaccharide **39**.[69]

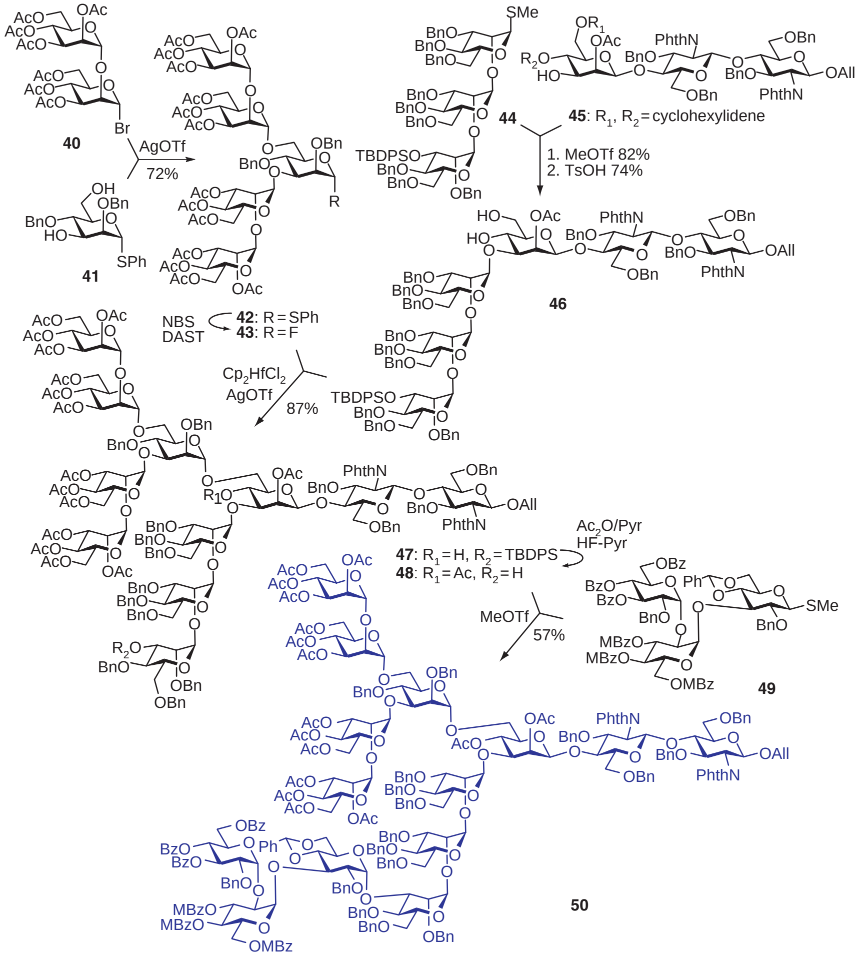
40
AgOTf
72%
41
NBS
DAST
42: R = SPh
43: R = F
Cp$_2$HfCl$_2$
AgOTf
87%
44
45: R$_1$, R$_2$ = cyclohexylidene
1. MeOTf 82%
2. TsOH 74%
46
47: R$_1$ = H, R$_2$ = TBDPS
48: R$_1$ = Ac, R$_2$ = H
Ac$_2$O/Pyr
HF-Pyr
MeOTf
57%
49
50

SCHEME 8. A convergent synthesis[70] of endoplasmic reticulum membrane-associated oligosaccharide **50**.

residue was assembled using an intramolecular aglycone delivery approach to ensure excellent *β*-stereoselectivity. Building block **49** contains multiple 1,2-*cis* glucosyl residues, and so its synthesis alone represents a considerable challenge.

The final assembly was accomplished as follows: glycosyl acceptor diol **41** was bis-glycosylated with the bromide donor **40** in the presence of AgOTf to afford the pentasaccharide derivative **42** in 72% yield. The latter was then converted into a glycosyl fluoride donor **43**. The hexasaccharide acceptor **46** was assembled via sequential coupling of building blocks **44** and **45** in the presence of MeOTf, followed by acetal removal with TsOH. The liberated diol in the glycosyl acceptor **46** was then regioselectively glycosylated with the fluoride donor **43** in the presence of a Cp_2HfCl_2/AgOTf promoter system to afford oligosaccharide **47** in 87% yield. The latter was then subjected to sequential acetylation of the remaining hydroxyl group and removal of the temporary silyl protecting group, strategically placed on the terminal mannose residue, to afford the glycosyl acceptor **48**. The latter was then glycosylated with the trisaccharide donor **49** in the presence of MeOTf to afford the target oligosaccharide **50** in 57% yield.

A conceptually related convergent approach (Variation B, Scheme 9) has been proven particularly advantageous if the synthesis of two or more sequential repeating units is required. In this case, a single oligosaccharide corresponding to the repeating unit is obtained, and divided into two portions. One portion is converted into a glycosyl donor and another into a glycosyl acceptor. Subsequently, the two reactants are converged to afford a dimer. This manipulation can be then repeated for the synthesis of even larger structures.

An elegant synthesis of the Lewis X structure was reported that utilized an efficient convergent approach.[71] First, the azido-lactose acceptor **52**, obtained via

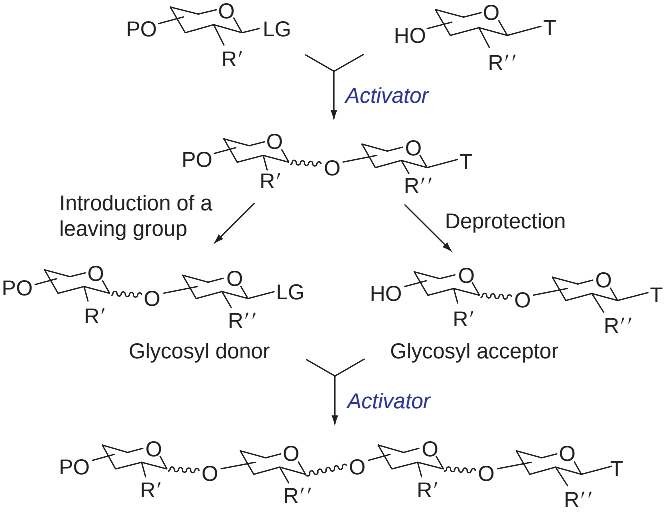

SCHEME 9. Convergent block synthesis. Variation B.

azidonitration of lactal, was glycosylated with the fucosyl trichloroacetimidate donor **51** in the presence of $ZnCl_2$ to obtain the trisaccharide **53** in 89% yield (Scheme 10). This trisaccharide was then split in two portions. The first portion was converted into the corresponding glycosyl donor **54** by sequential removal of the anomeric silyl protection, followed by the introduction of trichloroacetimidoyl anomeric leaving group. The second portion of the key building block **53** was treated with TFA, leading to the glycosyl acceptor **55**. The glycosidation of trichloroacetimidate donor **54** with glycosyl acceptor **55**, using $BF_3{\cdot}OEt_2$ as the promoter, provided hexasaccharide **56** in 78% yield.

The synthesis of pneumococcal oligosaccharides serotype 14 (consisting of multiple repeat units) utilizing a block synthesis strategy was reported by Oscarson.[72] In accordance with the strategy developed, galactosyl bromide donor **57** was

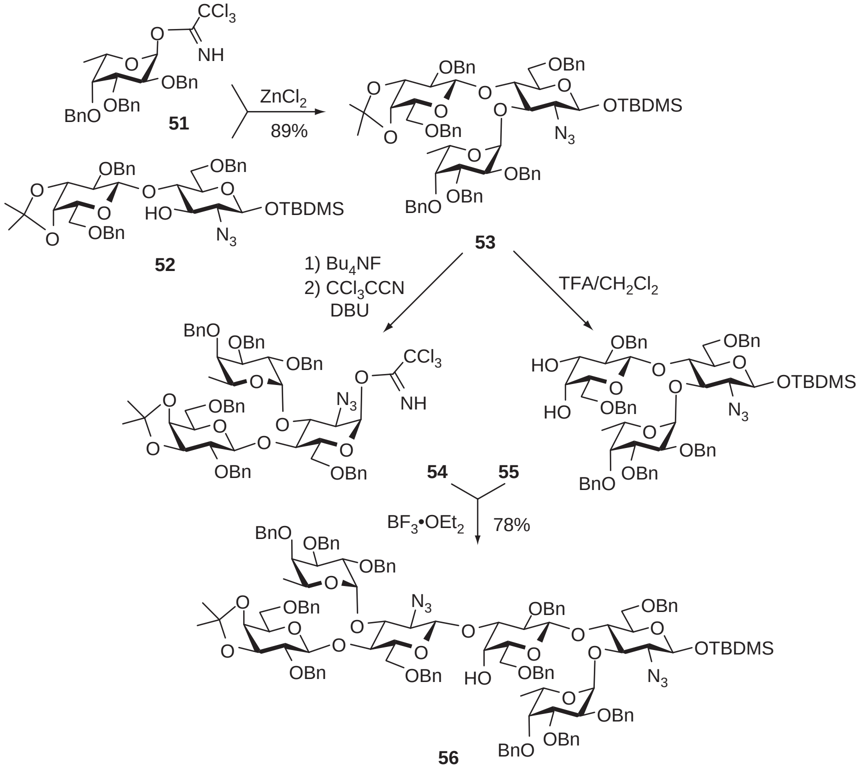

SCHEME 10. Convergent synthesis[71] of the dimeric Lewis-X **56**.

glycosidated with the glucosamine acceptor **58** using AgOTf as the promoter to obtain disaccharide **59** in 79% yield (Scheme 11). The TBDMS group was removed to provide glycosyl acceptor **60** in 95% yield. The latter was glycosylated with glycosyl donor **61** in the presence of AgOTf to give tetrasaccharide **62** in 88% yield. A portion of the key intermediate **62** was converted into the spacer-containing glycosyl acceptor **63**. This was accomplished by first installing the spacer by an *N*-iodosuccinimide–silver triflate (NIS/AgOTf)-promoted reaction with 3-azidopropanol in 87% yield, followed by acid hydrolysis in 84% yield of the bromoisopropylidene ketal. The remaining tetrasaccharide **62** was converted into the glycosyl bromide by the addition of bromine, and glycosidated directly with glycosyl acceptor **63** by the addition of AgOTf to provide octasaccharide **64** in 81% yield. The latter was converted into glycosyl acceptor **65** by hydrolysis of the bromoisopropylidene group in 59% yield. Finally, glycosyl acceptor **65** was glycosylated with the tetrasaccharide donor **62** via two-step activation of the thioglycoside moiety through reaction with bromine followed by treatment with AgOTf, providing the requisite dodecasaccharide **66** in 77% yield.

Despite the availability of more advanced techniques, the convergent block synthesis is still widely employed, and the following is only a short list of recent examples.[73–90]

III. SELECTIVE (LEAVING-GROUP BASED) STRATEGIES

It has become apparent that the linear, and even the convergent approaches, is too inefficient and lengthy because of the requirement to perform extensive protecting- or leaving-group manipulations between the glycosylation steps. As a result, the past two decades have witnessed a dramatic improvement of the methods and strategies used for expeditious oligosaccharide synthesis. Scientists working in the area of oligosaccharide synthesis have been persistently trying to raise (and answer) the key question: can we synthesize oligosaccharides more expeditiously by eliminating unnecessary synthetic steps?

1. Selective Activation

When the arsenal of the glycosylation techniques was limited to Fischer and Koenigs–Knorr approaches (or their variations), the oligosaccharide assembly was limited to the linear and block techniques. However, when such stable glycosyl donors as thioglycosides or *O*-alkenyl glycosides emerged, a question of selective activation of one leaving group over another arose. A schematic outline of this

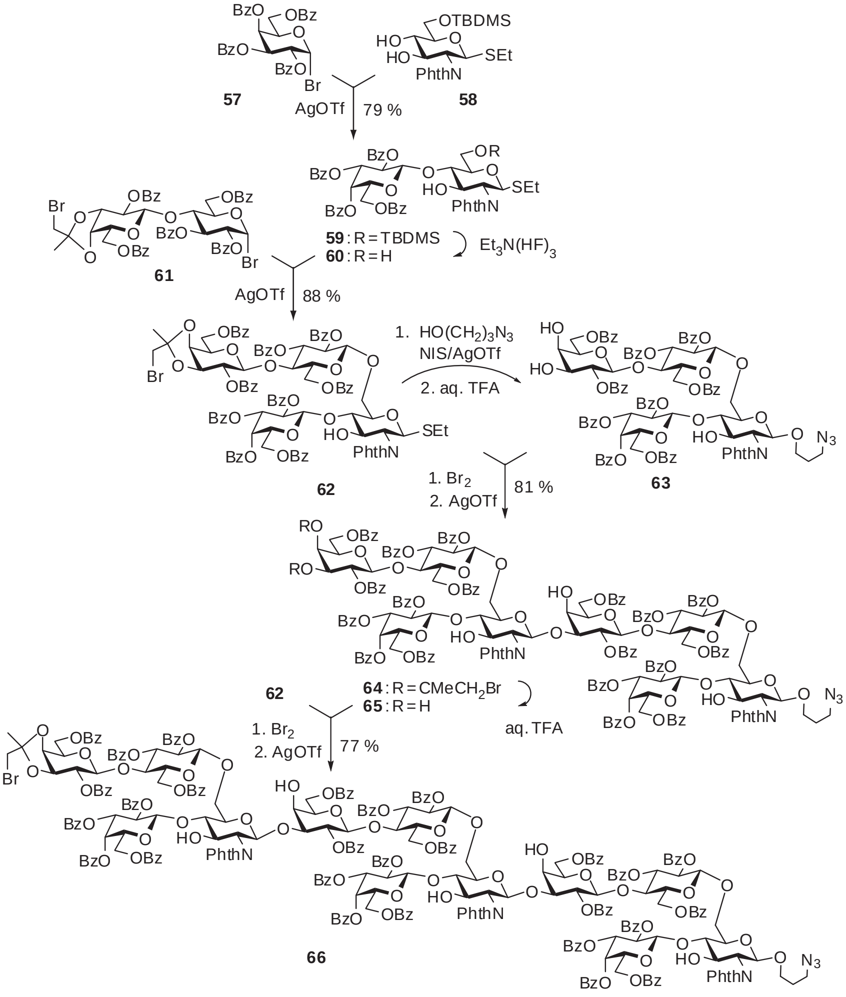
57
58
AgOTf
79 %
59 : R = TBDMS
60 : R = H
Et3N(HF)3
61
AgOTf
88 %
62
1. HO(CH2)3N3 NIS/AgOTf
2. aq. TFA
63
1. Br2
2. AgOTf
81 %
64 : R = CMeCH2Br
65 : R = H
aq. TFA
62
1. Br2
2. AgOTf
77 %
66

SCHEME 11. Block synthesis[72] of pneumococcal oligosaccharide serotype 14.

approach is shown in Scheme 12; wherein, a glycosyl donor, bearing a reactive leaving group (LG^a) is coupled with a glycosyl acceptor, bearing a relatively stable LG^b at the anomeric center. The major requirement for this reaction to take place is the use of a suitable activator that will selectively activate LG^a but not LG^b (Activator A). Clearly, LG^b has to withstand the reaction conditions associated with the LG^a activation. Pioneering research of Zen,[65] Nicolaou,[91,92] Lonn,[93,94]

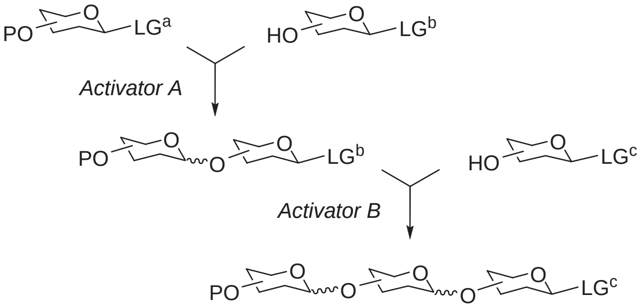

SCHEME 12. Stepwise selective activation.

Garegg,[95,96] and others[97,98] involved the activation of alkyl halides over *S*-alkyl/aryl glycosides. Subsequently, other examples of suitable LG^a for selective activations have become available: trichloroacetimidates,[99,100] phosphite,[101] phosphate,[102] thioimidate,[103–106] thiocyanate,[107,108] hemiacetal,[109,110] sulfoxide,[111,112] selenoglycoside,[113–116] orthoester,[76,117–119] *O*-hetaryl,[120–122] and others.[123–129] Many of these couplings were performed with the use of *S*-alkyl/aryl, fluoro, or *O*-alkenyl/hetaryl moieties as LG^b.

An example applying such selective-activation strategy is the synthesis of heparin-like oligosaccharides reported by van der Marel and co-workers (Scheme 13).[130] The synthesis of pentasaccharide **76** began by utilizing the diphenyl sulfoxide–triflic anhydride dehydrative activation of the 1-hydroxyl donor **67** developed by Gin[131] over thioglycoside acceptor **68**. The phenylthio moiety of the resulting disaccharide **69** was then directly activated with the benzenesulfinyl piperidine (BSP)–triflic anhydride system developed by Crich[132] for reaction with glycosyl acceptor **70** to give the trisaccharide **71** in only two direct glycosylation steps. The latter was then subjected to acetolysis of the 1,6-anhydride ring, followed by removal of the anomeric acetyl group to afford the hemiacetal derivative **72**. The latter was glycosidated with thioglycoside acceptor **73** in the presence of diphenyl sulfoxide–triflic anhydride to provide tetrasaccharide **74** in 51% yield, which was glycosidated with glycosyl acceptor **75** in the presence of the BSP/Tf$_2$O promoter system to furnish the target pentasaccharide **76** in 53% yield.

In principle, the activation sequence can be continued providing that there is an LG^c that would withstand reaction conditions for the LG^b activation (Activator B, Scheme 12). However, these elongated multi-step sequences are not yet routinely available.[133,134] An example of such a synthesis is presented in Scheme 14 (synthesis of **81**), in which bromine is used as LG^a, phenylselenyl as LG^b, and

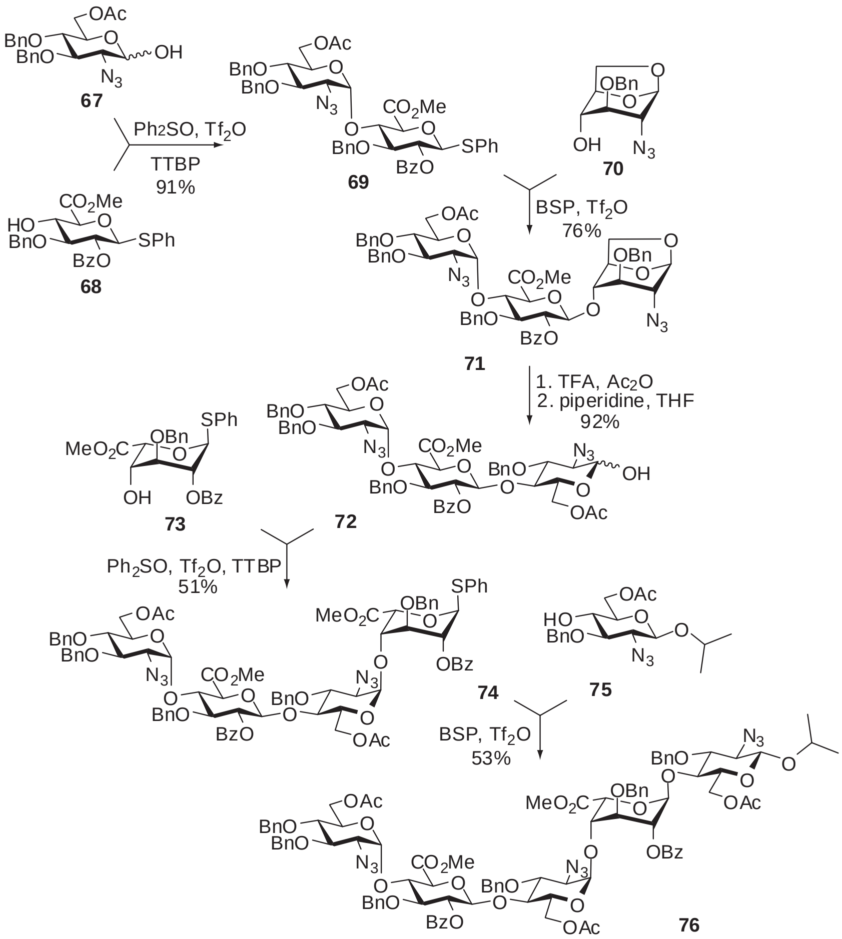
67
Ph2SO, Tf2O
TTBP
91%
68
69
70
BSP, Tf2O
76%
71
1. TFA, Ac2O
2. piperidine, THF
92%
73
72
Ph2SO, Tf2O, TTBP
51%
74
75
BSP, Tf2O
53%
76

SCHEME 13. Selective activation approach to the synthesis of heparin analogues.[130]

S-ethyl as LG^c.[114] First, the bromide donor **77** was activated over the phenylselenide acceptor **78** in the presence of AgOTf/γ-collidine to give the desired disaccharide **79** in 60% yield. The latter was then directly activated over the SEt acceptor **80** by the addition of AgOTf/K_2CO_3 to produce the desired trisaccharide **81** in 81% yield. Apparently, the trisaccharide **81** can be directly activated for subsequent glycosylations. A similar activation sequence was reported by Ley's group.[116]

Another relevant example is the use of the *S*-benzoxazolyl (SBox) moiety as LG^a, *S*-ethyl as LG^b, and *O*-pentenyl as LG^c depicted in Scheme 15.[104,135] The SBox

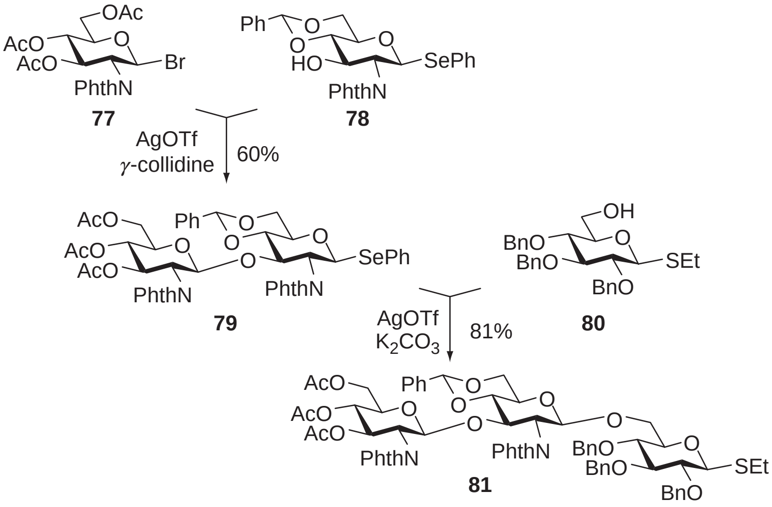
77
78
AgOTf
γ-collidine
60%
79
80
AgOTf
K$_2$CO$_3$
81%
81

SCHEME 14. Selective activation utilizing three leaving groups.[114]

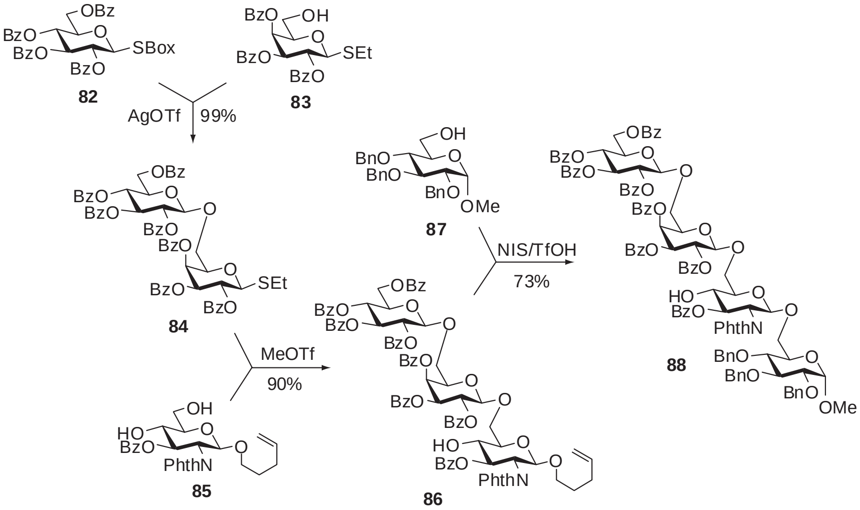
82
83
AgOTf
99%
84
85
MeOTf
90%
86
87
NIS/TfOH
73%
88

SCHEME 15. Three-step sequential selective activation.[104]

glycosyl donor **82** was activated over the SEt acceptor **83** by the addition of AgOTf to produce disaccharide **84** in 99% yield. This disaccharide was then glycosidated with the *O*-pentenyl acceptor **85** by the addition of MeOTf to provide trisaccharide **86** in 90% yield. The leaving *O*-pentenyl moiety of the trisaccharide donor **86** was then activated with NIS/TMSOTf for the coupling with glycosyl acceptor **87**, resulting in the formation of tetrasaccharide **88** in 73% yield. A similar example includes the following three-step activation sequence performed in a one-pot fashion: SBox as LG^a, *S*-thiazolinyl (STaz) as LG^b, and *S*-ethyl as LG^c.[106]

2. Two-Step Activation and the *In situ* Preactivation

According to the two-stage activation approach, both glycosyl donor and glycosyl acceptor initially bear the same type of a leaving group (LG^a). However, to couple these two reactants, the LG^a of the potential glycosyl donor unit is first converted into an LG^b, which is then selectively activated over LG^a of the glycosyl acceptor in the presence of a selective activator (Activator B, Scheme 16). This two-step activation sequence can be reiterated: for this purpose the leaving group LG^a of the obtained disaccharide is converted into LG^b. This allows the coupling with the glycosyl acceptor bearing LG^a, and so on.

This concept was discovered by Zen for *S*-ethyl (LG^a) and bromo (LG^b) groups[65] and further expanded by Nicolaou for *S*-phenyl (LG^a) and fluoro (LG^b) groups.[91,136]

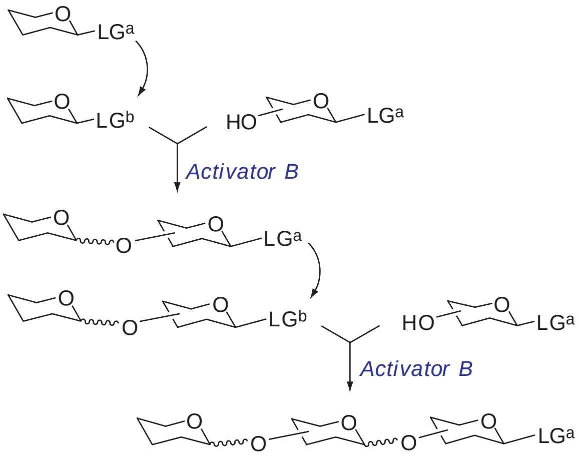

Scheme 16. Two-step activation concept.

For a relevant example, see the synthesis of **95** depicted in Scheme 17.[91] This procedure is based on the fact that such thioglycosides, as **89**, could be readily converted into glycosyl fluorides (**90**) by treatment with NBS/DAST. The glycosyl

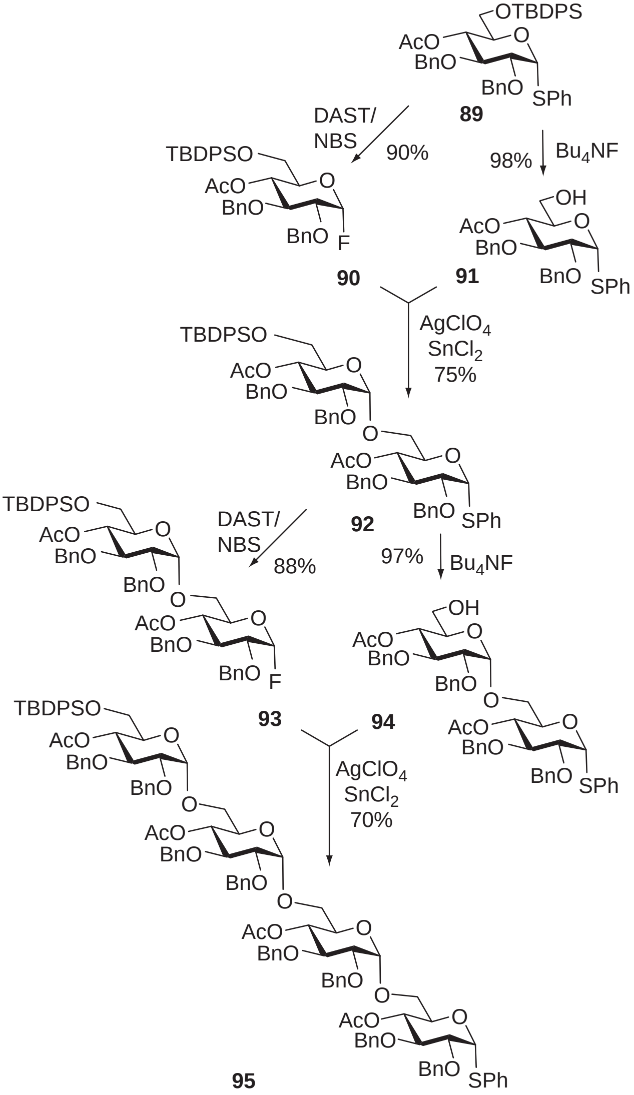
OTBDPS
AcO
BnO
BnO
SPh
89
DAST/
NBS
90%
98%
Bu_4NF
TBDPSO
AcO
BnO
BnO
F
OH
90
91
$AgClO_4$
$SnCl_2$
75%
92
DAST/
NBS
88%
97%
Bu_4NF
93
94
$AgClO_4$
$SnCl_2$
70%
95

SCHEME 17. Two-step activation of phenyl 1-thioglycosides via fluorides.[91]

fluoride donor **90** could be then coupled with a thioglycoside acceptor **91**, also generated from **89** by the treatment with tetrabutylammonium fluoride, in the presence of $SnCl_2/AgClO_4$ to provide disaccharide **92** in 75% yield. This procedure could then be repeated to furnish the desired fluoride donor **93** and thioglycoside acceptor **94**, followed by glycosylation to provide tetrasaccharide **95**. This approach combines advantages offered by the two-step activation and convergent strategies.

A number of other pathways have been developed, which include *in situ* conversion of *O*-pentenyl glycosides[117] or selenoglycosides.[137] The same principle was applied by Danishefsky and coworkers in their reiterative glycal-assembly approach.[138–140] The latter technique involves the transformation of glycals into 1,2-anhydro sugars, which can be readily glycosidated with partially protected glycal-based glycosyl acceptors. See for example the synthesis[138] of **101** depicted in Scheme 18. This strategy utilizes the epoxidation of glycals by treatment with dimethyldioxirane (DMDO, Murray's reagent).[141] The resulting 1,2-anhydro derivatives can then be employed as very potent glycosyl donors for 1,2-*trans* glycosylations. Thus, the glycosyl donor **97**, obtained from the glycal precursor **96**, was coupled to the acceptor glycal **98** in the presence of an electrophilic promoter ($ZnCl_2$) to afford the disaccharide **99** in 71% yield over two steps. The reaction sequence can be then reiterated: the disaccharide **99** is converted

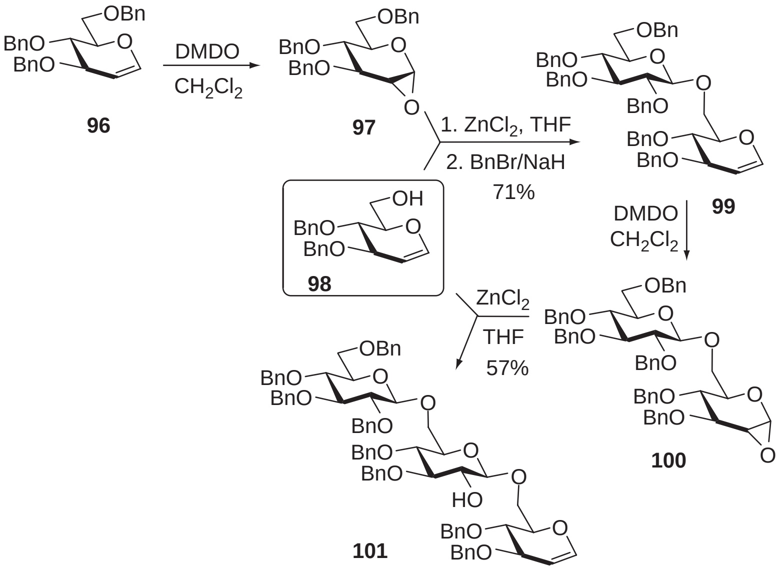

SCHEME 18. Two-step activation of glycals via epoxides.[138]

into the epoxide **100**, which is then reacted with glycosyl acceptor **98** to produce a trisaccharide derivative **101** in 57% yield. Very efficient solid-phase syntheses based on this methodology have been also performed.[142]

In situ preactivation of thioglycosides with BSP/Tf_2O, initially developed by Crich for the synthesis of β-mannosides,[21] was applied to expeditious oligosaccharide synthesis by van der Marel and co-workers.[20] For a representative example, see the synthesis[110] of **106** depicted in Scheme 19. The thiogalactosyl donor **102** was preactivated with BSP/Tf_2O and then allowed to react with thiomannoside **103** to yield disaccharide **104** in 73% yield. The latter then reacted with glycosyl acceptor **105** in the presence of the Ph_2SO/Tf_2O promoter system to furnish the trisaccharide **106** in 64% yield. Overall, this approach combines expeditious synthesis of the oligosaccharide sequence while also providing excellent stereocontrol in two challenging 1,2-*cis* glycosylation steps.

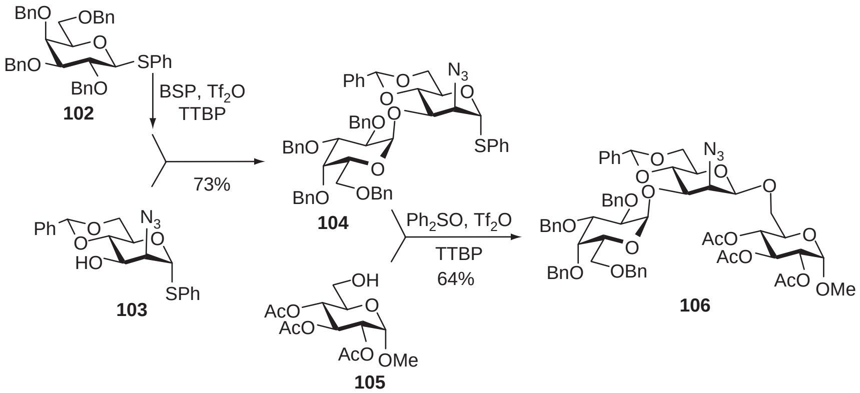

SCHEME 19. Two-step activation–preactivation of thioglycosides.[110]

A number of other pathways have been developed, which include *in situ* utilization of *O*-pentenyl glycosides[117,143] and selenoglycosides.[137] The versatility of the two-step preactivation concept was further expanded by development of a one-pot procedure based on the preactivation of tolyl thioglycosides. This strategy is discussed[18,137] in Section VI.1.

3. Active–Latent Strategy

According to this concept, an active leaving-group LG^a can be selectively activated over a latent (unreactive) LG^b in the presence of a suitable activator A (Scheme 20). Subsequently, the latent LG^b of the disaccharide is converted into the LG^a: this is

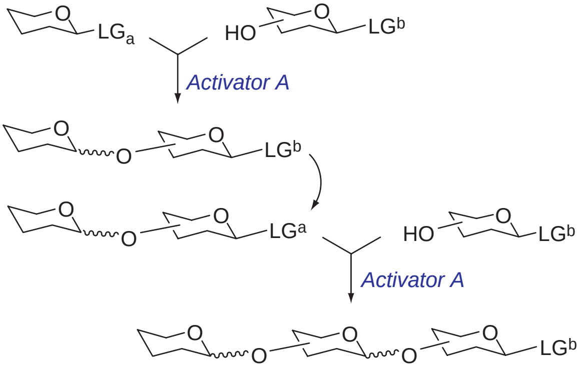

SCHEME 20. Active–latent approach.

achieved by modifying the leaving group rather than by replacing it with another leaving group. Thus, the conversion between LG^b and LG^a in the active–latent approach does not involve substitution at the anomeric center as in the two-step activation–preactivation strategy just discussed. Instead, a simple modification of the leaving group, usually at a remote reactive center, is executed.

The active–latent strategy was invented by Roy for active *p*-acetamidophenylthio (LG^a) and latent *p*-nitrophenylthio (LG^b) glycosides.[6] The conversion LG^b → LG^a is achieved by a simple reduction of the nitro group followed by acetylation of the resulting amine. Initially developed for the synthesis of sialosides,[6] the scope of this approach has been broadened.[144] Fraser-Reid has demonstrated that a similar outcome can be achieved with the use of active pentenyl glycosides and latent 4,5-dibromopentyl glycosides.[117] The latent 4,5-dibromopentyl moiety can be then converted into the active *O*-pentenyl leaving group under reductive conditions. Thus, it was demonstrated that the reactive double bond of *O*-pentenyl glycosides may be temporary protected as the dibromo derivative by the reaction with Br_2/Et_4NBr or $CuBr_2$/LiBr. The resulting anomeric moiety is unreactive as the leaving group, and therefore it is able to act as the temporary anomeric protection of the glycosyl acceptor. The backward conversion can be performed by reductive debromination through the treatment with Zn/Bu_4NI or NaI.[117,145]

A representative example of this strategy is depicted[146] in Scheme 21. The glycosyl donor **107** was glycosylidated with glycosyl acceptor **108** in the presence of triethylsilyl (TES) triflate to produce disaccharide **109** in 89% yield. The acceptor **108** can be also converted into a glycosyl donor by simple acylation, to afford pentenyl donor **110**

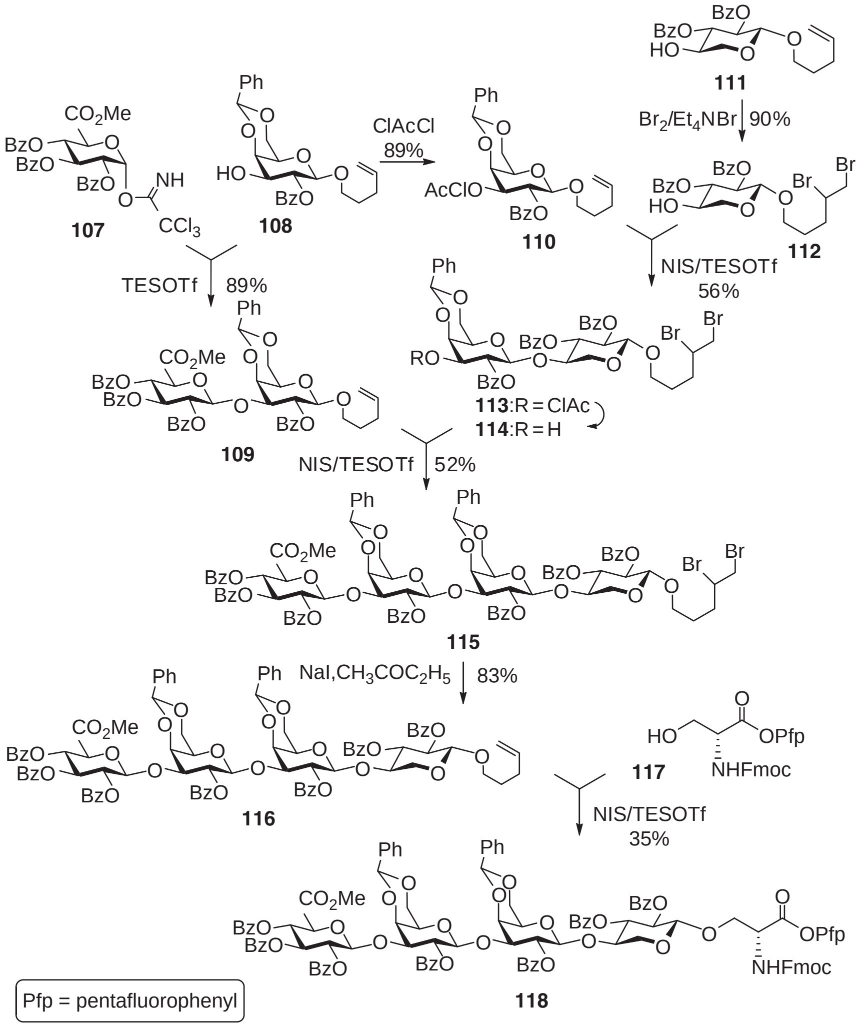
111
Br2/Et4NBr 90%
107
108
ClAcCl 89%
110
112
TESOTf 89%
NIS/TESOTf 56%
109
113:R = ClAc
114:R = H
NIS/TESOTf 52%
115
NaI,CH3COC2H5 83%
116
117
NIS/TESOTf 35%
118
Pfp = pentafluorophenyl

SCHEME 21. Synthesis of oligosaccharide **118** of the proteoglycan linkage-region via active–latent strategy.[146]

in 89% yield. This active glycosyl donor **110** is subsequently glycosylidated with the building block **112** bearing a latent dibromopentyl anomeric moiety. The latent moiety was obtained in one step from the pentenyl glycoside **111**. The coupling between the building blocks **110** and **112** was performed in the presence of

NIS/TESOTf, leading to the disaccharide **113** in 56% yield. The latter was then converted into a glycosyl acceptor **114** by a simple deacylation. Another active–latent coupling was executed between glycosyl donor **109** and glycosyl acceptor **114**. The resulting tetrasaccharide derivative **115**, bearing the latent dibromopentyl moiety, was then converted into its active state by elimination with NaI in butanone. The resulting *O*-pentenyl glycosyl donor **116** was then activated for the reaction with serine acceptor **117** in the presence of NIS/TESOTf, leading to the formation of the target compound **118** in 35% yield. This synthesis combines advantageous features of both active–latent and convergent building-block strategies.

Boons has developed a conceptually similar approach with the use of the latent substituted allyl glycosides (1-methyl-2-propenyl), which can be isomerized into the corresponding active vinyl glycosides.[7] An extension of this approach that utilizes the anomeric allyl moiety as the latent group and the corresponding vinyl moiety as its active counterpart has recently emerged.[147] As is evident from the example depicted in Scheme 22, the anomeric allyl moiety of compound **119** can be isomerized *in situ* to the active vinyl moiety (**120**) by the addition of a catalytic amount of [Ir(COD)-$(PMePh_2)_2]PF_6$. The resulting active glycosyl donor **120** could be glycosidated with allyl glycoside acceptor **121** in the presence of NIS to afford disaccharide **122**. Subsequently, the isomerization (**122** → **123**)–glycosylation (**123** + **124**) sequence can be reiterated to afford trisaccharide **125** in 85% yield.

Kim discovered that 2-(benzyloxycarbonyl)benzyl glycosides (see **127**, Scheme 23) are perfectly stable (latent) compounds, whereas the corresponding 2-(hydroxycarbonyl)benzyl analogues (for example **126**) are active glycosyl donors. It was thus, demonstrated that 2-(hydroxycarbonyl)benzyl glycoside **126** can be readily activated over glycosyl acceptor **127** in the presence of di(*t*-butyl)methylpyridine (DTBMP) and Tf_2O to provide disaccharide **128** in 85% yield.[148] The resulting disaccharide **128** bearing the 2-(benzyloxycarbonyl)benzyl aglycone could be converted by mild hydrogenation into the active donor **129** in 92% yield. The glycosyl donor **129** was then glycosidated with glycosyl acceptor **127** to provide trisaccharide **130** in 72% yield. This and other conceptually similar recent discoveries[17,149] open new exciting perspectives for further development of the active–latent strategy.

4. Orthogonal and Semi-orthogonal Strategies

The combination of two chemically distinct glycosylation reactions, in which one of the leaving groups is activated while the other one remains intact, and *vice versa*, has led to the discovery of the orthogonal strategy for oligosaccharide synthesis.[4]

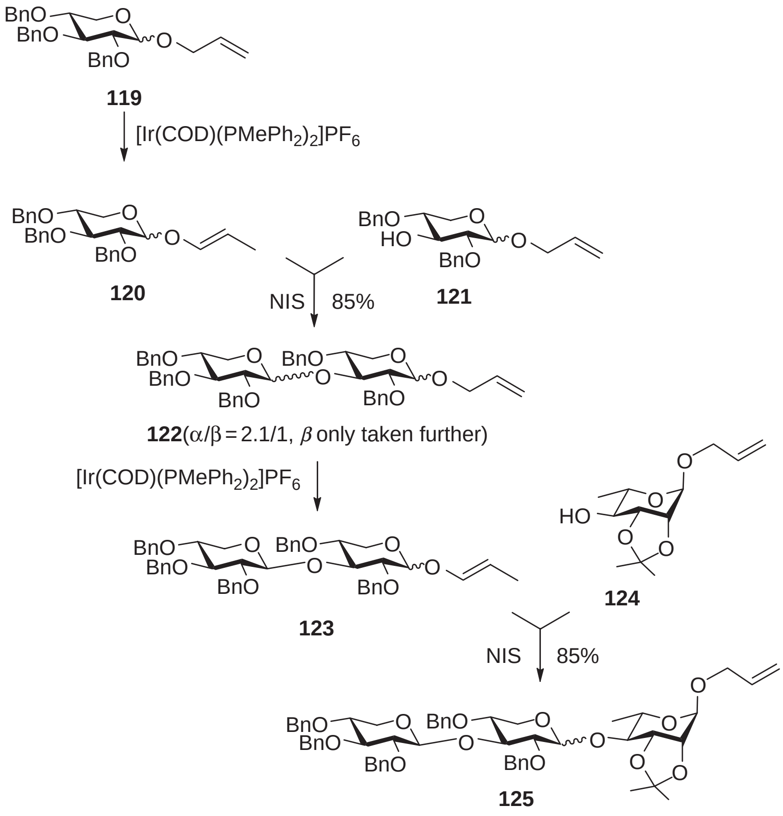

SCHEME 22. Allyl glycosides in the active–latent strategy for oligosaccharide synthesis.[147]

This unique, and virtually one of the most conceptually attractive techniques for expeditious oligosaccharide synthesis, requires the use of two orthogonal classes of glycosyl donors.[33,150] As with the selective activation strategy, at the first step the glycosyl donor bearing LG^a is activated over the glycosyl acceptor bearing LG^b. Uniquely to the orthogonal strategy, however, the LG^b is then activated over LG^a of the new glycosyl acceptor (Scheme 24). This activation sequence can then be reiterated to give straightforward access to larger oligosaccharides.

The classic variation of the orthogonal activation route involves building blocks bearing *S*-phenyl and fluoro leaving groups. These reactions have been performed both in solution[4,151] and on the polymer support.[5,152] Thus, Ogawa and co-workers illustrated that the phenyl thioglycoside **131** can be selectively activated over glycosyl

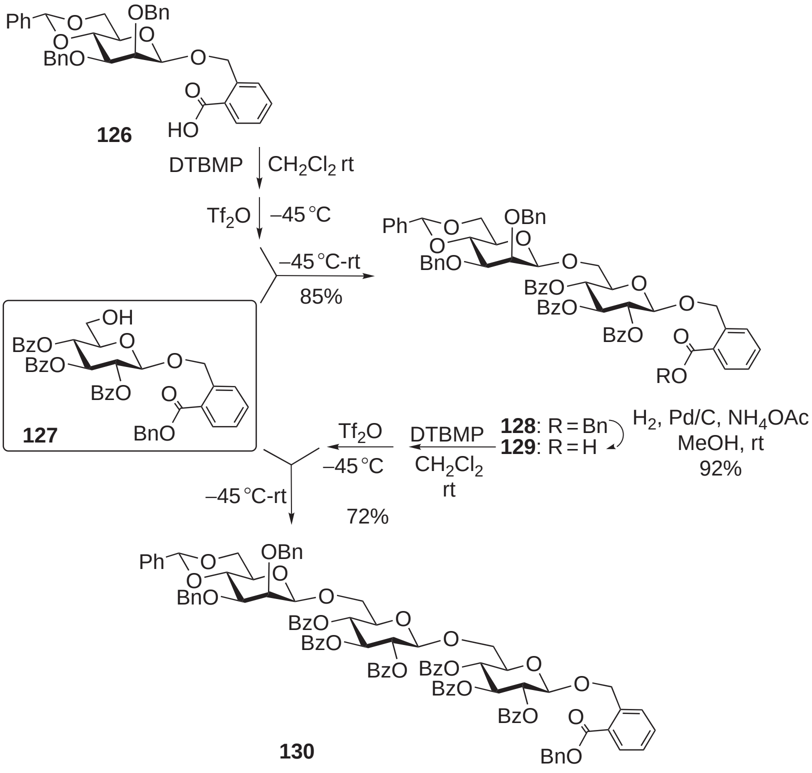
126
DTBMP
CH2Cl2 rt
Tf2O
–45 °C
–45 °C-rt
85%
127
128: R = Bn
129: R = H
H2, Pd/C, NH4OAc
MeOH, rt
92%
Tf2O
–45 °C
DTBMP
CH2Cl2
rt
–45 °C-rt
72%
130

SCHEME 23. Active–latent strategy with (2-hydroxycarbonyl)benzyl glycosides.[148]

fluoride **132** in the presence of NIS/AgOTf to afford the disaccharide **133** (Scheme 25).[4] The fluoro leaving group of the glycosyl donor **133** can then be activated over the SPh moiety of the glycosyl acceptor **134** in the presence of $Cp_2Hf_2Cl_2$ and AgOTf to afford the trisaccharide **135** in 72% yield. This sequence can be then reiterated, and to illustrate this, the phenylthio donor **135** was activated over the fluoride acceptor **132** to provide tetrasaccharide **136** in 66% yield.

Recently, it was discovered that a combination of *S*-ethyl glycosides and *S*-thiazolinyl (STaz) glycosides also allow for efficient orthogonal activation. Thus, STaz glycosides could be activated selectively over ethyl thioglycosides with AgOTf, whereas the ethyl thioglycoside could be significantly activated over the STaz moiety by using NIS in conjunction with catalytic TfOH.[105] This finding was later verified by

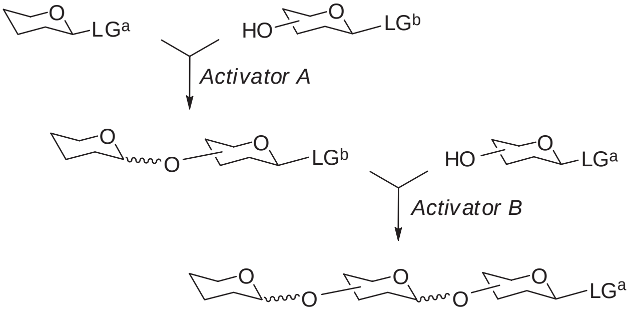
LG^a
HO
LG^b
Activator A
LG^b
HO
LG^a
Activator B
LG^a

SCHEME 24. Orthogonal strategy for oligosaccharide synthesis.

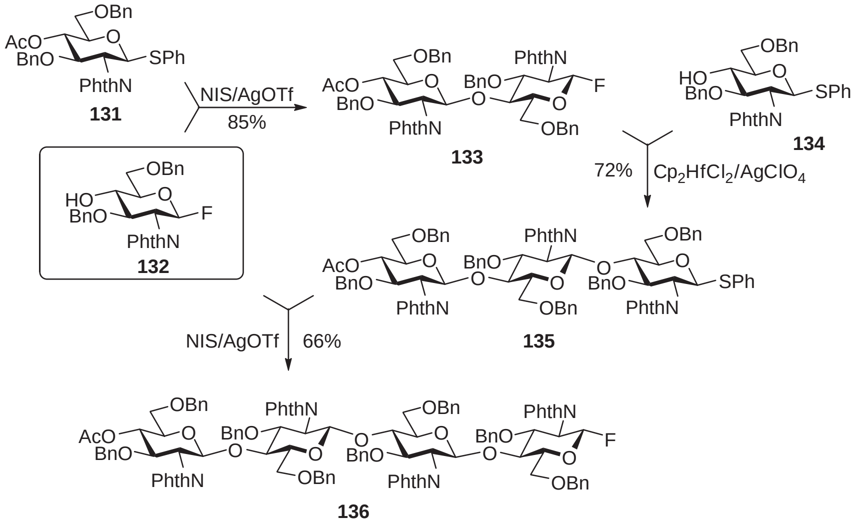
131
NIS/AgOTf
85%
132
133
134
72%
Cp2HfCl2/AgClO4
135
NIS/AgOTf
66%
136

SCHEME 25. Orthogonality of thioglycosides and fluorides.[4]

the synthesis of a pentasaccharide derivative **143**, as depicted in Scheme 26.[153] Thioglycoside donor **137** was activated over the STaz acceptor **138** by the addition of NIS and catalytic TfOH to provide disaccharide **139** in 98% yield. The latter, in turn, was activated over a thioglycoside acceptor **140** by the addition of AgOTf to give trisaccharide **141** in 93% yield. This thioglycoside building block was then

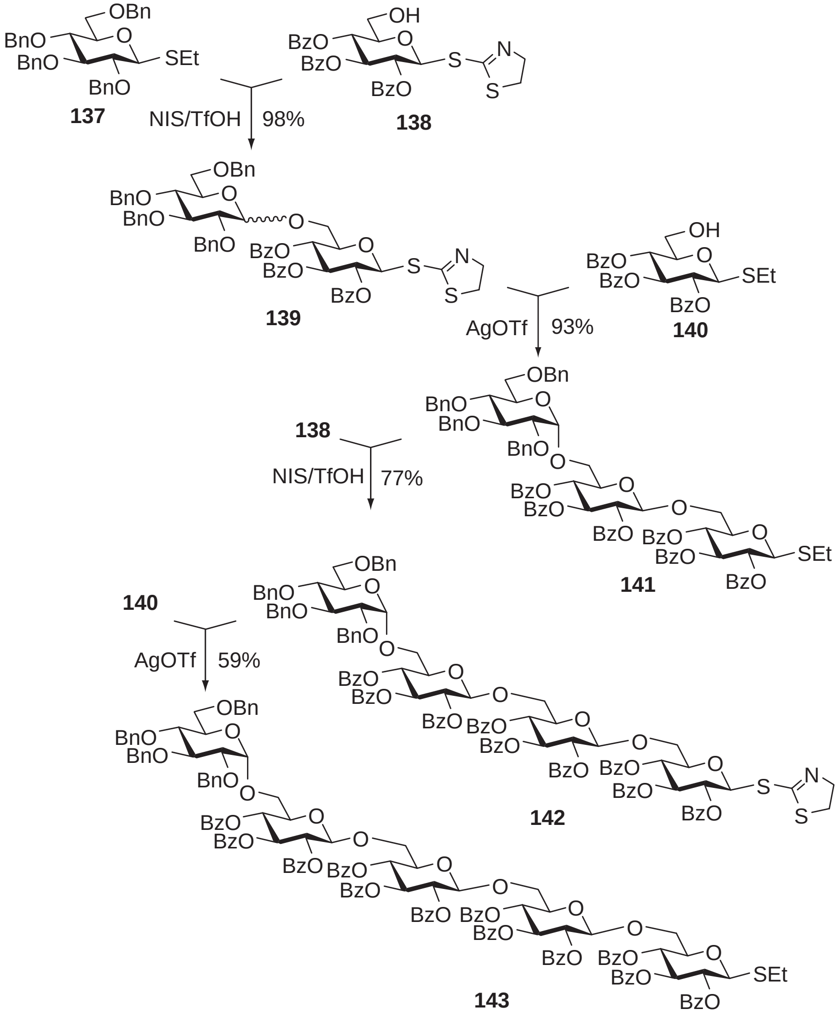
137
138
NIS/TfOH
98%
139
140
AgOTf
93%
141
138
NIS/TfOH
77%
142
140
AgOTf
59%
143

SCHEME 26. Orthogonality of ethyl and thiazolinyl thioglycosides.[153]

activated over the STaz acceptor **138** by NIS/TfOH to provide tetrasaccharide **142** in 77% yield. Finally, the tetrasaccharide **142** was activated over thioglycoside acceptor **140** by the addition of AgOTf to give the desired pentasaccharide **143** in 59% yield. A related approach involving orthogonal activation of STaz and SBox glycosides has also recently emerged.[154]

Ideally, the orthogonal approach allows for an unlimited number of reiterations of the two orthogonal leaving groups. In practice, however, the efficiency of glycosidation is usually inversely correlated to the size of the glycosyl donor involved. As is evident from the two examples quoted, the yields decrease dramatically for oligosaccharide glycosyl donors as compared to their monosaccharide counterparts.

A conceptually related approach, whereby *S*-ethyl glycosides could be activated over *O*-pentenyl glycosides and *vice versa*, has been developed.[155] The drawback of this technique is in its *semi*-orthogonality: while either armed or disarmed *S*-ethyl glycosides can be activated over armed/disarmed *O*-pentenyl glycosides, only armed *O*-pentenyl glycoside can be activated over disarmed *S*-ethyl glycoside. This semi-orthogonal concept was recently extended to another suitable pair of leaving groups, namely fluoro and *O*-pentenyl.[143] The armed–disarmed concept is thoroughly discussed in Section IV.1.

5. Deactivation by Steric Hindrance

Boons and co-workers developed an interesting concept for oligosaccharide synthesis (Scheme 27) by demonstrating that the increase of steric hindrance around the active site of the leaving group has a dramatic effect on the leaving-group ability.[156] Thus, it was shown that an *S*-ethyl glycoside **144** can be selectively activated with NIS/TMSOTf at −70 °C over the dicyclohexylmethyl thioglycoside **145** to afford trisaccharide derivative **146** in 50% yield. Presumably, the sulfur atom of the dicyclohexylmethylthio moiety is sterically hindered by two bulky cyclohexyl substituents and, evidently is significantly less accessible for the promoter activation than its ethylthio counterpart.[157] The less-reactive, bulky thioglycoside moiety can also be activated by using the same reagents under similar reaction conditions. Thus, activation of the dicyclohexylmethyl trisaccharide **146** with NIS/TMSOTf could be accomplished at room temperature in a matter of minutes. This was illustrated by reacting glycosyl donor **146** with trisaccharide acceptor **148** (also obtained from compound **146**) that resulted in the formation of hexasaccharide **149**.

6. Temporary Deactivation Concept

Demchenko and co-workers demonstrated that STaz glycosides can be engaged in stable non-ionizing transition-metal complexes. This observation served as a basis for the development of a temporary deactivation technique for oligosaccharide synthesis (Scheme 28).[158] The deactivation of the otherwise reactive building block was

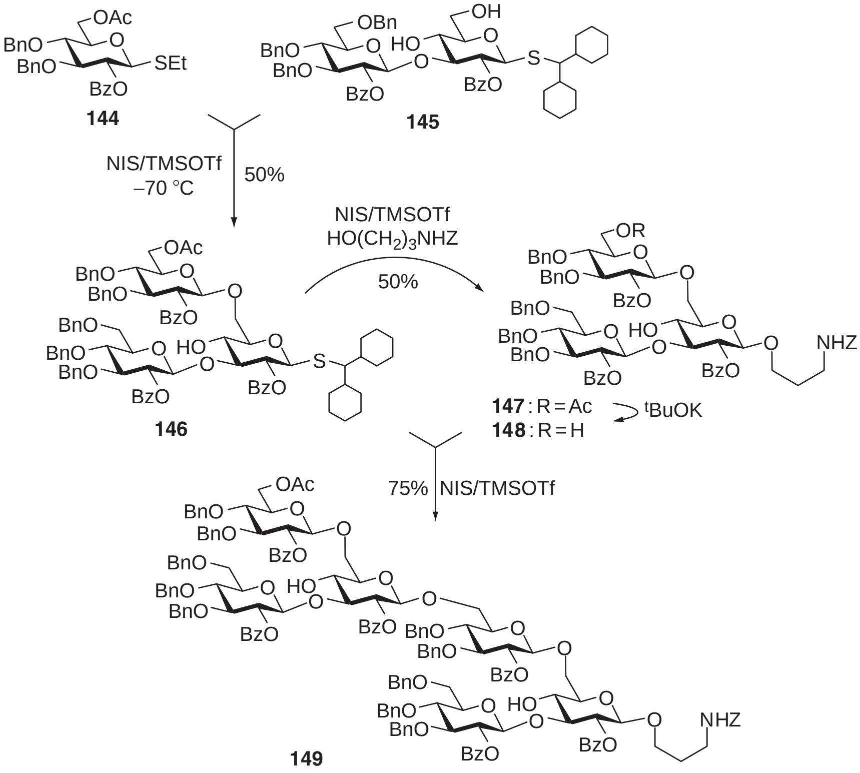

SCHEME 27. Steric hindrance-facilitated synthesis[157] of phytoalexin-elicitor active oligosaccharide **149**.

achieved by engaging its leaving group into a stable, non-ionizing metal complex with $PdBr_2$. This allowed selective activation of a ‘‘free’’ leaving group of the glycosyl donor over the deactivated (capped) leaving group of the complexed acceptor. Since the ‘‘leaving group’’ of the acceptor is deactivated, practically any type of leaving group could be used in the glycosyl donor unit, as long as its activation does not disrupt the complex. Another valuable outcome of this technique is the fact that even electronically disarmed glycosyl donors can be activated over electronically armed, but temporarily deactivated, acceptors.[158] The armed–disarmed approach is described in Section IV. Upon glycosylation, the disaccharide is released from the complex by treatment with a ligand-exchange reagent to liberate ‘‘free’’ disaccharide, which can be used in subsequent transformations.

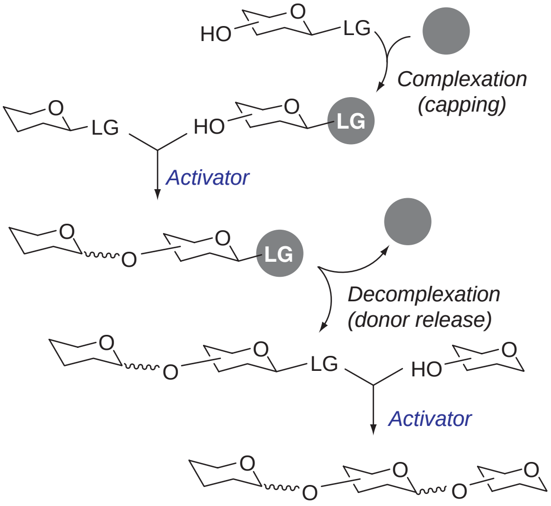

SCHEME 28. Temporary deactivation concept.

A relevant example illustrating the versatility of this approach is depicted in Scheme 29.[159] Specifically designed (2-pyridyl)thiazolyl glycosides were found to be excellent bidentate ligands for the complexation with platinum group metals. The pre-complexed stable glycosyl acceptor **151** was glycosylated with the STaz glycosyl donor **150** in the presence of AgOTf. Subsequent removal of the temporary TBDMS group led to disaccharide **152** in 79% yield. The latter was glycosylated with the SBox disaccharide donor **153** in the presence of AgOTf to give tetrasaccharide **154** in 89% yield. The tetrasaccharide **154** represents the repeating unit of pneumococcal polysaccharide serotype 14. To elongate the sequence, building block **154** was split into two portions. The first portion was treated with NaCN to remove the Pd(II) complex and provide tetrasaccharide donor **155** in 95% yield. The second portion was treated with TFA to remove the isopropylidene protective group to provide tetrasaccharide acceptor **156** in 89% yield. Coupling of the two tetrasaccharide building blocks provided octasaccharide **157** in 73% yield. This synthetic approach combines advantageous features of the temporary deactivation, convergent-block synthesis (Section II.3) and bidirectional strategy (Section V.3). It is important to note that the (2-pyridyl)thiazolyl glycoside-based platinum(II) complexes were found to be very stable under a variety of reaction conditions, ranging from strong acids (TFA) to strong bases (NaOMe).[159]

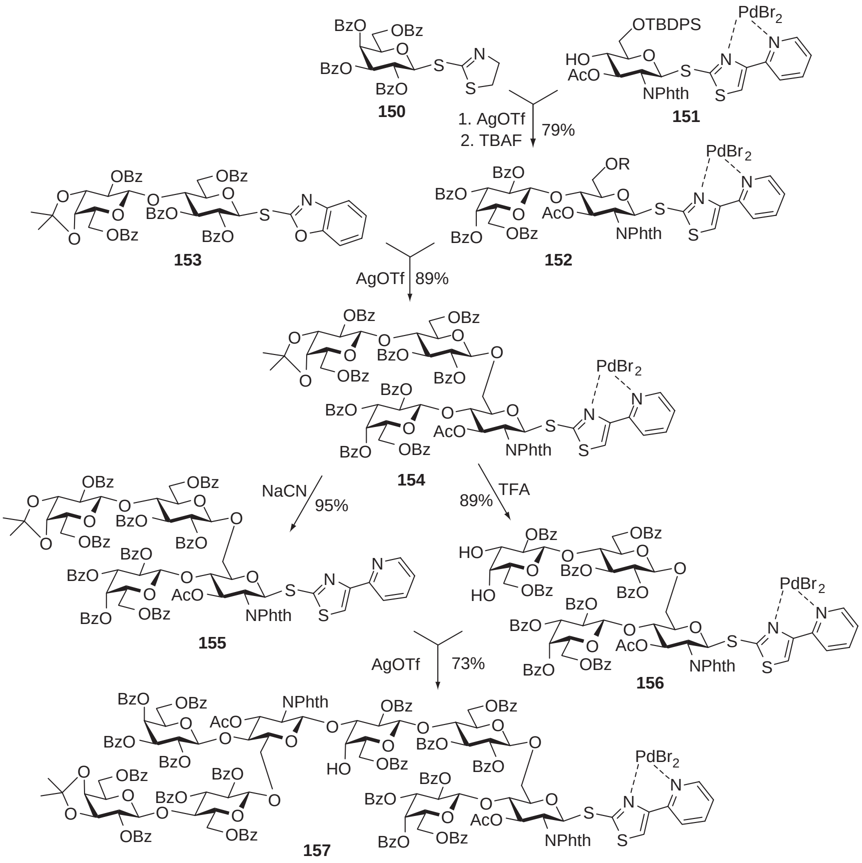
150
151
1. AgOTf
2. TBAF
79%
153
152
AgOTf
89%
154
NaCN
95%
TFA
89%
155
156
AgOTf
73%
157
BzO
OBz
AcO
HO
NPhth
OTBDPS
OR
PdBr2

SCHEME 29. Synthesis of pneumococcal oligosaccharides serogroup 14 by temporary deactivation technique.[159]

IV. CHEMOSELECTIVE (PROTECTING-GROUP BASED) STRATEGIES

The chemoselective approach and its variations discussed in this section make use of only one class of leaving group for both the glycosyl donor and glycosyl acceptor, which is either activated (armed) or deactivated (disarmed), respectively, by the influence of the protecting groups. Usually, protecting groups in both reaction components have to be taken into consideration. This allows for direct coupling, according to which the armed glycosyl donor is chemoselectively activated over the disarmed derivative bearing the same type of LG in the presence of a mild promoter (Scheme 30). The disaccharide obtained can then be used for subsequent direct glycosylation in the presence of a more-powerful promoter capable of activating the disarmed leaving group. In some applications, the same promoter as for step 1 could be used for step 2 performed at elevated temperature.

Experimentally, the chemoselective strategies are simpler than previously described selective or orthogonal activations, because one needs to operate with only one class of compounds (leaving groups); however the necessity for fine tuning of the leaving-group reactivity and the reaction conditions for its activation comes to the fore. Along with selective approaches, the chemoselective strategies have become valuable techniques for expeditious oligosaccharide synthesis. The majority of strategies discussed in this subsection allows efficient oligosaccharide assembly without the necessity to perform additional synthetic steps between the glycosylation steps.

The classic *armed–disarmed approach*, developed by Fraser-Reid, has created a solid basis for extensive studies and applications, and all strategies discussed in this section are related to (or derived from) this elegant concept. The key factor for the armed–disarmed activation to take place is the availability of a suitable promoter that differentiates between the armed and disarmed building blocks. While in most cases the differentiation of the reactivity between armed and disarmed species is maintained by the choice of promoter or temperature, the solvent effect observed by Oscarson may become a useful technique for future assemblies.[160] Thus, it was demonstrated that highly reactive substrates could be activated in diethyl ether, whereas poorly reactive disarmed derivatives had to be activated in CH_2Cl_2.

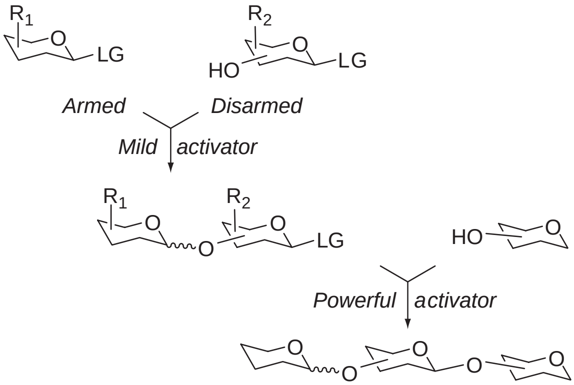

SCHEME 30. Armed–disarmed concept.

1. Arming and Disarming with Neighboring Substituents

The effect of protecting groups on the leaving-group ability has been known for long time, but it was Fraser-Reid and co-workers, who developed a new strategy for chemoselective oligosaccharide synthesis.[2,117,161–163] This concept utilizes the fact that the protective groups present on the sugar molecule dictate its reactivity. It was discovered that armed glycosides, sugar molecules that are protected with an ether moiety at C-2, can be readily activated by mild promoters. On the other hand, disarmed glycosides that are protected by an ester group at C-2 require stronger promoters. This allows for direct coupling according to which a benzylated (electronically activated, armed) glycosyl donor is chemoselectively activated over the acylated (electronically deactivated, disarmed) derivative bearing the same type of LG in the presence of a mild promoter (Scheme 31). For example, iodonium (di-γ-collidine) perchlorate (IDCP) was used as a mild electrophilic activator for *O*-pentenyl glycosides.[161] Since the anomeric configuration of the product is also determined by the protective group at O-2, a 1,2-*cis*-linked disaccharide is preferentially obtained at the first step, due to the use of the ether-type arming substituent, a non-participating group (*O*-benzyl). The disaccharide obtained can then be used for 1,2-*trans* glycosylation directly in the presence of a more potent promoter (such as NIS/TfOH for *O*-pentenyl glycosides), capable of activating the disarmed leaving

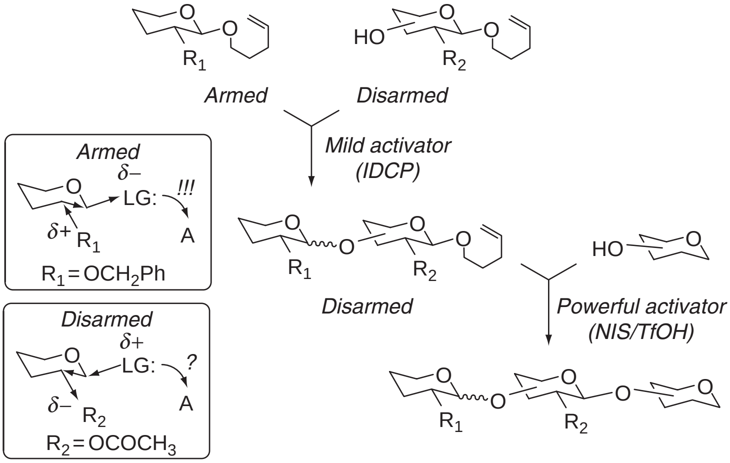

SCHEME 31. Arming–disarming by neighboring substituents.

group. As discussed in Section II.1, this selectivity takes place because of formation of the acyloxonium intermediate that coordinates the 1,2-*cis* face of the ring.

This concept was further explored for the chemoselective glycosidations of other classes of compounds, including thioglycosides,[164] selenoglycosides,[116] fluorides,[165] phosphoroamidates,[166] substituted thioformimidates,[167] glycals,[168] and thioimidates.[169,170] For example, Hashimoto *et al*. reported the synthesis of a glycosphingolipid **165** using phosphoroamidate building blocks (Scheme 32).[166] The armed galactosyl donor **158** was activated over the disarmed galactosyl acceptor **159** by activation with TMSOTf at −46 °C to provide disaccharide **160** in 85% yield. Glucosyl donor **161** was glycosidated with lipid **162** in the presence of TMSOTf at 0 °C to generate **163** in 74% yield. The latter was then converted into a glycosyl acceptor **164** by removal of the chloroacetyl group with thiourea–lutidine. Glycosyl donor **160** was then glycosidated with glycosyl acceptor **164** in the presence of TMSOTf at 0 °C to provide the requisite glycosphingolipid **165** in 85% yield.

Overall, the armed–disarmed strategy offers an efficient tool for the synthesis of oligosaccharides having a *cis*–*trans* glycosylation pattern.[58,117] The synthesis of *cis*–*cis*-linked derivatives is also possible, but additional reprotection at the

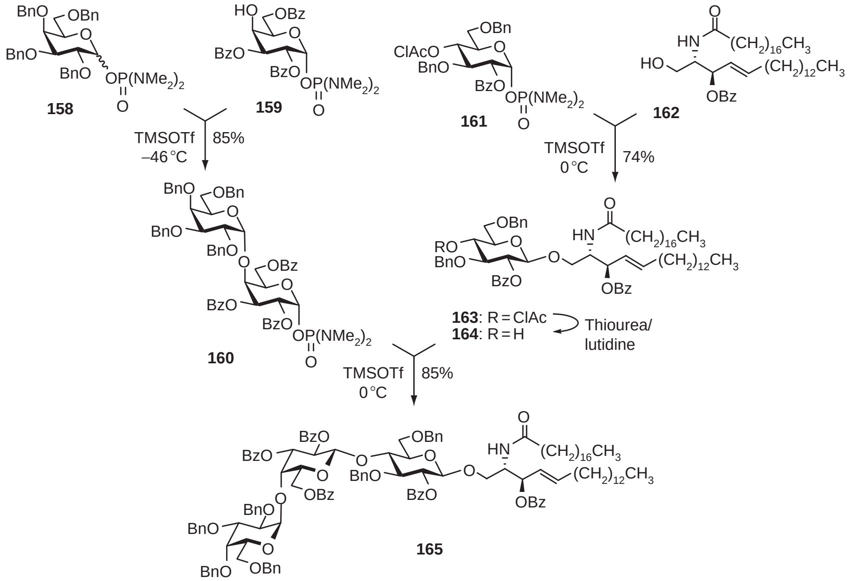
BnO
OBn
BnO
BnO
OP(NMe$_2$)$_2$
O
158
HO
OBz
BzO
BzO
OP(NMe$_2$)$_2$
O
159
TMSOTf
−46 °C
85%
ClAcO
BnO
OBn
BzO
OP(NMe$_2$)$_2$
O
161
HN
O
(CH$_2$)$_{16}$CH$_3$
HO
(CH$_2$)$_{12}$CH$_3$
OBz
162
TMSOTf
0 °C
74%
160
RO
BnO
163: R = ClAc
164: R = H
Thiourea/
lutidine
TMSOTf
0 °C
85%
165

SCHEME 32. Armed-disarmed synthesis[166] of glycosphingolipid **165**.

disaccharide stage (OBz → OBn) is required. A representative example of this strategy is shown in Scheme 33.[164] The armed glycosyl donor **166** was selectively activated over the disarmed glycosyl acceptor **167** in the presence of IDCP to provide disaccharide **168** in 91% yield. The latter was debenzoylated and then benzylated to provide the armed disaccharide donor **169**, which was then glycosidated with acceptor **167** to provide the *cis–cis* trisaccharide **170** in 72% yield. Because of the conversion of the second-generation glycosyl donor into the armed state, the second-step coupling could be also performed with the mild promoter IDCP.

A related concept was developed by the Demchenko group. Thus, it was demonstrated that, with the use of a 2-*O*-picolyl substituent as a novel *arming participating* group on glycosyl donor **171**, upon coupling with the disarmed acceptor **172** by the addition of Cu(OTf)$_2$, the 1,2-*trans*-glycosidic linkage can be chemo- and stereoselectively introduced at the first glycosylation step (Scheme 34). The resulting disaccharide **173** is isolated in 74% yield.[170] Due to the reverse outcome of this glycosylation in comparison that of classic armed–disarmed approach leading to the formation of 1,2-*cis* glycosides, this approach is called the *inverse armed–disarmed* strategy. Subsequent glycosidation of the disarmed disaccharide **173** with glycosyl acceptor **174** could be achieved in the presence of the more-powerful activator AgOTf, leading to the *trans–trans*-linked trisaccharide **175** in 88% yield.[170]

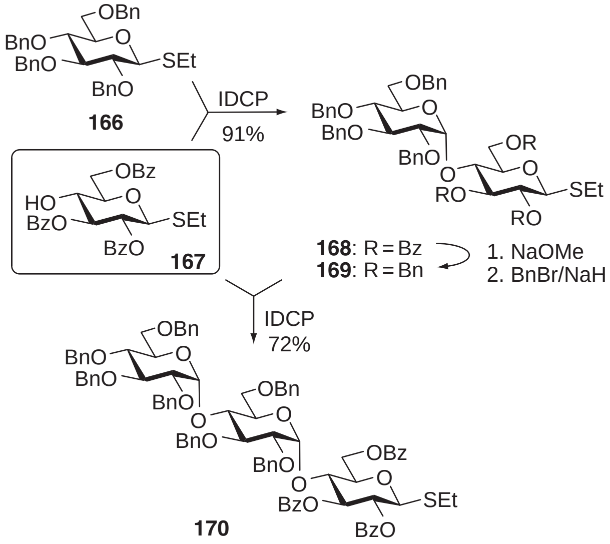

SCHEME 33. Synthesis of *cis–cis*-patterned oligosaccharide **170** via armed–disarmed approach.[164]

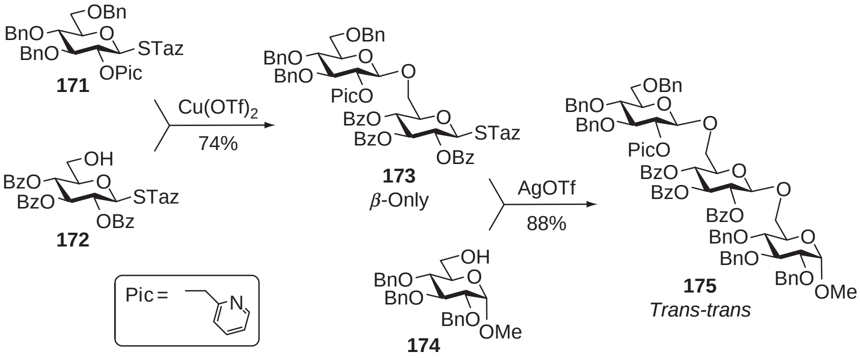

SCHEME 34. Arming participating group mediated inverse armed–disarmed strategy.

2. Reactivity-Based Programmable Strategy

Significant progress in the area of chemoselective oligosaccharide synthesis has emerged with the development of programmable oligosaccharide strategy, which became a logic extension of studies pioneered in Fraser-Reid's, van Boom's, Ley's, and Wong's groups. Attempts to classify, and even predict the outcome of, a glycosylation reaction (or a sequence) have led to the development of approaches to quantify the reactivity of building blocks.[8,9,171–173] Among these, a vast database of relative reactivity values (RRVs) has been assembled; and the data collected have been compiled into a predictive computer program called Optimer.[9] The determination of RRVs was performed with standard reaction conditions using tolyl thioglycoside donors in the presence of NIS/TfOH as the promoter system. It was noted that optimal chemoselective couplings generally occurred when there was a large difference in the RRVs. A particularly illustrative example is shown in Scheme 35 (synthesis of **179**). Thus, selective activation of glycosyl donor **176** (RRV = 17,000) over building block **177** (RRV = 28.9) in the presence of NIS/TfOH resulted in formation of the disaccharide derivative. The latter was not isolated; instead, glycosyl acceptor **178** and additional NIS were added to the reaction mixture. As a result of this two-step sequential activation, trisaccharide **179** was isolated in 58% overall yield.[9] This approach combining two (or more) glycosylation steps, based on the *in situ* activation of one donor over another, is termed the one-pot technique. One-pot strategies offer the shortest pathway to oligosaccharides, as the sequential glycosylation reactions are performed in a single flask (pot) and do not require isolation and purification of the intermediates. A more extensive discussion of this technique is detailed in Section VI.3.

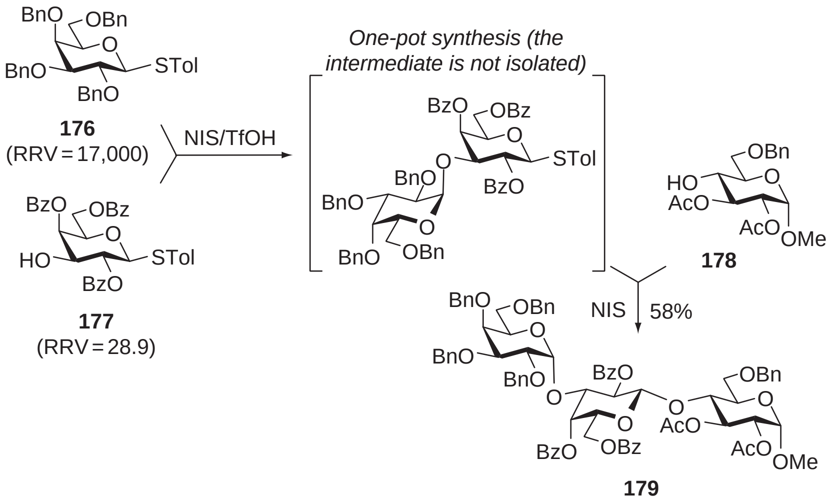

SCHEME 35. Programmable synthesis[9] of trisaccharide **179**.

3. Disarming by the Remote Substituents

Madsen's group observed that a single electron-withdrawing moiety at the remote C-6 position was sufficient to disarm a glycosyl acceptor by comparison with the peralkylated glycosyl donor.[174] This effect was especially pronounced with the use of a potent electron-withdrawing functionality, such as the pentafluorobenzoyl (PFBz) ester.[175] For example, benzylated thioglycoside **180** could be chemoselectively activated over the 6-*O*-pentafluorobenzoyl acceptor **181** in the presence of NIS/TESOTf to provide disaccharide **182** (Scheme 36). The latter could then be glycosidated with glycosyl acceptor **183** the presence of NIS/TESOTf to give trisaccharide **184** in 61% yield.

Further insight to the armed–disarmed approach came with the observation of the unusual reactivity pattern of the SBox glycosides. Thus, it was demonstrated that glycosyl donors having the 2-*O*-benzyl-3,4,6-*O*-triacyl pattern of protecting groups are even more deactivated than the corresponding ''disarmed'' peracylated derivatives.[169] Although the exact nature of this interesting effect, termed the O-2/O-5 cooperative effect, is not yet understood, it has been postulated that the intermediate carbocation stabilization via the acyloxonium ion of the peracylated donor is favored over the oxacarbenium ion stabilization of the 2-benzyl-3,4,6-triacylated donors (see

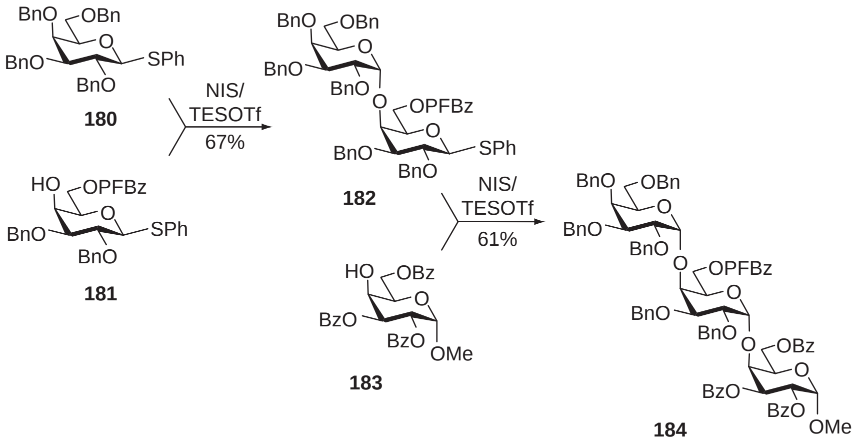

SCHEME 36. Disarming the glycosyl acceptor with the remote 6-*O*-pentafluorobenzoyl moiety.[175]

the synthesis of **189**, Scheme 37). This effect is especially profound with glycosyl donors having the 1,2-*trans* anomeric configuration, which is known to greatly facilitate anchimeric assistance by the neighboring substituent.[176] This stabilization presumably takes place with concerted displacement of the leaving group, resulting in the formation of the acyloxonium intermediate. Armed glycosyl donor **185** was activated over the disarmed SBox acceptor **186** by the addition of $Cu(OTf)_2$ to provide disaccharide **187** in 64% yield. The disarmed disaccharide **187** was then chemoselectively activated over glycosyl acceptor **188** by the addition of $Cu(OTf)_2$/TfOH to produce the trisaccharide **184** in 70% yield. To differentiate the two levels of the disarmed building blocks, the ''disarmed'' acceptor **186** was termed ''moderately disarmed''.[169]

4. Disarming by Torsional Effects

Fraser-Reid[171] and Ley[177] found that the anomeric deactivation can be also achieved by the torsional effect of cyclic acetal and dispiroketal protecting groups. The acetal and ketal groups impart rigidity into the structure. This rigidity hinders the flattening of the ring during formation of the oxacarbenium ion, thereby increasing the activation energy for formation of the intermediate. Ley and co-workers reported the synthesis of a GPI anchor utilizing the disarming effects of the cyclic dispiroketal

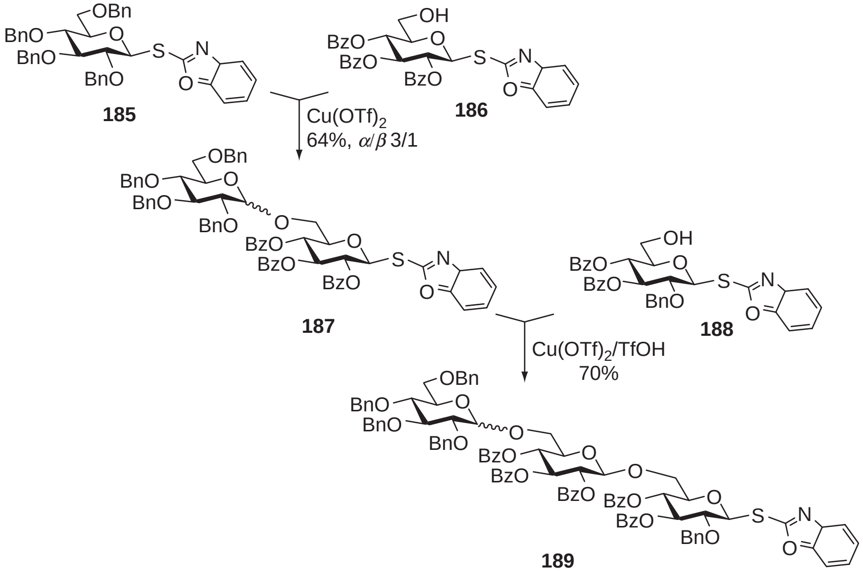

SCHEME 37. Sequential activation of armed → moderately disarmed → disarmed building blocks **185**, **186**, **188**, respectively.[169]

protecting moieties (Scheme 38).[116,178] Thus, the armed mannosyl donor **190** was activated over the torsionally disarmed mannosyl acceptor **191**, bearing the same leaving group (SePh), in the presence of NIS/TMSOTf. The resulting disaccharide **192** was obtained in 98% yield. In similar fashion, the armed galactosyl donor **193** was activated over the torsionally disarmed galactosyl acceptor **194** to provide disaccharide **195** in 71% yield. Selective activation of glycosyl donor **195** over thioglycoside acceptor **196** in the presence of MeOTf and subsequent desilylation with HF, led to trisaccharide **197** in 67% yield over two steps. It should be noted that, although MeOTf can in principle also activate the SEt group, in this instance it was found too weak an activator to activate the strongly electronically disarmed SEt group in compound **196** and also in **197**. The latter was glycosylated with the disaccharide donor **192** in the presence of MeOTf to provide pentasaccharide **198** in 75% yield. Finally, the pentasaccharide donor **198** was glycosidated with disaccharide acceptor **199** in the presence of NIS/TfOH to provide the corresponding heptasaccharide **200** in 50% yield.

More recently, Boons demonstrated that thioglycosides protected with the cyclic 2,3-carbonate group are even less reactive than traditional disarmed acylated derivatives.[179]

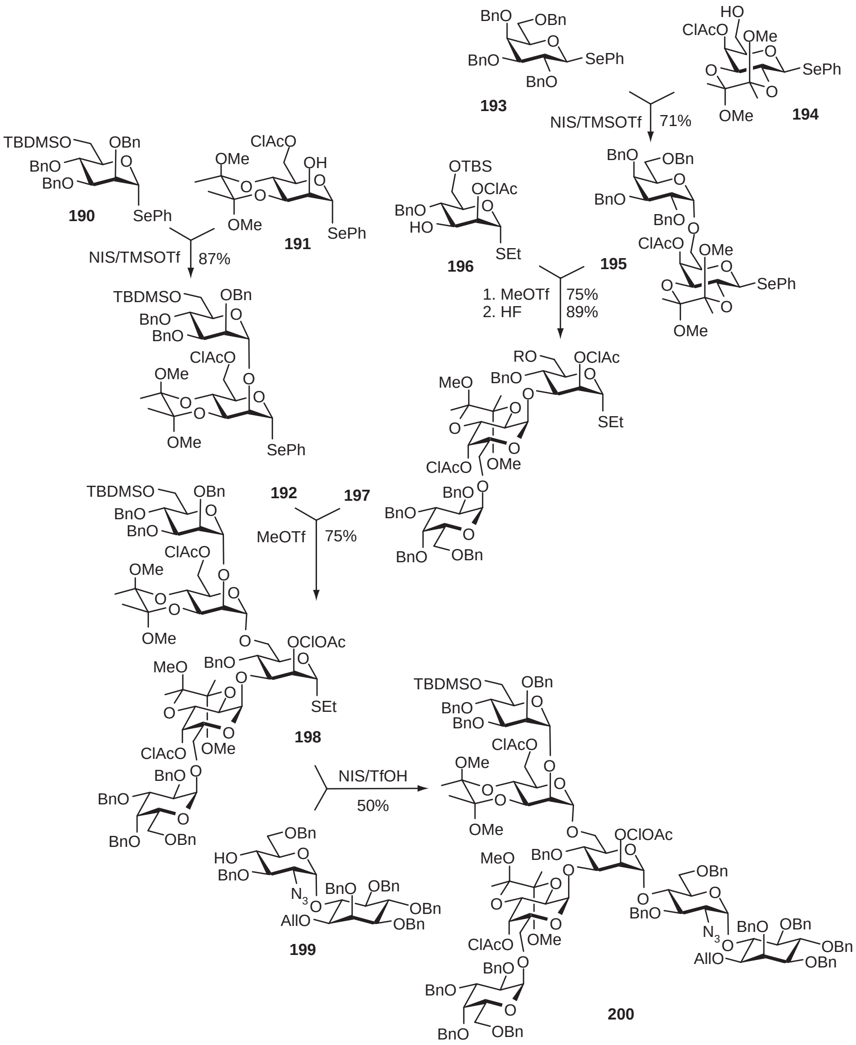
193
194
NIS/TMSOTf
71%
190
191
NIS/TMSOTf
87%
196
195
1. MeOTf
2. HF
75%
89%
192
197
MeOTf
75%
198
NIS/TfOH
50%
199
200

SCHEME 38. Synthesis of the GPI anchor oligosaccharide by employing torsionally disarmed building blocks.[116,178]

The ester/acetal groups are disarmed by different mechanisms: while esters disarm electronically, benzylidene and isopropylidene acetals were considered to be disarmed by torsional strain. This deactivation was extensively studied by Bols,[180] who used the acid hydrolysis of methyl glycosides and the spontaneous hydrolysis of 2,4-dinitrophenyl glycosides as their models to study the source of this deactivation. This study concluded that there is roughly equal deactivation from both torsional and electronic effects.

5. Super-Armed Glycosyl Donors

Bols and co-workers discovered a new phenomenon, according to which conformationally modified glycosyl donors are exceptionally reactive (super-armed).[181,182] Glycosyl donors protected with bulky TBDMS groups at 2, 3, and 4 positions were found to have superior reactivity by comparison with the classic armed perbenzylated glycosyl donors. The enhanced reactivity was explained by favorable stereoelectronic effects associated with conformational change (as in compound **201**, Scheme 39) induced by the bulky silyl protecting groups. Apparently, structurally modified glycosyl donors having axial OR protecting groups provide a more-favorable charge–dipole geometry in comparison to the conventional glycosyl donors that adopt the $^4C_1$ chair conformation. This concept was clearly illustrated by performing the one-pot coupling with all three reaction components (thioglycosides **201–203**) mixed from the very beginning (Scheme 39).[182] This type of one-pot technique

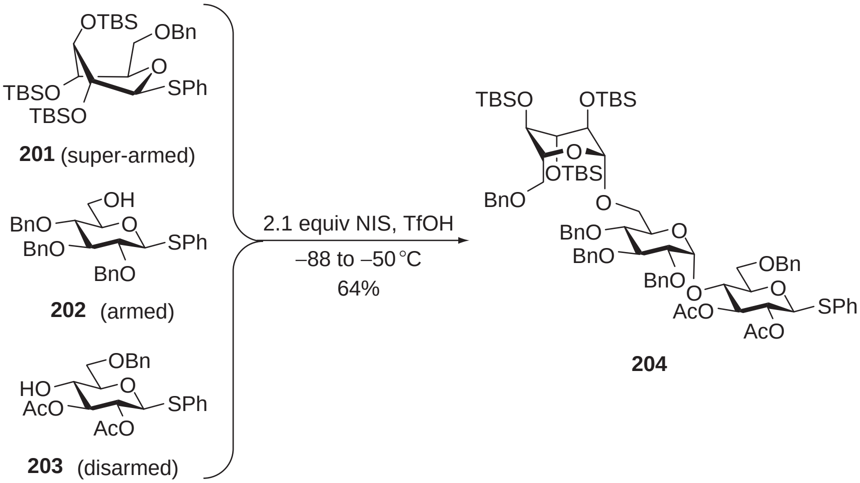
OTBS
OBn
O
SPh
TBSO
TBSO
201 (super-armed)
OH
BnO
O
BnO
SPh
BnO
202 (armed)
OBn
HO
O
AcO
SPh
AcO
203 (disarmed)
2.1 equiv NIS, TfOH
−88 to −50 °C
64%
TBSO
OTBS
O
OTBS
BnO
O
BnO
O
BnO
BnO
O
OBn
O
AcO
SPh
AcO
204

SCHEME 39. Conformationally super-armed glycosyl donors in comparative one-pot glycosylations.[182]

required differentiation between the reactivity levels of both glycosyl donors (**201** and **202**) and glycosyl acceptors (**202** and **203**)—all bear the same anomeric leaving group (phenylthio). The first reaction took place between the super-armed glycosyl donor **201** and the more reactive primary (and also more electron rich due to the neighboring benzyl substituents) glycosyl acceptor **202**. The resulting disaccharide derivative then reacted with the remaining glycosyl acceptor **203**. As a result of this one-pot coupling in the presence of NIS/TfOH, trisaccharide **204** was obtained in 64% yield.

Mydock and Demchenko have expanded the scope of this approach by determining that the strategic placement of common protecting groups opens up a new method for ‘‘super-arming’’ the glycosyl donors.[183,184] Thus, it was observed that *S*-benzoxazolyl (SBox) glycosyl donors possessing both a participating moiety at C-2 (benzoyl) and an electronically armed lone pair at O-5, achieved with the 3,4,6-tri-*O*-benzyl protection pattern, were super-armed. To illustrate this, super-armed glycosyl donor **205** was activated over ‘‘armed’’ acceptor **206** by the addition of DMTST to provide disaccharide **207** in 70% yield (Scheme 40). This disaccharide was then glycosidated with acceptor **208** to provide trisaccharide **209** in 85% yield.

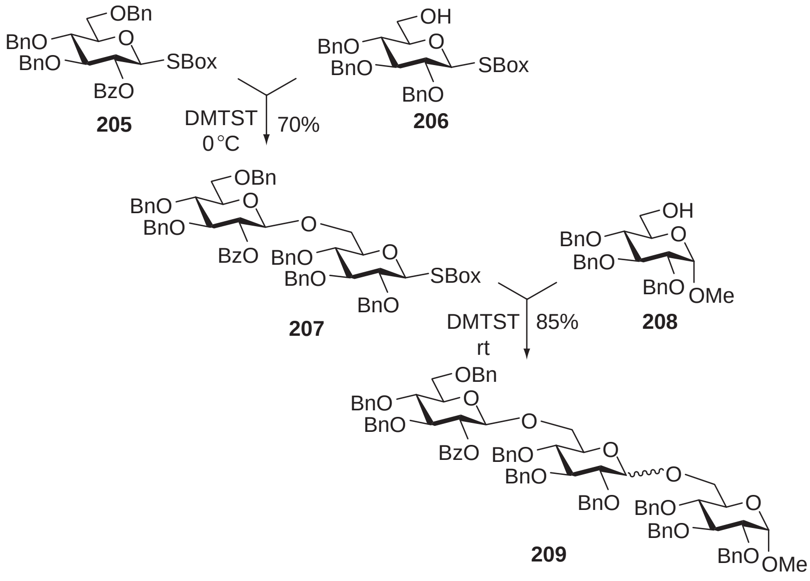

SCHEME 40. Investigation of 2-*O*-benzoyl-tri-*O*-benzyl-protected ‘‘super-armed’’ glycosyl donor.[183,184]

V. REGIOSELECTIVITY-BASED STRATEGIES

1. Hydroxyl Reactivity

Many common chemical reactions such as oxidation, acylation, or alkylation allow for the differentiation between various hydroxyl groups. Most commonly, the reactivity difference between primary and secondary alcohols has been explored. It should be noted that syntheses via these strategies are so numerous that only representative recent citations could be included in this subsection. Although the first regioselective glycosylations of primary hydroxyl groups over the secondary ones were performed decades ago, this approach is still among the most common techniques to obtain branched oligosaccharides (Scheme 41).[86,185–190]

A representative example, in which a tetrasaccharide was synthesized in a one-pot fashion, is depicted in Scheme 42.[191] Glycosyl acceptor diol **210** was selectively glycosylated at the primary hydroxyl group with glycosyl donor **211** in the presence of AgOTf to provide disaccharide **212**. The latter was used as a glycosyl donor for glycosidation with glycosyl acceptor **213** in the presence of MeOTf to provide trisaccharide **214**. The remaining hydroxyl group on compound **214** was then glycosylated with glycosyl donor **215** to provide tetrasaccharide **216** in 48% overall yield. This approach combines advantageous features of the regioselective glycosylation and bidirectional approach discussed next.

Occasionally, it is possible to glycosylate one secondary alcohol over another, and the most common examples include preferential glycosylation of equatorial hydroxyl groups over their axial counterparts.[119,187,192–196] Among many applications, acceptor polyols are commonly used for the introduction of bulky

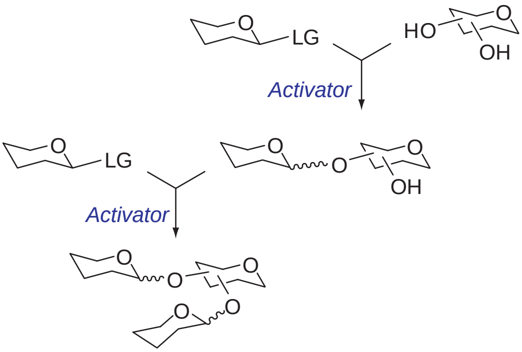

SCHEME 41. Reactivity-based regioselective glycosylation of polyols.

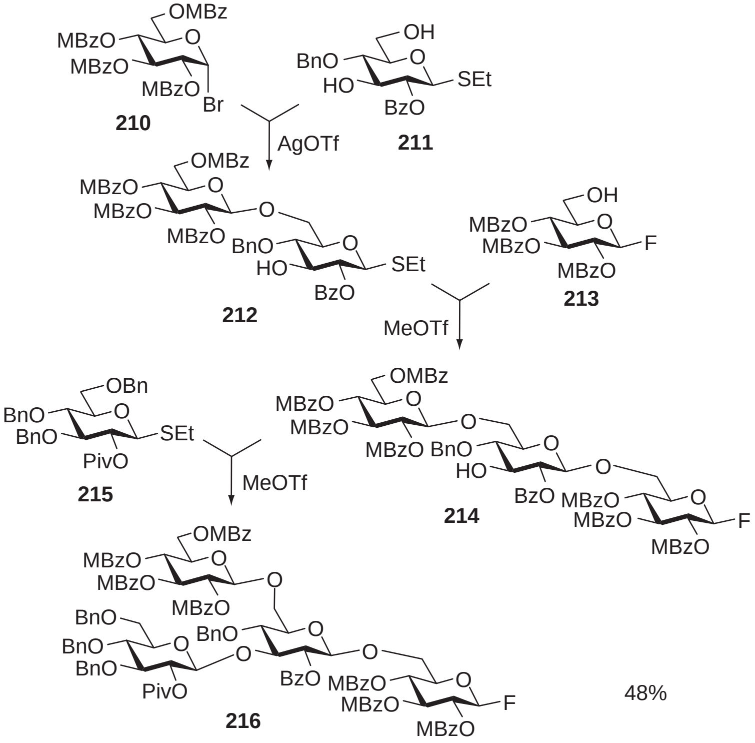

SCHEME 42. Regioselective synthesis[191] of branched oligosaccharide **216**.

N-acetylneuraminic acid residues.[197] For instance, the synthesis of fucosyl GM1 analogue **221**, a representative example of versatility of this approach, is depicted in Scheme 43.[198] The equatorial C-3′ hydroxyl of the lactosyl acceptor **217** was regioselectively glycosylated over the C-4′ hydroxyl by the glycosyl donor **218** in the presence of TMSOTf to provide trisaccharide **219** in 75% yield. The 4′-hydroxyl group of compound **219** was then glycosylated with the trisaccharide glycosyl donor **220** in the presence of MeOTf to produce the hexasaccharide **221** in 70% yield. Evidently, the versatility of this approach in this particular case has been additionally enhanced by applying the convergent strategic approach.

Glycosylation of acceptor polyols has also been used for the concomitant introduction of multiple copies of the same residue,[81,85,86,89] and for generating combinatorial libraries of oligosaccharides.[199–202] In a number of cases, the regioselectivity could be

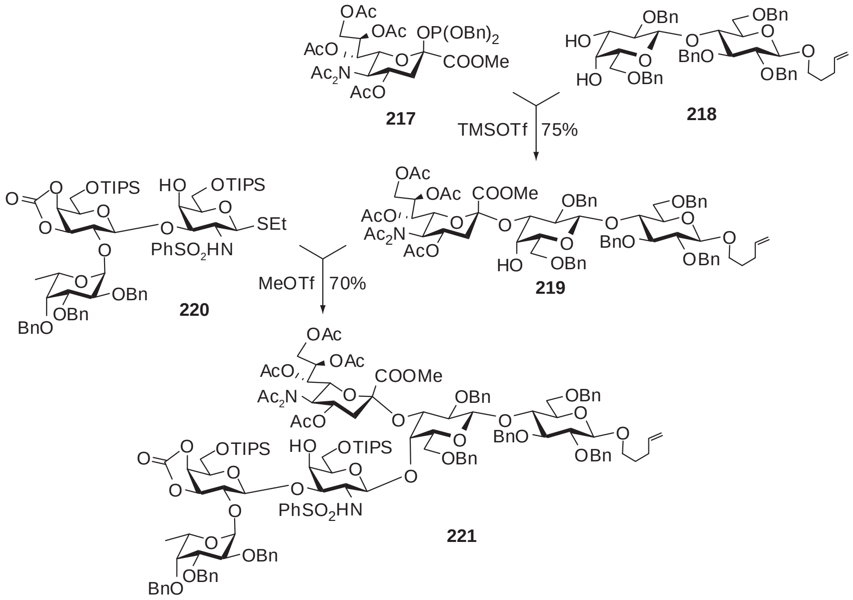

SCHEME 43. Regioselective synthesis[198] of fucosyl GM1 oligosaccharide **221**.

improved by the use of special techniques, such as regioselective (de)activation by tin-based reagents[203] or via boronic acid intermediates.[204]

Occasionally, unexpected (reverse) regioselectivity in glycosylations of polyols has been observed,[81,188,205] however, systematic studies that would explain these phenomena are yet to emerge.

2. Triphenylmethyl Reactivity

Kochetkov demonstrated that the reactivity of hydroxyl groups protected as triphenylmethyl (trityl) ethers is reversed in comparison to that of free alcohols.[206,207] Thus, it was shown that the secondary trityl can be regioselectively glycosylated in the presence of its primary counterpart. If the glycosyl donor used in excess, both positions are glycosylated.[76] This approach is especially useful for the synthesis of 4,6-branched oligosaccharides when the use of a 4,6-diol was less practical, as the bulky sugar unit at C-6 would further decrease the reactivity of 4-OH, if introduced at the earlier stage.

For a relevant example, see the synthesis of **228** shown in Scheme 44.[119] Glycosyl acceptor **223** was regioselectively glycosylated at C-4 by the glycosyl donor **223** in

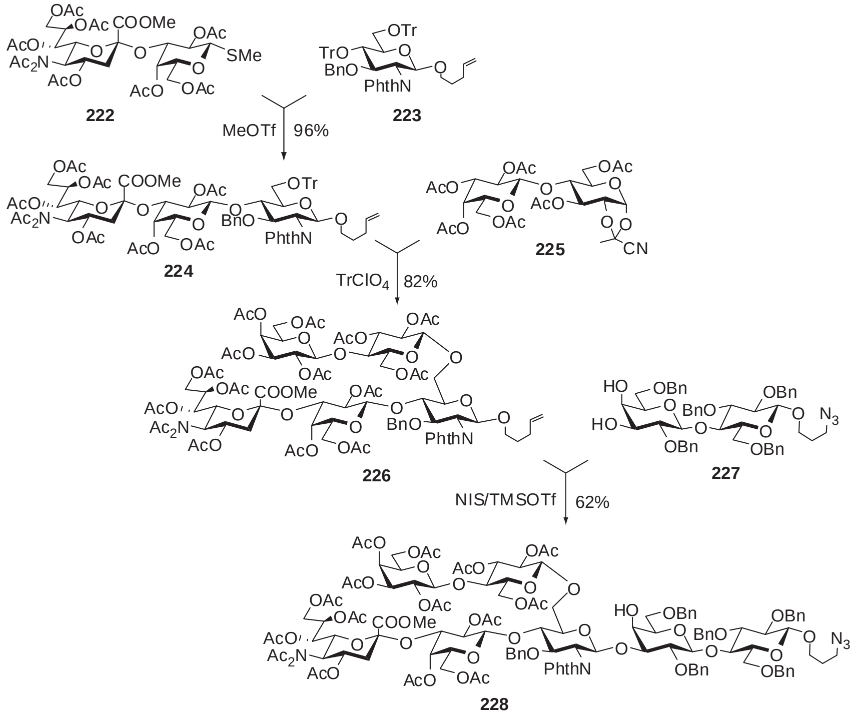

SCHEME 44. Inverse regioselectivity of the ditritylated acceptors in the synthesis[119] of Group B type III pneumococcal oligosaccharide **228**.

the presence of MeOTf to produce trisaccharide **224** in 96% yield. The primary trityl group in the trisaccharide **224** was subsequently glycosylated with disaccharide donor **225** in the presence of $TrClO_4$ to provide the pentasaccharide **226** in 82% yield. This pentasaccharide was then used as a glycosyl donor for the regioselective glycosylation of the lactose acceptor **227**, providing the target heptasaccharide **228** in 62% yield. In addition to the two regioselective glycosylation steps, this synthesis features selective activation and convergent assembly strategies.

3. Bidirectional Approaches

In a series of publications, Boons developed a bidirectional strategy for oligosaccharide synthesis. As highlighted in Scheme 45, the key building block bearing a leaving group and a deactivated hydroxyl group can first react as a glycosyl donor

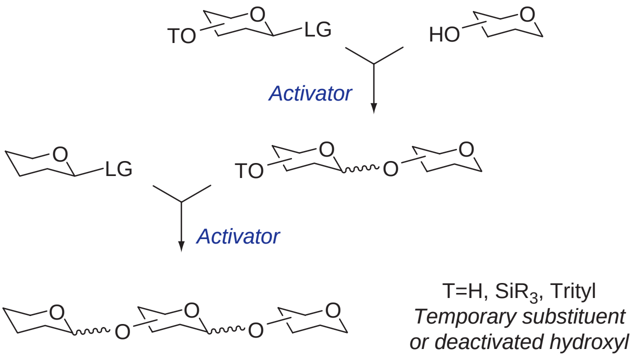

SCHEME 45. Bidirectional approach.

with a reactive glycosyl acceptor. Next, the same unit acts as the glycosyl acceptor that is glycosylated directly at the deactivated hydroxyl group. Hydroxyl deactivation can be achieved by employing electron-withdrawing protecting groups at surrounding positions.[208] Alternatively, either the silyl or trityl group can be used as the temporary masking functionality, which is then either glycosylated directly or removed during the next glycosylation step.

An example of this strategy is the synthesis of the Galili pentasaccharide **233** involved in tissue rejection in xenotransplantation, as shown in Scheme 46.[209] The key building block **229** bears both a leaving group and a hydroxyl group that would under certain reaction conditions allow for its use as either a glycosyl donor or glycosyl acceptor. In the synthesis described, compound **229** is glycosidated with the reactive glycosyl acceptor **230** by the addition of NIS/TMSOTf at −40 °C to provide trisaccharide **231** in 77% yield. At this stage it should be noted that the poorly nucleophilic hydroxyl groups in **229**, and in turn in **231**, remain unreactive. However at the elevated temperature (NIS/TMSOTf, 0 °C), compound **231** could be glycosylated at the deactivated position with the lactosyl donor **232** to provide pentasaccharide **233** in 61% yield. The use of convergent assembly allowed the authors to efficiently introduce the challenging 1,2-*cis* glycosidic linkage by pre-synthesizing the building block **232**, using the armed–disarmed approach.

Since the protecting-group dependence was an apparent limitation for this concept, the use of such temporary protecting groups (T, Scheme 45) as silyl.[111,210] or trityl,[211] has become a logical extension for this technique. It was anticipated that, under the initial mild reaction conditions (step 1) the temporary substituent would simply acts as a protecting group, while at the second step it can be glycosylated directly. A relevant

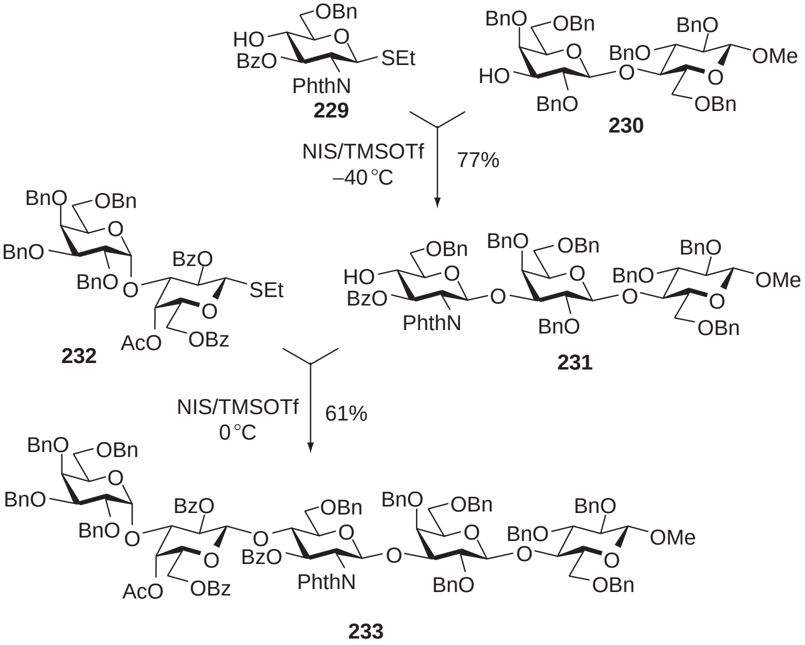

SCHEME 46. Bidirectional strategy for the synthesis[209] of Galili pentasaccharide **233**.

example is depicted in Scheme 47,[211] according to which the key building block **232** was glycosidated with glycosyl acceptor **235** by the addition of NIS/TfOH to provide disaccharide **236** in 62% yield. The latter was then concomitantly deprotected and glycosylated with thioglycoside donor **237** by the addition of NIS and a stoichiometric amount of TMSOTf, providing trisaccharide **238** in 70% yield. The use of the glycosyl donor/acceptor building on the solid support is another useful way to ‘‘deactivate’’ the hydroxyl group.[212] Apparently the polymer-supported glycosyl acceptor would be significantly less reactive in comparison to the solution-based acceptor.

VI. NOVEL TECHNOLOGIES FOR THE RAPID AND HIGH-THROUGHPUT OLIGOSACCHARIDE SYNTHESIS

Excellent innovations already surveyed here have allowed scientists to synthesize complex oligosaccharides and glycoconjugates that were practically inaccessible for decades. Nevertheless, these syntheses are still very far from simple: their successful

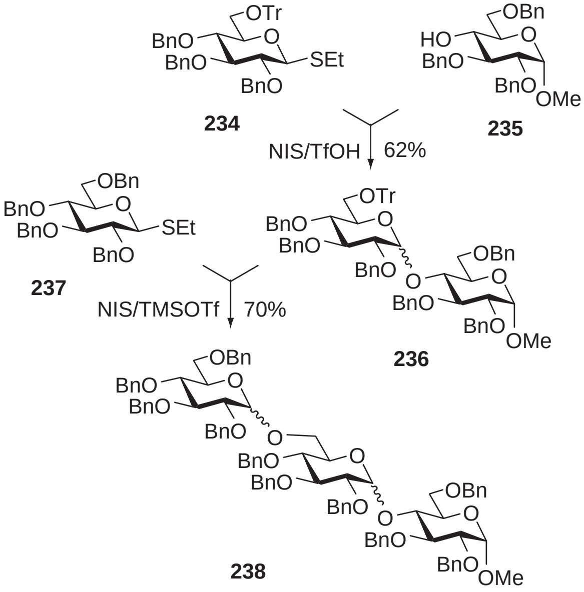

SCHEME 47. Bidirectional strategy with tritylated thioglycosides.[211]

accomplishment requires significant resources, keeping these targets accessible only to an elite circle of glycoscientists. Moreover, it has become apparent that only selected sequences can be accessed by these novel techniques. Furthermore, each target still requires careful selection of methods, conditions, and strategies.

These notable gaps have stimulated additional scientific efforts that have recently resulted in the development of a new pool of methods for the stereoselective synthesis of challenging glycosidic linkages, and strategies for expeditious oligosaccharide synthesis. Programmable synthesis, one-pot strategies including preactivation-based sequential couplings, polymer-supported and automated synthesis, as well as fluorous tag-assisted glycosylations in a microreactor are just a few examples of recent significant breakthroughs that are surveyed in this section.

1. One-Pot Strategies

One-pot techniques combining two or more (chemo)selective glycosylation steps have been developed. One-pot strategies offer the shortest pathway to oligosaccharides, as the sequential glycosylation reactions are performed in a single flask (pot) and do not require isolation and purification of the intermediates. Many variations of the one-pot strategy have been developed,[38] however, all of these protocols are based on four major concepts (Scheme 48) or combinations thereof. Approach A is based on selective activation of one leaving group over another. Since this is the leaving group-based concept, flexibility needs to be exercised with the protecting groups. Unfortunately, the number of leaving groups suitable for multi-step, sequential selective activation is still limited to too few examples. Approach B relies on the chemoselectivity principle, according to which the reactivity difference between the glycosyl donor and the glycosyl acceptor is achieved by varying the electronic properties of protecting groups in one or in both of the reaction components.

Approach C is independent of the building-block reactivity, since the leaving group of the glycosyl donor is first converted into a highly reactive species (preactivation), and then the acceptor is added. Although this approach involves a number of additional steps, as the glycosylation is virtually a two-step reaction, it offers more flexibility with the leaving and/or protecting groups. Approach D, is performed in the pure one-pot fashion with all reaction components present from the very beginning. It requires fine tuning of all reaction components, according to which the most reactive leaving-group reacts with the most reactive hydroxyl group.

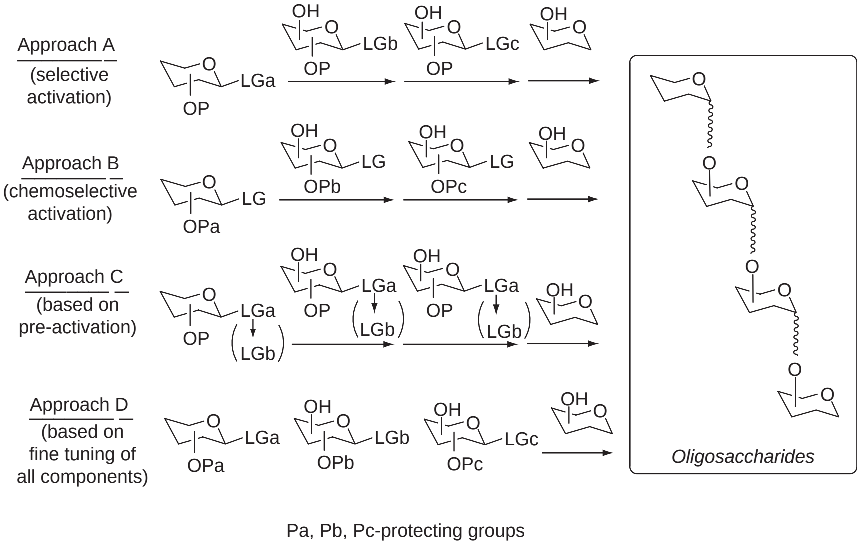
Approach A
(selective activation)
Approach B
(chemoselective activation)
Approach C
(based on pre-activation)
Approach D
(based on fine tuning of all components)
OH
O
OP
OPa
OPb
OPc
LGa
LGb
LGc
LG
Oligosaccharides
Pa, Pb, Pc-protecting groups

SCHEME 48. Major concepts for one-pot oligosaccharide assembly.

Subsequent reaction takes place between the most reactive LG and the hydroxyl group remaining after the first step has been completed. These concepts are illustrated by the relevant examples that follow.

Included are two examples of the two- and three-step sequential oligosaccharide assembly to illustrate Approach A. The first synthesis makes use of trichloroacetimidate **239**, which is selectively activated over the thioglycoside acceptor **240** with TMSOTf (Scheme 49). The SPh moiety of the resulting tetrasaccharide is then activated over the added glycosyl acceptor **241** by addition of NIS and TfOH to provide hexasaccharide **242** in 50% yield over two steps.[100] This approach combines advantages of the selective activation, convergent block strategy, and one-pot synthesis.

Another example involves an efficient synthesis of a linear tetrasaccharide derivative **247** in 73% yield over three sequential glycosylation steps (Scheme 50).[106] This was achieved by the stepwise activation of the SBox glycoside **243** over the *S*-ethyl glycoside **244** by addition of AgOTf. The ethylthio group of the resulting disaccharide intermediate is then activated over the added STaz glycoside **245** by the addition of NIS and catalytic TfOH. Finally, the STaz moiety of the trisaccharide intermediate is allowed to react with freshly added glycosyl acceptor **246**. This is achieved by addition of AgOTf; as a result, the tetrasaccharide **247** was obtained in 73% yield over three steps.

Approach B in its conventional mode requires a set of building blocks having the same type of leaving group, the reactivity of which is differentiated by the protecting-group pattern. Progress in this area has been possible through the development of armed–disarmed strategy by Fraser-Reid and the consequent programmable oligosaccharide strategies developed by Ley's and Wong's groups.[8,9,173,213] A relevant

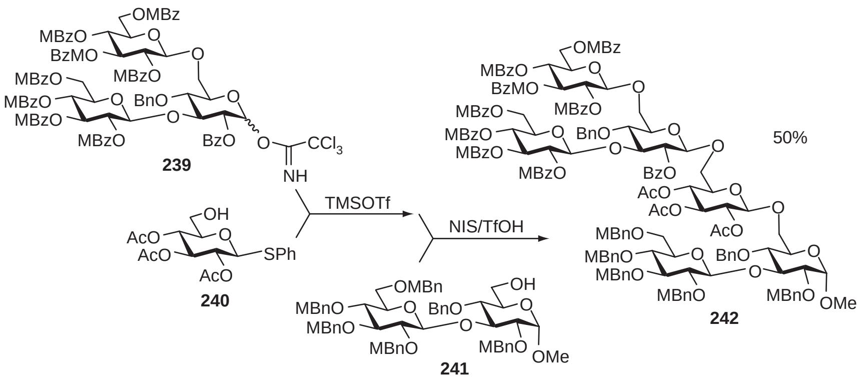

SCHEME 49. Two-step one-pot synthesis of hexasaccharide **242** by selective activation.[100]

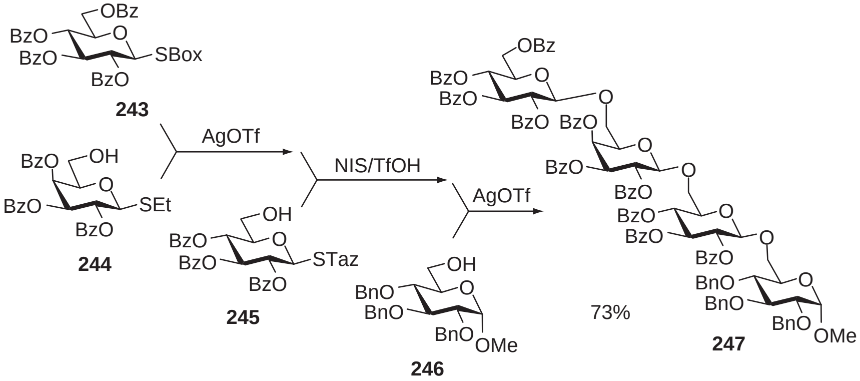
243
244
245
246
247
AgOTf
NIS/TfOH
AgOTf
73%
SBox
SEt
STaz
OMe

SCHEME 50. One-pot synthesis of tetrasaccharide **247** by the three-step sequential selective activation.[106]

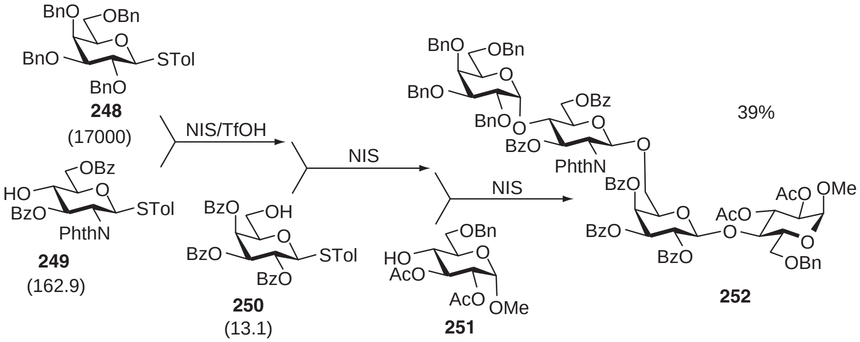
248
(17000)
249
(162.9)
250
(13.1)
251
252
NIS/TfOH
NIS
NIS
39%
STol
PhthN
OMe

The value in parentheses indicates relative reactivity of the building block

SCHEME 51. Synthesis of tetrasaccharide **252** via programmable one-pot synthesis.[9]

example is shown in Scheme 51 (synthesis of **252**),[9] which follows a programmable approach based on a predictive computer program Optimer, discussed in Section IV.2. Also in this case, the selection of building blocks **248**, **249**, and **250** was based on their RRVs, which were found to be 17,000, 162.8, and 13.1, respectively. Indeed, glycosyl donor **248** was efficiently activated over glycosyl acceptor **249** in the presence of NIS and TfOH. The resulting disaccharide intermediate then reacted with the freshly added glycosyl acceptor **250** and NIS. The trisaccharide intermediate was then glycosidated with added acceptor **251** to provide tetrasaccharide **252** in 39% yield overall. Generally, the reactivity difference between similarly protected sugars of different series has also to be taken into consideration. For example, the reactivity ratio between perbenzylated tolyl thioglycosides of the 6-deoxy-L-*galacto*, D-*galacto*, and D-*gluco* series was found to be 27.1/6.4/1 respectively.[9] Further exploration of this approach by Wong's group has resulted in a well-rounded and extremely useful technology for one-pot oligosaccharide synthesis.[10,15,214–218]

A relevant example illustrating Approach C is shown in Scheme 52 (synthesis of tetrasaccharide **257**).[18] Glycosyl donor **253** was cooled to −60 °C and the promoter system AgOTf and *p*-toluenesulfenyl chloride was added. After 5 min, glycosyl acceptor **254** was added and the reaction mixture was warmed to room temperature (rt) for 15 min to generate a disaccharide intermediate. The mixture was then cooled to −60 °C and another portion of the promoter was added. After 5 min, glycosyl acceptor **255** was added, and the reaction mixture was warmed to rt. Upon formation of the trisaccharide intermediate, the preactivation–glycosylation sequence was repeated once again with the glycosyl acceptor **256** to produce tetrasaccharide **257** in 55% overall yield in only 2 h.

Approach D can be illustrated by Kahne's synthesis depicted in Scheme 53.[111] The strategy takes advantage of the difference in reactivities of phenyl sulfoxide donors **258** and **259**, as well as glycosyl acceptors **259** (masked as the TMS ether)

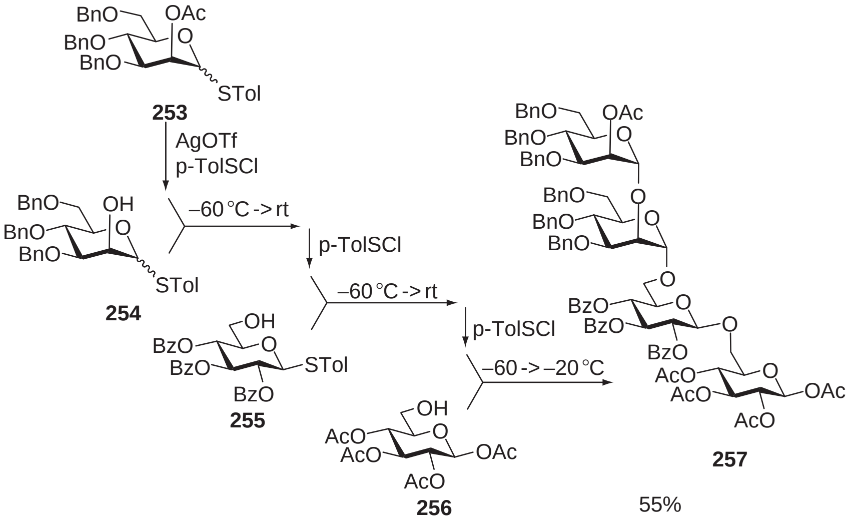
BnO
OAc
O
BnO
BnO
STol
253
AgOTf
p-TolSCl
BnO
OH
O
BnO
BnO
STol
254
−60 °C -> rt
p-TolSCl
−60 °C -> rt
OH
O
BzO
BzO
STol
BzO
255
p-TolSCl
−60 -> −20 °C
OH
O
AcO
AcO
OAc
AcO
256
BnO
OAc
O
BnO
BnO
BnO
O
O
BnO
BnO
O
O
BzO
BzO
O
BzO
O
AcO
AcO
OAc
AcO
257
55%

SCHEME 52. One-pot synthesis via *in situ* preactivation.[18]

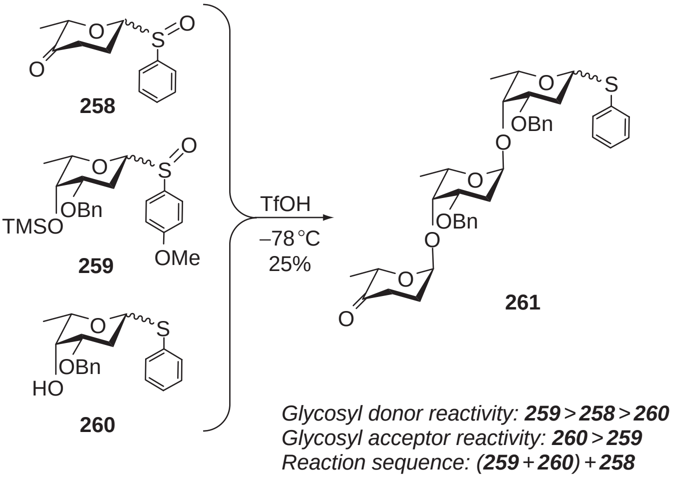

Glycosyl donor reactivity: ***259* > *258* > *260***
Glycosyl acceptor reactivity: ***260* > *259***
*Reaction sequence: (**259* + *260**)* + ***258***

SCHEME 53. One-pot synthesis of Ciclamycin 0 trisaccharide **261** by fine tuning of all reaction components.[111]

and **260**. Since the building block **259** can act as both glycosyl donor and glycosyl acceptor, this synthesis can serve as an illustrative example for the bidirectional strategy already discussed. In this instance, all three building blocks were mixed, the reaction mixture was cooled to −78 °C, and the activator (TfOH) was added. The less-reactive glycosyl donor **258** then slowly reacted with the TMS-protected hydroxyl group of the disaccharide intermediate to provide trisaccharide **261** in 25% yield. Another example of approach D was discussed previously (see Section IV.5).

A number of one-pot syntheses that rely on mixed conventions,[191,219] for instance selective and chemoselective activations, as well as acceptor-[187,220] and bidirectional strategy-based approaches[221,222] have also been developed. These techniques offer further advantages for the synthesis of longer or branched oligosaccharide sequences.

2. Polymer-Supported, Solid-Phase, and Automated Synthesis

Further breakthroughs in the area of synthetic chemistry emerged with the development of organic synthesis on solid phase.[223–226] As a consequence, the past decade has witnessed dramatic improvements in the area of solid phase-supported oligosaccharide synthesis.[202,227–230] Polymer-supported synthesis is a very attractive techniques as it allows for rapid synthesis of oligosaccharide sequences without the necessity of purifying (and characterizing) the intermediates. Another important advantage of oligosaccharide synthesis on solid-phase support is the ease of excess reagent removal (by filtration).

Among multiple methods and approaches that have been developed to date,[23,26,36,231–245] two main strategies for solid-phase saccharide synthesis that differ in the type of the attachment can be identified (Scheme 54).[246] In strategy A, the glycosyl acceptor unit is bound to the solid support, most commonly at the anomeric position, however, attachments to other hydroxyl groups have also been used. In this case, the excess of the glycosyl donor and promoter are present in the solution phase. In the approach B, the glycosyl donor unit, linked to the solid support via a suitable hydroxyl group, reacts with the solution-phase acceptor.

The reiteration for the repetitive glycosylation is usually performed in the conventional linear fashion and involves removal of the temporary protecting groups or anomeric substituents. Nevertheless, a number of improvements, allowing more-expeditious oligosaccharide assembly, are also available, including convergent synthesis,[247] two-step,[142] selective,[248,249] and orthogonal activations,[5,152,248] as well as the bidirectional approach,[14,212]

An elegant synthesis that combined advantages of the polymer-supported technology and convergent building-block strategy was applied to the synthesis of a hexasaccharide **274** (Scheme 55).[247] The key feature of this assembly is the use of an anomerically connected spacer-linker that can be removed under unique reaction conditions. This approach also allows flexible manipulation with the remaining

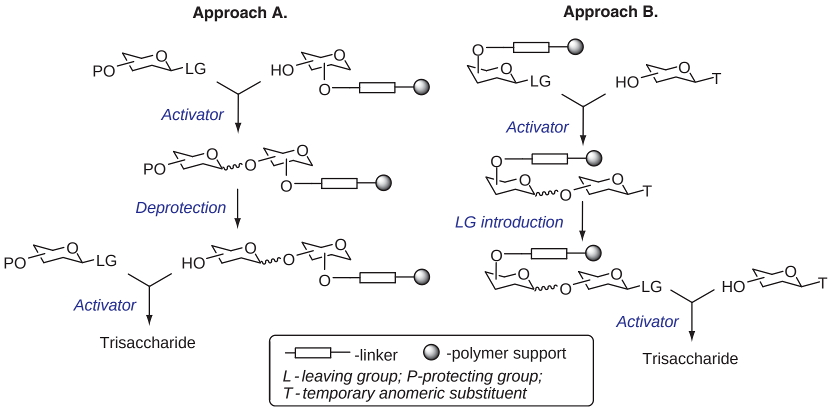

SCHEME 54. Major concepts for the polymer-supported/solid-phase oligosaccharide synthesis: glycosyl acceptor bound approach (A) and glycosyl donor bound approach (B).

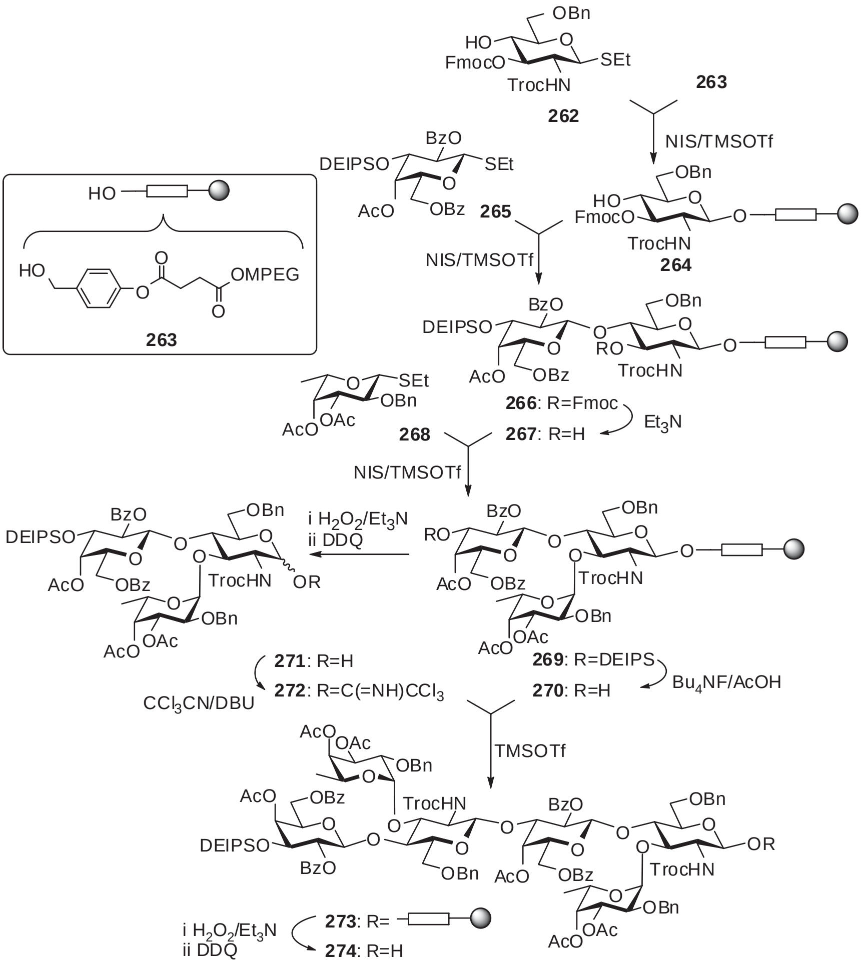
262
263
264
265
266: R=Fmoc
267: R=H
268
269: R=DEIPS
270: R=H
271: R=H
272: R=C(=NH)CCl3
273
274: R=H
NIS/TMSOTf
Et3N
Bu4NF/AcOH
CCl3CN/DBU
TMSOTf
i H2O2/Et3N
ii DDQ

SCHEME 55. Solid-phase synthesis of dimeric Lewis X hexasaccharide **274**.[247]

protecting groups. For example, the fluorenylmethoxycarbonyl (Fmoc) and diethylisopropylsilyl (DEIPS) groups could be removed without affecting the linker. Thus, the scheme involved the use of thioglycoside **262** as glycosyl donor for the anomeric attachment to the resin **263**. This was accomplished in the presence of NIS/TMSOTf and resulted in the formation of the polymer-bound acceptor **264**. The latter was then glycosylated with the solution-based glycosyl donor **265**, and the resulting polymer-bound disaccharide **266** was converted into a glycosyl acceptor **267** by removing the Fmoc protection with triethylamine. The resulting disaccharide acceptor **267** was then glycosylated with fucose donor **268** in the presence of NIS and TMSOTf to give the trisaccharide **269**. The yield of all steps up to the trisaccharide **273** was determined to be 35% (based of loading of the polymer). The trisaccharide common pool was then split into two portions: the first was treated with Bu_4NF to afford the polymer-bound glycosyl acceptor **270**. The second portion was cleaved from the polymer support with DDQ, and the resulting hemiacetal **271** was then converted into trichloroacetimidate donor **272**. The solution-phase donor **272** was then glycosidated with the polymer-bound acceptor **270** to generate the hexasaccharide **273**. Upon cleavage from resin, hexasaccharide **274** was obtained in 20% overall yield (based on loading).

Danishefsky reported the solid-phase synthesis of oligosaccharide **281**, based on the glycosyl donor-bound approach (Scheme 56).[142] First, glycal **275** was attached to a divinylbenzene–styrene copolymer resin via a silyl linkage that was formed in the presence of diisopropylethylamine (DIPEA) to provide polymer-bound **276**. The glucal was then epoxidized with DMDO and the resulting 1,2-anhydro sugar was glycosidated with **275** in the presence of $ZnCl_2$ to provide the attached disaccharide intermediate **277**. The latter was then epoxidized and glycosidated with **275** in the presence of $ZnCl_2$ to provide the attached trisaccharide **278**. Once again, epoxidation with DMDO was executed and the resulting 1,2-anhydride was glycosidated with disaccharide acceptor **279** in the presence of $ZnCl_2$ to provide the attached pentasaccharide **280**. The latter was then cleaved from the resin by the treatment with Bu_4NF/-AcOH to provide the pentasaccharide **281** in 58% overall yield.

Schmidt reported the synthesis of a branched N-glycan hexasaccharide **290** using the acceptor-bound strategy (Scheme 57).[250] The glucosamine derivative **282** was attached glycosidically to the Merrifield resin support in the presence of TMSOTf, and the Fmoc protective group was removed by treatment with Et_3N, providing glycosyl acceptor **283**. Glycosyl donor **284** was then reacted with the polymer-bound acceptor **283** in the presence of TMSOTf to give a trisaccharide, which was then treated with Et_3N to remove the Fmoc group. The resulting glycosyl acceptor **285** was glycosylated with mannosyl donor **286** in the presence of TMSOTf to produce the tetrasaccharide, which was treated with Et_3N to remove the Fmoc group. The tetrasaccharide acceptor **287** was glycosylated with glycosyl donor **288** to provide the pentasaccharide, which was debenzoylated by treatment with NaOMe in CH_2Cl_2/MeOH. The resulting glycosyl acceptor **289** was then glycosylated with glycosyl donor **286** in the presence of TMSOTf to give the requisite hexasaccharide. Upon cleavage from the resin, achieved by treatment with NaOMe/MeOH, and subsequent acetylation with Ac_2O/pyridine the hexasaccharide **290** was obtained in 19% overall yield.

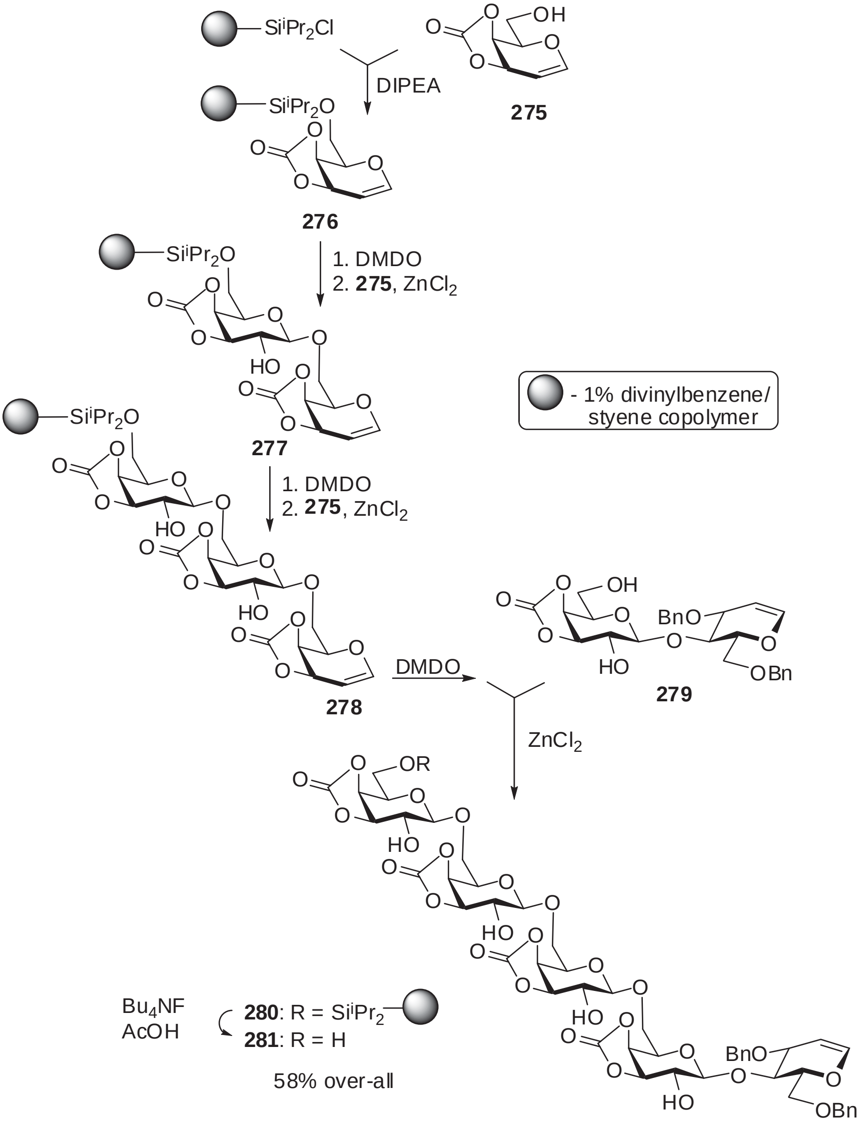

SiiPr2Cl
OH
275
DIPEA
SiiPr2O
276
1. DMDO
2. 275, ZnCl2
HO
277
- 1% divinylbenzene/ styene copolymer
1. DMDO
2. 275, ZnCl2
278
DMDO
OH
BnO
HO
OBn
279
ZnCl2
OR
Bu4NF
AcOH
280: R = SiiPr2
281: R = H
58% over-all

SCHEME 56. Donor-bound approach for the synthesis[142] of oligosaccharide **281**.

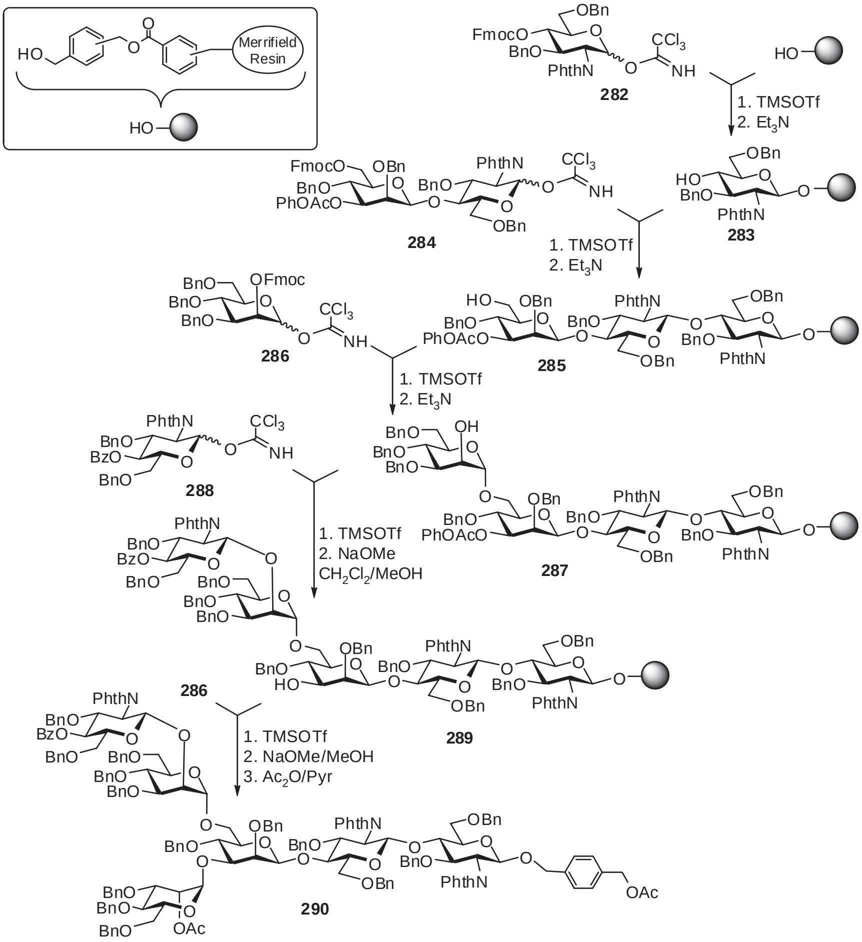
Merrifield Resin
HO
282
1. TMSOTf
2. Et$_3$N
283
284
1. TMSOTf
2. Et$_3$N
285
286
1. TMSOTf
2. Et$_3$N
287
288
1. TMSOTf
2. NaOMe
CH$_2$Cl$_2$/MeOH
289
286
1. TMSOTf
2. NaOMe/MeOH
3. Ac$_2$O/Pyr
290

SCHEME 57. Acceptor-bound approach to the synthesis[250] of oligosaccharide **290**.

To expedite and simplify oligosaccharide synthesis even further, Seeberger and coworkers developed a method for the automated synthesis of oligosaccharides.[23,251–253] Automation was accomplished by using a peptide synthesizer that had been modified to be compatible with oligosaccharide assembly using the trichloroacetimidate or phosphate glycosyl donors that normally require low temperature. Although a relatively new technique, this approach has already been applied to the synthesis of a variety of oligosaccharide sequences.

For example, the synthesis of a tetrasaccharide derivative **296**, a fragment of the GPI malarial toxin, was achieved in a highly efficient, automated fashion (Scheme 58).[254] High conversion was achieved by repeating the key reaction steps, of glycosylation and deprotection, and the use of reagents in excess. The resin **291** was glycosylated with glycosyl donor **292** (five equiv) in the presence of TMSOTf, followed by washing the resin with CH_2Cl_2. The glycosylation was repeated to maximize the conversion. The bound monosaccharide was then deacetylated with NaOMe (10 equiv) to liberate the hydroxyl group and the resin was washed successively with AcOH/MeOH/THF solution, THF, and CH_2Cl_2. The resulting polymer-bound acceptor was then glycosylated with glycosyl donor **293**, and the process repeated for glycosylations with glycosyl donors **294** and **295**. The resulting tetrasaccharide was cleaved from the resin by Grubbs' catalyst to provide the tetrasaccharide **296**.

A later example of an automated solid-phase synthesis is the synthesis of Globo-H hexasaccharide **304** (Scheme 59).[255] This synthesis is particularly significant because of the fact that the introduction of 1,2-*cis*-linked glycosidic residues is not yet routinely available in polymer-supported reactions in general, and in automated

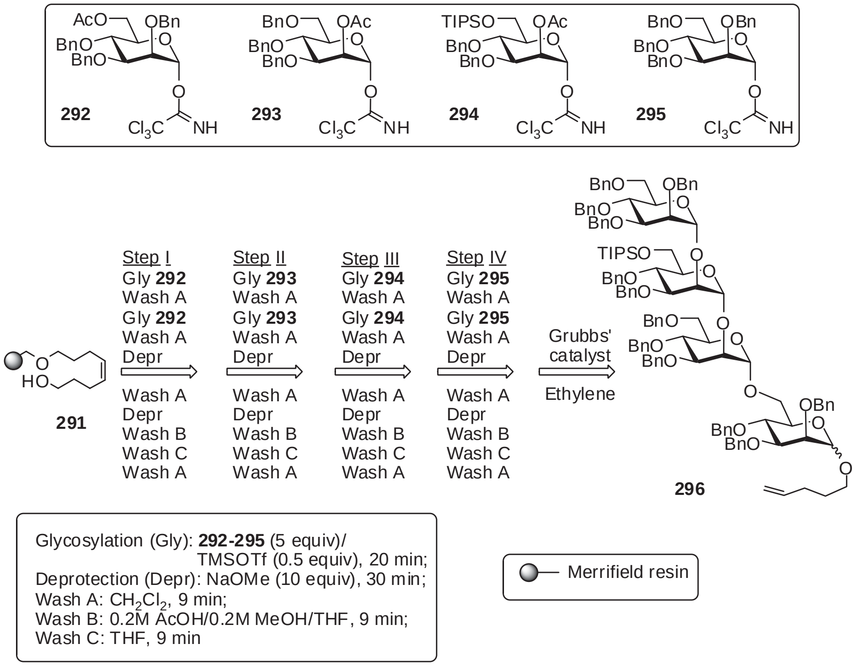
292
293
294
295
291
296
Step I
Gly 292
Wash A
Gly 292
Wash A
Depr
Wash A
Depr
Wash B
Wash C
Wash A
Step II
Gly 293
Step III
Gly 294
Step IV
Gly 295
Grubbs' catalyst
Ethylene
Glycosylation (Gly): 292-295 (5 equiv)/ TMSOTf (0.5 equiv), 20 min;
Deprotection (Depr): NaOMe (10 equiv), 30 min;
Wash A: CH2Cl2, 9 min;
Wash B: 0.2M AcOH/0.2M MeOH/THF, 9 min;
Wash C: THF, 9 min
Merrifield resin

SCHEME 58. Automated synthesis[254] of a tetrasaccharide fragment **296** of GPI malarial toxin.

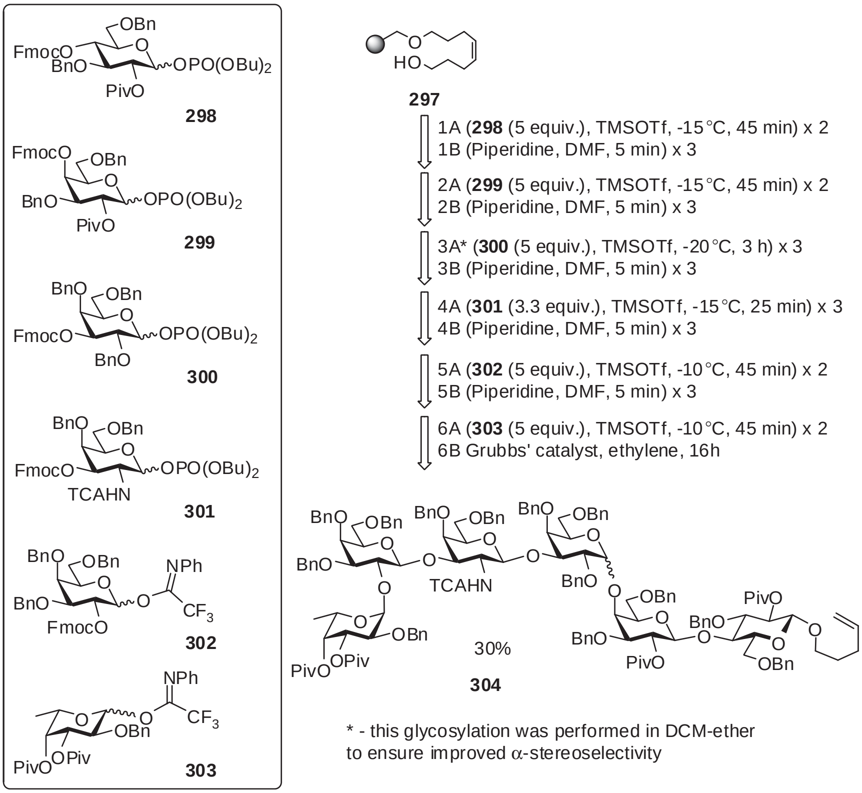
298
299
300
301
302
303
297
1A (298 (5 equiv.), TMSOTf, -15 °C, 45 min) x 2
1B (Piperidine, DMF, 5 min) x 3
2A (299 (5 equiv.), TMSOTf, -15 °C, 45 min) x 2
2B (Piperidine, DMF, 5 min) x 3
3A* (300 (5 equiv.), TMSOTf, -20 °C, 3 h) x 3
3B (Piperidine, DMF, 5 min) x 3
4A (301 (3.3 equiv.), TMSOTf, -15 °C, 25 min) x 3
4B (Piperidine, DMF, 5 min) x 3
5A (302 (5 equiv.), TMSOTf, -10 °C, 45 min) x 2
5B (Piperidine, DMF, 5 min) x 3
6A (303 (5 equiv.), TMSOTf, -10 °C, 45 min) x 2
6B Grubbs' catalyst, ethylene, 16h
30%
304

* - this glycosylation was performed in DCM-ether
to ensure improved α-stereoselectivity

SCHEME 59. Automated synthesis[255] of tumor-associated antigen Globo-H hexasaccharide **304**.

syntheses in particular. Glycosyl donor **298** was bound to the resin **297** via glycosylation using TMSOTf (repeated once) as the promoter, followed by deprotection of the Fmoc substituent with piperidine (repeated twice) to provide polymer-bound acceptor. Subsequent application of glycosyl donors **299–303**, followed by removal from the resin by cross-metathesis completed of the synthesis of oligosaccharide **304** in 30% overall yield.

3. Fluorous Tag-Supported and Microreactor Synthesis

During the long history of oligosaccharide synthesis, numerous improvements have been incorporated. Among these, fluorous protecting groups (groups incorporating a long perfluorinated alkyl chain) allow the simple separation of fluorinated species (glycosyl acceptor) from non-fluorinated (glycosyl donor) by simple partitioning between perfluorohexanes and methanol (or toluene). For a representative example, refer to the synthesis[256] of a linear oligosaccharide **315** shown in Scheme 60. Triol **305** was protected at the O-2,O-3, and O-4 positions with fluorous protecting groups, using DCC/DMAP mediated coupling with the fluorous acid **306**, and the resulting ‘‘tagged’’ compound was detritylated with camphorsulfonic acid/lithium chloride (CSA/LiCl) to provide glycosyl acceptor **307**. The latter was glycosylated with glycosyl donor **308** in the presence of TMSOTf in $EtOC_4F_9$–diethyl ether to provide disaccharide **309**. Desilylation of disaccharide **309** with HF–pyridine led to

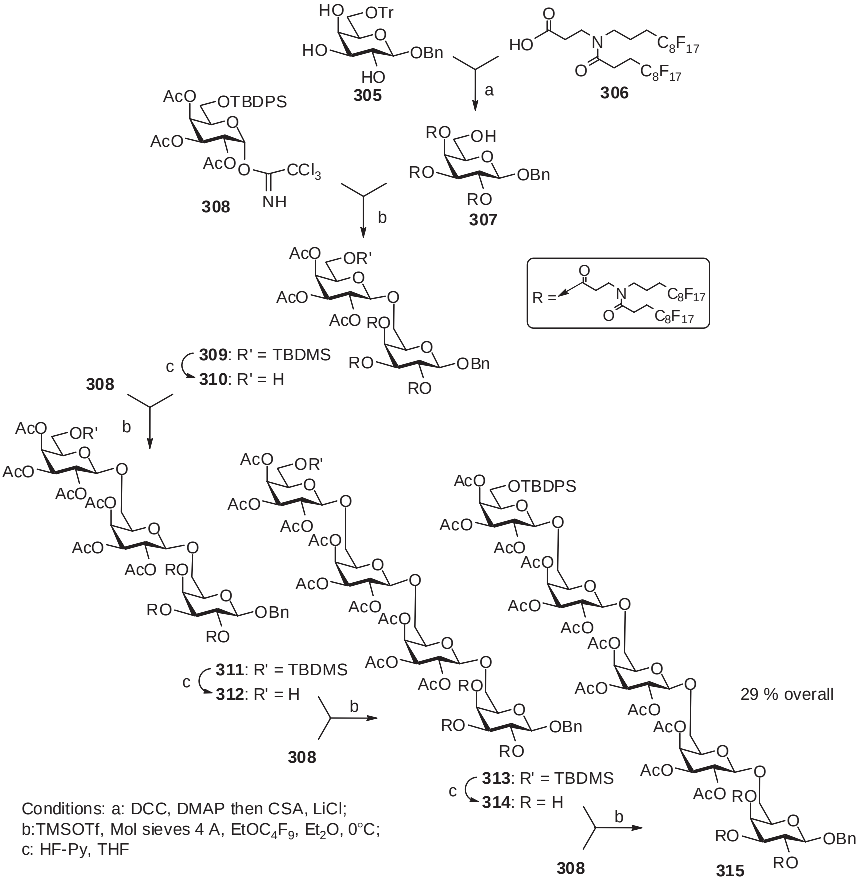
305
306
a
307
308
b
309: R' = TBDMS
310: R' = H
c
R =
311: R' = TBDMS
312: R' = H
313: R' = TBDMS
314: R = H
315
29 % overall
AcO
RO
OBn
OTr
OTBDPS
OR'
CCl3
NH
C8F17

Conditions: a: DCC, DMAP then CSA, LiCl;
b:TMSOTf, Mol sieves 4 A, $EtOC_4F_9$, Et_2O, 0°C;
c: HF-Py, THF

SCHEME 60. Fluorous tag-assisted synthesis[256] of a linear oligosaccharide **315**.

glycosyl acceptor **310**, which was then glycosylated with glycosyl donor **308** to afford trisaccharide **311**. The sequence was then reiterated until the desired pentasaccharide **315** had been assembled, with a 29% yield overall.

The chemistry of solution-based microreactors, developed in the late 1990s, has now been applied to carbohydrate chemistry. Seeberger utilized a five-port silicon microfluidic microreactor to investigate whether such a complex reaction as glycosylation can be performed in a microreactor.[257] The benefits of using a microreactor include: safety, a much greater control of reaction temperature, the capability of integration of analytical techniques, applicability to automation, ease of scale up (by simply increasing the number of reactors), and the ability to readily optimize and study/optimize reactions by varying the flow rate and amounts of reagent in the process. The drawbacks include: possible longer times if a low flow-rate is required, along with lack of compatibility with solids.

Recently, the microreactor setup was utilized for the synthesis of a homotetramer **322** (Scheme 61).[258] Glycosyl donor **316** was first glycosidated to a fluorous linker **317** in the presence of TMSOTf. This was followed by the removal of the Fmoc group with piperidine and TBAF to afford fluorous glycosyl acceptor **318**. Tetrabutylammonium fluoride proved necessary for removal of the 6-O-TMS by-products. The fluorous acceptor **318** was then glycosylated with glycosyl donor **316** and the deprotection–glycosylation sequence was repeated until the desired tetrasaccharide **321** has been assembled. The tetrasaccharide was then cleaved from the fluorous support by treatment with Grubbs' second-generation catalyst to provide tetrasaccharide **322**. The reaction times for the glycosylations were 20 s for the formation of the disaccharide, and 60 s each for the tri- and tetra-saccharides. The yields for the reactions after purification were 97, 90, and 95% for the di-, tri-, and tetra-saccharides, respectively.

A promising technique for the tagged oligosaccharide synthesis that makes use of an ionic-liquid support has recently emerged.[259] As with the polymer-supported and fluorous tag-supported syntheses, ionic liquid-supported assembly expedites oligosaccharide synthesis by eliminating the need for chromatographic purification of the intermediates.

VII. ENZYMATIC APPROACH

The need for increasingly efficient methods for organic synthesis has stimulated the development of enzymatic approaches.[260–262] These techniques help in solving various challenges of carbohydrate chemistry in general[34,263] and the synthesis

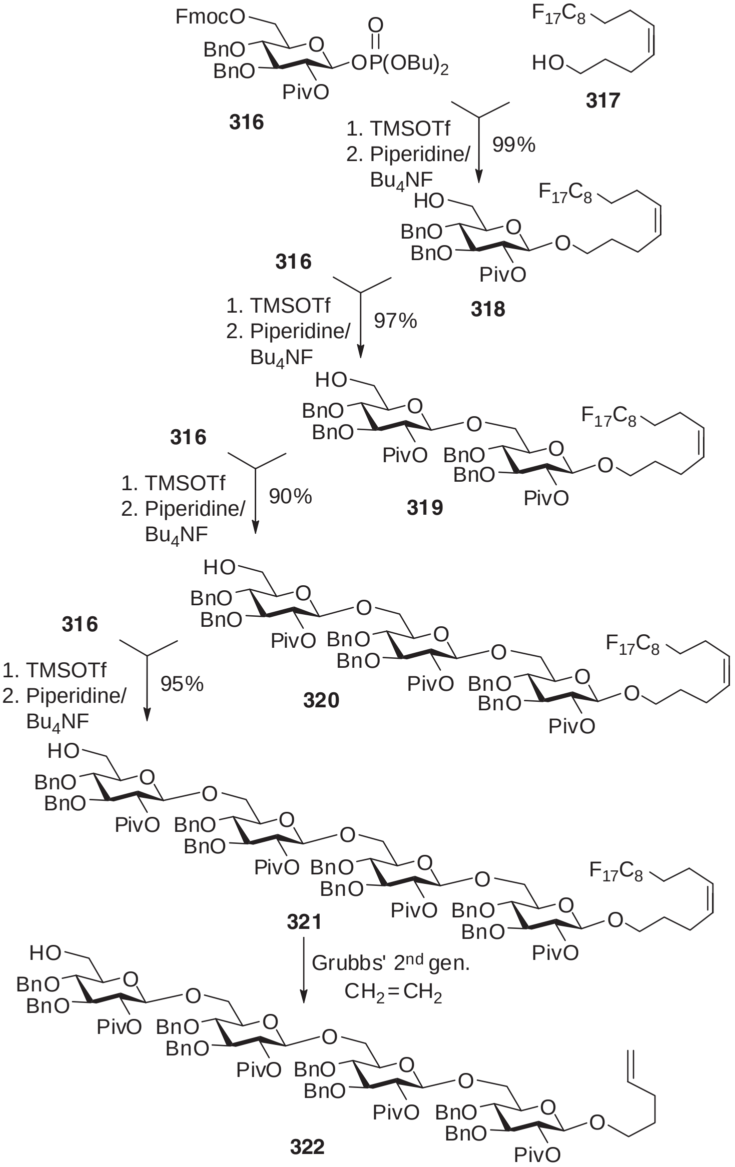
FmocO
BnO
BnO
O
PivO
OP(OBu)2
316
F17C8
HO
317
1. TMSOTf
2. Piperidine/
Bu4NF
99%
HO
318
316
97%
319
316
90%
320
316
95%
321
Grubbs' 2nd gen.
CH2=CH2
322

SCHEME 61. Fluorous tag-assisted synthesis of a tetrasaccharide **322** in a microreactor.[258]

of oligosaccharides in particular.[264,265] Enzymatic approaches are often used to overcome the difficulties associated with chemical glycosylations, and the related multi-step protecting-group manipulations, especially when the introduction of ‘‘difficult’’ glycosidic linkages is required. The enzymatic reactions offer an important advantage for ‘‘green’’ chemists because these reactions can often be performed in the absence of organic solvents. Two fundamentally different approaches for enzymatic oligosaccharide synthesis are outlined here: the use of glycosyltransferases and the application of glycosyl hydrolases. The drawbacks of using enzymatic synthesis include: lack of availability of a wide choice of enzymes, the high cost of some enzymes (especially transferases), as well as low reaction yields and the occasional lack of specificity (especially with hydrolases).

1. Oligosaccharide Synthesis with Glycosyltransferases

Glycosyltransferases are essential enzymes for oligosaccharide biosynthesis. They are classified as enzymes of the Leloir and those of the non-Leloir pathway.[266–269] The glycosyltransferases of the *Leloir pathway* are involved in the biosynthesis of most glycoconjugates and oligosaccharides in mammalians and utilize sugar nucleotide mono- or diphosphates as glycosyl donors. Several glycosyltransferases have been used for oligosaccharide synthesis, however thus far only few of them are commercially available. These enzymes transfer the sugar moiety of activated sugar nucleotides such uridine 5′-(α-D-galactopyranosyl diphosphate) (UDP-Gal, Fig. 2) and its D-glucose analogue (UDP-Gly), the guanosine L-fucose

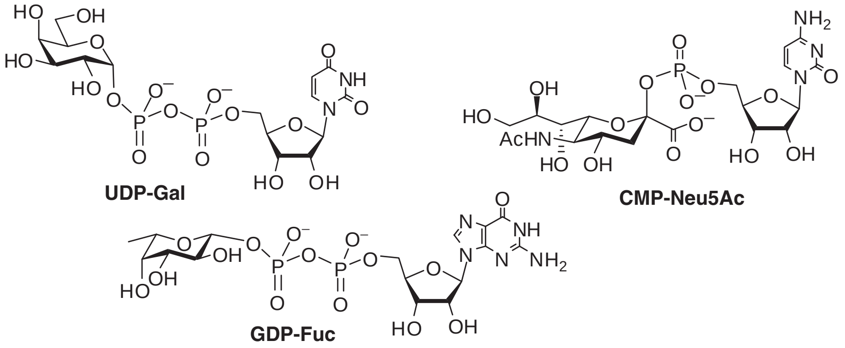

FIG. 2. Common nucleotide donors for glycosyltransferases of the Leloir pathway.

and D-mannose analogues (GDP-Fuc and GDP-Man), and cytidine 5′-(neuraminyl phosphate) (CMP-Neu5Ac) to a specific hydroxyl group of the glycosyl acceptor. These enzymes are highly substrate-specific and, therefore, the ‘‘one enzyme–one linkage’’ concept is widely accepted. Nevertheless, some minor modifications of acceptor or donor are typically tolerated, widening therefore the applicability of a particular enzyme.[270–272]

Depending on the structure of the nucleotide donor, there are two main catalytic mechanisms for glycosyltransferases of the Leloir pathway: inversion and retention of the anomeric configuration. Retention of the anomeric configuration corresponds to a two-step mechanism involving first the formation of a glycosyl–enzyme intermediate and the release of the nucleotide (di)phosphate, followed by attack by the glycosyl acceptor (Scheme 62). Conversely, inversion of the anomeric configuration most probably follows a single displacement mechanism wherein the acceptor affects a nucleophilic attack at C-1 of the glycosyl donor.

Sugar nucleotides have been obtained by both chemical and enzymatic approaches, [273] however, a very attractive approach to enzymatic synthesis of oligosaccharides involves the *in situ* formation and/or regeneration of sugar nucleotides.[274] For example, the synthesis of the GM3 trisaccharide **325** was accomplished with the use of a three-enzyme system via *in situ* generation of CMP-Neu5Ac from *N*-acetylmannosamine (**323**), followed by coupling with the lactose acceptor **324** (Scheme 63).[275] The sialyltransferase from *Pasteurella multocida* (tPm0188Ph)

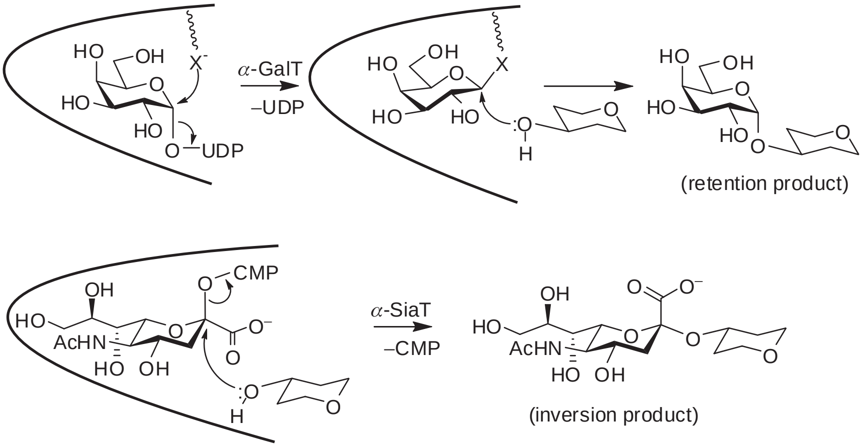

SCHEME 62. Retention and inversion pathways for glycosyltransferase-mediated glycosylations.

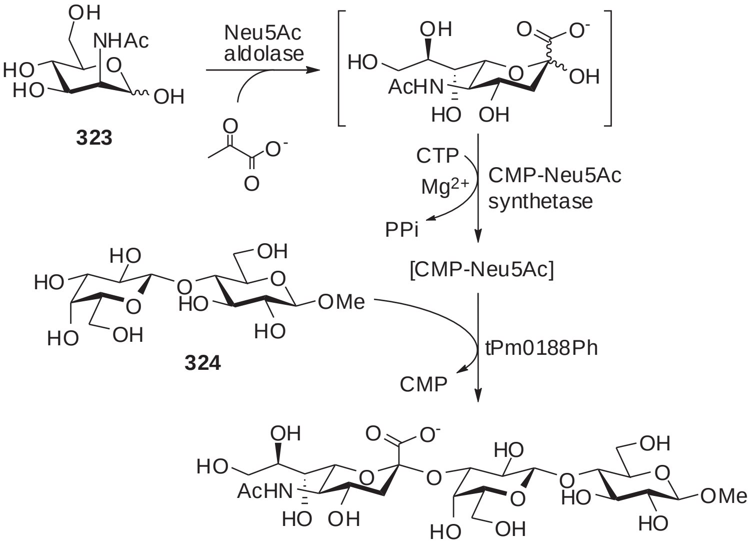

Scheme 63. Enzymatic one-pot synthesis of GM3 oligosaccharide **325**.[275]

proved to be very efficient and allowed trisaccharide **325** to be obtained in 91% yield. In addition, it was shown to be applicable to a broad range of substrates in tolerating significant modifications of both donor and acceptor components.

Multiple current studies have demonstrated that microbial glycosyltransferases can serve as alternative enzymes, with the advantage of ready expression in active form without the necessity for the complicated gene manipulation required for mammalian enzymes. For example, Wang and co-workers discovered that the sequence of enzyme reactions to synthesize blood-group antigens in bacteria is essentially the same as that in humans.[276] This discovery was applied to the enzymatic synthesis of blood-group B antigen **329** using cloned, over-expressed, and purified bacterial glycosyltransferases (Scheme 64). Starting with the glycosyl acceptor **326**, galactosylation was performed with the use of β-1,3-galactosyltransferase (WbnJ) to afford the disaccharide **327** in 85% yield. The latter, in turn, was fucosylated with α-1,2-fucosyltransferase (WbnK) to afford trisaccharide **328** in 75% yield. The sequence was completed by galactosylation in the presence of α-1,3-galactosyltransferase (WbnI) to afford blood-group B antigen tetrasaccharide **329** in 93% yield.

A variety of linear oligo- and polysaccharides can be also prepared using glycosyltransferases of the *non-Leloir pathway*, which utilize sugar α-phosphates as

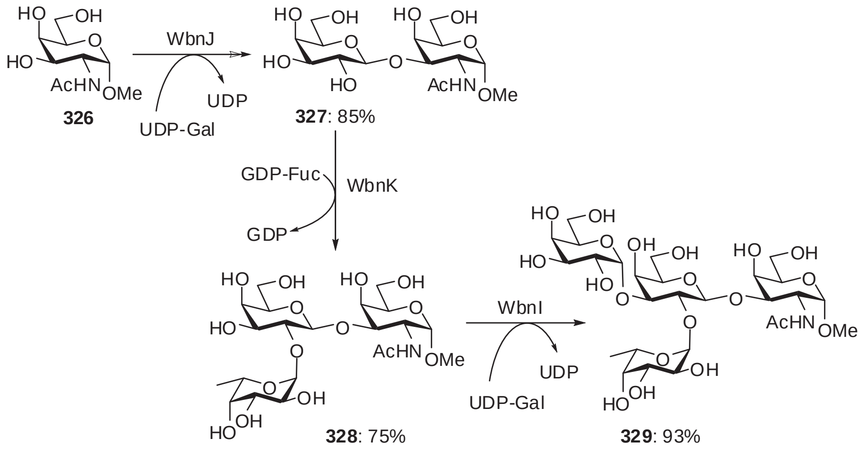

SCHEME 64. Stepwise enzymatic synthesis[276] of blood-group B antigen **329**.

glycosyl donors.[264,266] Another group of non-Leloir glycosyltransferases, cyclodextrin glucanotransferases, catalyze the synthesis of cyclodextrins. These enzymes are typically characterized by broad acceptor specificity.[277]

2. Oligosaccharide Synthesis with Glycosidases (Hydrolases)

In the natural environment, these enzymes hydrolyze glycosidic bonds and therefore are responsible for degradation of oligosaccharides. However, the reverse hydrolytic activity of hydrolases can also be exploited for the glycosidic bond-formation process.[278,279] Glycosyl hydrolases are much more readily available than glycosyltransferases, but also are typically less regioselective, and the transformation yields are lower. By analogy with glycosyltransferases, there are two main catalytic mechanisms for hydrolases: one leading to inversion of the anomeric configuration and the other leading to retention.[264,280] The easiest way to employ this approach is to perform the glycosylation under thermodynamically controlled conditions, where reverse hydrolysis is achieved at equilibrium (Scheme 65A). In spite of considerable progress made in this area, the major limitations of this approach are the low isolated yields, which rarely exceed 10–20%.[281] A significantly improved outcome (yields are typically ranging from 20 to 40%) can be achieved under kinetically controlled glycosylation conditions. In this case, activated glycosyl donors are employed, such

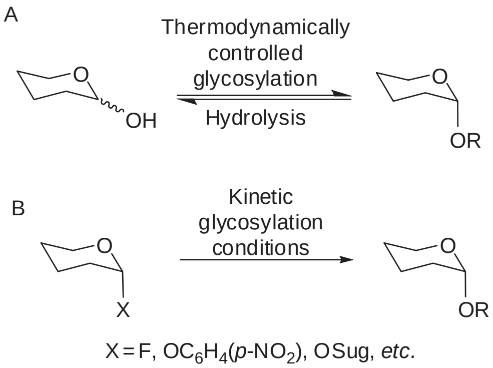
A
Thermodynamically controlled glycosylation
Hydrolysis
OH
OR
B
Kinetic glycosylation conditions
X
OR
X = F, OC6H4(p-NO2), OSug, etc.

SCHEME 65. Common catalytic mechanisms of glycosidases.

as glycosyl fluorides, aryl glycosides, disaccharides, oxazolines, and so on (Scheme 65B). Kinetically controlled glycosylation employing glycosidases (often called ‘‘transglycosylation’’ reactions) have been employed for the synthesis of a variety of oligosaccharides.[279]

A major drawback of the hydrolase-catalyzed enzymatic approach in general is the ‘‘relaxed’’ and often unpredictable regioselectivity, which occasionally can be improved by varying the reaction conditions, as by the use of organic co-solvents, by acceptor modification, and others.[282–284] The discovery and application of other, more-selective enzymes is another efficient approach to achieve improved regioselectivity.[278,285] For example, application of glycosynthase, a synthetic enzyme derived from a retaining glycosidase, allowed irreversible glycosidation of glycosyl fluoride donor **330** with the dixyloside acceptor **331** (Scheme 66).[286] The enzyme modification was achieved by mutation of the catalytic nucleophile into a glycine moiety. Application of the glycosynthase derived from the β-1,4-xylanase of *Cellulomonas fimi* resulted in a very efficient and high-yielding synthesis of xylans. The (1→4)-linked xylooligosaccharides **332**, ranging from tetra- to dodecasaccharides, were obtained regio- and stereoselectively in excess of 60% combined yield.

VIII. OUTLOOK

It is critical to make complex carbohydrates more accessible to the general chemical, biochemical, and industrial audience to keep pace with the exploding area of glycobiology. This can be only achieved by the development of methods

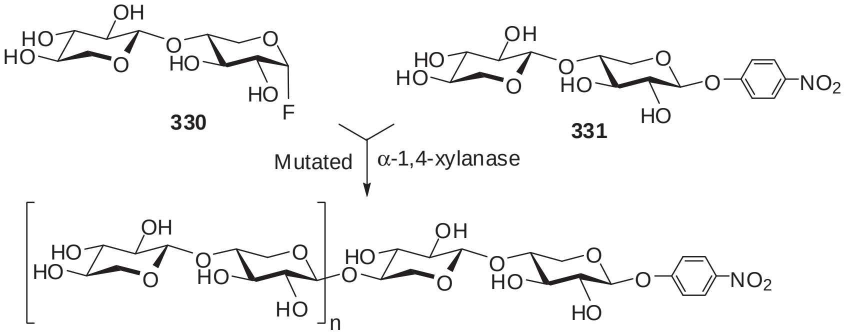

330

331

332: n = 1, 30%
n = 2, 19%
n = 3, 7%
n = 4, 4%
n = 5, 1%

SCHEME 66. Synthesis of xylans **332** using an engineered xylanase.[286]

and strategies for efficient oligosaccharide synthesis that would be applicable for both laboratory and industrial preparation. A number of excellent strategies that offer a reasonably efficient route to oligosaccharide assembly have already emerged. Important discoveries surveyed in this chapter have already allowed scientists to synthesize complex oligosaccharides and glycoconjugates for structural, biological, and medical studies. Nevertheless, carbohydrates of even moderate complexity still present a considerable challenge, even to experts. No expeditious strategy developed to date can offer an easy and reliable access to all full range of compounds of interest. Some strategies offer a very efficient approach to certain sequences, but in general each target still requires careful selection of methods, conditions, and strategies.

The development of efficient and general methods for the expeditious synthesis of complex carbohydrates will undoubtedly remain an important and active arena for scientific endeavors during the twenty-first century. In the coming years, glycoscientists are expected to have developed simple, efficient, and flexible approaches to oligosaccharide assembly that will complement existing methodologies and bring our ability to obtain complex oligosaccharides up to a significantly higher level. The recent innovations surveyed herein make contemporary glycoscientists well positioned to undertake further studies. Future developments may be expected to incorporate existing methodologies, and combinations thereof, while blending in new concepts and technologies.

REFERENCES

1. K. C. Nicolaou and H. Ueno, Oligosaccharide synthesis from glycosyl fluorides and sulfides, in S. Hanessian, (Ed.), *Preparative Carbohydrate Chemistry,* Marcel Dekker, Inc., New York, 1997, pp. 313–338.
2. B. Fraser-Reid, Z. Wu, U. E. Udodong, and H. Ottosson, Armed/disarmed effects in glycosyl donors: rationalization and sidetracking, *J. Org. Chem.*, 55 (1990) 6068–6070.
3. L. J. Williams, R. M. Garbaccio, and S. J. Danishefsky, Iterative assembly of glycals and glycal derivatives: The synthesis of glycosylated natural products and complex oligosaccharides, in B. Ernst, G. W. Hart, and P. Sinay, (Eds.), *Carbohydrates in Chemistry and Biology*, Vol. 1, Wiley-VCH, Weinheim, 2000, pp. 61–92.
4. O. Kanie, Y. Ito, and T. Ogawa, Orthogonal glycosylation strategy in oligosaccharide synthesis, *J. Am. Chem. Soc.*, 116 (1994) 12073–12074.
5. Y. Ito, O. Kanie, and T. Ogawa, Orthogonal glycosylation strategy for rapid assembly of oligosaccharides on a polymer support, *Angew Chem. Int. Ed.*, 35 (1996) 2510–2512.
6. R. Roy, F. O. Andersson, and M. Letellier, ''Active'' and ''latent'' thioglycosyl donors in oligosaccharide synthesis. Application to the synthesis of α-sialosides, *Tetrahedron Lett.*, 33 (1992) 6053–6056.
7. G.-J. Boons and S. Isles, Vinyl glycosides in oligosaccharide synthesis. Part 1: A new latent-active glycosylation strategy, *Tetrahedron Lett.*, 35 (1994) 3593–3596.
8. N. L. Douglas, S. V. Ley, U. Lucking, and S. L. Warriner, Tuning glycoside reactivity: New tool for efficient oligosaccharides synthesis, *J. Chem. Soc., Perkin Trans.*, 1 (1998) 51–65.
9. Z. Zhang, I. R. Ollmann, X. S. Ye, R. Wischnat, T. Baasov, and C.-H. Wong, Programmable one-pot oligosaccharide synthesis, *J. Am. Chem. Soc.*, 121 (1999) 734–753.
10. X. S. Ye and C.-H. Wong, Anomeric reactivity-based one-pot oligosaccharide synthesis: A rapid route to oligosaccharide libraries, *J. Org. Chem.*, 65 (2000) 2410–2431.
11. L. G. Green and S. V. Ley, Protecting groups: Effects on reactivity, glycosylation specificity and coupling efficiency, in B. Ernst, G. W. Hart, and P. Sinaÿ, (Eds.), *Carbohydrates in Chemistry and Biology*, Vol. 1, Wiley-VCH, Weinheim, 2000, pp. 427–448.
12. M. T. Bilodeau, T. K. Park, S. Hu, J. T. Randolph, S. J. Danishefsky, P. O. Livingston, and S. Zhang, Total synthesis of a human breast tumor associated antigen, *J. Am. Chem. Soc.*, 117 (1995) 7840–7841.
13. J. Lassaletta and R. R. Schmidt, Glycosyl imidates. Part 75. Synthesis of the hexasaccharide moiety of globo H (human breast cancer) antigen, *Liebigs Ann.*, (1996) 1417–1423.
14. T. Zhu and G.-J. Boons, A two-directional and highly convergent approach for the synthesis of the tumor-associated antigen Globo-H, *Angew. Chem., Int. Ed. Engl.*, 38 (1999) 3495–3497.
15. F. Burkhart, A. Zhang, S. Wacowich-Sgarbi, and C.-H. Wong, Synthesis of the globo H hexasaccharide using the programmable reactivity-based one-pot strategy, *Angew. Chem. Int. Ed.*, 40 (2001) 1274–1277.
16. F. Bosse, L. A. Marcaurelle, and P. H. Seeberger, Linear synthesis of the tumor-associated carbohydrate antigens Globo-H, SSEA-3, and Gb3, *J. Org. Chem.*, 67 (2002) 6659–6670.
17. L. Huang, Z. Wang, and X. Huang, One-pot oligosaccharide synthesis: Reactivity tuning by post-synthetic modification of aglycone, *Chem. Commun.*, (2004) 1960–1961.
18. X. Huang, L. Huang, H. Wang, and X. S. Ye, Iterative one-pot synthesis of oligosaccharides, *Angew Chem., Int. Ed.*, 43 (2004) 5221–5224.
19. Z. Wang, L. Zhou, K. Ei-Boubbou, X. S. Ye, and X. Huang, Multi-component one-pot synthesis of the tumor-associated carbohydrate antigen Globo-H based on preactivation of thioglycosyl donors, *J. Org. Chem.*, 72 (2007) 6409–6420.

20. J. D. C. Codée, R. E. J. N. Litjens, L. J. van den Bos, H. S. Overkleeft, and G. A. van der Marel, Thioglycosides in sequential glycosylation strategies, *Chem. Soc. Rev.*, 34 (2005) 769–782.
21. D. Crich, Chemistry of glycosyl triflates: Synthesis of β-mannopyranosides (reprinted from Glycochemistry: Principles, Synthesis, and Applications, pp. 53–75, 2001), *J. Carbohydr. Chem.*, 21 (2002) 667–690.
22. D. Gin, Dehydrative glycosylation with 1-hydroxy donors (reprinted from Glycochemistry: Principles, Synthesis, and Applications, pp. 33–52, 2001), *J. Carbohydr. Chem.*, 21 (2002) 645–665.
23. O. J. Plante, E. R. Palmacci, and P. H. Seeberger, Automated solid-phase synthesis of oligosaccharides, *Science*, 291 (2001) 1523–1527.
24. P. H. Seeberger, Automated carbohydrate synthesis to drive chemical glycomics, *Chem. Commun.*, (2003) 115–1121.
25. T. L. Lowary, D-Arabinofuranosides from mycobacteria: Synthesis and conformation (reprinted from Glycochemistry: Principles, Synthesis, and Applications, pp. 133–162, 2001), *J. Carbohydr. Chem.*, 21 (2002) 691–722.
26. S. N. Lam and J. Gervay-Hague, Solution- and solid-phase oligosaccharide synthesis using glucosyl iodides: A comparative study, *Carbohydr. Res.*, 337 (2002) 1953–1965.
27. M. J. Hadd and J. Gervay, Glycosyl iodides are highly efficient donors under neutral conditions, *Carbohydr. Res.*, 320 (1999) 61–69.
28. C. C. Wang, J. C. Lee, S. Y. Luo, H. F. Fan, C. L. Pai, W. C. Yang, L. D. Lu, and S.-C. Hung, Synthesis of biologically potent $\alpha 1 \rightarrow 2$-linked disaccharide derivatives via regioselective one-pot protection-glycosylation, *Angew. Chem. Int. Ed.*, 41 (2002) 2360–2362.
29. C. C. Wang, J. C. Lee, S. Y. Luo, S. S. Kulkarni, Y. W. Huang, C. C. Lee, K. L. Chang, and S.-C. Hung, Regioselective one-pot protection of carbohydrates, *Nature*, 446 (2007) 896–899.
30. J. H. Kim, H. Yang, J. Park, and G.-J. Boons, A general strategy for stereoselective glycosylations, *J. Am. Chem. Soc.*, 127 (2005) 12090.
31. J. H. Kim, H. Yang, and G.-J. Boons, Stereoselective glycosylation reactions with chiral auxiliaries, *Angew. Chem. Int. Ed.*, 44 (2005) 947–949.
32. G.-J. Boons, Strategies in oligosaccharide synthesis, *Tetrahedron*, 52 (1996) 1095–1121.
33. O. Kanie, Orthogonal strategy in oligosaccharide synthesis, in B. Ernst, G. W. Hart, and P. Sinaÿ, (Eds.), *Carbohydrates in Chemistry and Biology*, Vol. 1, Wiley-VCH, Weinheim, 2000, pp. 407–426.
34. K. M. Koeller and C.-H. Wong, Synthesis of complex carbohydrates and glycoconjugates: Enzyme-based and programmable one-pot strategies, *Chem. Rev.*, 100 (2000) 4465–4493.
35. B. G. Davis, Recent developments in oligosaccharide synthesis, *J. Chem. Soc., Perkin Trans.*, 1 (2000) 2137–2160.
36. T. Kanemitsu and O. Kanie, Recent developments in oligosaccharide synthesis: Tactics, solid-pase synthesis and library synthesis, *Comb. Chem. High Throughput Screen.*, 5 (2002) 339–360.
37. A. V. Demchenko, Strategic approach to the chemical synthesis of oligosaccharides, *Lett. Org. Chem.*, 2 (2005) 580–589.
38. Y. Wang, X. S. Ye, and L. H. Zhang, Oligosaccharide assembly by one-pot multi-step strategy, *Org. Biomol. Chem.*, 5 (2007) 2189–2200.
39. A. V. Demchenko, (Ed.), *Handbook of Chemical Glycosylation: Advances in Stereoselectivity and Therapeutic Relevance*, Wiley-VCH, Weinheim, 2008, .
40. H. Kunz and M. Schultz, Glycopeptide synthesis in solution and on the solid phase, in B. Ernst, G. W. Hart, and P. Sinay, (Eds.), *Carbohydrates in Chemistry and Biology*, Vol. 1, Wiley-VCH, Weinheim, 2000, pp. 267–304.
41. H. C. Hang and C. R. Bertozzi, Chemoselective approaches to glycoprotein assembly, *Acc. Chem. Res.*, 34 (2001) 727–736.

42. K. M. Koeller and C.-H. Wong, Glycoproteins: Synthesis and applications of biologically relevant glycopeptides, in B. Fraser-Reid, K. Tatsuta, and J. Thiem, (Eds.), *Glycoscience: Chemistry and Chemical Biology*, Vol. 3, Springer, Berlin, 2001, pp. 2305–2352.
43. B. G. Davis, Synthesis of glycoproteins, *Chem. Rev.*, 102 (2002) 579–601.
44. L. A. Marcaurelle and C. R. Bertozzi, Mini review recent advances in the chemical synthesis of mucin-like glycoproteins, *Glycobiology*, 12 (2002) 69R–77R.
45. M. R. Pratt and C. R. Bertozzi, Synthetic glycopeptides and glycoproteins as tools for biology, *Chem. Soc. Rev.*, 34 (2005) 58–68.
46. D. Kahne, C. Leimkuhler, W. Lu, and C. Walsh, Glycopeptide and lipoglycopeptide antibiotics, *Chem. Rev.*, 105 (2005) 425–448.
47. I. Tvaroška and T. Bleha, Anomeric and exo-anomeric effects in carbohydrate chemistry, *Adv. Carbohydr. Chem. Biochem.*, 47 (1989) 45–123.
48. L. Goodman, Neighboring-group participation in sugars, *Adv. Carbohydr. Chem. Biochem.*, 22 (1967) 109–175.
49. T. Nukada, A. Bérces, M. Z. Zgierski, and D. M. Whitfield, Exploring the mechanism of neighboring group assisted glycosylation reactions, *J. Am. Chem. Soc.*, 120 (1998) 13291–13295.
50. K. Toshima and K. Tatsuta, Recent progress in O-glycosylation methods and its application to natural-products synthesis, *Chem. Rev.*, 93 (1993) 1503–1531.
51. M. Nitz and D. R. Bundle, Oligosaccharides: Synthesis: Glycosyl halides in oligosaccharide synthesis, in B. Fraser-Reid, K. Tatsuta, and J. Thiem, (Eds.), *Glycoscience: Chemistry and Chemical Biology*, Vol. 2, Springer, Berlin, 2001, pp. 1497–1542.
52. K. Igarashi, The Koenigs–Knorr reaction, *Adv. Carbohydr. Chem. Biochem.*, 34 (1977) 243–283.
53. R. R. Schmidt and K. H. Jung, Trichloroacetimidates, in B. Ernst, G. W. Hart, and P. Sinaÿ, (Eds.), *Carbohydrates in Chemistry and Biology*, Vol. 1, Wiley-VCH, Weinheim, 2000, pp. 5–59.
54. T. Mukaiyama, Explorations into new reaction chemistry, *Angew. Chem. Int. Ed.*, 43 (2004) 5590–5614.
55. P. J. Garegg, Thioglycosides as glycosyl donors in oligosaccharide synthesis, *Adv. Carbohydr. Chem. Biochem.*, 52 (1997) 179–205.
56. S. Oscarson, Thioglycosides, in B. Ernst, G. W. Hart, and P. Sinaÿ, (Eds.), *Carbohydrates in Chemistry and Biology*, Vol. 1, Wiley-VCH, Weinheim, 2000, pp. 93–116.
57. B. Fraser-Reid and R. Madsen, Oligosaccharide synthesis by *n*-pentenyl glycosides,, in S. Hanessian, (Ed.), *Preparative Carbohydrate Chemistry,* Marcel Dekker, Inc., New York, 1997, p. 339.
58. B. Fraser-Reid, G. Anilkumar, M. B. Gilbert, S. Joshi, and R. Kraehmer, Glycosylation methods: Use of *n*-pentenyl glycosides, in B. Ernst, G. W. Hart, and P. Sinaÿ, (Eds.), *Carbohydrates in Chemistry and Biology*, Vol. 1, Wiley-VCH, Weinheim, 2000, pp. 135–154.
59. J. Lu and B. Fraser-Reid, Preparation, properties, and applications of *n*-pentenyl arabinofuranosyl donors, *Org. Lett.*, 6 (2004) 3051–3054.
60. L. J. van den Bos, J. Dinkelaar, H. S. Overkleeft, and G. A. van der Marel, Stereocontrolled synthesis of β-D-mannuronic acid esters: synthesis of an alginate trisaccharide, *J. Am. Chem. Soc.*, 128 (2006) 13066–13067.
61. S. Hanashima, B. Castagner, D. Esposito, T. Nokami, and P. H. Seeberger, Synthesis of a sialic acid α(2–3) galactose building block and Its use in a linear synthesis of sialyl Lewis X, *Org. Lett.*, 9 (2007) 1777–1779.
62. A. Ishiwata, Y. Munemura, and Y. Ito, Synergistic solvent effect in 1,2-*cis*-glycosides formation, *Tetrahedron*, 64 (2008) 92–102.
63. T. M. Slaghek, A. H. van Oijen, A. A. M. Maas, J. P. Kamerling, and J. F. G. Vliegenthart, Synthesis of structural elements of the capsular polysaccharides of *Streptococcus pneumoniae* types 6A and 6B, *Carbohydr. Res.*, 207 (1990) 237–248.

64. K. R. Love, R. B. Andrade, and P. H. Seeberger, Linear synthesis of a protected h-type II pentasaccharide using glycosyl phosphate building blocks, *J. Org. Chem.*, 66 (2001) 8165–8176.
65. S. Koto, T. Uchida, and S. Zen, Syntheses of isomaltose, isomaltotetraose, and isomaltooctaose, *Bull. Chem. Soc. Jpn.*, 46 (1973) 2520–2523.
66. H. Paulsen, Advances in selective chemical syntheses of complex oligosaccharides, *Angew. Chem. Int. Edit. Engl.*, 21 (1982) 155–173.
67. T. Ogawa, H. Yamamoto, T. Nukada, T. Kitajima, and M. Sugimoto, Synthetic approach to glycan chains of a glycoprotein and proteoglycan, *Pure Appl. Chem.*, 56 (1984) 779–795.
68. G. Gu and Y. Du, Synthesis of a pentasaccharide derivative corresponding to a triterpenoid saponin isolated from *Spergularia ramosa*, *J. Chem. Soc., Perkin Trans.*, 1 (2002) 2075–2079.
69. D. Depre, A. Düffels, L. G. Green, R. Lenz, S. V. Ley, and C.-H. Wong, Synthesis of glycans from the glycodelins: Two undeca-, two deca-, three nona-, an octa- and a heptasaccharide, *Chem. Eur. J.*, 5 (1999) 3326–3340.
70. I. Matsuo, K. Totani, A. Tatami, and Y. Ito, Comprehensive synthesis of ER related high-mannose-type sugar chains by convergent strategy, *Tetrahedron*, 62 (2006) 8262–8277.
71. R. Bommer, W. Kinzy, and R. R. Schmidt, Glycosyl imidates. 49. Synthesis of the octasaccharide moiety of the dimeric Le^x antigen, *Liebigs Ann. Chem.*, (1991) 425–433.
72. A. Sundgren, M. Lahmann, and S. Oscarson, Block synthesis of *Streptococcus pneumoniae* type 14 capsular polysaccharide structures, *J. Carbohydr. Chem.*, 24 (2005) 379–391.
73. M. Iida, A. Endo, S. Fujita, M. Numata, M. Sugimoto, S. Nunomura, and T. Ogawa, Total synthesis of glycohexa- and nonaosyl ceramide with a sialyl Le^a and sialyl dimeric Le^a sequence, *J. Carbohydr. Chem.*, 17 (1998) 647–672.
74. T. Mukaiyama, K. Ikegai, H. Jona, T. Hashihayata, and K. Takeuchi, A convergent total synthesis of the mucin related F1a antigen by one-pot sequential stereoselective glycosylation, *Chem. Lett.*, (2001) 840–841.
75. A. R. Chowdhury, A. Siriwardena, and G.-J. Boons, A highly convergent approach for the synthesis of disaccharide repeating units of peptidoglycan, *Tetrahedron Lett.*, 43 (2002) 7805–7807.
76. L. V. Backinowsky, P. I. Abronina, A. S. Shashkov, A. A. Grachev, N. K. Kochetkov, S. A. Nepogodiev, and J. F. Stoddart, An efficient approach towards the convergent synthesis of ''fully-carbohydrate'' mannodendrimers, *Chem. Eur. J.*, 8 (2002) 4412–4423.
77. V. Y. Dudkin, J. S. Miller, and S. J. Danishefsky, A concise route to the core pentasaccharide of N-linked glycoproteins, *Tetrahedron Lett.*, 44 (2003) 1791–1793.
78. J. Xue and Z. Guo, Convergent synthesis of a GPI containing an acylated inositol, *J. Am. Chem. Soc.*, 125 (2003) 16334–16339.
79. J. D. Warren, J. S. Miller, S. J. Keding, and S. J. Danishefsky, Toward fully synthetic glycoproteins by ultimately convergent routes: A solution to a long-standing problem, *J. Am. Chem. Soc.*, 126 (2004) 6576–6578.
80. X. Liu, Y. U. Kwon, and P. H. Seeberger, Convergent synthesis of a fully lipidated glycosylphosphatidylinositol anchor of *Plasmodium falciparum*, *J. Am. Chem. Soc.*, 127 (2005) 5004–5005.
81. B. Fraser-Reid, J. Lu, K. N. Jayaprakash, and J. C. Lopez, Synthesis of a 28-mer oligosaccharide core of mycobacterial lipoarabinomannan (LAM) requires only two *n*-pentenyl orthoester progenitors, *Tetrahedron Asymmetry*, 17 (2006) 2449–2463.
82. D. Crich, B. Wu, and P. Jayalath, Convergent synthesis of a β-(1→3)-mannohexaose, *J. Org. Chem.*, 72 (2007) 6806–6815.
83. M. L. Gening, Y. E. Tsvetkov, G. B. Pier, and N. E. Nifantiev, Synthesis of β-(1→6)-linked glucosamine oligosaccharides corresponding to fragments of the bacterial surface polysaccharide poly-*N*-acetylglucosamine, *Carbohydr. Res.*, 342 (2007) 567–575.
84. Y. Rao and G.-J. Boons, A highly convergent chemical synthesis of conformational epitopes of rhamnogalactan II, *Angew. Chem. Int. Ed.*, 46 (2007) 6148–6151.

85. M. Joe, Y. Bai, R. C. Nacario, and T. L. Lowary, Synthesis of the docosanasaccharide arabinan domain of mycobacterial arabinogalactan and a proposed octadecasaccharide biosynthetic precursor, *J. Am. Chem. Soc.*, 129 (2007) 9885–9901.
86. K. N. Jayaprakash, S. R. Chaudhuri, C. V. S. R. Murty, and B. Fraser-Reid, Regioselective strategies mediated by lanthanide triflates for efficient assembly of oligomannans, *J. Org. Chem.*, 72 (2007) 5534–5545.
87. H. S. Cheon, Y. Lian, and Y. Kishi, Highly stereoselective and iterative synthesis of α-(1→4)-linked polysaccharides composed of 3-*O*-methyl-D-mannose, *Org. Lett.*, 9 (2007) 3323–3326.
88. S. Manabe, K. Ishii, and Y. Ito, Synthesis of a natural oligosaccharide antibiotic active against Helicobacter pylori, *J. Org. Chem.*, 72 (2007) 6107–6115.
89. M. A. Oberli, P. Bindschadler, D. B. Werz, and P. H. Seeberger, Synthesis of a hexasaccharide repeating unit from *Bacillus anthracis* vegetative cell wall, *Org. Lett.*, 10 (2008) 905–908.
90. K. Deng, M. M. Adams, and D. Y. Gin, Synthesis and structure verification of the vaccine adjuvant QS-7-Api. Synthetic access to homogeneous *Quillaja saponaria* immunostimulants, *J. Am. Chem. Soc.*, 130 (2008) 5860–5861.
91. K. C. Nicolaou, R. E. Dolle, D. P. Papahatjis, and J. L. Randall, Practical synthesis of oligosaccharides. Partial synthesis of avermectin B1a, *J. Am. Chem. Soc.*, 106 (1984) 4189–4192.
92. J. L. Randall and K. C. Nicolaou, Preparation and reactions of glycosyl fluorides, *ACS Symp. Ser.*, 374 (1988) 13–28.
93. H. Lönn, Synthesis of a tri- and a heptasaccharide which contain α-L-fucopyranosyl groups and are part of the complex type of carbohydrate moiety of glycoproteins, *Carbohydr. Res.*, 139 (1985) 105–113.
94. H. Lönn, Synthesis of a tetra- and a nona-saccharide which contain α-L-fucopyranosyl groups and are part of the complex type of carbohydrate moiety of glycoproteins, *Carbohydr. Res.*, 139 (1985) 115–121.
95. P. J. Garegg and S. Oscarson, A synthesis of 8-methoxycarbonyloct-1-yl *O*-α-D-galactopyranosyl-(1→3)-*O*-*β*-D-galactopyranosyl-(1→4)-2-acetamido-2-deoxy-*β*-D-glucopyranoside, *Carbohydr. Res.*, 136 (1985) 207–213.
96. P. Fügedi, P. J. Garegg, H. Lonn, and T. Norberg, Thioglycosides as glycosylating agents in oligosaccharide synthesis, *Glycoconjugate J.*, 4 (1987) 97–108.
97. K. Leontein, M. Nilsson, and T. Norberg, Synthesis of the methyl and 1-octyl glycosides of the P-antigen tetrasaccharide (globotetraose), *Carbohydr. Res.*, 144 (1985) 231–240.
98. H. Paulsen, M. Heume, and H. Nurnberger, Synthese der verzwiegten Nonasaccharid-Sequenz der ‘‘bisected’’ Structur von N-Glycoproteinen, *Carbohydr. Res.*, 200 (1990) 127–166.
99. T. Ziegler, E. Eckhardt, and V. Birault, Synthetic studies toward pyruvate acetal containing saccharides. Synthesis of the carbohydrate part of the *Mycobacterium smegmatis* pentasaccharide glycolipid and fragments thereof for the preparation of neoantigens, *J. Org. Chem.*, 58 (1993) 1090–1099.
100. H. Yamada, T. Harada, and T. Takahashi, Synthesis of an elicitor-active hexaglucoside analogue by a one-pot, two-step glycosidation procedure, *J. Am. Chem. Soc.*, 116 (1994) 7919–7920.
101. S. Aoki, H. Kondo, and C.-H. Wong, Glycosyl phosphites as glycosylation reagents, *Methods Enzymol.*, 247 (1994) 193–211.
102. O. J. Plante, E. R. Palmacci, R. B. Andrade, and P. H. Seeberger, Oligosaccharide synthesis with glycosyl phosphate and dithiophosphate triesters as glycosylating agents, *J. Am. Chem. Soc.*, 123 (2001) 9545–9554.
103. A. V. Demchenko, N. N. Malysheva, and C. De Meo, S-Benzoxazolyl (SBox) glycosides as novel, versatile glycosyl donors for stereoselective 1,2-*cis* glycosylation, *Org. Lett.*, 5 (2003) 455–458.
104. A. V. Demchenko, M. N. Kamat, and C. De Meo, S-Benzoxazolyl (SBox) glycosides in oligosaccharide synthesis: novel glycosylation approach to the synthesis of *β*-D-glucosides, *β*-D-galactosides, and α-D-mannosides, *Synlett*, (2003) 1287–1290.
105. A. V. Demchenko, P. Pornsuriyasak, C. De Meo, and N. N. Malysheva, Potent, versatile, and stable: thiazolyl thioglycosides as glycosyl donors, *Angew. Chem., Int. Ed.*, 43 (2004) 3069–3072.

106. P. Pornsuriyasak and A. V. Demchenko, Glycosyl thioimidates in a highly convergent one-pot strategy for oligosaccharide synthesis, *Tetrahedron Asymmetry*, 16 (2005) 433–439.
107. N. K. Kochetkov, N. N. Malysheva, E. M. Klimov, and A. V. Demchenko, Synthesis of polysaccharides with 1,2-*cis*-glycosidic linkages by trityl-thiocyanate polycondensation-stereoregular α-(1→6)-D-glucan, *Tetrahedron Lett.*, 33 (1992) 381–384.
108. E. M. Klimov, N. N. Malysheva, A. V. Demchenko, and N. K. Kochetkov, Synthesis of 1,2-*cis*-linked regular heteropolysaccharide – rhamnoglucan, *Dokl. Akad. Nauk*, 330 (1993) 331–332.
109. J. D. C. Codée, L. J. van den Bos, R. E. J. N. Litjens, H. S. Overkleeft, J. H. van Boom, and G. A. van der Marel, Sequential one-pot glycosylations using 1-hydroxyl and 1-thiodonors, *Org. Lett.*, 5 (2003) 1947–1950.
110. J. D. C. Codée, R. E. J. N. Litjens, R. Heeten, H. S. Overkleeft, J. H. van Boom, and G. A. van der Marel, Ph_2SO/Tf_2O: A powerful promotor system in chemoselective glycosylations using thioglycosides, *Org. Lett.*, 5 (2003) 1519–1522.
111. S. Raghavan and D. Kahne, A one-step synthesis of ciclamycin trisaccharide, *J. Am. Chem. Soc.*, 115 (1993) 1580–1581.
112. L. Yan, C. M. Taylor, R. Goodnow, and D. Kahne, Glycosylation on the Merrifield resin using anomeric sulfoxides, *J. Am. Chem. Soc.*, 116 (1994) 6953–6954.
113. S. Mehta and B. M. Pinto, Phenylselenoglycosides as novel, versatile glycosyl donors. selective activation over thioglycosides, *Tetrahedron Lett.*, 32 (1991) 4435–4438.
114. S. Mehta and B. M. Pinto, Novel glycosidation methodology. The use of phenylselenoglycosides as glycosyl donors and acceptors in oligosaccharide synthesis, *J. Org. Chem.*, 58 (1993) 3269–3276.
115. H. M. Zuurmond, P. H. van der Meer, P. A. M. van der Klein, G. A. van der Marel, and J. H. van Boom, Iodonium-promoted glycosylations with phenyl selenoglycosides, *J. Carbohydr. Chem.*, 12 (1993) 1091–1103.
116. D. K. Baeschlin, A. R. Chaperon, V. Charbonneau, L. G. Green, S. V. Ley, U. Lucking, and E. Walther, Rapid assembly of oligosaccharides: Total synthesis of a glycosylphosphatidylinositol anchor of *Trypanosoma brucei*, *Angew. Chem. Int. Edit.*, 37 (1998) 3423–3428.
117. B. Fraser-Reid, U. E. Udodong, Z. F. Wu, H. Ottosson, J. R. Merritt, C. S. Rao, C. Roberts, and R. Madsen, *n*-Pentenyl glycosides in organic chemistry: A contemporary example of serendipity, *Synlett*, (1992) 927–942,and references therein.
118. A. Demchenko and G.-J. Boons, A highly convergent synthesis of a hexasaccharide derived from the oligosaccharide of group B type III *Streptococcus*, *Tetrahedron Lett.*, 38 (1997) 1629–1632.
119. A. V. Demchenko and G.-J. Boons, A highly convergent synthesis of a complex oligosaccharide derived from group B type III *Streptococcus*, *J. Org. Chem.*, 66 (2001) 2547–2554.
120. S. Hanessian, H. K. Huynh, G. V. Reddy, R. O. Duthaler, A. Katopodis, M. B. Streiff, W. Kinzy, and R. Oehrlein, Synthesis of Gal determinant epitopes, their glycomimetic variants, and trimeric clusters-relevance to tumor associated antigens and to discordant xenografts, *Tetrahedron*, 57 (2001) 3281–3290.
121. B. Lou, G. V. Reddy, H. Wang, and S. Hanessian, Glycoside and oligosaccharide synthesis with unprotected glycosyl donors based on the remote activation concept, in S. Hanessian, (Ed.), *Preparative Carbohydrate Chemistry,* Marcel Dekker, Inc., New York, 1997, p. 389.
122. B. Lou, E. Eckhardt, and S. Hanessian, Oligosaccharide synthesis by selective anomeric activation with MOP- and TOPCAT-leaving groups, in S. Hanessian, (Ed.), *Preparative Carbohydrate Chemistry,* Marcel Dekker, Inc., New York, 1997, p. 449.
123. M. Kiso and L. Anderson, Protected glycosides and disaccharides of 2-amino-2-deoxy-D-glucopyranose by ferric chloride-catalyzed coupling, *Carbohydr. Res.*, 136 (1985) 309–323.
124. P. Fügedi, P. J. Garegg, S. Oscarson, G. Rosen, and B. A. Silvanis, Glycosyl 1-piperidinecarbodithioates in the synthesis of glycosides, *Carbohydr. Res.*, 211 (1991) 157–162.

125. A. Marra, F. Gauffeny, and P. Sinaÿ, A novel class of glycosyl donors: anomeric S-xanthates of 2-azido-2-deoxy-D-galactopyranosyl derivatives, *Tetrahedron*, 47 (1991) 5149–5160.
126. H. K. Chenault and A. Castro, Glycosyl transfer by isopropenyl glycosides: Trisaccharide synthesis in one pot by selective coupling of isopropenyl and *n*-pentenyl glycopyranosides, *Tetrahedron Lett.*, 35 (1994) 9145–9148.
127. R. V. Stick, D. M. G. Tilbrook, and S. J. Williams, The selective activation of telluro- over seleno-*β*-D-glucopyranosides as glycosyl donors: A reactivity scale for various telluro, seleno and thio sugars, *Aust. J. Chem.*, 50 (1997) 237–240.
128. K. Takeuchi, T. Tamura, and T. Mukaiyama, The trityl tetrakis(pentafluorophenyl)borate catalyzed stereoselective glycosylation using new glycosyldonor, 3,4,6-tri-*O*-benzyl-2-*O*-*p*-toluoyl-*β*-D-glucopyranosyl phenylcarbonate, *Chem. Lett.*, (2000) 122–123.
129. J. Bogusiak and W. Szeja, Block synthesis of oligosaccharides. Part 1: Preparation of furanosyl-1-thiopyranosides, *Tetrahedron Lett.*, 42 (2001) 2221–2223.
130. J. D. C. Codée, B. Stubba, M. Schiattarella, H. S. Overkleeft, C. A. A. van Boeckel, J. H. van Boom, and G. A. van der Marel, A modular strategy toward the synthesis of heparin-like oligosaccharides using monomeric building blocks in a sequential glycosylation strategy, *J. Am. Chem. Soc.*, 127 (2005) 3767–3773.
131. B. A. Garcia, J. L. Poole, and D. Y. Gin, Direct glycosylations with 1-hydroxy glycosyl donors using trifluoromethanesulfonic anhydride and diphenyl sulfoxide, *J. Am. Chem. Soc.*, 119 (1997) 7597–7598.
132. D. Crich and M. Smith, 1-Benzenesulfinyl piperidine/trifluoromethanesulfonic anhydride: a potent combination of shelf-stable reagents for the low-temperature conversion of thioglycosides to glycosyl triflates and for the formation of diverse glycosidic linkages, *J. Am. Chem. Soc.*, 123 (2001) 9015–9020.
133. T. Kondo, T. Tomoo, H. Abe, M. Isobe, and T. Goto, Total synthesis of GD_3, a ganglioside, *Chem. Lett.*, (1996) 337–338.
134. T. Kondo, T. Tomoo, H. Abe, M. Isobe, and T. Goto, Simple construction of Neu5Ac(α2–8)Neu5Ac and total synthesis of ganglioside GD_3, *J. Carbohydr. Chem.*, 15 (1996) 857–878.
135. M. N. Kamat, C. De Meo, and A. V. Demchenko, *S*-Benzoxazolyl as a stable protecting moiety and a potent anomeric leaving group in oligosaccharide synthesis, *J. Org. Chem.*, 72 (2007) 6947–6955.
136. K. C. Nicolaou, T. Caulfield, H. Kataoka, and T. Kumazawa, A practical and enantioselective synthesis of glycosphingolipids and related compounds. Total synthesis of globotriaosylceramide (Gb_3), *J. Am. Chem. Soc.*, 110 (1988) 7910–7912.
137. S. Yamago, T. Yamada, O. Hara, H. Ito, Y. Mino, and J. Yoshida, A new, iterative strategy of oligosaccharide synthesis based on highly reactive *β*-bromoglycosides derived from selenoglycosides, *Org. Lett.*, 3 (2001) 3867–3870.
138. R. L. Halcomb and S. J. Danishefsky, On the direct epoxidation of glycals: Application of a reiterative strategy for the synthesis of *β*-linked oligosaccharides, *J. Am. Chem. Soc.*, 111 (1989) 6661–6666.
139. S. J. Danishefsky and M. T. Bilodeau, Glycals in organic synthesis: The evolution of comprehensive strategies for the assembly of oligosaccharides and glycoconjugates of biological consequence, *Angew. Chem. Int. Ed. Engl.*, 35 (1996) 1380–1419.
140. P. P. Deshpande, H. M. Kim, A. Zatorski, T. K. Park, G. Ragupathi, P. O. Livingston, D. Live, and S. J. Danishefsky, Strategy in oligosaccharide synthesis: An application to a concise total synthesis of the KH-1(adenocarcinoma) antigen, *J. Am. Chem. Soc.*, 120 (1998) 1600–1614.
141. R. W. Murray and R. Jeyaraman, Dioxiranes: synthesis and reactions of methyldioxiranes, *J. Org. Chem.*, 50 (1985) 2847–2853.
142. J. T. Randolph, K. F. McClure, and S. J. Danishefsky, Major simplifications in oligosaccharide syntheses arising from a solid-phase based method: An application to the synthesis of the Lewis b antigen, *J. Am. Chem. Soc.*, 117 (1995) 5712–5719.

143. J. C. Lopez, C. Uriel, A. Guillamon-Martin, S. Valverde, and A. M. Gomez, IPy_2BF_4-Mediated transformation of *n*-pentenyl glycosides to glycosyl fluorides: A new pair of semiorthogonal glycosyl donors, *Org. Lett.*, 9 (2007) 2759–2762.

144. S. Cao, F. Hernandez-Mateo, and R. Roy, Scope and applications of ''active and latent'' thioglycosyl donors. Part 4, *J. Carbohydr. Chem.*, 17 (1998) 609–631.

145. R. Rodebaugh, J. S. Debenham, B. Fraser-Reid, and J. P. Snyder, Bromination of alkenyl glycosides with copper (II) bromide and lithium bromide: synthesis, mechanism, and DFT calculations, *J. Org. Chem.*, 64 (1999) 1758–1761.

146. J. G. Allen and B. Fraser-Reid, *n*-Pentenyl glycosyl orthoesters as versatile intermediates in oligosaccharide synthesis. The proteoglycan linkage region, *J. Am. Chem. Soc.*, 121 (1999) 468–469.

147. P. G. Wang, P. Haldar, Y. Wang, and H. Hu, Simple glycosylation reaction of allyl glycosides, *J. Org. Chem.*, 72 (2007) 5870–5873.

148. K. S. Kim, J. H. Kim, Y. J. Lee, Y. J. Lee, and J. Park, 2-(Hydroxycarbonyl)benzyl glycosides: A novel type of glycosyl donors for highly efficient *β*-mannopyranosylation and oligosaccharide synthesis by latent-active glycosylation, *J. Am. Chem. Soc.*, 123 (2001) 8477–8481.

149. R. J. Hinklin and L. L. Kiessling, Glycosyl sulfonylcarbamates: New glycosyl donor with tunable reactivity, *J. Am. Chem. Soc.*, 123 (2001) 3379–3380.

150. H. Paulsen, Progress in oligosaccharide synthesis through a new orthogonal glycosylation strategy, *Angew. Chem. Int. Ed. Engl.*, 34 (1995) 1432–1434.

151. O. Kanie, Y. Ito, and T. Ogawa, Orthogonal glycosylation strategy in synthesis of extended blood group B determinant, *Tetrahedron Lett.*, 37 (1996) 4551–4554.

152. O. Kanie, I. Ohtsuka, T. Ako, S. Daikoku, Y. Kanie, and R. Kato, Orthogonal glycosylation reactions on solid phase and synthesis of a library consisting of a complete set of fucosyl galactose isomers, *Angew Chem. Int. Ed.*, 45 (2006) 3851–3854.

153. P. Pornsuriyasak and A. V. Demchenko, *S*-Thiazolinyl (STaz) glycosides as versatile building blocks for convergent selective, chemoselective, and orthogonal oligosaccharide synthesis, *Chem. Eur. J.*, 12 (2006) 6630–6646.

154. S. Kaeothip, P. Pornsuriyasak, N. P. Rath, and A. V. Demchenko, Unexpected orthogonality of the *S*-benzoxazolyl and *S*-thiazolinyl derivatives: Application to expeditious oligosaccharide assembly. *Org. Lett.*, 11 (2009) 799–802.

155. A. V. Demchenko and C. De Meo, semi-Orthogonality of *O*-pentenyl and *S*-ethyl glycosides: Application for the oligosaccharide synthesis, *Tetrahedron Lett.*, 43 (2002) 8819–8822.

156. G.-J. Boons, R. Geurtsen, and D. Holmes, Chemoselective glycosylations (Part 1): Differences in size of anomeric leaving groups can be exploited in chemoselective glycosylations, *Tetrahedron Lett.*, 36 (1995) 6325–6328.

157. R. Geurtsen, F. Cote, M. G. Hahn, and G.-J. Boons, Chemoselective glycosylation strategy for the convergent assembly of phytoalexin-elicitor active oligosaccharides and their photoreactive derivatives, *J. Org. Chem.*, 64 (1999) 7828–7835.

158. P. Pornsuriyasak, U. B. Gangadharmath, N. P. Rath, and A. V. Demchenko, A novel strategy for oligosaccharide synthesis via temporarily deactivated S-thiazolyl glycosides as glycosyl acceptors, *Org. Lett.*, 6 (2004) 4515–4518.

159. P. Pornsuriyasak, N. P. Rath, and A. V. Demchenko, 4-(Pyridin-2-yl)thiazol-2-yl thioglycosides as bidentate ligands for oligosaccharide synthesis via temporary deactivation, *Chem. Commun.*, (2008) 5633–5635.

160. M. Lahmann and S. Oscarson, One-pot oligosaccharide synthesis exploiting solvent reactivity effects, *Org. Lett.*, 2 (2000) 3881–3882.

161. D. R. Mootoo, P. Konradsson, U. E. Udodong, and B. Fraser-Reid, ''Armed'' and ''disarmed'' *n*-pentenyl glycosides in saccharide couplings leading to oligosaccharides, *J. Am. Chem. Soc.*, 110 (1988) 5583–5584.

162. P. Konradsson, D. R. Mootoo, R. E. McDevitt, and B. Fraser-Reid, Iodonium ion generated in situ from *N*-iodosuccinimide and trifluoromethanesulphonic acid promotes direct linkage of ''disarmed'' pent-4-enyl glycosides, *J. Chem. Soc., Chem. Commun.*, (1990) 270–272.
163. A. J. Ratcliffe, P. Konradsson, and B. Fraser-Reid, *n*-Pentenyl glycosides as efficient synthons for promoter-mediated assembly of N-α-linked glycoproteins, *J. Am. Chem. Soc.*, 112 (1990) 5665–5667, and references therein.
164. G. H. Veeneman and J. H. van Boom, An efficient thioglycoside-mediated formation of a-glycosidic linkages promoted by iodonium dicollidine perchlorate, *Tetrahedron Lett.*, 31 (1990) 275–278.
165. M. I. Barrena, R. Echarri, and S. Castillón, Synthesis of disaccharides by selective metallocene promoted activation of glycosyl fluorides, *Synlett*, (1996) 675–676.
166. S. I. Hashimoto, H. Sakamoto, T. Honda, H. Abe, S. I. Nakamura, and S. Ikegami, ''Armed-disarmed'' glycosidation strategy based on glycosyl donors and acceptors carrying phosphoroamidate as a leaving group: a convergent synthesis of globotriaosylceramide, *Tetrahedron Lett.*, 38 (1997) 8969–8972.
167. H. Chiba, S. Funasaka, K. Kiyota, and T. Mukaiyama, Catalytic and chemoselective glycosylation between armed and disarmed glycosyl *p*-trifluoromethylbenzylthio-*p*-trifluoromethylphenyl formimidates, *Chem. Lett.*, (2002) 746–747.
168. R. W. Friesen and S. J. Danishefsky, On the controlled oxidative coupling of glycals: A new strategy for the rapid assembly of oligosaccharides, *J. Am. Chem. Soc.*, 111 (1989) 6656–6660.
169. M. N. Kamat and A. V. Demchenko, Revisiting the armed-disarmed concept rationale: Chemoselective activation of the *S*-benzoxazolyl glycosides in oligosaccharide synthesis, *Org. Lett.*, 7 (2005) 3215–3218.
170. J. T. Smoot, P. Pornsuriyasak, and A. V. Demchenko, Development of an arming participating group for stereoselective glycosylation and chemoselective oligosaccharide synthesis, *Angew. Chem. Int. Ed.*, 44 (2005) 7123–7126.
171. B. Fraser-Reid, Z. Wu, C. W. Andrews, and E. Skowronski, Torsional effects in glycoside reactivity: Saccharide couplings mediated by acetal protecting groups, *J. Am. Chem. Soc.*, 113 (1991) 1434–1435.
172. B. G. Wilson and B. Fraser-Reid, n-Pentenyl glycoside based methodology for determining the relative reactivities of variously protected pairs of glycosides, *J. Org. Chem.*, 60 (1995) 317–320.
173. M. Fridman, D. Solomon, S. Yogev, and T. Baasov, One-pot synthesis of glucosamine oligosaccharides, *Org. Lett.*, 4 (2002) 281–283.
174. M. H. Clausen and R. Madsen, Synthesis of hexasaccharide fragments of pectin, *Chem. Eur. J.*, 9 (2003) 3821–3832.
175. T. Schmidt and R. Madsen, Glycosylations directed by the armed-disarmed effect with acceptors containing a single ester group, *Eur. J. Org. Chem.*, 2007 (2007) 3935–3941.
176. D. Crich and M. Li, Revisiting the armed-disarmed concept: The importance of anomeric configuration in the activation of S-benzoxazolyl glycosides, *Org. Lett.*, 9 (2007) 4115–4118.
177. G.-J. Boons, P. Grice, R. Leslie, S. V. Ley, and L. L. Yeung, Dispiroketals in synthesis (Part 5): A new opportunity for oligosaccharide synthesis using differentially activated glycosyl donors and acceptors, *Tetrahedron Lett.*, 34 (1993) 8523–8526.
178. D. K. Baeschlin, A. R. Chaperon, L. G. Green, M. G. Hahn, S. J. Ince, and S. V. Ley, 1,2-Diacetals in synthesis: Total synthesis of a glycosylphosphatidylinositol anchor of *Trypanosoma brucei*, *Chem. Eur. J.*, 6 (2000) 172–186.
179. T. Zhu and G.-J. Boons, Thioglycosides protected as Trans-2,3-cyclic carbonates in chemoselective glycosylations, *Org. Lett.*, 3 (2001) 4201–4203.
180. H. H. Jensen, L. U. Nordstrom, and M. Bols, The disarming effect of the 4,6-acetal group on glycoside reactivity: Torsional or electronic? *J. Am. Chem. Soc.*, 126 (2004) 9205–9213.

181. C. M. Pedersen, L. U. Nordstrom, and M. Bols, ''Super armed'' glycosyl donors: Conformational arming of thioglycosides by silylation, *J. Am. Chem. Soc.*, 129 (2007) 9222–9235.
182. H. H. Jensen, C. M. Pedersen, and M. Bols, Going to extremes: ''Super'' armed glycosyl donors in glycosylation chemistry, *Chem. Eur. J.*, 13 (2007) 7576–7582.
183. L. K. Mydock and A. V. Demchenko, Superarming the *S*-benzoxazolyl glycosyl donors by simple 2-*O*-benzoyl-3,4,6-tri-*O*-benzyl protection, *Org. Lett.*, 10 (2008) 2103–2106.
184. L. K. Mydock and A. V. Demchenko, Application of the superarmed glycosyl donor to chemoselective oligosaccharide synthesis, *Org. Lett.*, 10 (2008) 2107–2110.
185. B. Fraser-Reid, J. C. Lopez, K. V. Radhakrishnan, M. V. Nandakumar, A. M. Gomez, and C. Uriel, One pot/two donors/one diol give one differentiated trisaccharide: Powerful evidence for reciprocal donor-acceptor selectivity (RDAS), *Chem. Commun.*, (2002) 2104–2105.
186. M. Adachi, H. Tanaka, and T. Takahashi, An effective sialylation method using N-Troc and N-Fmoc-protected β-thiophenyl sialosides and application to the one-pot two-step synthesis of 2,6-sialyl-T antigen, *Synlett*, (2004) 609–614.
187. K. N. Jayaprakash and B. Fraser-Reid, One-pot chemo-, regio-, and stereoselective double-differential glycosidation mediated by lanthanide triflates, *Org. Lett.*, 6 (2004) 4211–4214.
188. T. W. D. F. Rising, C. D. Heidecke, and A. J. Fairbanks, *Synlett*, (2007) 1421–1425.
189. S. Eller, R. Schuberth, G. Gundel, J. Seifert, and C. Unverzagt, Synthesis of pentaantennary N-glycans with bisecting GlcNAc and core fucose, *Angew. Chem. Int. Ed.*, 46 (2007) 4173–4175.
190. C. Unverzagt, S. Eller, S. Mezzato, and R. Schuberth, A double regio- and stereoselective glycosylation strategy for the synthesis of N-glycans, *Chem. Eur. J.*, 14 (2008) 1304–1311.
191. H. Tanaka, M. Adachi, H. Tsukamoto, T. Ikeda, H. Yamada, and T. Takahashi, Synthesis of di-branched heptasaccharide by one-pot glycosylation using seven independent building blocks, *Org. Lett.*, 4 (2002) 4213–4216.
192. R. Windmuller and R. R. Schmidt, Efficient synthesis of lactoneo series antigens H, Lewis X(Le^x), and Lewis Y(Le^y), *Tetrahedron Lett.*, 35 (1994) 7927–7930.
193. G. Anilkumar, L. G. Nair, and B. Fraser-Reid, Targeted glycosyl donor delivery for site-selective glycosylation, *Org. Lett.*, 2 (2000) 2587–2589.
194. C. Uriel, A. M. Gomez, J. C. Lopez, and B. Fraser-Reid, Further insight into 'matching' of donors and acceptors via reciprocal donor acceptor selectivity (RDAS) studies, *Synlett*, (2003) 2203–2207.
195. Y. Du, G. Gu, G. Wei, Y. Hua, and R. J. Linhardt, Synthesis of saponins using partially protected glycosyl donors, *Org. Lett.*, 5 (2003) 3627–3630.
196. G. Gu, Y. Du, and R. J. Linhardt, Facile synthesis of saponins containing 2,3-branched oligosaccharides by using partially protected glycosyl donors, *J. Org. Chem.*, 69 (2004) 5497–5500.
197. G.-J. Boons and A. V. Demchenko, Recent advances in *O*-sialylation, *Chem. Rev.*, 100 (2000) 4539–4565.
198. S. J. Danishefsky and J. R. Allen, From the laboratory to the clinic: A retrospective on fully synthetic carbohydrate-based anticancer vaccines, *Angew. Chem. Int. Ed.*, 39 (2000) 836–863.
199. Z. G. Wang and O. Hindsgaul, Combinatorial carbohydrate chemistry, in Axford, (Ed.), *Glycoimmunology 2,* Plenum Press, New York, 1998, pp. 219–236.
200. G.-J. Boons, Combinatorial approaches in oligosaccharide synthesis, *Carbohydr. Eur.*, (1999) 28–32.
201. F. Schweizer and O. Hindsgaul, Combinatorial synthesis of carbohydrates, *Curr. Opin. Chem. Biol.*, 3 (1999) 291–298.
202. K. Fukase, Oligosaccharides: Synthesis: Combinatorial and solid phase methods in oligosaccharide synthesis, in B. Fraser-Reid, K. Tatsuta, and J. Thiem, (Eds.), *Glycoscience: Chemistry and Chemical Biology*, Vol. 2, Springer, Berlin, 2001, pp. 1621–1660.
203. P. J. Garegg, J. L. Maloisel, and S. Oscarson, Stannylene activation in glycoside synthesis: Regioselective glycosidations at the primary position of galactopyranosides unprotected in the 2-,3-,4-, and 6-positions, *Synthesis*, (1995) 409–414.

204. K. Oshima and Y. Aoyama, Regiospecific glycosidation of unprotected sugars via arylboronic activation, *J. Am. Chem. Soc.*, 121 (1999) 2315–2316.
205. J. C. Lopez, A. Agocs, C. Uriel, A. M. Gomez, and B. Fraser-Reid, Iterative, orthogonal strategy for oligosaccharide synthesis based on the regioselective glycosylation of polyol acceptors with partially unprotected *n*-pentenyl-orthoesters: further evidence for reciprocal donor acceptor selectivity (RDAS), *Chem. Commun.*, (2005) 5088–5090.
206. Y. E. Tsvetkov, P. I. Kitov, L. V. Backinowsky, and N. K. Kochetkov, Unusual regioselective glycosylation of sugar secondary trityloxy function in the presence of primary one, *Tetrahedron Lett.*, 34 (1993) 7977–7980.
207. Y. E. Tsvetkov, P. I. Kitov, L. V. Backinowsky, and N. K. Kochetkov, Highly regioselective glycosylation of a secondary position in sugar primary-secondary ditrityl ethers, *J. Carbohydr. Chem.*, 15 (1996) 1027–1050.
208. G.-J. Boons and T. Zhu, Novel regioselective glycosylations for the convergent and chemoselective assembly of oligosaccharides, *Synlett*, (1997) 809–811.
209. T. Zhu and G.-J. Boons, Two-directional, convergent synthesis of a pentasaccharide that is involved in the hyperacute rejection response in xenotransplantation from pig to man, *J. Chem. Soc., Perkin Trans.*, 1 (1998) 857–862.
210. T. Zhu and G.-J. Boons, A two directional glycosylation strategy for the convergent assembly of oligosaccharides, *Tetrahedron Lett.*, 39 (1998) 2187–2190.
211. G.-J. Boons, S. Bowers, and D. M. Coe, Trityl ethers in oligosaccharide synthesis: A novel strategy for the convergent assembly of oligosaccharides, *Tetrahedron Lett.*, 38 (1997) 3773–3776.
212. T. Zhu and G.-J. Boons, A two-directional approach for the solid-phase synthesis of trisaccharide libraries, *Angew. Chem. Int. Ed.*, 37 (1998) 1898–1900.
213. P. Grice, S. V. Ley, J. Pietruszka, H. W. M. Priepke, and E. P. E. Walther, Tuning the reactivity of glycosides: efficient one-pot oligosaccharide synthesis, *Synlett*, (1995) 781–784.
214. T. K.-K. Mong and C.-H. Wong, Reactivity-based one-pot synthesis of a Lewis Y carbohydrate hapten: a colon-rectal cancer antigen determinant, *Angew. Chem. Int. Ed.*, 41 (2002) 4087–4090.
215. T. K.-K. Mong, C.-Y. Huang, and C.-H. Wong, A new reactivity-based one-pot synthesis of *N*-acetyllactosamine oligomers, *J. Org. Chem.*, 68 (2003) 2135–2142.
216. T. K.-K. Mong, H.-K. Lee, S. G. Duron, and C.-H. Wong, Reactivity-based one-pot total synthesis of fucose GM1 oligosaccharide: A sialylated antigenic epitope of small-cell lung cancer, *Proc. Nat. Acad. Sci. USA*, 100 (2003) 797–802.
217. J. C. Lee, C. Y. Wu, J. V. Apon, G. Siuzdak, and C.-H. Wong, Reactivity-based one-pot synthesis of the tumor-associated antigen N3 minor octasaccharide for the development of a photocleavable DIOS-MS sugar array, *Angew. Chem. Int. Ed.*, 45 (2006) 2753–2757.
218. T. Polat and C.-H. Wong, Anomeric reactivity-based one-pot synthesis of heparin-like oligosaccharides, *J. Am. Chem. Soc.*, 129 (2007) 12795–12800.
219. D. K. Baeschlin, L. G. Green, M. G. Hahn, B. Hinzen, S. J. Ince, and S. V. Ley, Rapid assembly of oligosaccharides: 1,2-diacetal-mediated reactivity tuning in the coupling of glycosyl fluorides, *Tetrahedron Asymmetry*, 11 (2000) 173–197.
220. S. Valverde, M. Garcia, A. M. Gomez, and J. C. Lopez, A combined intramolecular–intermolecular one-pot glycosylation approach for the synthesis of a branched trisaccharide, *Chem. Commun.*, (2000) 813–814.
221. T. Hiroshi, N. Matoba, and T. Takahashi, Effective one-pot synthesis of H type 1 and 2 trisaccharide derivatives using glycal epoxide, *Chem. Lett.*, 34 (2005) 400–401.
222. S. Bhattacharyya, B. G. Magnusson, U. Wellmar, and U. J. Nilsson, The *p*-methoxybenzyl ether as an *in situ* -removable carbohydrate-protecting group: a simple one-pot synthesis of the globotetraose tetrasaccharide, *J. Chem. Soc. Perkin Trans. 1*, 8 (2001) 886–890.

223. M. Winter, Support for solid-phase organic synthesis, in G. Jung, (Ed.), *Combinatorial Peptide and Nonpeptide Libraries,* VCH, Weinheim, 1996, pp. 465–510.
224. J. S. Fruchtel and G. Jung, Organic chemistry on solid supports, *Angew. Chem. Int. Ed. Engl.*, 35 (1996) 17–42.
225. P. H. H. Hermkens, H. C. J. Ottenheijm, and D. Rees, Solid-phase organic reactions: A review of the recent literature, *Tetrahedron*, 52 (1996) 4527–4554.
226. R. C. D. Brown, Recent developments in solid-phase organic synthesis, *J. Chem. Soc., Perkin Trans.*, 1 (1998) 3293–3320.
227. H. M. I. Osborn and T. H. Khan, Recent developments in polymer supported syntheses of oligosaccharides and glycopeptides, *Tetrahedron*, 55 (1999) 1807–1850.
228. J. J. Krepinsky and S. P. Douglas, Polymer-supported synthesis of oligosaccharides, in B. Ernst, G. W. Hart, and P. Sinaÿ, (Eds.), *Carbohydrates in Chemistry and Biology*, Vol. 1, Wiley-VCH, Weinheim, 2000, pp. 239–265.
229. P. H. Seeberger and W. C. Haase, Solid-phase oligosaccharide synthesis and combinatorial carbohydrate libraries, *Chem. Rev.*, 100 (2000) 4349–4393.
230. P. H. Seeberger, Solid phase oligosaccharide synthesis (reprinted from Glycochemistry: Principles, synthesis, and applications, pp. 1–32, 2001), *J. Carbohydr. Chem.*, 21 (2002) 613–643.
231. H. Ando, S. Manabe, Y. Nakahara, and Y. Ito, Tag-reporter strategy for facile oligosaccharide synthesis on polymer support, *J. Am. Chem. Soc.*, 123 (2001) 3848–3849.
232. P. Sears and C.-H. Wong, Toward automated synthesis of oligosaccharides and glycoproteins, *Science*, 291 (2001) 2344–2350.
233. D. Crich and M. Smith, Solid-phase synthesis of β-mannosides, *J. Am. Chem. Soc.*, 124 (2002) 8867–8869.
234. S. Manabe and Y. Ito, On-resin real-time reaction monitoring of solid-phase oligosaccharide synthesis, *J. Am. Chem. Soc.*, 124 (2002) 12638–12639.
235. D. Majumdar, T. Zhu, and G.-J. Boons, Synthesis of oligosaccharides on soluble high-molecular-weight branched polymers in combination with purification by nanofiltration, *Org. Lett.*, 5 (2003) 3591–3594.
236. R. Ojeda, J. L. de Paz, and M. Martin-Lomas, Synthesis of heparin-like oligosaccharides on a soluble polymer support, *Chem. Commun.*, (2003) 2486–2487.
237. R. Ojeda, O. Terenti, J. L. de Paz, and M. Martin-Lomas, Synthesis of heparin-like oligosaccharides on polymer supports, *Glycoconjugate J.*, 21 (2004) 179–195.
238. X. Wu and R. R. Schmidt, Solid-phase synthesis of complex oligosaccharides using a novel capping reagent, *J. Org. Chem.*, 69 (2004) 1853–1857.
239. J. Bauer and J. Rademann, Hydrophobically assisted switching phase synthesis: The flexible combination of solid-phase and solution-phase reactions employed for oligosaccharide preparation, *J. Am. Chem. Soc.*, 127 (2005) 7296–7297.
240. A. Dondoni, A. Marra, and A. Massi, Hybrid solution/solid-phase synthesis of oligosaccharides by using trichloroacetyl isocyanate as sequestration-enabling reagent of sugar alcohols, *Angew. Chem. Int. Ed.*, 44 (2005) 1672–1676.
241. S. Hanashima, S. Manabe, and Y. Ito, Divergent synthesis of sialylated glycan chains: Combined use of polymer support, resin capture-release, and chemoenzymatic strategies, *Angew Chem. Int. Ed.*, 44 (2005) 4218–4228.
242. T. Ako, S. Daikoku, I. Ohtsuka, R. Kato, and O. Kanie, A method of orthogonal oligosaccharide synthesis leading to a combinatorial library based on stationary solid-phase reaction, *Chem. Asian J.*, 1 (2006) 798–813.
243. S. Jonke, K.-g. Liu, and R. R. Schmidt, Solid-phase oligosaccharide synthesis of a small library of N-glycans, *Chem. Eur. J.*, 12 (2006) 1274–1290.

244. H. A. Branderhorst, R. A. J. Liskamp, and R. J. Pieters, Solid-phase carbohydrate synthesis via on-bead protecting group chemistry, *Tetrahedron*, 63 (2007) 4290–4296.
245. T. Doi, A. Kinbara, H. Inoue, and T. Takahashi, Donor-bound glycosylation for various glycosyl acceptors: Bidirectional solid-phase semisynthesis of vancomycin and its derivatives, *Chem. Asian J.*, 2 (2007) 188–198.
246. O. J. Plante, E. R. Palmacci, and P. H. Seeberger, Development of an automated oligosaccharide synthesizer, *Adv. Carbohydr. Chem. Biochem.*, 58 (2003) 35–54.
247. T. Zhu and G.-J. Boons, A novel and efficient synthesis of a dimeric Le^x oligosaccharide on polymeric support, *J. Am. Chem. Soc.*, 122 (2000) 10222–10223.
248. J. Ferguson and C. Marzabadi, On-resin generation and reactions of orthogonal glycosyl donors, *Tetrahedron Lett.*, 44 (2003) 3573–3577.
249. M. C. Parlato, M. N. Kamat, H. Wang, K. J. Stine, and A. V. Demchenko, Application of glycosyl thioimidates in polymer-supported oligosaccharide synthesis, *J. Org. Chem.*, 73 (2008) 1716–1725.
250. X. Wu, M. Grathwohl, and R. R. Schmidt, Efficient solid-phase synthesis of a complex, branched N-glycan hexasaccharide: Use of a novel linker and temporary-protecting-group pattern, *Angew. Chem. Int. Ed.*, 41 (2002) 4489–4493.
251. P. H. Seeberger and D. B. Werz, Automated synthesis of oligosacchraides as a basis for drug discovery, *Nat. Rev.*, 4 (2005) 751–763.
252. P. H. Seeberger and D. B. Werz, Synthesis and medical applications of oligosaccharides, *Nature*, 446 (2007) 1046–1051.
253. P. H. Seeberger, Automated oligosaccharide synthesis, *Chem. Soc. Rev.*, 37 (2008) 19–28.
254. M. C. Hewitt, D. A. Snyder, and P. H. Seeberger, Rapid synthesis of a glycosylphosphatidylinositol-based malaria vaccine using automated solid-phase oligosaccharide synthesis, *J. Am. Chem. Soc.*, 124 (2002) 13434–13436.
255. D. B. Werz, B. Castagner, and P. H. Seeberger, Automated synthesis of the tumor-associated carbohydrate antigens Gb-3 and Globo-H: Incorporation of α-galactosidic linkages, *J. Am. Chem. Soc.*, 129 (2007) 2770–2771.
256. T. Miura, K. Goto, H. Waragai, H. Matsumoto, Y. Hirose, M. Ohmae, H. Ishida, A. Satoh, and T. Inazu, Rapid oligosaccharide synthesis using a fluorous protective group, *J. Org. Chem.*, 69 (2004) 5348–5353.
257. D. M. Ratner, E. R. Murphy, M. Jhunjhunwala, D. A. Snyder, K. F. Jensen, and P. H. Seeberger, Microreactor-based reaction optimization in organic chemistry – glycosylation as a challenge, *Chem. Comm.*, (2005) 578–580.
258. F. R. Carrel, K. Geyer, J. D. C. Codée, and P. H. Seeberger, Oligosaccharide synthesis in microreactors, *Org. Lett.*, 9 (2007) 2285–2288.
259. A. K. Pathlak, C. K. Yerneni, Z. Young, and V. Pathlak, Oligomannan synthesis using ionic liquid supported glycosylation, *Org. Lett.*, 10 (2008) 145–148.
260. C.-H. Wong, R. L. Halcomb, Y. Ichikawa, and T. Kajimoto, Enzymes in organic synthesis: Application to the problems of carbohydrate recognition (part 1), *Angew. Chem., Int. Ed. Engl.*, 34 (1995) 412–432.
261. C.-H. Wong, R. L. Halcomb, Y. Ichikawa, and T. Kajimoto, Enzymes in organic synthesis: Application to the problems of carbohydrate recognition (part 2), *Angew. Chem., Int. Ed. Engl.*, 34 (1995) 521–546.
262. A. J. Kirby, Enzyme mechanisms, models, and mimics, *Angew. Chem., Int. Ed. Engl.*, 35 (1996) 707–724.
263. S. David, C. Augé, and C. Gautheron, Enzymic methods in preparative carbohydrate chemistry, *Adv. Carbohydr. Chem. Biochem.*, 49 (1991) 175–237.
264. V. Kren and J. Thiem, Glycosylation employing bio-systems: From enzymes to whole cells, *Chem. Soc. Rev.*, 26 (1997) 463–473.

265. E. J. Hehre, Glycosyl transfer: a history of the concept's development and view of its major contributions to biochemistry, *Carbohydr. Res.*, 331 (2001) 347–368.
266. U. Gambert and J. Thiem, Chemical transformations employing glycosyltransferases, *Topics Curr. Chem.*, 186 (1997) 21–43.
267. D. H. van den Eijnden, On the origin of oligosaccharide species – glycosyltransferases in action, in B. Ernst, G. W. Hart, and P. Sinay, (Eds.), *Carbohydrates in Chemistry and Biology*, Vol. 1, Wiley-VCH, Weinheim, 2000, pp. 589–624.
268. O. Renkonen, Enzymatic glycosylations with glycosyltransferases, in B. Ernst, G. W. Hart, and P. Sinay, (Eds.), *Carbohydrates in Chemistry and Biology*, Vol. 1, Wiley-VCH, Weinheim, 2000, pp. 647–662.
269. C. Augé, C. Le Narvor, and A. Lubineau, Solid-phase synthesis with glycosyltransferases,, in B. Ernst, G. W. Hart, and P. Sinay, (Eds.), *Carbohydrates in Chemistry and Biology*, Vol. 1, Wiley-VCH, Weinheim, 2000, pp. 705–722.
270. X. Qian, K. Sujino, A. Otter, M. M. Palcic, and O. Hindsgaul, Chemoenzymatic synthesis of α-(1- > 3)-Gal(NAc)-terminating glycosides of complex tertiary sugar alcohols, *J. Am. Chem. Soc.*, 121 (1999) 12063–12072.
271. X. Qian, K. Sujino, and M. M. Palcic, Enzymatic glycosylations with non-natural donors and acceptors,, in B. Ernst, G. W. Hart, and P. Sinaÿ, (Eds.), *Carbohydrates in Chemistry and Biology*, Vol. 1, Wiley-VCH, Weinheim, 2000, pp. 685–704.
272. K. Sujino, T. Uchiyama, O. Hindsgaul, N. O. L. Seto, W. W. Wakarchuk, and M. M. Palcic, Enzymatic synthesis of oligosaccharide analogues: evaluation of UDP-Gal analogues as donors for three retaining α-galactosyltransferases, *J. Am. Chem. Soc.*, 122 (2000) 1261–1269.
273. R. Ohrlein, Synthesis of sugar nucleotides, in B. Ernst, G. W. Hart, and P. Sinaÿ, (Eds.), *Carbohydrates in Chemistry and Biology*, Vol. 1, Wiley-VCH, Weinheim, 2000, pp. 625–646.
274. K. M. Koeller and C.-H. Wong, Recycling of sugar nucleotides in enzymatic glycosylation,, in B. Ernst, G. W. Hart, and P. Sinaÿ, (Eds.), *Carbohydrates in Chemistry and Biology*, Vol. 1, Wiley-VCH, Weinheim, 2000, pp. 663–684.
275. H. Yu, H. Chokhawala, R. Karpel, H. Yu, B. Wu, J. Zhang, Y. Zhang, Q. Jia, and X. Chen, A multifunctional *Pasteurella multocida* sialyltransferase: A powerful tool for the synthesis of sialoside libraries, *J. Am. Chem. Soc.*, 127 (2005) 17618–17619.
276. W. Yi, J. Shao, L. Zhu, M. Li, Y. Lu, S. Lin, H. Li, K. Ryu, J. Shen, H. Guo, Q. Yao, C. A. Bush, and P. G. Wang, *E. coli* O86 O-antigen biosynthetic gene cluster and stepwise enzymatic synthesis of human blood group B antigen tetrasaccharide, *J. Am. Chem. Soc.*, 127 (2005) 2040–2041.
277. Y. Tachibana, T. Takaha, S. Fujiwara, M. Takagi, and T. Imanaka, Acceptor specificity of 4-α-glucanotransferase from *Pyrococcus kodakaraensis* KOD1, and synthesis of cycloamylose, *J. Biosci. Bioeng.*, 90 (2000) 406–409.
278. M. Scigelova, S. Singh, and D. H. G. Crout, Glycosidases – a great synthetic tool, *J. Mol. Catal. B-Enzym.*, 6 (1999) 483–494.
279. D. J. Vocadlo and S. G. Withers, Glycosidase-catalyzed oligosaccharide synthesis, in B. Ernst, G. W. Hart, and P. Sinaÿ, (Eds.), *Carbohydrates in Chemistry and Biology*, Vol. 1, Wiley-VCH, Weinheim, 2000, pp. 723–844.
280. E. J. Hehre, A fresh understanding of the stereochemical behavior of glycosylases: Structural distinction of ''inverting'' (2-MCO-type) versus ''retaining'' (1-MCO-type) enzymes, *Adv. Carbohydr. Chem. Biochem.*, 55 (2000) 265–310.
281. G. Vic, J. J. Hastings, and D. H. G. Crout, Glycosidase-catalysed synthesis of glycosides by an improved procedure for reverse hydrolysis: Application to the chemoenzymatic synthesis of galactopyranosyl-(1→4)-*O*-α-galactopyranoside derivatives, *Tetrahedron Asymmetry*, 7 (1996) 1973–1984.
282. K. G. I. Nilsson, A simple strategy for changing the regioselectivity of glycosidase-catalyzed formation of disaccharides, *Carbohydr. Res.*, 167 (1987) 95–103.

283. S. Singh, M. Scigelova, and D. H. G. Crout, Glycosidase-catalysed synthesis of α-galactosyl epitopes important in xenotransplantation and toxin binding using the α-galactosidase from *Penicillium multicolor*, *Chem. Commun.*, (1999) 2065–2066.
284. M. Dion, A. Nisole, P. Spangenberg, C. Andre, A. Glottin-Fleury, R. Mattes, C. Tellier, and C. Rabiller, Modulation of the regioselectivity of a *Bacillus* α-galactosidase by direct evolution, *Glycoconjugate J.*, 18 (2001) 215–223,and references therein.
285. P. Spangenberg, C. Andre, M. Dion, C. Rabiller, and R. Mattes, Comparative study of new α-galactosidases in transglycosylation reactions, *Carbohydr. Res.*, 329 (2000) 65–73.
286. Y. W. Kim, D. T. Fox, O. Hekmat, T. Kantner, L. P. McIntosh, R. A. J. Warren, and S. G. Withers, Glycosynthase-based synthesis of xylo-oligosaccharides using an engineered retaining xylanase from *Cellulomonas fimi*, *Org. Biomol. Chem.*, 4 (2006) 2025–2032.

STEREOCONTROLLED SYNTHESIS OF MANNANS AND RHAMNANS

By Feng Cai, Baolin Wu and David Crich

Department of Chemistry, Wayne State University, Detroit, MI 48202, USA

- I. Introduction 251
- II. The α-Mannans and α-Rhamnans 252
  - 1. α-Mannan Synthesis in the Absence of Neighboring-Group Participation 252
  - 2. Neighboring Group-Directed α-Mannan Synthesis 262
  - 3. Synthesis of α-Rhamnans 281
- III. The β-Mannans and β-Rhamnans 286
  - 1. Introduction 286
  - 2. β-Mannan Synthesis by Indirect Methods 286
  - 3. β-Rhamnan Synthesis by Indirect Methods 291
  - 4. β-Mannan Synthesis by Direct Methods 291
  - 5. β-Rhamnan Synthesis by Direct Methods 299
- References 301

I. INTRODUCTION

The mannans and rhamnans, glycans composed of multiple mannopyranosyl and rhamnopyranosyl monomers, are widespread in Nature and present a very diverse set of biological properties. As with most oligosaccharides and glycoconjugates, the study of these properties is often hindered by the heterogeneity of natural isolates and the small quantities in which they are available. The chemical synthesis of homogeneous mannans and rhamnans is therefore an area of both considerable interest and importance. The α-mannans and rhamnans contain multiple 1,2-*trans*-axial glycosidic units and might be considered some of the more facile glycans accessible by synthesis. This is evident from the considerable amount of work in this area, and it is for this reason that this chapter opens with this subgroup. Nevertheless two approaches, those avoiding the use of neighboring-group participation and

ISBN: 978-0-12-374743-3
DOI: 10.1016/S0065-2318(09)00006-7

© 2009 Elsevier Inc. All rights reserved.

those relying on it for the stereocontrolled formation of the 1,2-*trans*-axial glycosidic bonds, are discernible, along with considerable ingenuity directed toward the development of ever more efficient strategies. The *β*-mannans and rhamnans on the other hand are examples of glycans based on the 1,2-*cis*-equatorial class of glycosidic bond, which, until recently, was considered to be one of the more difficult linkages to prepare. Less work has therefore been directed at the synthesis of the *β*-mannans and rhamnans, but the existing syntheses testify to the creativity and adaptability of organic synthesis in the service of carbohydrate chemistry.

To contain the chapter within manageable limits, for both authors and readers, the material has been arbitrarily limited, with occasional exceptions, to pure mannans and pure rhamnans. Consequently the synthesis of the GPI anchors, which has been reviewed recently[1,2] and which feature a trimannan at the center of a longer glycan chain, is not covered. The minimum chain length considered is three monosaccharide units, and, for the most part, final deprotections have been omitted from the reaction schemes.

II. THE α-MANNANS AND α-RHAMNANS

1. *α*-Mannan Synthesis in the Absence of Neighboring-Group Participation

The seemingly straightforward task of α-mannan synthesis in the absence of neighboring-group participation has been the subject of considerable creativity. This is illustrated through the labors of Ley and co-workers who, setting the stage for their groundbreaking work on one-pot oligosaccharide synthesis,[3] constructed a high mannose-type nonasaccharide in a highly efficient manner.[4] A series of five mannosyl donors (Fig. 1) was constructed whose relative reactivities were determined by the nature of the anomeric substitutent, pheynlseleno or alkylthio glycosides, and by the protecting-group array.

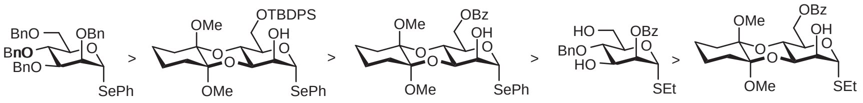

1 **2** **3** **4** **5**

FIG. 1. Donors employed by Ley and their relative reactivity.

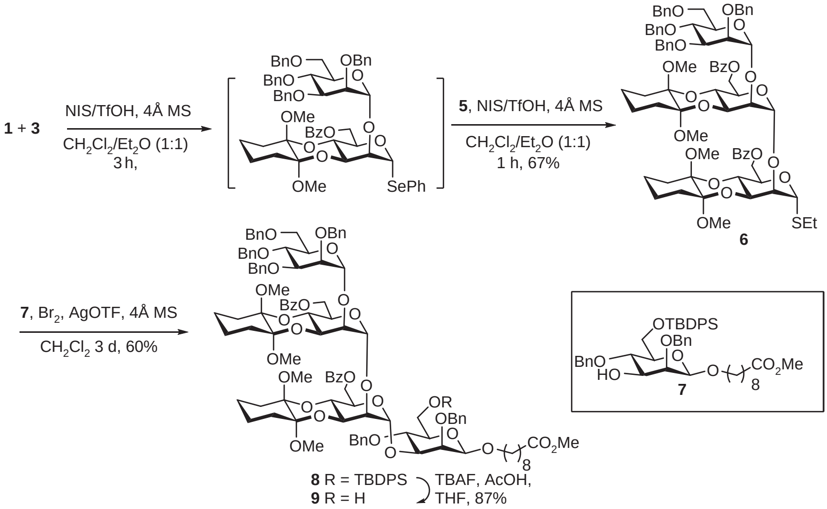

SCHEME 1. Tetrasaccharide assembly.

Activation of the perbenzylated selenoglycoside **1** by NIS (*N*-iodosuccinimide)* and triflic acid in the presence of the monohydroxy bisacetal-protected selenoglycoside **2** took advantage of the greater reactivity of the perbenzyl system and afforded a disaccharide. This disaccharide was not isolated, but was activated with further NIS and triflic acid in the presence of the bisacetal-protected monohydroxy thioglycoside **5** to give a trisaccharide in 67% isolated yield (Scheme 1). The lower reactivity of the thioglycoside was reflected in the fact that the trisaccharide **6** could not be activated by the NIS/TfOH combination for coupling to the acceptor **7**, meaning that recourse had to be made to the more powerful combination of silver triflate and bromine, when the tetrasaccharide **8** was obtained in 60% yield. Removal of the single silyl ether protecting group cleared the way for introduction of the second arm of the biantennary nonsaccharide target (Scheme 1).[4]

A second disaccharide was assembled similarly to the first, again taking advantage of the lower reactivity of the bisacetal protecting group over the perbenzylated system, before coupling to 3,6-dihydroxy thioglycoside **4** to give a pentasaccharide **11** in the form of a thioglycoside (Scheme 2).[4]

Activation of this pentasaccharide with the NIS/TfOH combination in the presence of the tetrasaccharide acceptor **9** gave the target nonasaccharide in 89% yield (Scheme 3). The subtle influence of protecting groups on glycoside reactivity is

---

*For a list of many abbreviations commonly used in glycoside synthesis, see page 162 of the article by Smoot and Demchenko in the current volume.

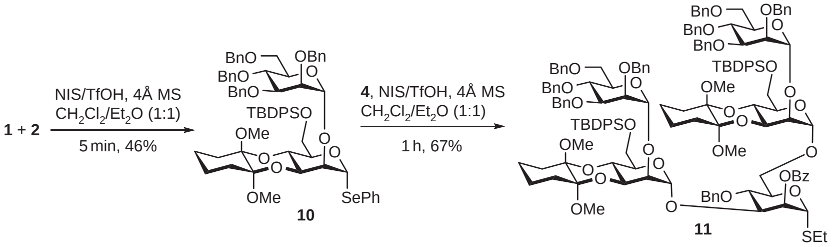

SCHEME 2. Assembly of a pentasaccharide.

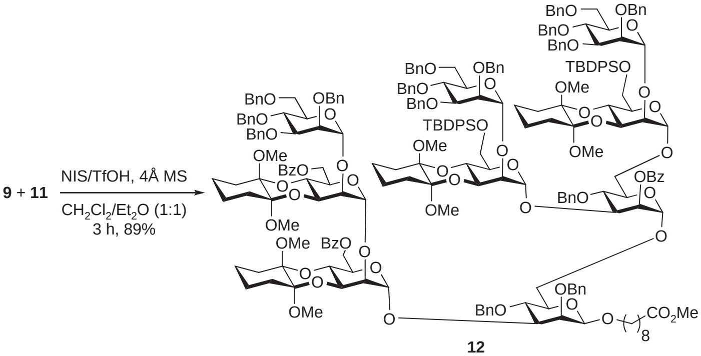

SCHEME 3. Completion of the synthesis.

underlined by the comparison of the two donors, trisaccharide **6** and pentasaccharide **11**, with the first requiring the more powerful bromine/AgOTf activating system, while the second succumbed to NIS/TfOH. The careful design of the entire reaction scheme leading to the protected nonasaccharide is emphasized by the need for only a single protecting-group manipulation after the preparation of the monosaccharide building blocks. The final deprotection of the entire nonasaccharide (not shown) required only four steps, but was hampered by complications in the hydrogenolysis of certain benzyl ethers with competing reduction to cyclohexylmethyl ethers.[4]

Ito and coworkers assembled a series of α-mannans working under frozen solvent conditions, and observed striking rate accelerations when compared to the same reactions in fluid media.[5] For example, the trisaccharide thioglycoside **14** was coupled to the hexasaccharide **13** at 4 °C with activation by methyl triflate to give the nonasaccharide[15] (Scheme 4). When toluene was employed as solvent, after 22 h at 4 °C only 6% of the product was obtained, whereas in frozen xylene under the same

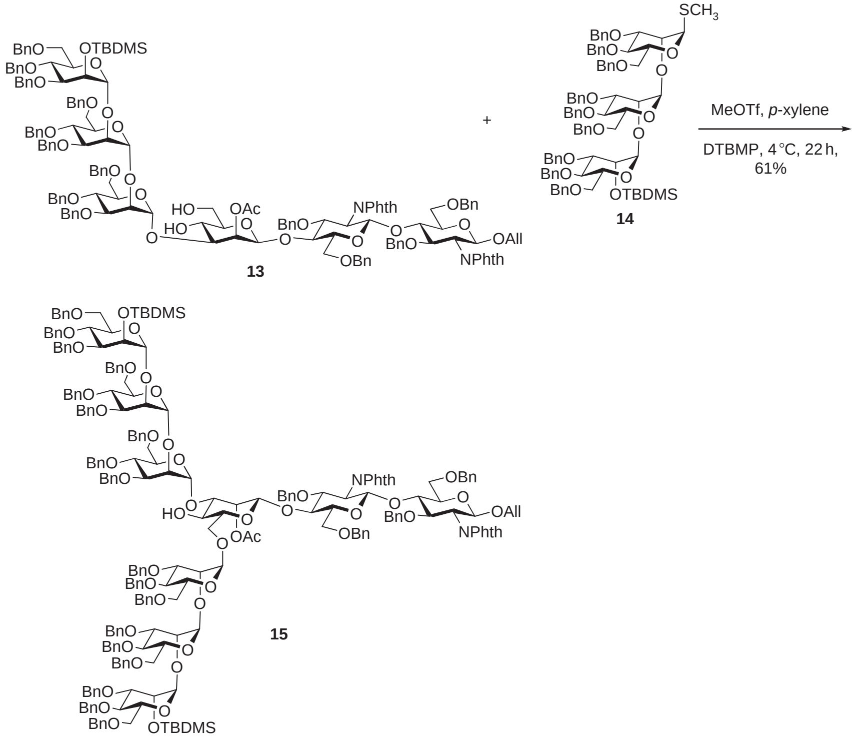

SCHEME 4. α-Mannan synthesis in a frozen solvent.

conditions of temperature and time the yield increased dramatically to 61%. The results were rationalized by invoking concentration of the reactants in the small volume of the liquid phase that exists in equilibrium with the solid phase below the freezing point, but above the eutectic temperature of the reaction mixture.[5] Unfortunately, in some examples, the acceleration in rate was accompanied by an unexplained loss of stereoselectivity for the α anomer that we speculate may be due to reduced mobility of the reactants within the small volume of the liquid phase. This would have the effect of hindering solvation of the key oxacarbenium ion/leaving group ion-pairs and/or of positioning the acceptor ideally for attack on the β face.

Several other syntheses of α-mannans have been reported that concentrate for the most part on glycosidic bond formation in the absence of neighboring-group participation but which, nevertheless, fall back on this concept for one or more linkages. Included in this class is the Ley synthesis of a series of high mannose-type neoglycolipids prepared with the aim of targeting liposomes to macrophages for gene therapy.[6] Thus, activation of the 2-*O*-acetyl selenoglycoside **16** with NIS/TfOH in the presence of the thioglycoside mono-ol **17** gave disaccharide **18** in 75% yield, thereby illustrating the superior reactivity of selenoglycosides over thioglycosides, even in the presence of a disarming 2-*O*-acetyl group (Scheme 5).[6]

Coupling of disaccharide **18** with acceptor **7** gave a trisaccharide **19** which, after removal of the distal acetate ester, was again coupled to the perbenzylated selenoglycoside donor giving a tetrasaccharide **21** (Scheme 6). Finally, after removal of a silyl ether, a further α-mannosidic linkage was crafted through the use of the 4,6-*O*-benzylidene-protected selenomannoside **23** to give the hexasaccharide **24** (Scheme 6). It is of some interest to note that this last coupling gave the α-mannosidic linkage, despite the presence of the strongly disarming 4,6-*O*-benzylidene acetal in the donor, a result that is presumably due to the premixing of the donor and acceptor and the use of the mixed solvent containing 50% diethyl ether, which was known to be detrimental to acetal-directed *β*-mannoside synthesis.[7,8]

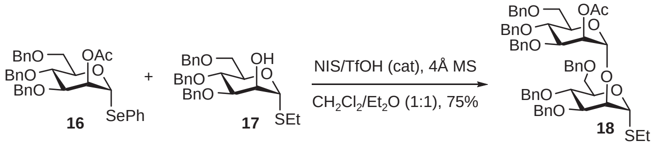
BnO
BnO
BnO
OAc
O
SePh
16
+
BnO
BnO
BnO
OH
O
SEt
17
NIS/TfOH (cat), 4Å MS
CH2Cl2/Et2O (1:1), 75%
BnO
BnO
BnO
OAc
O
BnO
O
O
BnO
BnO
18
SEt

SCHEME 5. Preferential activation of an acetylated selenoglycoside.

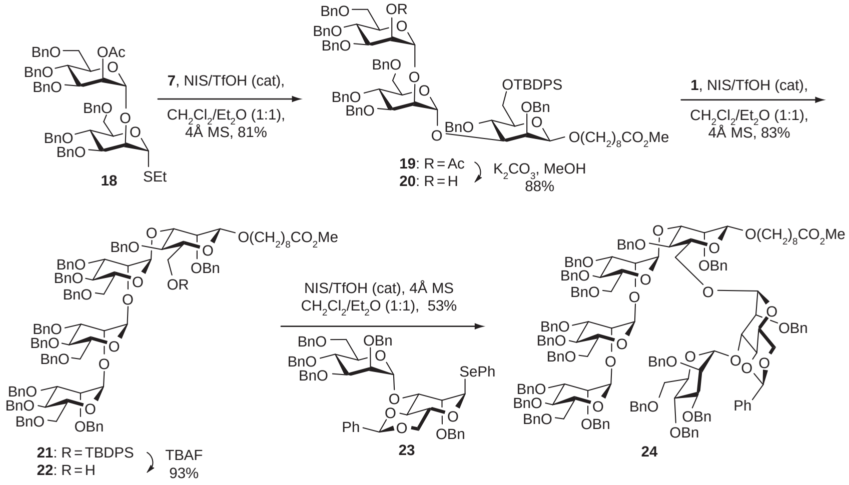
18
SEt
7, NIS/TfOH (cat),
CH2Cl2/Et2O (1:1), 4Å MS, 81%
OR
OTBDPS
OBn
O(CH2)8CO2Me
19: R = Ac
20: R = H
K2CO3, MeOH 88%
1, NIS/TfOH (cat),
CH2Cl2/Et2O (1:1), 4Å MS, 83%
21: R = TBDPS
22: R = H
TBAF 93%
NIS/TfOH (cat), 4Å MS
CH2Cl2/Et2O (1:1), 53%
SePh
Ph
23
24

SCHEME 6. Construction of a heptasaccharide.

Kong and coworkers developed an approach to a branched α-mannan from a *Saccharomyces cerevisiae* strain employing the Schmidt trichloroacetimidate glycosylation method in conjunction with the use of allyl glycoside-based acceptors.[9] In this synthesis a disaccharide donor **25** benefiting from neighboring-group participation was coupled to the allyl disaccharide **26** to give a tetrasaccharide **27** (Scheme 7). A two-step process was then required to convert the allyl glycoside into the corresponding trichloroacetimidate **28** ready for coupling to the allyl monosaccharide **29**. The single acetate ester present in the resulting pentasaccharide **30** was then removed selectively in the presence of 15 benzoate esters with a combination of acetyl chloride and methanol in dichloromethane. A final disaccharide was introduced onto the alcohol released in this manner to give a heptasaccharide **32** (Scheme 7).[9] The ability to achieve global deprotection of the heptasaccharide **32** in a single step is a noteworthy feature of this synthesis, but the requirement for the two-step conversion of the allyl ether into the trichloroacetimidate midway through the synthesis detracts from the efficiency of the route as compared to those of the Ley group.

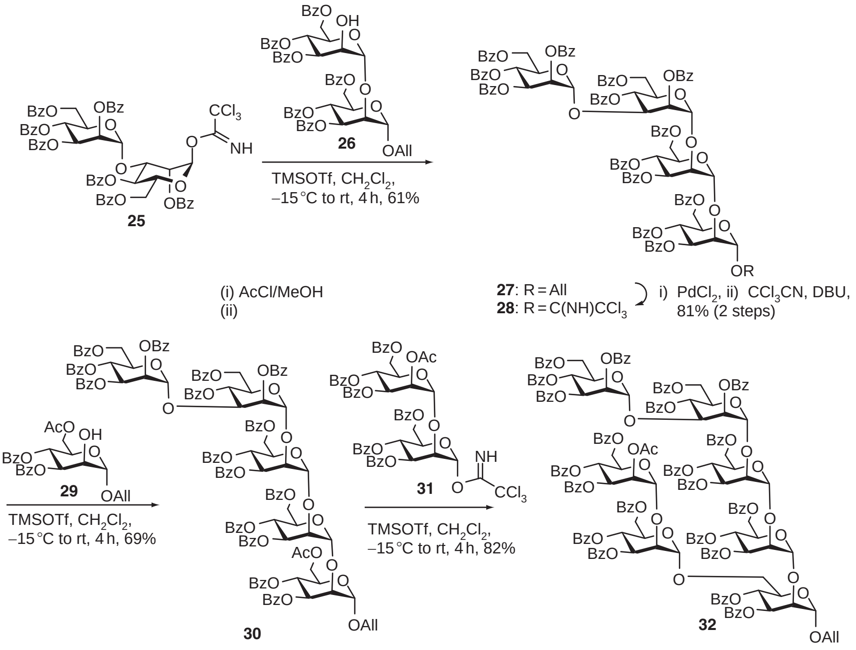
25
26
OAll
TMSOTf, CH_2Cl_2, –15 °C to rt, 4 h, 61%
27: R = All
28: R = C(NH)CCl_3
i) $PdCl_2$, ii) CCl_3CN, DBU, 81% (2 steps)
(i) AcCl/MeOH
(ii)
29
TMSOTf, CH_2Cl_2, –15 °C to rt, 4 h, 69%
30
31
TMSOTf, CH_2Cl_2, –15 °C to rt, 4 h, 82%
32

SCHEME 7. The allyl glycoside to trichloroacetimidate approach.

In a synthesis of an α-mannan containing tetrasaccharide **38** comprising the binding domain of an N-glycan recognized by the lectin calreticulin/calnexin, Oscarson and coworkers first employed neighboring-group participation to affect coupling of the very readily available mannosyl chloride **33** to acceptor **34** with mediation by silver triflate (Scheme 8). Cleavage of the then redundant acetate provided a glycosyl acceptor **36**, which was coupled to the highly armed mannosyl thioglycoside **37** to give the protected target **38** (Scheme 8), which on hydrogenolysis afforded the free tetrasaccharide.[10]

Kishi and co-workers described an iterative synthesis of the 3-*O*-methyl-(1→4)-α-D-mannan from *Mycobacterium smegmatis* in which an anomeric 2-carbomethoxybenzoate served as glycosyl donor under activation conditions developed by Mukaiyama, using silver perchlorate and tin(IV) chloride.[11] In an exploratory model study it was found that coupling of donor **40** ($n = 1$) with the trimethylsilyl ether **41** ($n = 1$) in the presence of the $AgClO_4/SnCl_4$ promoter in diethyl ether at 0 °C afforded, after 1 h, an α:β mixture of disaccharides **42** ($n = 1$) with an anomeric ratio of 3:1 in favor of the desired α anomer. However, over time, the ratio improved to the extent that after 30 h it had reached 22:1, leading to the conclusion that under the reaction conditions the undesired β anomer was undergoing slow epimerization to its α counterpart. Submission of the isolated β-disaccharide to the coupling conditions confirmed this hypothesis, but also revealed that cleavage of the glycosidic bond was a competing reaction, albeit a minor one. With these and other model experiments in hand, conditions were optimized for the

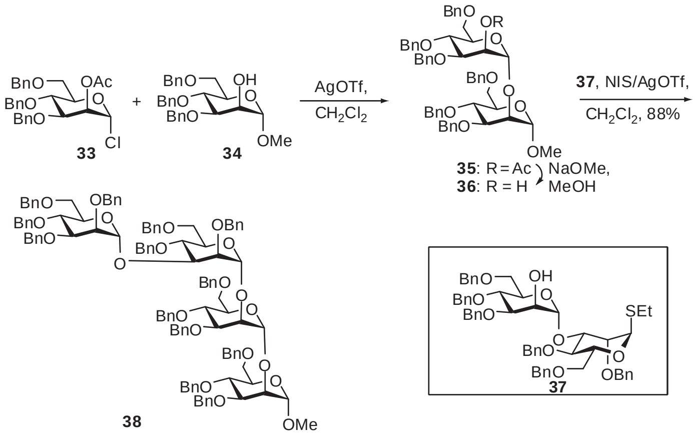

SCHEME 8. Block synthesis of a tetrasaccharide.

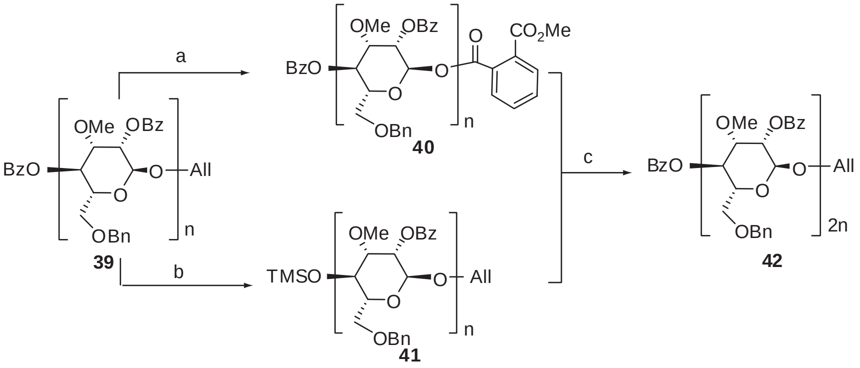

42 Glycosylation Products (2*n*)	Selectivity (α:β)	Isolated Yield (α only)
2	>20:1	76%
4	>50:1	76%
8	>50:1	79%
12	>50:1	75%
16	>50:1	74%

Reagent and conditions: (a) (1) (i) $(Ph_3P)_3RhCl$, DABCO; (ii) HCl, 77–81%; (2) monomethyl phthalate, EDCI, DMAP 94–100%; (b) (1) NaOH, MeOH, 83–92%; (2) TMSOTf, Et_3N, 98–100%; (c) $SnCl_4$–$AgClO_4$, Et_2O, 0 °C.

SCHEME 9. Iterative synthesis of an α-(1→4)-mannan.

epimerization-assisted α-selective glycosidic bond-forming reaction and applied to a block synthesis, as set out in Scheme 9. In this synthesis a standard type of oligomeric allyl 4-*O*-benzoyl mannoside **39** served as building block and was converted into the donor by isomerization of the allyl glycoside with Wilkinson's catalyst, subsequent acidic hydrolysis and carbodimide-mediated esterification with monomethyl phthalate. The same building block was saponified and then silylated to give the 4-*O*-trimethylsilyl ether employed as acceptor. Coupling of the two species thus obtained gave a disaccharide to which the same two protocols could be applied, to access a disaccharide donor and acceptor for preparation of a tetrasaccharide. Two further iterations of this process eventually lead to the formation of a hexadecasaccharide (Scheme 9).[11]

Iadonisi and coworkers developed a clever block-synthesis approach to the antitumor α-(1→3)-pentamannan known as PI-88, illustrating the selective activation of a trichloroacetimidate **43** in the presence of a *N*-phenyl trifluoroacetimidate **44** (Scheme 10).[12] This useful selectivity enabled assembly of the complete pentasaccharide with the adjustment of only a single protecting group in the course of the entire sequence.

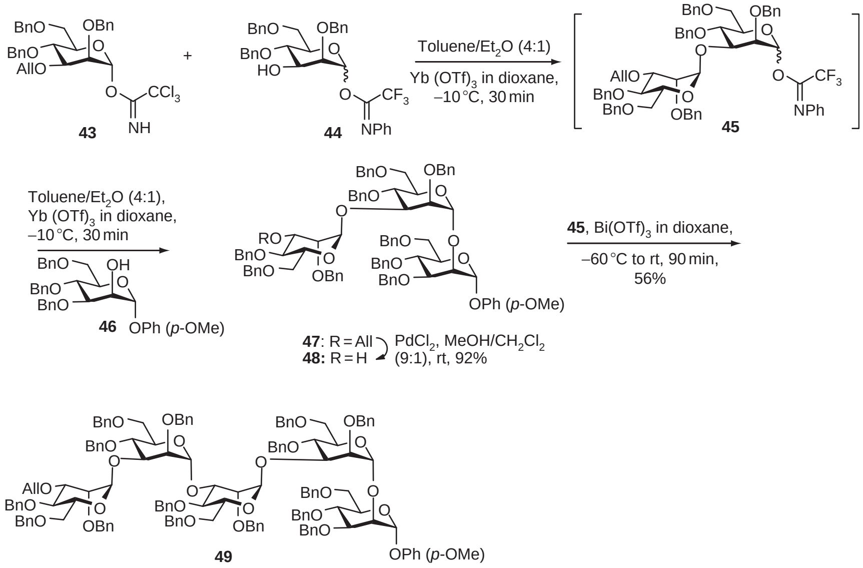
43
44
Toluene/Et$_2$O (4:1)
Yb (OTf)$_3$ in dioxane, −10 °C, 30 min
45
Toluene/Et$_2$O (4:1), Yb (OTf)$_3$ in dioxane, −10 °C, 30 min
46
47: R = All
48: R = H
PdCl$_2$, MeOH/CH$_2$Cl$_2$ (9:1), rt, 92%
45, Bi(OTf)$_3$ in dioxane, −60 °C to rt, 90 min, 56%
49

SCHEME 10. Combined use of trichloroacetimidates and *N*-phenyl trifluoroacetimidates.

O'Doherty and coworkers, shadowed by the groups of Feringa and Lee,[13,14] developed a *de novo* approach to glycosidic-bond formation that is ideally suited to the synthesis of α-mannans and which, of essence, completely avoids the issue of the use of neighboring-group participation.[15] In this chemistry, the Achmatowicz rearrangement of a 2-[2-(*t*-butyldimethylsiloxy)-1-hydroxyalkyl]furan, available in either enantiomeric modification by asymmetric dihydroxylation of 2-vinylfuran, gives, after protection as a *t*-butyloxycarbonyl derivative, the allylic carbonate **50**. Reaction of this derivative with benzyl alcohol in the presence of a palladium(0) catalyst affords the corresponding benzyl glycoside **51** with excellent yield, regio-, and stereo-selectivity (Scheme 11). Removal of the silyl ether then provides an alcohol **52** to be employed as nucleophile in a second palladium-catalyzed allylic substitution with the allylic carbonate **50**. Iteration of the desilylation, palladium-catalyzed coupling sequence then gave a trisaccharide **55**, sodium borohydride reduction of which took place with excellent stereoselectivity to give the equatorial triol **56**. Finally, osmium tetraoxide-mediated dihydroxylation took place with excellent selectivity on the opposite to the glycosidic bonds, giving the (1→6)-α-L-mannan **57** in excellent yield (Scheme 11).

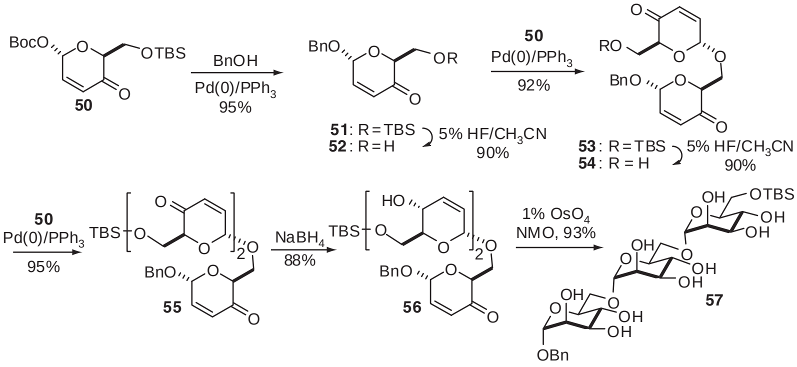
BocO
O
OTBS
O
50
BnOH
Pd(0)/PPh3
95%
BnO
OR
51: R = TBS
52: R = H
5% HF/CH3CN
90%
50
Pd(0)/PPh3
92%
RO
53: R = TBS
54: R = H
5% HF/CH3CN
90%
50
Pd(0)/PPh3
95%
TBS
2
55
NaBH4
88%
HO
56
1% OsO4
NMO, 93%
OH
OTBS
57
OBn

SCHEME 11. *De novo* synthesis of an α-(1→6)-L-mannan.

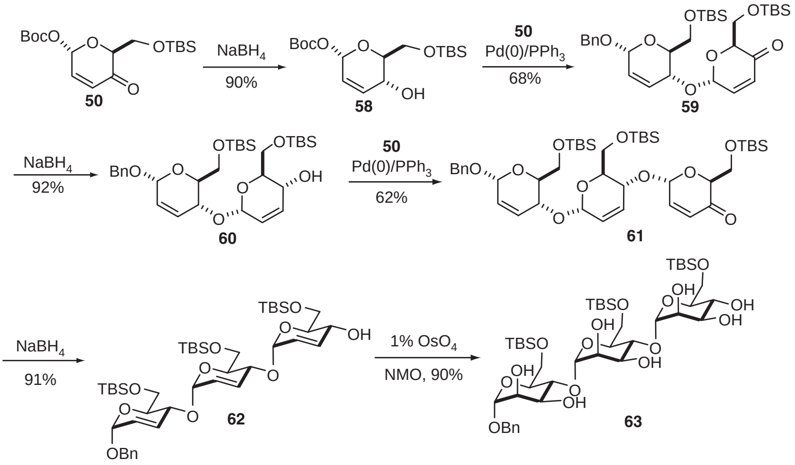
BocO
OTBS
50
NaBH4
90%
OH
58
50
Pd(0)/PPh3
68%
BnO
59
NaBH4
92%
60
50
Pd(0)/PPh3
62%
61
NaBH4
91%
TBSO
62
1% OsO4
NMO, 90%
OBn
63

SCHEME 12. *De novo* synthesis of an α-(1→4)-L-mannan.

α-(1→4)-L-Mannans were obtained by a modification in this protocol whereby the initial allylic carbonate **50** was reduced with sodium borohydride to afford an equatorial alcohol **58** ready for use as nucleophile in a subsequent palladium-catalyzed glycosylation reaction (Scheme 12). Iteration of the process gave a (1→4)-linked trisaccharide **62** that, when subjected to catalytic dihydroxylation, provided the target α-(1→4)-L-mannan **63**.[15]

2. Neighboring Group-Directed *α*-Mannan Synthesis

Somewhat predictably, in view of the ease with which α-mannopyranosides are formed with the aid of a participating 2-ester, most syntheses of α-mannans make use of the concept of neighboring-group participation. This being the case, the efficiency of any given synthesis is determined by the orchestration of the protecting-group strategy with the need generate glycosyl donors at the apposite moment.

The early synthesis of a branched mannohexoside described by Ogawa and Nukada[16] began with a tri-*O*-benzoyl allyl orthoaceate **64** that underwent stereospecific rearrangement to the allyl 2-*O*-acetyl α-mannoside **65** in the presence of TMSOTf (Scheme 11). Replacement of the acetyl group by the more-labile trichloroacetate was followed by liberation of the allyl glycoside with catalytic $PdCl_2$ and conversion of the resulting hemiacetal **68** into the anomeric chloride **69**. Coupling of this chloride with disaccharide **70** gave a branched tetrasaccharide **71** in 69% yield. Removal of the chloroacetate groups by treatment with thiourea was followed by a second coupling with the mannosyl chloride **69** to give the branched hexasaccharide **73** (Scheme 13).[16]

This is to be contrasted with a more convergent approach employed by the same group, but which necessarily eschews the use of neighboring-group participation. Here, the mannobiosyl chloride was coupled with the diol **70** with promotion by mercuric cyanide in the presence of 4 Å molecular sieves in 1,2-dichloroethane to give a 91% yield of a mixture of tetrasaccharides (not shown) and two hexasaccharides, one of which was the required all α-system. The second hexasaccharide, which

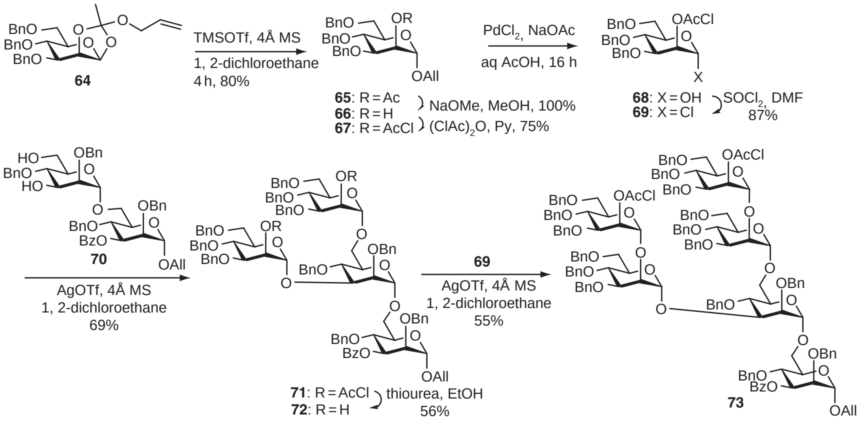
64
TMSOTf, 4Å MS
1, 2-dichloroethane
4 h, 80%
65: R = Ac
66: R = H
67: R = AcCl
NaOMe, MeOH, 100%
(ClAc)2O, Py, 75%
PdCl2, NaOAc
aq AcOH, 16 h
68: X = OH
69: X = Cl
SOCl2, DMF
87%
70
AgOTf, 4Å MS
1, 2-dichloroethane
69%
69
AgOTf, 4Å MS
1, 2-dichloroethane
55%
71: R = AcCl
72: R = H
thiourea, EtOH
56%
73
BnO
BzO
HO
OBn
OR
OAcCl
OAll
X
O

SCHEME 13. Early synthesis employing allyl glycoside to glycosyl chlorides.

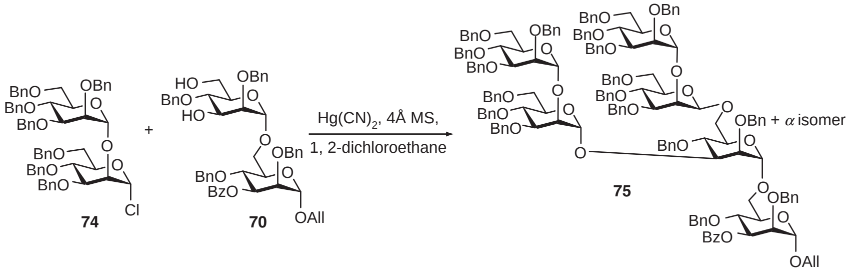

SCHEME 14. Inadvertent β-mannoside formation.

was obtained in a comparable amount, was determined to contain a β-mannopyranosyl linkage **75** (Scheme 14), thereby illustrating the failings of the classical Helferich-type glycosylation in the absence of neighboring-group participation.

In each of Ogawa and Nukada's syntheses, the glycosyl chlorides required for the coupling steps were obtained by a two-step protocol from the corresponding allyl glycosides, involving treatment with palladium chloride and sodium acetate to yield the hemiacetal, followed by reaction with the Vilsmeier combination of thionyl chloride and DMF originally introduced to carbohydrate chemistry by Hanessian.[17]

A variation on the general Ogawa strategy of the employment of allyl mannosides as glycosyl acceptors, with subsequent conversion to a mannosyl donor for application in a further coupling, has been widely adopted by the Kong group.[18–21] In the numerous mannan syntheses from this group the allyl glycoside is released in the standard manner with palladium chloride, and the resulting hemiacetal converted into the corresponding glycosyl trichloroacetimdate for use in the next iteration. One example of this kind began with the regioselective tritylation and silylation of allyl α-D-mannopyranoside leading, after benzoylation, to the glycoside **76** in high yield.[22] This monotritylation followed by a regioselective monsilylation is a useful variant on the 3,6-di-*O*-tritylation employed by Ogawa and Nukada in their α-mannan synthesis. Treatment of **76** with trifluoroacetic acid gave the 3,6-diol **77**, while exposure to tetrabutylammonium fluoride selectively afforded the 3-ol **81** (Scheme 15). Coupling of diol **77** with perbenzoyl mannopyranosyl trichloroacetimidate in the presence of TMSOTf gave the trimannan **79** in 85% yield, while application of the same donor to 3-ol **81** followed by removal of the trityl ether with an excess of TMSOTf afforded disaccharide **82** in 80% yield. Conversion of the allyl trisaccharide **79** to the corresponding trichloroacetimidate **80** was achieved in 80% yield for the two steps, and was followed by a final coupling with the allyl disaccharide **82** to

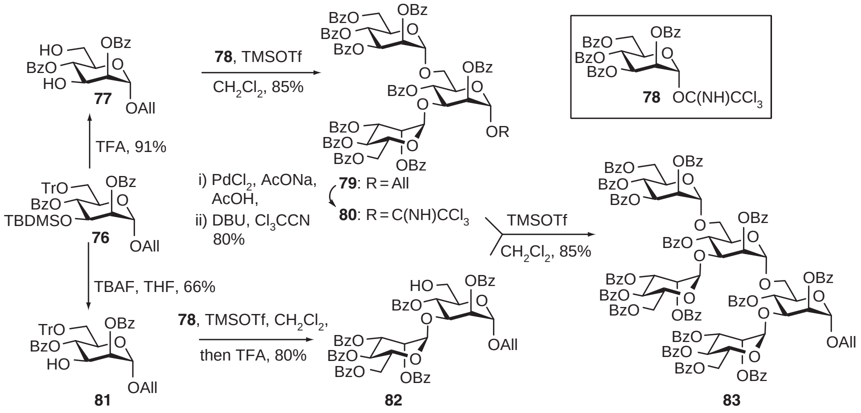

SCHEME 15. Block synthesis by means of allyl glycosides.

afford the doubly branched pentasaccharide **83** in 85% yield (Scheme 15). A number of other α-mannans were synthesized by the same group with subtle adaptation of the protecting-group strategy to the particular target.[22] Yet further variations on the theme of allyl glycoside to trichloroacetimidates have been employed by the Seeberger group in their synthesis of a phosphatidylinosityl mannan from *Mycobacterium tuberculosis*.[23]

The antiangiogenic α-(1→3)-pentamannan PI-88 has been assembled twice through the aegis of trichloroacetimidate donors bearing stereodirecting carboxylate esters at the 2-position. The synthesis of Ferro and coworkers proceeded in a linear fashion from the reducing terminus, employing 3-*O*-allyl-2,4,6-tri-*O*-benzoyl-α-D-mannopyranosyl trichloroacetimidate **84** as the key building block in a two-step iterative sequence of coupling and deallylation (Scheme 16).[24] Du and coworkers, on the other hand, used a block-synthesis approach, but had to fall back on the conversion of allyl glycosides to trichloroacetimidates in order to do so, thereby increasing the number of steps.[25]

A Fraser-Reid synthesis of biantennary mannans [26,27] exemplifies the protection of pentenyl glycosides as the corresponding vicinal dibromides, at which point they may be carried through a coupling reaction. Thus, the pentenyl 3,6-diol **93** was brominated and selectively chloroacetylated to give the acceptor **94** (Scheme 17) that was subsequently coupled with the 2-*O*-acetyl pentenyl glycoside **95** under activation with NIS/Et_3SiOTf to give the α-disaccharide **96** in 96% yield. Removal of the

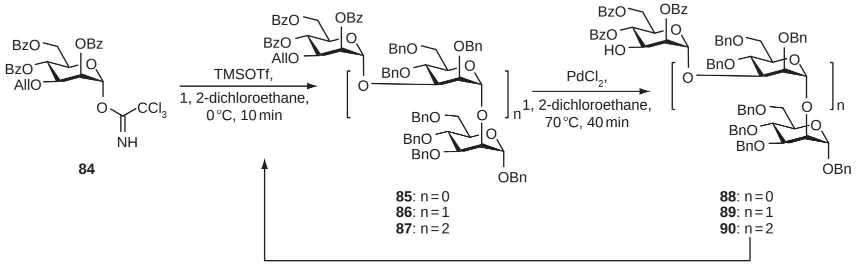
84
TMSOTf,
1, 2-dichloroethane,
0 °C, 10 min
85: n = 0
86: n = 1
87: n = 2
PdCl₂,
1, 2-dichloroethane,
70 °C, 40 min
88: n = 0
89: n = 1
90: n = 2

Acceptor	Glycosylation (% Yield)	Deallylation (% Yield)
Benzyl 3,4,6-tri-*O*-benzyl-α-D-mannopyranoside	**85** (84)	**88** (91)
88	**86** (90)	**89** (84)
89	**87** (94)	**90** (64)

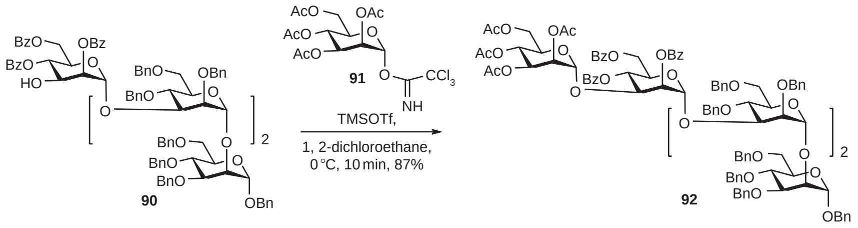
90
91
TMSOTf,
1, 2-dichloroethane,
0 °C, 10 min, 87%
92

SCHEME 16. Iterative synthesis of an α-(1→3)-D-mannan.

chloroacetate group and a second coupling with **95** then gave the trisaccharide **98** from which the two acetates were cleaved to yield diol **99**. Caution had to be exercised in the deacetylation stage to avoid elimination of HBr from the vicinal dibromide functionality, giving rise to the corresponding bromovinyl derivative. Double glycosylation of **99** with pentenyl glycoside **95** gave the pentasaccharide **100**. Treatment of this pentasaccharide with zinc and tetrabutylammonium bromide finally liberated the pentenyl pentasaccharide **101** (Scheme 17).

In a closely analogous manner a trisaccharide **102** was assembled and then coupled to pentenyl glycoside **95** to give the tetrasaccharide **103** in 72% yield (Scheme 18). Removal of the chloroacetate from this tetrasaccharide was followed by glycosylation with the pentenyl pentasaccharide **101** to give the branched nonasaccharide **105** in 57% yield (Scheme 18).

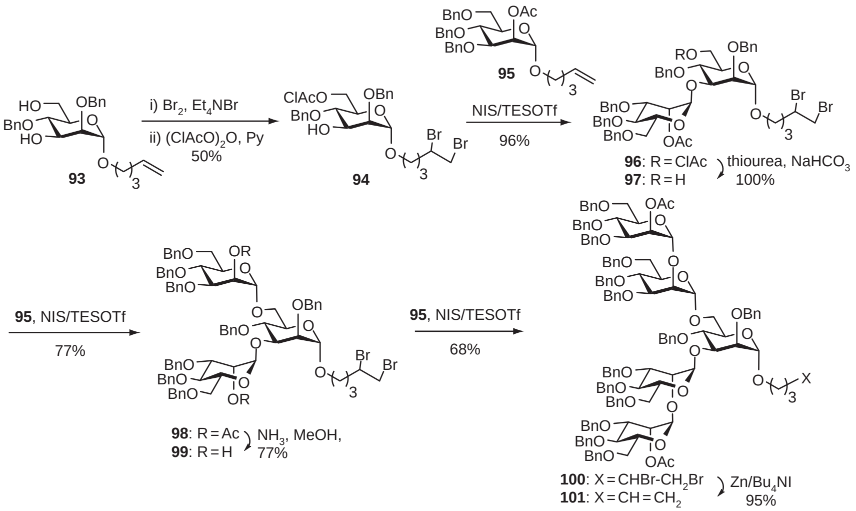

SCHEME 17. Pentenyl glycoside-based approach to a biantennary pentasaccharide.

1,2-Orthoesters have featured prominently in the neighboring-group participation-directed synthesis of α-mannans, including the work of Ogawa and Nukada, as they afford a ready means of selective preparation of 2-*O*-acyl mannopyranosyl donors. This is illustrated by the work of the Fraser-Reid group toward a series of glycolipids suitable for multivalent presentation.[28] In this example the pentenyl orthoester **106** was converted into the 3,4,6-tri-*O*-benzyl derivative **107** in the usual manner or was selectively silylated at the primary position followed by benzylation to give **110** (Scheme 19). Exposure of the tribenzyl orthoester to TBDMSOTf bought about rearrangement to the corresponding pentenyl 2-*O*-benzoate derivative **108** from which the ester was removed to provide a glycosyl acceptor **109**. The pentenyl orthoester **110** was directly coupled to this alcohol in 81% yield on activation by NIS in the presence of ytterbium triflate, thereby displaying the dual possibility of employing the orthoester as a precursor to a pentenyl glycoside by rearrangement, and as a glycosyl donor for an α-selective coupling depending on the Lewis acid and the presence or absence of an external alcohol. Removal of the benzoate ester from **111** set the stage for a second orthoester-type glycosylation to give the trisaccharide **113** (Scheme 19), which was ultimately manipulated into a number of phospholipid analogues by osmylation and derivatization, or metathesis followed by osmylation and derivatization.[28]

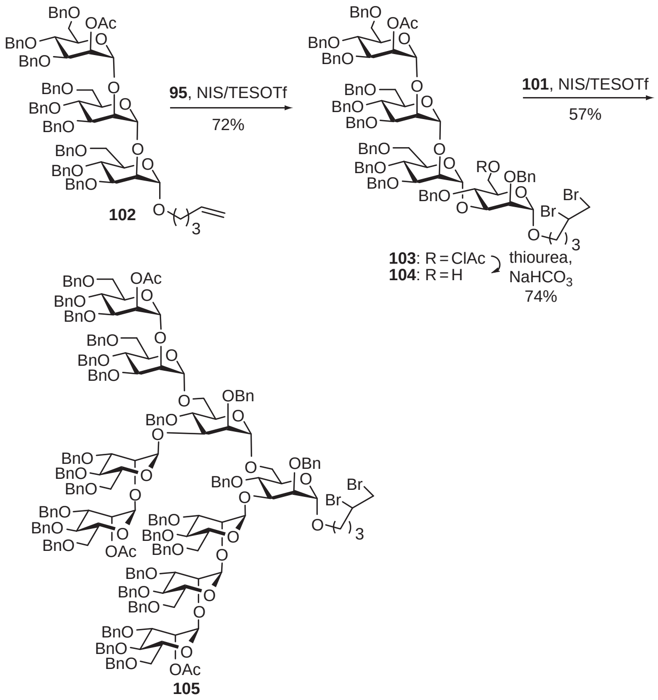

SCHEME 18. Pentenyl glycoside-based approach to a highly branched nonasaccharide.

Cyanoethylidene orthoesters were employed in α-mannan synthesis by Backinowsky and coworkers, in the first instance as a protecting group for a glycosyl donor, and subsequently as donor in a coupling reaction, resulting in a very efficient reaction scheme.[29] Thus, coupling of the cyanoethylidene derivative **114** with tetraacetyl α-D-mannopyranosyl bromide in the presence of mercuric cyanide and mercuric bromide in acetonitrile at room temperature directly afforded the branched trisaccharide **117** in 62% yield, whose remaining alcohol was acetylated to give **118** (Scheme 20).

Activation of trisaccharide cyanoethylidene derivative **118** with catalytic trityl perchlorate in the presence of a stiochiometric amount of the 3,6-di-*O*-trityl ether **119** afforded the tetrasaccharide **120** in 55% yield, whereas carrying out the same reaction with a half-molar equivalent of the bis trityl ether gave the heptasaccharide **121** in 60% yield (Scheme 21).

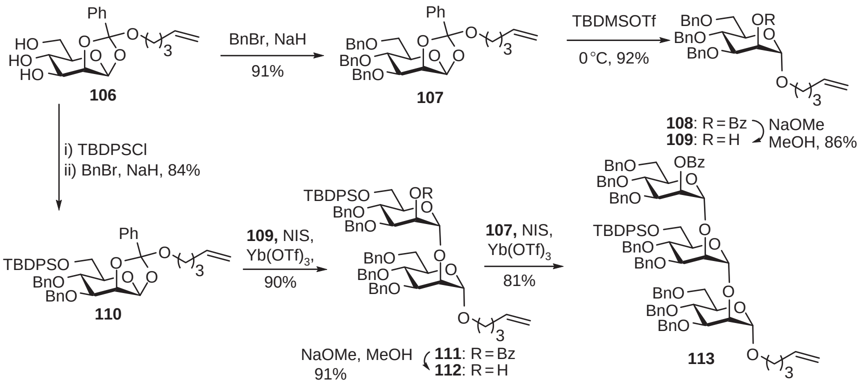
106
BnBr, NaH
91%
107
TBDMSOTf
0°C, 92%
108: R = Bz
109: R = H
NaOMe
MeOH, 86%
i) TBDPSCl
ii) BnBr, NaH, 84%
110
109, NIS,
Yb(OTf)3,
90%
NaOMe, MeOH
91%
111: R = Bz
112: R = H
107, NIS,
Yb(OTf)3
81%
113

SCHEME 19. Pentenyl orthoester approach to α-(1→2)-mannans.

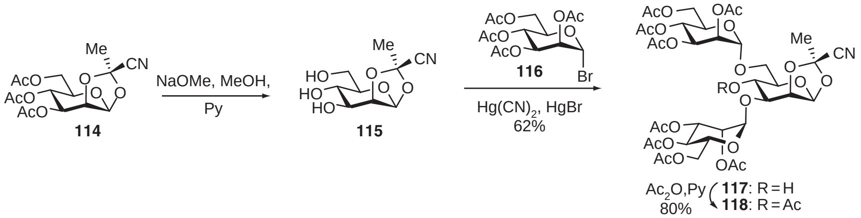
114
NaOMe, MeOH,
Py
115
116
Hg(CN)2, HgBr
62%
Ac2O,Py
80%
117: R = H
118: R = Ac

SCHEME 20. Use of a cyanoorthoacetate-protected acceptor.

An interesting twist on the orthoester approach was uncovered by Fraser-Reid and coworkers in which it was revealed that a 4-pentenyl orthobenzoate **123**, on activation with ytterbium triflate in dichloromethane, was able to selectively glycosylate the primary hydroxyl group in a mannopyranosyl 2,6-diol **122**. Treatment with a 2-*O*-benzoyl mannosyl trichloroacetimidate **126** in diethyl ether with the same promoter then introduced a second α-mannosidic linkage to the remaining secondary hydroxyl group (Scheme 22).[30] This selectivity pattern was central to the development of a very efficient synthesis of a branched pentadecamannan **129**.

In another synthesis of a nonamannan, Seeberger and coworkers preferred the use of trichloroacetimidates as glycosyl donors.[31] This opus began with the pentenyl *β*-mannoside **131**, which was constructed in 10 steps from D-glucal via a route involving *β*-glucosylation, oxidation, and reduction typical of classical routes to the *β*-mannosides. Neighboring group-directed coupling with the trichloroacetimidate **130** and removal of the triisopropylsilyl ether provided the alcohol **133**, ready to

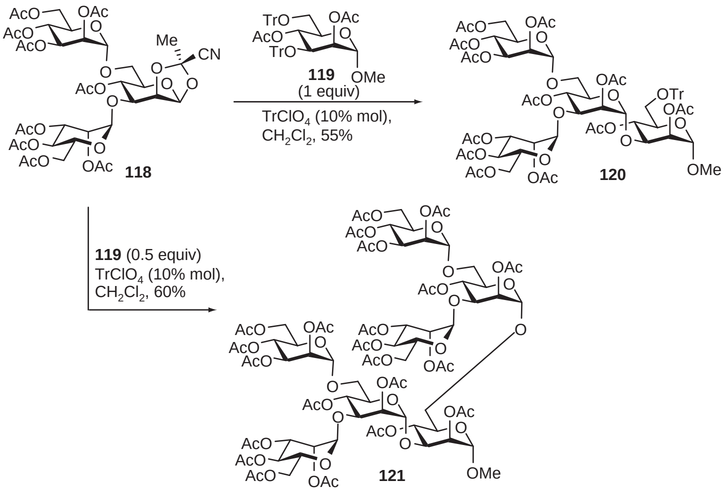

SCHEME 21. Use of a cyanoorthoacetate as donor.

accept a second donor (Scheme 23). The second coupling was again conducted by the trichloroacetimidate method, but without neighboring-group participation and afforded the trisaccharide **135**. Saponification then enabled removal of the three carboxylate esters and gave a triol **136**, which was subjected to treatment with an excess of donor **130** and TBSOTf in ether, leading to the formation of the hexasaccharide **137** in 94% yield. Further treatment with sodium methoxide removed the three newly introduced acetate esters and final exposure to trichloroacetimidate **130** and TBSOTf gave the target nonasaccharide **139** in 80% yield (Scheme 23).[31]

Lam and Gervay-Hague obtained a selectively protected 2,4-di-*O*-benzyl mannopyranoside acceptor **144** in several steps, beginning with the borane-THF reduction of methyl 2,3;4,6-di-*O*-benzylidene-α-D-mannopyranoside (Scheme 24).[32] With the endo-phenyl isomer illustrated the 2,4-di-benzyl ether is obtained in good yield and selectivity. It must be noted, however, that borane reduction of the exo-phenyl isomer gives exclusively the 3,4-di-benzyl ether, thereby somewhat diminishing the utility of this method, as the endo- and exo-isomers are invariably formed together. This regioselective opening of the 1,2-*O*-benzylidene acetal is thus related to the partial hydrolysis of mannopyranosyl 1,2;4,6-di-orthobenzoates reported by Oscarson, which gives the 2,6-dibenzoate ester preferentially with moderate selectivity over the corresponding 2,4-dibenzoate.[33]

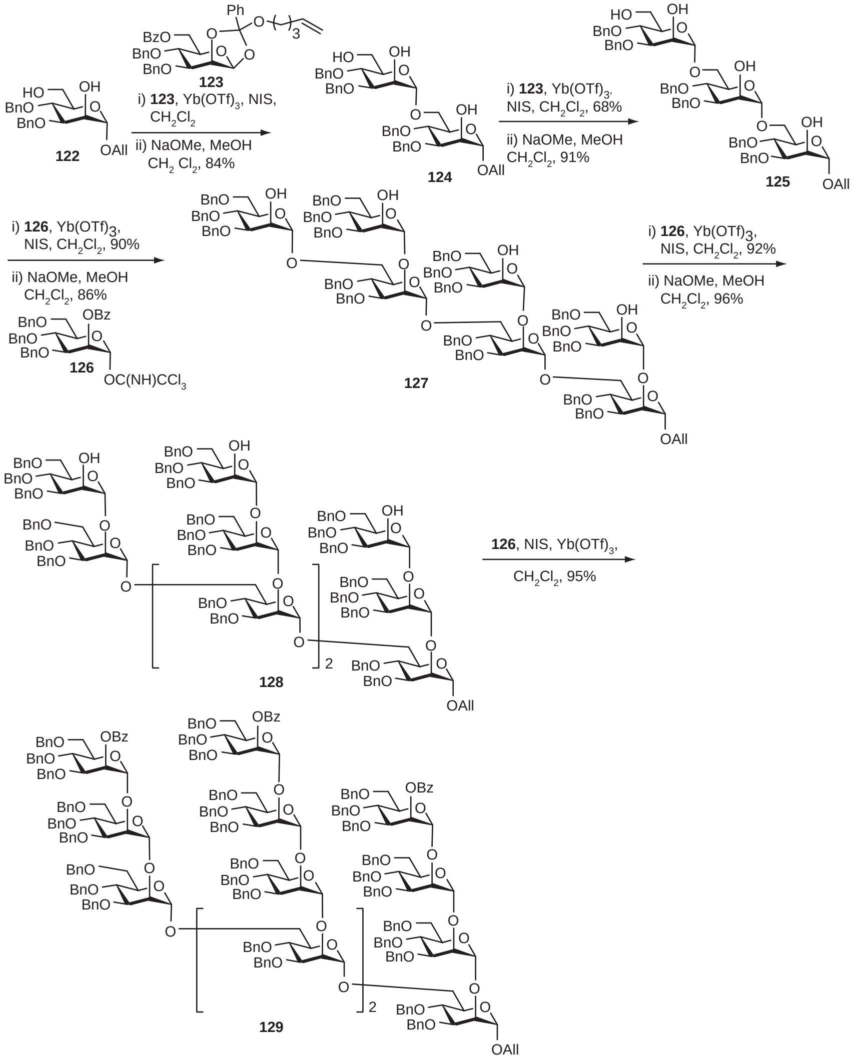
122
123
i) 123, Yb(OTf)3, NIS, CH2Cl2
ii) NaOMe, MeOH CH2 Cl2, 84%
124
i) 123, Yb(OTf)3, NIS, CH2Cl2, 68%
ii) NaOMe, MeOH CH2Cl2, 91%
125
i) 126, Yb(OTf)3, NIS, CH2Cl2, 90%
ii) NaOMe, MeOH CH2Cl2, 86%
126
127
i) 126, Yb(OTf)3, NIS, CH2Cl2, 92%
ii) NaOMe, MeOH CH2Cl2, 96%
128
126, NIS, Yb(OTf)3, CH2Cl2, 95%
129

SCHEME 22. Pentenyl orthoester-based approach to an undecasaccharide.

Continuing on with their synthesis of biantennary mannans, Lam and Gervay-Hague treated diol **144** with the mannosyl iodide **145**, obtained in quantitative yield from the corresponding 1,2-(ethoxyethylidene) orthoester with trimethylsilyl iodide, and silver triflate in dichloromethane at −40 °C to gain access to the α,α-trisaccharide

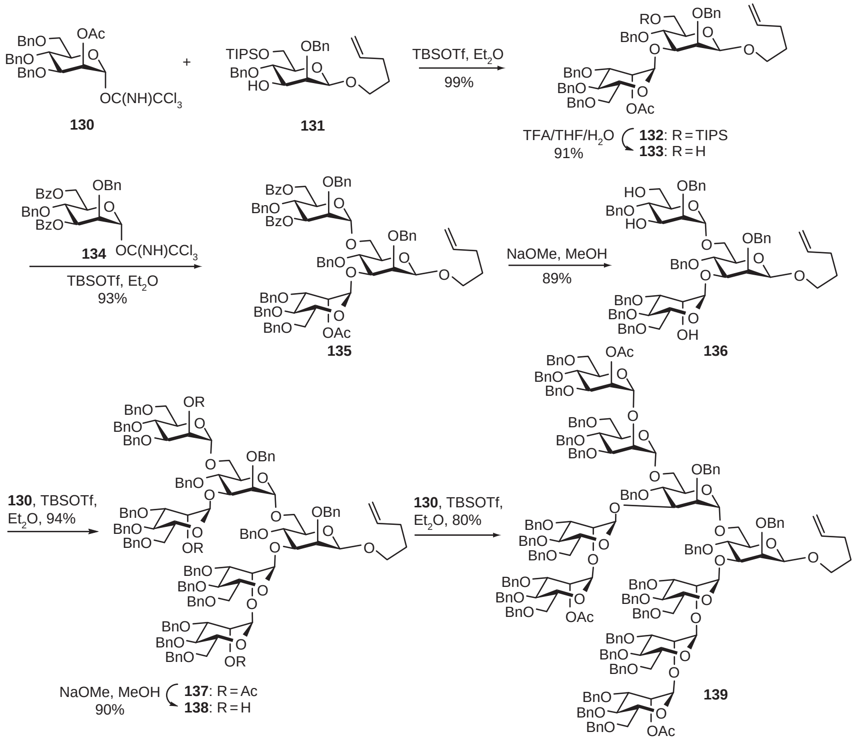
130
131
TBSOTf, Et$_2$O
99%
TFA/THF/H$_2$O
91%
132: R = TIPS
133: R = H
134
TBSOTf, Et$_2$O
93%
135
NaOMe, MeOH
89%
136
130, TBSOTf, Et$_2$O, 94%
137: R = Ac
138: R = H
NaOMe, MeOH
90%
130, TBSOTf, Et$_2$O, 80%
139

SCHEME 23. Nonamannan synthesis by the trichloroacetimidate method.

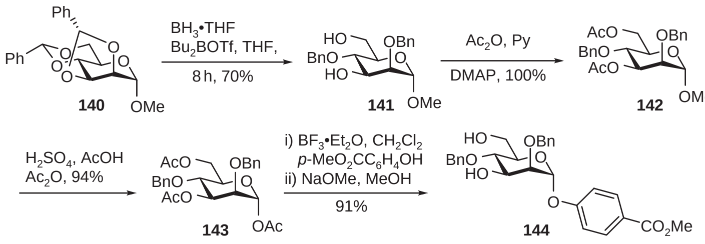
140
BH$_3$•THF
Bu$_2$BOTf, THF,
8 h, 70%
141
Ac$_2$O, Py
DMAP, 100%
142
H$_2$SO$_4$, AcOH
Ac$_2$O, 94%
143
i) BF$_3$•Et$_2$O, CH$_2$Cl$_2$
p-MeO$_2$CC$_6$H$_4$OH
ii) NaOMe, MeOH
91%
144

SCHEME 24. Chemoselective cleavage of a 2,3;4,6-di-benzylidene acetal.

146 in 91% yield (Scheme 25).[32] According to the authors, silver-mediated couplings conducted in this manner proceed significantly faster than analogous reactions with the corresponding glycosyl chlorides. Zemplén deesterification of the two acetates

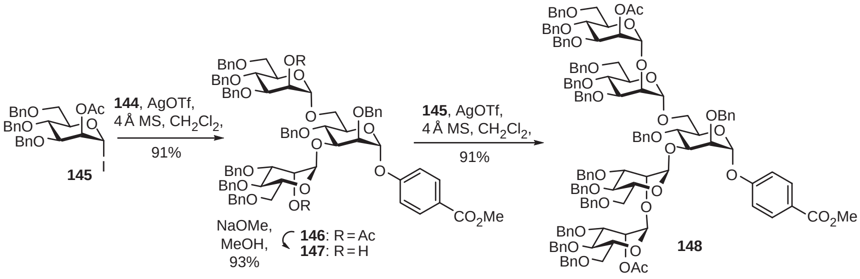
145
144, AgOTf, 4 Å MS, CH2Cl2, 91%
NaOMe, MeOH, 93%
146: R = Ac
147: R = H
145, AgOTf, 4 Å MS, CH2Cl2, 91%
148
BnO
OAc
OR
OBn
CO2Me

SCHEME 25. Use of a mannosyl iodide as donor.

gave the diol **147**, to which a further two α-mannosides were appended with mannosyl iodide **145** in the same manner to give the pentasaccharide **148** in 91% yield.[32]

Preliminary to a second-generation synthesis of the 3-*O*-methyl-α-(1→4)-mannans, Kishi and co-workers screened a series of mannosyl phosphates for the influence of the O-2 protecting group and the anomeric stereochemistry of the donor on the outcome of the glycosylation reaction. As may be seen from Scheme 26, the use of benzyl ether protection under these homogeneous solution-phase conditions gave selectivities that were insufficient, whereas the 2-benzoates gave exquisite α-selectivity.[34]

Armed with this knowledge, an allyl 2-*O*-benzoyl 4-*O*-triisopropylsilyl mannoside **149** ($n = 1$) was constructed as a single building block for employment in the α-(1→4)-mannan synthesis. Treatment of this building block with Wilkinson's catalyst and DABCO in a mixture of ethanol and toluene at reflux brought about isomerization of the allyl ether to the corresponding enol ether, which was then cleaved with iodine in wet THF (Scheme 27). Reaction of the thus-formed hemiacetal with dibenzyl *N*,*N*-diethylphosphoramidite followed by oxidative workup with hydrogen peroxide afforded the glycosyl donor **150** ($n = 1$). Desilylation of building block **149** ($n = 1$) with Bu_4NF afforded the glycosyl acceptor **151** ($n = 1$) that was then coupled with the phosphate **150** ($n = 1$) by exposure to TBSOTf leading to the formation of the disaccharide **152** ($n + m = 2$) with greater than 20:1 $\alpha:\beta$ selectivity. This disaccharide building block could then be converted into either a glycosyl phosphate or a glycosyl acceptor in a similar manner to the monosaccharide **149**, thereby affording access to an efficient block-synthesis approach to the α-(1→4)-mannan, marred only by the cumbersome multistep transformation of the allyl glycoside to the glycosyl phosphate (Scheme 27). Iterations of this process enabled preparation of an eicosaccharide with impressive yields and >20:1 $\alpha:\beta$ selectivity at each of the coupling steps.[34]

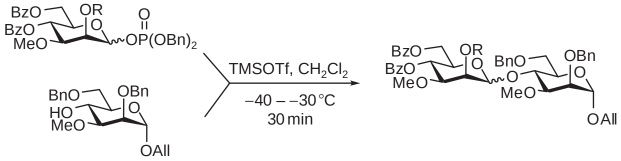
BzO
BzO
MeO
OR
O
O
OP(OBn)$_2$
BnO
HO
MeO
OBn
O
OAll
TMSOTf, CH$_2$Cl$_2$
−40 – −30 °C
30 min
BzO
BzO
MeO
OR
O
BnO
O
MeO
OBn
O
OAll

Donor R	Stereochemistry	Glycosylation Yield (%)	α:β Ratio
Bn	α	92	1.3:1
Bn	β	93	1.2:1
Bz	α	90	>20:1
Bz	β	91	>20:1

SCHEME 26. Influence of the O-2-protecting group and anomeric stereochemistry on glycosylation.

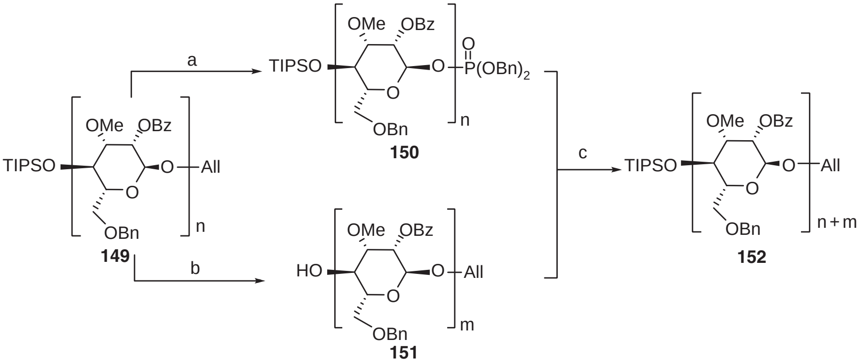
a
TIPSO
OMe
OBz
O
O
P(OBn)$_2$
O
OBn
n
150
TIPSO
OMe
OBz
O
All
O
OBn
n
149
b
HO
OMe
OBz
O
All
O
OBn
m
151
c
TIPSO
OMe
OBz
O
All
O
OBn
n+m
152

150 *n*	**151** *m*	**152** *n* + *m*	Glycosylation Yield (α only)
1	1	2	90%
2	2	4	87%
4	2	6	85%
4	4	8	83%
8	2	10	80%
8	4	12	78%
8	6	14	83%
8	8	16	75%
12	6	18	80%
12	8	20	76%

Reagent and conditions: (a) (1) $(Ph_3P)_3RhCl$, Dabco, EtOH/toluene, reflux, followed by treatment with I_2, THF/CH_2Cl_2/H_2O, 80–88%. (2) $Et_2NP(OBn)_2$, 1*H*-1,2,4-triazole, $NaHCO_3$, CH_2Cl_2, followed by workup with 30% H_2O_2, THF/CH_2Cl_2, 83–89%. (b) TBAF, THF, 83–92%. (c) TBSOTf, −40→−30 °C, 30 min, CH_2Cl_2.

SCHEME 27. Iterative synthesis of an α-(1→4)-eicomannan.

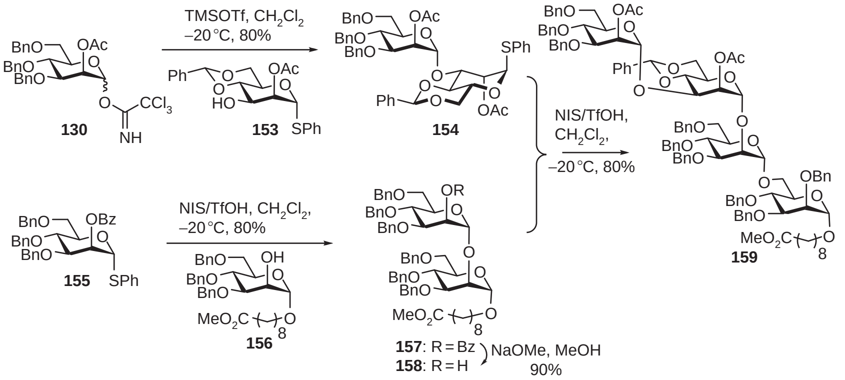
TMSOTf, CH_2Cl_2, −20 °C, 80%
130
153
154
NIS/TfOH, CH_2Cl_2, −20 °C, 80%
155
156
157: R = Bz
158: R = H
NaOMe, MeOH 90%
NIS/TfOH, CH_2Cl_2, −20 °C, 80%
159

SCHEME 28. Combined use of trichloroacetimidate and thioglycoside donors.

The compatibility of thioglycosides with the conditions for the trichloroacetimidate glycosylation protocol was exploited by Mallet and co-workers in their block synthesis of a potential tetramannan marker for Crohn's disease.[35] Thus, activation of trichloroacetimidate **130** in the presence of the monohydroxy thioglycoside **153** gave the α disaccharide **154** in 89% yield (Scheme 28). A second disaccharide **157** was constructed from the thioglycoside **155** and acceptor **156** on activation with *N*-iodosuccinimide and triflic acid (Scheme 28). Following cleavage of the benzoate from this latter species, it was coupled with the thiodisaccharide **154**, also with activation by NIS/TfOH to give the tetrasaccharide **159** in 80% yield.

Exploiting their observation that in an otherwise identical thioglycoside, a free 2-OH group confers greater reactivity than an ether-protected O-2 on activation with *N*-iodosuccinimide, Wong and co-workers investigated the autocondensation of the 2-hydroxythioglycoside **160** over a range of temperature and reaction times. Operating at −50 °C and with 0.7 equivalents of NIS, the reaction could be optimized to give 70% of the disaccharide **161** along with only 5% of the trisaccharide **162**. On the other hand, at −40 °C and with the shorter reaction time of 1 h, as much as 30% of the trisaccharide could be obtained, albeit accompanied by 38% of the disaccharide (Scheme 29). The use of higher temperatures resulted in diminished yield of either product owing to the onset of polymerization.[36]

After adjustment of the protecting groups, the thiotrisaccharide **163** was coupled to a series of further acceptors, with *N*-iodosuccinimide and triflic acid, to yield, for example, the heptasaccharide **165** in 63% yield (Scheme 30).[36]

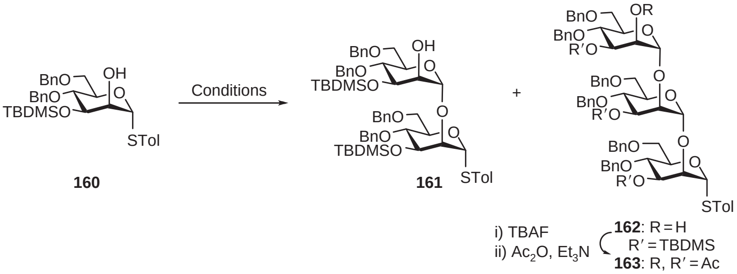
Conditions
160
161
+
STol
i) TBAF
ii) Ac₂O, Et₃N
162: R = H
R′ = TBDMS
163: R, R′ = Ac

T (°C)	NIS (Molar Equiv.)	*T* (h)	161 (% Yield)	162 (% Yield)
−50	0.7	24	70[a]	5[a]
−40	0.6	1	38	30

[a] Based on recovered starting material.

SCHEME 29. Controlled oligomerization of a hydroxythioglycoside.

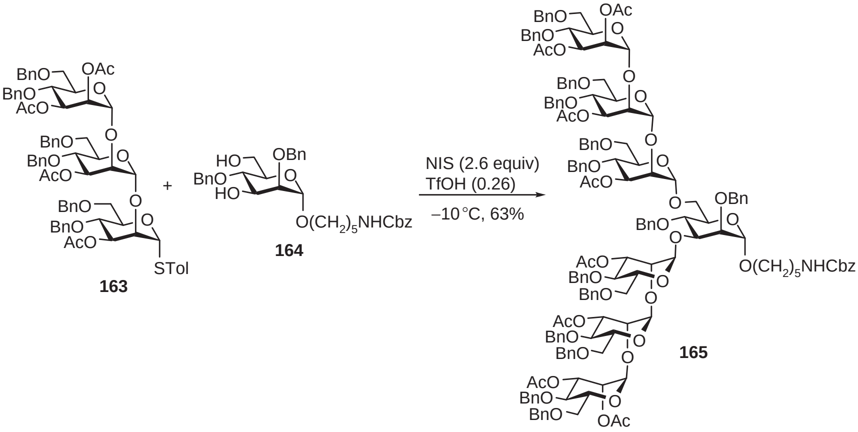
163
+
164
NIS (2.6 equiv)
TfOH (0.26)
−10 °C, 63%
165
O(CH₂)₅NHCbz

SCHEME 30. Completion of a heptasaccharide.

The concept of preactivation of a thioglycoside with a sulfenyl triflate or related reagent leading to the formation of a highly reactive glycosyl triflate,[37] as introduced originally by Kahne for glycosyl sulfoxides[38] and adapted to thioglycosides by Crich,[39] permits an even simpler strategy using a single type of thioglycoside. This approach has been productively applied by Huang and coworkers to a branched pentamannan. Thus, reaction of the *S*-tolyl thioglycoside **166** with toluene sulfenyl triflate, preformed from the sulfenyl chloride and silver triflate, in ether at −78 °C followed by the addition of the diol **167** gave the α,α-trisaccharide **168**. After removal of the two acetates, a second glycosylation reaction under the same conditions gave the pentasaccharide **170** in good overall yield (Scheme 31).[40]

This is to be contrasted with a block-synthesis approach to the same target in which Huang and his co-workers noted a highly unusual β-selective coupling in the key step. The synthesis began uneventfully with the preactivation of donor **166** and coupling to the monohydroxy thioglycoside **171** in 63% yield and the anticipated α-selectivity. However, combination of the thiodisaccharide **172** with diol **167** gave two major products, the anticipated all α-pentasaccharide **170** and the somewhat unexpected isomer **173** with two β-mannoside linkages. Curiously, this last product predominated and no mention was made the two intermediate isomers containing a single β-mannoside (Scheme 32).

Jiang and Chan employed a monomethylpolyethylene glycol-supported (MPEG) glycoside in the synthesis of a branched mannan, taking advantage of the ability of the MPEG chain to retain its conjugates at the baseline on silica gel chromatography while less-polar impurities are eluted.[41] Elution with methanol–dichloromethane mixtures then permits isolation of the MPEG glycosides. Thus, activation of thioglycoside **178** with NIS and TMSOTf in dichloromethane at 0 °C in the presence of the MPEG glycoside **177** gave the trisaccharide **179** (Scheme 33) after filtration on silica gel. Saponification was followed by further glycosylation under the same conditions leading to the pentasaccharide **181**.[41]

Furneaux and coworkers carried out a comparative study of the synthesis of an α-(1→6)-mannan, using both a phenyl glycoside **183** and an MPEG glycoside **184** as acceptor, by the trichloroacetimidate method (Scheme 34). It was generally found that

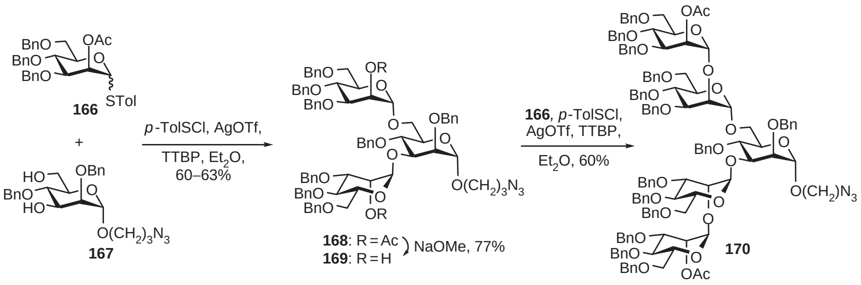

SCHEME 31. Thioglycoside activation with a sulfenyl chloride/silver triflate combination.

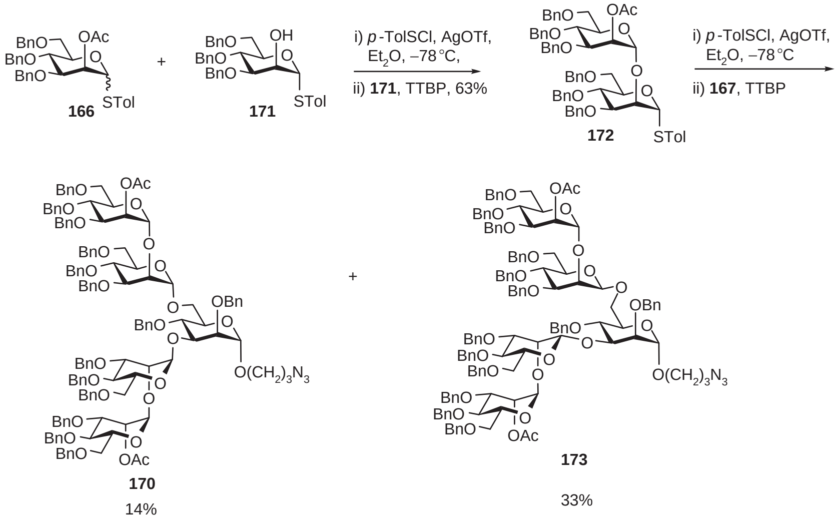
166
171
i) p-TolSCl, AgOTf, Et$_2$O, −78 °C,
ii) 171, TTBP, 63%
172
i) p-TolSCl, AgOTf, Et$_2$O, −78 °C
ii) 167, TTBP
O(CH$_2$)$_3$N$_3$
170
14%
173
33%

SCHEME 32. Unanticipated β-mannoside synthesis.

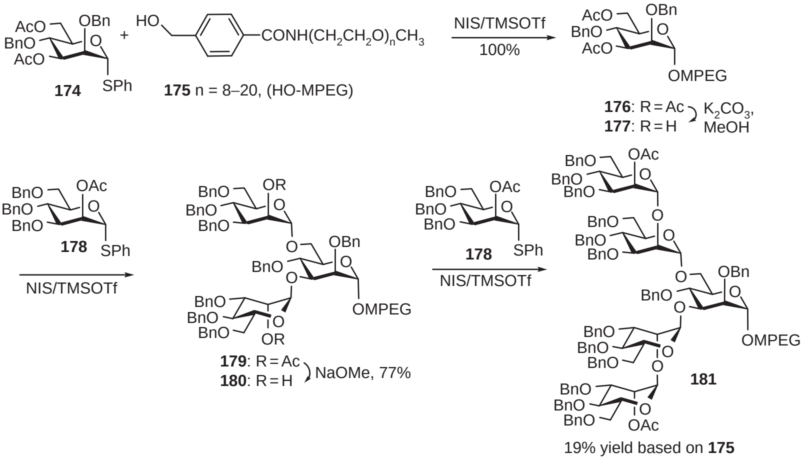
174
175 n = 8–20, (HO-MPEG)
HO–CH$_2$–C$_6$H$_4$–CONH(CH$_2$CH$_2$O)$_n$CH$_3$
NIS/TMSOTf
100%
OMPEG
176: R = Ac
177: R = H
K$_2$CO$_3$, MeOH
178
NIS/TMSOTf
179: R = Ac
180: R = H
NaOMe, 77%
178
NIS/TMSOTf
181
19% yield based on 175

SCHEME 33. MPEG-Supported pentamannan synthesis.

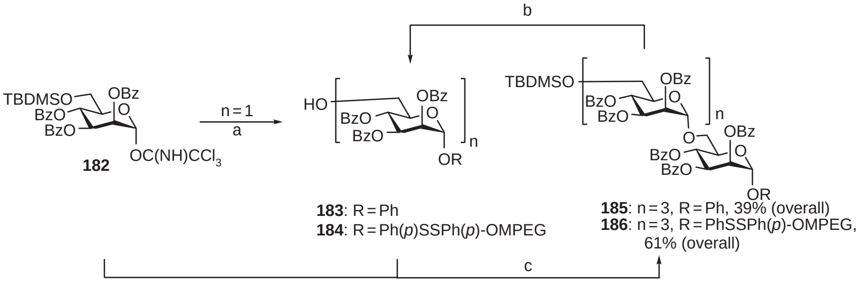
b
TBDMSO
OBz
BzO
BzO
O
OC(NH)CCl3
182
n = 1
a
HO
OBz
BzO
BzO
O
OR
n
TBDMSO
OBz
BzO
BzO
O
n
O
OBz
BzO
BzO
O
OR
183: R = Ph
184: R = Ph(p)SSPh(p)-OMPEG
185: n = 3, R = Ph, 39% (overall)
186: n = 3, R = PhSSPh(p)-OMPEG, 61% (overall)
c

Reagents and conditions: (a) Phenol, TMSOTf, or HOPh(*p*)SSPh(*p*)-OMPEG, BF_3•Et_2O, CH_2Cl_2; (b) AcOH, H_2O; (c) TMSOTf, CH_2Cl_2

SCHEME 34. Comparison of MPEG-supported and solution-phase syntheses for the preparation of an α-(1→6)-mannan.

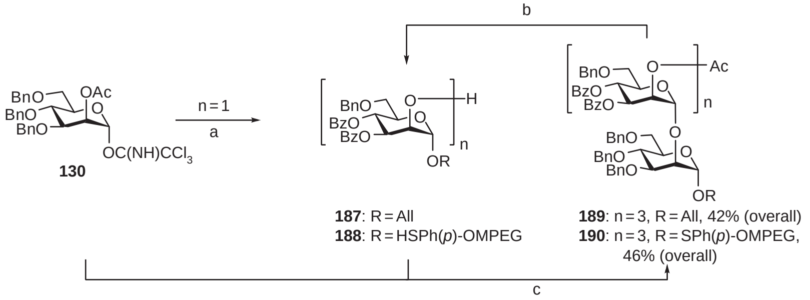
b
BnO
OAc
BnO
BnO
O
OC(NH)CCl3
130
n = 1
a
BnO
O
H
BzO
BzO
O
OR
n
BnO
O
Ac
BzO
BzO
O
n
O
BnO
BnO
BnO
O
OR
187: R = All
188: R = HSPh(p)-OMPEG
189: n = 3, R = All, 42% (overall)
190: n = 3, R = SPh(p)-OMPEG, 46% (overall)
c

Reagents and conditions: (a) (i) AllOH, TMSOTf, or HOPh(*p*)SSPh(*p*)-OMPEG, BF_3•Et_2O, CH_2Cl_2; (ii) DBU, MeOH; (b) DBU, MeOH; (c) TMSOTf, CH_2Cl_2

SCHEME 35. Comparison of MPEG-supported and solution-phase syntheses for the preparation of an α-(1→2)-mannan.

both syntheses proceeded with comparable ease, but that the MPEG-supported method facilitated purification, both chromatographically and by crystallization (Scheme 34).[42]

A similar comparison was conducted for the synthesis of an α-(1→2)-mannan, but using a different, thioglycoside-derived MPEG derivative as acceptor (Scheme 35). Interestingly, while no problems were reported with the standard solution-phase approach, it was noted that appreciable amounts of an α-mannoside (**190**, $n = 3$) were formed at the level of the disaccharide in the MPEG-supported approach.[42] A further variation on the PEG-supported approach to the α-(1→2)-mannan has also been described by Wu and Guo, who used a 2-levulinate-protected trichloroacetimidate as the mannosyl donor.[43]

An approach to the α-(1→6)-mannan employing an "ionic liquid" tag to facilitate purification has been described recently. In this chemistry[44] imidazolium-labeled glycosyl fluoride **191** was coupled with the monohydroxy thioglycoside **192** under activation with dicyclopentadienylhafnium dichloride in dichloromethane at room temperature to afford the disaccharide **193** in 92% yield (Scheme 36). Somewhat analogously to the MPEG-supported approach, purification of the imidazolium-labeled product was achieved by washing with diethyl ether. After removal of the imidazolium-labeled ester, an alcohol **194** was obtained that was employed as acceptor in a subsequent coupling to give a trisaccharide **195**. A further iteration of the same protocol eventually gave a thiotetrasaccharide **198**.

α-Mannans have also been prepared on the solid phase. Thus, Rademann and Schmidt prepared a polystyrene-supported thiol **199** and coupled it to the α-mannosyl

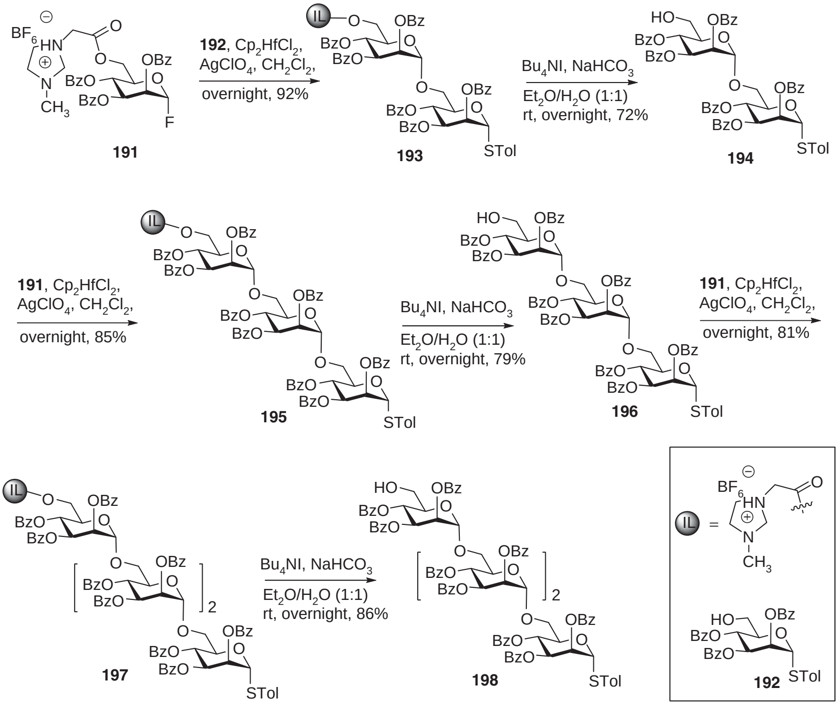
191
192, Cp2HfCl2, AgClO4, CH2Cl2, overnight, 92%
193
Bu4NI, NaHCO3 Et2O/H2O (1:1) rt, overnight, 72%
194
191, Cp2HfCl2, AgClO4, CH2Cl2, overnight, 85%
195
Bu4NI, NaHCO3 Et2O/H2O (1:1) rt, overnight, 79%
196
191, Cp2HfCl2, AgClO4, CH2Cl2, overnight, 81%
197
Bu4NI, NaHCO3 Et2O/H2O (1:1) rt, overnight, 86%
198
IL =
192

SCHEME 36. Use of an ionic tag to facilitate purification.

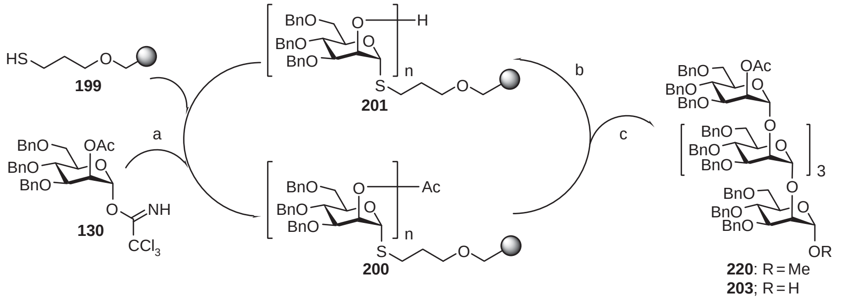

(a) **130** (3 equiv), TMSOTf (0.3 equiv), CH_2Cl_2; (b) NaOMe/CH_2Cl_2; (c) NBS (4 equiv), THF/MeOH (9:1) or acetone/water (9:1).

SCHEME 37. α-(1→2)-mannan synthesis with a polymer-supported acceptor.

trichloroacetimidate **130** under neighboring-group participation conditions with TMSOTf as promoter, followed by deacetylation with sodium methoxide in dichloromethane to liberate an acceptor **201** ($n = 1$). Three iterations of the protocol lead to a polymer-bound α-(1→2)-mannotetraose **200** ($n = 4$) that was cleaved from the support with *N*-bromosuccinimide in methanolic tetrahydrofuran or wet acetone (Scheme 37).[45]

A (1→2)-α-mannopentaosyl lipid, closely related to **202**, was constructed by Whitfield and coworkers by a pathway analogous to that of Scheme 37 but under more traditional solution-phase conditions, using the trichloroacetimidate donor **130** and 1,2-di-*O*-(geranylgeranyl)glycerol (achaeol) as the first acceptor.[46]

In later work, Grathwohl and Schmidt prepared an α-(1→2)-mannohexaoside **208** by a related protocol in which the initiating acceptor **204** was tethered to the support by means of an ester at O-6 (Scheme 38). A trichloroacetimidate-based donor **205** was again used in this iterative protocol, but the O-2 protecting group employed, somewhat unusually,[47] was the 9-fluorenylmethylcarbonate.[48] It is not clear whether the 9-fluorenylmethyl group directs the α-mannosylation reaction actively by neighboring-group participation or not.

In another variation on the same theme Seeberger and coworkers employed 2-*O*-acetyl-3,4,6-tri-*O*-benzyl-α-D-mannopyranosyl trichloroacetimidate **130** to construct the α-(1→2)-mannoheptaose **209** bound to the support by means of a *cis*-4-octenyl linker.[49] Cleavage from the resin was achieved with the first-generation Grubb's metathesis catalyst in the presence of ethylene, ultimately leading to the isolation of the heptasaccharide **210** in the form of a pentenyl glycoside ready for further transformations (Scheme 39).

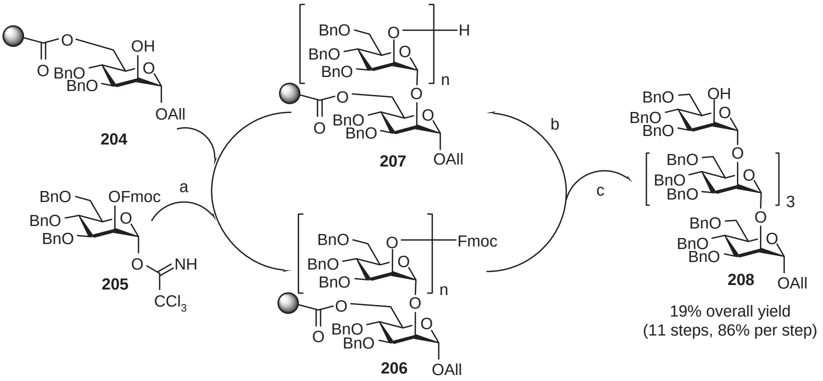

(a) TMSOTf, CH_2Cl_2; (b) Et_3N/CH_2Cl_2 (4:1); (c) NaOMe, CH_2Cl_2/MeOH (9:1).

SCHEME 38. α-(1→2)-mannan synthesis with a polymer-supported donor.

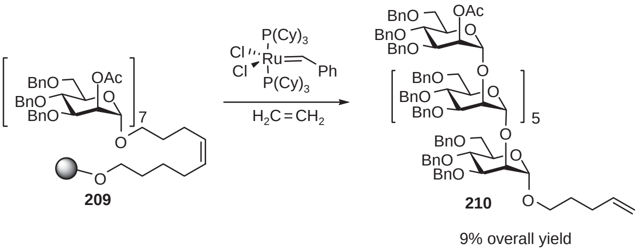

SCHEME 39. Conversion of a 4-octenyl linker to a pentenyl glycoside.

3. Synthesis of α-Rhamnans

The α-rhamnans, both D- and L-, have been accessed by many of the methods employed to synthesize the α-mannans, with and without the aid of neighboring-group participation. Accordingly, the various syntheses of the α-rhamnans described in the literature have been collated in Tables I and II.

In addition to the foregoing syntheses employing classical glycosylation strategies, ingenious approaches have also been devised to the α-rhamnans by O'Doherty[96,97] using palladium-mediated allylation reactions followed by osmylation corresponding to his α-mannan syntheses described in Schemes 11 and 12. As with the α-mannan syntheses, the α-rhamnan assembly begins by Achmatowicz rearrangement of a substituted furan. Thus, exposure of 2-(1-hydroxyethyl)furan to *N*-bromosuccinimide

TABLE I
α-Rhamnan Synthesis in the Absence of Neighboring-Group Participation

α-Rhamnan	**Coupling Method and Activating Agent**	**References**
[L-Rhap-(1→4)-α]$_5$	TCA[a], BF$_3$·OEt$_2$; Thiorhamnoside, DMTST[b]	50
[L-Rhap-(1→4)-α]$_6$	Rhamnosyl chloride, α-methylstyrene; Thiorhamnoside, PhSeOTf	51
2,3-*O*-CMe$_2$–4-*O*-Ac-L-Rha*p*-[(1→4)-α-2,3-*O*-CMe$_2$-L-Rha*p*]$_3$	Rhamnosyl hemiacetal, Ph$_2$SO[c], Tf$_2$O	52
β-Ant[d]-(1→3)-α-L-Rha*p*-(1→3)-α-L-Rha*p*-(1→2)-α-L-Rha*p*-OPent[e]	Thiorhamnoside, Ph$_2$SO, Tf$_2$O, TTBP[f]; Thioanthroside, NIS, TfOH	53
β-Ant[d]-(1→3)-α-L-Rha*p*-(1→3)-α-L-Rha*p*-(1→2)-α-L-Rha*p*	Rhamnosyl hemiacetal, Bu$_2$SnO, ROTf, CsF[g]; Thiorhamnoside, NIS, AgOTf; rhamnosyl chloride, AgOTf; thioanthroside, NIS, AgOTf	54–56
L-Rha*p*-(1→2)-α-L-Rha*p*-(1→2)-α-L-Rha*p*	Thiorhamnoside, IDCP[h]	57

[a] Trichloroacetimidate.
[b] Dimethyl(methylthio)sulfonium triflate.
[c] Diphenyl sulfoxide.
[d] Anthrose (2-*O*-methyl-4-(3-hydroxy-3-methylbutylamino)-4,6-dideoxy-D-glucopyranose).
[e] 1-Pent-4-enyl.
[f] 2,4,6-tri-*tert*-butylpyrimidine.
[g] Alkylation with dibutyltin acetal.
[h] Iodonium dicollidine perchlorate.

TABLE II
Neighboring Group-Directed α-Rhamnan Synthesis

α-Rhamnan	**Coupling Method and Activating Agent**	**Directing Group**	**References**
L-Rha*p*-(1→4)-α-L-Rha*p*-(1→4)-α-L-Rha*p*-(1→2)-α-D-Fuc*p*-β-(11S)-(+)-jalapinolic acid	TCA[a], BF$_3$.Et$_2$O	Acetate	58
α-L-Rha*p*-(1→2)-α-L-Rha*p*-(1→2)-α-L-Rha*p*	Rhamnosyl acetate, TMSOTf	Acetate	59
α-L-Rha*p*-(1→2)-α-L-Rha*p*-(1→2)-α-L-Rha*p*-(1→2)-α-L-Rha*p*-OAll	TCA[a], or Orthoester, TMSOTf	Acetate, orthoester	60
α-L-Rha*p*-(1→3)-α-L-Rha*p*-(1→2)-α-L-Rha*p*-(1→2)-α-L-Rha*p*-(1→3)-α-L-Rha*p*-(1→3)-α-L-Rha*p*-(1→2)-α-L-Rha*p*-OPr	TCA[a], BF$_3$.Et$_2$O	Benzoate	61
α-L-Rha*p*-(1→3)-α-L-Rha*p*-(1→2)-α-L-Rha*p*-(1→2)-(D-Fuc*p*3NAc-(1→3))-α-L-Rha*p*-OMe	TCA[a], BF$_3$.Et$_2$O	Benzoate	62
α-L-Rha*p*-(1→3)-α-L-Rha*p*-(1→2)-α-L-Rha*p*-(1→2)-(β-D-Glc*p*NAc-(1→3))-α-L-Rha*p*-OBn	TCA[a], BF$_3$.Et$_2$O; Thiorhamnoside, NIS, TfOH	Benzoate	63

(continued)

TABLE II (*continued*)

***α*-Rhamnan**	**Coupling Method and Activating Agent**	**Directing Group**	**References**
α-L-Rha*p*-(1→2)-α-L-Rha*p*-(1→2)-α-L-Rha*p*-OPr	Glycosyl phosphate, TMSOTf	Acetate, orthoester	64
α-L-Rha*p*-(1→2)-α-L-Rha*p*-(1→2)-α-L-Rha*p*-(1→2)-α-L-Rha*p*-(1→2)-α-L-Rha*p*	TCA[a], TMSOTf	Phenoxyacetyl group	65
α-L-Rha*p*-(1→2)-[β-D-Glc*p*NAc-(1→3)]-α-L-Rha*p*-(1→3)-α-L-Rha*p*-(1→3)-α-L-Rha*p*-(1→2)- α-L-Rha*p*-(1→2)-[β-D-Glc*p*NAc-(1→3)]-α-L-Rha*p*-(1→3)-α-L-Rha*p*-(1→3)-α-L-Rha*p*-OMe	TCA[a], TMSOTf;	Benzoate	66
α-L-Rha*p*-(1→3)-α-L-Rha*p*-(1→2)-α-L-Rha*p*-(1→2)-α-L-Rha*p*-O-Oct[b]	TCA[a], TMSOTf;	Benzoate, acetate	67
α-L-Rha*p*-(1→2)-α-L-Rha*p*-(1→2)-α-L-Rha*p*-(1→1)-D-Glucitol	Thiorhamnoside, $NOBF_4$	Benzoate, acetate,	68
α-L-Rha*p*-(1→2)-α-L-Rha*p*-(1→2)-α-L-Rha*p*-OPent[c]	TCA[a], TMSOTf; Solid phase, Automated synthesis	Acetate	69
4-*O*-Ac-α-L-Rha*p*-(1→3)-4-*O*-Ac-α-L-Rha*p*-(1→3)-4-*O*-Ac-α-L-Rha*p*-(1→4)-α-L-Rha*p*-$OC_{12}H_{25}$	Thiorhamnoside, NIS, AgOTf or TfOH, TCA[a], TMSOTf	Levulinate	70
α-L-Rha*p*-(1→2)-α-L-Rha*p*-(1→3)-[β-D-Glc*p*NAc-(1→2)]-α-L-Rha*p*-(1→3)-α-L-Rha*p*-OPr	TCA[a], TMSOTf	Benzoate	71
α-L-Rha*p*-(1→3)-[β-L-Xyl*p*(1→2)][β-L-Xyl*p* (1→4)]-α-L-Rha*p*-(1→3)-α-L-Rha*p*-OMe	TCA[a], TMSOTf	Benzoate, acetate,	72
α-L-Rha*p*-(1→3)-[β-L-Xyl*p*(1→2)]-α-L-Rha*p*-(1→3)-[β-L-Xyl*p*(1→4)]-α-L-Rha*p*	TCA[a], TMSOTf	Benzoate, acetate,	73
3-MHB-NH-3,6-dideoxy-β-D-Glcp-(1→3)-α-L-Rha*p*-(1→3)-α-L-Rha*p*-(1→3)-α-L-Rha*p*-(1→2)-α-L-Fuc*p*-OPNP[d]	Thioglycoside, NIS, TfOH; TCA[a], TMSOTf	Benzoate,	74
α-L-Rha*p*-(1→3)-α-L-Rha*p*-(1→3)-α-L-Rha*p*-(1→3)-α-L-Rha*p*-(1→4)-β-D-Glc*p*-O-saponin	Thiorhamnoside, NIS, TfOH; TCA[a], TMSOTf	Benzoate, acetate,	75
Ant[e]-(1→3)-α-L-Rha*p*-(1→3)-α-L-Rha*p*-(1→2)-α-L-Rha*p*-O-linkers-BSA[f]	Glycosyl Chloride, AgOTf, DBMP; thiorhamnoside, NIS, AgOTf.	Benzoate, acetate,	76
β-Ant[e]-(1→3)-α-L-Rha*p*-(1→3)-α-L-Rha*p*-O-$C_3H_6NH_2$	Thiorhamnoside, NIS, TfOH	Benzoate	77
β-Ant[e]-(1→3)-α-L-Rha*p*-(1→3)-α-L-Rha*p*-(1→2)-α-L-Rha*p*-(1→3)-D-Gla*p*NAc-OC_5H_9	TCA[a], TMSOTf	Benzoate, acetate,	78,79
α-L-Rha*p*-(1→3)-[β-D-Glc*p*-(1→2)]-α-L-Rha*p*-(1→2)-[β-D-Glc*p*-(1→2)]-α-L-Rha*p*-(1→3)-α-L-Rha*p*-OAll	TCA[a], TMSOTf	Benzoate, acetate	80

(continued)

Table II (*continued*)

α-Rhamnan	**Coupling Method and Activating Agent**	**Directing Group**	**References**
β-D-Glc*p*-(1→2)-[β-D-Rib*f* -(1→3)]-α-L-Rha*p*-(1→3)-α-L-Rha*p*-(1→2)-α-L-Rha*p*-OAll	TCA[a], TMSOTf	Benzoate,	81
α-L-Rha*p*-(1→3)-α-L-Rha*p*-(1→2)-α-L-Rha*p*-(1→3)-[β-L-Xyl*p*(1→2)][β-L-Xyl*p*(1→4)]-α-L-Rha*p*-(1→3)-α-L-Rha*p*-OMe	TCA[a], TMSOTf	Benzoate	82
α-L-Rha*p*-(1→2)-α-L-Rha*p*-(1→3)-α-L-Rha*p*-(1→2)-[β-D-Gla*p*NAc-(1→3)]-α-L-Rha*p*-OAll	TCA[a], TESOTf	Benzoate, acetate	83
[α-L-Rha*p*-(1→2)-α-L-Rha*p*-(1→3)-α-L-Rha*p*-(1→3)-[α-D-Glc*p*-(1→3)]-α-L-Rha*p*-(1→3)-β-d-Glc*p*NAc-(1→2))]$_n$-$C_2H_4NHCOCH_2SAc$($n = 3$) or PADRE[g]-Lys-(thiomethyl)carbonylaminoethyl ($n = 1$)	TCA[a], TfOH or TMSOTf	Benzoate, acetate	84–87
β-D-Glc*p*NAc-(1→3)-α-L-Rha*p*-(1→2)-[β-L-Xyl*p*(1→4)]-α-L-Rha*p*-(1→3)-α-L-Rha*p*	TCA[a], TMSOTf	Benzoate, acetate	88
[3-α-L-Rha*p*-(1→3)-α-L-Rha*p*-(1→2)-α-L-Rha*p*]$_3$	TCA[a], TMSOTf	Benzoate	89
α-L-Rha*p*-(1→2)-α-L-Rha*p*-(1→3)-α-L-Rha*p*-(1→3)-β-D-Glc*p*NAc-(1→2)-α-L-Rha*p*-(1→2)-α-L-Rha*p*-OPr	Glycosyl Chloride, AgOTf, TMU; Glycosyl Bromide, AgOTf, collidine;	Benzoate	90,91
[3-β-D-Glc*p*-(1→2)-α-L-Rha*p*-(1→2)-α-L-Rha*p*-(1→3)-α-L-Rha*p*]$_{10}$	Glycosyl Bromide, $Hg(CN)_2$ and $HgBr_2$	Acetate	92
α-L-Rha*p*-(1→2)-[α-D-Glc*p*-(1→3)]-α-L-Rha*p*-(1→3)-α-L-Rha*p*-(1→3)-β-d-Glc*p*NAc	TCA[a], TMSOTf,	Benzoate	93
β-d-Glc*p*NAc-(1→2)-α-L-Rha*p*-(1→2)-α-L-Rha*p*-(1→3)-[α-D-Glc*p*-(1→3)]-α-L-Rha*p*-OMe	TCA[a], TMSOTf	Benzoate, acetate	94
β-d-Glc*p*NAc-(1→2)-α-L-Rha*p*-(1→2)-[α-D-Glc*p*-(1→3)]-α-L-Rha*p*-(1→3)-α-L-Rha*p*-OMe	Glycosyl fluoride, TiF_4; TCA[a], TMSOTf	Benzoate	95

[a] Trichloroacetimidate.
[b] Octyl.
[c] 1-pent-4-enyl.
[d] C_6H_4NH-TFA.
[e] Anthrose (2-*O*-methyl-4-(3-hydroxy-3-methylbutylamino)-4,6-dideoxy-D-glucopyranose).
[f] Bovine serum albumin.
[g] Pan HLA DR-binding epitope.

followed capping with a *t*-butyloxycarbonyl group affords the key dihydropyranone building block **211**. As the initial substituted furan is available in either enantiomeric series by asymmetric synthesis, this approach provides a convenient access to both the D- and the L-α-rhamnans. The method is illustrated in Scheme 40 for the synthesis of the *Bacillus anthracis* tetrasaccharide **225**, which has also been accessed by more conventional means by the Seeberger,[78,79] Boons,[77] Kováč,[55,76] and Crich groups.[53]

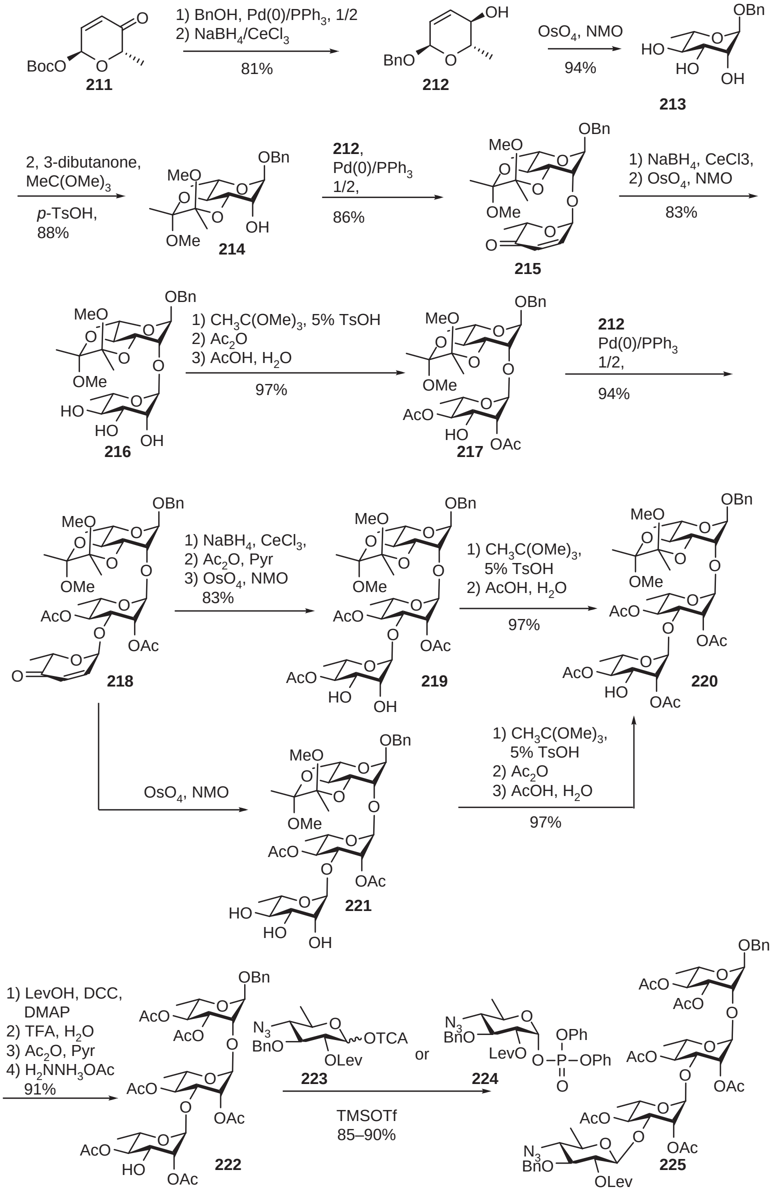
211
1) BnOH, Pd(0)/PPh3, 1/2
2) NaBH4/CeCl3
81%
212
OsO4, NMO
94%
213
2, 3-dibutanone,
MeC(OMe)3
p-TsOH,
88%
214
212,
Pd(0)/PPh3
1/2,
86%
215
1) NaBH4, CeCl3,
2) OsO4, NMO
83%
216
1) CH3C(OMe)3, 5% TsOH
2) Ac2O
3) AcOH, H2O
97%
217
212
Pd(0)/PPh3
1/2,
94%
218
1) NaBH4, CeCl3,
2) Ac2O, Pyr
3) OsO4, NMO
83%
219
1) CH3C(OMe)3,
5% TsOH
2) AcOH, H2O
97%
220
OsO4, NMO
221
1) CH3C(OMe)3,
5% TsOH
2) Ac2O
3) AcOH, H2O
97%
1) LevOH, DCC,
DMAP
2) TFA, H2O
3) Ac2O, Pyr
4) H2NNH3OAc
91%
222
223
or
224
TMSOTf
85–90%
225

SCHEME 40. *De novo* synthesis of the rhamnan from *Bacillus anthracis*.

III. THE β-MANNANS AND β-RHAMNANS

1. Introduction

With the need to overcome the kinetic anomeric effect and the additional steric hindrance presented by the protected axial O-2 group, while avoiding neighboring-group participation completely, the synthesis of β-mannopyranosides was long recognized as one of the more challenging aspects of carbohydrate chemistry. Consistent with this line of thinking, the β-mannans, in which the difficulties are multiplied many fold, can be considered to be an extremely challenging class of glycan to synthesize. Numerous ingenious methods were devised for the indirect synthesis of β-mannopyranosides avoiding the difficulties considered inherent in the direct approach, as summarized in several review articles and book chapters,[98–102] and most of these have been applied to the indirect synthesis of β-mannans. More recently, however, a very efficient direct approach to the β-mannopyranosides was developed in Chicago, rendering the synthesis of this class of glycosidic bond as simple as that of the β-glucopyranosides.[8,103] This method has also been applied to the preparation of β-mannans. In the following discussion, β-mannan syntheses by "classical" indirect methods are presented first, before consideration of those obtained more directly.

2. *β*-Mannan Synthesis by Indirect Methods

Nikolaev and coworkers prepared a β-(1→4)-linked mannobiose and triose adopting a classical approach[104] in which β-glucosidic linkages, prepared by neighboring-group participation,[105–107] are converted into the corresponding β-mannosides by subsequent nucleophilic displacement at C-2. Thus, cellobiose was converted through a number of steps into the protected form **226**, which was selectively tribenzoylated to give **227**. Reaction with trifluoromethanesulfonic anhydride then gave the ditriflate, which was subjected to tetrabutylammonium benzoate in toluene at reflux to give the mannobiose derivative **228** in 76% yield (Scheme 41).[104] Hydrolysis of the benzylidene acetal was followed by selective benzoylation of the primary alcohol with benzoyl cyanide, affording the glycosyl acceptor **230** in 92% yield. Neighboring group-directed β-glucosylation by the trichloroacetimidate method then gave the trisaccharide **233**, which was subjected to several reaction steps to give the triflate **235**. Finally, a second S_N2 displacement with tetrabutylammonium benzoate gave access to the β-(1→4)-linked mannotriose **236** in 88% yield (Scheme 41).

Lichtenthaler and coworkers developed a method for β-mannoside synthesis based upon the β-selective coupling reactions of an α-2-glyculosyl bromide with catalysis

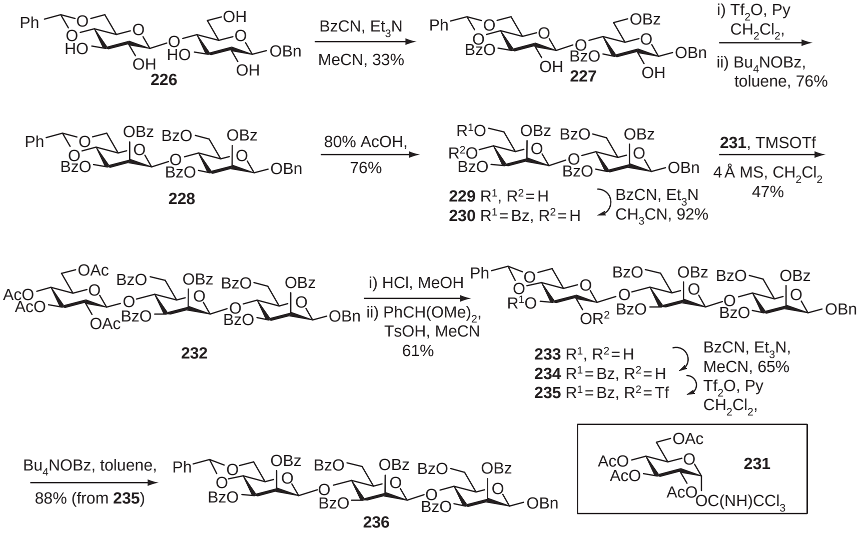
226
BzCN, Et$_3$N
MeCN, 33%
227
i) Tf$_2$O, Py CH$_2$Cl$_2$,
ii) Bu$_4$NOBz, toluene, 76%
228
80% AcOH, 76%
229 R^1, R^2=H
230 R^1=Bz, R^2=H
BzCN, Et$_3$N CH$_3$CN, 92%
231, TMSOTf
4 Å MS, CH$_2$Cl$_2$
47%
232
i) HCl, MeOH
ii) PhCH(OMe)$_2$, TsOH, MeCN
61%
233 R^1, R^2=H
234 R^1=Bz, R^2=H
235 R^1=Bz, R^2=Tf
BzCN, Et$_3$N, MeCN, 65%
Tf$_2$O, Py CH$_2$Cl$_2$,
Bu$_4$NOBz, toluene,
88% (from 235)
236
231

SCHEME 41. Synthesis of a β-(1→4)-mannotriose by a glucosylation/oxidation/reduction route.

with silver ions. This chemistry is based on the assumptions that the ketone functionality at C-2 (i) eliminates the problem of steric hindrance to β-face attack, (ii) accelerates S_N2 attack on the anomeric bromide, and (iii) retards selectivity-diminishing solvolysis of the anomeric bromide.[108–110] This method was applied in the Bundle group's first synthesis of the β-(1→2)-linked mannan from *Candida albicans*. The synthesis began with the coupling of the Lichtenthaler donor **238** to acceptor **237** with silver zeolite, followed by reduction with L-selectride to give the β-mannobiose **239** in 78% yield (Scheme 42). Adaptation of the protocol to the β-mannotriose required modification of Lichtenthaler's donor to avoid competing formation of a 1,6-anhydro sugar. This was achieved through replacement of the benzyl ethers with *p*-chlorobenzyl ethers, as in donor **240**. The conditions were also modified at this stage to incorporate the use of the soluble silver triflate promoter and the use of acetonitrile as solvent, in the expectation that participation by the solvent[111–117] would enhance the β-selectivity of the reaction. When the synthesis was taken forward to the level of the tetrasaccharide, the intermediate nitrilium ion arising from participation by acetonitrile was quenched in part by attack of the acceptor on the *sp*-carbon in competition with the desired displacement at the anomeric center. This problem was overcome by the use of pivalonitrile. Two further iterations of the sequence eventually provided a β-(1→2)-linked mannohexaose **244** (Scheme 42).[118,119]

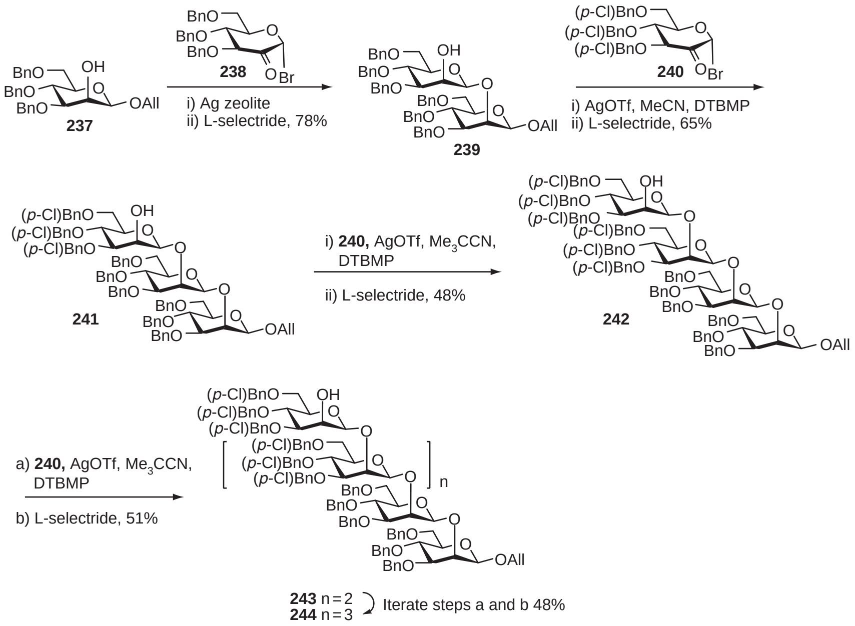
237
238
i) Ag zeolite
ii) L-selectride, 78%
239
240
i) AgOTf, MeCN, DTBMP
ii) L-selectride, 65%
241
i) 240, AgOTf, Me$_3$CCN, DTBMP
ii) L-selectride, 48%
242
a) 240, AgOTf, Me$_3$CCN, DTBMP
b) L-selectride, 51%
243 n = 2
244 n = 3
Iterate steps a and b 48%

SCHEME 42. β-(1→2)-Mannan synthesis by the glyculosyl bromide method.

Detailed studies on the reduction of the β-glyculosides to β-mannopyranosides have been reported by the Lichtenthaler group. Bundle and his coworkers noted in the course of their studies that the application of sodium borohydride as reducing agent gave less than perfect manno/gluco selectivity, but that the bulky reducing agent L-selectride performed ideally.

Seeking to introduce a hydrolytically stable thio-β-mannoside linkage into their β-(1→2)-linked mannans, Nitz and Bundle introduced[119] a modification of the nucleophilic glucose-to-mannose inversion protocol.[105–107] In this chemistry, the mannobiose **239** was subjected to neighboring group-directed β-glucosylation to give the trisaccharide **246**. Cleavage of the acetate and triflation was followed by nucleophilic displacement with potassium thioacetate to give **249** in good overall yield (Scheme 43). After removal of the labile thioacetate, application of the Lichtenthaler protocol[108–110] gave the monothio β-(1→2)-mannotetraose in modest yield, along with a certain amount of the corresponding 1-thio-α-epimer, thereby revealing a limitation of the glyculosyl bromide approach.[119] In subsequent work toward further β-(1→2)-linked mannans containing thioglycoside linkages, Bundle and his coworkers employed the β-glucosylation, selective 2-acetate deprotection,

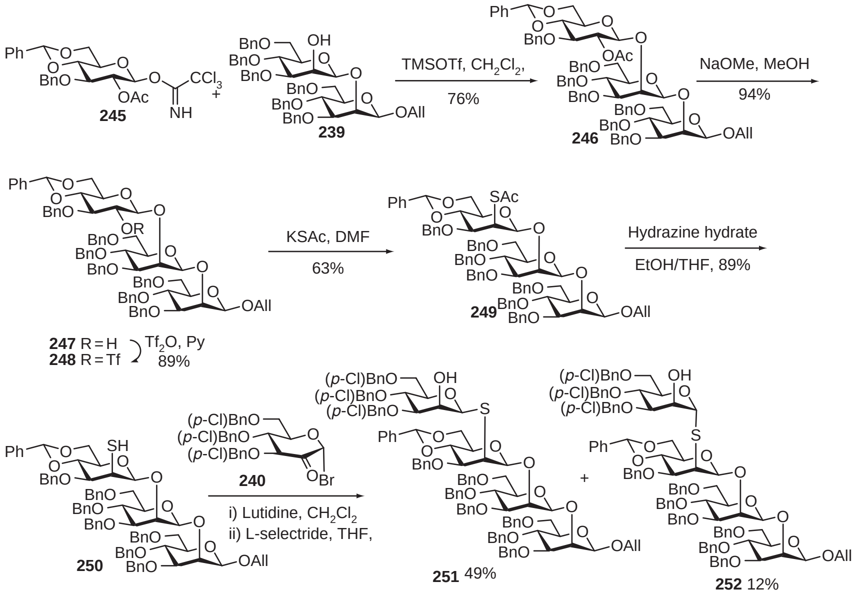

SCHEME 43. Synthesis of a thioglycoside-containing β-(1→2)-mannan.

oxidation, reduction protocol to achieve the β-mannosidic linkage.[120] Although not yet applied to β-mannan synthesis, it is noted here that a number of thio β-mannosides have been obtained in excellent yields and selectivity by the 4,6-*O*-benzylidene-controlled direct β-mannosylation protocol.[121]

Sinaÿ and coworkers were the first to prepare a β-(1→2)-mannotetraose,[122] which they did by adapting the classical approach[123,124] to β-mannosides in which a β-glucoside is selectively oxidized at C-2 to the glyculoside and then selectively reduced to the manno-isomer. Thus, NIS/triflic acid-mediated coupling of the thioglucoside **254** with acceptor **253** gave disaccharide **255**, from which the stereodirecting benzoate ester was removed under Zemplén conditions (Scheme 44). Swern oxidation was followed by L-selectride reduction to give the corresponding β-mannobiose **257**. Two iterations of the protocol finally gave the β-(1→2)-mannotetraose **259**.

Fraser-Reid and coworkers took a very similar tack using, however, the orthoester approach to prepare the β-glucosidic bond. The Swern oxidation/L-selectride reduction approach to inversion subsequently applied was identical to that of the Sinaÿ laboratory, but further iterations of the process were applied until a β-(1→2)-mannooctaose **270** was obtained (Scheme 45).[125] Yet another variation on the theme

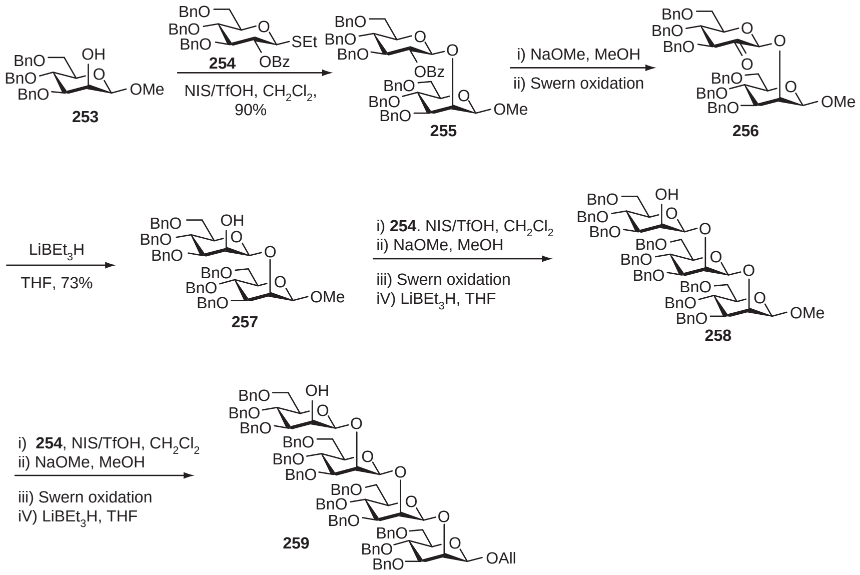
253
254
NIS/TfOH, CH2Cl2, 90%
255
i) NaOMe, MeOH
ii) Swern oxidation
256
LiBEt3H
THF, 73%
257
i) 254. NIS/TfOH, CH2Cl2
ii) NaOMe, MeOH
iii) Swern oxidation
iV) LiBEt3H, THF
258
i) 254, NIS/TfOH, CH2Cl2
ii) NaOMe, MeOH
iii) Swern oxidation
iV) LiBEt3H, THF
259

SCHEME 44. Synthesis of a β-(1→2)-mannan by a glucosylation/oxidation/reduction route.

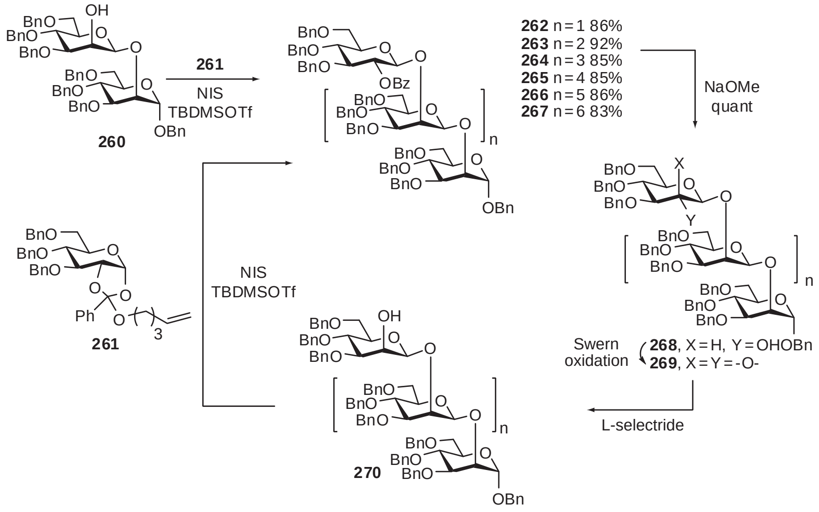
260
261
NIS
TBDMSOTf
262 n = 1 86%
263 n = 2 92%
264 n = 3 85%
265 n = 4 85%
266 n = 5 86%
267 n = 6 83%
NaOMe
quant
Swern
oxidation
268, X = H, Y = OHOBn
269, X = Y = -O-
L-selectride
261
NIS
TBDMSOTf
270

SCHEME 45. Indirect, pentenyl glycoside-based synthesis of a β-(1→2)-mannan.

was advanced by Wu and Bundle in the preparation of a *β*-(1→2)-mannotetraose, with the main difference being the use of the neighboring group-directed trichloroacetimidate protocol to access the *β*-glucoside.[120]

3. *β*-Rhamnan Synthesis by Indirect Methods

As with the *β*-mannans, and for the same reasons, the stereocontrolled synthesis of the *β*-rhamnans is one of the more challenging goals in oligosaccharide synthesis. Rather less attention has been devoted to the *β*-rhamnans than to the *β*-mannans, perhaps because of their lower incidence in Nature, and the range of methods applied is correspondingly shorter even if most approaches documented for the mannans have been applied to the preparation of single *β*-rhamnosidic units.[126–132] A rhamnotriose **277** containing a single *β*-L-rhamnopyranosidic linkage has been assembled by the Lichtenthaler group, employing a modification of their glycos-2-ulosyl bromide approach to access the key linkage (Scheme 46).[133]

4. *β*-Mannan Synthesis by Direct Methods

The direct synthesis of a *β*-(1→2)-mannooctaose was achieved by a two-step iterative protocol from the key sulfoxide donor **275**. After an initial coupling to cyclohexanol to cap the reducing end of the chain, the 2-*O*-(4-methoxybenzyl) ether

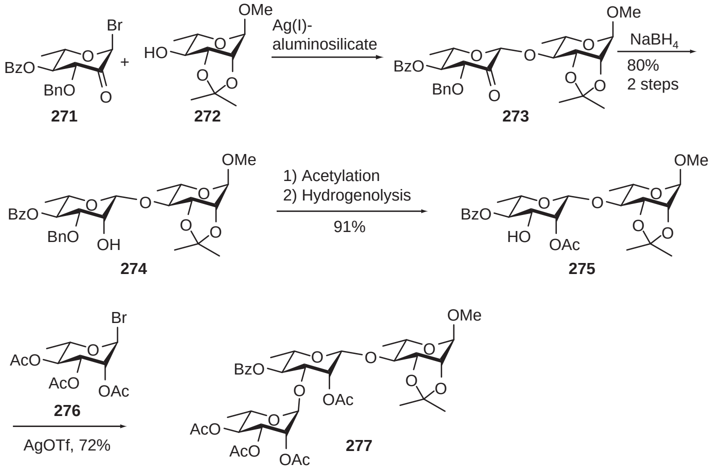

Br
BzO
BnO
O
271
+
OMe
HO
O
272
Ag(I)-
aluminosilicate
BzO
BnO
O
OMe
273
NaBH$_4$
80%
2 steps
OMe
BzO
BnO
OH
274
1) Acetylation
2) Hydrogenolysis
91%
OMe
BzO
HO
OAc
275
Br
AcO
AcO
OAc
276
AgOTf, 72%
OMe
BzO
OAc
AcO
AcO
OAc
277

SCHEME 46. Synthesis of a rhamnan containing a single *β*-linkage.

was removed with DDQ, thereby revealing an acceptor **279** ($n = 0$) primed for the first repetition of the sequence. Several iterations afforded the octaose **279** ($n = 7$), with the only impediment to the process being the drop off in yield and selectivity between the introduction of the third and fourth sugar units (Scheme 47). The X-ray crystal structure of the tetrasaccharide revealed a collapsed helical structure in which the fourth sugar sits obliquely above the first, hinting at an explanation for the fall off in selectivity at that stage of the synthesis.[134,135] A related structure was determined by NMR methods by Bundle and Nitz[136] for the *β*-(1→2)-mannhexaose obtained by the indirect methods and in whose synthesis the difficulties also became apparent at the level of the tetrasaccharide.

β-(1→2)-Mannans of various lengths were subsequently accessed by several groups, all using variations on the method introduced by Crich and co-workers and relying on the use of the 4,6-*O*-benzylidene acetal to control the anomeric stereochemistry. Thus, Mallet and coworkers adopted a block-synthesis approach in which a sulfoxide donor **282** was activated and coupled to a monohydroxy thioglycoside **281** (Scheme 48).[137] The moderate yield observed in the coupling of the two disaccharides is presumably due to the benzenesulfenyl triflate byproduct from activation of the sulfoxide reacting in part with the thioglycoside, as had been determined by Crich and Sun in their studies on the mechanism of this reaction, and which lead them to develop the arenesulfenyl triflates for thioglycoside activation.[37,39]

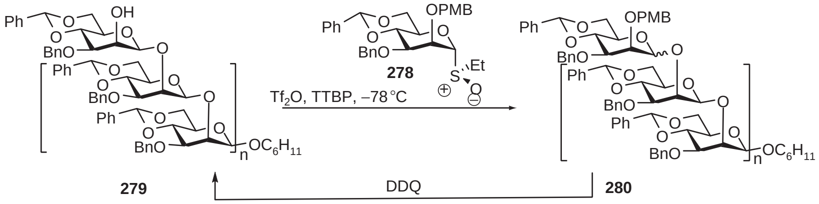

Acceptor (*n*)	280*β* *n* (% Yield)	280*α* *n* (% Yield)	*β*/*α* Ratio	279 (% Yield)
Cyclohexanol	$n = 0$ (77)	$n = 0$ (0)	100:0	$n = 0$ (85)
279 $n = 1$	$n = 1$ (94)	$n = 1$ (0)	100:0	$n = 1$ (97)
279 $n = 2$	$n = 2$ (89)	$n = 2$ (9)	9.9:1	$n = 2$ (91)
279 $n = 3$	$n = 3$ (77)	$n = 3$ (20)	3.9:1	$n = 3$ (85)
279 $n = 4$	$n = 4$ (69)	$n = 4$ (16)	4.3:1	$n = 4$ (80)
279 $n = 5$	$n = 5$ (68)	$n = 5$ (15)	4.5:1	$n = 5$ (85)
279 $n = 6$	$n = 6$ (64)	$n = 6$ (13)	4.9:1	$n = 6$ (81)
279 $n = 7$	$n = 7$ (64)	$n = 7$ (14)	4.5:1	$n = 7$ (71)

SCHEME 47. Direct synthesis of a *β*-(1→2)-mannan.

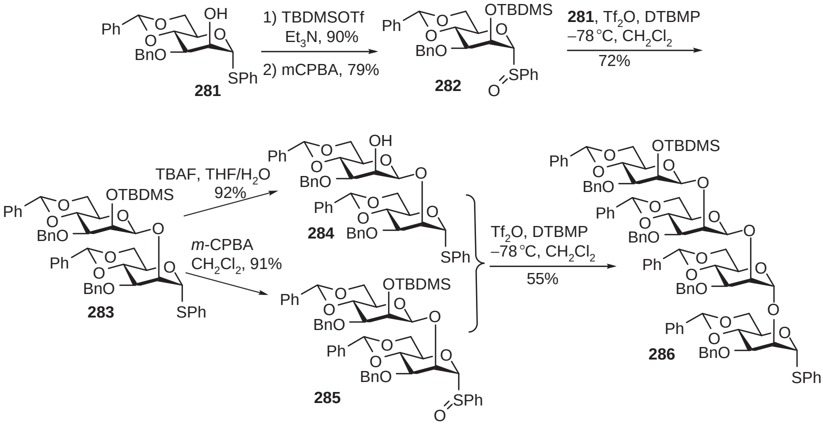

SCHEME 48. Block synthesis of a β-(1→2)-mannan.

The synthesis of a β-(1→4)-mannan by the 4,6-*O*-benzylidene-directed β-mannosylation is not quite so straightforward as that of the 1→2 isomers as it requires the conversion of the 4,6-benzylidene acetal at the nonreducing end of the growing chain into an acceptor in which the 6-hydroxy group has been selectively protected. The obvious approach here is the application of one the several sets of reducing conditions described in the literature[138–144] for the regioselective cleavage of a benzylidene acetal into a monobenzylated diol. This approach was investigated by Crich and coworkers employing sodium cyanoborohydride as reducing agent in the presence of hydrogen chloride.[135] While the reaction functioned according to plan at level of the monosaccharide, large excesses of both reagents and unexpectedly long reaction times were required in application of this protocol in a disaccharide, resulting in the onset of competing decomposition processes. It was reasoned that the diminished reactivity observed was due to the presence of 10 ether oxygens of similar basicity in the disaccharide, as opposed to the six in the monosaccharide, which decreased the overall level of protonation at the acetal required for reduction. A two-step process was therefore developed involving cleavage of the benzylidene acetal with neopentyl glycol and camphorsulfonic acid, followed by selective monopivaloylation of the resulting diol **291**. The chain was then extended by coupling to a standard thioglycoside donor **287**, with preactivation using the 1-benzenesulfinyl piperidine/trifluoromethanesulfonic acid conditions leading to the preparation of the β-(1→4)-mannohexaose (Scheme 49).[135]

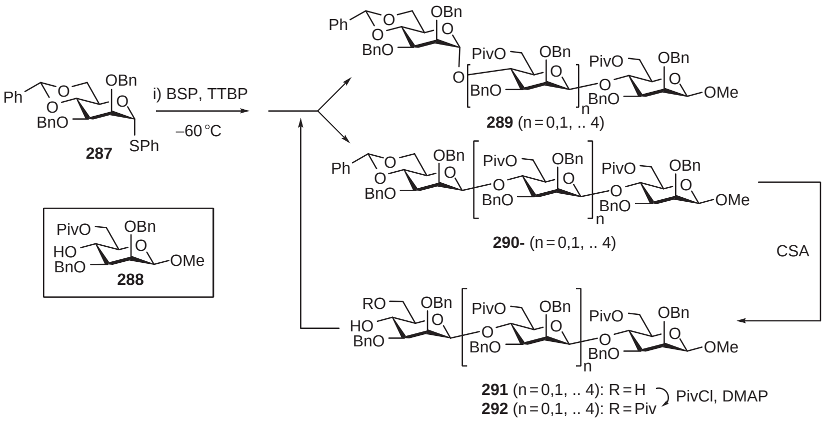

Acceptor	**290 (% Yield)**	**289 (% Yield)**	***β*/*α* Ratio**	**291 (% Yield)**	**292 (% Yield)**
288	$n = 0$ (80)	$n = 0$ (8)	1/9	$n = 0$ (85)	$n = 0$ (88)
292 ($n = 0$)	$n = 1$ (77)	$n = 1$ (8)	1/9	$n = 1$ (85)	$n = 1$ (88)
292 ($n = 1$)	$n = 2$ (72)	$n = 2$ (8)	1/9	$n = 2$ (87)	$n = 2$ (89)
292 ($n = 2$)	$n = 3$ (71)	$n = 3$ (8)	1/9	$n = 3$ (88)	$n = 3$ (86)
292 ($n = 3$)	$n = 4$ (73)	$n = 4$ (7)	1/10		

SCHEME 49. Direct synthesis of a *β*-(1→4)-mannan.

Kim and co-workers carried out a closely related synthesis of a *β*-(1→4)-mannotetraose **300**, using their method for the *in situ* conversion of hemiacetals to glycosyl triflates by means of reaction with phthalic anhydride (“phthalan”) followed by trifluoromethanesulfonic anhydride. In this instance cleavage of the benzylidene acetal was effected with trifluoroacetic acid, and regioselective reprotection of the diol employed benzoyl chloride (Scheme 50).[145]

The synthesis of an alternating antigenic *β*-(1→3)-*β*-(1→4)-mannan common to *Rhodotorula glutinis*, *Rhodotorula mucilaginosa*, and *Leptospira biflexa* provided the occasion for the comparison of linear and block approaches. A linear synthesis was first undertaken and provided a relatively straightforward access to the hexaose **313** (Scheme 51).[134,146] The most noteworthy feature of this synthesis was the protection of the *β*-donor **305** destined to become the →4)-D-mannopyranosyl-*β*-(1→ unit in the polymer as the 4-methoxybenzylidene acetal rather than as the simple benzylidene acetal employed in the *β*-donor **301** precursor to the ultimate →3)-D-mannopyranosyl-*β*-(1→ moiety. This protecting-group adjustment enabled selective cleavage of

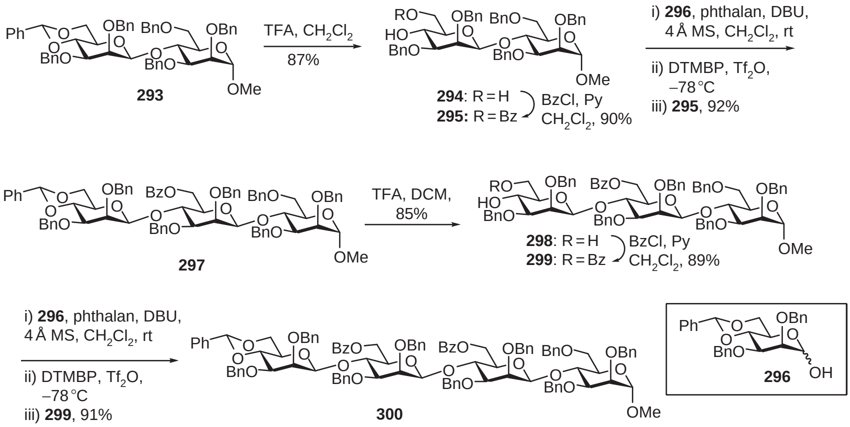
293
TFA, CH2Cl2
87%
294: R = H
295: R = Bz
BzCl, Py
CH2Cl2, 90%
i) 296, phthalan, DBU, 4 Å MS, CH2Cl2, rt
ii) DTMBP, Tf2O, −78 °C
iii) 295, 92%
297
TFA, DCM, 85%
298: R = H
299: R = Bz
BzCl, Py
CH2Cl2, 89%
i) 296, phthalan, DBU, 4 Å MS, CH2Cl2, rt
ii) DTMBP, Tf2O, −78 °C
iii) 299, 91%
300
296

SCHEME 50. Direct synthesis of a β-(1→2)-mannan employing a hemiacetal donor.

the 4-methoxybenzylidene acetal with acetic acid in the presence of one or more benzylidene acetals. The ensuing diol was selectively benzylated at the primary site with benzyl bromide and dibutyltin oxide.

The subsequent 3 + 3 block synthesis of the same mannohexaose, while successful and more efficient than the linear approach in terms of number of steps and overall yield, highlighted a limitation in the 4,6-*O*-benzylidene directed β-mannosylation reaction; namely the deleterious effect of large groups at O-3 in the donor. Activation of the 4-methoxybenzylidene-protected thiomannoside **314** with 1-benzenesulfinyl piperidine and trifluoromethanesulfonic anhydride, followed by coupling to the monohydroxy thioglycoside **315** gave disaccharide **316** in 62% yield and excellent selectivity. After protecting-group adjustment, alcohol **318** served as acceptor in a coupling with the 4,6-*O*-benzylidene-protected donor **287** to give the trisaccharide donor **319** in good yield and selectivity (Scheme 53).[146] The effect of the bulky group at O-3 became apparent when disaccharide **316** was coupled to acceptor **302** under the BSP/Tf_2O conditions, giving trisaccharide **320** in excellent yield but only 1:1 β:α selectivity. Nevertheless, the 4-methoxybenzylidene acetal was converted to the corresponding 6-*O*-benzyl-4-ol **321** ready for application as the acceptor in the final step of the block synthesis (Scheme 52).

The coupling of the two trisaccharides **319** and **321**, conducted under the BSP/Tf_2O conditions, proceeded in 88% overall yield but with poor selectivity (β:α = 1:1.5) (Scheme 53),[146] leaving no doubt of the negative impact of a bulky substituent on O-3 of the donor in these 4,6-*O*-benzylidene-directed β-mannosylation reactions.

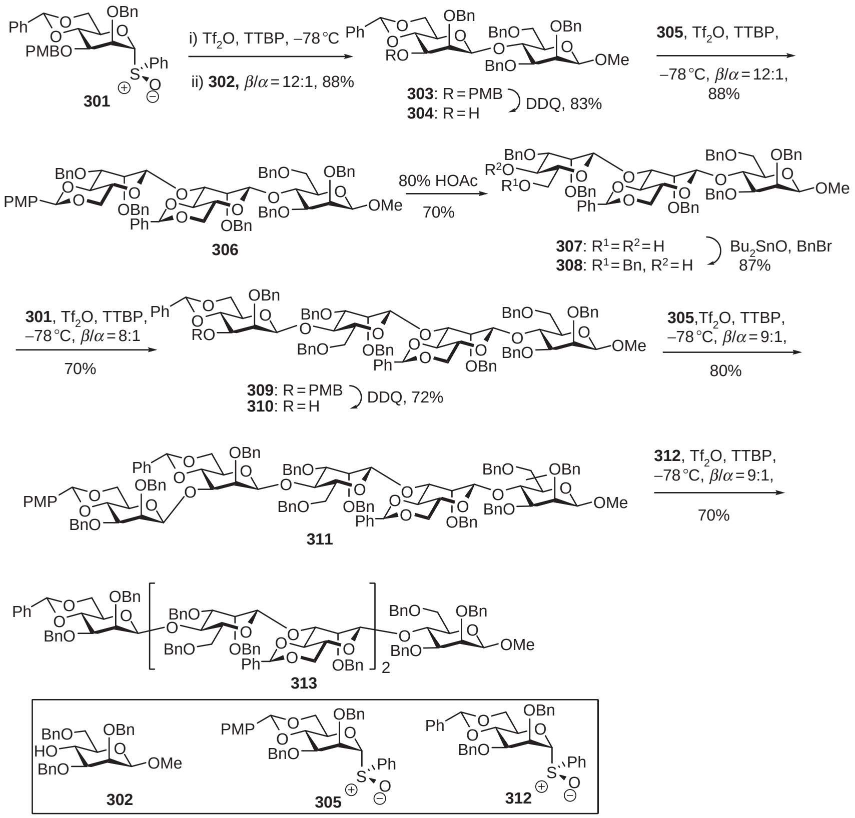
301
i) Tf2O, TTBP, −78 °C
ii) 302, β/α = 12:1, 88%
303: R = PMB
304: R = H
DDQ, 83%
305, Tf2O, TTBP,
−78 °C, β/α = 12:1,
88%
306
80% HOAc
70%
307: R1 = R2 = H
308: R1 = Bn, R2 = H
Bu2SnO, BnBr
87%
301, Tf2O, TTBP,
−78 °C, β/α = 8:1
70%
309: R = PMB
310: R = H
DDQ, 72%
305, Tf2O, TTBP,
−78 °C, β/α = 9:1,
80%
311
312, Tf2O, TTBP,
−78 °C, β/α = 9:1,
70%
313
302
305
312

SCHEME 51. Direct synthesis of an alternating β-(1→4)-β-(1→3)-mannan.

In spite of the poor selectivity in two of the coupling reactions, the overall yield of the mannohexaose **321** from the block synthesis was higher than that achieved previously in the linear synthesis, thereby clearly highlighting the well-known advantages of convergent syntheses.

In view of this limitation, the ultimate challenge in the field of β-mannan synthesis is necessarily that of a β-(1→3)-mannan such as was subsequently undertaken by Crich and his coworkers. Consideration of the poor selectivities outlined in Scheme 52, and of similarly poor selectivities noted with 4,6-*O*-benzylidene-protected mannosyl doors carrying the large *tert*-butyldimethylsilyl ether group at O-3[147,148] led to the hypothesis of steric buttressing between the bulky O-3 group and the protecting group on O-2, resulting in the latter hindering the β-face of the donor to an unusually large extent.

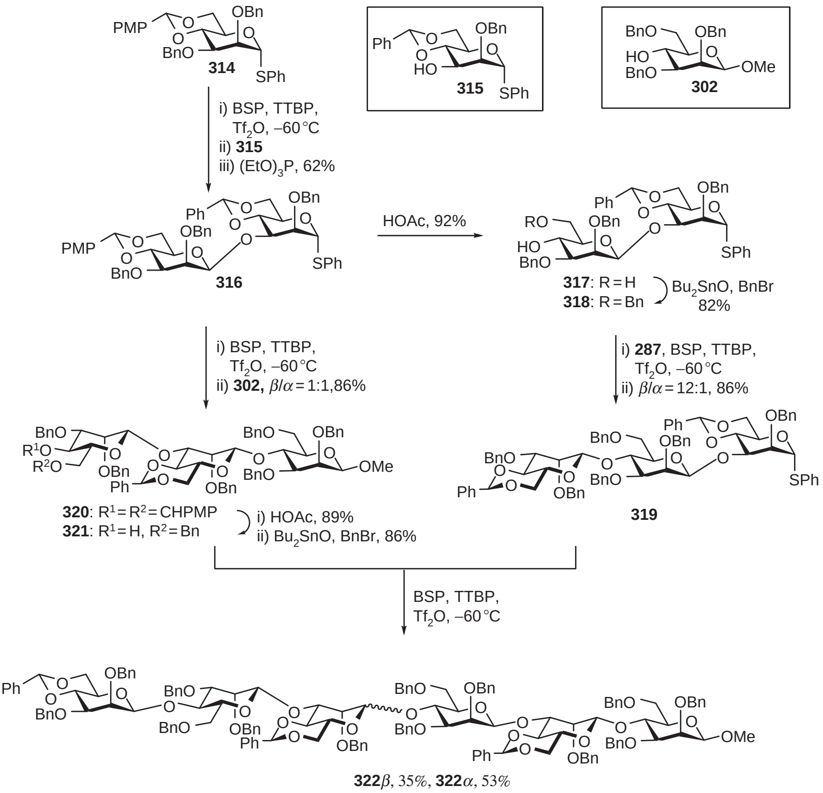
PMP
OBn
BnO
SPh
314
Ph
HO
315
BnO
OBn
HO
BnO
OMe
302
i) BSP, TTBP,
Tf$_2$O, –60 °C
ii) 315
iii) (EtO)$_3$P, 62%
316
HOAc, 92%
RO
317: R = H
318: R = Bn
Bu$_2$SnO, BnBr
82%
i) BSP, TTBP,
Tf$_2$O, –60 °C
ii) 302, β/α = 1:1,86%
i) 287, BSP, TTBP,
Tf$_2$O, –60 °C
ii) β/α = 12:1, 86%
R^{1}O
R^{2}O
320: R^1 = R^2 = CHPMP
321: R^1 = H, R^2 = Bn
i) HOAc, 89%
ii) Bu$_2$SnO, BnBr, 86%
319
BSP, TTBP,
Tf$_2$O, –60 °C
322β, 35%, 322α, 53%

SCHEME 52. Block synthesis of an alternating β-(1→4)-β-(1→3)-mannan.

This in turn resulted in the introduction of the sterically minimal 2-propargyl ether group to compensate for the presence of a bulky group at O-3, with positive results in a number of systems.[149] Unfortunately even this innovation was not sufficient for the β-(1→3)-mannan synthesis, as is clear from the contrast in the selectivities of the di- and trisaccharide preparations presented in Scheme 53.[150]

The problem was reduced to a minimum in a redesigned approach for which the only coupling employing a 3-*O*-glycosylated donor was the final block assembly of two trisaccharides to afford a hexamannan. This solution also made use of the novel 3-naphthylpropargyl ether for protection of the 3-position at a number of reaction stages. This system[151] enjoys the minimal steric bulk of the propargyl ether, but is more easily removed in a single step by exposure to DDQ under conditions akin to

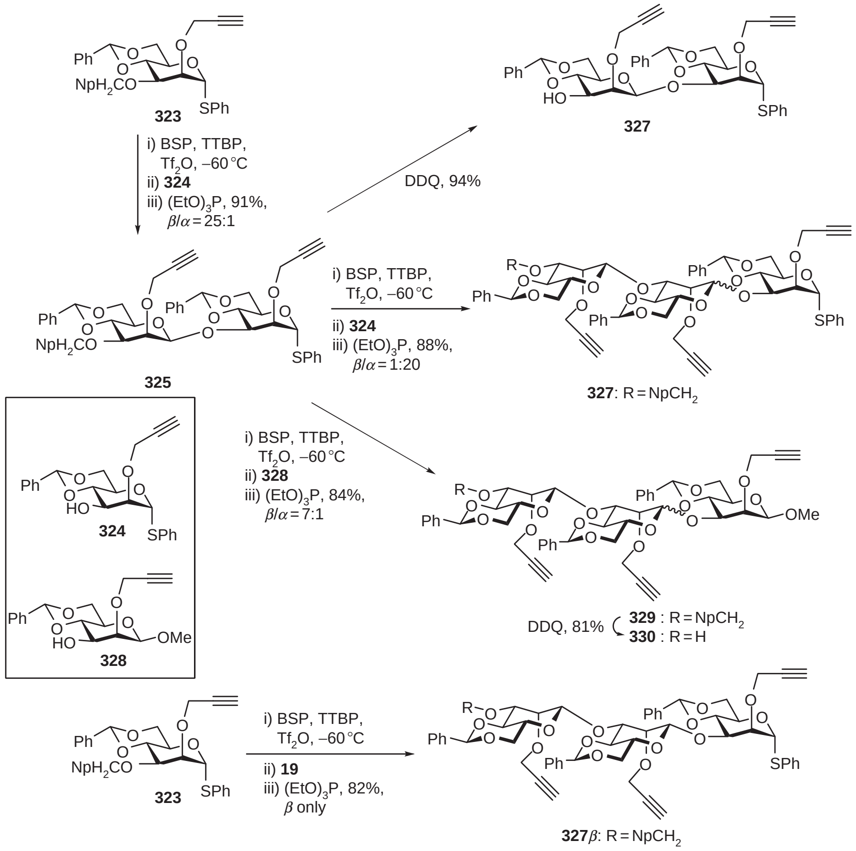
323
i) BSP, TTBP, Tf2O, −60 °C
ii) 324
iii) (EtO)3P, 91%, β/α = 25:1
DDQ, 94%
327
325
i) BSP, TTBP, Tf2O, −60 °C
ii) 324
iii) (EtO)3P, 88%, β/α = 1:20
327: R = NpCH2
324
328
i) BSP, TTBP, Tf2O, −60 °C
ii) 328
iii) (EtO)3P, 84%, β/α = 7:1
DDQ, 81%
329 : R = NpCH2
330 : R = H
323
i) BSP, TTBP, Tf2O, −60 °C
ii) 19
iii) (EtO)3P, 82%, β only
327β: R = NpCH2

SCHEME 53. Direct synthesis of a β-(1→3)-mannotroise using the propargyl ether protecting group.

those employed for cleavage of 4-methoxybenzyl ethers and naphthylmethyl ethers. The trisaccharide donor **335** and the acceptor **336** were assembled uneventfully in linear fashion and excellent selectivity (Scheme 54), with 1-octene deployed as a sacrifical alkene to trap the benzenesulfinyl triflate byproduct of the sulfoxide activation reaction and prevent its addition to either the electron-rich propargyl system or the thioglycoside present in one of the acceptors.

Finally, the two trisaccharides were combined to yield the mannohexaose **337** in 61% yield and the somewhat modest selectivity by now expected, of 1:1 for the two anomers (Scheme 55).[150]

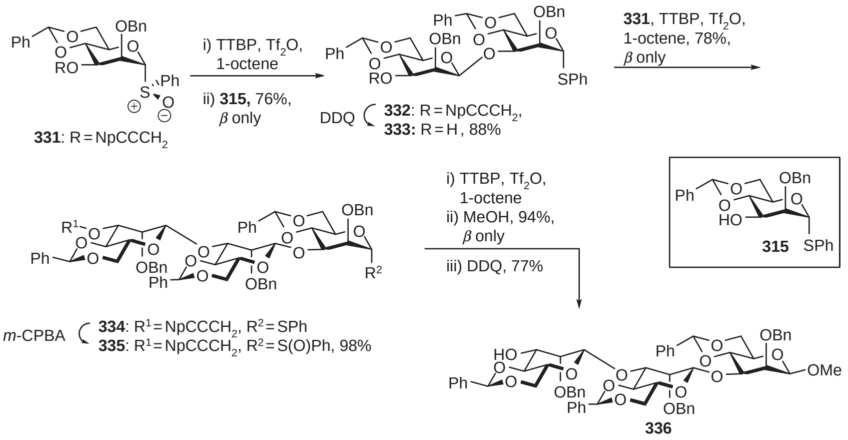
Ph
OBn
O
RO
Ph
S
O
331: R = NpCCCH$_2$
i) TTBP, Tf$_2$O, 1-octene
ii) 315, 76%, β only
Ph
OBn
RO
SPh
DDQ
332: R = NpCCCH$_2$,
333: R = H, 88%
331, TTBP, Tf$_2$O, 1-octene, 78%, β only
Ph
HO
OBn
315
SPh
R^1
Ph
OBn
R^2
i) TTBP, Tf$_2$O, 1-octene
ii) MeOH, 94%, β only
iii) DDQ, 77%
m-CPBA
334: R^1 = NpCCCH$_2$, R^2 = SPh
335: R^1 = NpCCCH$_2$, R^2 = S(O)Ph, 98%
HO
OMe
336

SCHEME 54. Assembly of two trisaccharides for subsequent coupling.

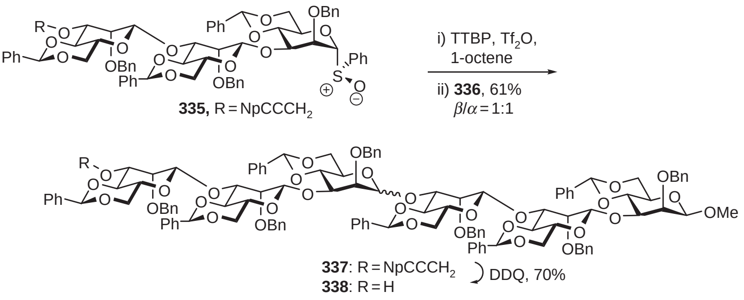
R
Ph
OBn
Ph
S
O
335, R = NpCCCH$_2$
i) TTBP, Tf$_2$O, 1-octene
ii) 336, 61%
β/α = 1:1
R
OMe
337: R = NpCCCH$_2$
338: R = H
DDQ, 70%

SCHEME 55. Block synthesis of a β-(1→3)-mannan.

5. β-Rhamnan Synthesis by Direct Methods

Paulsen and Kutschker employed the classical insoluble silver salt method to prepare the β-(1→4)-β-(1→2)-rhamnotriose characteristic of the lipopolysaccharide from *Shigella flexneri*.[152] Accordingly, the rhamnosyl bromide **340** dissolved in toluene was added dropwise to a solution of acceptor **339** stirred in dichloromethane in the presence of the insoluble silver silicate promoter (Scheme 56) to give exclusively the β-rhamnoside **341** in 77% yield. Interestingly in view of subsequent claims of the β-directing effects of 4-*O*-carboxyl esters in related glycosylation reactions,[100] the arming 2-allyl and 3-benzyl ethers were considered to counteract the disarming

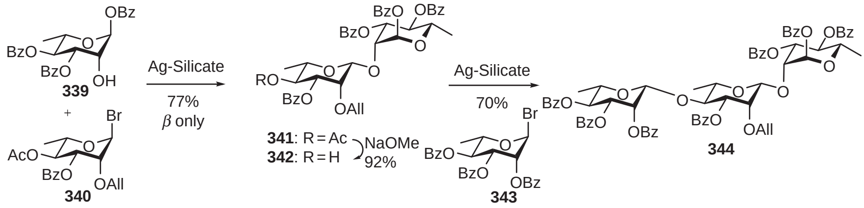
OBz
BzO
BzO
OH
339
+
Br
AcO
BzO
OAll
340
Ag-Silicate
77%
β only
BzO OBz
BzO
RO
BzO
OAll
341: R = Ac
342: R = H
NaOMe
92%
Ag-Silicate
70%
Br
BzO
BzO
OBz
343
BzO OBz
BzO
BzO
BzO
OBz
BzO
OAll
344

SCHEME 56. Direct synthesis of an alternating β-rhamnan by the insoluble silver salt method.

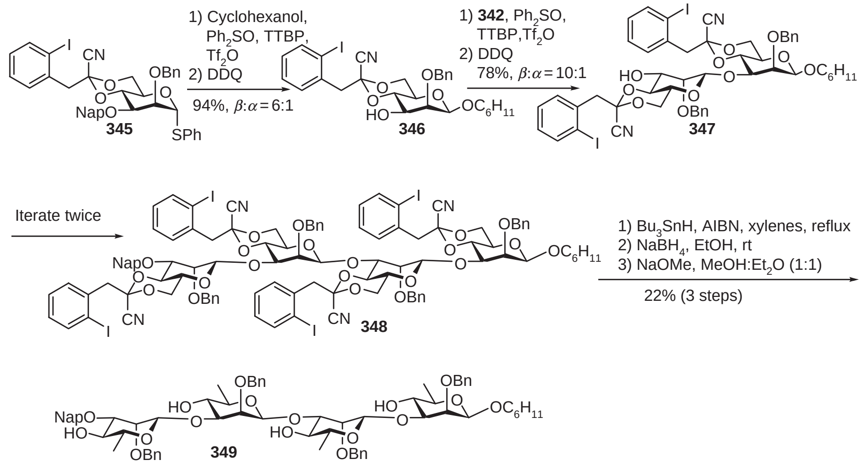
I
CN
OBn
NapO
345
SPh
1) Cyclohexanol, Ph$_2$SO, TTBP, Tf$_2$O
2) DDQ
94%, β:α = 6:1
I
CN
OBn
HO
OC$_6$H$_{11}$
346
1) 342, Ph$_2$SO, TTBP, Tf$_2$O
2) DDQ
78%, β:α = 10:1
I
CN
OBn
HO
OC$_6$H$_{11}$
OBn
CN
I
347
Iterate twice
I
CN
OBn
NapO
OBn
CN
I
I
CN
OBn
OC$_6$H$_{11}$
OBn
CN
I
348
1) Bu$_3$SnH, AIBN, xylenes, reflux
2) NaBH$_4$, EtOH, rt
3) NaOMe, MeOH:Et$_2$O (1:1)
22% (3 steps)
OBn
NapO
HO
HO
OBn
349
OBn
HO
HO
OC$_6$H$_{11}$
OBn

SCHEME 57. Direct synthesis of a β-rhamnan by deoxygenation of a β-mannan.

effect of the 4-acetate group and to facilitate this particular coupling. After removal of the acetate ester, a second silver silicate-promoted β-rhamnosylation was conducted with donor **343**, leading to the formation of the trisaccharide **344** in 70% yield (Scheme 56).[152]

The application of the 4,6-benzylidene acetal-controlled β-mannoside synthesis to the preparation of the β-rhamnans is rendered more complex by the 6-deoxy nature of rhamnose. In the D series this problem was circumvented by Crich and Bowers, who applied a novel free-radical fragmentation to convert a 4,6-acetal linkage directly to a 6-deoxy sugar subsequent to the glycosylation step. Thus, in the first step of an iterative sequence, thioglycoside **345** was coupled first with cyclohexanol to cap the reducing end of the target tetrasaccharide (Scheme 57). After oxidative removal of the naphthylmethyl ether, a further coupling with **345** gave a disaccharide which led, after two more iterations of the deprotection/coupling sequence, to a β-mannotetraose **348**. Treatment with tributyltin hydride and azoisobutyronitrile in xylene at reflux then afforded, after work-up with sodium borohydride and Zemplén deacylation, the β-rhamnotetraose **349** in 22% yield (Scheme 57).[153] Although the fragmentation employed in this synthesis to convert the β-mannan into the β-rhamnan is reminiscent of the well-known Hanessian–Hullar *N*-bromosuccinimide-mediated fragmentation of 4,6-benzylidene acetals to their 4-*O*-benzoyl-6-bromo-6-deoxy congeners[154–156] it differs in so far as it is a purely radical fragmentation, as opposed to the radical ionic crossover of the NBS process.[157] The radical fragmentation employed by Crich and Bowers follows the contrathermodynamic path to the less stable primary radical, owing to the greater relief of strain in the fragmentation transition than that required for the formation of the more-stable secondary radical at the 4-position.[158–160]

REFERENCES

1. Z. Guo and L. Bishop, Chemical synthesis of GPIs and GPI-anchored glycopeptides, *Eur. J. Org. Chem.* (2004) 3585–3596.
2. Z. Guo and L. Bishop, in B. Fraser-Reid, K. Tatsuta, and J. Thiem, (Eds.). *Glycoscience,* Springer-Verlag, Berlin, 2008.
3. N. L. Douglas, S. Ley, U. Lucking, and S. L. Warriner, Tuning glycoside reactivity: New tool for efficient oligosaccharide synthesis, *J. Chem. Soc., Perkin Trans.*, 1 (1998) 51–65.
4. P. Grice, S. V. Ley, J. Pietruszka, H. M. I. Osborn, H. W. M. Priepke, and S. L. Warriner, A new strategy for oligosaccharide assembly exploiting cyclohexane-1,2-diacetal methodology: A efficient synthesis of a high mannose type nonasaccharide, *Chem. Eur. J.*, 3 (1997) 431–446.
5. M. Takatani, J. Nakano, M. A. Arai, A. Ishiwata, H. Ohta, and Y. Ito, Accelerated glycosylation under frozen conditions, *Tetrahedron Lett.*, 45 (2004) 3929–3932.
6. A. Düffels, L. G. Green, S. V. Ley, and A. D. Miller, Synthesis of high-mannose type neoglycolipids: Active targeting of liposomes to macrophages in gene therapy, *Chem. Eur. J.*, 6 (2000) 1416–1430.
7. D. Crich and S. Sun, Direct synthesis of β-mannopyranosides by the sulfoxide method, *J. Org. Chem.*, 62 (1997) 1198–1199.
8. D. Crich and S. Sun, Direct chemical synthesis of β-mannopyranosides and other glycosides via glycosyl triflates, *Tetrahedron*, 54 (1998) 8321–8348.
9. Y. L. Zeng, J. J. Zhang, J. Ning, and F. Z. Kong, Synthesis of a mannose heptasaccharide existing in baker's yeast, *Saccharomyces cerevisiae* X2180–1A wild-type strain, *Carbohydr. Res.*, 338 (2003) 5–9.
10. E. Gemma, M. Lahmann, and S. Oscarson, Synthesis of the tetrasaccharide α-D-Glc*p*(1→3)-α-D-Man*p*-(1→2)-α-D-Man*p*-(1→2)-α-D-Man*p* recognized by calreticulin/calnexin, *Carbohydr. Res.*, 340 (2005) 2558–2562.
11. M. C. Hsu, J. Lee, and Y. Kishi, Synthetic 3-*O*-methylmannose-containing polysaccharides (sMMPs): Design and synthesis, *J. Org. Chem.*, 72 (2007) 1931–1940.
12. S. Valerio, A. Pastore, M. Adinolfi, and A. Iadonisi, Sequential one-pot glycosidations catalytically promoted: Unprecedented strategy in oligosaccharide synthesis for the straightforward assemblage of the antitumor PI-88 pentasaccharide, *J. Org. Chem.*, 73 (2008) 4496–4503.

13. A. C. Comely, R. Eelkema, A. J. Minnaard, and B. L. Feringa, *De novo* asymmetric bio- and chemocatalytic synthesis of saccharides – Stereoselective formal *O*-glycoside bond formation using palladium catalysis, *J. Am. Chem. Soc.*, 125 (2003) 8714–8715.
14. H. J. Kim, H. Men, and C. Lee, Stereoselective Palladium-catalyzed *O*-glycosylation using glycals, *J. Am. Chem. Soc.*, 126 (2004) 1336–1337.
15. R. S. Babu, M. Zhou, and G. A. O'Doherty, *De novo* synthesis of oligosaccharides using a palladium-catalyzed glycosylation reaction, *J. Am. Chem. Soc.*, 126 (2004) 3428–3429.
16. T. Ogawa and T. Nukada, Synthesis of a branched mannohexaose, a part structure of a high-mannose-type glycan of a glycoprotein, *Carbohydr. Res.*, 136 (1985) 135–152.
17. S. Hanessian and N. R. Plessas, A new synthesis of chlorodeoxy-sugars, *Chem. Commun.* (1967) 1152–1155.
18. J. J. Zhang, Z. Ma, and F. Kong, Efficient synthesis of a 3,6-branched mannose hepta- and octasaccharide, *Carbohydr. Res.*, 338 (2003) 2039–2046.
19. J. J. Zhang, Z. Ma, and F. Kong, Synthesis of a mannose nonasaccharide existing in the exopolysaccharide of *Cryphonectria parasitica*, *Carbohydr. Res.*, 338 (2003) 1711–1718.
20. Z. C. Ma, J. J. Zhang, and F. Z. Kong, Convergent synthesis of a galactofuranosylated mannan, the repeating unit of *Trichophyton mentagrophytes* IFO 5466 and Trichophyton rubrum IFO 5467, *Tetrahedron Asymmetry*, 15 (2004) 1517–1525.
21. J. Ning, L. S. Heng, and F. Z. Kong, Facile syntheses of D-mannose hexa- and nonasaccharides: The di- and trimer of the trisaccharide repeating unit of the cell-wall mannans of *Epidermophyton floccosum, Trychophyton mentagrophytes, Microsporum canis* and related species of Microsporum, *Tetrahedron Lett.*, 43 (2002) 673–675.
22. Y. Du, M. Zhang, and F. Kong, Highly efficient and practical synthesis of 3,6-branched oligosaccharides, *Org. Lett.*, 2 (2000) 3797–3800.
23. X. Y. Liu, B. L. Stocker, and P. H. Seeberger, Total synthesis of phosphatidylinositol mannosides of *Mycobacterium tuberculosis*, *J. Am. Chem. Soc.*, 128 (2006) 3638–3648.
24. J. K. Fairweather, E. Hammond, and V. Ferro, Synthesis and heparanase inhibitory activity of sulfated mannooligosaccharides related to the antiangiogenic agent PI-88, *Bioorg. Med. Chem.*, 16 (2008) 699–799.
25. G. Gu and Y. Du, Synthesis of a 6V-sulfated mannopentasaccharide analogue related to PI-88, *Carbohydr. Res.*, 339 (2004) 1155–1162.
26. J. R. Merritt and B. Fraser-Reid, *n*-Pentenyl glycoside methodology for rapid assembly of homoglycans exemplified with the nonasaccharide component of a high-mannose glycoprotein, *J. Am. Chem. Soc.*, 114 (1992) 8334–8336.
27. J. R. Merritt, E. Naisang, and B. Fraser-Reid, *n*-Pentenyl mannoside precursors for synthesis of the nonamannan component of high mannose glycoproteins, *J. Org. Chem.*, 59 (1994) 4443–4449.
28. J. Lu, B. Fraser-Reid, and C. Gowda, A strategy for ready preparation of glycolipids for multivalent presentation, *Org. Lett.*, 7 (2005) 3841–3843.
29. L. V. Backinowsky, P. I. Abronina, A. S. Shashkov, A. A. Grachev, N. K. Kochetkov, S. A. Nepogodiev, and J. F. Stoddart, An efficient approach towards the convergent synthesis of "fully-carbohydrate" mannodendrimers, *Chem. Eur. J.*, 8 (2002) 4412–4423.
30. K. N. Jayaprakash, S. R. Chaudhuri, C. V. S. R. Murty, and B. Fraser-Reid, Regioselective strategies mediated by lanthanide triflates for efficient assembly of oligomannans, *J. Org. Chem.*, 72 (2007) 5534–5545.
31. D. M. Ratner, O. J. Plante, and P. H. Seeberger, A linear synthesis of branched high-mannose oligosaccharides from the HIV-1 viral surface envelop glycoprotein gp120, *Eur. J. Org. Chem.*, (2002) 826–833.
32. S. N. Lam and J. Gervay-Hague, Efficient synthesis of man$_2$, man$_3$, man$_5$ oligosaccharides, using mannosyl iodide donors, *J. Org. Chem.*, 70 (2005) 8772–8779.

33. S. Oscarson and A.-K. Tidén, Synthesis of the octyl and tetradecyl glycosides of 3,6-di-*O*-α-D-mannopyranosyl-α-D-mannopyranose and of 3,4-di-*O*-α-D-mannopyranosyl-α-D-mannopyranose. A new way for 2,4-di-*O*-protection of mannopyranosides, *Carbohydr. Res.*, 247 (1993) 323–328.
34. H. S. Cheon, Y. Lian, and Y. Kishi, Highly stereoselective and iterative synthesis of α-(1→4)-linked polysaccharides composed of 3-*O*-methyl-D-mannose, *Org. Lett.*, 9 (2007) 3323–3326.
35. R. Chevalier, J. Esnault, P. Vandewalle, B. Sendid, J. F. Colombel, D. Poulain, and J.-M. Mallet, Synthetic yeast oligomannosides as biological probes: α-D-Man*p* (1→3) α-D-Man*p* (1→2) α-D-Man*p* and α-D-Man*p* (1 →3) α-D-Man*p* (1→2) α-D-Man*p* (1→2) α-D-Man*p* as Crohn's disease markers, *Tetrahedron*, 61 (2005) 7669–7677.
36. H.-K. Lee, C. N. Scanlan, C.-Y. Huang, A. Y. Chang, D. A. Calarese, R. A. Dwek, P. M. Rudd, D. R. Burton, I. A. Wilson, and C.-H. Wong, Reactivity-based one-pot synthesis of oligomannose: Defining antigens recognized by 2G12, a broadly neutralizing anti-HIV-1 antibody, *Angew. Chem. Int. Ed.*, 43 (2004) 1000–1003.
37. D. Crich and S. Sun, Are glycosyl triflates intermediates in the sulfoxide glycosylation method? A chemical and ^{1}H, ^{13}C, and ^{19}F NMR spectroscopic investigation, *J. Am. Chem. Soc.*, 119 (1997) 11217–11223.
38. D. Kahne, S. Walker, Y. Cheng, and D. Van Engen, Glycosylation of unreactive substrates, *J. Am. Chem. Soc.*, 111 (1989) 6881–6882.
39. D. Crich and S. Sun, Direct formation of *β*-mannopyranosides and other hindered glycosides from thioglycosides, *J. Am. Chem. Soc.*, 120 (1998) 435–436.
40. N. Teumelsan and X. Huang, Synthesis of branched man5 oligosaccharides and an unusual stereochemical observation, *J. Org. Chem.*, 72 (2007) 8976–8979.
41. L. Jiang and T. H. Chan, Efficient synthesis of the nonamannoside residue of high mannose glycoproteins, *Can. J. Chem.*, 83 (2005) 693–701.
42. R. Blattner, R. H. Furneaux, and M. Ludewig, Synthesis of oligomannosides in solution and on a soluble polymer support: a comparison, *Carbohydr. Res.*, 341 (2006) 299–321.
43. J. Wu and Z. Guo, Cap and capture-release techniques applied to solid-phase synthesis of oligosaccharides, *J. Org. Chem.*, 71 (2006) 7067–7070.
44. A. K. Pathlak, C. K. Yerneni, Z. Young, and V. Pathlak, Oligomannan synthesis using ionic liquid supported glycosylation, *Org. Lett.*, 10 (2008) 145–148.
45. J. Rademann and R. R. Schmidt, Repetitive solid phase glycosylation on an alkyl thiol polymer leading to sugar oligomers containing 1,2-*trans*- and 1,2-*cis*-glycosidic linkages, *J. Org. Chem.*, 62 (1997) 3650–3653.
46. D. M. Whitfield, E. E. Eichlera, and G. D. Sprott, Synthesis of archaeal glycolipid adjuvants – What is the optimum number of sugars? *Carbohydr. Res.*, 343 (2008) 2349–2300.
47. F. Roussel, L. Knerr, M. Grathwohl, and R. R. Schmidt, *O*-Glycosyl trichloroacetimidates bearing Fmoc as temporary hydroxy protecting group: A new access to solid-phase oligosaccharide synthesis, *Org. Lett.*, 2 (2000) 3043–3046.
48. M. Grathwohl and R. R. Schmidt, Solid phase synthesis of oligomannosides and of a lactosamine containing milk trisaccharide using a benzoate linker, *Synthesis*, 15 (2001) 2263–2272.
49. R. B. Andrade, O. J. Plante, L. G. Melean, and P. H. Seeberger, Solid-phase oligosaccharide synthesis: Preparation of complex structures using a novel linker and different glycosylating agents, *Org. Lett.*, 1 (1999) 1811–1814.
50. M. Nishizawa, H. Imagawa, E. Morikuni, S. Hatakeyama, and H. Yamada, Synthesis of cyclo-L-rhamnopentaose, *Chem. Pharm. Bull.*, 42 (1994) 1365–1366.
51. M. Nishizawa, H. Imagawa, Y. Kan, and H. Yamada, Total synthesis of cyclo-L-rhamnohexaose by a stereoselective thermal glycosylation, *Tetrahedron Lett.*, 32 (1991) 5551–5554.
52. H. M. Nguyen, J. L. Poole, and D. Y. Gin, Chemoselective iterative dehydrative glycosylation, *Angew. Chem., Int. Ed.*, 40 (2001) 414–417.

53. D. Crich and O. Vinogradova, Synthesis of the antigenic tetrasaccharide side chain from the major glycoprotein of *Bacillus anthracis* exosporium, *J. Org. Chem.*, 72 (2007) 6513–6520.
54. R. Adamo, R. Saksena, and P. Kováč, Synthesis of the β-anomer of the spacer-equipped tetrasaccharide side chain of the major glycoprotein of the *Bacillus anthracis* exosporium, *Carbohydr. Res.*, 340 (2005) 2579–2582.
55. R. Adamo, R. Saksena, and P. Kováč, Studies towards a conjugate vaccine for anthrax: Synthesis of the tetrasaccharide side chain of the *Bacillus anthracis* exosporium, *Helv. Chim. Acta*, 89 (2006) 1075–1089.
56. R. Saksena, R. Adamo, and P. Kováč, Synthesis of the tetrasaccharide side chain of the major glycoprotein of the *Bacillus anthracis* exosporium, *Bioorg. Med. Chem. Lett.*, 16 (2006) 615–617.
57. S. V. Ley and H. W. M. Priepke, Cyclohexane 1,2-diacetals in synthesis. A facile one-pot synthesis of a trisaccharide unit from the common polysaccharide antigen of group B Streptococci using cyclohexane-1,2-diacetal protected rhamnosides, *Angew. Chem. Int. Ed;* 33 (1994) 2290–2292.
58. I. Kitagawa, N. I. Baek, K. Ohashi, M. Sakagami, M. Yoshikawa, and H. Shibuya, Mammosides B and H1, new ionophoric resin-glycosides from the tuber of *Merremia mammosa,* an Indonesian folk medicine, *Chem. Pharm. Bull.*, 37 (1989) 1131–1133.
59. V. Pozsgay, J. R. Brisson, and H. J. Jennings, Synthetic oligosaccharides related to group B streptococcal polysaccharides. The rhamnotriose moiety of the common antigen, *Can. J. Chem.*, 65 (1987) 2764–2769.
60. Y. Zhu and F. Kong, Concise and effective synthesis of α (1→2)-linked manno- and rhamnopyranosyl oligosaccharides and related antigenic factor 4 and dominant of antigenic factor 6, *Synlett*, (2000) 1783–1787.
61. E. Bedini, A. Carabellese, D. Comegna, C. De Castro, and M. Parrilli, Synthetic oligorhamnans related to the most common O-chain backbone from phytopathogenic bacteria, *Tetrahedron*, 62 (2006) 8474–8483.
62. E. Bedini, A. Carabellese, M. Schiattarella, and M. Parrilli, First synthesis of an α-D-Fucp3NAc containing oligosaccharide: A study on D-Fucp3NAc glycosylation, *Tetrahedron*, 61 (2005) 5439–5448.
63. E. Bedini, G. Barone, C. Unverzagt, and M. Parrilli, Synthesis of the pentasaccharide repeating unit of the major O-antigen component from *Pseudomonas syringae* pv. ribicola NVPPB 1010, *Carbohydr. Res.*, 339 (2004) 393–400.
64. A. Ravidà, X. Liu, L. Kovacs, and P. H. Seeberger, Synthesis of glycosyl phosphates from 1,2-orthoesters and application to *in situ* glycosylation reactions, *Org. Lett.*, 8 (2006) 1815–1818.
65. J. Bauer and J. Rademann, Hydrophobically assisted switching phase synthesis: The flexible combination of solid-phase and solution-phase reactions employed for oligosaccharide preparation, *J. Am. Chem. Soc.*, 127 (2005) 7296–7297.
66. J. J. Zhang and F. Kong, A general method for the synthesis of oligosaccharides consisting of α-(1→2)- and α-(1→3)-linked rhamnan backbones and GlcNAc side chains, *Tetrahedron*, 59 (2003) 1429–1441.
67. J. J. Zhang, Y. Zhu, and F. Kong, Synthesis of an L-rhamnose tetrasaccharide, the common and major structure of the repeating unit of the O-antigenic polysaccharide of a strain of *Klebsiella pneumoniae* and *Pseudomonas holci*, *Carbohydr. Res.*, 336 (2001) 229–235.
68. V. Pozsgay and H. J. Jennings, Synthetic oligosaccharides related to group B streptococcal polysaccharides. 3. Synthesis of oligosaccharides corresponding to the common polysaccharide antigen of group B streptococci, *J. Org. Chem.*, 53 (1988) 4042–4052.
69. E. R. Palmacci, O. J. Plante, M. C. Hewitt, and P. H. Seeberger, Automated synthesis of oligosaccharides, *Helv. Chim. Acta*, 86 (2003) 3975–3990.
70. Z. Zhang, P. G. Wang, N. Ding, G. Song, and Y. Li, Total synthesis of cleistetroside-2, partially acetylated dodecanyl tetra-rhamnoside derivative isolated from *Cleistopholis patens* and *Cleistopholis glauca*, *Carbohydr. Res.*, 342 (2007) 1159–1168.

71. Z. Ma, J. J. Zhang, and F. Kong, A concise synthesis of two isomeric pentasaccharides, the O repeat units from the lipopolysaccharides of *P. syringae* pv. porri NCPPB 3364T and NCPPB 3365, *Carbohydr. Res.*, 339 (2004) 43–49.
72. J. J. Zhang and F. Kong, Synthesis of a xylosylated rhamnose pentasaccharide-the repeating unit of the O-specific side chain of lipopolysaccharides from the reference strains for *Stenotrophomonas maltophilia* serogroup O18, *J. Carbohydr. Chem.*, 21 (2002) 89–97.
73. J. J. Zhang and F. Kong, Synthesis of an xylosylated rhamnose pentasaccharide, the repeating unit of the O-chain polysaccharide of the lipopolysaccharide of *Xanthomonas campestris* pv. begoniae GSPB 525, *Carbohydr. Res.*, 337 (2002) 391–396.
74. Z. Varga, I. Bajza, G. Batta, and A. Lipták, Synthesis of the pentasaccharide hapten from the glycopeptidolipid antigen of *Mycobacterium avium* serovar 17, *Tetrahedron Lett.*, 42 (2001) 5283–5286.
75. H. Yu, B. Yu, X. Y. Wu, Y. Z. Hui, and X. W. Han, Synthesis of a group of diosgenyl saponins with combined use of glycosyl trichloroacetimidate and thioglycoside donors, *J. Chem. Soc., Perkin Trans.*, 19 (2000) 1445–1453.
76. R. Saksena, R. Adamo, and P. Kováč, Immunogens related to the synthetic tetrasaccharide side chain of the *Bacillus anthracis* exosporium, *Bioorg. Med. Chem.*, 15 (2007) 4283–4310.
77. A. S. Mehta, E. Saile, W. Zhong, T. Buskas, R. Carlson, E. Kannenberg, Y. Reed, C. P. Quinn, and G.-J. Boons, Synthesis and antigenic analysis of the BclA glycoprotein oligosaccharide from the *Bacillus anthracis* exosporium, *Chem. Eur. J.*, 12 (2006) 9136–9149.
78. D. B. Werz, A. Adibekian, and P. H. Seeberger, Synthesis of a spore surface pentasaccharide of *Bacillus anthracis*, *Eur. J. Org. Chem.* (2007) 1976–1982.
79. D. B. Werz and P. H. Seeberger, Total synthesis of antigen *Bacillus anthracis* tetrasaccharide-creation of an anthrax vaccine candidate, *Angew. Chem., Int.l Ed.*, 44 (2005) 6315–6318.
80. Y. Zeng and F. Kong, Synthesis of a hexasaccharide fragment of group E streptococci polysaccharide and the tetrasaccharide repeating unit of *E. coli* O7:K98:H6, *Carbohydr. Res.*, 339 (2004) 1503–1510.
81. J. J. Zhang and F. Kong, Synthesis of β-D-Glc*p*-(1→2)-[β-D-Rib*f*-(1→3)-]-α-L-Rha*p*-(1→3)-α-L-Rha*p*-(1→2)-α-L-Rha*p*, the repeating unit of the lipopolysaccharide of *Acetobacter diazotrophicus* PAL 5, *J. Carbohydr. Chem.*, 21 (2002) 579–589.
82. J. J. Zhang, J. Ning, and F. Kong, Efficient synthesis of a heptasaccharide, the repeating unit of the O-chain lipopolysaccharide produced by *Xanthomonas campestris* strain 642, *Carbohydr. Res.*, 338 (2003) 1023–1031.
83. C. Höög, A. Rotondo, B. D. Johnston, and B. M. Pinto, Synthesis and conformational analysis of a pentasaccharide corresponding to the cell-wall polysaccharide of the Group A *Streptococcus*, *Carbohydr. Res.*, 337 (2002) 2023–2036.
84. F. Bélot, C. Guerreiro, F. Baleux, and L. A. Mulard, Synthesis of two linear PADRE conjugates bearing a deca- or pentadecasaccharide B epitope as potential synthetic vaccines against *Shigella flexneri* serotype 2a infection, *Eur. J. Chem.*, 11 (2005) 1625–1635.
85. F. Bélot, K. Wright, C. Costachel, A. Phalipon, and L. A. Mulard, Blockwise approach to fragments of the O-specific polysaccharide of *Shigella flexneri* serotype 2a: Convergent synthesis of a decasaccharide representative of a dimer of the branched repeating unit, *J. Org. Chem.*, 69 (2004) 1060–1074.
86. F. Bélot, C. Costachel, K. Wright, A. Phalipon, and L. A. Mulard, Synthesis of the methyl glycoside of a branched octasaccharide fragment specific for the *Shigella flexneri* serotype 2a O-antigen, *Tetrahedron Lett.*, 43 (2002) 8215–8218.
87. K. Wright, C. Guerreiro, I. Laurent, F. Baleux, and L. A. Mulard, Preparation of synthetic glycoconjugates as potential vaccines against *Shigella flexneri* serotype 2a disease, *Org. Biomol. Chem.*, 2 (2004) 1518–1527.

88. J. J. Zhang and F. Kong, Synthesis of β-D-GlcpNAc-(1→3)-α-L-Rhap-(1→2)-[β-L-Xylp-(1→4)]-α-L-β-(1→3)-α-L-Rhap, the repeating unit of the O-antigen produced by *Pseudomonas solanacearum* ICMP 7942, *Carbohydr. Res.*, 338 (2003) 19–27.
89. E. Bedini, M. Parrilli, and C. Unverzagt, Oligomerization of a rhamnanic trisaccharide repeating unit of O-chain polysaccharides from phytopathogenic bacteria, *Tetrahedron Lett.*, 43 (2002) 8879–8882.
90. B. M. Pinto, K. B. Reimer, D. G. Morissette, and D. R. Bundle, Oligosaccharides corresponding to biological repeating units of *Shigella flexneri* variant Y polysaccharide. IV. Synthesis and 2D-NMR analysis of a pentasaccharide glycoside of the biological repeating units of *Shigella flexneri* variant Y polysaccharide and the preparation of a synthetic antigen, *Carbohydr. Res.*, 196 (1990) 156–166.
91. B. M. Pinto, K. B. Reimer, D. G. Morissette, and D. R. Bundle, Oligosaccharides corresponding to biological repeating units of *Shigella flexneri* variant-Y Polysaccharide.2. Synthesis and two-dimensional NMR analysis of a hexasaccharide hapten, *J. Org. Chem.*, 54 (1989) 2650–2656.
92. N. E. Byramova, Y. E. Tsvetkov, L. V. Bakinovskii, and N. K. Kochetkov, Synthesis of the basic chain of the O-specific polysaccharides of *Shigella flexneri*, *Carbohydr. Res.*, 137 (1985) C8–C13.
93. L. A. Mulard, M.-J. Clement, A. Imberty, and M. Delepierre, Synthesis of ligands related to the O-specific polysaccharides of *Shigella flexneri* serotype 2a and *Shigella flexneri* serotype 5a. Part 7. Convergent synthesis, NMR and conformational analysis of tetra- and pentasaccharide haptens of the *Shigella flexneri* serotype 5a O-specific polysaccharide, *Eur. J. Org. Chem*, (2002) 2486–2498.
94. C. Costachel, P. J. Sansonetti, and L. A. Mulard, Synthesis of ligands related to the O-specific polysaccharides of *Shigella flexneri* serotype 5a. 5. Linear synthesis of the methyl glycosides of tetra- and pentasaccharide fragments specific for the *Shigella flexneri* serotype 2a O-antigen, *J. Carbohydr. Chem.*, 19 (2000) 1131–1150.
95. L. A. Mulard and J. Ughetto-Monfrin, Linear synthesis of the methyl glycosides of tri-, tetra-, and pentasaccharide fragments of the *Shigella flexneri* serotype 5a O-antigen, *J. Carbohydr. Chem.*, 19 (2000) 503–526.
96. H. Guo and G. A. O'Doherty, *De novo* asymmetric synthesis of the anthrax tetrasaccharide by a palladium-catalyzed glycosylation reaction, *Angew. Chem., Int. Ed.*, 46 (2007) 5206–5208.
97. H. Guo and G. A. O'Doherty, *De novo* asymmetric synthesis of anthrax tetrasaccharide and related tetrasaccharide, *J. Org. Chem.*, 73 (2008) 5211–5220.
98. F. Barresi and O. Hindsgaul, in S. H. Khan and R. A. O'Neill, (Eds.), *Modern Methods in Carbohydrate Synthesis,* Harwood Academic Publishers, Amsterdam, 1996, pp. 251–276.
99. Y. Ito and Y. Ohnishi, in B. Fraser-Reid, T. Kuniaki, and J. Thiem, (Eds.), Glycoscience: Chemistry and Chemical Biology, Springer-Verlag, Berlin, 2001, pp. 1589–1619.
100. A. V. Demchenko, Stereoselective chemical 1,2-cis-*O*-glycosylation: From sugar Ray to modern techniques of the 21st century, *Synlett*, (2003) 1225–1240.
101. V. Pozsgay, in B. Ernst, G. W. Hart, and P. Sinaÿ, (Eds.) *Carbohydrates in Chemistry and Biology,* Wiley-VCH, Weinheim, 2000, pp. 319–343.
102. J. J. Gridley and H. M. I. Osborn, Recent advances in the construction of β-D-mannose and β-D-mannosamine linkages, *J. Chem. Soc., Perkin Trans.*, 1 (2000) 1471–1491.
103. J. D. C. Codée, L. J. Van den Bos, R. E. J. N. Litjens, H. S. Overkleeft, C. A. A. Van Boeckel, J. H. Van Boom, and G. A. Van der Marel, Chemoselective glycosylations using sulfonium triflate activator systems, *Tetrahedron*, 60 (2004) 1057–1064.
104. G. W. J. Twaddle, D. V. Yashunsky, and A. V. Nikolaev, The chemical synthesis of β-(1→4)-linked D-mannobiose and D-mannotriose, *Org. Biomol. Chem.*, 1 (2003) 623–628.
105. K. Sato, A. Yoshitomo, and Y. Takai, A novel method for constructing β-D-mannosidic, 2-acetamido-2-deoxy-β-D-mannosidic, and 2-deoxy-D-*arabino*-hexopyranosidic units from the bis(triflate) derivative of β-D-galactoside, *Bull. Chem. Soc. Jpn.*, 70 (1997) 885–890.

106. S. David, A. Malleron, and C. Dini, Preparation of oligosaccharides with β-D-mannopyranosyl and 2-azido-2-deoxy-β-D-mannopyranosyl residues by inversion at C-2 after coupling, *Carbohydr. Res.*, 188 (1989) 193–200.
107. J. Alais and S. David, Preparation of disaccharides having a β-D-mannopyranosyl group from *N*-phthaloyllactosamine derivatives by double or triple S_N2 substitution, *Carbohydr. Res.*, 201 (1990) 69–77.
108. F. W. Lichtenthaler, T. Schneider-Adams, and S. Immel, Practical synthesis of β-D-Xyl-(1→2)-β-D-Man-(1→4)-α-D-Glc-OMe, a trisaccharide component of the hyriopsis-Schlegelii glycosphingolipid, *J. Org. Chem.*, 59 (1994) 6735–6738.
109. F. W. Lichtenthaler, U. Klares, Z. Szurmai, and B. Werner, 4,6-di-*O*-benzoyl-3-*O*-benzyl-α-D-arabino-hexo-pyranos-2-ulosyl bromide: A conveniently accessible glycosyl donor for the expedient construction of diantennary β-D-mannosides branched at O-3 and O-6, *Carbohydr. Res.*, 305 (1997) 293–303.
110. F. W. Lichtenthaler and T. Schneider-Adams, 3,4,6-Tri-*O*-benzyl-α-D-*arabino*-hexopyranos-2-ulosyl bromide – A versatile glycosyl donor for the efficient generation of β-D-mannopyranosidic linkages, *J. Org. Chem.*, 59 (1994) 6728–6734.
111. R. U. Lemieux and R. M. Ratcliffe, The azidonitration of tri-*O*-acetyl-D-galactal, *Can. J. Chem.*, 57 (1979) 1244–1251.
112. J.-R. Pougny and P. Sinaÿ, Reaction d'imidates de glucopyranosyle avec l'acetonitrile. Applications synthetiques, *Tetrahedron Lett.*, 17 (1976) 4073–4076.
113. I. Braccini, C. Derouet, J. Esnault, C. H. de Penhoat, J.-M. Mallet, and V. Michon, and P. Sinaÿ, *Carbohydr. Res.*, 246 (1993) 23–41.
114. R. R. Schmidt, M. Behrendt, and A. Toepfer, Nitriles as solvents in glycosylation reactions: highly selective β-glycoside synthesis, *Synlett*, (1990) 694–696.
115. A. J. Ratcliffe and B. Fraser-Reid, Generation of α-D-glucopyranosylacetonitrilium ions. Concerning the reverse anomeric effect, *J. Chem. Soc., Perkin Trans.*, 1 (1990) 747–750.
116. D. Majumdar and G.-J. Boons, in D. Crich, (Ed.), *Handbook of Reagents for Organic Synthesis: Reagents for Glycoside, Nucleotide, and Peptide Synthesis,* Wiley, Chichester, 2005, pp. 11–15.
117. D. Crich and M. Patel, On the nitrile effect in L-rhamnopyranosylation, *Carbohydr. Res.*, 341 (2006) 1467–1475.
118. M. Nitz, B. W. Purse, and D. R. Bundle, Synthesis of a β-1,2-mannopyranosyl tetrasaccharide found in the phosphomannan antigen of *Candida albicans*, *Org. Lett.*, 2 (2000) 2939–2942.
119. M. Nitz and D. R. Bundle, Synthesis of di- to hexasaccharide 1,2-linked β-mannopyranan oligomers, a terminal S-linked tetrasaccharide congener and the corresponding BSA glycoconjugates, *J. Org. Chem.*, 66 (2001) 8411–8423.
120. X. Y. Wu and D. R. Bundle, Synthesis of glycoconjugate vaccines for *Candida albicans* using novel linker methodology, *J. Org. Chem.*, 70 (2005) 7381–7388.
121. D. Crich and H. M. Li, Direct stereoselective synthesis of β-thiomannoside, *J. Org. Chem.*, 65 (2000) 801–805.
122. C. Fradin, T. Jouault, A. Mallet, J.-M. Mallet, D. Camus, P. Sinaÿ, and D. Poulain, β-1,2-linked oligomannosides inhibit *Candida albicans* binding to murine macrophage, *J. Leukocyte Biol.*, 60 (1996) 81–87.
123. G. Ekborg and B. Lindberg, and J. Lönngren, Synthesis of β-D-mannopyranosides, *Acta Chem. Scand. B.*, 26 (1972) 3287–3292.
124. M. A. E. Shaban and R. W. Jeanloz, The synthesis of 2-acetamido-2-deoxy-4-*O*-β-D-mannopyranosyl-D-glucose, *Carbohydr. Res.*, 52 (1976) 115–127.
125. F. Mathew, M. Mach, K. C. Hazen, and B. Fraser-Reid, Orthoester-based strategy for efficient synthesis of the virulent antigenic 1,2-linked oligomannans of *Candida albicans*, *Synlett*, 9 (2003) 1319–1322.

126. T. Iversen and D. R. Bundle, Direct and efficient synthesis of β-L-rhamnopyranosides, *J. Org. Chem.*, 46 (1981) 5389–5393.
127. V. K. Srivastava and C. Schuerch, Synthesis of some disaccharide derivatives containing a β-L-rhamnopyranosidic bond, *Carbohydr. Res.*, 100 (1982) 411–417.
128. L. V. Backinowsky, N. F. Balan, A. S. Shashkov, and N. K. Kochetkov, Synthesis and ^{13}C-NMR spectra of β-L-rhamnopyranosides, *Carbohydr. Res.*, 84 (1980) 225–235.
129. A. M. Szpilman, J. M. Manthorpe, and E. M. Carreira, Synthesis and biological studies of 35-deoxy amphotericin B methyl ester, *Angew. Chem. Int. Ed.*, 47 (2008) 4339–4342.
130. G. K. Packard and S. D. Rychnovsky, β-Selective glycosylations with masked D-mycosamine precursors, *Org. Lett.*, 3 (2001) 3393–3396.
131. R. Lau, G. Schüle, U. Schwaneberg, and T. Ziegler, Intramolecular glycosylation of prearranged saccharides as a novel strategy for the construction of β-L-rhamnopyranosidic linkages, *Liebigs Ann.*, (1995) 1745–1754.
132. T. Ziegler and G. Lemanski, Double asymmetric induction during intramolecular glycosylation, *Eur. J. Org. Chem.*, (1998) 163–170.
133. F. W. Lichtenthaler and T. Metz, Efficient generation of β-L-rhamnosidic linkages by the 2-ulosyl donor approach: Synthesis of a trisaccharide with a central β-L-rhamnose unit, *Eur. J. Org. Chem.*, (2003) 3081–3093.
134. D. Crich, H. M. Li, Q. J. Yao, D. J. Wink, R. D. Sommer, and A. L. Rheingold, Direct synthesis of β-mannans. A hexameric(1→3)-β-D-Man-(1→4)-β-D-Man-(1→3) subunit of the antigenic polysaccharides from *Leptospira biflexa* and the octameric (1→ 2)-linked β-D-mannan of the *Candida albicans* phospholipomannan. X-ray crystal structure of a protected tetramer, *J. Am. Chem. Soc.*, 123 (2001) 5826–5828.
135. D. Crich, A. Banerjee, and Q. J. Yao, Direct chemical synthesis of the β-D-mannans: The β-(1→2) end β-(1→4) series, *J. Am. Chem. Soc.*, 126 (2004) 14930–14934.
136. M. Nitz, C.-C. Ling, A. Otter, J. E. Cutler, and D. R. Bundle, The unique solution structure and immunochemistry of the *Candida albicans* β-1,2-mannopyranan cell wall antigens, *J. Biol. Chem.*, 277 (2002) 3440–3446.
137. F. Dromer, R. Chevalier, B. Sendid, L. Improvisi, T. Jouault, R. Robert, J.-M. Mallet, and D. Poulain, Synthetic analogues of β-1,2-oligomannosides prevent intestinal colonization by the pathogenic yeast *Candida albicans*, *Antimicrob. Agents Chemother.*, 46 (2002) 3869–3876.
138. P. J. Garegg, H. Hultberg, and S. Wallin, Novel, reductive ring-opening of carbohydrate benzylidene acetals, *Carbohydr. Res.*, 108 (1982) 97–101.
139. L. Jiang and T.-H. Chan, Borane/Bu_2BOTf: A mild reagent for the regioselective reductive ring opening of benzylidene acetals in carbohydrates, *Tetrahedron Lett.*, 39 (1998) 355–358.
140. M. Sakagami and H. Hamana, A selective ring opening reaction of 4,6-*O*-benzylidene acetals in carbohydrates using trialkylsilane derivatives, *Tetrahedron Lett.*, 41 (2000) 5547–5551.
141. R. Johansson and B. Samuelsson, Regioselective reductive ring-opening of 4-methoxybenzylidene acetals of hexopyranosides. Access to a novel protecting-group strategy, *J. Chem. Soc., Perkin Trans.*, 1 (1984) 2371–2374.
142. C. C. Wang, S. Y. Luo, C. R. Shie, and S.-C. Hung, Metal trifluoromethanesulfonate-catalyzed regioselective borane-reductive ring opening of benzylidene acetals: A concise synthesis of 1,4-dideoxy-1,4-imino-L-xylitol, *Org. Lett.*, 4 (2002) 847–849.
143. P. J. Garegg, in S. Hanessian, (Ed.), *Preparative Carbohydrate Chemistry,* Dekker, New York, 1993, pp. 53–67.
144. J. Hernández-Torres, J. Achkar, and A. Wei, Temperature-controlled regioselectivity in the reductive cleavage of *p*-methoxybenzylidene acetals, *J. Org. Chem.*, 69 (2004) 7206–7211.

145. K. S. Kim, D. B. Fulse, J. Y. Baek, B.-Y. Lee, and H. B. Jeon, Stereoselective direct glycosylation with anomeric hydroxy sugars by activation with phthalic anhydride and trifluoromethanesulfonic anhydride involving glycosyl phthalate intermediates, *J. Am. Chem. Soc.*, 130 (2008) 8537–8547.
146. D. Crich, W. Li, and H. Li, Direct chemical synthesis of the β-mannans: Linear and block synthesis of the alternating β-(1→3)-β-(1→4)-mannan common to *Rhodotorula glutinis*, *Rhodotorula mucilaginosa*, and *Leptospira biflexa*, *J. Am. Chem. Soc.*, 126 (2004) 15081–15086.
147. J. D. C. Codée, L. H. Hossain, and P. H. Seeberger, Efficient installation of β-mannosides using a dehydrative coupling strategy, *Org. Lett.*, 7 (2005) 3251–3254.
148. D. Crich and V. Y. Dudkin, An unusual example of steric buttressing in glycosylation, *Tetrahedron Lett.*, 41 (2000) 5643–5646.
149. D. Crich, P. Jayalath, and T. K. Hutton, Enhanced diastereoselectivity in β-mannopyranosylation through the use of sterically minimal propargyl ether protecting groups, *J. Org. Chem.*, 71 (2006) 3064–3070.
150. D. Crich, B. Wu, and P. Jayalath, Convergent synthesis of a β-(1→3)-mannohexaose, *J. Org. Chem.*, 72 (2007) 6806–6815.
151. D. Crich and B. Wu, 1-Naphthylpropargyl ether group: A readily cleaved and sterically minimal protecting system for stereoselective glycosylation, *Org. Lett.*, 8 (2006) 4879–4882.
152. H. Paulsen and W. Kutschker, Synthesis of β-L-rhamnoside linked oligosaccharides of lipopolysaccharides from *Shigella flexneri* serotype 6, *Carbohydr. Res.*, 120 (1983) 25–42.
153. D. Crich and A. A. Bowers, Synthesis of a β-(1→3)-D-rhamnotetraose by a one-pot, multiple radical fragmentation, *Org. Lett.*, 8 (2006) 4327–4330.
154. S. Hanessian and N. R. Plessas, The reaction of *O*-benzylidene sugars with *N*-bromosuccinimide. II. Scope and synthetic utility in the methyl 4,6-*O*-benzylidenehexopyranoside series, *J. Org. Chem.*, 34 (1969) 1035–1044.
155. D. Crich, Q. J. Yao, and A. A. Bowers, On the regioselectivity of the Hanessian–Hullar reaction in 4,6-*O*-benzylidene protected galactopyranosides, *Carbohydr. Res.*, 341 (2006) 1748–1752.
156. W. A. Szarek, Deoxyhalogeno sugars, *Adv. Carbohydr. Chem. Biochem.*, 28 (1973) 225–306.
157. J. McNulty, J. Wilson, and A. C. Rochon, Regiocontrol in the oxidative radical fragmentation of benzylidene acetals and its mechanistic applications, *J. Org. Chem.*, 69 (2004) 563–565.
158. Y. Cai, H. S. Dang, and B. P. Roberts, Regioselectivity in the ring opening β-scission of 2-phenyl-1,3-dioxan-2-yl radicals derived from bicyclic benzylidene acetals, *J. Chem. Soc., Perkin Trans.*, 1 (2002) 2449–2458.
159. A. J. Fielding, P. Franchi, B. P. Roberts, and T. M. Smits, EPR and computational studies of the formation and β-scission of cyclic and acyclic dialkoxyalkyl radicals, *J. Chem. Soc., Perkin Trans.*, 2 (2002) 155–163.
160. D. Crich and A. A. Bowers, 4,6-*O*-[1-Cyano-2-(2-iodophenyl)ethylidene] acetals. Improved second generation acetals for the stereoselective formation of β-D-mannopyranosides and regioselective reductive radical fragmentation to β-D-Rhamnopyranosides. scope and limitations, *J. Org. Chem.*, 71 (2006) 3452–3463.

GLYCOBIOLOGY OF *TRYPANOSOMA CRUZI*

BY ROSA M. DE LEDERKREMER and ROSALÍA AGUSTI

CHIDECAR, Departamento de Química Orgánica, Facultad de Ciencias Exactas y Naturales,
Universidad de Buenos Aires, Pabellón II, Ciudad Universitaria, 1428 Buenos Aires, Argentina

I. Introduction 312
II. Life Cycle of the Parasite 312
III. Specific Cell-Surface Glycoconjugates 313
  1. Glycoinositolphospholipids, Free and as Anchors of Proteins 313
  2. *Trypanosoma cruzi* Mucins 321
  3. *T. cruzi* Trans-sialidase (TcTS) 336
  4. Other Glycoproteins 352
IV. Concluding Remarks 354
References 355

ABBREVIATIONS

A., amastigotes; AAG, alkylacylglycerol; AEP, aminoethylphosphonic acid; CRD, cross reacting determinant; C-T, C terminus; DHS, dihydrosphingosine; E, epimastigotes; ER, endoplasmic reticulum; EtN, ethanolamine; GC–MS, gas chromatography–mass spectrometry; GIPLs, glycoinositolphospholipids; GPI, glycophosphatidylinositol; GPIT, glycophosphatidylinositol transamidase; HC, highly conserved N terminus; HPAEC-PAD, high pH anion-exchange chromatography–pulse amperometric detection; HV, hypervariable N-terminus; IPC, inositolphosphoceramide; IPL, inositol phospholipid; LPPG, lipopeptidophosphoglycan; MASP, mucin-associated surface proteins; PI, phosphatidylinositol; PI-PLC, phosphatidylinositol phospholipase C; PLD, phospholipase D; SDS–PAGE, sodium dodecylsulfate–polyacrylamide gel electrophoresis; SP, sphingosine; T, cell-derived trypomastigotes; TBDPC, *tert*-butylchlorodiphenylsilane; TcMUC, *T. cruzi* mucin gene family; TcSMUG,

ISBN: 978-0-12-374743-3
DOI: 10.1016/S0065-2318(09)00007-9

© 2009 Elsevier Inc. All rights reserved.

T. cruzi small mucin-like gene family; TcTS, *Trypanosoma cruzi* trans-sialidase; THF, tetrahydrofuran; TMSOTf, trimethylsilyl trifluoromethanesulfonate; TRR, Thr-rich región; TSSA, trypomastigote small surface antigen; UDP, uridine diphosphate; VSG, variant surface glycoprotein.

I. INTRODUCTION

Trypanosoma cruzi is the causative agent of Chagas' disease, American trypanosomiasis, endemic to many countries of South and Central America and affecting millions of people.[1] The parasite is transmitted to animals, including humans, by insect vectors of the family Reduviidae. Following the acute phase of the disease a chronic infection is usually established, and thus, the parasites may be transmitted during pregnancy or by blood transfusions and organ transplants. With increasing northbound immigration of people from Latin America, the disease is now of concern for the northern countries, which do not screen donors for Chagas' disease. Cardiomyopathy is the most common of the manifestations of chronic Chagas' disease.

The genome sequence of *T. cruzi* has been described,[2] but no vaccines or effective drugs are yet available to control the disease.

Studies on the cell-surface molecules of *T. cruzi* have revealed unique structures. Knowledge of the glycobiology of *T. cruzi* has contributed significantly to the identification of target enzymes responsible for the construction of these molecules. Efforts are now underway in several laboratories to find specific inhibitors for these enzymes. This task is complicated by the recognition of subpopulations of *T. cruzi* strains having characteristic individual properties.

According to biological, genetic, biochemical, and immunological studies, these strains have been classified into two major phylogenetic lineages.[3–4] The *T. cruzi* 1 group is associated with the sylvatic transmission cycle and infection of such small vertebrate animals as the opossum. Strains belonging to lineage 2 are associated with the domestic transmission cycle and chronic human disease.

Controversial results have been reported on the relation between the genetic group and the infectivity of an isolate.[5–7] Most *T. cruzi* proteins are heavily glycosylated, and the carbohydrate modification is strongly dependent on the life cycle and original lineage of the parasite, as described in the following sections of this chapter.

II. LIFE CYCLE OF THE PARASITE

T. cruzi differentiates during its life cycle as it travels from insects to humans, undergoing biochemical and morphological changes (Fig. 1).[8]

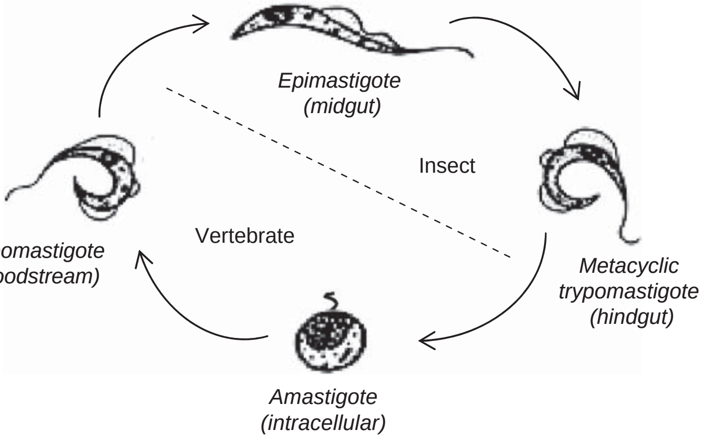

FIG. 1. Life cycle of *Trypanosoma cruzi*.

Epimastigotes replicate in the midgut of a triatomine insect, commonly *Triatoma infestans* (vinchuca) in Argentina and *Rhodnius prolixus* (barbeiro) in Brazil. In the intestine, they transform into non-proliferative metacyclic trypomastigotes that pass from the hindgut to the feces. The infective trypomastigotes enter the vertebrate host through a skin wound or through mucosal membranes. Inside the host, trypomastigotes invade cells and differentiate into amastigotes which, after several cycles of binary division, differentiate back into trypomastigotes. These non-replicative forms are released into circulation upon host-cell rupture. Trypomastigotes may then infect other cells or be taken by the blood-sucking insect vector. The ingested trypomastigotes transform into epimastigotes, thereby, closing the cycle. The different forms of *T. cruzi* differ not only in cell morphology but also, more importantly, in the molecular structure on the cell surface. In particular, specific carbohydrates characterize each stage.

III. SPECIFIC CELL-SURFACE GLYCOCONJUGATES

1. Glycoinositolphospholipids, Free and as Anchors of Proteins

a. Glycoinositolphospholipids.—The first glycoconjugate to be purified and completely characterized from *T. cruzi* was a glycoinositolphospholipid (GIPL). Earlier reviews on *T. cruzi* GIPLs have been published.[9,10] The GIPLs are the most abundant cell-surface molecules in the epimastigotes and metacyclic trypomastigotes.

Around 10^7 GIPLs/cell form a dense glycocalyx covering the surface.[11,12] The GIPL isolated from epimastigotes, strain Y, was originally called a lipopeptidophosphoglycan (LPPG),[13–14] since amino acids (3–5%) were found in early preparations.[13,15] It was later determined that an inositolphosphoceramide (IPC) was linked to the glycan.[14] After purification by hydrophobic chromatography, structural studies showed the characteristic features of glycophosphatidylinositol (GPI) anchors of glycoproteins (Fig. 2):[16]

1. Release of the lipid by bacterial phosphatidylinositol phospholipase C (PI-PLC)
2. Cross reacting determinant (CRD) activity in the phosphoinositolglycan liberated by PI-PLC
3. Presence of non-N-acylated glucosamine ($NaNO_2$/$NaBH_4$)

In a later paper it was established that ceramide 1-phosphate was released from the GIPLs by the PLD from rat blood plasma.[17]

The complete structure for the GIPLs[11,18] showed the glycan core of GPI anchors of proteins,[19] αMan-(1→2)-αMan-(1→6)-αMan-(1→4)-αGlcN-(1→6)-D-*myo*-inositol-

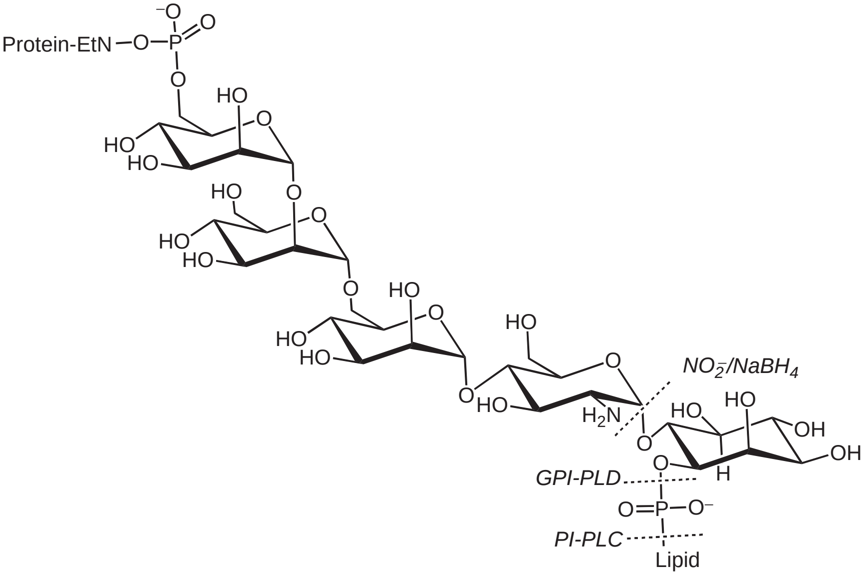

FIG. 2. Common features of glycophosphatidylinositol (GPIs) anchors of glycoproteins. Characteristic sites of chemical and enzymatic reactions of GPIs are shown. EtN, 2-aminoethanol (ethanolamine).

1PO$_4$-lipid, with one more mannose residue. The substitutions of this core, galactofuranose and aminoethylphosphonic acid (AEP), and the IPC moiety are xenobiotic to mammalian cells and are thus good targets for drugs. Microheterogeneity with respect to the glycan has been described, with three major oligosaccharide structures (Fig. 3),[11] and structural variations depending on the strain have been reported.[20] GIPLs isolated from epimastigotes in the exponential phase of growth showed a microheterogeneity in the lipid moiety, and 1-*O*-hexadecyl-2-*O*-hexadecanoylglycerol or a ceramide, mainly *N*-hexadecanoyl and *N*-lignoceroylsphinganines were identified.[21] However, ceramides alone were found in GIPLs isolated from parasites in the stationary phase of growth.

Decades after the first report on the LPPG,[13] the mystery of the peptide found in early preparations was solved by the work of Ferguson and coworkers.[22] These investigators purified a novel small glycopeptide termed NETNES, of low abundance (approx. 30,000 molecules/cell), which was extracted with the GIPLs. Accordingly, the amino acids analyzed in NETNES were the same as those previously found in LPPG with the addition of an isoleucine residue. The GPI anchor in NETNES lacks the Gal*f* and the lipid is 1-*O*-hexadecyl-2-*O*-hexadecanoylglycerol. The fine structure of NETNES is discussed later in this chapter.

The infective trypomastigotes have a lower content of GIPLs than the epimastigotes.[23,24] The structures of the trypomastigote free GIPLs were not described.

b. GIPL Anchors (GPIs) in *T. cruzi* Glycoproteins.—GIPLs perform the important function of anchoring proteins to the cell membrane. To accomplish this, a peptide linkage is formed, catalyzed by a transpeptidase, between the ethanolamine substituent in the third Man of the glycan and a carboxyl-terminal amino acid. The GIPLs attached to the protein are generally called GPIs because the first full

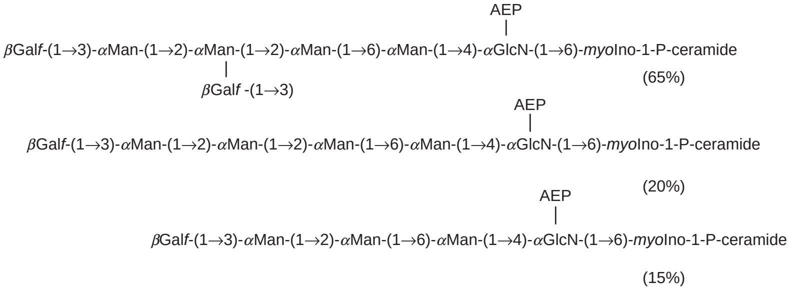

$$\beta\mathrm{Gal}f\text{-}(1\to3)\text{-}\alpha\mathrm{Man}\text{-}(1\to2)\text{-}\underset{\substack{|\\ \beta\mathrm{Gal}f\text{-}(1\to3)}}{\alpha\mathrm{Man}}\text{-}(1\to2)\text{-}\alpha\mathrm{Man}\text{-}(1\to6)\text{-}\alpha\mathrm{Man}\text{-}(1\to4)\text{-}\overset{\substack{\mathrm{AEP}\\ |}}{\alpha\mathrm{GlcN}}\text{-}(1\to6)\text{-}myo\mathrm{Ino}\text{-}1\text{-}\mathrm{P}\text{-}\mathrm{ceramide}\quad(65\%)$$

$$\beta\mathrm{Gal}f\text{-}(1\to3)\text{-}\alpha\mathrm{Man}\text{-}(1\to2)\text{-}\alpha\mathrm{Man}\text{-}(1\to2)\text{-}\alpha\mathrm{Man}\text{-}(1\to6)\text{-}\alpha\mathrm{Man}\text{-}(1\to4)\text{-}\overset{\substack{\mathrm{AEP}\\ |}}{\alpha\mathrm{GlcN}}\text{-}(1\to6)\text{-}myo\mathrm{Ino}\text{-}1\text{-}\mathrm{P}\text{-}\mathrm{ceramide}\quad(20\%)$$

$$\beta\mathrm{Gal}f\text{-}(1\to3)\text{-}\alpha\mathrm{Man}\text{-}(1\to2)\text{-}\alpha\mathrm{Man}\text{-}(1\to6)\text{-}\alpha\mathrm{Man}\text{-}(1\to4)\text{-}\overset{\substack{\mathrm{AEP}\\ |}}{\alpha\mathrm{GlcN}}\text{-}(1\to6)\text{-}myo\mathrm{Ino}\text{-}1\text{-}\mathrm{P}\text{-}\mathrm{ceramide}\quad(15\%)$$

FIG. 3. The three major oligosaccharide structures found in the LPPG from *T. cruzi* epimastigotes.

assignment of a GPI structure was that of the *T. brucei* VSG containing a phosphatidylinositol (PI) with diacylglycerol as the glycerolipid.[25] In mammals, a PI with an alkylacylglycerol (AAG) is usually found in the anchor.[26,27] An IPC, with sphinganine or sphingosine, is found more often as the lipid moiety of the anchors in the infective stages of *T. cruzi* (Fig. 4). Also, an IPC is commonly present in anchors of *Saccharomyces cerevisiae* glycoproteins.[28] Although the abbreviation GPI, would not be correct in these instances, it was adopted for all GIPLs anchoring glycoproteins.

A method for the quantification of GPIs in biological samples has been described.[12]

(i) GPI in Mucins. The mucins from all stages of *T. cruzi* are anchored by GPIs. Moreover, a recombinant mucin, obtained by transfection of a repetitive gene in epimastigotes, is anchored by a GPI and shed into the medium by an endogenous phospholipase C.[29] Structural variations in the inositolphospholipid (IPL) of the

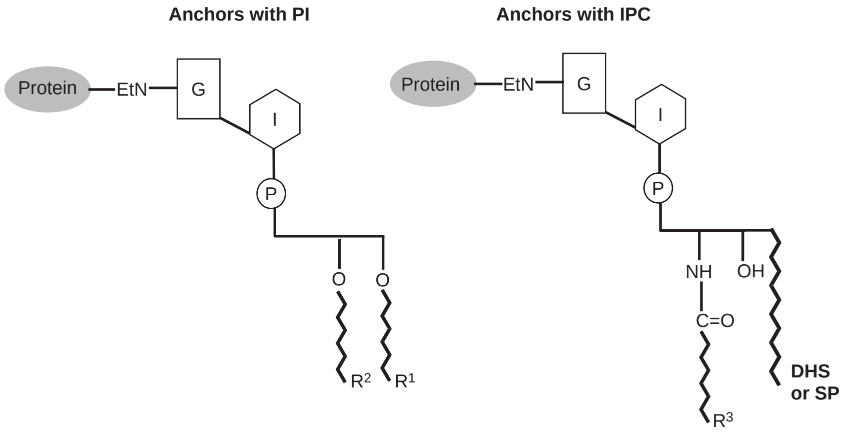

	R^1	R^2		R^3
Mucins (epi)[30, 31,]	Alkyl ($C_{16:0}$)	Acyl ($C_{16:0}$)	Ssp-4[42]	$C_{16:0}$
Mucins (trypo)[33]	Alkyl ($C_{16:0}$)	Acyl ($C_{16:0}$, $C_{18:2}$, $C_{18:1}$)	TcTS (trypo)[34]	$C_{16:0}$
1G7[41]	Alkyl ($C_{16:0}$)	Acyl ($C_{16:0}$, $C_{18:0}$)	TcTS (metacyclic)[35]	$C_{16:0}$, $C_{18:0}$
Tc85[38,39]	Alkyl ($C_{16:0}$)	-	Mucins (metacyclic)[31]	$C_{16:0}$, $C_{24:0}$
GIPLs[21]	Alkyl ($C_{16:0}$)	Acyl ($C_{16:0}$)	LPPG[16]	$C_{16:0}$, $C_{24:0}$
TcTS (trypo)[34]	Alkyl ($C_{16:0}$)	-		
NETNES (epi)[22]	Alkyl ($C_{16:0}$)	Acyl ($C_{16:0}$)		

FIG. 4. Structure of the lipid in the GPI anchors of the major glycoproteins of *T. cruzi*.

anchor must be emphasized, since the lipid has been associated with the infectivity of the parasite. Only the GPI anchors of the glycoproteins are discussed in this section.

The GPI in mucins of the epimastigote stage have the same mannose oligosaccharide, but lack the Gal*f* present in the free GIPLs.[30,31] Interestingly, in the IPL, 1-*O*-hexadecyl-2-*O*-hexadecanoylglycerol is replaced by ceramide when the parasites differentiate to metacyclic forms, whereas the glycan moiety remains unchanged.[31] The ceramide species are the same as those characterized in the free GIPLs.[21] Also, as in the GIPLs, the glucosamine is substituted at O-6 by 2-aminoethylphosphonic acid (AEP). The attachment to the protein is through an ethanolamine phosphate or another molecule of AEP that is linked to the third mannose. The GPI anchor of trypomastigote mucins is constituted by an AAG that contains mainly the unsaturated fatty acids, oleic and linoleic acid. The glycan is based on the $(\mathrm{Man})_4$ oligosaccharide, commonly found in *T. cruzi* GIPLs, substituted with, on average, 2.5 galactose units. The configuration and linkages of the galactoses were not established.[32] The GPI anchor of these mucins is responsible for their bioactivity. Treatment with nitrous acid, which cleaves the IPL, or mild alkaline hydrolysis, which affects the GPI structure, abolishes the cytokine-and nitric oxide-inducing activity of the mucins.[33]

(ii) GPI in Trans-Sialidases. The other family of surface glycoproteins, crucial for infection by *T. cruzi*, is the trans-sialidase (TcTS) family. The GPI anchor of these molecules enables their shedding by an endogenous PI-PLC into the bloodstream of the host, where it exerts different biological effects. The presence of a GPI anchor has been confirmed by incorporation of $[^3\mathrm{H}]$-hexadecanoic acid, immunoprecipitation with a monoclonal antibody, and release of the radioactivity by the action of a bacterial PI-PLC.[34] The lipid was characterized in both mammalian cell-derived and metacyclic trypomastigotes. While ceramide is the only constituent of the anchor of the trans-sialidase from metacyclic forms,[35] ceramide and alkylglycerol in 3:1 ratio were detected in the trypomastigote trans-sialidase.[34] The major ceramide was characterized as *N*-hexadecanoyl-sphinganine. Analysis of the glycan constituent of the GPI in the trans-sialidase of the metacyclic forms showed a major oligosaccharide having the trimannosyl core backbone substituted by α-galactose. The oligosaccharide in the trans-sialidase anchor of trypomastigote forms was not analyzed.

The gp85 glycoproteins are included in the trans-sialidase superfamily, although some members are enzymatically inactive.[36] The Tc-85 glycoprotein is specific for the trypomastigote forms[37] and is anchored by a GPI with 1-*O*-hexadecylglycerol.[38,39]

(iii) GPI in Minor Glycoproteins. 1G7 Antigen. The low-abundance cell-surface glycoprotein 1G7 is expressed by the metacyclic forms and is also anchored by a GPI.[40] Studies on the anchor showed that the glycan had the $\mathrm{Man}_4\mathrm{GlcN}$ basic

structure found in other *T. cruzi* anchors. Gal*f* and aminoethylphosphonate, constituents of the glycan in free GIPLs, were not found in 1G7. The lipid component is mainly *sn*-1-*O*-hexadecylglycerol, substituted with hexadecanoic or octadecanoic acids. A minor proportion of ceramide was shown by use of electrospray mass spectrometry.[41]

NETNES—The recently described unique glycopeptide NETNES is also anchored by a GPI with the glycan structure:

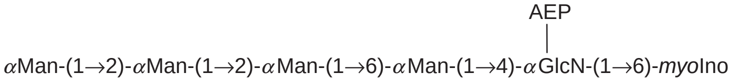

$$\alpha\text{Man-}(1\to2)\text{-}\alpha\text{Man-}(1\to2)\text{-}\alpha\text{Man-}(1\to6)\text{-}\alpha\text{Man-}(1\to4)\text{-}\alpha\overset{\overset{\text{AEP}}{|}}{\text{GlcN}}\text{-}(1\to6)\text{-}\mathit{myo}\text{Ino}$$

The AAG is *sn*-1-*O*-hexadecyl-2-*O*-hexadecanoylglycerol, as found in the free GIPLs of epimastigotes.[22]

Ssp4–The intracellular amastigote forms express the specific Ssp4 antigen, which is progressively shed by the action of an endogenous PI-PLC.[42] The lipid moiety in the GPI is the ceramide hexadecanoyl-sphinganine.

c. Biological and Immunological Properties of *T. cruzi* GIPLs.—It was shown that GIPLs are involved in the attachment to the luminal midgut surface of the vector *R. prolixus*.[43] Moreover, administration of 0.5 μM epimastigote GIPLs to the infected blood meal inhibited parasite infection in the insect by up to 90%. Apparently, the terminal β-D-Gal*f* groups present in the GIPLs are important for the interaction with the insect intestine. Previous partial acid hydrolysis, under conditions that selectively remove Gal*f*, diminishes the inhibitory effect of the GIPLs. Since GIPLs are less abundant in the metacyclic trypomastigotes, which are detached from the surface, a developmental regulation mediated by GIPLs was suggested.

A decreased expression of surface proteins in *T. cruzi* was observed on induction of GPI deficiency by heterologous expression of *T. brucei* GPI-PLC.[44] A different behavior was described for the different stages of the parasite. Whereas epimastigotes and metacyclic trypomastigotes from stationary-phase cultures were not drastically affected by GPI deficiency, the intracellular amastigote forms showed diminished replication and differentiation into trypomastigotes.[45] Accordingly, it was suggested that GPI-anchored proteins or free GIPLs act as mediators for signals necessary for amastigote development.[46] Related to this, activation of GIPL biosynthesis upon differentiation of trypomastigotes to amastigotes was demonstrated.[47]

Antibodies to the GIPLs were obtained in rabbits and were shown to be directed to Gal*f* epitopes.[23]

Studies have been made on the effect of *T. cruzi* GIPLs on the host immune system, and it was shown that the GIPLs downregulate T cell activation *in vivo* and *in vitro*. By controlling host cellular responses a chronic infection is maintained.[48]

On the other hand, it has been demonstrated that GIPLs purified from *T. cruzi* stimulate Ig production *in vitro*.[49]

A pro-apoptotic activity of the *T. cruzi* GIPLs was reported,[50] and the lipid and glycan moieties where shown to transmit different signals to the host.[51]

Purified GPIs, obtained by proteinase K digestion from the mucins of *T. cruzi* trypomastigotes (tGPIs), are potent inducers of nitric oxide, tumor necrosis factor-α and interleukin-12. The unsaturated fatty acid of the GPI alkylacyl-PI moiety is essential for bioactivity, but other features of the intact GPI are also necessary since the PI obtained by nitrous acid treatment was inactive.[32] Correlation between GPI structure and proinflammatory activity in macrophages has been reviewed.[52]

d. Biosynthesis of *T. cruzi* GIPLs.—Biosynthesis of the related GPI anchors has been studied in several organisms. The GPI anchor is the most ubiquitous of the lipid anchors for proteins, particularly favored by protozoal parasites, especially trypanosomatids.[9] Definition of the successive steps for the complex biosynthesis of GIPL precursors started with the work on the GPI anchor of the variant surface glycoprotein (VSG) of *Trypanosoma brucei*.[19,53,54] The glycan core is assembled on a phosphatidylinositol by initial addition of GlcNAc to give GlcNAc-PI, which is deacetylated to GlcN-PI, one of the crucial steps in the biosynthesis. The three mannose residues for construction of the core are donated by dolichol mannose phosphate. Ethanolamine phosphate, which is the linkage to the protein, is next linked to the third mannose. This entire process for the construction of the precursor glycolipid, $EtNPMan_3GlcNPI$, takes place in the endoplasmic reticulum (ER). Addition of other sugars, such as another mannose in the GIPLs and in some GPIs of *T. cruzi*, may take place also in the ER, as in yeast.

Most intriguing is the following lipid remodeling whereby the original fatty acids of the diacylglycerol in the PI are replaced in both positions by tetradecanoic (myristic) acid ($C_{14:0}$). This lipid remodeling has been well characterized in *T. brucei*.[53,55] The glycolipid precursor, termed glycolipid A may undergo acylation and deacylation of the inositol as a regulatory process.[56] Acylation of inositol precludes hydrolysis by PI-PLC,[57] a reaction usually used for detection of GPI anchors. The inositol deacylase gene has been characterized in *T. brucei*,[58] but inositol acylation in *T. cruzi* was not proved. The detailed enzymology of the individual steps for the assembly of the GPI in trypanosomes is not as well defined as that for mammals and *Saccharomyces*, for which genes encoding proteins involved in most of the steps and in the transfer of GPI to protein have been identified.[59]

An important difference between the GPI anchor in *T. brucei*, and the free GIPLs or those anchoring the proteins in *T. cruzi*, is the lipid linked to the glycan. IPC is commonly found in *T. cruzi*.[9] Ceramide is also the main lipid in the anchor of mature glycoproteins of yeast. Interestingly, this lipid is not found in mammals. In a series of papers, Conzelmann and coworkers described the remodeling that takes place in GPI anchors of yeast for introduction of the ceramide.[28,60–63] Biosynthetic studies showed that in *T. cruzi*, as in yeast, IPC is not a substrate for the first steps in the biosynthesis of the GIPLs. These results proved that a remodeling step must be also operating in *T. cruzi* to replace the glycerolipid by a ceramide, as found in the mature GIPLs.[64] Accordingly it was shown that glycolipids biosynthesized by membranes of *T. cruzi* showed only a PI with AAG as the lipid moiey.[65] In *S. cerevisiae* ceramide replaces the glycerolipid after its transfer to the protein in the ER.[61] This would not be a requisite for *T. cruzi*, since ceramide-containing GIPLs, not linked to protein, are abundant in the membrane of epimastigote cells.[11] Ceramide used for remodeling GIPL anchors in *S. cerevisiae* is newly synthesized and not taken from IPC.[28] The authors used the antibiotic aureobasidin A to block IPC biosynthesis and showed that it did not block remodeling of the GIPL. In *T. cruzi* amastigotes, the antibiotic inhibited not only the synthesis of IPC, but also the incorporation of [^{3}H]-hexadecanoic acid into GIPLs[47] suggesting that IPC is a substrate in the remodeling step. Moreover, as no lignoceric acid was found in free ceramides[42] or in IPC[66] and the $C_{24:0}$ is the major fatty acid in the LPPG, a remodeling step must be responsible for its introduction in the ceramide. In this respect, a ceramide lipase activity and IPC-fatty acid hydrolase and acyl transferase activities have been detected in a cell-free system of *T. cruzi*.[67] It is still not known what features of the GIPLs dictate remodeling of the glycerolipid by ceramide. By analogy with yeast, where it was found that branching with EtNP is important for remodeling,[68] the introduction of AEP at the O-6 of GlcN may play a similar role.

It was shown that the IPC synthase was induced upon differentiation,[47] providing an important target for antiprotozoal therapy, since no equivalent mammalian enzyme is known. In this respect, biosynthesis of radioactive IPC by metabolic labeling of *T. cruzi* epimastigotes,[66] trypomastigotes,[69] and amastigotes[47] could be used to study the action of potential inhibitors. Properties of the IPC synthase have been described,[70] but in contrast to earlier results,[47] the authors report no inhibition of the enzyme by aureobasidin. Elucidation of the structure of the *T. cruzi* enzyme would clarify its analogy with the yeast enzyme.

(i) Transfer of GPIs to Proteins. The products of more than 20 genes are involved in the assembly of GPI precursor and its transfer to protein and have been identified for yeast and mammal proteins.[59] Genes encoding GPI-anchored proteins can be identified by two signal sequences in the primary translation product, an N-terminal sequence that directs the protein to the lumen of the ER and a C-terminal sequence that directs attachment of a GPI anchor (GPIsp). Although there is no strict consensus

sequence for the C-terminal signal, its general properties were originally determined experimentally by site-directed mutagenesis studies with model proteins.[71] Slight variations have been noted in metazoan and protozoan signal sequences.[72] Both signal peptides are removed during processing in the ER. The N-terminal signal peptide is removed by a peptidase. The removal of the C-terminal GPI signal peptide and its replacement by GPI on the luminal face of the ER are catalyzed by a transamidase (GPIT), a multisubunit membrane-bound enzyme. The GPI is covalently attached through the amino group of EtNP to an internal residue (ω site) of the pro-protein, with the concomitant release of the C-terminal signal peptide. The GPIT in mammals and yeast is a complex of five proteins (reviewed in Ref. 59). All five subunits are needed for the nucleophilic attack on the ω residue of the pro-protein. The GPIT of *T. brucei* shares three subunits but have two novel subunits.[73,74] They have not yet been described for *T. cruzi*.

e. Chemical Synthesis of the *T. cruzi* GIPLs.—GIPLs of *T. cruzi* contain such structural motifs as Gal*f* and AEP, which make their synthesis a challenge. The heptasaccharyl *myo*-inositol **1** (Fig. 5) is the sugar moiety of the major GIPL in *T. cruzi* insect forms. Synthesis of **1** has been accomplished by a convergent assembly of three building blocks (Fig. 5).[75] In the following Schemes 1–3, synthesis of the complete glycan is depicted. The deprotection steps to afford **1** were crucial and included debenzylation with sodium in liquid ammonia, since the commonly used catalytic hydrogenation was not successful in this instance.[76] Removal of the acetal groups as the final step avoided the formation of a mixture of products resulting from phosphate migration. An earlier paper described the synthesis of the tetrasaccharide **2** and the pentasaccharide containing the two terminal Gal*f* groups.[77]

A complete GPI anchor of *T. cruzi* trypomastigote glycoproteins, lacking Gal*f* in the glycan, was synthesized (**13**, **14**, Scheme 4).[78] The Man_4GlcN*myo*-Inos is linked through phosphate to 1-*O*-hexadecyl-2-*O*-acyl-*sn*-glycerol, with oleoyl or linoleoyl as the acyl group. In Scheme 4 the key building blocks are shown. The presence of the unsaturated fatty acids was associated with the important biological activity of purified GPI from trypomastigote mucins.[32]

2. *Trypanosoma cruzi* Mucins

The most abundant surface glycoproteins of *T. cruzi* are the GPI anchored, highly glycosylated, mucin-like proteins.[24,79,80] They were first described by Alves and Colli in epimastigotes and termed glycoproteins A, B, and C.[81] Their surface location and the presence of Gal*p* in the glycan were shown by labeling whole cells with galactose

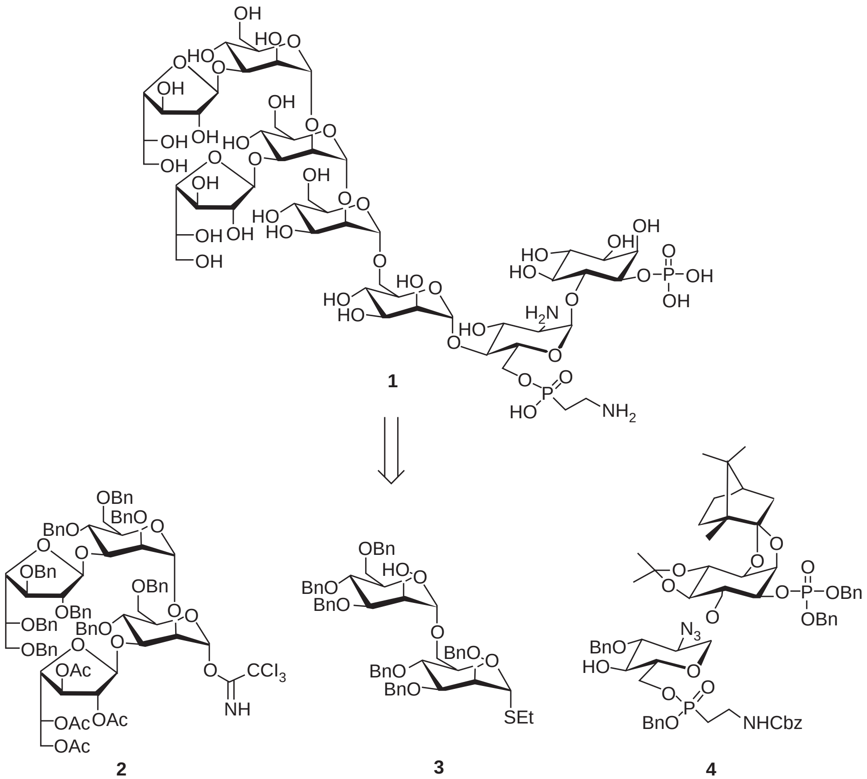

1

2

3

4

FIG. 5. Building blocks for the convergent synthesis of the heptasaccharyl *myo*-inositol **1** of *T. cruzi* insect forms.

oxidase–NaB$^3H_4$.[82] They were later found in other life stages, as discussed in the following sections.

a. Genetic Variability.—The mucin-gene repertoire in *T. cruzi* shows high complexity and heterogeneity. In a first approach, mucins may be divided in two types depending on the parasite host: those present in the insect stages and those identified in the mammalian stages (Table I). Hundreds of genes have been identified and arranged into two main families on the basis of sequence homology.[83]

The TcSMUG (*T. cruzi* small mucin gene) family is a homogeneous family of 70–80 genes encoding mucins in the insect stages. Members of this family were classified in two groups, S (small) and L (large) according to the size of the mRNAs. The group TcSMUG S products would correspond to the 35–50 kDa mucins that

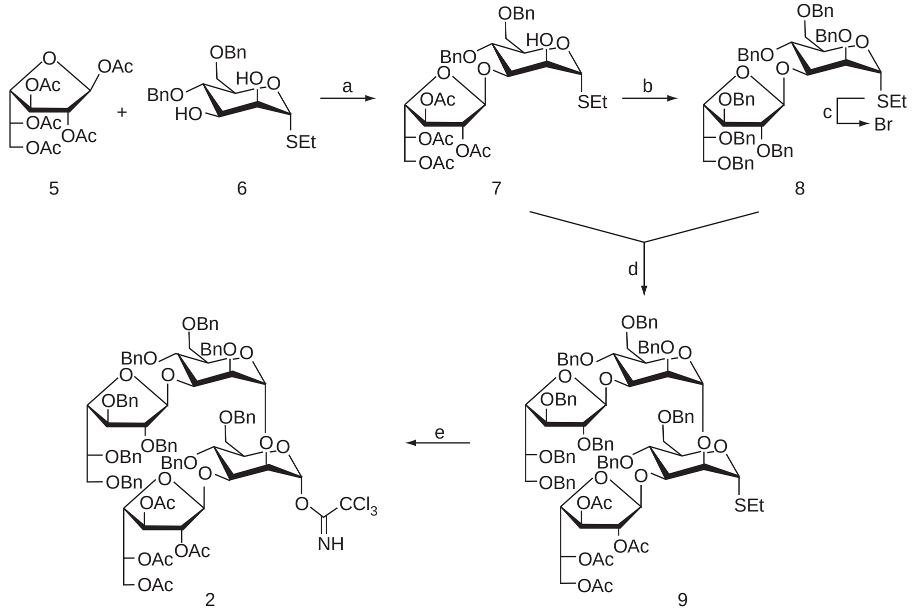

SCHEME 1. Synthesis of building block **2**. Conditions: (a) $SnCl_4$, 4 Å molecular sieves, −50 °C →rt, CH_2Cl_2, (70%); (b) 1. NaOMe, MeOH/CH_2Cl_2 (1:2); 2. BnBr, KI, Ag_2O, DMF, (86%); (c) Br_2, CH_2Cl_2; (d). AgOTf, 4 Å molecular sieves, CH_2Cl_2, −30 °C, (60%); (e) 1. n-Bu_4NIO_4, TfOH, H_2O, acetonitrile; 2. Cl_3CCN, DBU, CH_2Cl_2, (70%).

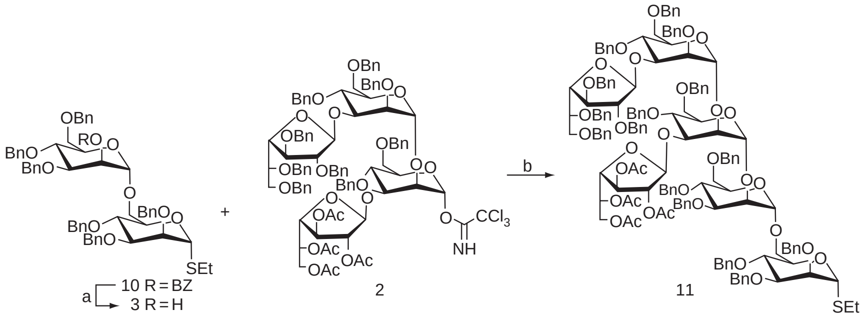

SCHEME 2. Synthesis of the hexasaccharide donor 11. Conditions: (a) NaOMe, CH_2Cl_2/MeOH (2:1) (90%); (b) TMSOTf, Et_2O, 4 Å molecular sieves, (89%).

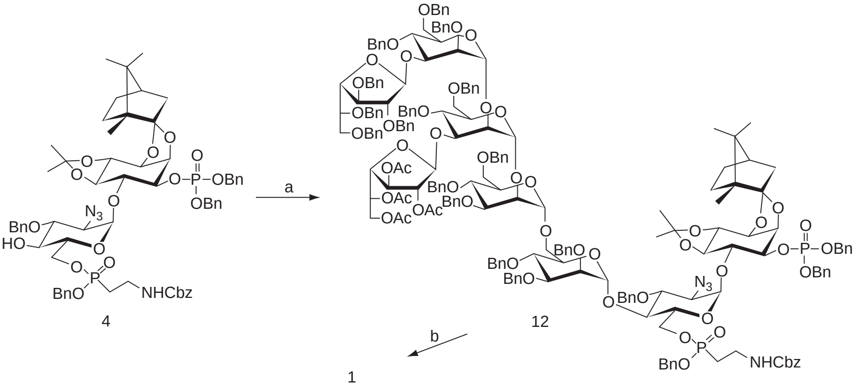

SCHEME 3. Assembly of the fully protected IPG and subsequent deprotection to **1**. Conditions: (a) 11, DMTST, 4 Å molecular sieves, Et_2O, (71%); (b) 1 NaOMe, CH_2Cl_2/MeOH (2:1); 2. Na (s), NH_3 (l); 3. 0.1 M HCl, (83%).

cover the surface of epimastigotes.[84] *In vivo* expression of group L has not been proved. The other gene family, named TcMUC, comprises 500–700 genes[2] and encodes mucins present in the mammal-dwelling stages.[29,85–87] The TcMUC proteins have conserved N- and C-termini corresponding to an ER signal and a GPI anchor signal, respectively. They differ mainly in the central domain (Fig. 6).[88] They were divided in three groups according to their structure. The TcMUC I group is characterized by a central domain composed of tandem repeats, with the consensus sequence T_8KP_2, providing suitable targets for O-glycosylation. TcMUC I products behave as functional mucins in transfected parasites, being glycosylated and displaying an antigenic hypervariable region in their mature N termini.[29] The TcMUC II has fewer repeats in the central region which, however, are rich in Thr, Ser, and Pro residues. The TcMUC I products are predominant in amastigotes, whereas the TcMUC II mucins are preponderant in bloodstream trypomastigotes, being less expressed in amastigotes.[88] The diversity in the length, sequence, and number of putative glycosylation-acceptor sites of TcMUC II genes can explain some of the molecular-mass heterogeneity observed for cell-derived trypomastigote mucins (tGPI-mucins). tGPI-mucins run on SDS–PAGE as a smear, spanning a wide range of molecular masses (60–200 kDa). They share the sialic acid-containing epitope Ssp-3, which is crucial for attachment to and invasion of mammalian cells.[89]

A third group, termed TcMUC III, yielded a very small protein, called trypomastigote small surface antigen (TSSA), because it is expressed on the surface of

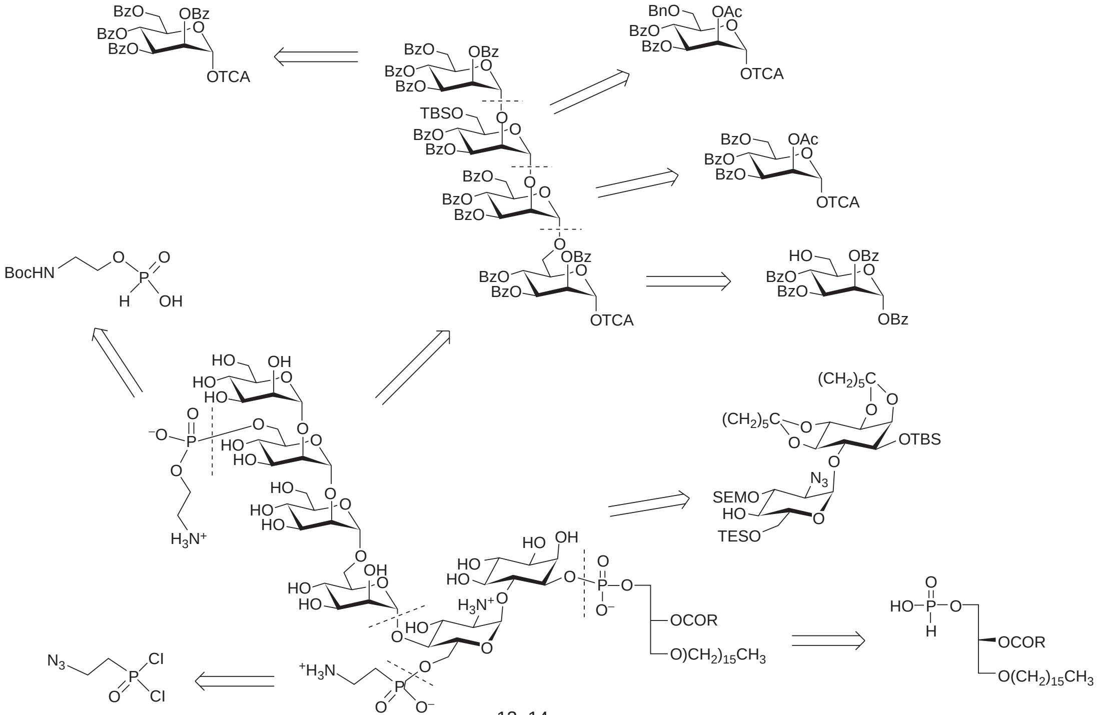
OTCA
BocHN
H_3N^+
OCOR
$O)CH_2)_{15}CH_3$
$O(CH_2)_{15}CH_3$
OTBS
SEMO
TESO
N_3
$(CH_2)_5C$
^+H_3N

13, 14

13: $R=(CH_2)_7CH=CH(CH_2)_7CH_3$
14: $R=(CH_2)_7CH=CHCH_2CH=CH(CH_2)_7CH_3$

SCHEME 4. Retrosynthetic scheme for the synthesis of the GPI-anchor of *T. cruzi* trypomastigote glycoproteins, lacking Gal*f* in the glycan, showing key building blocks and D-mannose monosaccharide intermediates.

TABLE I

Classification of Mucin-Like Gene Families in *Trypanosoma cruzi*

Host	Family	Group	Parasite Stage	Structural Features
Mammal	TcMUC	TcMUC I	A > T	60–200 kDa mucins. 2–10 tandem T_8KP_2 repeats for O-glycosylation
		TcMUC II	T > A	60–200 kDa mucins. 1–2 repeats, central Thr, Ser and Pro-rich region
		TSSA	T	20 kDa. Without repeats or central Thr, Ser and Pro-rich region
		MASP	T	Highly variable central region, with repeats
Insect	TcSMUG	TcSMUG S	E	35–50 kDa mucins. Thr runs, no repeats, no variable regions
?		TcSMUG L	?	Presence of repeats, no variable regions

Stages: A, amastigotes; T, cell-derived trypomastigotes; E, epimastigotes. Groups: TcMUC, *T. cruzi* mucin gene family; TcSMUG, *T. cruzi* small mucin-like gene family.

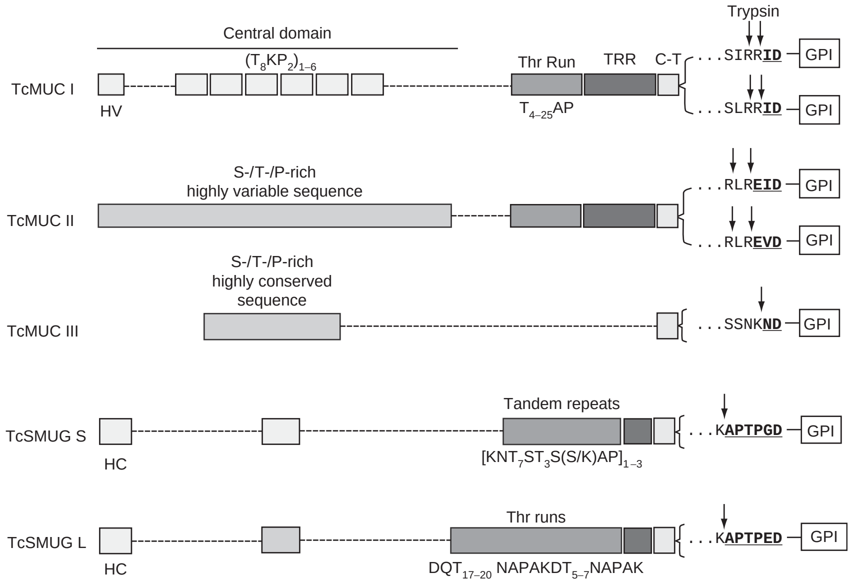
Trypsin
Central domain
(T8KP2)1–6
Thr Run
TRR
C-T
...SIRRID
GPI
TcMUC I
HV
T4–25AP
...SLRRID
GPI
S-/T-/P-rich
highly variable sequence
...RLREID
GPI
TcMUC II
...RLREVD
GPI
S-/T-/P-rich
highly conserved
sequence
TcMUC III
...SSNKND
GPI
Tandem repeats
TcSMUG S
...KAPTPGD
GPI
HC
[KNT7ST3S(S/K)AP]1–3
Thr runs
TcSMUG L
...KAPTPED
GPI
HC
DQT17–20 NAPAKDT5–7NAPAK

FIG. 6. Schematic representation of *T. cruzi* TcMUC and TcSMUG families and groups. Arrows indicate the putative trypsin-digestion site(s). HV, hypervariable N-terminus; HC, highly conserved N terminus; TRR, Thr-rich region; C-T, C terminus. Ref. 88.

cell-derived trypomastigotes.[90] This group is actually constituted by a dimorphic single-copy gene, with two alleles correlating with the two broad lineages postulated for *T. cruzi*.[91,92] These two alleles yield two different kinds of TSSA proteins, named TSSA-I and TSSA-II, which differ mainly in the central region. These sequence changes have major impact on TSSA antigenicity, leading to negligible cross-reactivity between the two isoforms. Sera from animals infected with *T. cruzi* 2 isolates showed an exclusive recognition toward the TSSA-II molecule. On the other hand, infection with *T. cruzi* 1 isolates displayed exclusive recognition toward TSSA-I, although the signal is much weaker. This result has great epidemiological value, as it allows for identification of the lineage of the infecting strain by simple serological methods.[90] On its C-terminus, TSSA-I and TSSA-II displayed a hydrophobic region compatible with a GPI-anchoring signal.

The genoma of *T. cruzi* revealed another family linked to TcMUC II, termed mucin-associated surface proteins (MASP),[2] which is predominant in the trypomastigote proteoma.[93] The members of this family are characterized by conserved N- and C-terminal domains that respectively encode a signal peptide and a GPI anchor addition site, suggesting a surface location in the parasite. The central region of these proteins is highly variable and often contains repeats. Only nine MASP gene family proteins were identified, suggesting that they are not as abundantly expressed or that they have extensive posttranslational modifications, which complicate their proteomic detection. A glycoproteomic analysis showed *N*-glycosylation in members of the MASP family.[94] However, about 25% of the mucin genes in *T. cruzi* are nonfunctional pseudogenes, with most disabling mutations being localized within the TcMUC II central domain.[86,95,96]

In summary, the transition from insect-dwelling to mammal-dwelling stages leads to the use of different, non-overlapping sets of mucin genes. As a consequence, when the parasite moves from the insect into the mammal, it switches from a mucin coat of rather homogeneous polypeptide composition to a highly heterogeneous one. One possible explanation is that the variable TcMUC apo-mucins function as redundant receptors that facilitate the attachment to, and/or invasion of, different cell types and mammalian hosts infected by this parasite. Furthermore, it is possible that their sequential expression might help the parasite to avoid host immune responses.[83]

b. Carbohydrate Structures in Mucins.—Mucins perform the crucial function of being acceptors of sialic acid, mediated by a parasite trans-sialidase, which is discussed later in this chapter.

The structures of the O-linked oligosaccharides have been elucidated for the mucins of the insect stages of the parasite. Both epimastigote and trypomastigote forms have about the same number of mucin molecules per cell (n 4 × 10^6).[24] Galactose is present in all mucin oligosaccharides, although it was reported that the surface hexose transporter expressed by *T. cruzi* is unable to transport galactose.[97] The UDP-Glc 4′-epimerase,[98] together with the UDP-Gal*p* mutase recently identified in *T. cruzi*, [99,100] provides the necessary Gal*p* and Gal*f* for the construction of the parasite glycoconjugates. The *T. cruzi* UDP-Glc 4′-epimerase is encoded by the *Tc GALE* gene. Null mutants could not be obtained, suggesting that the gene is essential. Two single-allele knockout clones showed biochemical and morphological aberrations.[101] Under diminished supply of UDP-Gal*p*, incorporation of Gal*p* into the mucins was more affected than biosynthesis of the Gal*f* containing GIPLs, suggesting that they play an important role for parasite survival in culture.

The striking feature of the O-linked chains is that they are linked to the protein by α-GlcNAc instead of the GalNAc common in vertebrate mucins. Indeed, GalNAc was not found in any of the *T. cruzi* glycoconjugates. The inability of the UDP-Glc 4′-epimerase of *T. cruzi* to convert UDP-GlcNAc into UDP-GalNAc, in contrast to the human epimerase, explains these findings.[98] It is also unusual for surface glycoproteins in that, in some strains, a significant amount of non-substituted O-linked GlcNAc was found.[31,102] The enzyme that transfers the GlcNAc from UDP-GlcNAc has been characterized.[103]

(i) Interstrain Variation of O-Linked Oligosaccharides in Mucins of the Insect Stages. Interstrain variations in the carbohydrates linked to the protein have been described, thus different patterns of the surface glycoproteins for the Y and Tulahuen strains was demonstrated by labeling with galactose oxidase–NaB^3H_4. Moreover, the mucins of two lines from the Tulahuen strain (T0 and T2), which differ in virulence, also showed a different pattern when analyzed by SDS–polyacrylamide gel electrophoresis.[104] By comparing structural data on the O-linked chains of the mucins from different strains it followed that the O-linked oligosaccharides may be derived from two cores, *β*Gal*p*-(1→4)-GlcNAc or *β*Gal*f*-(1→4)-GlcNAc. The cores are further branched with various units of Gal*f* and/or Gal*p*. Thus far, galactofuranose was found in the mucins of strains belonging to lineage 1 (Fig. 7),[31,105–107] whereas in the more infective Y[30] and CL[29,102,108] strains, galactose in the mucins is present only as pyranose. The mechanism whereby the presence of Gal*f* correlates with the parasite inactivation was not fully elucidated. Gal*f* is an antigenic epitope,[109] and an immunological reaction could influence the infection. The metabolic pathways involved in the transference of Gal*f* in *T. cruzi* were not elucidated.

(ii) Chemical Synthesis of Oligosaccharides Containing Galf O-Linked in Mucins of T. cruzi, Lineage 1. The structures of the oligosaccharides from the mucins (Fig. 7)

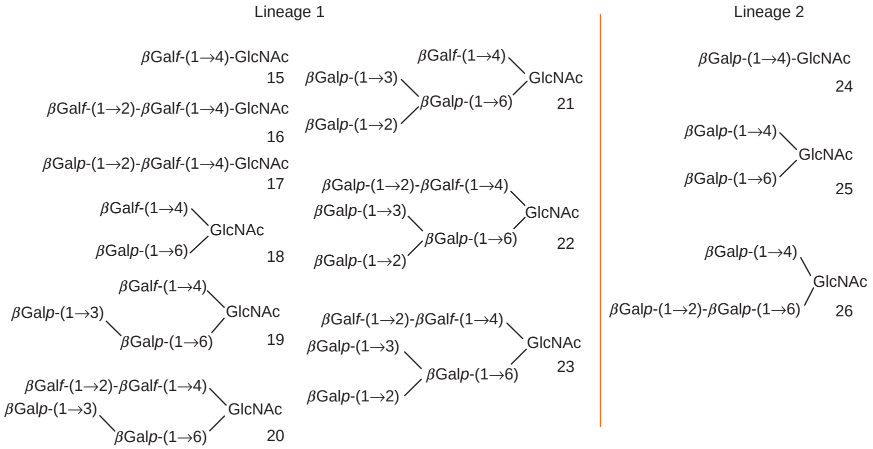
Lineage 1
Lineage 2
βGalf-(1→4)-GlcNAc
15
βGalf-(1→2)-βGalf-(1→4)-GlcNAc
16
βGalp-(1→2)-βGalf-(1→4)-GlcNAc
17
βGalf-(1→4)
GlcNAc
βGalp-(1→6)
18
βGalf-(1→4)
βGalp-(1→3)
GlcNAc
βGalp-(1→6)
19
βGalf-(1→2)-βGalf-(1→4)
βGalp-(1→3)
GlcNAc
βGalp-(1→6)
20
βGalf-(1→4)
βGalp-(1→3)
GlcNAc
βGalp-(1→6)
21
βGalp-(1→2)
βGalp-(1→2)-βGalf-(1→4)
βGalp-(1→3)
GlcNAc
βGalp-(1→6)
22
βGalp-(1→2)
βGalf-(1→2)-βGalf-(1→4)
βGalp-(1→3)
GlcNAc
23
βGalp-(1→6)
βGalp-(1→2)
βGalp-(1→4)-GlcNAc
24
βGalp-(1→4)
GlcNAc
βGalp-(1→6)
25
βGalp-(1→4)
GlcNAc
βGalp-(1→2)-βGalp-(1→6)
26

FIG. 7. Oligosaccharides from mucins of *T. cruzi* (lineage 1 and 2).

were identified by spectroscopic methods. The disaccharide core **15**, the trisaccharide **18**, and the tetra and pentasaccharides **19** and **21** have been synthesized as follows.

*Synthesis of β-D-Galf(1→4)GlcNAc (**15**).* A simple synthesis of the core disaccharide **15** has been described (Scheme 5),[110] using penta-*O*-benzoyl-α,β-D-galactofuranose (**27**) as the galactofuranosyl donor. This furanosyl derivative has the advantage of being accessible crystalline in one step from D-galactose (for details of its preparation see Ref. 111). Although the yield of **27** is only moderate (35%), it crystallizes from ethanol and a similar amount of the galactopyranosyl benzoate **34** is obtained crystalline from the mother liquors. Compound **34** was later used for the preparation of trisaccharide **18**.

The partially protected derivative of GlcNAc **28** was also prepared in one step from the benzyl glycoside, and the condensation of **27** with **28** to yield the disaccharide derivative was promoted by tin(IV) chloride.

The other two isomeric disaccharides, β-D-Gal*f*-(1→3)-D-GlcNAc and β-D-Gal*f*-(1→6)-D-GlcNAc were also prepared,[112] providing all of the disaccharides of Gal*f* necessary for unequivocal identification of the component found in the mucins of *T. cruzi*.

*Synthesis of β-D-Galf (1→4)[β-D-Galp(1→6)]GlcNAc (**18**).* For the preparation of trisaccharide **18**, the key glycosyl acceptor intermediate, benzyl 2-acetamido-3-*O*-benzoyl-2-deoxy-α-D-glucopyranoside (**33**) was prepared in 81% yield according to Scheme 6.[111] Trisaccharide derivative **36** could be obtained in a one-pot reaction, taking advantage of the lower reactivity of the galactopyranose benzoate with respect to the galactofuranose derivative in the glycosidation reaction as promoted by tin(IV)

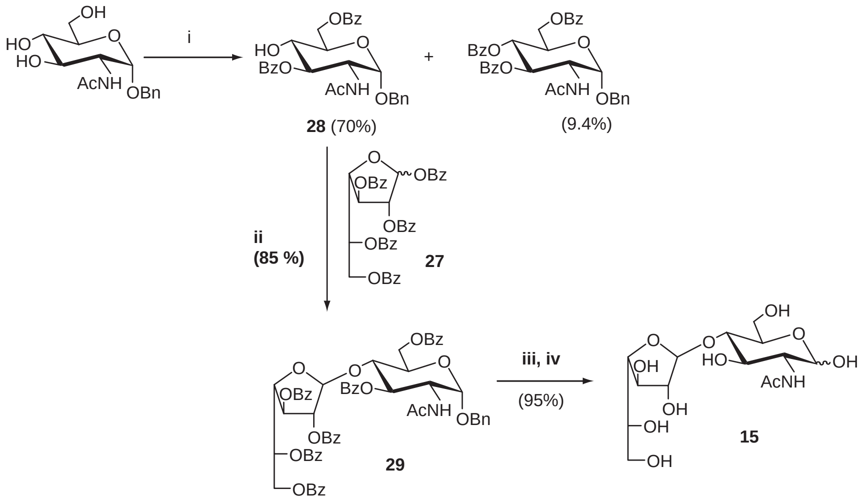
i
28 (70%)
(9.4%)
ii
(85 %)
27
iii, iv
(95%)
29
15
OBz
OBn
AcNH
BzO
HO
OH

Scheme 5. Synthesis of disaccharide **15**. Conditions: (i) *N*-benzoylimidazole, MeCN, reflux; (ii) $SnCl_4$, Cl_2CH_2, 20 h, 0 °C to rt.; (iii) NaOMe, MeOH; (iv) NH_4CO_2H, 10% Pd/C, MeOH, reflux, 1 h.

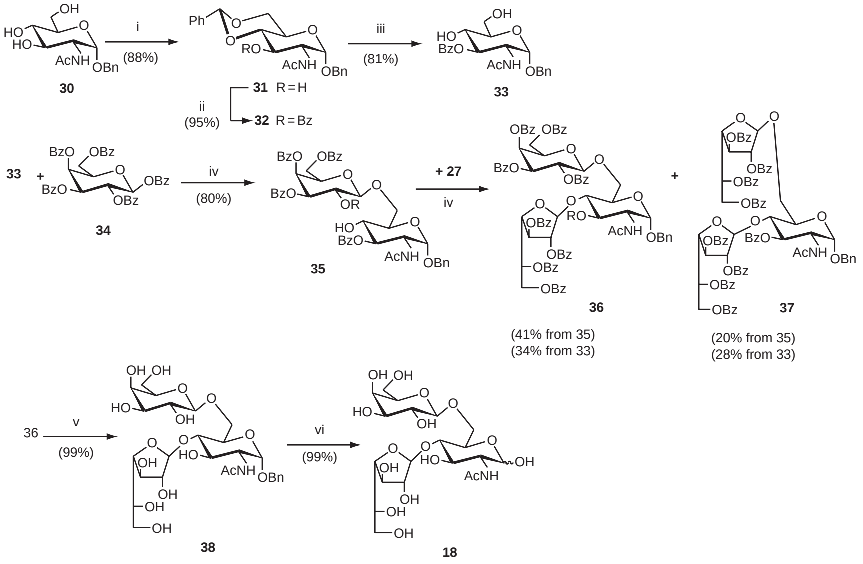
30
i
(88%)
Ph
iii
(81%)
33
ii
(95%)
31 R = H
32 R = Bz
33 +
34
iv
(80%)
35
+ 27
iv
36
37
(41% from 35)
(34% from 33)
(20% from 35)
(28% from 33)
36
v
(99%)
38
vi
(99%)
18
OBz
OBn
AcNH
BzO
HO
OR
RO
OH

Scheme 6. Synthesis of trisaccharide **18**. Conditions: (i) α-α-dimethoxytoluene, *p*-toluensulfonic acid, DMF, 60 °C; (ii) benzoyl chloride, C_5H_5N; (iii) AcOH, water, 100 °C; (iv) $SnCl_4$, CH_2Cl_2; (v) NaOMe, MeOH; (vi) NH_4CO_2H, 10% Pd/C, MeOH, reflux, 1 h.

chloride. The trisaccharide derivative 4,6-di-*O*-(*β*-D-Gal*f*)-GlcNAc (**37**) was obtained as byproduct.

*Synthesis of β-D-Galp-(1→3)-β-D-Galp-(1→6)-[β-D-Galf-(1→4)]-D-GlcNAc (**19**).* For the preparation of the tetrasaccharide **19**, a convergent route was employed, condensing the derivative of *β*-D-Gal*f*-(1→4)-D-GlcNAc with the *β*-D-Gal*p*-(1→3)-D-Gal*p* donor (Scheme 7).[113]

Starting from **30**, selective protection of OH-6 by treatment with *tert*-butylchlorodiphenylsilane (TBDPC) followed by regioselective benzoylation of the 3-OH group afforded the acceptor **40** in 65% overall yield. Glycosidation, to obtain the *β*-galactofuranosyl disaccharide **41**, gave better yields by using the trichloroacetimidate method. Removal of the silyl group was achieved with 5% HF (48%) in acetonitrile affording compound **42** in 89% yield.

For the synthesis of the *β*-D-Gal*p*-(1→3)-D-Gal*p* fragment, the glycosyl aldonolactone approach was used (Scheme 7). The 5,6-*O*-isopropylidene-2-*O*-pivaloyl-D-galactono-1,4 lactone **43** was obtained crystalline from the galactono-1,4-lactone[114] and was glycosylated with the tetra-*O*-acetyl-α-D-galactopyranosyl trichloroacetimidate **44**, affording the lactonic disaccharide **45** in 84% yield. Reduction with diisoamylborane was followed by hydrolysis of the isopropylidene group, which led to equilibration. The mixture of pyranose and furanose derivatives **47** and **49** was obtained in 8:2 ratio upon acetylation. After separation by column chromatography the anomeric acetate was hydrolyzed with ethylenediamine–acetic acid in THF, followed by preparation of the imidate **50**.

Glycosylation of acceptor **42** with **50** and deprotection afforded the tetrasaccharide **19** (Scheme 7).

*Synthesis of β-D-Galp(1→3)[β-D-Galp(1→2)]-β-D-Galp(1→6)[β-D-Galf(1→4)]-D-GlcNAc (**21**).* Pentasaccharide **21** (Fig. 7) is the major oligosaccharide in the mucins of the G strain.[31] It was synthesized by a convergent approach, condensing acceptor **42**, previously used for the synthesis of the tetrasaccharide **19**, with the derivative of the trisaccharide 2,3-di-*O*-(*β*-D-Gal*p*)-D-Gal*p* (Scheme 8).

The Gal*p* trisaccharide was synthesized starting from benzyl 4,6-di-*O*-benzylidene-*β*-D-Gal*p* (**53**) which was glycosylated at both free positions by the trichloroacetimidate method. Further hydrolysis of the benzylidene group of **54**, followed by acetylation, and hydrogenolysis of the benzyl glycoside, afforded the anomeric free trisaccharide **57**.[115]

Because of the absence of a participating group at C-2 of donor **57**, and in order to obtain the *β*-(1→6) linkage, glycosylation was performed in a participating solvent such as acetonitrile (nitrile effect).[116] The condensation of benzyl (2,3,5,6-

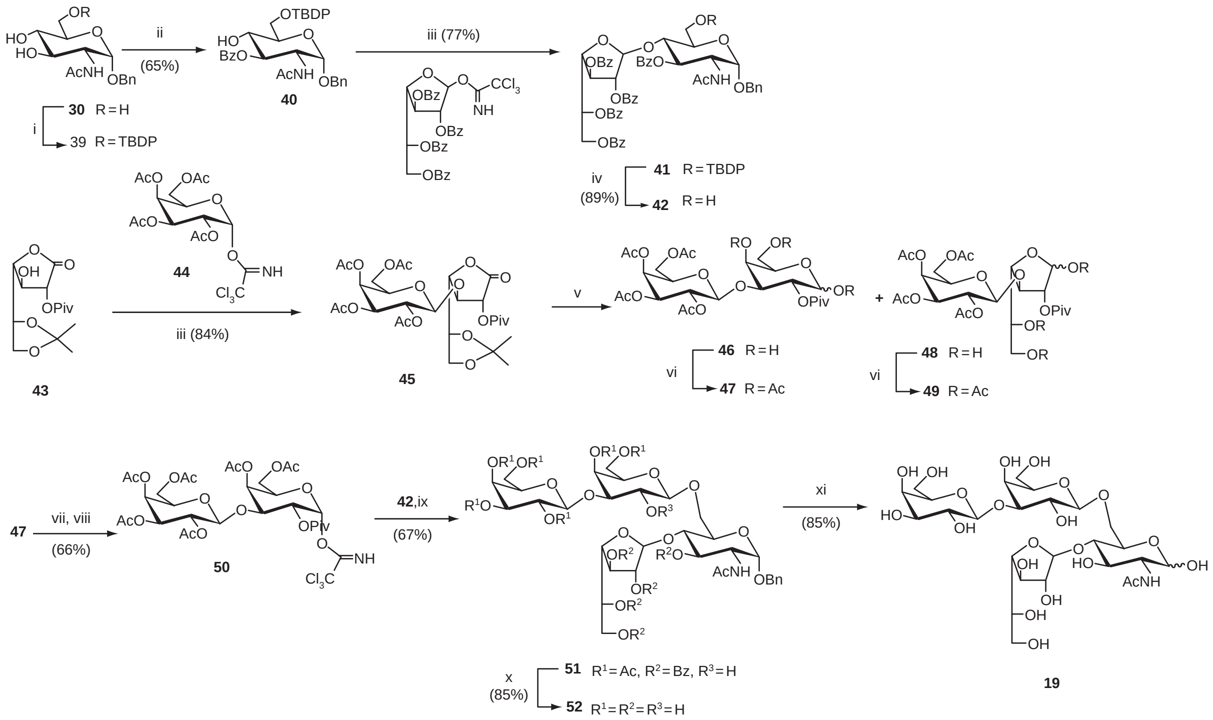
30 R = H
i
39 R = TBDP
ii
(65%)
40
iii (77%)
41 R = TBDP
iv
(89%)
42 R = H
43
44
iii (84%)
45
v
46 R = H
vi
47 R = Ac
+
48 R = H
vi
49 R = Ac
47
vii, viii
(66%)
50
42,ix
(67%)
51 R1 = Ac, R2 = Bz, R3 = H
x
(85%)
52 R1 = R2 = R3 = H
xi
(85%)
19

SCHEME 7. Synthesis of tetrasaccharide **19**. Conditions: (i) TBDPCl, DMF, imidazole; (ii) *N*-benzoylimidazole, MeCN; (iii) TMSOTf, Cl_2CH_2; (iv) HF, MeCN; (v) bis(2-butyl-3-methyl)borane, THF; (vi) Ac_2O, C_5H_5N; (vii) $(CH_2NH_2)_2$, AcOH; (viii) Cl_3CCN, DBU; (ix) 1-TMSOTf, Cl_2CH_2, 2-Ac_2O, C_5H_5N; (x) NaOMe; (xi) H_2, Pd(C).

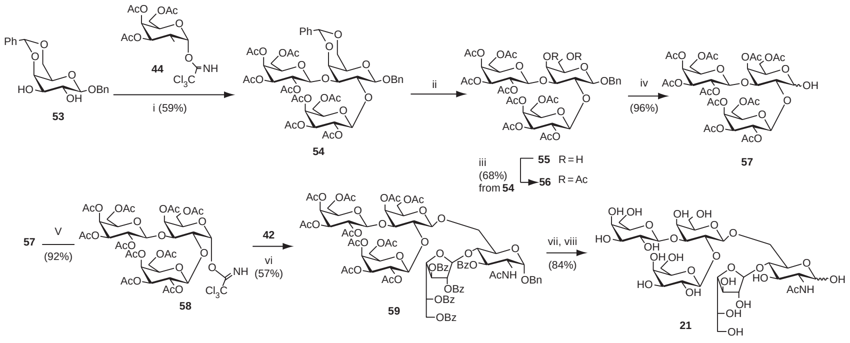

SCHEME 8. Synthesis of pentasaccharide 21. Conditions: (i) TMSOTf, Cl_2CH_2; (ii) AcOH–H_2O, 60 °C; (iii) Ac_2O, C_5H_5N; (iv) H_2, Pd(C); (v) Cl_3CCN, DBU; (vi) TMSOTf, MeCN; (vii) NaOMe; (viii) H_2, Pd(C).

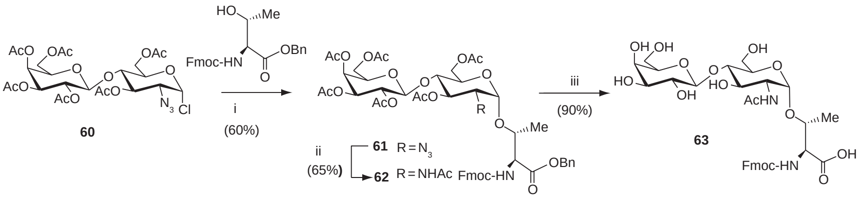

SCHEME 9. Synthesis of LacNAc-α-threonine. Conditions: (i) $HgBr_2$, $ClCH_2CH_2Cl$, rt 10 h then reflux 9 h; (ii) Zn powder, AcOH, Ac_2O, THF; (iii) 1-H_2, Pd(C), MeOH–AcOH (10:1), 10 h, 2-NaOMe, MeOH.

tetra-*O*-benzoyl-*β*-D-galactofuranosyl)-(1→4)-2-acetamido-3-*O*-benzoyl-2-deoxy-α-D-glucopyranoside (**42**) with imidate **58** in the presence of TMSOTf as catalyst, and employing acetonitrile as solvent at −40 °C, gave pentasaccharide **59** diastereoselectively in 57% yield. The α-glycosylation product was not detected, and unreacted acceptor **42** was also recovered. Deprotection of **59** afforded the pentasaccharide **21**.[117]

(iii) Chemical and Chemoenzymatic Synthesis of Glycosyl Amino Acids Related to Mucins of Lineage 2. The synthesis of *β*Gal*p*-(1→4)-GlcNAc-α-L-threonine (LacNAc-α-threonine), which represents the core in mucins of the more infective strains grouped in lineage 2, was recently described (Scheme 9).[118] Solid-phase synthesis of the glycopeptide Thr-Thr-[LacNAcThr]-Thr-Thr-Gly (**66**) was also reported (Scheme 10). Although tandem repeats containing Thr_5 were determined in the TcMUC I products, this sequence was not proved in the mucins isolated from epimastigotes or trypomastigotes.

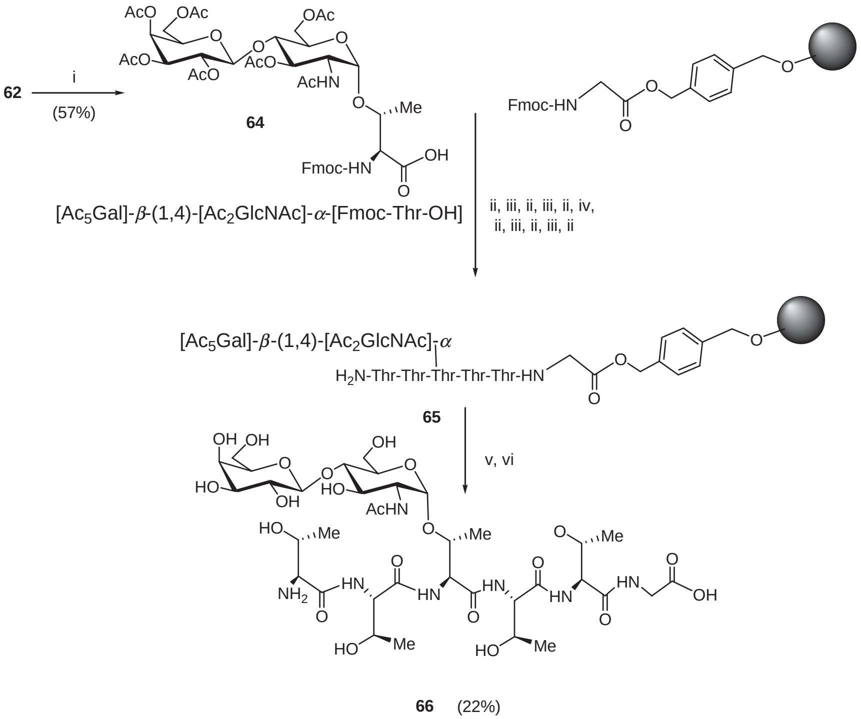
62
i
(57%)
64
[Ac5Gal]-β-(1,4)-[Ac2GlcNAc]-α-[Fmoc-Thr-OH]
Fmoc-HN
ii, iii, ii, iii, ii, iv,
ii, iii, ii, iii, ii
[Ac5Gal]-β-(1,4)-[Ac2GlcNAc]-α
H2N-Thr-Thr-Thr-Thr-Thr-HN
65
v, vi
66
(22%)

SCHEME 10. Synthesis of H_2N-(Thr)$_2$-(LacNAc-α-Thr)-(Thr)$_2$-Gly-OH. Conditions: (i) H_2, Pd(C), MeOH–AcOH (10:1), 1 h; (ii) 20% piperidine in DMF; (iii) Fmoc-Thr, (benzotriazol-1-yloxy)tripyrrolidinophosphonium hexafluorophosphate (PyBOP), *N*-hydroxybenzotriazole (HOBt), ethyldiisopropylamine (DIPEA); (iv) Glyco-amino acid **64**, PyBOP, HOBt, DIPEA; (v) TFA; (vi) NaOMe, MeOH.

(iv) Analysis of the Alditol Oligosaccharides of T. cruzi Mucins by HPAEC-PAD. Analysis of the O-chains released as oligosaccharitols from the mucins provides a sensitive method for identifying the original lineage of a *T. cruzi* strain. The chemically synthesized oligosaccharide alditols, containing Gal*f*, can be resolved by HPAEC-PAD.[119] Analysis of the isomeric disaccharides *β*Gal*p*-(1→X)-GlcNAc and *β*Gal*f*-(1→*X*)-GlcNAc ($X = 3$, 4, and 6) showed that all the Gal*f* disaccharides were more retained in the columns than their pyranose counterparts.[102] By this method it was proved that mucins from *T. cruzi* epimastigotes, clones CL14 and CL Brener, contained only Gal*p* oligosaccharides. When *T. cruzi* CL Brener parasites were transfected with TcMUC I genes with repeats in the central region, the product was highly O-glycosylated i*n vivo* and the oligosaccharides showed the same pattern as the endogenous mucins.[29]

(v) Carbohydrate Structures in Mucins of the Mammal Stages of T. cruzi. Information on the fine structure of the carbohydrates in the mucins from mammal-derived stages (tGPI mucins) is scarce. After reductive β-elimination, a complex mixture of structures was obtained.[120] The smallest structure was the trisaccharide αGal-(1→3)-βGal-(1→4)-GlcNAc-ol. The larger structures contained both 4-substituted GlcNAc-ol and 4,6-disubstituted GlcNAc-ol termini, together with non-reducing terminal Gal residues and 2-, 3-, 4- and 6-substituted and 2,6-disubtituted Gal residues. Unlike the trisaccharide, some of these structures may be sialylated. tGPI-mucins are anchored to the membrane via a glycosylphosphatidylinositol anchor containing 4–8 hexoses and mainly unsaturated ($C_{18:1}$ or $C_{18:2}$) fatty acids in their alkylacyl-PI moieties. Monosaccharide composition analysis of the GPI by GC-MS revealed the presence of mannose and galactose in the ratio 4.0:2.5, suggesting a substitution with an average of 2.5 galactose residues. The configuration of these units was not described.[32] The striking difference of the O-linked oligosaccharides in mucins of the insect and mammal stages is the presence of αGal-(1→3)-Gal epitopes in the latter.[120] These oligosaccharides are highly immunogenic and are the targets for lytic anti-α-galactosyl antibodies found in sera from patients with chronic Chagas disease. Lysis of trypomastigotes is prevented by sialylation of the mucins catalyzed by the parasite trans-sialidase (TcTS).[24]

c. Biological Functions of the Mucins.—Epimastigote mucins have a protective role against proteases in the intestine of the insect vector.[121] In the infective metacyclic trypomastigotes, mucins are involved in adhesion and invasion of host cells. It was proved that the binding was mediated by the carbohydrate constituents of the mucins.[122,123] Metacyclic mucins also act on Ca^{2+} mobilization in the host cell, and immunomodulatory roles have been also described.[124,125]

Each constituent of the trypomastigote mucins, namely, the GPI anchor, the polypeptide, and the linked carbohydrate has a distinct biological function which may contribute to the success of the infection. It was suggested that the heterogeneity of the polypeptide helps the parasite to evade the immune response. However, this effect would be neutralized *in vivo* by the activation of macrophages mediated by GPI and by the antigenicity of the linked sugars. Further studies are necessary to explain these apparent contradictions.

A 45-kDa mucin, expressed only in invasive trypomastigotes and shed to the medium, is involved in adhesion to mammalian cells.[126] It was recognized by the anti-*T-cruzi* mucin monoclonal antibody MabC20, although no structural data are included to support its classification as a mucin.

3. *T. cruzi* Trans-sialidase (TcTS)

T. cruzi is unable to incorporate sialic acid from the donor nucleotide, CMP-sialic acid, but sialylated molecules on the surface of the parasite perform crucial functions in the infection.[89] Sialylated glycoproteins anchored to the membrane by a GPI or shed into the bloodstream may bind to mammalian cell receptors to start infection,[127] and they also play an important role in resistance to complement-mediated host immune response.[128]

To acquire sialic acid, *T. cruzi* expresses a unique enzyme, the trans-sialidase which catalyzes the transfer of sialic acid from host glycoconjugates to glycans at the surface of the parasite, in particular to the mucins. In the early papers, a trans-sialidase activity that transferred sialic acid from fetuin to epimastigotes[129] or to surface molecules of trypomastigotes[130] was reported. The specific activity of the sialic acid transglycosylase in epimastigotes was 17% of that found in trypomastigotes. From then on results from studies on various aspects of this enzyme have emerged from several laboratories (reviewed in Ref. 83, 131–133).

Substrate specificity of the trans-sialidase was established by *in vitro* experiments using as acceptors oligosaccharides[134] or glycolipids and glycoproteins.[135] 3′-Sialyllactose or fetuin was used as donors of the sialic acid, and it was also shown that α-(2→6) or α-(2→8) sialic acid is not transferred by the enzyme. The reaction is specific and involves the sialic acid α-(2→3)-linked in the donor and the formation of the same linkage, with a terminal *β*-galactopyranosyl group in the acceptor substrate (Fig. 8). TcTS also transfers, efficiently, α-(2→3)-linked *N*-glycolylneuraminic acid to terminal *β*-galactosyl groups.[136,137]

The enzymatic activity was detected in the shed acute-phase antigen (SAPA) which contains tandem repeats of 12 amino acids in a C-terminal region.[138] Antibodies against SAPA appear very early after infection in humans[139] and mice.[140] The *T. cruzi* genoma[2] revealed a superfamily of trans-sialidase genes in *T. cruzi* which encodes hundreds of proteins ranging in size from 80 to 200 kDa, although not all showed enzymatic activity. Only about 70 genes code for trans-sialidase-active products. A second group having the same number of genes and the same protein size (120–200 kDa) encode products lacking enzymatic activity owing to a mutation in the key Tyr residue, but bind to *β*-galactose.[141] These two groups contain the SAPA repeats and are present in trypomastigotes. A third group, in epimastigotes, lacks the repeats but contains the catalytic region. Another group of glycoproteins, the gp 85 are included in the superfamily as a trans-sialidase-like family[83] because they have 30–40% homology, although they lack trans-sialidase activity. The Tc85

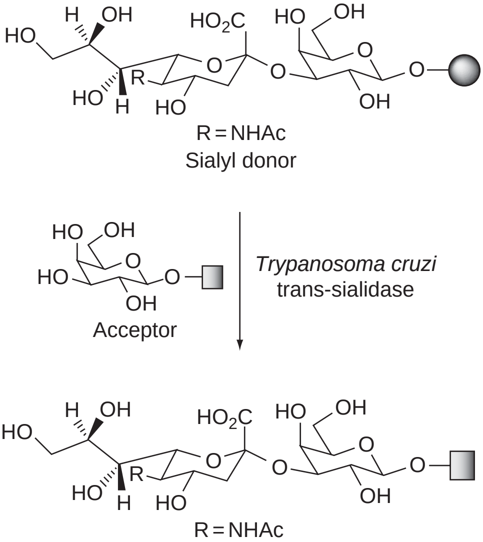

FIG. 8. Transfer of sialic acid by TcTS from host glycoconjugate to *β*-galactopyranosyl units in the acceptor substrate.

glycoprotein, specific to trypomastigotes, was the first described in this group[37] and the interaction with host structures has been recently reviewed.[36] The trans-sialidases from trypomastigotes, metacyclic trypomastigotes, as well as Tc85 are anchored by GPIs (see Section III.1.b.*ii*). Members of the trans-sialidase family show *N*-glycosylation sites[142] but the sugar chains play no role in the enzymatic activity since recombinant, non-glycosylated TcTS, retains its activity.[143] Apparently, the sugar chains have not been studied in the trans-sialidase-active members of the family. The N-glycosylic chain was released from the Tc85 glycoprotein, and the presence of sialic acid, fucose, and αGal-(1→3)-Gal was described.[144]

a. TcTS Structure and Mechanism of Catalysis.—According to its structure, TcTS was classified as a member of the glycoside hydrolase family 33;[143] however, in the presence of a suitable acceptor it behaves as a transferase and catalyzes the construction of the new linkage, αNeuAc-(2→3)-*β*Gal*p*-1 (Fig. 8).

The three-dimensional structure of TcTS was determined by crystallographic studies on a fully active TcTS mutant.[145–147] It consists of two domains: the N-terminal catalytic domain which forms a six-bladed *β* propeller, characteristic of microbial sialidases, connected through a long α helix to a C-terminal lectin-like domain which does not participate in the enzymatic reaction. The catalytic domain shares several features with the common sialidases, among them, the arginine triad (Arg 35, Arg 245, and Arg 314) that binds the carboxylate of the sialic acid, an aspartic acid (Asp 59) essential for catalysis, and two residues (Tyr 342 and Glu 230) well positioned for participation in the activation process. These similarities suggest that the ancestor of TcTS is a trypanosomal hydrolase.[145] However, TcTS exhibits some distinct units that could be responsible for the different enzymatic activities. Two tyrosine residues (Tyr119 and Tyr 248), together with Trp 120, Val 203, and Trp 312, define a hydrophobic environment in the binding pocket, favoring transglycosylation to hydrolysis.

Studies on crystals of TcTS in complexes with different ligands, such as the acceptor substrate lactose and the sialidase inhibitor 2,3-dehydro-3-deoxy-*N*-acetylneuraminic acid (Neu5Ac2en) showed that TcTS has two (sub)sites in the active center: the sialic acid-binding site and the galactose-binding site. The sialic acid (sub)site is present in all sialidases but in TcTS it is somewhat different. The sugar enters in a tilted position as compared with other sialidases, partially explaining the lack of inhibition observed with Neu5Ac2en. On the other hand, the lactose (sub)site is absent in all known sialidases and is formed upon binding of substrate. In Fig. 9 the interactions of TcTS with the sialic acid analogue and with the acceptor lactose are shown. The lactose is stabilized by water-mediated hydrogen-bond interactions with both monosaccharides constituents, the galactose and the glucose. The 3-OH of the Gal is conveniently situated for a nucleophilic attack on the sialyl intermediate and at hydrogen-bonding distance from

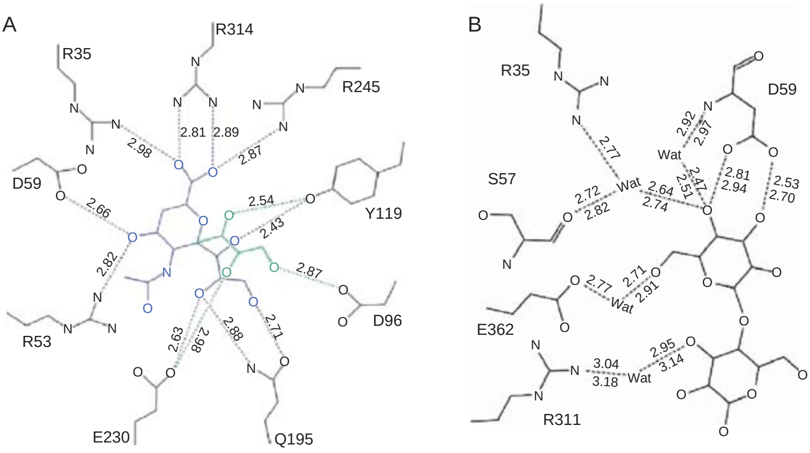

FIG. 9. Schematic diagram showing protein–ligand hydrogen-bonding interactions of TcTS with (A) Neu5Ac2en and (B) lactose. Ref. 145.

the catalytic Asp59 (Fig. 9). In order to better characterize the enzyme–substrate complex structure a mutant of the enzyme having Asp59 replaced by Ala was constructed to retard the acid–base catalysis. The structures of the $TcTS_{D59A}$ in complex with the natural substrate αNeuAc-(2→3)-lactose (3′SL) or the synthetic 2′-(4-methylumbelliferyl)-α-NeuAc (MUNeu5Ac) showed hydrogen bonding and stacking interactions with different amino acids and water molecules.[147]

Binding of the sialic acid moiety of the donor substrate in the TcTS reactive center triggers a conformational switch that creates the sugar acceptor-binding site for a terminal *β*-galactose. In the free enzyme, the Tyr119 points toward the floor of the catalytic pocket, filling the space of sialic acid. Upon binding of the donor substrate, the Tyr119 side chain suffers a displacement, leaving the sialic acid-binding cleft and forming a stacking interaction with lactose, which is placed against the Trp312. In addition to creating the acceptor-binding site, a second consequence of the binding of sialic acid is a conformational switch of a Tyr residue at position 342, which is the catalytic nucleophile making a covalent bond with the sialic acid intermediary state of the reaction.[148,149] The accepted mechanism of the trans-sialidase reaction is shown in Scheme 11.

A nucleophilic participation with the formation of a covalent intermediate enzyme-donor was suggested by *β*-dideuterium and ^{13}C isotope effects in acid hydrolysis and transfer reactions catalyzed by TcTS.[150] The first proof for a covalent sialyl-TcTS intermediate was reported by Withers and coworkers,[148] who analyzed by ES/MS peptide digests after the enzyme had been incubated with 3-F-α-NeuAc fluoride. The incorporation of a fluorine atom at C-3 adjacent to the anomeric center slows the reaction, allowing detection of the covalent intermediate. Moreover, formation of the covalent intermediate was confirmed by X-ray crystallography.[147] By using the mutant TcTS $_{D59A}$ lacking acid–base catalysis by the aspartic acid, the complex could be trapped and Tyr 342 was identified as the catalytic nucleophile.[148] Thus, the reaction starts with attack of the phenolic group in Tyr 342 with acid–base catalysis by Glu 230. The leaving group of the donor glycan is protonated by Asp 59, which is the base catalyst for the subsequent attack by 3-OH of the *β*-galactosyl acceptor, resulting in retention of the configuration for the new sialoside.

In some natural inactive members of the TcTS family Tyr 342 is substituted by Hys,[151] which abolishes the enzymatic activity but preserves sugar binding properties.[141,152]

b. Selective Sialylation of Oligosaccharides.—(*i*) *The Mucin Oligosaccharides as Acceptors of Sialic Acid.* TcTs has been used for the selective synthesis of oligosaccharides bearing the αNeuAc-(2→3)-*β*Gal motif. A recombinant enzyme and 3′-sialyllactose (SL) or an α-sialoside as donor are usually used.

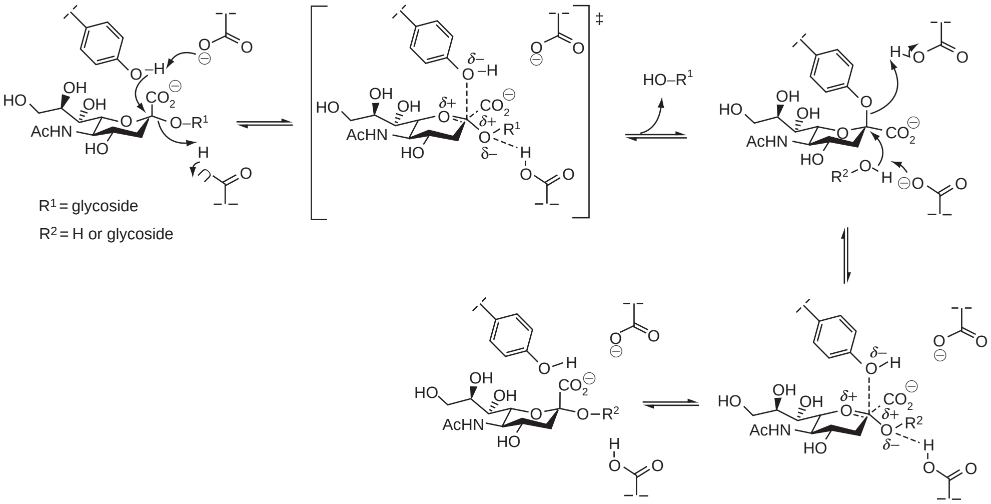
R1 = glycoside
R2 = H or glycoside
HO–R1
‡
HO
OH
AcHN
CO2
O–R1
O–R2
δ+
δ–

SCHEME 11. Mechanism of action of *T. cruzi* trans-sialidase (Ref. 149).

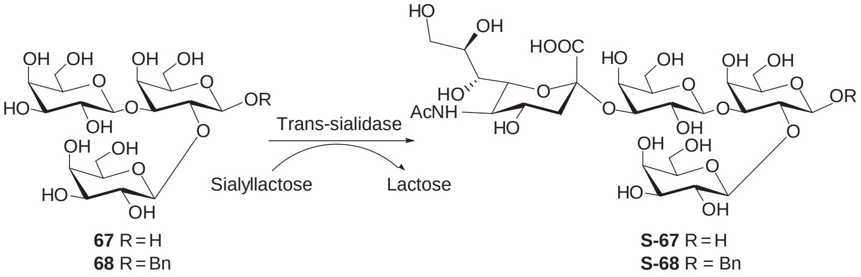

SCHEME 12. Selective sialylation of 2,3-di-*O*-(*β*-D-galactopyranosyl)-D-galactose catalyzed by *Trypanosoma cruzi* trans-sialidase.

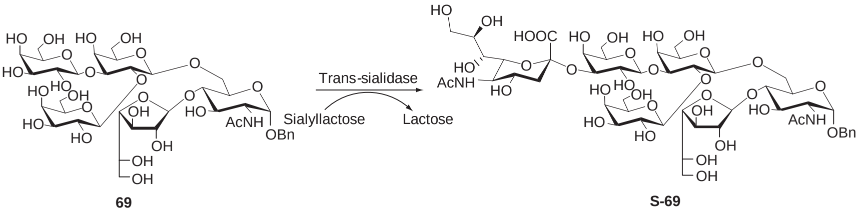

SCHEME 13. Selective sialylation of *β*-D-Gal*p*(1→2)[*β*-D-Gal*p*(1→3)]-*β*-D-Gal*p*(1→6)[*β*-D-Gal*f* (1→4)]-D-GlcNAc catalyzed by *Trypanosoma cruzi* trans-sialidase.

The pentasaccharide **21** and the hexasaccharide **22** in the mucins of *T. cruzi* (Fig. 7), lineage 1, contain 2,3-di-*O*-(*β*-D-Gal*p*)-*β*-D-Gal*p* as an external unit. This trisaccharide, **67** (Scheme 12),[115] presents two *β*-D-Gal*p* for possible sialylation. Analysis by HPAEC-PAD and NMR studies indicated that the trisaccharide **67** and the benzyl glycoside **68** were selectively monosialylated at the (1→3)-linked Gal*p* (Scheme 12), whereas the more flexible alditol was sialylated in both terminal Gal*p* groups.[153] Also, selective sialylation of the less-hindered (1→3)-linked Gal*p* occurred on trans-sialylation of the pentasaccharide benzyl glycoside (Scheme 13).[117] The hexasaccharide **22** in the mucins has three terminal Gal*p* as possible sites for sialylation. It was synthesized, and trans-sialylation experiments showed two monosialylated products in relative proportions varying with the time of the reaction (unpublished results).

A study on the comparative rates for sialylation of the synthetic oligosaccharides, found in mucins that contain Gal*f*, showed that the presence of Gal*f* did not impair the reaction. Thus, the diminished virulence of these strains is not related to interference of sialylation by Gal*f*.[119]

(ii) Sialylation of Other Oligosaccharides. Use of α-(2→3)Sialyllactose (3′SL) as Donor. The transfer reaction using sialyllactose as donor is reversible as the lactose formed could act as acceptor, depending on the relative affinities for the enzyme. A method was described introducing *β*-galactosidase together with the TcTS to hydrolyze the lactose formed in the reaction,[154] however this is practical only if the acceptor Gal*β*OR is not substrate for the *β*-galactosidase.

Use of Nonnatural Donors for the TcTS Reaction. Modification in the Acceptor Structure. Such nonnatural donors as the *p*-nitrophenyl (*p*NP) and methylumbelliyferyl (MU) α-sialosides have much lower activities than 3′SL as donors for the transfer reaction.[155] In contrast, the rate for hydrolysis of 2′-*O*-(4-methylumbelliferyl)-αNeu5Ac (MUNeu5Ac) was much higher than for 3′SL.[156] However, 2′-*O*-(*p*-nitrophenyl)-αNeu5Ac (*p*NPNeu5Ac) and the MU analogue have been used for the preparation of sialylated oligosaccharides, with the advantage that the reactions are not reversible.

The ability of αNeu5Ac-(2→3)-*β*GalO-*p*NP to act as donor substrate in the TcTS reaction was investigated using *β*Gal-(1→3)-*β*GlcNAc-1-octyl as acceptor.[157] A hydrolysis:transfer selectivity of 1:4 was observed, which was in between that observed for 3′SL (1:13)[155] and MUNeu5Ac.[156]

Vetere *et al*., used MUNeu5Ac and a recombinant TcTs for the synthesis of αNeu5Ac-(2→3)-*β*Gal-(1→4) GlcNAc (3′sialyl-*N*-acetyllactosamine)[158] and αNeu5Ac-(2→3)-*β*Gal-(1→3)-GlcNAc,[159] with 60 and 35% yields of isolated products respectively. In the first synthesis the authors claim that the yield was considerably higher than when using 3′SL as donor.

Yields of 85% were reported when the donor (*p*NPNeu5Ac) and recombinant TcTS were used for sialylation of lactose and lactosamine.[160] In the same communication the authors report some controversial results. Thus, they described that methyl α-D-Gal*p* could be sialylated in 54% yield and that αGal*p*-(1→6)-*β*Gal*p*OMe (**70**) was sialylated to give the branched trisaccharide αNeu5Ac-(2→3) [α Gal*p*-(1→6)] *β*Gal*p*OMe (**71**, Scheme 14) in good yield. On the other hand, it was reported that

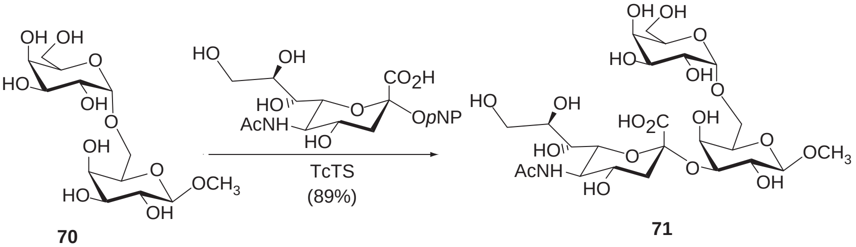

70 **71**

SCHEME 14. Sialylation of α-D-Gal*p*-(1→6)-*β*-D-Gal*p*-OMe by the trans-sialidase of *T. cruzi*.

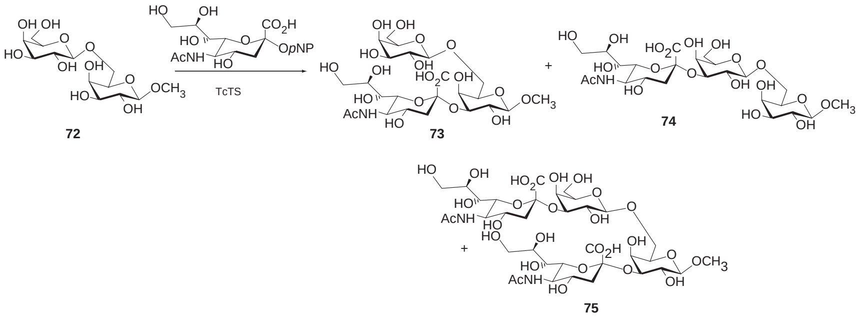

SCHEME 15. Sialylation of β-D-Gal*p*-(1→6)-β-D-Gal*p*-OMe by the trans-sialidase of *T. cruzi*.

βGal*p*-(1→6)-β-Gal*p*OMe (**72**) afforded a 1:1 mixture of the monosialylated products in 88% yield (**73** and **74**, Scheme 15) and that each of them could be converted into the bis-sialylated product **75**. However, no details of the reactions, nor full characterization of the compounds, were provided.

The labeled GM3 trisaccharide, αNeu5NAc-(2→3)-βGal-(1→4)-Glc was prepared by sialylation of [U-^{13}C]-lactose using *p*NPNeu5Ac as donor and a recombinant TcTS.[161] The same authors synthesized, by enzymatic trans-sialylation of lactosamine, followed by enzymatic fucosylation, the sialyl Lewis X tetrasaccharide, αNeu5NAc-(2→3)-βGal-(1→4)[αFuc-(1→3)]GlcNAc.

A water-soluble glycopolymer containing 3′-sialyl-lactosamineNAc was prepared from GlcNAc attached to polyacrylamide by sequential β-galactosidation with bovine galactosyltransferase followed by sialylation with TcTS using the donor *p*NPNeu5Ac. Sialic acid analysis showed 35% transfer.[162]

In recent works, Thiem and coworkers used *p*NPNeu5Ac and MUNeu5Ac for TcTS studies.[137,163–165] Several lactose derivatives have been sialylated, with yields of 30–60% (Scheme 16). βGal-(1→3)-Gal derivatives have been sialylated, but with lower yields (Scheme 17). In this way, the tumor-associated antigens αNeu5Ac-(2→3)-βGal*p*-(1→3)-αGal*p*NAc-(1→3)-threonine (**88**) and the serine glycoside analogue **89** were prepared.

Investigations of the influence of the hydroxy groups in the acceptor galactose ring on the trans-sialylation showed that the 2- or 6-deoxy, or even the replacement of β-Gal by β-L-Ara, did not impair the reaction, although a lower yield (30%) was obtained with the fucose disaccharide.[165]

Modifications of the Sialyl Donor. One of the first reports on the donor specificities of nonnatural substrates described transfer studies using MUNeu5Ac and derivatives, with lactose as acceptor, and the native enzyme.[166] Derivatives of C-7 MUNeu5Ac

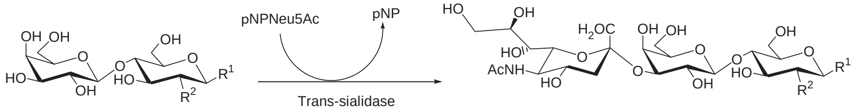

	R^1	R^2		Yield
76	SPh	N$_3$	**80**	32 %
77	OH	OH	**81**	49 %
78	OAll	OH	**82**	61 %
79	OMe	NHAc	**83**	42 %

SCHEME 16. Trans-sialylation of lactose and modified derivatives employing trans-sialidase.

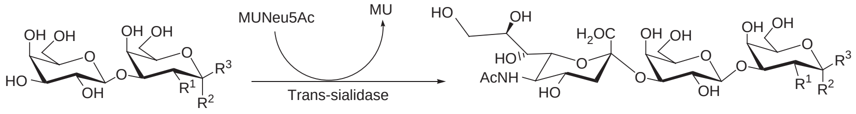

	R^1	R^2	R3		Yield
84	NHAc	Thr	H	**88**	25%
85	NHAc	Ser	H	**89**	22%
86	H	OMe	H	**90**	16%
87	N$_3$	H	OAll	**91**	31%

SCHEME 17. Trans-sialylations of βGal-(1→3)-Gal-R derivatives employing trans-sialidase.

were prepared by periodate oxidation of MUNeu5Ac and coupling of the C-7 aldehyde with various primary amines by reductive amination. The TcTS reactions for compounds **92–100** (Scheme 18) analyzed by HPAEC-PAD showed that only compounds **93**, **94**, and **99** served as donors but with a considerably low efficiency as compared with MUNeu5Ac (~50% transfer).

Using MUNeu5Ac as donor, the enzymatic sialylation of N-linked oligosaccharides released from the glycoproteins and derivatized with 2-aminopyridine has been reported, but no details on yields were provided.[167]

More recent works have described that the C-7 and C-8 analogues of *p*NPNeu5Ac obtained by periodate oxidation of the *p*-nitrophenyl α-sialoside, were efficient donors for sialylation of methyl β-lactoside, indicating that the exocyclic chain is not required for the enzymatic reaction.[164] Also, *N*-acyl-modified sialic acids were analyzed as donors, using βGal-(1→6)-α-GlcOMe as acceptor; substituents larger

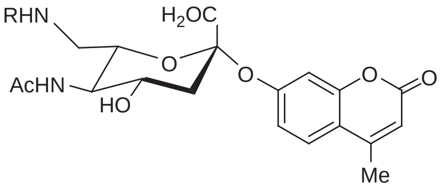

	R
92	H
93	$PHCH_2$
94	$MeOPhCH_2$
95	$PHCH_2O$
96	$NH_2(CH_2)_2$
97	Dansyl-NH-$(CH_2)_2$
98	Dansyl-NH
99	CF_3CO
100	$CF_3CONH(CH2)_2$

SCHEME 18. Trans-sialylation using MUNeu5Ac derivatives prepared by periodate oxidation followed by reductive amination with various primary amines.

than propanoyl were not transferred (Scheme 19).[137] Neu5Gc was efficiently transferred as described, when using a NeuGc oligosaccharide as donor (Scheme 20).[136]

c. Studies on Inhibition of TcTS.—The *T. cruzi* trans-sialidase meets one of the main requirements for a drug target, it is specific for the parasite with no equivalent in the human host. However, no efficient inhibitors have yet been reported. Besides their potential use for chemotherapy of Chagas disease, inhibitors should provide a tool for probing the biological functions of the enzyme.

Given the 3D structure of TcTS, inhibitors may be directed to the sialic acid binding site or to the galactose-acceptor site.

(i) Compounds Studied as Inhibitors for the Sialic Acid Binding Site. Although the sialic acid site for TcTS and microbial sialidases have common structural features, known inhibitors of sialidases as Neu5Ac2en (**109**) and zanamivir (**110**) are very weak inhibitors of TcTS (*Ki* for Neu5Ac2en 12.3 mM).[168] However, Neu5Ac2en co-crystallized with TcTS and the complex was used for 3D studies, indicating that

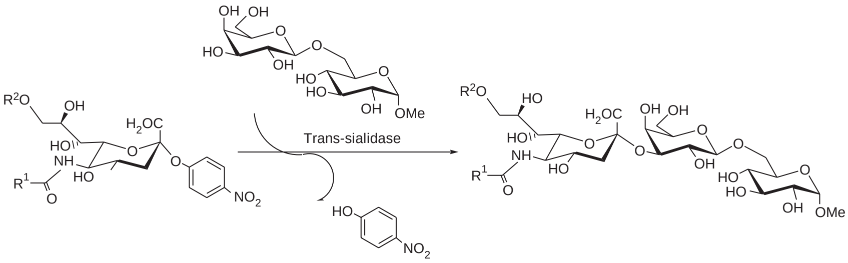

	R^1	R^2	Yield
101	CH_3	H	80%
102	CH_3	C_4H_7O	78%
103	C_2H_5	H	32%
104	C_3H_4	H	0%
105	$CH(CH_3)_2$	H	0%
106	CH_2OH	H	60%

SCHEME 19. Trans-sialylation with *p*NPNeu5Ac derivatives.

key aminoacids are different in both enzymes. Formulas for some compounds tested as inhibitors for their donor activity are shown in Fig. 10. The phosphonic acid derivatives **111** and **112**, in which a phosphonic acid replaces the carboxylic group of sialic acid, do not inhibit TcTS, neither does the analogue **113**, all competitive inhibitors of influenza sialidase and other sialidases.[169]

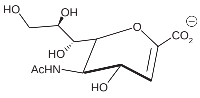
109
Neu5Ac2en Ki = 12 mM

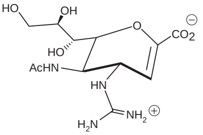
110
Zanamivir Ki not informed

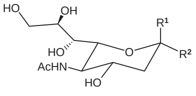
111 $R^1 = PO_3H_2$, $R^2 = H$
112 $R^1 = H$, $R^2 = PO_3H_2$
No inhibition

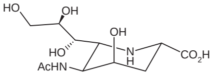
113
No inhibition

Taking in consideration that the anti-influenza drug and neuraminidase inhibitor GS-4071 has a cyclohexenecarboxylic acid structure, the cyclohexene phosphonate derivatives **114–123** (Fig. 10) were prepared and tested for TcTS activity.[170] Compounds **115** and **117**, containing the phosphonate as the monoethyl ester showed only weak inhibition (IC_{50} values of 4.7 and 5.7 mM, respectively).

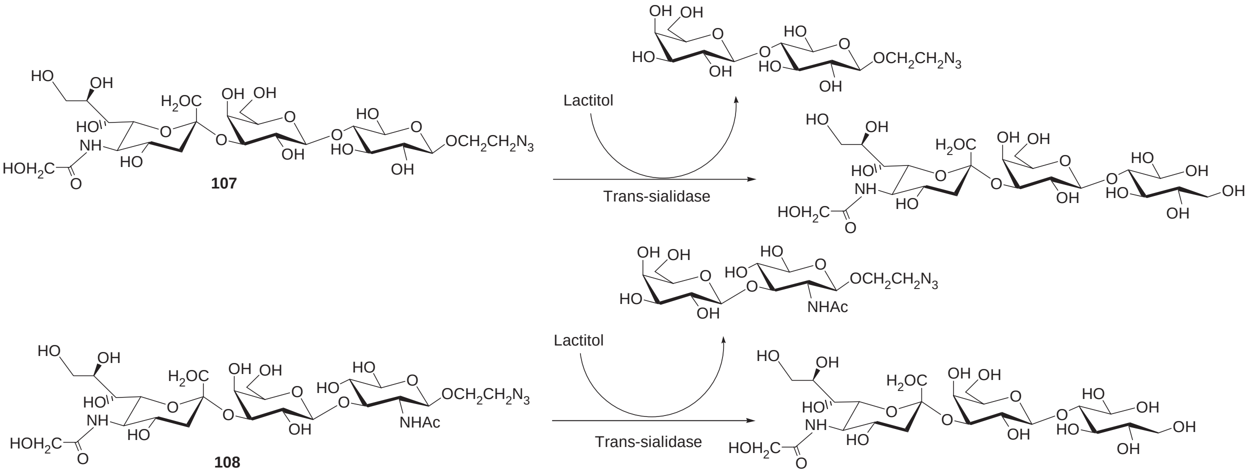
107
108
Lactitol
Trans-sialidase
Lactitol
Trans-sialidase

SCHEME 20. *N*-Glycolylneuraminic acid transfer by *Trypanosoma cruzi* trans-sialidase from donors **107** and **108** to lactitol.

Phosphonic acid derivatives

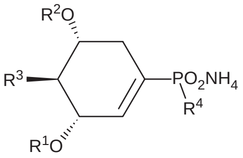

	R^1	R^2	R^3	R^4	
114	H	$CH_2CH(OH)CH_2OH$	NHAc	OEt	$IC_{20}>8mM$
115	H	CH_2CH_2OH	NHAc	OEt	$IC_{50}=4.7mM$
116	H	H	N_3	OEt	$IC_{20}>8mM$
117	H	H	NHAc	OEt	$IC_{50}=5.7mM$
118	H	$CH_2CH(OH)CH_2OH$	NHAc	$O^-NH_4^+$	No inhibition
119	H	CH_2CH_2OH	NHAc	$O^-NH_4^+$	No inhibition
120	H	H	NHAc	$O^-NH_4^+$	No inhibition
121	H	H	NHAc	6-*O*-Gal	No inhibition
122	H	H	NHAc	Benzyl	No inhibition
123	H	H	NHAc	n-octyl	No inhibition

Inhibition by aromatic derivatives

Pyridine derivatives

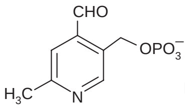

124

Ki 7.3 mM

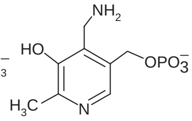

125

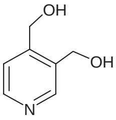

126

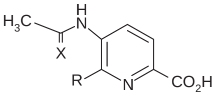

127 $R=NH_2$ $X=O$; IC_{50} 0.44 mM

128 $R=H$ $X=S$; IC_{50} 0.54 mM

FIG. 10. Continued

Aromatic compounds, in particular pyridine derivatives, have been tested for TcTS activity. One of the first reports describes a noncompetitive inhibition ($Ki = 7.3$ mM) with pyridoxal 5′-phosphate (**124**). Pyridoxamine (**125**) and pyridoxine (**126**) were still less efficient.[171] More recently, a series of benzoic acid and pyridine 2-carboxylic acid derivatives (Fig. 10, **129–135**) have been tested. Moderate inhibition was observed, with IC_{50} values between 0.4 and 1 mM.[172]

Covalent inhibitors were synthesized by Withers and coworkers.[148,149] The use of 3F-sialyl fluoride **136** as donor substrate allowed identification of the covalent mechanism for TcTS. Fluoride **136** completely inactivates the enzyme, but only at concentrations as high as 20 mM, and separation of excess inactivator caused recovery of the activity.[148] Since the 3D structure of TcTS showed that the donor site is more spacious and hydrophobic than in a human sialidase, derivatives at C-9 of the fluoride **136** were synthesized by a chemoenzymatic method and tested as inhibitors (Fig. 10).[149] Inhibition was analyzed with trifluoromethylumbelliferyl sialic acid for measuring hydrolase activity, however, as the site is the same for

Benzoic acid derivatives

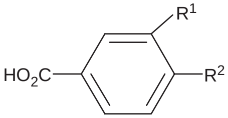

	R^1	R^2	IC50 (Mm)
129	CH_2OH	$NHCOCH_3$	0.54
130	$N{=}C(NH_2)_2$	$CONHCH_3$	0.76
131	NH_2	$NHCOCH_2Ph$	1.20
132	$NHCOCH_3$	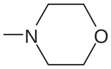	0.58
133	NH_2	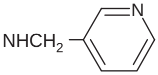	0.74
134	NH_2	SCH_2Ph	0.70
135	$NHCOCH_2NH_2$	SCH_2Ph	1.00

FIG. 10. Continued

hydrolase and trans-sialidase activity the results were extrapolated. Values for the compounds tested were of the same order of magnitude as for **136**, but in contrast with **136**, much higher concentrations of lactose were necessary to promote reactivation. The best inhibitors were compounds **137** and **141**.

(ii) Lactose Derivatives as Competitive Inhibitors of TcTS. Inhibitors of TcTS, binding to the *β*-galactosyl acceptor site should be more specific, as other sialidases lack this interaction. Lactose was normally used for measuring trans-sialidase activity and as acceptor in the crystallographic studies. The 3D structure showed water-mediated hydrogen bonds not only with the galactose unit, but also with the 3-OH of the reducing glucose.[145] Lactose derivatives analyzed as substrates and competitive inhibitors of the TcTS are shown in Fig. 11. Quantitative data were obtained by monitoring the reaction by HPAEC-PAD.[173] All of the compounds were shown to be good acceptors of sialic acid from the donor sialyllactose, with the exception of lactotetrazole derivative **147**. Lactitol was the preferred acceptor in comparison with lactose and *N*-acetyllactosamine, which suggests that better binding with the

Covalent derivatives

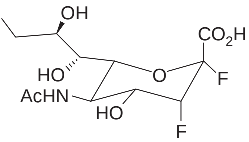

	R	$k_i/k_d \times 10^{-3}$ (min^{-1} mM^{-1})
136	OH	8.0
137	N_3	14.0
138	NH_2	n.d.
139	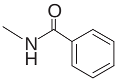	2.9
140	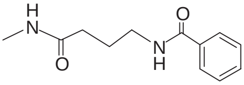	3.2
141	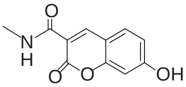	14.0

FIG. 10. Compounds tested as inhibitors of TcTS.

enzyme takes place with the open-chain alditol. Inhibition experiments showed that lactitol, the best competitive inhibitor, produced 75% inhibition in the sialylation of lactosamine. Lactitol also prevented parasite sialylation and partially inhibited cell infection. The use of inhibitors for the acceptor site unequivocally differentiates hydrolase from transfer activities as being responsible for biological events.

d. Biological Effects of TcTS.—TcTS is anchored by a GPI (see Section III.1.b.ii) and is shed into the bloodstream by the action of a PI-PLC. The enzyme in circulation exerts different biological effects on diverse cell types, probably by changing their surface sialylation. Strains belonging to lineage 2 secrete higher amounts of TS and induce 100% mortality in mouse.[174] During the acute phase of the disease, important hematological and immunological alterations are produced.

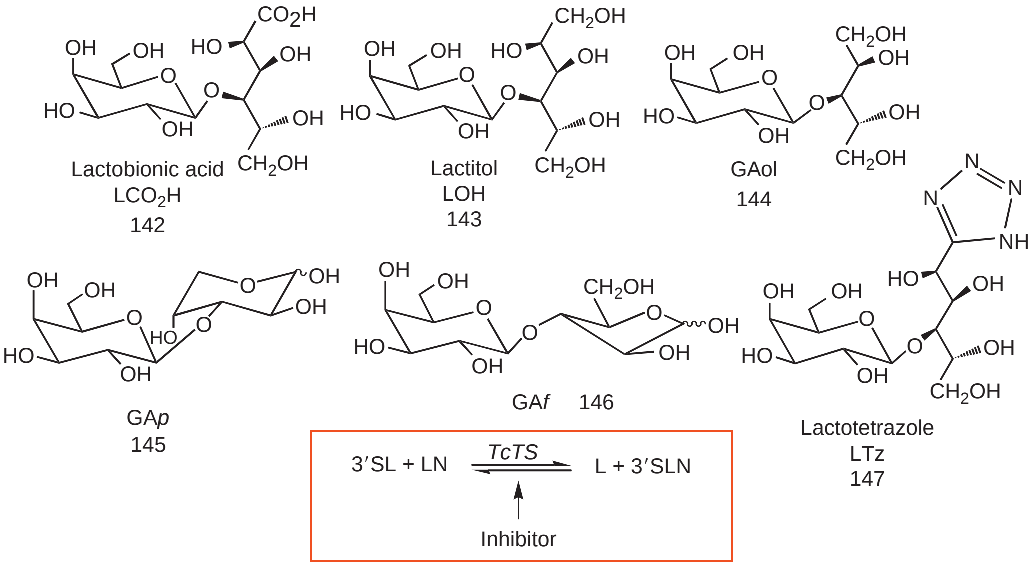
Lactobionic acid
LCO_2H
142
Lactitol
LOH
143
GAol
144
GA*p*
145
GA*f* 146
Lactotetrazole
LTz
147
3′SL + LN
TcTS
L + 3′SLN
Inhibitor

FIG. 11. Lactose derivatives analyzed as substrates and competitive inhibitors of TcTS.

TcTS was found to induce apoptosis in cells from the immune system.[175,176] Inhibition of this effect by lactitol indicated that sialylation of the surface thymocyte molecules, most probably CD43, was the cause for thymocyte depletion.[177] The TcTS is shed early during infection, damaging the immune system. Neutralizing antibodies prevent further damage,[178–180] allowing recovery, but they might not inhibit the enzyme at the surface of parasites present inside the tissues. On the other hand, it was reported that binding of TcTS or the inactive form of TcTS to CD43 inhibits T CD4 cell death[181] and that a recombinant inactive TcTS binding to the cell-surface sialic acid protects endothelial cells from apoptosis induced by growth-factor deprivation.[182] It was also reported that TcTS inhibits human lymphocyte proliferation by a non-apoptotic mechanism.[183] These apparent controversial results need to be clarified.

The inactive TcTS contains the two binding sites;[152] the difference is a His at position 342 instead of a Tyr as in active members.[151]

4. Other Glycoproteins

a. NETNES.—The name NETNES refers to the central peptide, from a total of 13 amino acids, of this GPI-anchored glycopeptide. NETNES is a minor component in the cell membrane of epimastigotes and it exists in two forms according to the number of glycosidic chains.[22] These are one or two N-linked mannose oligosaccharides and two linear α-mannose oligosaccharides linked to serine via phosphodiester linkages (Fig. 12). The GPI anchor is attached to the C-terminal aspartic acid via ethanolamine phosphate in the normal manner. The lipid in the IPL constituent is an alkyl acyl glycerol, with $C_{16:0}$ chains. There are four assumptions in the structural assignments.

It is assumed that AEP is attached to O-6 of the GlcN in the GPI by comparison with the GIPL structure (see Fig. 2). The α-(1→6) linkage of GlcN to *myo*-inositol and the position of the EtNP bridge are based on the structure of known anchors[54] and finally, the α configuration for the αManP-Ser was based on precedent for *Leishmania* phosphoglycans.

The biological functions for NETNES are not known.

b. GP72.—GP72 refers to *T. cruzi* glycoproteins that are recognized by the carbohydrate-specific monoclonal antibody WIC29.26.[184] It was first identified at the surface of epimastigote cells and later found in metacyclic trypomastigotes.[185] WIC29.26 did not react with amastigotes or tissue culture trypomastigotes, although the protein could be identified by expressing an epitope-tagged version of GP72 in all

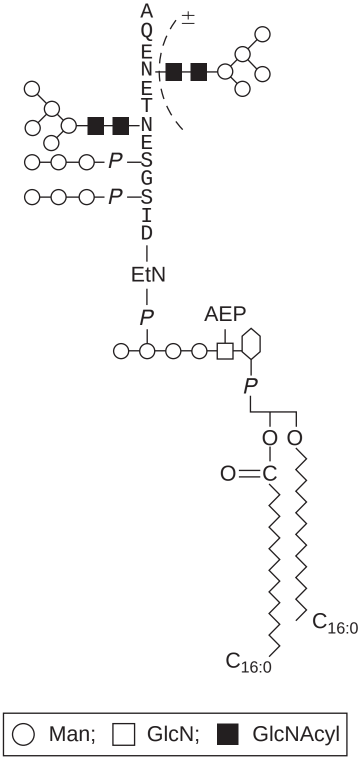

FIG. 12. Proposed primary structure of the NETNES glycoprotein isolated from *T. cruzi* (epimastigote). Ref. 22.

life stages of the parasite.[186] These results indicate developmental regulation of GP72 at the level of glycosylation rather than protein expression.

Studies on the carbohydrates have been performed on the glycoprotein isolated by monoclonal affinity chromatography,[187] and unusual structures were described for the carbohydrate moieties. No carbohydrates were released by the methods commonly used to cleave N- and O-glycosyl chains in glycoproteins. However, a series of oligosaccharides were released by mild acid hydrolysis, suggesting the presence of phosphodiester linkages between the carbohydrate and the protein, and supported by the detection of threonine phosphate. Phosphated hexa- and heptasaccharides were separated from a neutral fraction and they contained galactofuranose, xylose, fucose, and rhamnose, with galactofuranose being the most abundant. The unique structure of the carbohydrate in GP72 is illustrated by the partial structure of the hexasaccharide

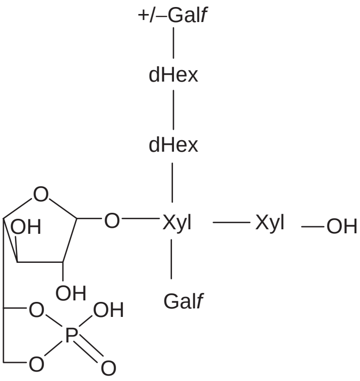

FIG. 13. Diagram of the partial structure deduced for the hexasaccharide of GP72. dHex, deoxyhexose.

(Fig. 13). Incorporation of galactofuranose, present also in GIPLs of epimastigotes and in the mucins of lineage 1, is a good candidate for involvement in developmental regulation. In this respect, an exo *β*-D-galactofuranosidase activity was detected in *T. cruzi* with an antibody against the enzyme from *Penicillium fellutanum*.[188]

The gene encoding GP72 has been cloned and sequenced.[189] Deletion of the gene caused drastic morphological changes and the flagellum was detached from the cell body, indicating that GP72 is involved in flagellar adhesion.[190] A null mutant was unable to survive in the insect vector.[191]

IV. CONCLUDING REMARKS

T. cruzi is an exceptional system for glycobiology studies; and the most unusual structures have been identified. From the medical point of view, the mucin and trans-sialidase families, which constitute ~15% of all predicted genes, are involved in the infection process.

Some of the unresolved subjects related to the glycobiology of *T. cruzi* are:

- The fine structure of the mucins from the trypomastigote stage
- The characterization of the glycosyltransferases and biosynthetic pathways involved in the construction of the O-chains in the mucins
- Why is Gal*f* incorporated only in mucins of strains belonging to lineage 1 and α-Gal*p* in mucins of trypomastigotes?

- What are the functions for the minor, unique glycoproteins, NETNES and GP72?
- The synthesis of efficient inhibitors for the trans-sialidase

And, not strictly glycobiology, but related to:

- The characterization of the remodelases that remodel the lipid in the biosynthetic pathways of the GPI anchor.

The answer to these matters may lead to the development of enzyme inhibitors effective as drugs for Chagas' disease.

REFERENCES

1. Z. Brener, Biology of *Trypanosoma cruzi*, *Ann. Rev. Microbiol.*, 27 (1973) 347–382; A. Moncayo, Chagas Disease: Current epidemiological trends after the interruption of vectorial and transfusional transmission in the southern cone countries, *Mem. Inst. Oswaldo Cruz*, 98 (2003) 577–591.
2. N. M. El-Sayed, *et al.*, The genome sequence of *Trypanosoma cruzi*, etiologic agent of Chagas disease, *Science*, 309 (2005) 409–415.
3. B. Zingales, R. P. Souto, R. H. Mangia, C. V. Lkboa, D. A. Campbell, J. R. Coura, A. Jansen, and O. Fernandes, Molecular epidemiology of American trypanosomiasis in Brazil based on dimorphisms of r&WA and mini-exon gene sequences, *Int. J. Parasitol.*, 28 (1998) 105–112.
4. M. R. S. Briones, R. P. Souto, B. S. Stolf, and B. Zingales, The evolution of two *Trypanosoma cruzi* subgroups inferred from rRNA genes can be correlated with the interchange of American mammalian faunas in the Cenozoic and has implications to pathogenicity and host specificity, *Mol. Biochem. Parasitol.*, 104 (1999) 219–232.
5. M. Bértoli, M. H. Andó, M. J. De Ornelas Toledo, S. M. De Araújo, and M. L. Gomes, Infectivity for mice of *Trypanosoma cruzi* I and II strains isolated from different hosts, *Parasitol Res.*, 99 (2006) 7–13.
6. M. J. de O. Toledo, M. de Lana, C. M. Carneiro, M. T. Bahia, G. L. L. Machado-Coelho, V. M. Veloso, C. Barnabé, M. Tibayrenc, and W. L. Tafuri, Impact of *Trypanosoma cruzi* clonal evolution on its biological properties in mice, *Exp. Parasitol.*, 100 (2002) 161–172.
7. A. B. Fernandes and R. A. Mortara, Invasion of MDCK epithelial cells with altered expression of Rho GTPases by *Trypanosoma cruzi* amastigotes and metacyclic trypomastigotes of strains from the two major phylogenetic lineages, *Microbes Infect.*, 6 (2004) 460–467.
8. W. De Souza, Basic cell biology of *Trypanosoma cruzi*, *Curr. Pharm. Des.*, 8 (2002) 269–285.
9. R. M. de Lederkremer and L. E. Bertello, Glycoinositolphospholipids free and as anchors of proteins, in *Trypanosoma cruzi*, *Curr. Pharm. Des.*, 7 (2001) 1165–1179.
10. J. O. Previato, R. Wait, C. Jones, A. R. Todeschini, N. Heise, and L. M. Previato, Glycoinositolphospholipid from *Trypanosoma cruzi*: structure, biosynthesis and immunobiology, *Adv. Parasitol*, 56 (2004) 1–41.
11. R. M. de Lederkremer, C. Lima, M. I. Ramirez, M. A. J. Ferguson, S. W. Homans, and J. Thomas-Oates, Complete structure of the glycan of lipopeptidophosphoglycan from *Trypanosoma cruzi* epimastigotes, *J. Biol. Chem.*, 266 (1991) 23670–23675.
12. J. L. MacRae and M. A. J. Ferguson, A robust and selective method for the quantification of glycosylphosphatidylinositols in biological samples, *Glycobiology*, 15 (2005) 131–138.

13. R. M. de Lederkremer, M. J. M. Alves, G. C. Fonseca, and W. Colli, A lipopeptidophosphoglycan from *Trypanosoma cruzi* (epimastigota). Isolation, purification and carbohydrate composition, *Biochim. Biophys. Acta.*, 444 (1976) 85–96.
14. R. M. de Lederkremer, O. L. Casal, C. T. Tanaka, and W. Colli, Ceramide and inositol content of the lipopeptidophosphoglycan from *Trypanosoma cruzi*, *Biochem. Biophys. Res. Commun.*, 85 (1978) 1268–1274.
15. R. M. de Lederkremer, O. L. Casal, M. J. M. Alves, and W. Colli, *Trypanosoma cruzi*: Aminoacid and phosphorus linkages in the lipopeptidophosphoglycan, *Biochem. Internat.*, 10 (1985) 89–96.
16. R. M. de Lederkremer, C. Lima, M. I. Ramirez, and O. L. Casal, Structural features of the lipopeptidophosphoglycan (LPPG) from *Trypanosoma cruzi* common with the glycophosphatidylinositol anchors, *Eur. J. Biochem.*, 192 (1990) 337–345.
17. R. M. de Lederkremer, C. Lima, and M. C. Vila, Ceramide 1-phosphate is released from a glycoinositolphosphoceramide of *Trypanosoma cruzi* by rat blood plasma, *Mol. Biochem. Parasitol.*, 79 (1996) 219–223.
18. J. O. Previato, P. A. Gorin, M. Mazurek, M. T. Xavier, B. Fournet, J. M. Wieruszesk, and L. Mendonça-Previato, Primary structure of the oligosaccharide chain of lipopeptidophosphoglycan of epimastigote forms of *Trypanosoma cruzi*, *J. Biol. Chem.*, 265 (1990) 2518–2526.
19. M. A. J. Ferguson, The structure, biosynthesis and functions of glycosylphosphatidylinositol anchors, and the contributions of trypanosome research, *J. Cell Sci.*, 112 (1999) 2799–2809.
20. J. C. Carreira, C. Jones, R. Wait, J. O. Previato, and L. Mendonça-Previato, Structural variation in the glycoinositolphospholipids of different strains of *Trypanosoma cruzi*, *Glycoconj. J.*, 13 (1996) 955–966.
21. R. M. de Lederkremer, C. Lima, M. I. Ramirez, M. F. Gonçalvez, and W. Colli, Hexadecylpalmitoylglycerol or ceramide is linked to similar glycophosphoinositol anchor-like structures in *Trypanosoma cruzi*, *Eur. J. Biochem.*, 218 (1993) 929–936.
22. J. I. MacRae, A. Acosta-Serrano, N. A. Morrice, A. Mehlert, and M. A. J. Ferguson, Structural Characterization of NETNES, a Novel Glycoconjugate in *Trypanosoma cruzi* Epimastigotes, *J. Biol. Chem.*, 280 (2005) 12201–12211.
23. D. B. Golgher, W. Colli, T. Souto-Padron, and B. Zingales, Galactofuranose-containing glycoconjugates of epimastigote and trypomastigote forms of *Trypanosoma cruzi*, *Mol. Biochem. Parasitol.*, 60 (1993) 249–264.
24. V. L. Pereira-Chioccola, A. Acosta-Serrano, I. Correira de Almeida, M. A. J. Ferguson, T. Souto-Padron, M. M. Rodrigues, L. R. Travassos, and S. Schenkman, Mucin-like molecules form a negatively charged coat that protects *Trypanosoma cruzi* trypomastigotes from killing by human anti-alpha-galactosyl antibodies, *J. Cell Sci.*, 113 (2000) 1299–1307.
25. M. A. J. Ferguson, S. W. Homans, R. A. Dwek, and T. W. Rademacher, Glycosyl-phosphatidylinositol moiety that anchors *Trypanosoma brucei* variant surface glycoprotein to the membrane, *Science*, 239 (1988) 753–759.
26. W. L. Roberts, B. H. Kim, and T. L. Rosenberry, Differences in the glycolipid membrane anchors of bovine and human erythrocyte acetylcholinesterases, *Proc. Natl. Acad. Sci. USA*, 84 (1987) 7817–7821.
27. J. Armesto, E. Hannappel, K. Leopold, W. Fischer, R. Bublitz, L. Langer, G. A. Cumme, and A. Horn, Microheterogeneity of the hydrophobic and hydrophilic part of the glycosylphosphatidylinositol anchor of alkaline phosphatase from calf intestine, *Eur. J. Biochem.*, 238 (1996) 259–269.
28. F. Reggiori and A. Conzelmann, Biosynthesis of inositol phosphoceramides and remodeling of glycosylphosphatidylinositol anchors in Saccharomyces cerevisiae are mediated by different enzymes, *J. Biol. Chem.*, 273 (1998) 30550–30559, and references therein.

29. G. D. Pollevick, J. M. Di Noia, M. L. Salto, C. Lima, M. S. Leguizamon, R. M. de Lederkremer, and A. C. C. Frasch, *Trypanosoma cruzi* surface mucins with exposed variant epitopes, *J. Biol. Chem.*, 275 (2000) 27671–27680.
30. J. O. Previato, C. Jones, L. P. B. Gonçalves, R. Wait, L. R. Travassos, A. J. Parodi, and L. Mendonça-Previato, Structural characterization of the major glycosylphosphatidylinositol membrane-anchored glycoprotein from epimastigote forms of *Trypanosoma cruzi* Y-strain, *J. Biol. Chem.*, 270 (1995) 7241–7250.
31. A. Acosta-Serrano, S. Schenkman, N. Yoshida, A. Mehlert, J. Richardson, and M. A. J. Ferguson, The lipid structure of the glycosylphosphatidylinositol-anchored mucin-like sialic acid acceptors of *Trypanosoma cruzi* changes during parasite differentiation from epimastigotes to infective metacyclic trypomastigote froms, *J. Biol. Chem.*, 270 (1995) 27244–27253.
32. I. C. Almeida, M. M. Camargo, D. O. Procopio, L. S. Silva, A. Mehlert, L. R. Travassos, R. T. Gazzinelli, and M. A. J. Ferguson, Highly purified glycosylphosphatidylinositols from *Trypanosoma cruzi* are potent proinflammatory agents, *EMBO J.*, 19 (2000) 1476–1485.
33. M. M. Camargo, I. C. Almeida, M. E. S. Pereira, M. A. J. Ferguson, T. Souto-Padrón, M. M. Rodrigues, L. R. Travassos, and S. Schenkman, Glycoconjugates isolated from *Trypanosoma cruzi* but not from Leishmania species membranes trigger nitric oxide synthesis as well as microbicidal activity in IFN-gamma-primed macrophages, *J. Immunol.*, 158 (1997) 5890–5901.
34. R. Agusti, A. S. Couto, O. E. Campetella, A. C. C. Frasch, and R. M. De Lederkremer, The trans-sialidase of *Trypanosoma cruzi* is anchored by two different lipids, *Glycobiology.*, 7 (1997) 731–735.
35. R. Agusti, A. S. Couto, O. Campetella, A. C. C. Frasch, and R. M. de Lederkremer, Structure of the glycosylphosphatidylinositol-anchor of the *trans*-sialidase from *Trypanosoma cruzi* metacyclic trypomastigote forms, *Mol. Biochem. Parasitol.*, 97 (1998) 123–131.
36. M. J. M. Alves and W. Colli, Role of the gp85/trans-sialidase superfamily of glycoproteins in the interaction of *Trypanosoma cruzi* with host structures, in B. A. Burleigh and D. Soldati-Favre, (Eds.), *Molecular Mechanisms of Parasite Invasion*, 47 pp. 58–96.
37. A. M. Katzin and W. Colli, Lectin receptors in *Trypanosoma cruzi*. An *N*-acetyl-D-glucosamine-containing surface glycoprotein specific for the trypomastigote stage, *Biochim. Biophys. Acta.*, 727 (1983) 403–411.
38. A. S. Couto, R. M. de Lederkremer, W. Colli, and M. J. M. Alves, The glycosylphosphatidylinositol anchor of the trypomastigote specific Tc 85 glycoprotein from *Trypanosoma cruzi*. Metabolic labeling and structural studies, *Eur. J. Biochem.*, 217 (1993) 597–602.
39. G. Abuin, A. S. Couto, R. M. Lederkremer, O. L. Casal, C. Galli, W. Colli, and M. J. M. Alves, *Trypanosoma cruzi*: the Tc-85 surface glycoprotein shed by trypomastigotes bears a modified glycosylphosphatidylinositol anchor, *Exp. Parasitol.*, 72 (1996) 290–297.
40. M. L. Guther, M. L. de Almeida, N. Yoshida, and M. A. J. Ferguson, Structural studies on the glycosylphosphatidylinositol membrane anchor of *Trypanosoma cruzi* 1G7-antigen. The structure of the glycan core, *J. Biol. Chem.*, 267 (1992) 6820–6828.
41. N. Heise, M. L. Cardoso de Almeida, and M. A. J. Ferguson, Characterization of the lipid moiety of the glycosylphosphatidylinositol anchor of *Trypanosoma cruzi* 1G7-antigen, *Mol. Biochem. Parasitol.*, 70 (1995) 71–84.
42. L. E. Bertello, N. W. Andrews, and R. M. Lederkremer, Developmentally regulated expression of ceramide in *Trypanosoma cruzi*, *Mol. Biochem. Parasitol.*, 79 (1996) 143–151.
43. N. F. Nogueira, M. S. Gonzalez, J. E. Gomes, W. de Souza, E. S. Garcia, P. Azambuja, L. L. Nohara, I. C. Almeida, B. Zingales, and W. Colli, *Trypanosoma cruzi*: involvement of glycoinositolphospholipids in the attachment to the luminal midgut surface of Rhodnius prolixus, *Exp. Parasitol.*, 116 (2007) 120–128.

44. N. Garg, R. L. Tarleton, and K. Mensa-Wilmot, Proteins with glycosylphosphatidylinositol (GPI) signal sequences have divergent fates during a GPI deficiency. GPIs are essential for nuclear division in *Trypanosoma cruzi*, *J. Biol. Chem.*, 272 (1997) 12482–12491.
45. N. Garg, M. Postan, K. Mensa-Wilmot, and R. L. Tarleton, Glycosylphosphatidylinositols are required for the development of *Trypanosoma cruzi* amastigotes, *Infect. Immun.*, 65 (1997) 4055–4060.
46. R. A. Mortara, L. M. Minelli, F. Vandekerckhove, V. Nussenzweig, and F. J. Ramalho-Pinto, Phosphatidylinositol-specific phospholipase C (PI-PLC) cleavage of GPI-anchored surface molecules of *Trypanosoma cruzi* triggers *in vitro* morphological reorganization of trypomastigotes, *J. Eukaryot. Microbiol.*, 48 (2002) 27–37.
47. M. L. Salto, L. E. Bertello, M. Vieira, R. Docampo, S. N. Moreno, and R. M. de Lederkremer, Formation and remodeling of inositolphosphoceramide during differentiation of *Trypanosoma cruzi* from trypomastigote to amastigote, *Eukaryot. Cell.*, 2 (2003) 756–768.
48. N. A. Gomes, J. O. Previato, B. Zingales, L. Mendonça-Previato, and G. A. DosReis, Down-regulation of T lymphocyte activation *in vitro* and *in vivo* induced by glycoinositolphospholipids from *Trypanosoma cruzi*. Assignment of the T cell-suppressive determinant to the ceramide domain, *J. Immunol.*, 156 (1996) 628–635.
49. C. A. Bento, M. B. Melo, J. O. Previato, L. Mendonça-Previato, and L. M. Peçanha, Glycoinositolphospholipids purified from *Trypanosoma cruzi* stimulate Ig production *in vitro*, *J. Immunol.*, 157 (1996) 4996–5001.
50. C. G. Freire de Lima, M. P. Nunes, S. Corte-Real, M. P. Soares, J. O. Previato, L. Mendonça-Previato, and G. A. DosReis, Proapoptotic activity of a *Trypanosoma cruzi* ceramide-containing glycolipid turned on in host macrophages by IFN-gamma, *J. Immunol.*, 161 (1998) 4909–4916.
51. G. A. DosReis, L. M. Peçanha, M. Bellio, J. O. Previato, and L. Mendonça-Previato, Glycoinositol phospholipids from *Trypanosoma cruzi* transmit signals to the cells of the host immune system through both ceramide and glycan chains, *Microbes Infect.*, 4 (2002) 1007–1013.
52. I. C. Almeida and R. T. Gazzinelli, Proinflammatory activity of glycosylphosphatidylinositol anchors derived from *Trypanosoma cruzi*: structural and functional analyses, *J. Leukoc. Biol.*, 70 (2001) 467–477.
53. W. J. Masterson, T. L. Doering, G. W. Hart, and P. T. Englund, A novel pathway for glycan assembly: biosynthesis of the glycosyl-phosphatidylinositol anchor of the trypanosome variant surface glycoprotein, *Cell.*, 56 (1989) 793–800.
54. M. A. J. Ferguson, J. S. Brimacombe, J. R. Brown, A. Crossman, A. Dix, R. A. Field, M. L. Güther, K. G. Milne, D. K. Sharma, and T. K. Smith, The GPI biosynthetic pathway as a therapeutic target for African sleeping sickness, *Biochim. Biophys. Acta.*, 1455 (1999) 327–340.
55. Y. S. Morita and P. T. Englund, Fatty acid remodeling of glycosyl phosphatidylinositol anchors in *Trypanosoma brucei*: incorporation of fatty acids other than myristate, *Mol. Biochem. Parasitol.*, 115 (2001) 157–164.
56. M. L. Guther and M. A. J. Ferguson, The role of inositol acylation and inositol deacylation in GPI biosynthesis in *Trypanosoma brucei*, *EMBO J.*, 14 (1995) 3080–3093.
57. W. L. Roberts, S. Santikarn, V. N. Reinhold, and T. L. Rosenberry, Structural characterization of the glycoinositol phospholipid membrane anchor of human erythrocyte acetylcholinesterase by fast atom bombardment mass spectrometry, *J. Biol. Chem.*, 263 (1988) 18776–18784.
58. M. L. Guther, S. Leal, N. A. Morrice, G. A. Cross, and M. A. J. Ferguson, Purification, cloning and characterization of a GPI inositol deacylase from *Trypanosoma brucei*, *EMBO J.*, 20 (2001) 4923–4934.
59. P. Orlean and A. K. Menon, Thematic review series: lipid posttranslational modifications. GPI anchoring of protein in yeast and mammalian cells, or: how we learned to stop worrying and love glycophospholipids, *J. Lipid Res.*, 48 (2007) 993–1011.

60. G. Sipos, A. Puoti, and A. Conzelmann, Glycosylphosphatidylinositol membrane anchors in *Saccharomyces cerevisiae*: absence of ceramides from complete precursor glycolipids, *EMBO J.*, 13 (1994) 2789–2796.
61. G. Sipos, F. Reggiori, C. Vionnet, and A. Conzelmann, Alternative lipid remodelling pathways for glycosylphosphatidylinositol membrane anchors in *Saccharomyces cerevisiae*, *EMBO J.*, 16 (1997) 3494–3505.
62. F. Reggiori, E. Canivenc-Gansel, and A. Conzelmann, Lipid remodeling leads to the introduction and exchange of defined ceramides on GPI proteins in the ER and Golgi of *Saccharomyces cerevisiae*, *EMBO J.*, 16 (1997) 3506–3518.
63. M. Pittet and A. Conzelmann, Biosynthesis and function of GPI proteins in the yeast *Saccharomyces cerevisiae*, *Biochim. Biophys Acta.*, 1771 (2007) 405–420.
64. L. E. Bertello, M. J. M. Alves, W. Colli, and R. M. de Lederkremer, Inositolphosphoceramide is not a substrate for the first steps in the biosynthesis of glycoinositolphospholipids in *Trypanosoma cruzi*, *Mol. Biochem. Parasitol.*, 133 (2004) 71–80.
65. N. Heise, J. Raper, L. U. Buxbaum, T. M. Peranovich, and M. L. de Almeida, Identification of complete precursors for the glycosylphosphatidylinositol protein anchors of *Trypanosoma cruzi*, *J. Biol. Chem.*, 271 (1996) 16877–16887.
66. L. E. Bertello, M. F. Goncalvez, W. Colli, and R. M. de Lederkremer, Structural analysis of inositol phospholipids from *Trypanosoma cruzi* epimastigote forms, *Biochem. J.*, 310 (1995) 255–261.
67. L. E. Bertello, M. J. M. Alves, W. Colli, and R. M. de Lederkremer, Evidence for phospholipases from *Trypanosoma cruzi* active on phosphatidylinositol and inositolphosphoceramide, *Biochem. J.*, 345 (2000) 77–84.
68. Y. Zhu, C. Vionnet, and A. Conzelmann, Ethanolaminephosphate side chain added to glycosylphosphatidylinositol (GPI) anchor by mcd4p is required for ceramide remodeling and forward transport of GPI proteins from endoplasmic reticulum to Golgi, *J. Biol. Chem.*, 281 (2006) 19830–19839.
69. M. L. Uhrig, A. S. Couto, W. Colli, and R. M. de Lederkremer, Characterization of inositolphospholipids in *Trypanosoma cruzi* trypomastigote forms, *Biochim. Biophys. Acta.*, 1300 (1996) 233–239.
70. J. M. Figueiredo, W. B. Dias, L. Mendonça-Previato, J. O. Previato, and N. Heise, Characterization of the inositol phosphorylceramide synthase activity from *Trypanosoma cruzi*, *Biochem. J.*, 387 (2005) 519–529.
71. S. Undenfriend and K. Kodukula, How glycosylphosphatidylinositol-anchored membrane proteins are made, *Annu. Rev. Biochem.*, 64 (1995) 563–591.
72. B. Eisenhaber, P. Bork, and F. Eisenhaber, Sequence properties of GPI-anchored proteins near the omega-site: constraints for the polypeptide binding site of the putative transamidase, *Protein Eng.*, 11 (1998) 1155–1161.
73. K. Nagamune, K. Ohishi, H. Ashida, Y. Hong, J. Hino, K. Kangawa, N. Inoue, Y. Maeda, and T. Kinoshita, GPI transamidase of *Trypanosoma brucei* has two previously uncharacterized (trypanosomatid transamidase 1 and 2) and three common subunits, *Proc. Natl. Acad. Sci. USA*, 100 (2003) 10682–10687.
74. Y. Hong, K. Nagamune, K. Ohishi, Y. S. Morita, H. Ashida, Y. Maeda, and T. Kinoshita, TbGPI16 is an essential component of GPI transamidase in *Trypanosoma brucei*, *FEBS Lett*, 580 (2006) 603–606.
75. M. Hederos and P. Konradsson, Synthesis of the *Trypanosoma cruzi* LPPG heptasaccharyl myo-inositol, *J. Am. Chem. Soc.*, 128 (2006) 3414–3419.
76. M. Hederos and P. Konradsson, Synthesis of the core tetrasaccharide of *Trypanosoma cruzi* glycoinositolphospholipids: Man*p*(α1→6)-Man*p*(α1→4)-6-(2-aminoethylphosphonic acid)-GlcN*p* (α1→6)-myo-Ins-1-PO4, *J. Org. Chem.*, 70 (2005) 196–207.

77. K. D. Randell, B. D. Johnston, P. N. Browin, and B. M. Pinto, Synthesis of galactofuranosyl-containing oligosaccharides corresponding to the glycosylinositolphospholipid of *Trypanosoma cruzi*, *Carbohydr. Res.*, 325 (2000) 253–264.
78. D. V. Yashunsky, V. S. Borodkin, M. A. J. Ferguson, and A. V. Nikolaev, The chemical synthesis of bioactive glycosylphosphatidylinositols from *Trypanosoma cruzi* containing an unsaturated fatty acid in the lipid, *Angew. Chem. Int. Ed. Engl.*, 45 (2006) 468–474.
79. S. Schenkman, M. A. J. Ferguson, N. Heise, M. L. de Almeida, R. A. Mortara, and N. Yoshida, Mucin-like glycoproteins linked to the membrane by glycosylphosphatidylinositol anchor are the major acceptors of sialic acid in a reaction catalyzed by trans-sialidase in metacyclic forms of *Trypanosoma cruzi*, *Mol. Biochem. Parasitol.*, 59 (1993) 293–303.
80. A. Acosta-Serrano, I. C. Almeida, L. H. G. Freitas-Junior, N. Yoshida, and S. Schenkman, The mucin-like glycoprotein super-family of *Trypanosoma cruzi*: structure and biological roles, *Mol. Biochem. Parasitol.*, 114 (2001) 143–150.
81. M. J. M. Alves and W. Colli, Glycoproteins from *Trypanosoma cruzi*: partial purification by gel chromatography, *FEBS Lett.*, 52 (1975) 188–190.
82. B. Zingales, N. F. Martin, R. M. de Lederkremer, and W. Colli, Endogenous and surface labeling of glycoconjugates from the three differentiation stages of *Trypanosoma cruzi*, *FEBS Lett.*, 142 (1982) 238–242.
83. C. A. Buscaglia, V. A. Campo, A. C. C. Frasch, and J. M. Di Noia, *Trypanosoma cruzi* surface mucins: host-dependent coat diversity, *Nat. Rev. Microbiol*, 4 (2006) 229–236; A. C. C. Frasch, Functional diversity in the trans-sialidase and mucin families in *Trypanosoma cruzi*, *Parasitol. Today*, 16 (2000) 282–286.
84. J. M. Di Noia, I. D'Orso, D. O. Sanchez, and A. C. C. Frasch, AU-rich elements in the $3'$-untranslated region of a new mucin-type family of *Trypanosoma cruzi* confers mRNA instability and modulates translation efficiency, *J. Biol. Chem.*, 275 (2000) 10218–10227.
85. J. M. Di Noia, D. O. Sanchez, and A. C. C. Frasch, The protozoan *Trypanosoma cruzi* has a family of genes resembling the mucin genes of mammalian cells, *J. Biol. Chem.*, 270 (1995) 24146–24149.
86. J. M. Di Noia, I. D'Orso, L. Aslund, D. O. Sanchez, and A. C. C. Frasch, The *Trypanosoma cruzi* mucin family is transcribed from hundreds of genes having hypervariable regions, *J. Biol. Chem.*, 273 (1998) 10843–10850.
87. L. H. G. Freitas-Junior, M. R.S. Briones, and S. Schenkman, Two distinct groups of mucin-like genes are differentially expressed in the developmental stages of *Trypanosoma cruzi*, *Mol. Biochem. Parasitol.*, 93 (1998) 101–114.
88. C. A. Buscaglia, V. A. Campo, J. M. Di Noia, A. C. T. Torrecillas, C. R. De Marchi, M. A. J. Ferguson, A. C. C. Frasch, and I. C. Almeida, The surface coat of the mammal-dwelling infective trypomastigote stage of *Trypanosoma cruzi* is formed by highly diverse immunogenic mucins, *J. Biol. Chem.*, 279 (2004) 15860–15869.
89. S. Schenkman and M. Jiang, G.W. Hart and V. Nussenzweig. A novel cell surface trans-sialidase of *Trypanosoma cruzi* generates a stage-specific epitope required for invasion of mammalian cells, *Cell*, 65 (1991) 1117–1125.
90. J. M. Di Noia, C. A. Buscaglia, C. R. De Marchi, I. C. Almeida, and A. C. C. Frasch, A *Trypanosoma cruzi* small surface molecule provides the first immunological evidence that Chagas' Disease is due to a single parasite lineage, *J. Exp. Med.*, 195 (2002) 401–413.
91. R. P. Souto, O. Fernandes, A. M. Macedo, D. A. Campbell, and B. Zingales, DNA markers define two phylogenetic lineages of *Trypanosoma cruzi*, *Mol. Biochem. Parasitol.*, 83 (1996) 141–152.
92. B. Zingales, B. S. Stolf, R. P. Souto, O. Fernandes, and M. R. S. Briones, Epidemiology, biochemistry and evolution of *Trypanosoma cruzi* lineages based on ribosomal RNA sequences, *Mem. Inst. Oswaldo Cruz.*, 94(Suppl. 1), (1999) 159–164.
93. J. A. Atwood, III, *et al.*, The *Trypanosoma cruzi* proteome, *Science*, 309 (2005) 473–476.

94. J. A. Atwood, III, *et al.*, Glycoproteomics of *Trypanosoma cruzi* trypomastigotes using subcellular fractionation, lectin affinity, and stable isotope labeling, *J. Proteome Res.*, 5 (2006) 3376–3384.
95. C. L. Allen and J. M. Kelly, *Trypanosoma cruzi*: mucin pseudogenes organized in a tandem array, *Exp. Parasitol.*, 97 (2001) 173–177.
96. V. A. Campo, J. M. Di Noia, C. A. Buscaglia, F. Aguero, D. O. Sanchez, and A. C. C. Frasch, Differential accumulation of mutations localized in particular domains of the mucin genes expressed in the vertebrate host stage of *Trypanosoma cruzi*, *Mol. Biochem. Parasitol.*, 133 (2004) 81–91.
97. E. Tetaud, M. P. Barret, F. Bringaud, and T. Baltz, Kinetoplastid glucose transporters, *Biochem. J.*, 325 (1997) 569–580.
98. J. R. Roper and M. A. J. Ferguson, Cloning and characterisation of the UDP-glucose 4′-epimerase of *Trypanosoma cruzi*, *Mol. Biochem. Parasitol.*, 132 (2003) 47–53.
99. S. M. Beverley, K. L. Owens, M. Showalter, C. L. Griffith, T. L. Doering, V. C. Jones, and M. R. McNeil, Eukaryotic UDP-galactopyranose mutase (GLF gene) in microbial and metazoal pathogens, *Eukaryot. Cell*, 4 (2005) 1147–1154.
100. H. Bakker, B. Kleczka, R. Gerardy-Schahn, and F. H. Routier, Identification and partial characterization of two eukaryotic UDP-galactopyranose mutases, *Biol. Chem.*, 386 (2005) 657–661.
101. J. I. MacRae, S. O. Obado, D. C. Turnock, J. R. Roper, M. Kierans, J. M. Kelly, and M. A. J. Ferguson, The suppression of galactose metabolism in *Trypanosoma cruzi* epimastigotes causes changes in cell surface molecular architecture and cell morphology, *Mol. Biochem. Parasitol.*, 147 (2006) 126–136.
102. M. L. Salto, C. Gallo-Rodriguez, C. Lima, and R. M. de Lederkremer, Separation of Gal*fβ*1-XGlcNAc and Gal*pβ*-XGlcNAc (X = 3, 4, and 6) as the alditols by high-pH anion-exchange chromatography and thin-layer chromatography: characterization of mucins from *Trypanosoma cruzi*, *Anal. Biochem.*, 279 (2000) 79–84.
103. J. O. Previato, M. Sola-Penna, O. A. Agrellos, C. Jones, T. Oekmann, L. R. Travassos, and L. Mendonça-Previato, Biosynthesis of O-N-acetylglucosamine-linked glycans in *Trypanosoma cruzi*. Characterization of the novel uridine diphospho-N-acetylglucosamine:polypeptide N-acetylglucosaminyltransferase-catalyzing formation of N-acetylglucosamine α1-O-threonine, *J. Biol. Chem.*, 273 (1998) 14982–14988.
104. R. M. de Lederkremer and A. N. Confalonieri, Different pattern of glycoproteins with unusual *O*-linked oligosaccharides in two strains of *Trypanosoma cruzi* epimastigotes, *Ciencia e cultura.*, 46 (1994) 286–289.
105. J. O. Previato, C. Jones, L. B. P. Goncalves, R. Wait, L. R. Travassos, and L. Mendonça-Previato, *O*-Glycosidically linked *N*-acetylglucosamine-bound oligosaccharides from glycoproteins of *Trypanosoma cruzi*, *Biochem. J.*, 301 (1994) 151–159.
106. O. A. Agrellos, C. Jones, A. R. Todeschini, J. O. Previato, and L. Mendonça-Previato, A novel sialylated and galactofuranose-containing O-linked glycan, Neu5Acα-3Gal*pβ*-6(Gal*fβ*-4)GlcNAc, is expressed on the sialoglycoprotein of *Trypanosoma cruzi* Dm28c, *Mol. Biochem. Parasitol.*, 126 (2003) 93–96.
107. C. Jones, A. R. Todeschini, O. A. Agrellos, J. O. Previato, and L. Mendonça-Previato, Heterogeneity in the biosynthesis of mucin O-glycans from *Trypanosoma cruzi* tulahuen strain with the expression of novel galactofuranosyl-containing oligosaccharides, *Biochemistry*, 43 (2004) 11889–11897.
108. A. R. Todeschini, E. X. da Silveira, C. Jones, R. Wait, J. O. Previato, and L. Mendonça-Previato, Structure of O-glycosidically linked oligosaccharides from glycoproteins of *Trypanosoma cruzi* CL-Brener strain: evidence for the presence of O-linked sialyl-oligosaccharides, *Glycobiology*, 11 (2001) 47–55.
109. M. V. de Arruda, W. Colli, and B. Zingales, Terminal β-D-galactofuranosyl epitopes recognized by antibodies that inhibit *Trypanosoma cruzi* internalization into mammalian cells, *Eur. J. Biochem.*, 182 (1989) 413–421.

110. C. Gallo-Rodriguez, O. Varela, and R. M. de Lederkremer, First Synthesis of β-D-Gal*f*(1-4)GlcNAc, a Structural Unit Attached O-Glycosidically in Glycoproteins of *Trypanosoma cruzi*, *J. Org. Chem.*, 61 (1996) 1886–1889.
111. C. Gallo-Rodriguez, O. Varela, and R. M. de Lederkremer, One-pot synthesis of β-D-Gal*f*(1-4)[β-D-Gal*p*(1-6)]-D-GlcNAc, a 'core' trisaccharide linked O-glycosidically in glycoproteins of *Trypanosoma cruzi*, *Carbohydr. Res.*, 305 (1998) 163–170.
112. C. Gallo-Rodriguez, L. Gandolfi, and R. M. de Lederkremer, Synthesis of β-D-Gal*f*-(1-3)-D-GlcNAc by the trichloroacetamidate method and of β-D-Gal*f*-(1-6)-D-GlcNAc by $SnCl_4$-promoted glycosylation, *Org. Lett.*, 1 (1999) 245–247.
113. C. Gallo-Rodriguez, M. A. Gil-Libarona, V. M. Mendoza, and R. M. de Lederkremer, Synthesis of β-D-Gal*p*-(1-3)- β-D-Gal*p*(1-6)-[β-D-Gal*f*(1-4)]-D-GlcNAc, a tetrasaccharide component of mucins of *Trypanosoma cruzi*, *Tetrahedron*, 58 (2002) 9373–9380.
114. L. Gandolfi-Donadio, C. Gallo-Rodriguez, and R. M. de Lederkremer, Synthesis of α-D-Gal*p*(1-3)-β-D-Gal*f*(1-3)-D-Man, a terminal trisaccharide of Leishmania type-2 glycoinositolphospholipids, *J. Org. Chem.*, 67 (2002) 4430–4435.
115. V. M. Mendoza, C. Gallo-Rodriguez, and R. M. de Lederkremer, Syntheses of 2,3-di-*O*-(β-D-Galp)-D-Galp, a synthon for the mucin oligosaccharides of *Trypanosoma cruzi*, *Arkivoc*, (2003) 82–94.
116. R. R. Schmidt and K. H. Jung, Oligosaccharide synthesis with trichloroacetimidates, in S. Hanessian, (Ed.) *Preparative Carbohydrate Chemistry,* Marcel Dekker, Inc, New York, 1997, .
117. V. M. Mendoza, R. Agusti, C. Gallo-Rodriguez, and R. M. de Lederkremer, Synthesis of the *O*-linked pentasaccharide in glycoproteins of *Trypanosoma cruzi* and selective sialylation by recombinant *trans*-sialidase, *Carbohydr. Res.*, 341 (2006) 1488–1497.
118. V. A. Campo, I. Carvalho, S. Allman, B. G. Davis, and R. A. Field, Chemical and chemoenzymatic synthesis of glycosyl-amino acids and glycopeptides related to *Trypanosoma cruzi* mucins, *Org. Biomol. Chem.*, 5 (2007) 2645–2657.
119. R. Agusti, M. E. Giorgi, V. M. Mendoza, C. Gallo-Rodriguez, and R. M. de Lederkremer, Comparative rates of sialylation by recombinant *trans*-sialidase and inhibitor properties of synthetic oligosaccharides from *Trypanosoma cruzi* mucins-containing galactofuranose and galactopyranose, *Bioorg. Med. Chem.*, 15 (2007) 2611–2617.
120. I. C. Almeida, M. A. J. Ferguson, S. Schenkman, and L. R. Travassos, Lytic anti- α-galactosyl antibodies from patients with chronic Chagas' disease recognize novel *O*-linked oligosaccharides on mucin-like glycosylphosphatidylinositol-anchored glycoproteins of *Trypanosoma cruzi*, *Biochem J.*, 304 (1994) 793–802.
121. R. A. Mortara, S. da Silva, M. F. Araguth, S. A. Blanco, and N. Yoshida, Polymorphism of the 35- and 50-kilodalton surface glycoconjugates of *Trypanosoma cruzi* metacyclic trypomastigotes, *Infect. Immun.*, 60 (1992) 4673–4678.
122. N. Yoshida, R. A. Mortara, M. F. Araguth, J. C. Gonzalez, and M. Russo, Metacyclic neutralizing effect of monoclonal antibody 10D8 directed to the 35- and 50-kilodalton surface glycoconjugates of *Trypanosoma cruzi*, *Infect. Immun.*, 57 (1989) 1663–1667.
123. R. de C Ruiz, V. L. Rigoni, J. Gonzalez, and N. Yoshida, The 35/50 kDa surface antigen of *Trypanosoma cruzi* metacyclic trypomastigotes, an adhesion molecule involved in host cell invasion, *Parasite Immunol.*, 15 (1993) 121–125.
124. R. C. Ruiz, S. Jr. Favoreto, M. L. Dorta, M. E. Oshiro, A. T. Ferreira, P. M. Manque, and N. Yoshida, Infectivity of *Trypanosoma cruzi* strains is associated with differential expression of surface glycoproteins with differential Ca2+ signalling activity, *Biochem. J.*, 330 (1998) 505–511.
125. S. N. Moreno, J. Silva, A. E. Vercesi, and R. Docampo, Cytosolic-free calcium elevation in *Trypanosoma cruzi* is required for cell invasion, *J. Exp. Med.*, 180 (1994) 1535–1540.
126. C. W. Turner, M. F. Lima, and F. Villalta, *Trypanosoma cruzi* uses a 45-KDa mucin for adhesion to mammalian cells, *Biochem. Biophys. Res. Commun.*, 290 (2002) 29–34.

127. M. Chuenkova and M. E. S. Pereira, *Trypanosoma cruzi trans*-sialidase: enhancement of virulence in a murine model of Chagas' disease, *J. Exp. Med.*, 181 (1995) 1693–1703.
128. S. Tomlinson and J. Raper, Natural human immunity to trypanosomes, *Parasitol. Today*, 14 (1998) 354–359.
129. J. O. Previato, A. F. Andrade, M. C. Pessolani, and L. Mendonça-Previato, Incorporation of sialic acid into *Trypanosoma cruzi* macromolecules. A proposal for a new metabolic route, *Mol. Biochem. Parasitol.*, 16 (1985) 85–96.
130. B. Zingales, C. Carniol, R. M. de Lederkremer, and W. Colli, Direct sialic acid transfer from a protein donor to glycolipids of trypomastigote forms of *Trypanosoma cruzi*, *Mol. Biochem. Parasitol.*, 26 (1987) 135–144.
131. W. Colli, *Trans*-sialidase: a unique enzyme activity discovered in the protozoan *Trypanosoma cruzi*, *FASEB J.*, 7 (1993) 1257–1264.
132. G. A. Cross and G. B. Takle, The surface *trans*-sialidase family of *Trypanosoma cruzi*, *Annu. Rev. Microbiol.*, 47 (1993) 385–411.
133. S. Schenkman, D. Eichinger, M. E. S. Pereira, and V. Nussenzweig, Structural and functional properties of *Trypanosoma trans*-sialidase, *Annu. Rev. Microbiol.*, 48 (1994) 499–523.
134. F. Vandekerckhove, S. Schenkman, L. Pontes de Carvalho, S. Tomlinson, M. Kiso, M. Yoshida, A. Hasegawa, and V. Nussenzweig, Substrate specificity of the *Trypanosoma cruzi* trans-sialidase, *Glycobiology*, 2 (1992) 541–548.
135. M. A. Ferrero-Garcia, S. E. Trombetta, D. O. Sanchez, A. Reglero, A. C. C. Frasch, and A. J. Parodi, The action of *Trypanosoma cruzi* trans-sialidase on glycolipids and glycoproteins, *Eur. J. Biochem.*, 213 (1993) 765–771.
136. R. Agusti, M. E. Giorgi, and R. M. de Lederkremer, The *trans*-sialidase from *Trypanosoma cruzi* efficiently transfers alpha-(2-->3)-linked N-glycolylneuraminic acid to terminal beta-galactosyl units, *Carbohydr. Res.*, 342 (2007) 2465–2569.
137. A. Schroven, S. Meinke, P. Ziegelmuller, and J. Thiem, Transsialidase from *Trypanosoma cruzi* for regio- and stereoselective synthesis of N-acyl-modified sialylated oligosaccharides and measurement of transfer rates, *Chem. Eur. J.*, 13 (2007) 9012–9021.
138. A. J. Parodi, G. D. Pollevick, M. Mautner, A. Buschiazzo, D. O. Sanchez, and A. C. C. Frasch, Identification of the gene(s) coding for the *trans*-sialidase of *Trypanosoma cruzi*, *EMBO J.*, 11 (1992) 1705–1710.
139. J. L. Affranchino, C. F. Ibañez, A. O. Luquetti, A. Rassi, M. B. Reyes, R. A. Macina, L. Aslund, U. Pettersson, and A. C. C. Frasch, Identification of a *Trypanosoma cruzi* antigen that is shed during the acute phase of Chagas' disease, *Mol. Biochem. Parasitol.*, 34 (1989) 221–228.
140. M. B. Reyes, M. Lorca, P. Muñoz, and A. C. C. Frasch, Fetal IgG specificities against *Trypanosoma cruzi* antigens in infected newborns, *Proc. Natl. Acad. Sci. USA*, 87 (1990) 2846–2850.
141. M. L. Cremona, O. Campetella, D. O. Sanchez, and A. C. C. Frasch, Enzymically inactive members of the *trans*-sialidase family from *Trypanosoma cruzi* display beta-galactose binding activity, *Glycobiology*, 9 (1999) 581–587.
142. A. Buschiazzo, G. A. Tavares, O. Campetella, S. Spinelli, M. L. Cremona, G. Paris, M. F. Amaya, A. C. C. Frasch, and P. M. Alzari, Structural basis of sialyltransferase activity in *trypanosomal sialidases*, *EMBO J.*, 19 (2000) 16–24.
143. O. E. Campetella, A. K. Uttaro, A. J. Parodi, and A. C. C. Frasch, A recombinant *Trypanosoma cruzi* trans-sialidase lacking the amino acid repeats retains the enzymatic activity, *Mol. Biochem. Parasitol.*, 64 (1994) 337–340.
144. A. S. Couto, M. F. Goncalves, W. Colli, and R. M. de Lederkremer, The N-linked carbohydrate chain of the 85-kilodalton glycoprotein from *Trypanosoma cruzi* trypomastigotes contains sialyl, fucosyl and galactosyl (alpha 1-3)galactose units, *Mol. Biochem. Parasitol.*, 39 (1990) 101–107.

145. A. Buschiazzo, M. F. Amaya, M. L. Cremona, A. C. C. Frasch, and P. M. Alzari, The crystal structure and mode of action of trans-sialidase, a key enzyme in *Trypanosoma cruzi* pathogenesis, *Mol. Cell*, 10 (2002) 757–768.
146. M. F. Amaya, A. Buschiazzo, T. Nguyen, and P. M. Alzari, The high resolution structures of free and inhibitor-bound *Trypanosoma rangeli* sialidase and its comparison with *T. cruzi trans*-sialidase, *J. Mol. Biol.*, 325 (2003) 773–784.
147. M. F. Amaya, A. G. Watts, I. Damager, A. Wehenkel, T. Nguyen, A. Buschiazzo, G. Paris, A. C. C. Frasch, S. G. Withers, and P. M. Alzari, Structural insights into the catalytic mechanism of *Trypanosoma cruzi trans*-sialidase, *Structure*, 12 (2004) 775–784.
148. A. G. Watts, I. Damager, M. F. Amaya, A. Buschiazzo, P. Alzari, A. C. C. Frasch, and S. G. Withers, *Trypanosoma cruzi* Trans-sialidase operates through a covalent sialyl-enzyme intermediate: Tyrosine is the catalytic nucleophile, *J. Am. Chem. Soc.*, 125 (2003) 7532–7533.
149. S. Buchini, A. Buschiazzo, and S. G. Withers, A new generation of specific *Trypanosoma cruzi trans*-sialidase inhibitors, *Angew. Chem. Int. Ed.*, 47 (2008) 2700–2703.
150. J. Yang, S. Schenkman, and B. A. Horenstein, Primary 13C and beta-secondary 2H KIEs for trans-sialidase. A snapshot of nucleophilic participation during catálisis, *Biochemistry*, 39 (2000) 5902–5910.
151. M. L. Cremona, D. O. Sanchez, A. C. C. Frasch, and O. Campetella, A single tyrosine differentiates active and inactive *Trypanosoma cruzi* trans-sialidases, *Gene*, 160 (1995) 123–128.
152. A. R. Todeschini, W. B. Dias, M. F. Girard, J. M. Wieruszeski, L. Mendonça-Previato, and J. O. Previato, Enzymatically inactive *trans*-sialidase from *Trypanosoma cruzi* binds sialyl and beta-galactopyranosyl residues in a sequential ordered mechanism, *J. Biol. Chem.*, 279 (2004) 5323–5328.
153. R. Agusti, V. M. Mendoza, C. Gallo-Rodriguez, and R. M. de Lederkremer, Selective sialylation of 2,3-di-*O*-(β-D-galactopyranosyl)-D-galactose catalyzed by *Trypanosoma cruzi trans*-sialidase, *Tetrahedron: Asymmetry*, 16 (2005) 541–551.
154. S. Lee and B. H. Kim, *trans*-Sialidase catalyzed sialylation of beta-galactosyldisaccharide with an introduction of beta-galactosidase, *Enzyme Microb. Technol.*, 28 (2001) 161–167.
155. P. Scudder, J. P. Doom, M. Chenkova, I. D. Manger, and M. E. S. Pereira, Enzymatic characterization of beta-D-galactoside alpha 2,3-*trans*-sialidase from *Trypanosoma cruzi*, *J. Biol. Chem.*, 268 (1993) 9886–9891.
156. M. Ribeirao, V. L. Pereira-Chioccola, D. Eichinger, M. M. Rodrigues, and S. Schenkman, Temperature differences for *trans*-glycosylation and hydrolysis reaction reveal an acceptor binding site in the catalytic mechanism of *Trypanosoma cruzi trans*-sialidase, *Glycobiology*, 7 (1997) 1237–1246.
157. J. A. Harrison, K. P. Kartha, W. B. Turnbull, S. L. Scheuerl, J. H. Naismith, S. Schenkman, and R. A. Field, Hydrolase and sialyltransferase activities of *trypanosoma cruzi trans*-sialidase towards NeuAc-alpha-2,3-gal-Gal-beta-O-PNP, *Bioorg. Med. Chem. Lett.*, 11 (2001) 141–144.
158. A. Vetere and S. Paoletti, Complete synthesis of 3′-sialyl-N-acetyllactosamine by regioselective transglycosylation, *FEBS Lett.*, 399 (1996) 203–206.
159. A. Vetere, M. Miletich, M. Bosco, and S. Paoletti, Regiospecific glycosidase-assisted synthesis of lacto-N-biose I (Galβ1-3GlcNAc) and 3′-sialyl-lacto-N-biose I (NeuAcα2-3Galβ1-3GlcNAc), *Eur. J. Biochem.*, 267 (2000) 942–949.
160. S. Singh, M. Scigelova, M. L. Hallberg, O. W. Howarth, D. H. G. Crout, and S. Schenkman, Synthesis of sialyloligosaccharides using the *trans*-sialidase from *Trypanosoma cruzi*: novel branched and di-sialylated products from digalactoside acceptors, *Chem. Commun.*, 12 (2000) 1013–1014.
161. M. A. Probert, M. J. Milton, R. Harris, S. Schenkman, J. M. Brown, S. W. Homans, and R. A. Field, Chemoenzymatic synthesis of GM3, Lewis x and sialyl Lewis x oligosaccharides in ^{13}C-enriched form, *Tetrahedron Lett.*, 38 (1997) 5861–5864.

162. S. I. Nishimura, K. B. Lee, K. Matsuoka, and Y. C. Lee, Chemoenzymic preparation of a glycoconjugate polymer having a sialyloligosaccharide: Neu5Acα(2-3)Galβ (1-4)GlcNAc, *Biochem. Biophys. Res. Commun.*, 199 (1994) 249–254.
163. B. Neubacher, D. Schmidt, P. Ziegelmuller, and J. Thiem, Preparation of sialylated oligosaccharides employing recombinant trans-sialidase from *Trypanosoma cruzi*, *Org. Biomol. Chem.*, 3 (2005) 1551–1556.
164. B. Neubacher, S. Scheid, S. Kelm, A. C. C. Frasch, B. Meyer, and J. Thiem, Synthesis of Neu5Ac oligosaccharides and analogues by transglycosylation and their binding properties as ligands to MAG, *Chem Bio Chem.*, 7 (2006) 896–899.
165. L. Kroger, A. Scudlo, and J. Thiem, Subsequent enzymatic galactosylation and sialylation towards sialylated Thomsen-Friedenreich antigen components, *Adv. Synth. Catal.*, 348 (2006) 1217–1227.
166. K. B. Lee and Y. C. Lee, Transfer of modified sialic acids by *Trypanosoma cruzi trans*-sialidase for attachment of functional groups to oligosaccharide, *Anal. Biochem.*, 216 (1994) 358–364.
167. N. Takahashi, K. B. Lee, H. Nakagawa, Y. Tsukamoto, Y. Kawamura, and Y. C. Lee, Enzymatic sialylation of N-linked oligosaccharides using an alpha-(2,3)-specific *trans*-sialidase from *Trypanosoma cruzi*: structural identification using a three-dimensional elution mapping technique, *Anal. Biochem.*, 230 (1995) 333–342.
168. G. Paris, L. Ratier, M. F. Amaya, T. Nguyen, P. A. Alzari, and A. C. C. Frasch, A sialidase mutant displaying *trans*-sialidase activity, *J. Mol. Biol.*, 345 (2005) 923–934.
169. M. Engstler, R. Schauer, M. A. Ferrero-Garcia, A. J. Parodi, T. Storz-Eckerlin, A. Vasella, C. Witzig, and X. Zhu, N-(4-Nitrophenyl)oxamic Acid and Related N-Acylanilines Are Non-competitive Inhibitors of *vibrio cholerae* sialidase but do not inhibit *trypanosoma cruzi* or *trypanosoma brucei* trans-sialidases, *Helv. Chim. Acta.*, 77 (1994) 1166–1174.
170. H. Streicher and H. Busse, Building a successful structural motif into sialylmimetics-cyclohexenephosphonate monoesters as pseudo-sialosides with promising inhibitory properties, *Bioorg. Med. Chem.*, 14 (2006) 1047–1057.
171. M. A. Ferrero-Garcia, D. O. Sanchez, A. C. C. Frasch, and A. J. Parodi, The effect of pyridoxal 5′-phosphate and related compounds on *Trypanosoma cruzi* trans-sialidase, *An. Asoc. Quim. Argent*, 81 (1993) 127–132.
172. J. Neres, P. Bonnet, P. N. Edwards, P. L. Kotian, A. Buschiazzo, P. M. Alzari, R. A. Bryce, and K. T. Douglas, Benzoic acid and pyridine derivatives as inhibitors of *Trypanosoma cruzi trans*-sialidase, *Bioorg. Med. Chem.*, 15 (2007) 2106–2119; J. Neres, R. A. Bryce, and K. T. Douglas, Racional drug design in parasitology: *trans*-sialidase as a case of study for Chagas disease, *Drug. Discov. Today*, 13 (2008) 110–117.
173. R. Agusti, G. Paris, L. Ratier, A. C. C. Frasch, and R. M. de Lederkremer, Lactose derivatives are inhibitors of *Trypanosoma cruzi* trans-sialidase activity toward conventional substrates *in vitro* and *in vivo*, *Glycobiology*, 14 (2004) 659–670.
174. M. G. Risso, G. B. Garbarino, E. Mocetti, O. Campetella, S. M. Gonzalez Cappa, C. A. Buscaglia, and M. S. Leguizamon, Differential expression of a virulence factor, the *trans*-sialidase, by the main *Trypanosoma cruzi* phylogenetic lineages, *J. Infect. Dis.*, 189 (2004) 2250–2259.
175. M. S. Leguizamon, E. Mocetti, H. García Rivello, P. F. Argibay, and O. Campetella, *trans*-sialidase from *Trypanosoma cruzi* induces apoptosis in cells from the immune system *in vivo*, *J. Infect. Dis.*, 180 (1999) 1398–1402.
176. J. Mucci, A. Hidalgo, E. Mocetti, P. F. Argibay, M. S. Leguizamon, and O. Campetella, Thymocyte depletion in *Trypanosoma cruzi* infection is mediated by *trans*-sialidase-induced apoptosis on nurse cells complex, *Proc. Natl. Acad. Sci. USA*, 99 (2002) 3896–3901.
177. J. Mucci, M. G. Risso, M. S. Leguizamon, A. C. C. Frasch, and O. Campetella, The *trans*-sialidase from *Trypanosoma cruzi* triggers apoptosis by target cell sialylation, *Cell Microbiol.*, 8 (2006) 1086–1095.

178. M. S. Leguizamon, O. E. Campetella, S. M. Gonzalez-Cappa, and A. C. C. Frasch, Mice infected with *Trypanosoma cruzi* produce antibodies against the enzymatic domain of *trans*-sialidase that inhibit its activity, *Infect. Immun.*, 62 (1994) 3441–3446.
179. M. S. Leguizamon, O. Campetella, G. Russomando, M. Almiron, I. Guillen, S. M. Gonzalez Cappa, and A. C. C. Frasch, Antibodies inhibiting *Trypanosoma cruzi trans*-sialidase activity in sera from human infections, *J. Infect. Dis.*, 170 (1994) 1570–1574.
180. M. G. Risso, T. A. Pitcovsky, R. L. Caccuri, O. Campetella, and M. S. Leguizamon, Immune system pathogenesis is prevented by the neutralization of the systemic *trans*-sialidase from *Trypanosoma cruzi* during severe infections, *Parasitology*, 134 (2007) 503–510.
181. A. R. Todeschini, M. P. Nunes, R. S. Pires, M. F. Lopes, J. O. Previato, L. Mendonça-Previato, and G. A. DosReis, Costimulation of host T lymphocytes by a trypanosomal *trans*-sialidase: involvement of CD43 signaling, *J. Immunol.*, 168 (2002) 5192–5198.
182. W. B. Dias, F. D. Fajardo, A. V. Graça-Souza, L. Freire-de-lima, F. Vieira, M. F. Girard, B. Bouteille, J. O. Previato, L. Mendonça-Previato, and A. R. Todeschini, Endothelial cell signalling induced by *trans*-sialidase from *Trypanosoma cruzi*, *Cell. Microbiol.*, 10 (2008) 88–99.
183. C. A. Vercelli, A. M. Hidalgo, S. H. Hyon, and P. F. Argibay, *Trypanosoma cruzi trans*-sialidase inhibits human lymphocyte proliferation by nonapoptotic mechanisms: implications in pathogenesis and transplant immunology, *Transplant. Proc.*, 37 (2005) 4594–4597.
184. D. Snary, M. A. J. Ferguson, M. T. Scott, and A. K. Allen, Cell surface antigens of *Trypanosoma cruzi*: use of monoclonal antibodies to identify and isolate an epimastigote specific glycoprotein, *Mol. Biochem. Parasitol.*, 3 (1981) 343–356.
185. L. V. Kirchhoff and A. Sher, Modifications of a 72 k surface glycoprotein (GP-72) of *Trypanosoma cruzi* during development, *Fed. Proc.*, 44 (1985) 1332.
186. P. A. Haynes and G. A. Cross, Differential glycosylation of epitope-tagged glycoprotein Gp72 during the *Trypanosoma cruzi* life cycle, *Mol. Biochem. Parasitol.*, 83 (1996) 253–256.
187. P. A. Haynes, M. A. J. Ferguson, and G. A. Cross, Structural characterization of novel oligosaccharides of cell-surface glycoproteins of *Trypanosoma cruzi*, *Glycobiology*, 6 (1996) 869–878.
188. L. C. Miletti, K. Mariño, C. Marino, W. Colli, M. J. M. Alves, and R. M. de Lederkremer, Evidence for exo beta-D-galactofuranosidase in *Trypanosoma cruzi*, *Mol. Biochem. Parasitol.*, 127 (2003) 85–88.
189. R. Cooper, J. A. Inverso, M. Espinosa, N. F. Nogueira, and G. A. Cross, Characterization of a candidate gene for GP72, an insect stage-specific antigen of *Trypanosoma cruzi*, *Mol. Biochem. Parasitol.*, 49 (1991) 45–59.
190. R. Cooper, A. R. de Jesus, and G. A. Cross, Deletion of an immunodominant *Trypanosoma cruzi* surface glycoprotein disrupts flagellum-cell adhesion, *J. Cell Biol.*, 122 (1993) 149–156.
191. A. R. de Jesus, R. Cooper, M. Espinosa, J. E. Gomes, E. S. Garcia, S. Paul, and G. A. Cross, Gene deletion suggests a role for *Trypanosoma cruzi* surface glycoprotein GP72 in the insect and mammalian stages of the life cycle, *J. Cell Sci.*, 106 (1993) 1023–1033.

AUTHOR INDEX

Page numbers in roman type indicate that the listed author is cited on that page; page numbers in italic denote the page where the literature citation is given.

A

Abboud, J.-L. M., 104, *153*
Abe, H., 179, 199, *242*, *244*
Abraham, R. J., 18, 22–23, 26, *73–75*
Abronina, P. I., 177, 179, 210, *239*, 267, *302*
Abuin, G., 317, *357*
Achkar, J., 293, *308*
Acosta-Serrano, A., 315, 317–318, 321, 328, 331, 335, 352, *356–357*, *360*
Adachi, M., 208–209, 219, *245*
Adamo, R., 282–284, *304–305*
Adams, M. M., 177, *240*
Adamson, J., 62–63, *81*
Adcock, W., 104, *153*
Adibekian, A., 283–284, *305*
Adinolfi, M., 259, *301*
Affranchino, J. L., 336, *363*
Agocs, A., 210, *246*
Agrellos, O. A., 328, *361*
Aguero, F., 327, *361*
Agusti, R., 317, 333–334, 336, 341, 345, 349, *357*, *362–365*
Ako, T., 189, 220, *243*, *247*
Alabugin, I. V., 118, *155*
Alais, J., 286, 288, *307*
Alcázar, E., 118–119, *155*
Alkorta, I., 104, *153*
Allen, A. K., 352, *366*
Allen, C. L., 327, *361*
Allen, J. G., 186–187, *243*
Allen, J. R., 209–210, *245*
Allinger, N. L., 119, *155*
Allman, S., 333, *362*
Almeida, I. C., 317–319, 321, 324, 326–327, 335, *357–358*, *360*, *362*
Almiron, M., 352, *366*
Almond, A., 33, *77*
Altona, C., 23, 25–29, 31, 47–50, 71, *75–76*, *79*
Alves, M. J. M., 314–315, 317, 320–321, 337, 354, *356–357*, *359–360*, *366*
Alzari, P., 339, 348, *364*
Alzari, P. A., 345, *365*
Alzari, P. M., 113–114, *154*, 337–339, 348–349, *363–365*
Amaya, M. F., 337–339, 345, 348–349, *363–365*
Amyes, T. L., 84, 99, 104, *147*, *152–153*
Anderson, J. E., 118, *155*
Anderson, L., 179, *241*
Anderson, W. A., 19, *74*
Andersson, F. O., 163, 186, *236*
Ando, H., 121, *157*, 220, *247*
Andó, M. H., 312, *355*
Andrade, A. F., 336, *363*
Andrade, R. B., 169–170, 179, *239–240*, 280, *303*
Andre, C., 234, *250*
André, I., 130–131, *158*
Andrews, C. W., 97, 102, 120, *151–152*, *156*, 201, 203, *244*
Andrews, N. W., 318, 320, *357*
Andrews, T., 121, *156*
Anilkumar, G., 167, 199, 208, *238*, *245*
Anteunis, M. J. O., 36, *77*
Antony, J., 88, *150*
Antz, C., 72, *82*
Aoki, S., 179, *240*
Aoyama, Y., 210, *246*
Apon, J. V., 218, *246*

Araguth, M. F., 335, *362*
Arai, M. A., 254–255, *301*
Ardèvol, A., 113, *154*
Argibay, P. F., 352, *365–366*
Armesto, J., 316, *356*
Ashida, H., 321, *359*
Aslund, L., 324, 327, 336, *360*, *363*
Atkins, P., 71, *82*
Atwood III, J. A., 327, *360–361*
Augé, C., 228, 230, *248–249*
Aydin, R., 41–42, *78*
Azambuja, P., 318, *357*

B

Baasov, T., 120, *156*, 163, 201–202, 216–218, *236*, *244*
Babu, R. S., 254, 260–261, *302*
Backinowsky, L. V., 177, 179, 210, *239*, *246*, 267, 291, *302*, *308*
Baek, J. Y., 294, *309*
Baek, N. I., 282, *304*
Baer, H. H., 103, *153*
Baeschlin, D. K., 179–180, 199, 204–205, 219, *241*, *244*, *246*
Bahia, M. T., 312, *355*
Bai, Y., 177, 209, *240*
Bain, A. D., 113–114, *154*
Bajza, I., 283, *305*
Baker, J., 90, *150*
Bakinovskii, L. V., 284, *306*
Bakker, H., 328, *361*
Bakker, J. M., 85, *148*
Balacco, G., 25, *75*
Balan, N. F., 291, *308*
Balashova, T. L., 33, *77*
Baleux, F., 284, *305*
Ball, G. E., 39, *78*
Baltz, T., 328, *361*
Balza, F., 37, *77*
Banait, N. S., 84, *147*
Banerjee, A., 292–293, *308*
Banoub, J., 123, *157*
Barfield, M., 28, 32–33, 54–57, 65–69, 71–72, *76*, *80–82*
Barnabé, C., 312, *355*
Barone, G., 282, *304*
Barone, V., 63, *81*
Barrena, M. I., 199, *244*
Barresi, F., 286, *306*
Barret, M. P., 328, *361*
Barrows, S. E., 85, *148*
Bartolotti, L. J., 85, *148*
Basma, M., 87, *149*
Batta, G., 43, 45, *78*, 283, *305*
Bauer, J., 220, *247*, 283, *304*
Bax, A., 52, *79*
Beaulieu, C., 88, *149*
Becalski, A., 121, *156*
Becke, A. D., 89, *150*
Bedini, E., 282, 284, *304*, *306*
Béguin, C., 60, *80*
Béguin, P., 113–114, *154*
Behrendt, M., 287, *307*
Bellio, M., 319, *358*
Bélot, F., 284, *305*
Beneicke, W., 72, *82*
Bennet, A. J., 83, 135, *147*, *158*
Bento, C. A., 319, *358*
Bérces, A., 87–88, 90, 102, 104, 110, 112–114, 123, *149*, *151*, *154*, *157*, 166, *238*
Berger, S., 57–58, *80*
Bermejo, F., 31, *76*
Bermel. W., 29, *76*
Bernardi, F., 119, *155*
Bernstein, E. R., 88, *149*
Bernstein, H. J., 18, *73*
Bertello, L. E., 313, 318–320, *355*, *357–359*
Berti, P. J., 113–114, *154*
Bértoli, M., 312, *355*
Bertozzi, C. R., 165, *237–238*
Betaneli, V. I., 123, *158*
Beverley, S. M., 328, *361*
Bhacca, N. S., 23–24, *75*
Bhattacharyya, S., 219, *246*
Biarmés, X., 113, 131, *154, 158*
Bilodeau, M. T., 163, 184, *236*, *242*
Bindschadler, P., 177, 209, *240*

Birault, V., 179, *240*
Bishop, L., 252, *301*
Blanc-Muesser, M., 42–43, *78*
Blanco, S. A., 335, *362*
Blattner, R., 276, 278, *303*
Bleha, T., 166, *238*
Blériot, Y., 102, *152*
Bo, C., 118–119, *155*
Bochkov, A. F., 123, *158*
Bock, K., 19, 41, 62, 71, *74*, *78*, *80*, *82*
Boebel, T. A., 102, *152*
Boeggeman, E., 113–114, *154*
Bogusiak, J., 179, *242*
Böhm, M., 85, *149*
Bols, M., 85, 95, 110, 137, *148*, *151*, *153*, *159*, 205–206, *244–245*
Bommer, R., 175–176, *239*
Bondo, G., 51, 53–54, 57–58, *79–80*
Bondo, P. B., 51–54, 57–58, *80*
Bonnet, P., 348, *365*
Boons, G.-J., 99–100, 114–115, *151–152*, *154*, 163, 165, 177, 179, 188, 193–194, 203–204, 208–214, 220–221, *236–237*, *239*, *241, 243–247*, 283–284, 287, *305*, *307*
Booth, H., 24, 26, *75*
Bork, P., 321, *359*
Borodkin, V. S., 321, *360*
Bosco, M., 342, *364*
Bose, B., 53–54, 57–58, *80*
Bosma, W. B., 88, *149*
Bossa, M., 104, *153*
Bosse, F., 163, *236*
Bouteille, B., 352, *366*
Bowden, T., 100, *152*
Bowen, J. P., 97, 102, *151–152*
Bowers, A. A., 301, *309*
Bowers, S., 212–214, *246*
Braccini, I., 99, *151*, 287, *307*
Brady, J. W., 87, *149*
Brahimi, M., 104, *153*
Branderhorst, H. A., 220, *248*
Brass, A., 33, *77*
Bravo, F., 118–119, *155*
Brener, Z., 312, *355*
Breton, C., 87, *149*
Brignole, A., 71, *82*
Brimacombe, J. S., 319, 352, *358*
Bringaud, F., 328, *361*
Brinkmann, A., 21, *74*
Briones, M. R. S., 312, 324, 327, *355, 360*
Brisson, J. R., 282, *304*
Brooks, B. R., 89, *150*
Browin, P. N., 321, *360*
Brown, J. M., 343, *364*
Brown, J. R., 319, 352, *358*
Brown, R. C. D., 219, *247*
Bryce, R. A., 102, *152*, 348, *365*
Bublitz, R., 316, *356*
Buchini, S., 339, 348, *364*
Buckles, R. E., 121, *156*
Bullpitt, M., 64, *81*
Bülow, A., 137, *159*
Bundle, D. R., 123, *157*, 166–167, *238*, 284, 287–289, 291–292, *306–308*
Burant, J. C., 120, *155*
Burfitt, I., 55, 64, *80–81*
Burke, K., 89, *150*
Burkhart, F., 163, 218, *236*
Burton, D. R., 274, 287, *303*, *307*
Buscaglia, C. A., 322, 324, 326–327, 336, 350, *360–361*, *365*
Buschiazzo, A., 336–339, 343–345, 348–349, *363–365*
Bush, C. A., 52, *79*, 232–233, *249*
Buskas, T., 283–284, *305*
Busse, H., 346, *365*
Buxbaum, L. U., 320, *359*
Byramova, N. E., 284, *306*
Bystrov, V. F., 33, 47, 65, *77*, *79*, *81*

C

Caccuri, R. L., 352, *366*
Cai, Y., 301, *309*
Calarese, D. A., 274, *303*
Calgan, D., 87, *149*
Camargo, M. M., 317, 319, 321, 335, *357*
Campbell, D. A., 312, 327, *355*, *360*

Campestella, O. E., 317, 336–337, 339, 350, 352, *357*, *363–366*
Campo, V. A., 322, 324, 326–327, 333, 336, *360–361, 362*
Camus, D., 289, *307*
Canada, E. D., 55–56, *80*
Canivenc-Gansel, E., 320, *359*
Cao, S., 186, *243*
Carabellese, A., 282, *304*
Çarçabal, P., 85, *148*
Cardoso de Almeida, M. L., 318, *357*
Carleer, R., 36 *77*
Carlson, R., 283–284, *305*
Carmichael, I., 32, 34, 36, 38, 41, 43, 45, 51, 53–59, 71, *76–80*
Carneiro, C. M., 312, *355*
Carniol, C., 336, *363*
Carpenter, J. E., 120, *155*
Carreira, E. M., 291, *308*
Carreira, J. C., 315, *356*
Carrel, F. R., 228–229, *248*
Carvalho, I., 333, *362*
Carver, J. P., 89, 117, 130–131, 140, *150*, *155*, *158–159*
Casal, O. L., 314, 317, *356–357*
Casanueva, J., 31–32, *76*
Castagner, B., 167, 225–226, *238*, *248*
Castillón, S., 118–119, *155*, 199, *244*
Castro, A., 179, *242*
Casu, B., 19, *74*
Caulfield, T., 182, *242*
Cerda-Garcia-Rojas, C. M., 25, *75*
Chan, T. H., 276, *303*
Chan, T.-H., 293, *308*
Chandrasegaran, S., 61–62, *80*
Chandrasekera, N. S., 116–117, *155*
Chandrasekhar, J., 135, *158*
Chang, A. Y., 274, *303*
Chang, K. L., 165, *237*
Chaperon, A. R., 179–180, 199, 204–205, *241*, *244*
Charbonneau, V., 179–180, 199, 204–205, *241*
Charlon, C., 60, *80*
Chattopadhyaya, J., 50–51, 60–61, *79–80*
Chaudhuri, S. R., 177, 208–209, *240*, 268, *302*
Chęcińska, L., 85, *148*
Cheeseman, J. R., 120, *155*
Cheetham, N. W. H., 39, *78*
Chen, K.-H., 119, *155*
Chen, L., 121, *157*
Chen, X., 231–232, *249*
Chenault, H. K., 179, *242*
Cheng, Y., 275, *303*
Chenkova, M., 342, *364*
Cheon, H. S., 177, *240*, 272, *303*
Chevalier, R., 274, 292, *303*, *308*
Chiba, H., 199, *244*
Chipman, D. M., 43, *78*
Chokhawala, H., 231–232, *249*
Chowdhury, A. R., 177, *239*
Chuenkova, M., 336, *363*
Church, T., 51, *79*
Clary, D. C., 85, *148*
Clausen, M. H., 202, *244*
Clement, M.-J., 284, *306*
Cloran, F., 38, 41, 53–58, *78*, *80*
Cobas, J. C., 71, *82*
Codée, J. D. C., 121, *156*, 164, 179–180, 185, 228–229, *237, 241–242*, *248*, 286, 296, *306, 309*
Coe, D. M., 212–214, *246*
Colli, W., 314–315, 317–318, 320–322, 328, 336–337, 354, *356–363*, *366*
Colombel, J. F., 274, *303*
Colucci, W. J., 26–27, 71, *75*
Comegna, D., 282, *304*
Comely, A. C., 260, *302*
Compagnon, I., 85, *148*
Confalonieri, A. N., 328, *361*
Conn, S. A., 54–57, 68–69, *80*
Considine, J. L., 64, *81*
Constantino, M. G., 67–68, *81*
Contreras, R. H., 63, *81*
Conzelmann, A., 316, 320, *356*, *359*
Cooper, R., 354, *366*
Corminboeuf, C., 88, *150*

Correira de Almeida, I., 315, 321, 328, 335, *356*
Corte-Real, S., 319, *358*
Coskuner, O., 110, *154*
Costabel, M., 113–114, *154*
Costachel, C., 284, *305–306*
Cote, F., 193–194, *243*
Coura, J. R., 312, *355*
Couto, A. S., 317, 320, 337, *357*, *359*, *363*
Cox, K. J., 88, *149*
Coxon, B., 21–22, 33–34, 37–38, 45–46, 51, 55, 64–65, 68–69, *77–79*, *81*
Cramer, C. J., 85, *148*
Cremer, D., 90, *151*
Cremona, M. L., 336–339, 349, 352, *363–364*
Crich, D., 99–100, 104, 116–117, 121, *151–155*, *157*, 164, 177, 179, 185, 203, 220, *237*, *239*, *242*, *244*, *247*, 256, 275, 282, 284, 286–287, 289, 292–298, 301, *301*, *303–304*, *307–309*
Cross, G. A., 319, 336, 352–354, *358*, *363*, *366*
Crossman, A., 319, 352, *358*
Crout, D. H. G., 233–234, *249–250*, 342, *364*
Csizmadia, I. G., 85, 118, 131, *149*, *155*, *158*
Csonka, G. I., 88, *149*
Cumme, G. A., 316, *356*
Cutler, J. E., 292, *308*
Cyr, N., 37, *77*

D

da Silva, C. O., 84, *147*
da Silva, G. V. J., 67–68, *81*
da Silva, S., 335, *362*
da Silveira, E. X., 328, *361*
Daalmans, G. J., 31, *76*
Dai, Z., 121, *157*
Daikoku, S., 189, 220, *243*, *247*
Dalton, L., 18, *73*
Damager, I., 337, 339, 348, *364*
Damberg, C., 38, *78*
Dang, H. S., 301, *309*
Danishefsky, S. J., 68, *81*, 163, 167, 177, 184–185, 199, 209–210, 220, 222–223, *236*, *239*, *242*, *244–245*
Dapprich, S., 120, *155*
Dasgupta, P., 39, *78*
Davalos, J. Z., 104, *153*
David, S., 228, *248*, 286, 288, *307*
Davies, D. B., 37–38, 53, *77*
Davies, G. J., 83, 85, 112–114, *147*, *149*, *154*
Davis, B. G., 85, *148*, 165, *237–238*, 333, *362*
de Almeida, M. L., 317, 320–321, *357*, *359–360*
De Araújo, S. M., 312, *355*
de Arruda, M. V., 328, *361*
De Bie, M. J. A., 22, *74*
de C Ruiz, R., 335, *362*
De Castro, C., 282, *304*
de Haan, R., 31, *76*
de Jesus, A. R., 354, *366*
de Lana, M., 312, *355*
de Lederkremer, R. M., 313–322, 324, 328–329, 331, 334, 336–337, 341, 345, 349, 354, *355–366*
de Leeuw, F. A. A. M., 23–25, 28–29, 71, *75–76*
de Leeuw, H. P. M., 23–25, 71, *75*
De Marchi, C. R., 324, 326–327, *360*
De Meo, C., 179–181, 193, *240*, *242–243*
De Ornelas Toledo, M. J., 312, *355*
de Paula, J., 71, *82*
de Paz,J. L., 220, *247*
de Penhoat, C. H., 287, *307*
de Souza, W., 312–313, 318, *355*, *357*
Dean, K. E. S., 110, *153*
Debenham, J. S., 186, *243*
Dejter-Juszynski, M., 104, *153*
Delepierre, M., 284, *306*
Deleuze, M. S., 88, *150*
Demchenko, A., 99, *151*, 179, *241*
Demchenko, A. V., 114, 121, *154*, *156*, 165–166, 179–182, 191–196, 199–200, 202–204, 207–211,

216–217, 220, *237*, *240–245*, *248*, 286, 299, *306*
Denekamp, C., 102, *152*
Deng, J. K., 88, *150*
Deng, K., 177, *240*
Denisov, A. Y., 58, *80*
Dennis, R. J., 83, *147*
Depre, D., 172–173, *239*
Deretey, E., 85, *149*
Derouet, C., 99, *151*, 287, *307*
Deshmukh, M. M., 85, *148*
Deshpande, P. P., 184, *242*
Deslongchamps, P., 85, 102, 140, *148*, *152*, *159*
Dewar, M. J. S., 100, *152*
Di Noia, J. M., 316, 322, 324, 326–328, 334, 336, *357*, *360–361*
Dias, W. B., 320, 339, 352, *359*, *364*, *366*
Díez, E., 31–32, 71, *76*
Ding, N., 283, *304*
Dini, C., 286, 288, *307*
Dinkelaar, J., 167, *238*
Dion, M., 234, *250*
Dix, A., 319, 352, *358*
do Santos, Z. I., 87, *149*
Docampo, R., 318, 320, 335, *358*, *362*
Doddrell, D., 55, 64, *80–81*
Doering, T. L., 319, 328, *358*, *361*
Doi, T., 220, *248*
Dolle, R. E., 178, 182–183, *240*
Donders, L. A., 27–28, 31, 71, *76*
Dondoni, A., 220, *247*
Doom, J. P., 342, *364*
Dorland, L., 22, *74*
D'Orso, I., 322, 324, 327, *360*
Dorta, M. L., 335, *362*
Dory, Y. L., 85, 102, 140, *148*, *152*, *159*
DosReis, G. A., 318–319, 352, *358*, *366*
Dougherty, R. C., 100, *152*
Douglas, K. T., 348, *365*
Douglas, N. L., 120, *156*, 163, 201, 216, *236*, 252, *301*
Douglas, S. P., 84, 118, 131, *147*, *155*, *158*, 219, *247*
Driguez, H., 42–43, *78*
Dromer, F., 292, *308*
du Penhoat, C. H., 99, *151*
Du, Y., 121, *157*, 171–172, 208, *239*, *245*, 263–264, *302*
Ducros, V. M.-A., 112–114, *154*
Dudkin, V. Y., 116, *154*, 177, *239*, 296, *309*
Düffels, A., 172–173, *239*, 255–256, *301*
Duker, J. M., 51, *79*
Dulles, F. J., 85, *148*
Durette, P. L., 22, *74*
Durier, V., 42, *78*
Duron, S. G., 218, *246*
Duthaler, R. O., 179, *241*
Duus, J. Ø., 71, *82*
Dwek, R. A., 87, *149*, 274, *303*, 316, *356*

E

Eby, R., 103, *153*
Echarri, R., 199, *244*
Eckhardt, E., 179, *240–241*
Edén, M., 21, *74*
Edge, C. J., 87, *149*
Edward, J. T., 84, *147*
Edwards, P. N., 348, *365*
Eelkema, R., 260, *302*
Ei-Boubbou, K., 164, *236*
Eichinger, D., 336, 342, *363–364*
Eichler, E., 129, *158*
Eichlera, E. E., 280, *303*
Eisenhaber, B., 321, *359*
Eisenhaber, F., 321, *359*
Ekborg, G., 289, *307*
Eller, S., 208, *245*
El-Sayed, N. M., 312, 324, 327, 336, *355*
Endo, A., 177, *239*
Englund, P. T., 319, *358*
Engstler, M., 346, *365*
Ensley, H. A., 129, *158*
Eriksson, L., 21, *74*
Erkelens, C., 27, 47–50, *76*, *79*
Ernst, B., 286, *306*
Ernst, R R., 19, *74*

Esnault, J., 99, *151*, 274, 287, *303*, *307*
Espinosa, M., 354, *366*
Esposito, D., 167, *238*
Esteban, A. L., 31, *76*
Ewig, C. S., 87, *149*

F

Faehl, L. G., 57, *80*
Fairbanks, A. J., 85, *148*, 208, 210, *245*
Fairweather, J. K., 264, *302*
Fajardo, F. D., 352, *366*
Fan, H. F., 165, *237*
Favoreto, S. J., 335, *362*
Fehér, K., 45, *78*
Ferguson, J., 220, *248*
Ferguson, M. A. J., 314–315, 317–321, 324, 326, 328, 331, 335, 352–353, *355–358*, *360–361*, *362*, *366*
Feringa, B. L., 260, *302*
Fernandes, A. B., 312, *355*
Fernandes, O., 312, 327, *355*, *360*
Fernandez, J. M., 112, *154*
Ferreira, A. T., 335, *362*
Ferrero-Garcia, M. A., 336, 346, 348, *363*, *365*
Ferro, V., 264, *302*
Field, R. A., 52–53, *80*, 319, 333, 342–343, 352, *358*, *362*, *364*
Fielding, A. J., 301, *309*
Figueiredo, J. M., 320, *359*
Filippi, A., 104, *153*
Fischer, W., 316, *356*
Flieg, T., 88, *150*
Flowers, H. M., 104, *153*
Fokin, A. A., 88, *150*
Fonseca, G. C., 314–315, *356*
Foster, A. B., 62–63, *81*
Fournet, B., 22, *74*, 314, *356*
Fox, D. T., 234–235, *250*
Fradin, C., 289, *307*
Franchi, P., 301, *309*
Francke, R., 31, *76*
François, J.-P., 88, *150*
Frank, M., 62, *80*
Frasch, A. C. C., 316–317, 322, 324, 326–328, 334, 336–339, 343–345, 348–349, 352, *357*, *360–361*, *363–366*
Fraschetti, C., 104, *153*
Fraser, R. R., 34, *77*
Fraser-Reid, B., 87, 102, 120, *149*, *152*, *155–156*, 163, 167, 177, 179, 184–187, 198–199, 201, 203, 208–210, 219, *236*, *238–241*, *243–246*, 252, 264, 268, 286–287, 289, *301–302*, *306–307*
Fréchet, J. M. J., 103, *153*
Freire de Lima, C. G., 319, *358*
Freire-de-lima, L., 352, *366*
Freitas-Junior, L. H. G., 321, 324, *360*
French, A. D., 85, 118, *148*, *155*
Frenkiel, T. A., 37–38, 53, *77*
Fridman, M., 201, 216, *244*
Friedrich, A., 29, *76*
Friesen, R. W., 199, *244*
Frisch, M. J., 120, *155*
Fruchtel, J. S., 219, *247*
Frush, H. L., 121, *156*
Fügedi, P., 179, *240–241*
Fujimoto, Y., 103, *153*
Fujita, S., 177, *239*
Fujiwara, S., 233, *249*
Fukase, K., 103, *153*, 209, 219, *245*
Fukuda, S., 118, *155*
Fulse, D. B., 294, *309*
Funasaka, S., 199, *244*
Furneaux, R. H., 276, 278, *303*

G

Gadre, S. R., 85, *148*
Gaffney, P. R. J., 118, *155*
Gajdoŝ J., 42, *78*
Galli, C., 317, *357*
Gallo-Rodriguez, C., 328–329, 331, 334, 341, *361–362*, *364*
Gambert, U., 230, 232–233, *249*
Gamblin, D. P., 85, *148*
Gandolfi, L., 329, *362*
Gandolfi-Donadio, L., 331, *362*

Gandour, R. D., 26–27, 71, *75*
Gangadharmath, U. B., 193–194, *243*
Garbaccio, R. M., 163, 167, *236*
Garbarino, G. B., 350, *365*
Garcia, B. A., 99, *151*, 179, *242*
Garcia, E. S., 318, 354, *357*, *366*
Garcia, M., 219, *246*
García Rivello, H., 352, *365*
Garegg, P. J., 100, 123, *152*, *157*, 167, 179, 210, *238*, *240–241*, *245*, 293, *308*
Garg, N., 318, *358*
Gastaldi, S., 121, *157*
Gatti, G., 23, 26, *75*
Gauffeny, F., 179, *242*
Gautheron, C., 228, *248*
Gavrilov, Y. D., 47, *79*
Gazzinelli, R. T., 317, 319, 321, 335, *357–358*
Gemma, E., 258, *301*
Gening, M. L., 177, *239*
Genre-Grandpierre, A., 102, *152*
Gerardy-Schahn, R., 328, *361*
Gerbst, A. G., 84, 114, *147*, *154*
Gervay, J., 165, *237*
Gervay-Hague, J., 165, 220, *237*, 269–272, *302*
Gerwick, W. H., 45, *78*
Geurtsen, R., 99, *151*, 193–194, *243*
Geyer, K., 228–229, *248*
Geyer, M., 72, *82*
Ghiasi, M., 32, 39, 40, 42–43, *76*
Gilbert, H. J., 113–114, *154*
Gilbert, M. B., 167, 199, *238*
Gildersleeve, J. C., 99, *151*
Gil-Libarona, M. A., 331, *362*
Gin, D. Y., 99, 102, *151–152*, 165, 177, 179, 237, *240*, *242*, 282, *303*
Giorgi, M. E., 334, 336, 341, 345, *362–363*
Girard, M. F., 339, 352, *364*, *366*
Glendening, E. D., 120, *155*
Gloster, T. M., 112, *154*
Glottin-Fleury, A., 234, *250*
Goerler, A., 72, *82*
Golgher, D. B., 315, 318, *356*
Gomes, J. E., 318, 354, *357*, *366*
Gomes, M. L., 312, *355*
Gomes, N. A., 318, *358*
Gomez, A. M., 185, 193, 208, 210, 219, *243*, *245–246*
Gonçalves, L. B. P., 317, 328, *357*, *361*
Gonçalves, M. F., 315, 317, 320, 337, *356*, *359*, *363*
Gonzalez, J. C., 335, *362*
Gonzalez, M. S., 318, *357*
Gonzalez-Cappa, S. M., 350, 352, *365–366*
Gonzalez-Outeiriño, J., 87, 118, *149*, *155*
Goodman, L., 166, *238*
Goodnow, R., 179, *241*
Gorin, P. A., 314, *356*
Goto, K., 227, *248*
Goto, T., 179, *242*
Gouvion, C., 42, *78*
Govil, G., 34, *77*
Gowda, C., 266, *302*
Graça-Souza, A. V., 352, *366*
Grachev, A. A., 84, 114, *147*, *154*, 177, 179, 210, *239*, 267, *302*
Grathwohl, M., 222, 224, *248*, 280, *303*
Green, L. G., 163, 172–173, 179–180, 199, 204–205, 219, *236*, *239*, *241*, *244*, *246*, 255–256, *301*
Greig, I. R., 83, *147*
Grice, P., 203, 216, *244*, *246*, 252–254, *301*
Gridley, J. J., 286, *306*
Griesinger, C., 49–50, *79*
Griffith, C. L., 328, *361*
Grimme, S., 88, 120, *150*, *156*
Groesbeek, M., 27, *76*
Grützmacher, H.-F., 102, *152*
Grutzner, J. B., 55, *80*
Gu, G., 171–172, 208, *239*, *245*, 264, *302*
Guérin, D. M. A., 113–114, *154*
Guerreiro, C., 284, *305*
Guillamon-Martin, A., 185, 193, *243*
Guilleme, J., 31–32, 71, *76*
Guillen, I., 352, *366*

Gundel, G., 208, *245*
Günther, H., 41–42, *78*
Guo, H., 232–233, *249*, 281, *306*
Guo, Z., 177, *239*, 252, 278–279, *301*, *303*
Güther, M. L., 317, 319, 352, *357–358*
Guvench, O., 88, *150*

H

Haase, W. C., 219, *247*
Haasnoot, C. A. G., 23–26, 47–50, 71, *75*, *79*
Hadad, C. M., 40–41, *78*
Hadd, M. J., 165, *237*
Hagler, A. T., 87, *149*
Hahn, M. G., 193–194, 204–205, 219, *243–244*, *246*
Hajgató, B., 88, *150*
Halcomb, R. L., 184, 228, *242*, *248*
Haldar, P., 188–189, *243*
Hall, L. D., 18, 60, 62–65, *73–74*, *80–81*
Hallberg, M. L., 342, *364*
Hamana, H., 293, *308*
Hamer, G. K., 37, *77*
Hamman, S., 60, *80*
Hammer, C. F., 61–62, *80*
Hammond, E., 264, *302*
Hamza, A., 88, *150*
Han, X. W., 283, *305*
Hanashima, S., 167, 220, *238*, *247*
Handlon, A. L., 120, *156*
Hanessian, S., 179, *241*, 263, 301, *302*, *309*
Hang, H. C., 165, *237*
Hannappel, E., 316, *356*
Hao, W., 130, *158*
Hara, O., 184–185, *242*
Harada, T., 179, 216, *240*
Harris, R., 52–53, *80*, 343, *364*
Harrison, J. A., 342, *364*
Hart, G. W., 286, *306*, 319, 324, 336, *358*, *360*
Hasegawa, A., 336, *363*
Hashihayata, T., 177, *239*
Hashimoto, S. I., 199, *244*
Hassel, O., 93, *151*
Hastings, J. J., 233, *249*
Hatakeyama, S., 282, *303*
Hättig, C., 88, *150*
Havenith, M., 85, *148*
Haynes, P. A., 352–353, *366*
Hazen, K. C., 289, *307*
He, H., 121, *157*
Hederos, M., 321–322, *359*
Heeschen, J. P., 18, *73*
Heeten, R., 179, 185, *241*
Hehre, E. J., 228, 230, 233, *249*
Heidecke, C. D., 208, 210, *245*
Hein, M., 62, *80*
Heise, N., 313, 318, 320–321, *355*, *357*, *359–360*
Heitmann, J. A., 64, *81*
Hekmat, O., 234–235, *250*
Hendrickson, J. B., 90, *151*
Hendriks, K. B., 104, *153*
Heng, L. S., 263, *302*
Heo, C. K., 121, *156*
Hermkens, P. H. H., 219, *247*
Hernandez-Mateo, F., 186, *243*
Hernández-Torres, J., 293, *308*
Hertz, B., 53–54, 57–59, *80*
Heume, M., 179, *240*
Hewitt, M. C., 225, *248*, 283, *304*
Hidalgo, A., 352, *365*
Hidalgo, A. M., 352, *366*
Hilbers, C. W., 50, *79*
Hillier, I. H., 102, *152*
Hindsgaul, O., 209, 231, *245*, *249*, 286, *306*
Hinklin, R. J., 188, *243*
Hino, J., 321, *359*
Hinzen, B., 219, *246*
Hirose, Y., 227, *248*
Hiroshi, T., 219, *246*
Hirsch, J., 102, *152*
Hodosi, G., 121, *157*
Holmes, D., 193, *243*
Homans, S. W., 52–53, *80*, 314–316, 320, 343, *355–356*, *364*
Honda, T., 199, *244*
Hong, Y., 321, *359*
Höög, C., 38–39, *78*, 284, *305*

Horenstein, B. A., 339, *364*
Horn, A., 316, *356*
Horton, D., 22, *74*
Hosie, L., 140, *159*
Hossain, L. H., 296, *309*
Houdier, S., 103, *153*
Hough, L., 18, 64, *73*, *81*
Houseknecht, J. B., 40–41, *78*
Howarth, O. W., 342, *364*
Hricovíni, M., 19, 37–39, 53, *74*, *77*, 89, *150*
Hsu, M. C., 258–259, *301*
Hu, H., 188–189, *243*
Hu, S., 163, *236*
Hua, Y., 208, *245*
Huang, C.-Y., 218, *246*, 274, *303*
Huang, L., 121, *156*, 164, 185, 188, 218, *236*
Huang, X., 121, *156*, 164, 185, 188, 218, *236*, 276, *303*
Huang, Y. R., 88, *150*
Huang, Y. W., 165, *237*
Huggins, M. L., 27, *75*
Hui, Y. Z., 283, *305*
Hull, W. E., 29, *76*
Hultberg, H., 293, *308*
Hünenberger, P. H., 87, *149*
Hung, S.-C., 121, *156*, 165, 237, 293, 308
Hünig, I., 85, *148*
Hutton, T. K., 116, *154*, 297, *309*
Huynh, H. K., 179, *241*
Hwang, M.-J., 87, *149*
Hyon, S. H., 352, *366*

I

Iadonisi, A., 259, *301*
Ibañez, C. F., 336, *363*
Ichikawa, Y., 228, *248*
Igarashi, K., 166–167, *238*
Iida, M., 177, *239*
Ikeda, T., 208–209, 219, *245*
Ikegai, K., 177, *239*
Ikegami, S., 199, *244*
Im, H.-S., 88, *149*
Imagawa, H., 282, *303*
Imai, K., 29–31, *76*
Imamura, A., 121, *157*
Imanaka, T., 233, *249*
Imberty, A., 87, 102, *149*, *152*, 284, *306*
Immel, S., 287–288, *307*
Improvisi, L., 292, *308*
Inazu, T., 227, *248*
Ince, S. J., 204–205, 219, *244*, *246*
Inoue, H., 220, *248*
Inoue, N., 321, *359*
Inoue, Y., 118, *155*
Inverso, J. A., 354, *366*
Ionescu, A. R., 89–90, 98, 112, 118, 135, *150–151*, *154–155*
Ippel, J. H., 27, 31, *76*
Isbell, H. S., 121, *156*
Ishida, H., 121, *157*, 227, *248*
Ishii, K., 177, *240*
Ishiwata, A., 167, *238*, 254–255, *301*
Iskrić, S., 99, *152*
Isles, S., 163, 188, *236*
Isobe, M., 179, *242*
Ito, H., 184–185, *242*
Ito, T., 64, *81*
Ito, Y., 163, 167, 173–174, 177, 188–191, 220, *236*, *238–240*, *243*, *247*, 254–255, 286, *301*, *306*
Ivanov, V. T., 33, *77*
Iversen, T., 291, *308*

J

James, K., 104, *153*
Jansen, A., 312, *355*
Jaradat, D. M. M., 85, *148*
Jayalath, P., 116, 121, *154*, *157*, 177, *239*, 297–298, *309*
Jayaprakash, K. N., 120, *156*, 177, 208–210, 219, *239*, *245*, 268, *302*
Jeanloz, R. W., 289, *307*
Jeanneau, C., 87, *149*
Jeffrey, G. A., 85, *148*
Jencks, W. P., 84, *147*
Jennings, H. J., 69, *81*, 282–283, *304*

Jensen, H. H., 85, 95, 110, *148*, *151*, *153*, 205–206, *244–245*
Jensen, K. F., 228, *248*
Jensen, K. J., 116–117, *155*
Jeon, H. B., 294, *309*
Jeyaraman, R., 184, *242*
Jhunjhunwala, M., 228, *248*
Jia, Q., 231–232, *249*
Jiang, L., 276, 293, *303*, *308*
Jiang, M., 324, 336, *360*
Jochims, J. C., 68, *81*
Jockusch, R. A., 85, *148*
Joe, M., 177, 209, *240*
Johansson, R., 293, *308*
Johnson, G. P., 118, *155*
Johnson, R. N., 62–63, *81*
Johnston, B. D., 284, *305*, 321, *360*
Jona, H., 177, *239*
Jones, C., 313, 315, 317, 328, *355–357*, *361*
Jones, D. L., 60, *80*
Jones, V. C., 328, *361*
Jonke, S., 220, *247*
Jorgensen, W. L., 135, *158*
Joseph-Nathan, P., 25, *75*
Joshi, S., 167, 199, *238*
Jouault, T., 289, 292, *307–308*
Juaristi, E., 90, *151*
Jung, G., 219, *247*
Jung, K. H., 167, *238*, 331, *362*
Jungk, S. J., 26–27, 71, *75*

K

Kaeothip, S., 192, *243*
Kahne, D., 165, 179, 212, 218–219, *238*, *241*, 275, *303*
Kajimoto, T., 228, *248*
Kalbitzer, H. R., 72, *82*
Kamat, M. N., 179–181, 199, 202–204, 220, *240*, *242*, *244*, *248*
Kamerling, J. P., 167–168, *238*
Kan, Y., 282, *303*
Kanemitsu, T., 165, 220, *237*
Kaneno, D., 104, *153*
Kangawa, K., 321, *359*
Kanie, O., 163, 165, 188–191, 220, *236–237*, *243*, *247*
Kanie, Y., 189, 220, *243*
Kannenberg, E., 283–284, *305*
Kantner, T., 234–235, *250*
Karpel, R., 231–232, *249*
Karplus, M., 18–20, 22, 32–33, *73–74*, *76*
Kartha, K. P., 342, *364*
Kataoka, H., 182, *242*
Kato, R., 189, 220, *243*, *247*
Katopodis, A., 179, *241*
Kattner, R., 57, *80*
Katzin, A. M., 317, 336–337, *357*
Kaufman, M., 34, *77*
Kawamura, K., 102, *152*
Kawamura, Y., 344, *365*
Keding, S. J., 177, *239*
Kelly, J. M., 327–328, *361*
Kelm, S., 343–344, *365*
Kessler, H., 29, *76*
Khan, S. H., 286, *306*
Khan, T. H., 219, *247*
Khatuntseva, E. A., 114, *154*
Khot, V., 115, *154*
Kierans, M., 328, *361*
Kiessling, L. L., 188, *243*
Kim, B. H., 316, 342, *356*, *364*
Kim, H. J., 260, *302*
Kim, H. M., 184, *242*
Kim, J. H., 165, 188, 190, *237*, *243*
Kim, J.-W., 115, *154*
Kim, K. S., 188, 190, *243*, 294, *309*
Kim, Y. W., 234–235, *250*
Kimura, A., 121, *157*
Kinbara, A., 220, *248*
King-Morris, M. J., 52, *79*
Kinoshita, T., 321, *359*
Kinzy, W., 175–176, 179, *239*, *241*
Kirby, A. J., 110, *153*, 228, *248*
Kirchhoff, L. V., 352, *366*
Kirschner, K. N., 85, 87, *148–149*
Kishi, Y., 177, *240*, 258–259, 272, *301*, *303*
Kiso, M., 121, *157*, 179, *241*, 336, *363*
Kitagawa, I., 282, *304*

Kitajima, T., 169, 171, 173, *239*
Kitching, W., 64, *81*
Kitos, T. E., 83, *147*
Kitov, P. I., 210, *246*
Kiyota, K., 199, *244*
Kjellberg, A., 38, *78*
Klares, U., 287–288, *307*
Kleczka, B., 328, *361*
Klein, R. A., 85, *148*
Kleinpeter, E., 118, *155*
Klepach, T., 59, *80*
Klimov, E. M., 98, 121, *151*, *157*, 179, *241*
Knak Jensen, S. J., 85, *149*
Knecht, S., 88, *150*
Knerr, L., 280, *303*
Knippenberg, S., 88, *150*
Koća, J., 87, *149*
Koch, A., 118, *155*
Koch, H. J., 42, *78*
Kochetkov, N. K., 84, 98, 121, 123, *147*, *151*, *157–158*, 177, 179, 210, *239*, *241*, *246*, 267, 284, 291, *302*, *306*, *308*
Kodukula, K., 321, *359*
Koeller, K. M., 165, 228, 231, *237–238*, *249*
Komarov, I. V., 110, *153*
Komori, M., 118, *155*
Kondo, H., 179, *240*
Kondo, T., 179, *242*
Kong, F. Z., 121, 123, *157–158*, 257, 263–264, 282–284, *301–302*, *304–306*
Konradsson, P., 100, 123, *152*, *157*, 198, *243–244*, 321–322, *359*
Korogi, S., 121, *157*
Kotian, P. L., 348, *365*
Koto, S., 169, 178, 182, *239*
Kováč, P., 282–284, *304–305*
Kovacik, V., 102, *152*
Kovacs, L., 283, *304*
Kövér, K. E., 43, 45, *78*
Kozmon, S., 131, *158*
Krack, G., 29, *76*
Kraehmer, R., 167, 199, *238*
Kren, V., 228, 230, 232–233, *248*
Krepinsky, J. J., 87, 118, 121, 131, 140, *149*, *155*, *157–159*, 219, *247*
Kroemer, R. T., 85, *148*
Kroger, L., 343, *365*
Kubota, M., 118, *155*
Kuivila, H. G., 64, *81*
Kulkarni, S. S., 121, *156*, 165, *237*
Kullnig, R. K., 18, *73*
Kumazawa, T., 182, *242*
Kuniaki, T., 286, *306*
Kunz, H., 165, *237*
Kurihara, Y., 88, *149*
Kurimoto, M., 118, *155*
Kurtkaya, S., 63, *81*
Kusumoto, S., 103, *153*
Kutschker, W., 299–300, *309*
Kuttel, M., 87, *149*
Kvarnström, I., 123, *157*
Kveder, S., 99, *152*
Kwon, O., 68, *81*
Kwon, Y. U., 177, *239*

L

Laaksonen ,A., 68, *81*
Lacerda Jr., V., 67–68, *81*
Lahmann, M., 176, 178, 197, *239*, *243*, 258, *301*
Laine, R. A., 118, *155*
Laio, A., 113, *154*
Lam, S. N., 165, 220, *237*, 269–272, *302*
Lamzin, V., 113–114, *154*
Langer, L., 316, *356*
Lankhorst, P. P., 47–50, *79*
Larsen, K., 116–117, *155*
Larsson, E. A., 68, *81*
Lascombe, M. B., 113–114, *154*
Lassaletta, J., 163, *236*
Lau, R., 291, *308*
Laurent, I., 284, *305*
Lavaitte, S., 42–43, *78*
Le Narvor, C., 230, *249*
Leal, S., 319, *358*
Lee, B.-Y., 294, *309*
Lee, C., 260, *302*

Lee, C. C., 165, *237*

Lee, C.-H., 64, *81*

Lee, H.-K., 218, *246*, 274, *303*

Lee, J., 258–259, *301*

Lee, J. C., 165, 218, *237*, *246*

Lee, J. K., 113–114, *154*

Lee, K. B., 343–344, *365*

Lee, S., 342, *364*

Lee, Y. C., 343–344, *365*

Lee, Y. J., 188, 190, *243*

Leguizamon, M. S., 316, 324, 328, 334, 350, 352, *357*, *365–366*

Leimkuhler, C., 165, *238*

Lemanski, G., 291, *308*

Lemieux, R. U., 18, 36, *73*, *77*, 90, 104, 121, *150*, *153*, 287, *307*

Lenz, J. W., 18, *73*

Lenz, R., 172–173, *239*

Leontein, K., 179, *240*

Leopold, K., 316, *356*

Leslie, R., 203, *244*

Letellier, M., 163, 186, *236*

Levitt, M. H., 21, *74*

Ley, S. V., 120, *156*, 163, 172–173, 179–180, 199, 201, 203–205, 216, 219, *236*, *239*, *241*, *244*, *246*, 252–256, 282, *301*, *304*

Li, H. M., 112, 121, *154*, *157*, 203, 232–233, *244*, *249*, 289, 292, 294–295, *307–309*

Li, S., 102, 140, *152*, *159*

Li, W., 294–295, *309*

Li, Y., 283, *304*

Li, Z., 99, *151*

Lian, Y., 177, *240*, 272, *303*

Lichtenthaler, F. W., 287–288, 291, *307–308*

Lii, J.-H., 119, *155*

Lima, C., 314–316, 320, 324, 328, 334, *355–357*, *361*

Lima, M. F., 335, *362*

Lin, S., 232–233, *249*

Lin, X., 135, *158*

Lindberg, B., 289, *307*

Ling, C.-C., 292, *308*

Linhardt, R. J., 208, *245*

Lins, R. D., 87, *149*

Liptàk, A., 283, *305*

Liskamp, R. A. J., 220, *248*

Litjens, R. E. J. N., 121, *156*, 164, 179, 185, *237*, *241*, 286, *306*

Liu, B., 85, *148*

Liu, K.-G., 220, *247*

Liu, X. Y., 177, *239*, 264, 283, *302*, *304*

Liu, Y.-H., 121, *156*

Live, D., 184, *242*

Livingston, P. O., 163, 184, *236*, *242*

Lkboa, C. V., 312, *355*

Loftus, P., 26, *75*

Lönn, H., 178–179, *240*

Lönngren, J., 289, *307*

Lopes, M. F., 352, *366*

Lopez, J. C., 177, 185, 193, 208–210, 219, *239*, *243*, *245–246*

Lorca, M., 336, *363*

Lou, B., 179, *241*

Love, K. R., 169–170, *239*

Lowary, T. L., 40–41, *78*, 165, 177, 209, *237*, *240*

Lu, J., 120, *156*, 167, 177, 209–210, *238–239*, 266, *302*

Lu, L. D., 165, *237*

Lü, M., 121, *157*

Lu, W., 165, *238*

Lu, Y., 232–233, *249*

Lubineau, A., 230, *249*

Lucas, T. J., 103, *152*

Lucero, C. G., 85, *148*

Lucking, U., 120, *156*, 163, 179–180, 199, 201, 204–205, 216, *236*, *241*, 252, *301*

Ludewig, M., 276, 278, *303*

Luger, P., 85, *148*

Lundt, I., 19, *74*

Luo, S. Y., 165, *237*, 293, *308*

Luquetti, A. O., 336, *363*

Luthman, H., 21, *74*

Luu-Duc, C., 60, *80*

M

Ma, Z. C., 263, 283, *302*, *305*
Maas, A. A. M., 167–168, *238*
Macauley, M. S., 83, *147*
Macedo, A. M., 327, *360*
Mach, M., 120, *156*, 289, *307*
Mach, P., 85, *149*
Machado-Coelho, G. L. L., 312, *355*
Macina, R. A., 336, *363*
MacKerell Jr., A. D., 88–89, *150*
Macleod, N. A., 85, *148*
MacRae, J. I., 315, 318, 328, 352, *356*, *361*
MacRae, J. L., 314, 316, *355*
Madsen, R., 104, 120, *153*, *155*, 167, 179, 184–186, 198–199, 202–203, *238*, *241*, *244*
Maeda, Y., 321, *359*
Magnus, V., 99, *152*
Magnusson, B. G., 219, *246*
Majumdar, D., 220, *247*, 287, *307*
Makarova, Z. G., 121, *157*
Malleron, A., 286, 288, *307*
Mallet, A., 289, *307*
Mallet, J.-M., 99, *151*, 274, 287, 289, 292, *303*, *307–308*
Maloisel, J. L., 100, *152*, 210, *245*
Malysheva, N. N., 98, 121, *151*, *157*, 179, *240–241*
Mamatyuk, V. I., 58, *80*
Manabe, S., 177, 220, *240*, *247*
Manger, I. D., 342, *364*
Mangia, R. H., 312, *355*
Manoharan, M., 118, *155*
Manque, P. M., 335, *362*
Manthorpe, J. M., 291, *308*
Manville, J. F., 65, *81*
Marcaurelle, L. A., 163, 165, *236*, *238*
Marchand, A. P., 28, *76*
Marchand, N. W., 28, *76*
Marino, C., 354, *366*
Marino, J. P., 49–50, *79*
Mariño, K., 354, *366*
Maroušek, V., 103, *152*
Márquez, B. L., 45, *78*
Marra, A., 179, 220, *242*, *247*
Marshall, J. L., 28, 54–57, 68–69, *76*, *80*
Marshall, P. J., 140, *159*
Marszalek, P. E., 112, *154*
Martin, N. F., 321–322, *360*
Martin-Lomas, M., 220, *247*
Marx, D., 110, *154*
Marzabadi, C., 220, *248*
Marzabadi, C. H., 118, *155*
Massi, A., 220, *247*
Masterson, W. J., 319, *358*
Mathew, F., 289, *307*
Matoba, N., 121, *156*, 219, *246*
Matsumoto, H., 227, *248*
Matsumoto, K., 102, *152*
Matsuo, I., 173–174, *239*
Matsuoka, K., 343, *365*
Mattes, R., 234, *250*
Mautner, M., 336, 343–345, *363*
Max, D., 52, *79*
Mazeau, K., 42–43, *78*
Mazurek, 314, *356*
McCall, D. A., 121, *156*
McCarter, J. D., 121, *156*
McClure, K. F., 185, 220, 222–223, *242*
McDevitt, R. E., 198, *244*
McIntosh, L. P., 234–235, *250*
McLauchlan, K. A., 18, 69, *73*, *81*
McNeil, M. R., 328, *361*
McNulty, J., 301, *309*
Meah, M. Y., 131, *158*
Mebs, S., 85, *148*
Mehlert, A., 315, 317–319, 321, 328, 331, 335, 352, *356–357*
Mehta, A. S., 283–284, *305*
Mehta, S., 179–181, *241*
Meier, R. J., 110, *153*
Meijer, G., 85, *148*
Meinke, S., 336, 343–345, *363*
Melean, L. G., 280, *303*
Melo, M. B., 319, *358*
Meloncelli, P., 112, *154*
Men, H., 260, *302*
Mendonca, A., 118, *155*

Mendonça-Previato, L., 314–315, 317–320, 328, 336, 339, 352, *356–359*, *361*, *363–364*, *366*
Mendoza, V. M., 331, 333–334, 341, *362*, *364*
Menon, A. K., 319–320, *358*
Mensa-Wilmot, K., 318, *358*
Merritt, J. R., 120, *155–156*, 179, 184–186, 198–199, *241*, 264, *302*
Messick, J., 68, *81*
Metz, T., 291, *308*
Meyer, B., 343–344, *365*
Meyer, T., 137, *159*
Meyer zu Reckendorf, W. M., 68, *81*
Mezzato, S., 208, *245*
Michalik, M., 62, *80*
Michon, V., 99, *151*, 287, *307*
Miiller, D. E., 55–57, 68–69, *80*
Miletich, M., 342, *364*
Miletti, L. C., 354, *366*
Miljković, M., 85, *148*
Millam, J. M., 120, *155*
Miller, A. D., 255–256, *301*
Miller, J. S., 177, *239*
Milne, K. G., 319, 352, *358*
Milton, M. J., 52–53, *80*, 343, *364*
Minelli, L. M., 318, *358*
Minnaard, A. J., 260, *302*
Mino, Y., 184–185, *242*
Miura, N., 88, *149*
Miura, T., 227, *248*
Mobli, M., 33, *77*
Mocetti, E., 350, 352, *365*
Mohr, M., 102, *152*
Moir, R. Y., 18, *73*
Molas, P., 118–119, *155*
Momany, F. A., 88, *149*
Monde, K., 88, *149*
Mong, T. K.-K., 218, *246*
Montgomery Jr., J. A., 120, *155*
Montreuil, J., 22, *74*
Moolten, F. L., 131, *158*
Mooren, M. M. W., 50, *79*
Mootoo, D. R., 198, *243–244*
Moran, D., 89, *150*
Morand, P., 34, *77*
Moreno, S. N., 318, 320, 335, *358*, *362*
Morier, C. L., 88, *149*
Morikuni, E., 282, *303*
Morissette, D. G., 284, *306*
Morita, Y. S., 319, 321, *358–359*
Morpurgo, G. O., 104, *153*
Morpurgo, S., 104, *153*
Morrice, N. A., 315, 318–319, 352, *356*, *358*
Mortara, R. A., 312, 318, 321, 335, *355*, *358*, *360*, *362*
Mucci, J., 352, *365*
Mukaiyama, T., 167, 177, 179, 199, *238–239*, *242*, *244*
Mulard, L. A., 284, *305–306*
Müller, P., 104, *153*
Mulloy, B., 37–38, 53, *77*
Munemura, Y., 167, *238*
Muñoz, P., 336, *363*
Muraoka, O., 121, *157*
Murphy, E. R., 228, *248*
Murray, R. W., 184, *242*
Murshudov, G. N., 113–114, *154*
Murty, C. V. S. R., 177, 208–209, *240*, 268, *302*
Mydock, L. K., 207, *245*
Mynott, R. J., 64, *81*

N

Nacario, R. C., 177, 209, *240*
Nagabhushan, T. L., *77*
Nagamune, K., 321, *359*
Naidoo, K. J., 87, *149*
Nair, L. G., 208, *245*
Naisang, E., 264, *302*
Naismith, J. H., 342, *364*
Nakagawa, H., 344, *365*
Nakahara, Y., 220, *247*
Nakamura, S. I., 199, *244*
Nakano, J., 254–255, *301*
Nakayama, H., 87, *149*
Namchuk, M. N., 121, *156*

Nandakumar, M. V., 208, *245*
Navarro-Vázquez, A., 71, *82*
Neidig, K.-P., 72, *82*
Nepogodiev, S. A., 177, 179, 210, *239*, 267, *302*
Neres, J., 348, *365*
Neubacher, B., 343–344, *365*
Newth, F. H., 85, *148*
Nguyen, H. M., 282, *303*
Nguyen, T., 337, 339, 345, *364–365*
Ni, X., 87, *149*
Nicolaou, K. C., 163, 167, 178, 182–183, *236*, *240*, *242*
Nieto, J., 131, *158*
Nifantiev, N. E., 84, 114, *147*, *154*, 177, *239*
Nikolaev, A. V., 286, *306*, 321, *360*
Nilsson, K. G. I., 234, *249*
Nilsson, M., 179, *240*
Nilsson, U. J., 219, *246*
Ning, J., 121, *157*, 257, 263, 284, *301–302*, *305*
Nishida, T., 38, *78*
Nishimura, S. I., 88, *149*, 343, *365*
Nishizawa, M., 282, *303*
Nisole, A., 234, *250*
Nitz, M., 166–167, *238*, 287–288, 292, *307–308*
Nogueira, N. F., 318, 354, *357*, *366*
Nohara, L. L., 318, *357*
Nokami, T., 167, *238*
Norberg, T., 123, *157*, 179, *240*
Nordstrøm, L. U., 95, 110, *151*, *153*, 205–206, *244–245*
Novara, F. R., 104, *153*
Nukada, T., 87–90, 94, 97–98, 102, 104, 110, 112, 116, 123, 135, *149–151*, *153–154*, *157*, 166, 169, 171, 173, *238–239*, 262, *302*
Numata, M., 177, *239*
Nunes, M. P., 319, 352, *358*, *366*
Nunomura, S., 177, *239*
Nurnberger, H., 179, *240*
Nusair, M., 89, *150*
Nussenzweig, V., 318, 324, 336, *358*, *360*, *363*

O

Obado, S. O., 328, *361*
Oberhauser, A. F., 112, *154*
Oberli, M. A., 177, 209, *240*
Obuchowska, A., 87, *149*
O'Doherty, G. A., 254, 260–261, 281, *302*, *306*
Oehrlein, R., 179, *241*
Oekmann, T., 328, *361*
Ogawa, T., 163, 169, 171, 173, 177, 188–191, 220, *236*, *239*, *243*, 262, *302*
Ohashi, K., 282, *304*
Ohishi, K., 321, *359*
Ohmae, M., 227, *248*
Ohnishi, Y., 286, *306*
Ohrlein, R., 231, *249*
Ohta, H., 254–255, *301*
Ohtsuka, I., 189, 220, *243*, *247*
Ojeda, R., 220, *247*
Oku, K., 118, *155*
Ollman, I. R., 120, *156*
Ollmann, I. R., 163, 201–202, 216–218, *236*
Olszewski, T. K., 137, *159*
O'Neill, R. A., 286, *306*
Orlean, P., 319–320, *358*
Ōsawa, E., 29–31, *76*
Osborn, H. M. I., 219, *247*, 252–254, 286, *301*, *306*
Oscarson, S., 167, 176, 178–179, 197, 210, *238–241*, *243*, *245*, 258, 269, *301*, *303*
Oshima, K., 210, *246*
Oshiro, M. E., 335, *362*
Ott, A. Y., 121, *157*
Ottar, B., 93, *151*
Ottenheijm, H. C. J., 219, *247*
Otter, A., 231, *249*, 292, *308*
Ottosson, H., 120, *155*, 163, 179, 184–186, 198–199, *236*, *241*
Ovchinnikov, Y. A., 33, *77*

Overkleeft, H. S., 121, *156*, 164, 167, 179, 185, *237–238*, *241–242*, 286, *306*
Owens, K. L., 328, *361*

P

Pachler, K. G. R., 23–24, *74–75*
Packard, G. K., 291, *308*
Padrta, P., 72, *82*
Pai, C. L., 165, *237*
Palcic, M. M., 231, *249*
Palmacci, E. R., 165, 179, 220, 224, *237*, *240*, *247*, 283, *304*
Pan, Q., 34, 36, 43, 45 *77*
Pang, H. Y. S., 131, *158*
Pánková, M., 121, *156*
Paoletti, S., 342, *364*
Papahatjis, D. P., 178, 182–183, *240*
Pápai, I., 88, *150*
Paris, G., 337, 339, 345, 349, *363–365*
Park, J., 165, 188, 190, *237*, *243*
Park, T. K., 163, 184, *236*, *242*
Parker, V. D., 130, *158*
Parlato, M. C., 220, *248*
Parodi, A. J., 317, 328, 336–337, 343–346, 348, *357*, *363*, *365*
Parrilli, M., 282, 284, *304*, *306*
Parrinello, M., 113, *154*
Pastor, R. W., 89, *150*
Pastore, A., 259, *301*
Patel, M., 287, *307*
Pathlak, A. K., 228, *248*, 279, *303*
Pathlak, V., 228, *248*, 279, *303*
Paul, B., 36, *77*
Paul, S., 354, *366*
Pauling, L., 27, *76*
Paulsen, H., 84, 120–121, *147*, *155*, *157*, 169, 171, 173, 179, 189, *239–240*, *243*, 299–300, *309*
Peçanha, L. M., 319, *358*
Pedersen, C. M., 19, 41, 62, *74*, *78*, *80*, 110, *153*, 206, *245*
Penner, G. H., 88, *149*
Peralta, J. E., 63, *81*
Peranovich, T. M., 320, *359*
Perdew, J. P., 89, *150*
Pereira, M. E. S., 317, 336, 342, *357*, *363–364*
Pereira-Chioccola, V. L., 315, 321, 328, 335, 342, *356*, *364*
Perlin, A. S., 19, 37, 42, *74*, *77–78*
Perst, H., 102, *152*
Pessolani, M. C., 336, *363*
Petráková, E., 37–39, 53, *77*
Pettersson, U., 336, *363*
Phalipon, A., 284, *305*
Phillips, D. L., 135, *158*
Phillips, G. O., 85, *148*
Phillips, L., 23, *75*
Piacenza, M., 120, *156*
Pier, G. B., 177, *239*
Pieters, R. J., 220, *248*
Pietruszka, J., 216, *246*, 252–254, *301*
Pinto, B. M., 179–181, *241*, 284, *305–306*, 321, *360*
Pires, R. S., 352, *366*
Pitcovsky, T. A., 352, *366*
Pittet, M., 320, *359*
Planas, A., 113, 131, *154*, *158*
Plante, O. J., 165, 179, 220, 224, *237*, *240*, *248*, 268–269, 280, 283, *302–304*
Plavec, J., 50–51, 60–61, *79–80*
Plessas, N. R., 263, 301, *302*, *309*
Podlasek, C. A., 43, *78*
Polat, T., 218, *246*
Pollevick, G. D., 316, 324, 328, 334, 336, 343–345, *357*, *363*
Pontes de Carvalho, L., 336, *363*
Poole, J. L., 179, *242*, 282, *303*
Pople, J. A., 90, *151*
Poppe, L., 34, *77*
Pornsuriyasak, P., 179, 182, 191–196, 199–200, 216–217, *240–241*, *243–244*
Portnova, S. L., 33, *77*
Postan, M., 318, *358*
Pougny, J.-R., 287, *307*
Poulain, D., 274, 289, 292, *303*, *307–308*
Pozsgay, V., 38, *78*, 282–283, 286, *304*, *306*
Pratt, M. R., 165, *238*

Previato, J. O., 313–315, 317–320, 328, 336, 339, 352, *355–359*, *361*, *363–364*, *366*

Previato, L. M., 313, *355*

Priepke, H. W. M., 216, *246*, 252–254, 282, *301*, *304*

Probert, M. A., 52–53, *80*, 343, *364*

Procopio, D. O., 317, 319, 321, 335, *357*

Puoti, A., 320, *359*

Purse, B. W., 287, *307*

Q

Qasba, P. K., 113–114, *154*

Qian, X., 231, *249*

Quinn, C. P., 283–284, *305*

Quintanilla, E., 104, *153*

R

Raab, M., 131, *158*

Rabiller, C., 234, *250*

Rademacher, T. W., 316, *356*

Rademann, J., 220, *247*, 280, 283, *303–304*

Radhakrishnan, K. V., 208, *245*

Raghavan, S., 179, 212, 218–219, *241*

Ragupathi, G., 184, *242*

Ramakrishnan, B., 113–114, *154*

Ramalho-Pinto, F. J., 318, *358*

Ramey, K. C., 68, *81*

Ramirez, M. I., 314–315, 320, *355–356*

Randall, J. L., 178, 182–183, *240*

Randell, K. D., 321, *360*

Randolph, J. T., 163, 185, 220, 222–223, *236*, *242*

Rao, C. S., 120, *155*, 179, 184–186, 198–199, *241*

Rao, Y., 177, *239*

Raper, J., 320, 336, *359*, *363*

Rassi, A., 336, *363*

Ratcliffe, A. J., 198, *244*, 287, *307*

Ratcliffe, R. M., 287, *307*

Rath, N. P., 192–196, *243*

Ratier, L., 345, 349, *365*

Ratner, D. M., 228, *248*, 268–269, *302*

Ravidà, A., 283, *304*

Reddy, G. V., 179, *241*

Reed, A. E., 120, *155*

Reed, Y., 283–284, *305*

Rees, D., 219, *247*

Reggiori, F., 316, 320, *356*, *359*

Reglero, A., 336, *363*

Reimer, K. B., 284, *306*

Reinhold, V. N., 319, *358*

Renkonen, O., 230, *249*

Reyes, M. B., 336, *363*

Reynolds, R. C., 45–46, *79*

Rheingold, A. L., 292, 294, *308*

Rhind-Tutt, A. J., 100, *152*

Ribeirao, M., 342, *364*

Richard, J. P., 99–100, 104, 121, *152–153*, *156*

Richards, G. F., 64, *81*

Richardson, J., 317, 328, 331, *357*

Rigoni, V. L., 335, *362*

Rising, T. W. D. F., 208, 210, *245*

Risso, M. G., 350, 352, *365–366*

Rittner, R., 67–68, *81*

Robb, M. A., 120, *155*

Robert, R., 292, *308*

Roberts, B. P., 301, *309*

Roberts, C., 120, *155*, 179, 184–186, 198–199, *241*

Roberts, W. L., 316, 319, *356*, *358*

Rochon, A. C., 301, *309*

Rodebaugh, R., 186, *243*

Rodrigues, M. M., 315, 317, 321, 328, 335, 342, *356–357*, *364*

Röhle, G., 99, *151*

Rokob, T. A., 88, *150*

Rolla, N., 118, *155*

Roper, J. R., 328, *361*

Rosen, G., 179, *241*

Rosenberry, T. L., 316, 319, *356*, *358*

Rossier, J.-C., 104, *153*

Rotondo, A., 284, *305*

Roussel, F., 280, *303*

Rousson, E., 114, *154*

Routier, F. H., 328, *361*

Rovira, C., 113, 131, *154*, *158*
Roy, R., 163, 186, *236*, *243*
Rudd, P. M., 274, *303*
Ruiz, R. C., 335, *362*
Rundlöf, H., 85, *149*
Rundlöf, T., 38, *78*
Russo, M., 335, *362*
Russomando, G., 352, *366*
Ruzicka, C. J., 140, *159*
Rychnovsky, S. D., 291, *308*
Ryu, K., 232–233, *249*

S

Saffrich, R., 72, *82*
Saile, E., 283–284, *305*
Sakagami, M., 282, 293, *304*, *308*
Sakamoto, H., 199, *244*
Saksena, R., 282–284, *304–305*
Sakurai, M., 118, *155*
Salpin, J.-Y., 85, *148*
Salto, M. L., 316, 318, 320, 324, 328, 334, *357–358*, *361*
Samoshina, N. F., 123, *158*
Samuelsson, B., 293, *308*
Sanchez, D. O., 322, 324, 327, 336, 339, 343–345, 348, 352, *360–361*, *363–365*
Sandlers, Y., 102, *152*
Sandor, P., 38, *78*
San-Fabián, J., 31–32, 63, 71, *76*, *81*
Sansonetti, P. J., 284, *306*
Santikarn, S., 319, *358*
Sardina, F. J., 71, *82*
Sari, N., 38, *78*
Sarma, R. H., 64, *81*
Sato, K., 286, 288, *306*
Sato, T., 87, *149*
Satoh, A., 227, *248*
Scanlan, C. N., 274, *303*
Schaefer, T., 88, *149*
Schauer, R., 346, *365*
Scheid, S., 343–344, *365*
Schenkman, S., 315, 317, 321, 324, 328, 331, 335–336, 339, 342–343, *356–357*, *360*, *362*, *364*
Scheuerl, S. L., 342, *364*
Schiattarella, M., 179–180, *242*, 282, *304*
Schlegel, H. B., 119, 120, *155*
Schlueter, U., 120, *156*
Schmidt, D., 343, *365*
Schmidt, R. R., 116–117, *155*, 163, 167, 175–176, 208, 220, 222, 224, *236*, *238–239*, *245*, *247–248*, 280, 287, *303*, *307*, 331, *362*
Schmidt, T., 202–203, *244*
Schmidt, T. H., 104, *153*
Schneider, W. G., 18, *73*
Schneider-Adams, T., 287–288, *307*
Schnupf, U., 88, *149*
Schramm, V. L., 83, *147*
Schreiner, P. R., 88, *150*
Schroeder, L. R., 64, *81*, 121, *157*
Schroven, A., 336, 343–345, *363*
Schuberth, R., 208, *245*
Schuerch, C., 103, *152–153*, 291, *308*
Schüle, G., 291, *308*
Schultz, M., 165, *237*
Schut, B. L., 22, *74*
Schüttpelz, E., 121, *157*
Schwaneberg, U., 291, *308*
Schweizer, F., 209, *245*
Scigelova, M., 233–234, *249–250*, 342, *364*
Scott, M. T., 352, *366*
Screen, J., 85, *148*
Scudder, P., 342, *364*
Scudlo, A., 343, *365*
Scuseria, G. E., 120, *155*
Sealy, J., 129, *158*
Sears, P., 220, *247*
Sebastian, R., 88, *149*
Secor, H. V., 88, *149*
Seeberger, P. H., 163, 165, 167, 169–170, 177, 179, 209, 219–220, 224–226, 228–229, *236–240*, *247–248*, 264, 268–269, 280, 283–284, 296, *302–305*, *309*
Seeman, J. I., 88, *149*
Segre, A. L., 28, *76*
Seifert, J., 208, *245*

Sendid, B., 274, 292, *303*, *308*

Serianni, A. S., 32, 34, 36, 38, 41, 43, 45, 51–52, 55–56, 58–59, 71, *76–80*

Seto, N. O. L., 231, *249*

Shaban, M. A. E., 289, *307*

Shao, J., 232–233, *249*

Sharma, D. K., 319, 352, *358*

Shashkov, A. S., 84, *147*, 177, 179, 210, *239*, 267, 291, *302*, *308*

Sheehan, J. K., 33, *77*

Shen, J., 232–233, *249*

Shenoy, S. R., 85, 110, *148*, *153*

Sher, A., 352, *366*

Shibuya, H., 282, *304*

Shie, C. R., 293, *308*

Showalter, M., 328, *361*

Sigurskjold, B. W., 71, *82*

Silva, J., 335, *362*

Silva, L. S., 317, 319, 321, 335, *357*

Silvanis, B. A., 179, *241*

Simons, J. P., 85, *148*

Sinaÿ, P., 99, *151*, 179, *242*, 286–287, 289, *306–307*

Singh, S., 233–234, *249–250*, 342, *364*

Sinnott, M. L., 83, 135, 140, *147*, *158–159*

Sipos, G., 320, *359*

Siriwardena, A., 177, *239*

Siuzdak, G., 218, *246*

Sklenář, V., 72, *82*

Skowronski, E., 201, 203, *244*

Skylaris, C.-K., 85, *148*

Sládkovićová, M., 85, *149*

Slaghek, T. M., 167–168, *238*

Smith, D. M., 85, *148*

Smith, M., 179, 220, *242*, *247*

Smith, S. F., 135, *158*

Smith, T. K., 319, 352, *358*

Smith, W. B., 71–72, *82*

Smits, T. M., 301, *309*

Smoot, J. T., 199–200, *244*

Smrćok, L., 85, *149*

Šnajdrová, L., 87, *149*

Snary, D., 352, *366*

Snoek, L. C., 85, *148*

Snyder, D. A., 225, 228, *248*

Snyder, J. P., 63, *81*, 186, *243*

Soares, M. P., 319, *358*

Sola-Penna, M., 328, *361*

Solkan, V. N., 47, *79*

Solomon, D., 201, 216, *244*

Sommer, R. D., 292, 294, *308*

Song, G., 283, *304*

Sorensen, T. S., 104, *153*

Souchon, H., 113–114, *154*

Souto, R. P., 312, 327, *355*, *360*

Souto-Padrón, T., 315, 317–318, 321, 328, 335, *356–357*

Spangenberg, P., 234, *250*

Spear, R. J., 69, *81*

Speranza, M., 104, *153*

Spijker, N. M., 120, *156*

Spik, G., 22, *74*

Spinelli, S., 337, *363*

Sprott, G. D., 280, *303*

Srivastava, V. K., 291, *308*

Stanca-Kaposta, E. C., 85, *148*

Stauch, T., 99–100, *151–152*

Stenutz, R., 32, 53–54, 57–59, 70–71, *76*, *80*, *82*

Stepanyants, A. U., 65, *81*

Sternhell, S., 64, 68–69, *81–82*

Stick, R. V., 104, 112, *153–154*, 179, *242*

Stine, K. J., 220, *248*

Stocker, B. L., 264, *302*

Stoddart, J. F., 90, *151*, 177, 179, 210, *239*, 267, *302*

Stolf, B. S., 312, 327, *355*, *360*

Stoll, D., 113–114, *154*

Storz-Eckerlin, T., 346, *365*

Stratmann, R. E., 120, *155*

Strecker, G., 22, *74*

Streefkerk, D. G., 22, *74*

Streicher, H., 346, *365*

Streiff, M. B., 179, *241*

Stubba, B., 179–180, *242*

Stubbs, J. M., 110, *154*

Stubbs, K. A., 83, *147*

Sturdy, Y. K., 85, *148*

Suga, S., 102, *152*
Sugimoto, M., 169, 171, 173, 177, *239*
Sujino, K., 231, *249*
Sun, S., 99, 104, *151*, 256, 275, 286, 292, *301*, *303*
Sundara, S., 87, *149*
Sundaralingam, M., 25, *75*
Sundgren, A., 176, 178, *239*
Suzuki, S., 102, *152*
Svensson, S. C. T., 123, *157*
Szabó, L., 113–114, *154*
Szarek, W. A., 301, *309*
Szeja, W., 179, *242*
Szpilman, A. M., 291, *308*
Szurmai, Z., 287–288, *307*

T

Tachibana, Y., 233, *249*
Taddei, F., 118, *155*
Tafazzoli, M., 32, 39, 40, 42–43, *76*
Tafuri, W. L., 312, *355*
Taigel, G., 68, *81*
Takagi, M., 233, *249*
Takaha, T., 233, *249*
Takahashi, N., 344, *365*
Takahashi, T., 121, *156*, 179, 208–209, 216, 219–220, *240*, *245–246*, *248*
Takai, Y., 286, 288, *306*
Takatani, M., 254–255, *301*
Takeuchi, K., 177, 179, *239*, *242*
Takimoto, H., 121, *156*
Takle, G. B., 336, *363*
Talbot, F. O., 85, *148*
Tamura, T., 179, *242*
Tanabe, G., 121, *157*
Tanaka, C. T., 314, *356*
Tanaka, H., 121, *156*, 208–209, 219, *245*
Tanaka, S. E., 113–114, *154*
Tang, T.-H., 85, 118, 131, *149*, *155*, *158*
Taniguchi, T., 88, *149*
Taravel, F. R., 19, 42–43, *74*, *78*, 117, *155*
Tarleton, R. L., 318, *358*
Tasic, L., 67–68, *81*
Tatami, A., 173–174, *239*
Tatsuta, K., 166, *238*, 252, *301*
Tavares, G. A., 337, *363*
Taylor, C. M., 179, *241*
Taylor, E. J., 83, *147*
Tellier, C., 102, *152*, 234, *250*
Terenti, O., 220, *247*
Terinek, M., 121, *156*
Tetaud, E., 328, *361*
Teumelsan, N., 276, *303*
Thibaudeau, C., 59–61, *80*
Thiem, J., 228, 230, 232–233, *248–249*, 252, 286, *301*, *306*, 336, 343–345, *363*, *365*
Thobhani, S., 87, *149*
Thölmann, D., 102, *152*
Thomas, W. A., 26, *75*
Thomas-Oates, J., 314–315, 320, *355*
Tibayrenc, M., 312, *355*
Tichý, M., 121, *156*
Tidén, A.-K., 269, *303*
Tilbrook, D. M. G., 179, *242*
Timell, T. E., 135, *159*
Tkachev, A. V., 58, *80*
Tocher, D. A., 118, *155*
Todaro, L. J., 118, *155*
Todeschini, A. R., 313, 328, 339, 352, *355*, *361*, *364*, *366*
Toepfer, A., 287, *307*
Tokimoto, H., 103, *153*
Tomlinson, S., 336, *363*
Tomoda, S., 104, *153*
Tomoo, T., 179, *242*
Torgov, V. I., 98, *151*
Torrecillas, A. C. T., 324, 326, *360*
Tortajada, J., 85, *148*
Toshima, K., 166, *238*
Totani, K., 173–174, *239*
Toteva, M. M., 104, 121, *153*, *156*
Travassos, L. R., 315, 317, 319, 321, 328, 335, *356–357*, *361–362*
Trombetta, S. E., 336, *363*
Trout, N. A., 104, *153*
Trucks, G. W., 120, *155*

Truhlar, D. G., 85, 88, *148*, *150*
Tschumper, G. S., 89, *150*
Tsuji, Y., 99, *152*
Tsujisaka, Y., 118, *155*
Tsukamoto, H., 121, *156*, 208–209, 219, *245*
Tsukamoto, Y., 344, *365*
Tsvetkov, D. E., 114, *154*
Tsvetkov, Y. E., 177, 210, *239*, *246*, 284, *306*
Turnbull, W. B., 342, *364*
Turner, C. W., 335, *362*
Turnock, D. C., 328, *361*
Tvaroška, I., 19, 37–39, 42–43, 53, *74*, *77–78*, 87, 89, 117, 130–131, *149–150*, *155*, *158*, 166, *238*
Twaddle, G. W. J., 286, *306*

U

Uchida, T., 169, 178, 182, *239*
Uchiyama, T., 231, *249*
Udodong, U. E., 120, *155*, 163, 179, 184–186, 198–199, *236*, *241*, *243*
Ueda, K., 87, 88, *149*
Ueda, T., 87, *149*
Ueno, H., 163, 167, *236*
Ueoka, K., 102, *152*
Ughetto-Monfrin, J., 284, *306*
Uhrig, M. L., 320, *359*
Ulicny, J., 68, *81*
Undenfriend, S., 321, *359*
Unverzagt, C., 208, *245*, 282, 284, *304*, *306*
Uriel, C., 185, 193, 208, 210, *243*, *245–246*
Ustuzhanina, N. E., 114, *154*
Utille, J. P., 117, *155*
Uttaro, A. K., 337, *363*
Uvarova, N. I., 123, *158*

V

Václavík, L., 37, *77*
Valerio, S., 259, *301*
Valverde, S., 185, 193, 219, *243*, *246*
van Beuzekom, A. A., 28–29, *76*
van Boeckel, C. A. A., 120, *156*, 179–180, *242*, 286, *306*
van Boom, J. H., 49–50, *79*, 179, 199–200, *241–242*, *244*, 286, *306*
van den Bos, L. J., 121, *156*, 164, 167, 179, 185, *237–238*, *241*, 286, *306*
van den Eijnden, D. H., 230, *249*
van der Klein, P. A. M., 179, *241*
van der Marel, G. A., 49–50, *79*, 121, *156*, 164, 167, 179, 185, *237–238*, *241–242*, 286, *306*
van der Meer, P. H., 179, *241*
van Engen, D., 275, *303*
van Halbeek, H., 34, *77*
van Oijen, A. H., 167–168, *238*
van Speybroeck, V., 110, *153*
van Wijk, J., 31, *76*
Vandekerckhove, F., 318, 336, *358*, *363*
Vandewalle, P., 274, *303*
Varela, O., 329, *362*
Varga, Z., 283, *305*
Varrot, A., 112, *154*
Vasella, A., 85, 112, 121, *149*, *154*, *156*, 346, *365*
Veeneman, G. H., 199–200, *244*
Veloso, V. M., 312, *355*
Vercelli, C. A., 352, *366*
Vercesi, A. E., 335, *362*
Vernali, T., 87, *149*
Vernon, C. A., 100, *152*
Vetere, A., 342, *364*
Vic, G., 233, *249*
Vickrey, T. L., 89, *150*
Vieira, F., 352, *366*
Vieira, M., 318, 320, *358*
Vikić-Topić, D., 99, *152*
Vila, M. C., 314, *356*
Villalta, F., 335, *362*
Vinogradova, O., 99–100, *152*, 282, 284, *304*
Vionnet, C., 320, *359*
Viso, A., 118–119, *155*
Vliegenthart, J. F. G., 22, *74*, 167–168, *238*
Vocadlo, D. J., 83, *147*, 233–234, *249*

von Helden, G., 85, *148*
von Ragué Schleyer, P. R., 88, *150*
Vosko, S. H., 89, *150*
Vottero, P. J. A., 103, *153*
Vuorinen, T., 52, 58, *79*

W

Wacowich-Sgarbi, S., 163, 218, *236*
Wait, R., 313, 315, 317, 328, *355–357*, *361*
Wakarchuk, W. W., 231, *249*
Waldman, M., 87, *149*
Walker, S., 275, *303*
Wallace, J. E., 121, *157*
Wallin, S., 293, *308*
Walsh, C., 165, *238*
Walter, S. R., 28, *76*
Walther, E., 179–180, 199, 204–205, *241*
Walther, E. P. E., 216, *246*
Wang, C. C., 165, *237*, 293, *308*
Wang, H., 121, *156*, 179, 220, *241*, *248*
Wang, L.-J., 89–90, 104, *150–151*
Wang, P. G., 188–189, 232–233, *243*, *249*, *283*, *304*
Wang, Y., 89, 121, *150*, *156*, 165, 188–189, 215, *237*, *243*
Wang, Z., 164, 188, *236*
Wang, Z. G., 209, *245*
Waragai, H., 227, *248*
Warren, J. D., 177, *239*
Warren, R. A. J., 234–235, *250*
Warriner, S. L., 120, *156*, 163, 201, 216, *236*, 252–254, *301*
Watanabe, H., 118, *155*
Watts, A. G., 337, 339, 348, *364*
Wehenkel, A., 337, 339, *364*
Wei, A., 293, *308*
Wei, G., 208, *245*
Weingart, R., 116–117, *155*
Weinhold, F., 120, *155*
Weldon, A. J., 89, *150*
Wellmar, U., 219, *246*
Werner, B., 287–288, *307*
Werz, D. B., 177, 209, 224–226, *240–248*, 283–284, *305*
Westerduin, P., 120, *156*
Westerink, H. P., 49, *79*
Westra Hoekzema, A. J. A., 27, 31, 63, *76*, *81*
Whangbo, M.-H., 119, *155*
Wheat, P. E., 103, *152*
White, C. G. H., 118, *155*
Whitfield, D. M., 84–85, 87–90, 94, 97–98, 102, 104, 110, 112–115, 116, 118, 123, 129, 131, 135, 140, *147–151*, *153–155*, *157–159*, 166, *238*, 280, *303*
Whitworth, G. E., 83, *147*
Widmalm, G., 32, 38–39, 68, 71, *76*, *78*, *81*
Wieruszeski, J. M., 314, 339, 352, *356*, *364*
Wigilius, B., 123, *157*
Wijmenga, S. S., 50, *79*
Wilk, L., 89, *150*
Willcott, III, M. R., 55–56, *80*
Willet, J. L., 88, *149*
Williams, D. H., 23–24, *75*
Williams, D. L., 129, *158*
Williams, K. B., 99, *152*
Williams, L. J., 163, 167, *236*
Williams, S. J., 179, *242*
Williamson, R. T., 45, *78*
Wilson, B. G., 201, *244*
Wilson, I. A., 274, *303*
Wilson, J., 301, *309*
Windmuller, R., 208, *245*
Wink, D. J., 292, 294, *308*
Winstein, S., 121, *156*
Winter, M., 219, *247*
Wischnat, R., 120, *156*, 163, 201–202, 216–218, *236*
Withers, S. G., 113–114, 121, *154*, *156*, 233–234, *249–250*, 337, 339, 348, *364*
Witzig, C., 346, *365*
Wodrich, M. D., 88, *150*
Woerpel, K. A., 85, 110, *148*, *153*
Wolfe, S., 119, *155*
Wong, C.-H., 84, 120, *147*, *156*, 163, 165, 172–173, 179, 201–202, 216–218, 220, 228, 231, *236–240*, *246–249*, 274, *303*
Woodcock, H. L., 89, *150*

Woods, R. J., 85, 87, 97, *148–149*, *151*
Worm-Leonhard, K., 116–117, *155*
Wray, V., 23, 56, *75*, *80*
Wright, K., 284, *305*
Wu, B., 177, 231–232, *239*, *249*, 297–298, *309*
Wu, C. Y., 218, *246*
Wu, J., 52, *79*, 278–279, *303*
Wu, Q., 58–59, *80*
Wu, X. Y., 220, 222, 224, *247–248*, 283, 288–289, 291, *305*, *307*
Wu, Z., 120, *155*, 163, 198, 201, 203, *236*, *244*
Wu, Z. F., 179, 184–186, 198–199, *241*
Wulff, G., 99, *151*

X

Xavier, M. T., 314, *356*
Xu, H., 104, *153*
Xu, Q., 52, *79*
Xue, J., 177, *239*

Y

Yamada, H., 121, *156*, 179, 208–209, 216, 219, *240*, *245*, 282, *303*
Yamada, T., 184–185, *242*
Yamago, S., 184–185, *242*
Yamamoto, H., 169, 171, 173, *239*
Yan, F., 129, *158*
Yan, L., 179, *241*
Yang, F., 121, *157*
Yang, H., 115, *154*, 165, *237*
Yang, J., 339, *364*
Yang, W. C., 165, *237*
Yao, Q., 232–233, *249*
Yao, Q. J., 292–294, 301, *308–309*
Yashunsky, D. V., 286, *306*, 321, *360*
Ye, X. S., 163–165, 185, 201–202, 215–218, *236–237*
Ye, X.-S., 120–121, *156*
Yeagley, D., 85, *148*
Yerneni, C. K., 228, *248*, 279, *303*
Yeung, L. L., 203, *244*
Yi, W., 232–233, *249*
Yogev, S., 201, 216, *244*
Yoshida, J., 184–185, *242*
Yoshida, J.-I., 102, *152*
Yoshida, M., 317, 328, 331, 336, *357*, *363*
Yoshida, N., 317, 321, 335, *357*, *360*, *362*
Yoshikawa, M., 282, *304*
Yoshitomo, A., 286, 288, *306*
Young, Z., 228, *248*, 279, *303*
Yu, B., 283, *305*
Yu, H., 129, *158*, 231–232, *249*, 283, *305*

Z

Zajicek, J., 51, *79*
Zakrzewski, V. G., 120, *155*
Zatorski, A., 184, *242*
Zax, D., 52, *79*
Zechel, D. L., 112–114, *154*
Zeidan, T. A., 118, *155*
Zen, S., 169, 178, 182, *239*
Zeng, Y., 121, *157*, 283, *305*
Zeng, Y. L., 257, *301*
Zepeda, L. G., 25, *75*
Zgierski, M. Z., 87–90, 98, 104, 112, 118, 123, 135, *149–151*, *154–155*, 166, *238*
Zhang, A., 163, 218, *236*
Zhang, J. J., 231–232, *249*, 257, 263, 283–284, *301–302*, *304–306*
Zhang, L. H., 165, 215, *237*
Zhang, L.-H., 121, *156*
Zhang, M., 263–264, *302*
Zhang, S., 163, *236*
Zhang, W., 34, 36, 43, 45, *77*
Zhang, Y., 231–232, *249*
Zhang, Z., 120, *156*, 163, 201–202, 216–218, *236*, 283, *304*
Zhao, C., 135, *158*
Zhao, H., 34, 36, 43, 45, 55, *77*, *80*
Zhao, S., 51, 53–54, 57–59, *79–80*
Zhao, Y., 88, *150*
Zhong, W., 283–284, *305*
Zhou, L., 164, *236*
Zhou, M., 254, 260–261, *302*
Zhu, L., 232–233, *249*

Zhu, T., 163, 204, 212–213, 220–221, *236*, *244*, *246–248*
Zhu, X., 346, *365*
Zhu, Y., 282–283, *304*, 320, *359*
Zhulin, V. M., 121, *157*
Ziegelmuller, P., 336, 343–345, *363–365*
Ziegler, T., 179, *240*, 291, *308*
Zimmer, D. P., 49–50, *79*
Zingales, B., 312, 315, 318, 321–322, 327–328, 336, *355–358*, *360–361*, *363*
Zuurmond, H. M., 120, *156*, 179, *241*

SUBJECT INDEX

A

Ab initio MO methods, 21
Ab initio molecular dynamics (AIMD) studies
  1,6-anhydrodioxolenium from and, 98
  for finding ring-inversion barrier, 110–114, 111f, 112f, 112t
Acceptor-bound approach, to solid-phase synthesis, 220, 222, 224
p-Acetamidophenylthio glycosides, active-latent strategy for, 186
3-Acetoxy-2,2-dimethylpropanoate protecting group, acyl-transfer side reaction and, 129–130
Acetylated selenoglycoside, activation of, 255–256
Achmatowicz rearrangement, for α-mannans synthesis, 260–261
Activator, for selective activation, 178–179
Active–latent strategy, for oligosaccharide synthesis, 185–188
Acyl-transfer side reaction
  in 3-acetoxy-2,2-dimethylpropanoate protecting group, 129–130
  in 2,6-dimethoxybenzoyl, 129
  in galactopyranosyl oxacarbenium ions, 123, 126–128
  proton transfer and, 131–132
Additives, oxacarbenium ions and, 99
ADF. *See* Amsterdam density functional
Aerobacter aerogenes, 5
AFM. *See* Atomic force microscopy
AIM. *See* Atoms in molecules study
AIMD. *See Ab initio* molecular dynamics studies
Alditol oligosaccharides, of *T. cruzi* mucins, HPAEC-PAD analysis of, 334
Allinger's MM1 force field, 24
Allinger's MM2/MMP2 program, 29–30
Allyl glycosides, in stereocontrolled synthesis of α-mannans, 263–264
Allylic couplings, 68
ALTONA, 25
Altona equation, 24, 40, 61
Amsterdam density functional (ADF), for galactopyranoside study, 89
1,6-Anhydrodioxolenium, stability of, 97–98
Antiprotozoal therapy, targets of, 315, 320, 345–350, 348f–351f
Armed–disarmed approach
  inverse, 200–201
  for oligosaccharide synthesis, 197–201
Armed–disarmed effect, in galactopyranosyl oxacarbenium ions, 120
Aspinall, Gerald, 2–9
Atomic force microscopy (AFM), for ring-inversion barrier, 112–113
Atoms in molecules (AIM) study, for galactopyranosyl oxacarbenium, 85
Automated synthesis, of oligosaccharides, 224–226

B

Bacillus anthracis tetrasaccharide, synthesis of, 281, 284–285
Barfield transmission effect, 28–30
Barton/Cookson generalization, 5–6
Benzenesulfinyl piperidine-triflic anhydride system, for selective activation, 179–181
Benzoic acid derivatives, TcTS inhibition with, 348, 349f
S-Benzoxazolyl (SBox) glycosides
  disarming by, 202–203
  in orthogonal strategy, 192

S-Benzoxazolyl (SBox) glycosides (*cont.*)
  for selective activation, 180–182
  as super-armed glycosyl donors, 207
  temporary deactivation concept, 195
2-*O*-Benzoyl-tri-*O*-benzoyl-protected glycosyl donor, investigation of, 207
Benzyl ethers, for glycosylation reactions, 116
Biallylic couplings, 68
Biantennary heptasaccharide, convergent block synthesis of, 172–173
Bidirectional approaches
  to oligosaccharide synthesis, 211–213
  in solid-phase synthesis, 220
Biological effects, of TcTS, 350–352
Biological functions, of *T. cruzi* mucins, 335
Biological properties, of *T. cruzi* GIPLs, 318–319
Blood-group B antigen, synthesis of, 232–233
Bohlmann effect, in galactopyranosyl oxacarbenium ions, 119
Bromine
  for selective activation, 179–181
  for two-step activation, 182–184

C

CAGPLUS, 25
Campylobacter jejuni, 7
Campylobacter spp., 7
Candida albicans, 287
Canonical vector representation
  development of, 110
  of galactopyranosyl oxacarbenium ions, 95, 96t, 97
  pseudorotation in, 111, 111f
Carbohydrate structures, in *T. cruzi* mucins, 327–335, 329f
Carbon–carbon couplings, 51–59
  $^3J_{CCCC}$, 55–59
  $^3J_{CCOC}$, 52–55, 56f
Carbon–tin couplings, $^3J_{CCCSn}$, 64
Catalytic mechanism, of TcTS, 336–340, 337f–338f
CBS calculation. *See* Complete basis set calculation
Cell surface glycoconjugates, of *T. cruzi*, 313–354
  glycoinositolphospholipids, 313–321, 314f–316f, 322f
  mucins, 321–335, 322f, 326f, 326t, 329f
  other glycoproteins, 352–354, 353f–354f
  trans-sialidase, 336–352, 337f–338f, 348f–351f
Cellulomonas fimi, enzyme from, 234
Ceramides, of *T. cruzi*, 314–315, 317, 319–320
Chagas' disease, 312
CHARMM force field, 38–39, 50
CHARMM molecular modeling, 52
Chemical synthesis
  of glycosyl amino acids of *T. cruzi* mucins, 333–334
  of oligosaccharides in *T. cruzi* mucins, 328–333
  of *T. cruzi* GIPL, 321–325, 322f
Chemoenzymatic, of glycosyl amino acids of *T. cruzi* mucins, 333–334
Chemoselective strategies
  for oligosaccharide synthesis, 196–207
    armed–disarmed approach, 197–201
    disarming by remote substituents, 202–203
    disarming by torsional effects, 203–206
    inverse armed–disarmed approach, 200–201
    reactivity–based programmable strategy, 201–202
    super-armed glycosyl donors, 206–207
  in one-pot glycosylation strategies, 215
  for stereocontrolled synthesis of α-mannans, 269, 271
CHYMESA, 59
CIP. *See* Contact ion pair
Complete basis set (CBS) calculation, for glycopyranoside study, 89, 145
Contact ion pair (CIP)
  methodology development for, 146

  - oxacarbenium ion
    - equilibrium with, 99
    - facial selectivity and, 100–101
    - ionization and, 137
- Convergent block synthesis, 169–177
  - advantages of, 173
  - of alternating *β*-(1→3)-*β*-(1→4)-mannan, 295–297
  - of biantennary heptasaccharide, 172–173
  - of high mannose-type oligosaccharide, 173–175
  - of Lewis X structure, 175–176
  - linear v., 171
  - of α-mannans, 258
  - of *β*-mannans, 292–293
  - in one-pot glycosylation strategies, 216
  - of pneumococcal oligosaccharide serotype 14, 176–177
  - polymer-supported synthesis with, 220–222
  - in solid-phase synthesis, 220
  - of *Spergularia ramosa* pentasaccharide, 171–172
  - variation A, 169–171
  - variation B, 175
- COSY-45 method, 51
- Coupling constants
  - angular dependence of, 18–19, 21
  - online calculators for, 70–72
  - over five bonds, 68–69, 69f
  - over four bonds, 64–68
  - summary for, 72–73
  - vicinal, 21–59
    - carbon–carbon, 51–59
    - fluorine, 60–63
    - proton–carbon, 36–45
    - proton–nitrogen, 45–47
    - proton–phosphorus, 47–51, 48f
    - proton–proton, 21–36
- Coupling reactions, development of, 167
- Covalent inhibitors, TcTS inhibition with, 348–349, 350f
- Cremer–Pople representation, canonical vector representation v., 110
- Crescenzi, Vittorio, 12–16
- CS MOPAC PRO, 67
- Cyanoethylidene orthoester, in stereocontrolled synthesis of α-mannans, 267–269
- Cyanoorthoacetate, in stereocontrolled synthesis of α-mannans, 267–269
- Cyclohexane phosphonate derivatives, TcTS inhibition with, 346
- Cyclohexanes, $^3J_{\mathrm{HCCH}}$ values in, 25

D

- DEMON-KS program, 40
- DEMON-NMR procedure, 40
- Density functional theory (DFT) methods
  - for galactopyranosyl oxacarbenium ions, 88
    - rotation and, 119
  - $^3J_{\mathrm{CCCC}}$, 59
  - $^3J_{\mathrm{CCOC}}$, 55, 56f
  - $^3J_{\mathrm{FCCF}}$, 63
  - $^4J_{\mathrm{HCCCH}}$, 65–66, 66f
  - $^4J_{\mathrm{HC=CCH}}$, 68
  - $^3J_{\mathrm{HCNC}}$, 32–33
  - $^3J_{\mathrm{HCOC}}$, 39–40
  - $^3J_{\mathrm{HCOH}}$, 33–35, 35f
  - $^3J_{\mathrm{HOCC}}$, 43, 44f
- DFT. *See* Density functional theory methods
- Dihedral angle
  - couplings over four bonds, 64–68
  - $^3J_{\mathrm{CCCC}}$, 57–59
  - $^3J_{\mathrm{CCOC}}$, 52–54
  - $^3J_{\mathrm{FCCF}}$, 62–63
  - $^3J_{\mathrm{HCCC}}$, 41
  - $^5J_{\mathrm{HCCCCH}}$, 68–69
  - $^4J_{\mathrm{HCCCH}}$, 65, 66f
  - $^3J_{\mathrm{HCCH}}$, 22–26, 30
  - $^3J_{\mathrm{HCCN}}$, 46, 46f–47f
  - $^3J_{\mathrm{HCNF}}$ and $^4J_{\mathrm{HCCNF}}$, 62
  - $^3J_{\mathrm{HCNH}}$, 33
  - $^3J_{\mathrm{HCOC}}$, 37, 39, 39f
  - $^3J_{\mathrm{HCOP}}$, 48, 50
  - $^3J_{\mathrm{HCSC}}$, 42
  - $^3J_{\mathrm{HOCC}}$, 43, 44f

Dihedral angle (*cont.*)
  Karplus equation and, 30–31
  NMR coupling constants and, 18–21
2,6-Dimethoxybenzoyl (DMOB), synthesis and testing of, 129
Dimethyldioxirane (DMDO), for two-step activation, 184–185
2,4-Dinitrophenyl glycosides, torsional disarming of, 205–206
2,3-Di-*O*-(*β*-D-galactopyranosyl)-D-galactose, sialylation of, 341
Disarming by remote substituents, for oligosaccharide synthesis, 202–203
Disarming by torsional effects, for oligosaccharide synthesis, 203–206
2,6-Di-*tert*-butyl-4-methylpyridine (DTMP), for glycosylation reactions, 140–141
DMDO. *See* Dimethyldioxirane
DMOB. *See* 2,6-Dimethoxybenzoyl
Donor substrates, for TcTS reaction, 342–347
Donor-bound approach, to solid-phase synthesis, 220, 222–223
Double stereo-differentiation, in galactopyranosyl oxacarbenium ions, 120–121
DTMP. *See* 2,6-Di-*tert*-butyl-4-methylpyridine

E

EHT-MO calculations, for $^3J_{\mathrm{HCCH}}$, 25
α-(1→4)-Eicomannan, stereocontrolled synthesis of, 272–273
Electronegativity orientation
  $^3J_{\mathrm{CCOC}}$, 54
  $^3J_{\mathrm{HCCF}}$, 60
  $^3J_{\mathrm{HCCH}}$, 23–24, 23f–24f
  in Karplus equation, 30–31
Endoplasmic reticulum membrane-associated oligosaccharide, convergent block synthesis of, 173–175
Enzymatic approach, to oligosaccharide synthesis, 228–234
  with glycosidases, 233–234
  with glycosyltransferases, 230–233
2-Ethoxytetrahydropyran, studies of, 89
S-Ethyl glycosides
  in orthogonal strategy, 190–193
  for selective activation, 179–182
  for two-step activation, 182–184
Extended W couplings, 68–69, 69f

F

Facial selectivity, of galactopyranosyl oxacarbenium ions, 98–109, 141
  CIPs and SSIPs and, 100–101
  ionization and, 137, 138f
  leaving groups, 104
  methanol complexes, 101–102
  protecting-group strategies, 103–104
  proton transfer in, 102, 103f
  reactivity order and, 99–100
  reversibility, 109
Fischer approach, selective activation v., 177
Five bond coupling constants
  $^5J_{\mathrm{HCCCCH}}$, 68–69, 69f
  $^5J_{\mathrm{HCC=CCH}}$, 69
Fluorine
  in orthogonal strategy, 189–191
  for two-step activation, 182–184
Fluorine couplings, 60–63
  $^3J_{\mathrm{CCCF}}$ and $^3J_{\mathrm{COCF}}$, 62
  $^3J_{\mathrm{FCCF}}$, 62–63
  $^3J_{\mathrm{HCCF}}$, 60–61
  $^3J_{\mathrm{HCNF}}$ and $^4J_{\mathrm{HCCNF}}$, 61–62
Fluorous tag-supported synthesis, of oligosaccharides, 226–229
Force field
  Allinger's MM1, 24
  CHARMM, 38–39, 50
  MM2–85, 31
  for molecular mechanic calculations, 87
Four bond coupling constants
  $^4J_{\mathrm{HCCCH}}$, 64–68, 66f
  $^4J_{\mathrm{HC=CCH}}$, 68
FPT-INDO calculations, 38, 42
Free energy, in geometry optimization, 110

Frequency calculations, for galactopyranosyl oxacarbenium ions, 91–92, 93t, 94, 94f, 95f
Fucosyl GM1 oligosaccharide, synthesis of, 209–210

G

1G7 antigen, GPI in, 317–318
β-Gal-(1→3)-Gal-R derivatives, trans-sialylation of, 343–344
Galactofuranose, 354
Galactopyranosyl oxacarbenium ions
  background for, 84–89
    galactose derivative selection, 85, 87
    reactivity of, 84–86
    study methods for, 87–89
  facially selective complexes, 98–109, 141
    CIPs and SSIPs and, 100–101
    leaving groups, 99, 104
    linear transit, 105, 106–107f, 107–108f, 109
    methanol complexes, 101–102
    protecting-group strategies, 103–104
    proton transfer in, 102, 103f, 141
    reactivity order and, 99–100
    reversibility, 109
  ionization in, 136–140, 142
    facial selectivity and, 137, 138f
    stereoselectivity and, 137–138, 139f, 142
    thermal vibrational excitation, 140–141
  ring conformations of, 89–98, 141
    geometric parameters of, 95–97, 96t
    geometry optimization, 91–95, 93t, 94f, 95f
    starting geometry for, 89–91, 91f, 92, 94
  rotation role in, 118–130, 119f
    acyl-transfer side reaction, 123, 126–128
    hyperconjugative interactions, 118–119, 119f, 120f
    neighboring-group participation, 122–123, 122f, 124f, 125–126t, 141
    protecting groups, 119–121
    substituents, 121
  side-chain orientation and conformation, 109–118
    protecting group interactions, 118
    reactivity, 109–110
    ring-inversion barrier, 110–114, 111f, 112f, 112t
    steric buttressing, 116–117
    through-bond activation, 115, 115f
    through-space interaction efficiency, 114
Galactose-binding site, of TcTS, 338–339
  inhibition of, 349–350, 351f
β-D-Gal*f* (1→4)[β-D-Gal*p*(1→6)]GlcNAc, synthesis of, 329–331
β-D-Gal*f*(1→4)GlcNAc, synthesis of, 329–330
Galili pentasaccharide, bidirectional strategy for synthesis of, 212–213
Gal*p*, of *T. cruzi* GIPLs, 328
β-D-Gal*p*(1→3)-β-D-Gal*p*-(1→6)-[β-D-Gal*f*-(1→4)]-D-GlcNAc, synthesis of, 331–332
β-D-Gal*p*(1→2)[β-D-Gal*p*(1→3)]-β-D-Gal*p* (1→6)[β-D-Gal*f*(1→4)]-D-GlcNAc, sialylation of, 341
β-D-Gal*p*(1→3)[β-D-Gal*p*(1→2)]-β-D-Gal*p* (1→6)[β-D-Gal*f*(1→4)]-D-GlcNAc, synthesis of, 331–333
α-D-Gal*p*-(1→6)-β-D-Gal*p*-OMe, sialylation of, 342
β-D-Gal*p*-(1→6)-β-D-Gal*p*-OMe, sialylation of, 343
β-Gal*p*-(1→4)-GlcNAc-α-L-threonine (LacNAc-α-threonine), synthesis of, 333
GAUSSIAN94 program
  for $^3J_{\mathrm{CCOC}}$, 53
  for $^3J_{\mathrm{HCCF}}$, 61
GAUSSIAN98 program
  for $^3J_{\mathrm{HCOC}}$, 40
  for $^4J_{\mathrm{HCCCH}}$, 67
GAUSSIAN03 program
  for $^3J_{\mathrm{CCOC}}$, 55
  for $^3J_{\mathrm{HOCC}}$, 43–45

Genetic variability, of *T. cruzi* mucins, 322–327, 326f, 326t
Geometrical factors, ${}^{3}J_{\mathrm{CCOC}}$, 54–55
Geometry optimization
  free energy in, 110
  for galactopyranosyl oxacarbenium ions, 91–95, 93t, 94f, 95f
GIPL. *See* Glycoinositolphospholipids
Globo-H hexasaccharide, automated synthesis of, 225–226
Glycobiology, of *T. cruzi*, 311–355
  concluding remarks, 354–355
  glycoinositolphospholipids, 313–321, 314f–316f, 322f
  introduction, 312
  life cycle of the parasite, 312–313, 313f
  mucins, 321–335, 322f, 326f, 326t, 329f
  other glycoproteins, 352–354, 353f–354f
  trans-sialidase, 336–352, 337f–338f, 348f–351f
Glycofuranosyl groups, oxacarbenium ions and, 84
Glycoinositolphospholipids (GIPL), of *T. cruzi*, 313–321
  biological and immunological properties of, 318–319
  biosynthesis of, 319–321
  chemical synthesis of, 321–325, 322f
  as GPI anchors in *T. cruzi* glycoproteins, 315–318, 316f
Glycophosphatidylinositol (GPI)
  in minor *T. cruzi* glycoproteins, 317–318
  of *T. cruzi* anchors
    lipid remodeling of, 319–320
    structure of, 314, 314*f*
    in *T. cruzi* glycoproteins, 315–318, 316f
    transfer of, 320–321
  of tGPI mucins, 335
  in trans-sialidases, 317
Glycopyranosyl groups, oxacarbenium ions and, 84
Glycopyranosyl oxacarbenium ions, importance of, 83–84
Glycosidases, oligosaccharide synthesis with, 233–234
Glycosidic bonds
  breakage of, 84
  formation of, 84
    α-mannans stereocontrolled synthesis with, 255–256, 260–261
    stereocontrol of, 165
Glycosphingolipid, armed–disarmed approach for synthesis of, 199
Glycosyl amino acids, of *T. cruzi* mucins, chemical and chemoenzymatic synthesis of, 333–334
Glycosyl chlorides, in stereocontrolled synthesis of α-mannans, 262–263
Glycosyl donors, super-armed, for oligosaccharide synthesis, 206–207
Glycosyl processing enzymes (GPEs). *See also* Galactopyranosyl oxacarbenium ions
  applications of, 83–84
  glycosylation by, 130
  KIE studies for TSs of, 113–114
  reactivity of, 121
  study of, 85, 87
Glycosylation reactions. *See also* One-pot glycosylation strategies
  1,6-anhydrodioxolenium from, 97–98
  calculations for
    based on existing methodologies, 145
    requiring methodology development, 145–146
  charge neutralization in, 137
  coupling reactions, 167
  DTMP for, 140–141
  enzymatic approach to, 228–230
  experimental studies of, 146–147
  oxacarbenium ions and, 98
  principles of, 165–167
  proton transfer in, 105, 106–107f, 109, 130–136
    energetic magnitude of, 135–136
    neighboring-group participation, 131–132, 133–134f, 135

    rates of, 131
    timing of, 130–131
  reactivity order in, 99–100
    manipulation of, 136
  stereoselectivity of, 103–104, 103f
    control of, 165
    factors influencing, 166–167
    manipulation of, 136
    steric buttressing, 116–117
  summary of, 140–144
  transition states of, 141
Glycosyltransferase mechanisms, modeling of, 130–131
Glycosyltransferases, oligosaccharide synthesis with, 230–233
Glycosynthase, oligosaccharide synthesis with, 234–235
GM3 trisaccharide, synthesis of, 231–232
gp 85, 336
GP72, 352–354, 354f
GPEs. *See* Glycosyl processing enzymes
GPI. *See* Glycophosphatidylinositol
GPI malarial toxin, automated synthesis of, 225
GS-4071, 346

H

Haasnoot equation, 24, 31, 40, 61
Hartree–Fock (HF) methods, for galactopyranosyl oxacarbenium ions, 88
Hassel–Ottar effect, galactopyranosyl oxacarbenium ions and, 93, 95, 95f, 117
H-bonds. *See* Hydrogen bonds
Helferich-type glycosylation, α-mannans synthesis with, 262–263
Helicobacter pylori, 7–8
Helicobacter spp., 7
Heparin-like oligosaccharides, selective activation synthesis of, 179–180
Heptasaccharyl *myo*-inositol, of *T. cruzi*, synthesis of, 321, 322f, 323–325
HF. *See* Hartree–Fock methods
High mannose-type oligosaccharide, convergent block synthesis of, 173–175
Homotetramer, synthesis of, 228
H-type II pentasaccharide, traditional linear synthesis of, 169–170
Huggins electronegativity scale, 27, 51, 60
Hydrogen bonds (H-bonds)
  in galactopyranosyl oxacarbenium ions, 85
    facial selectivity, 102, 103f
    methodology development for, 145
    selectivities of, 116–117
  proton transfer rates and, 131, 135–136
  study of, 85, 87
Hydrolysis, of galactopyranosides v. glucopyranosides, 84–86
Hydroxyl reactivity, in oligosaccharide synthesis, 208–210
Hyperconjugative interactions, in galactopyranosyl oxacarbenium ions, 118–119, 119f, 120f

I

IDCP. *See* Iodonium (di-γ-collidine) perchlorate
Immunological properties, of *T. cruzi* GIPLs, 318–319
In situ preactivation
  for oligosaccharide synthesis, 182–185
  in one-pot glycosylation strategies, 218
1D INADEQUATE, 58
2D INEPT experiment, 37
Inhibitors, of TcTS, 345–350, 348f–351f
Inositolphosphoceramide (IPC), of *T. cruzi*, in lipid remodeling, 319–320
Inositolphospholipid (IPL), of GPI anchors, 316–317
Intermolecular processes, with oxacarbenium ions, 99
Intramolecular processes, with oxacarbenium ions, 99
Intrinsic reaction coordinate (IRC) calculation,
    for galactopyranosyl oxacarbenium ions, 92

Inverse armed–disarmed approach, 200–201
Iodonium (di-γ-collidine) perchlorate (IDCP), for armed–disarmed approach, 198–199
Ionic liquid-supported oligosaccharide synthesis, 228, 279
Ionization, in galactopyranosyl oxacarbenium ions, 136–140, 142
  facial selectivity and, 137, 138f
  leaving groups, 99, 104, 145
  stereoselectivity and, 137–138, 139f
  thermal vibrational excitation, 140–141
IPC. *See* Inositolphosphoceramide
IPC synthase, 320
IPL. *See* Inositolphospholipid
IRC. *See* Intrinsic reaction coordinate calculation

J

$^{3}J_{\mathrm{CCCC}}$, 55–59
$^{3}J_{\mathrm{CCCF}}$, 62
$^{3}J_{\mathrm{CCCSn}}$, 64
$^{3}J_{\mathrm{CCOC}}$, 52–55, 56f
$^{3}J_{\mathrm{COCF}}$, 62
$^{3}J_{\mathrm{FCCF}}$, 62–63
$^{3}J_{\mathrm{HCCC}}$, 41–42
$^{5}J_{\mathrm{HCCCCH}}$, 68–69
$^{5}J_{\mathrm{HCC{=}CCH}}$, 69
$^{4}J_{\mathrm{HCCCH}}$, 64–68, 66f
$^{4}J_{\mathrm{HC{=}CCH}}$, 68
$^{3}J_{\mathrm{HCCF}}$, 60–61
$^{3}J_{\mathrm{HCCH}}$, 21–32
$^{3}J_{\mathrm{HCCN}}$, 45–47, 46f–47f
$^{4}J_{\mathrm{HCCNF}}$, 61–62
$^{3}J_{\mathrm{HCNF}}$, 61–62
$^{3}J_{\mathrm{HCNH}}$, 32–33
$^{3}J_{\mathrm{HCOC}}$, 37–41, 39f
$^{3}J_{\mathrm{HCOH}}$, 33–36
$^{3}J_{\mathrm{HCOP}}$, 47–51, 48f
$^{3}J_{\mathrm{HCSC}}$, 42–43
$^{3}J_{\mathrm{HCSiH}}$, 36
J-HMBC NMR, 39
$^{3}J_{\mathrm{HOCC}}$, 43–45, 44f

K

Karplus equation
  couplings over five bonds, 68–69, 69f
  couplings over four bonds, 64–68, 66f
  introduction to, 18–19
  molecular modeling impact, 20–21
  NMR spectroscopy improvements, 19–20
  online calculators for coupling constants and torsions, 70–72
  summary for, 72–73
  vicinal coupling constants, 21–59
    carbon–carbon couplings, 51–59
    fluorine couplings, 60–63
    proton–carbon couplings, 36–45
    proton–nitrogen couplings, 45–47
    proton–phosphorus couplings, 47–51, 48f
    proton–proton couplings, 21–36
KIE. *See* Kinetic isotope effect studies
Kinetic isotope effect (KIE) studies, for GPE transition states, 113–114
Koenigs–Knorr approach, selective activation v., 177

L

LacNAc-α-threonine. *See* β-Gal*p*-(1→4)-GlcNAc-α-L-threonine
Lactitol, 349–350, 352
Lactose derivatives
  TcTS inhibition with, 349–350, 351f
  trans-sialylation of, 343–344
Leaving groups
  active–latent strategy for, 185–188
  armed–disarmed approach for, 198–201
  bidirectional approaches with, 211–213
  chemoselective strategies for, 196–197
  galactopyranosyl oxacarbenium ions and, 99
    ionization, 104, 145
  orthogonal and semi-orthogonal strategies for, 188–193
  selective activation of, 177–188
    heparin-like oligosaccharides, 179–180

with three leaving groups, 179–181
three-step sequential, 180–182
steric hindrance deactivation, 193–194
temporary deactivation concept, 193–196
two-step activation and *in situ* preactivation of, 182–185
Leloir pathway, for oligosaccharide synthesis with glycosyltransferases, 230–233
Lewis X structure
convergent block synthesis of, 175–176
solid-phase synthesis of, 220–222
Life cycle, of *T. cruzi*, 312–313, 313f
Linear oligosaccharide synthesis, 167–169
convergent block v., 171
of H-type II pentasaccharide, 169–170
of pneumococcal oligosaccharide serotype 6A, 167–169
Linear transit (LT), for galactopyranosyl oxacarbenium ions, 105, 106–107f, 107–108f, 109
β-(1→3)-Linked glucan, 5
Lipid remodeling, of GPI, 319–320
Lipopeptidophosphoglycan (LPPG), of *T. cruzi*, 314–315
oligosaccharide structures found in, 315, 315f
LPPG. *See* Lipopeptidophosphoglycan

M

α-(1→2)-Mannan, synthesis of, 278–281
α-(1→4)-L-Mannan, synthesis of, 261
α-(1→6)-Mannan, synthesis of, 279
β-(1→2)-Mannan, synthesis of, 286–289
β-(1→3)-Mannan, *β*-(1→4)-mannan alternating with
block synthesis, 295–297
direct synthesis, 294–296
β-(1→4)-Mannan
β-(1→3)-mannan alternating with
block synthesis, 295–297
direct synthesis, 294–296
synthesis of, 293–294
Mannans, stereocontrolled synthesis of
introduction to, 251–252, 286
α-mannans
in absence of neighboring-group participation, 252–261
neighboring group-directed, 262–281
β-mannans
by direct methods, 291–299
by indirect methods, 286–291
α-Mannans, stereocontrolled synthesis of
in absence of neighboring-group participation, 252–261
block synthesis, 258
in frozen solvent conditions, 254–255
glycosidic bond formation for, 255–256, 260–261
Helferich-type glycosylation, 262–263
α-(1→4)-L-Mannan, 261
3-*O*-methyl-(1→4)-α-D-mannan, 258–259
one-pot strategy for, 252–254
α-(1→3)-Pentamannan, 259–260
trichloroacetimidate approach to, 257
neighboring group-directed, 262–281
with allyl glycosides, 263–264
chemoselective cleavage, 269, 271
cyanoethylidene orthoester approach to, 267–269
α-(1→4)-eicomannan, 272–273
with glycosyl chlorides, 262–263
α-(1→2)-mannan, 278–281
α-(1→6)-mannan, 279
mannosyl iodide for, 270–272
MPEG glycosides for, 276–278
O-2-protecting group in, 272–723
α-(1→3)-pentamannan, 264–265
pentenyl glycoside approach to, 264–267
pentenyl orthoester approach to, 266, 268, 270
polymer-supported, 279–280
thioglycoside activation for, 275–276
trichloroacetimidate method for, 268–269, 271
trichloroacetimidate with thioglycoside donors, 274–275

β-Mannans, stereocontrolled synthesis of
  by direct methods, 291–299
    alternating β-(1→3)-β-(1→4)-mannan, 294–296
      block synthesis, 295–297
    block-synthesis, 292–293
    β-(1→4)-mannan, 293–294
    β-(1→3)-mannohexaose, 297–299
    β-(1→2)-mannooctaose, 291–292
    β-(1→4)-mannotetraose, 294–295
    β-(1→3)-mannotriose, 296–298
  by indirect methods, 286–291
    β-(1→2)-mannan synthesis, 286–289
    β-(1→2)-mannooctaose synthesis, 289–291
    β-(1→2)-mannotetraose synthesis, 288–290
    β-(1→4)-mannotriose synthesis, 286–287
β-(1→2)-Mannohexaose, synthesis of, 286–288
β-(1→3)-Mannohexaose, synthesis of, 297–299
β-(1→4)-Mannohexaose, synthesis of, 293–294
β-(1→2)-Mannooctaose, synthesis of
  direct methods, 291–292
  indirect methods, 289–291
Mannosyl donors, 252, 252f
Mannosyl iodide, for stereocontrolled synthesis of α-mannans, 270–272
β-(1→2)-Mannotetraose, synthesis of, 288–290
β-(1→4)-Mannotetraose, synthesis of, 294–295
β-(1→3)-Mannotriose, synthesis of, 296–298
β-(1→4)-Mannotriose, synthesis of, 286–287
MCSCF *ab initio* calculations, 31–32, 63
MD/MM methods, 21
MestRe-J, 71
Methanol complexes, facial selectivity of galactopyranosyl oxacarbenium ions, 101–102
2-Methoxytetrahydropyran, studies of, 89
Methyl glycosides, torsional disarming of, 205–206
3-*O*-Methyl-(1→4)-α-D-mannan, synthesis of, 258–259
2′-*O*-(4-Methylumbelliferyl)-αNeu5Ac (MUNeu5Ac) derivatives
  as donors for TcTS reaction, 342–344
  trans-sialylation with, 345
Methylumbelliyferyl α-sialosides, as donor for TcTS reaction, 342
Microreactor synthesis, of oligosaccharides, 228–229
MM. *See* Molecular mechanics
MM2–85 force field, 31
MO calculations, for $^{3}J_{\mathrm{CCCC}}$, 55–56
Molecular mechanics (MM), oxacarbenium ions and, 87
Molecular modeling
  CHARMM, 52
  impact of, 20–21
Monomethylpolyethylene (MPEG) glycoside, for α-mannans stereocontrolled synthesis, 276–278
MPEG glycoside. *See* Monomethylpolyethylene glycoside
Mucin oligosaccharides, as acceptors of sialic acid, 339–341
Mucin-associated surface proteins (MASP), 327
Mucins, of *T. cruzi*, 321–335, 322f, 326f, 326t, 329f
  biological functions of, 335
  carbohydrate structures in, 327–335, 329f
  genetic variability of, 322–327, 326f, 326t
  GPI in, 316–317
MUNeu5Ac derivatives. *See* 2′-*O*-(4-Methylumbelliferyl)-αNeu5Ac derivatives
Murray's reagent. *See* Dimethyldioxirane
Mycobacterium smegmatis, 258
Mycobacterium spp., 7

N

Neighboring-group participation
  in galactopyranosyl oxacarbenium ions, 122–123, 122f, 124f, 125–126t, 141

methodology development for, 145
proton transfer and, 131–132, 133–134f, 135
in stereocontrolled synthesis of α-mannans, 262–281
with allyl glycosides, 263–264
chemoselective cleavage, 269, 271
cyanoethylidene orthoester approach to, 267–269
α-(1→4)-eicomannan, 272–273
with glycosyl chlorides, 262–263
α-(1→2)-mannan, 278–281
α-(1→6)-mannan, 279
mannosyl iodide for, 270–272
MPEG glycosides for, 276–278
O-2-protecting group in, 272–723
α-(1→3)-pentamannan, 264–265
pentenyl glycoside approach to, 264–267
pentenyl orthoester approach to, 266, 268, 270
polymer-supported, 279–280
thioglycoside activation for, 275–276
trichloroacetimidate method for, 268–269, 271
trichloroacetimidate with thioglycoside donors, 274–275
in stereocontrolled synthesis of α-rhamnans, 282t–284t
NETNES, 315, 352, 353f
GPI in, 318
Neu5Ac2en, 345
Neutral species, oxacarbenium ion equilibrium with, 99
N-Glycolylneuraminic acid, TcTS transfer of, 345, 347
p-Nitrophenylthio glycosides, active–latent strategy for, 186
NMR coupling constants, angular dependence of, 18–19, 21
NMR spectroscopy, improvements of, 19–20
Non-Leloir pathway, for oligosaccharide synthesis with glycosyltransferases, 232–233
Nonnatural donors, for TcTS reaction, 342–343
Nucleophiles, in glycosylation reactions, 99
methodology development for, 146

O

Oligosaccharide synthesis
automated synthesis, 224–226
chemical glycosylation principles, 165–167
chemoselective strategies for, 196–207
armed–disarmed approach, 197–201
disarming by remote substituents, 202–203
disarming by torsional effects, 203–206
inverse armed–disarmed approach, 200–201
reactivity-based programmable strategy, 201–202
super-armed glycosyl donors, 206–207
cis-cis patterned, 199–200
convergent block, 169–177
advantages of, 173
of biantennary heptasaccharide, 172–173
of high mannose-type oligosaccharide, 173–175
of Lewis X structure, 175–176
of pneumococcal oligosaccharide serotype 14, 176–177
of *Spergularia ramosa* pentasaccharide, 171–172
variation A, 169–171
variation B, 175
enzymatic approach to, 228–234
with glycosidases, 233–234
with glycosyltransferases, 230–233
fluorous tag-supported synthesis, 226–229
introduction to, 162–165, 164f
challenges of, 163
new methods for, 163–165
ionic liquid-supported, 228
linear, 167–169
of H-type II pentasaccharide, 169–170

Oligosaccharide synthesis (*cont.*)
    of pneumococcal oligosaccharide serotype 6A, 167–169
  microreactor synthesis, 228–229
  one-pot glycosylation strategies, 214–219
    development of, 121
    by *in situ* preactivation, 218
    major concepts of, 214–216
    by programmable strategy, 216–218
    regioselective synthesis, 208–209
    by selective activation, 216–217
  outlook for, 234–235
  polymer-supported synthesis, 219–222
  rapid and high-throughput technologies for, 213–228
    fluorous tag-supported and microreactor synthesis, 226–229
    one-pot glycosylation strategies, 214–219
    polymer-supported, solid-phase, and automated synthesis, 219–226
  regioselectivity-based strategies for, 208–213
    bidirectional approaches, 211–213
    hydroxyl reactivity, 208–210
    triphenylmethyl reactivity, 210–211
  selective strategies for, 177–196
    active–latent strategy, 185–188
    orthogonal and semi-orthogonal strategies, 188–193
    selective activation, 177–182
    steric hindrance deactivation, 193–194
    temporary deactivation concept, 193–196
    two-step activation and *in situ* preactivation, 182–185
  solid-phase synthesis, 219–224
    acceptor-bound approach, 220, 222, 224
    donor-bound approach, 220, 222–223
    types of, 220
  trans-trans patterned, 200
Oligosaccharides
  of *T. cruzi*, sialylation of, 339–347
  of *T. cruzi* LPPG, 315, 315f
  of *T. cruzi* mucins
    chemical synthesis of, 328–333
    HPAEC-PAD analysis of, 334
    interstrain variation of, 328, 329f
O-linked oligosaccharides,
    of *T. cruzi* mucins
  chemical synthesis of, 328–333
  interstrain variation of, 328, 329f
One-pot glycosylation strategies, 214–219
  development of, 121
  by *in situ* preactivation, 218
  major concepts of, 214–216
  α-mannan synthesis with, 252–254
  by programmable strategy, 216–218
  reactivity-based programmable strategy for, 201–202
  regioselective synthesis, 208–209
  by selective activation, 216–217
  super-armed glycosyl donors for, 206–207
Orthoesters, neutral, galactopyranosyl oxacarbenium ions, 123, 126–128
Orthogonal strategies
  for oligosaccharide synthesis, 188–193
  in solid-phase synthesis, 220
Oxacarbenium ions
  glycosidic bonds and, 84
  nucleophile reactions with, 99

P

Pasteurella multocida, enzyme from, 231–232
PC MODEL, 67
PCILO quantum chemical method, 42–43
Pentafluorobenzoyl ester, disarming by, 202–203
α-(1→3)-Pentamannan, synthesis of, 259–260
Pentenyl glycoside, in stereocontrolled synthesis of α-mannans, 264–267
O-Pentenyl glycosides
  active–latent strategy for, 186
  armed–disarmed approach for, 198–199
  in orthogonal strategy, 192
  selective activation, 180–182

  two-step activation for, 184–185
Pentenyl orthoester, in stereocontrolled synthesis of α-mannans, 266, 268, 270
S-Phenyl glycosides
  in orthogonal strategy, 189–191
  for two-step activation, 182–184
Phenylselenyl, for selective activation, 179–181
Phosponic acid derivatives, TcTS inhibition with, 346, 348f
Phytoalexin-elicitor active oligosaccharide, steric hindrance deactivation synthesis of, 193–194
PI-88. *See* α-(1→3)-Pentamannan
PIROUETTE, 67
Pneumococcal oligosaccharide group B type III, inverse regioselectivity synthesis of, 210–211
Pneumococcal oligosaccharide serotype 6A, traditional linear synthesis of, 167–169
Pneumococcal oligosaccharide serotype 14
  convergent block synthesis of, 176–177
  temporary deactivation concept synthesis of, 195–196
p–Nitrophenyl α-sialosides, as donor for TcTS reaction, 342
2′-*O*-(*p*–Nitrophenyl)-αNeu5Ac (*p*NPNeu5Ac) derivatives
  as donors for TcTS reaction, 342–344
  trans-sialylation with, 344–346
*p*NPNeu5Ac derivatives. *See* 2′-*O*-(*p*–nitrophenyl)-αNeu5Ac derivatives
Polymer-supported synthesis
  convergent building-block strategy with, 220–222
  of α-mannans, 279–280
  of oligosaccharides, 219–222
Polyols, reactivity-based regioselective glycosylation of, 208–210
Pople–Santry LCAO-MO method, 23
Potential energy surface (PES)
  of galactopyranosyl oxacarbenium ions, 96t, 97
  hydronium ions on, 130
Programmable strategy
  for oligosaccharide synthesis, 201–202
  in one-pot glycosylation strategies, 216–218
Promoter, for armed–disarmed approach, 197–198
Propargyl ethers, for glycosylation reactions, 116
Protecting groups
  for galactopyranosyl oxacarbenium ions, 87–88
    facial selectivity, 103–104
    interaction of, 118
    methodology development for, 145
    reactivity and, 119–120
    rotation and, 119
  in glycosylation reactions, 165–166
  product purity and, 129
Proton transfer
  in galactopyranosyl oxacarbenium ions, 141
    facial selectivity, 102, 103f
    methodology development for, 145
    neutral orthoesters, 123, 126–128
  in glycosylation reactions, 105, 106–107f, 109, 130–136
    acyl-transfer and, 131–132
    energetic magnitude of, 135–136
    methodology development for, 145
    neighboring-group participation, 131–132, 133–134f, 135
    rates of, 131
    timing of, 130–131
Proton–carbon couplings, 36–45
  $^3J_{HCCC}$, 41–42
  $^3J_{HCOC}$, 37–41, 39f
  $^3J_{HCSC}$, 42–43
  $^3J_{HOCC}$, 43–45, 44f
Proton–nitrogen couplings, $^3J_{HCCN}$, 45–47, 46f–47f
Proton–phosphorus couplings, $^3J_{HCOP}$, 47–51, 48f

Proton–proton couplings, 21–36
  $^3J_{\mathrm{HCCH}}$, 21–32
  $^3J_{\mathrm{HCNH}}$, 32–33
  $^3J_{\mathrm{HCOH}}$, 33–36
  $^3J_{\mathrm{HCSiH}}$, 36
  $^4J_{\mathrm{HCCCH}}$, 64–68, 66f
  $^4J_{\mathrm{HC=CCH}}$, 68
  $^5J_{\mathrm{HCCCCH}}$, 68–69, 69f
  $^5J_{\mathrm{HCC=CCH}}$, 69
Pseudorotation, in canonical vector representation, 111, 111f
PSEUROT program, 29, 41, 60
Pyranose rings
  $^3J_{\mathrm{HCCH}}$ values in, 26
  $^3J_{\mathrm{HCOH}}$ values in, 34–35, 35f
Pyridine derivatives, TcTS inhibition with, 348, 348f

Q

QM. *See* Quantum mechanical studies
QM-MM. *See* Quantum mechanical-molecular mechanics studies
Quantum mechanical (QM) studies
  deficiencies of, 89
  of oxacarbenium ions, 84, 87–89
Quantum mechanical–molecular mechanics (QM-MM) studies, of oxacarbenium ions, 87
  experimental agreement, 117
  for structure study, 89–90

R

Reactivity-based programmable strategy, for oligosaccharide synthesis, 201–202
Regioselectivity-based strategies, for oligosaccharide synthesis, 208–213
  bidirectional approaches, 211–213
  hydroxyl reactivity, 208–210
  triphenylmethyl reactivity, 210–211
Remote substituents disarming, for oligosaccharide synthesis, 202–203
Rhamnans, stereocontrolled synthesis of
  introduction to, 251–252, 286
  α-rhamnans, 281–285, 282t–284t
  β-rhamnans
    by direct methods, 299–301
    by indirect methods, 291
α-Rhamnans, stereocontrolled synthesis of, 281–285
  in absence of neighboring-group participation, 282t
  neighboring group-directed, 282t–284t
β-Rhamnans, stereocontrolled synthesis of
  by direct methods, 299–301
    β-rhamnotetraose, 300–301
    β-(1→4)-β-(1→2)-rhamnotriose, 299–300
  by indirect methods, 291
β-rhamnotetraose, synthesis of, 300–301
β-(1→4)-β-(1→2)-Rhamnotriose, synthesis of, 299–300
Ring conformation, of galactopyranosyl oxacarbenium ions, 89–98, 141
  geometric parameters of, 95–97, 96t
  geometry optimization, 91–95, 93t, 94f, 95f
  leaving groups, 104
  protecting groups and, 104
  starting geometry for, 89–91, 91f, 92, 94
Ring-inversion barrier
  atomic force microscopy for, 112–113
  in galactopyranosyl oxacarbenium ions, 110–114, 111f, 112f, 112t
3D ROESY-HSQC technique, 52
Rotation, role in galactopyranosyl oxacarbenium ions, 118–130, 119f
  acyl-transfer side reaction, 123, 126–128
  hyperconjugative interactions, 118–119, 119f, 120f
  neighboring-group participation, 122–123, 122f, 124f, 125–126t
  protecting groups, 119–121
  substituents, 121

S

Saccharomyces cerevisiae, 257
SAPA. *See* Shed acute-phase antigen
SBox. *See* *S*-Benzoxazolyl
SCPT-INDO calculations, 58

Selective activation
  for oligosaccharide synthesis, 177–182
    heparin-like oligosaccharides, 179–180
    with three leaving groups, 179–181
    three step sequential, 180–182
  in one-pot glycosylation strategies, 215–217
  orthogonal strategies v., 189
  in solid-phase synthesis, 220
Selective strategies, for oligosaccharide synthesis, 177–196
  active–latent strategy, 185–188
  orthogonal and semi-orthogonal strategies, 188–193
  selective activation, 177–182
  steric hindrance deactivation, 193–194
  temporary deactivation concept, 193–196
  two-step activation and *in situ* preactivation, 182–185
Selenoglycosides, two-step activation for, 184–185
Semi-orthogonal strategies, for oligosaccharide synthesis, 188–193
Shed acute-phase antigen (SAPA), 336
Sialic acid
  mucin oligosaccharides as acceptors of, 339–341
  TcTS transfer of, 336, 337f
Sialic acid-binding site
  compounds studied as inhibitors of, 345–349, 348f–350f
  of TcTS, 338–339
Sialyl donor, for TcTS reaction, modifications of, 343–347
Sialylation, of *T. cruzi* oligosaccharides, 339–347
α-(2→3)-Sialyllactose, as donor for sialylation of *T. cruzi* oligosaccharides, 341
Sialyltransferase, oligosaccharide synthesis with, 231–232
Side-chain orientation and conformation, in galactopyranosyl oxacarbenium ions, 109–118
  reactivity, 109–110
  ring-inversion barrier, 110–114, 111f, 112f, 112t
  steric buttressing, 116–117
  through-bond activation, 115, 115f
  through-space interaction efficiency, 114
Solid-phase synthesis
  acceptor-bound approach, 220, 222, 224
  donor-bound approach, 220, 222–223
  of α-mannans, 279–280
  types of, 220
Solvation energy, for CBS calculation, 89
Solvents
  α-mannan stereocontrolled synthesis in frozen, 254–255
  oxacarbenium ions and, 99
Solvent-separated ion pair (SSIP)
  methodology development for, 146
  oxacarbenium ion
    equilibrium with, 99
    facial selectivity and, 100–101
    ionization and, 137
SOPPA *ab initio* calculations, 63
Spergularia ramosa pentasaccharide, convergent block synthesis of, 171–172
SSIP. *See* Solvent-separated ion pair
Ssp4, GPI in, 318
STaz. *See* *S*-Thiazolinyl
Stereocontrolled synthesis of mannans and rhamnans, 251–301
  introduction to, 251–252, 286
  α-mannans
    in absence of neighboring-group participation, 252–261
    neighboring group-directed, 262–281
  α-rhamnans, 281–285, 282t–284t
Stereoselectivity, of glycosylation reactions, 103–104, 103f
  manipulation of, 136
  steric buttressing, 116–117
Stereospecificity, of galactopyranosyl oxacarbenium ions, 103–105, 109, 142
  ionization and, 137–138, 139f

Stereospecificity, of galactopyranosyl oxacarbenium ions (*cont.*)
  pressure dependence of, 121
Steric buttressing, in glycosylation reactions, 116–117
Steric hindrance deactivation, for oligosaccharide synthesis, 193–194
Sucrose, electron density of, 85
Super-armed glycosyl donors, for oligosaccharide synthesis, 206–207

T

Tc85 glycoprotein, 336–337
TcMUC family. *See Trypanosoma cruzi* mucin gene family
TcSMUG family. *See Trypanosoma cruzi* small mucin gene family
TcTS. *See Trypanosoma cruzi* trans-sialidases
Temporary deactivation concept, for oligosaccharide synthesis, 193–196
2,3,4,6-Tetra-*O*-methyl-D-glycopyranosides, 87. *See also* Galactopyranosyl oxacarbenium
tGPI mucins, carbohydrate structures in, 335
Thermal vibrational excitation, ionization of galactopyranosyl oxacarbenium ions by, 140–141
S-Thiazolinyl (STaz)
  in orthogonal strategy, 190–192
  for selective activation, 182
  temporary deactivation concept, 193–195
Thioglycosides
  for α-mannans stereocontrolled synthesis
    activation for, 275–276
    in trichloroacetimidate approach, 274–275
  in situ preactivation for, 185
Through-space stabilizing electronic effect, in galactopyranosyl oxacarbenium, 85
  efficiency of, 114
  energetics of, 103–104
Thr-Thr-[LacNAcThr]-Thr-Thr-Gly, synthesis of, 333–334
Torsional angles
  of oligonucleotides, 48–49, 48f
  online calculators for, 70–72
Torsional effects disarming, for oligosaccharide synthesis, 203–206
Transition states (TS), of glycosylation reactions, 141
Trialkylsilyl ethers, for glycosylation reactions, 116
Trichloroacetimidate approach,
  to α-mannans stereocontrolled synthesis, 257, 259–260, 268–269, 271
  with thioglycoside donors, 274–275
Trifluoroacetimidate approach, to α-mannans stereocontrolled synthesis, 259–260
Triphenylmethyl reactivity, in oligosaccharide synthesis, 210–211
Tritylated thioglycosides, for bidirectional strategy of synthesis, 213–214
Trypanosoma cruzi, 311–355
  cell surface glycoconjugates of, 313–354
    glycoinositolphospholipids, 313–321, 314f–316f, 322f
    mucins, 321–335, 322f, 326f, 326t, 329f
    other glycoproteins, 352–354, 353f–354f
    trans-sialidase, 336–352, 337f–338f, 348f–351f
  concluding remarks, 354–355
  introduction to glycobiology of, 312
  life cycle of, 312–313, 313f
Trypanosoma cruzi mucin gene (TcMUC) family, 324, 326f, 326t, 327
Trypanosoma cruzi small mucin gene (TcSMUG) family, 322–324, 326f, 326t
Trypanosoma cruzi trans-sialidases (TcTS), 52, 336–352, 337f–338f, 348f–351f
  biological effects of, 350–352
  GPI in, 317
  inhibition of, 345–350, 348f–351f

- in selective sialylation of oligosaccharides, 339–347
- structure and catalytic mechanism, 336–340, 337f–338f

Trypomastigote small surface antigen (TSSA), of *T. cruzi*, 324, 327

TSSA. *See* Trypomastigote small surface antigen

Two-step activation
- active–latent strategy v., 186
- for oligosaccharide synthesis, 182–185
- in solid-phase synthesis, 220

V

VB calculations, 21
- for $^3J_{HCCH}$, 21–22
- for $^3J_{CCCC}$, 55–57
- for $^4J_{HCCCH}$, 65

Vicinal coupling constants, 21–59
- carbon–carbon couplings, 51–59
  - $^3J_{CCCC}$, 55–59
  - $^3J_{CCOC}$, 52–55, 56f
- carbon–tin couplings, $^3J_{CCCSn}$, 64
- fluorine couplings, 60–63
  - $^3J_{CCCF}$ and $^3J_{COCF}$, 62
  - $^3J_{FCCF}$, 62–63
  - $^3J_{HCCF}$, 60–61
  - $^3J_{HCNF}$ and $^4J_{HCCNF}$, 61–62
- proton–carbon couplings, 36–45
  - $^3J_{HCCC}$, 41–42
  - $^3J_{HCOC}$, 37–41, 39f
  - $^3J_{HCSC}$, 42–43
  - $^3J_{HOCC}$, 43–45, 44f
- proton–nitrogen couplings, $^3J_{HCCN}$, 45–47
- proton–phosphorus couplings, $^3J_{HCOP}$, 47–51, 48f
- proton–proton couplings, 21–36
  - $^3J_{HCCH}$, 21–32
  - $^3J_{HCNH}$, 32–33
  - $^3J_{HCOH}$, 33–36
  - $^3J_{HCSiH}$, 36

W

W couplings, 64–68, 66f
- extended, 68–69, 69f

X

Xylanase, oligosaccharide synthesis with, 234–235

Xylans, synthesis of, 234–235

2-*O*-*β*-D-Xylopyranosyl-D-xylose, 6

2-*O*-*β*-D-Xylopyranosyl-L-arabinose, 6

Z

Zanamivir, 345

Zero point energy (ZPE), for CBS calculation, 89

ZPE. *See* Zero point energy